



Cardiff School of Pharmacy and Pharmaceutical Sciences
Cardiff University
Cardiff

Phosphorus Prodrugs of S1P Receptor Modulators as a Novel Therapeutic Opportunity

A thesis submitted to Cardiff University for the degree of
Philosophiæ Doctor

Edward William James

Supervisors: Prof. Chris McGuigan, Prof. Yves-Alain Barde & Dr Andrea Brancale

February 2017

Acknowledgements

First and foremost I need to acknowledge Prof. Chris McGuigan for offering me the opportunity to work on this exciting project. It is with great sorrow that he is unable able to see the completion of the project. However, over his many decades of excellent scientific work he has left what could be described as a legacy that many have followed and will continue to follow in his examples of excellent scientific research and building of positive and productive professional interpersonal relationships. He had every right to believe that he has made a positive contribution to the world.

Dr Andrea Brancale, Prof. Andrew Westwell, Prof. Yves-Alain Barde and his PhD student Katharina Säuberli have all been supportive and provided me with numerous constructive conversations. My colleagues have been helpful, especially Salvatore Ferla in the first year and with the homology modelling in the final year. Fabrizio Pertusati, Magdalena Slusarczyk and Michaela Serpi have consistently been very helpful with technical difficulties such as with the HPLC or enzymatic NMR experiments. Valentina Ferrari was also very helpful as were the rest of Prof. Chris McGuigan's, Dr Andrea Brancale's and Prof. Andrew Westwell's research groups including the post-doctoral researchers Dr Sahar Kandil and Dr Martin Schepelmann.

The technicians Tom Robertshaw and Calvin Smith provided me with entertaining conversation and friendship, as did Julie Hayward, Hywel Edwards and Steph Larkin of the NRN administrative team. A number of Erasmus students who were around for roughly half a year were also good to chat to including Nicolo Santi, Principe Azzurro, Sara Serafini and Massimiliano Renzi.

“Nothing has such power to broaden the mind as the ability to investigate systematically and truly all that comes under thy observation in life.”

Marcus Aurelius

Abstract

The sphingosine 1-phosphate receptor modulator fingolimod / Gilenya / FTY720 has become an effective and commercially available therapeutic agent for the treatment of relapsing-remitting multiple sclerosis. Fingolimod is phosphorylated by sphingosine kinase *in vivo* to the pharmacologically active S-fingolimod phosphate. The original aim of the work was to synthesise novel phosphate delivery prodrug analogues of fingolimod and determine whether or not these novel analogues could provide an improved therapeutic profile. The principal phosphate delivery prodrug method to be investigated was phosphoramidate "ProTide" chemistry.

ProTide fingolimod analogues were found to have a poor level of stability and readily degrade to unwanted cyclised structures at room temperature and when exposed to very mildly basic conditions. In order to mitigate the poor stability issues it was considered possible that forming ProTide analogues of mono-alcohol S1P receptor modulators, as opposed to diol fingolimod, would lead to greater stability. The synthesis of mono-alcohol S1P receptor modulator benzyl ether derivative analogues published by Tsuji *et al* was attempted and successfully achieved.

Previously reported ProTide synthesis and *in vitro* testing methods were employed. Carboxypeptidase, human serum, base stability, acid stability and cell lysate processing experiments were conducted in the School of Pharmacy. Homology modelling was employed to determine S1P₁ selectivity of benzyl ether derivative analogues and novel structures.

ProTide benzyl ether derivative analogues were found to have a far greater level of stability than ProTide fingolimod analogues and *in vitro* processing experiments showed that they are processed to the desired pharmacologically active monophosphate. The research signifies the development of an entirely new family of potential therapeutic agents.

Abbreviations and Acronyms

ACN	Acetonitrile
AcOEt	Ethyl acetate
ADME	Absorption, distribution, metabolism and excretion
AMBER	Assisted Model Building with Energy Refinement
BBB	Blood-brain barrier
BDNF	Brain-derived neurotrophic factor
BED	Benzyl ether derivative
Bzl	Benzyl
^{13}C NMR	Carbon-13 nuclear magnetic resonance spectroscopy
CNS	Central nervous system
Cosy	Homonuclear correlation spectroscopy
CREB	cAMP response-element binding protein
DCM	Dichloromethane
EBV	Epstein-Barr virus
ELISA	Enzyme-linked immunosorbent assay
EMA	European Medicines Agency
ES cells	Embryonic stem cells
Et	Ethyl
Eq	Equivalent
FDA	Food and Drug Administration
Gly	Glycine
GPCR	G protein-coupled receptor
HCV	Hepatitis C virus
HDAC	Histone deacetylase

HIV	Human immunodeficiency virus
¹ H NMR	Proton nuclear magnetic resonance spectroscopy
HPLC	High performance liquid chromatography
HSQC	Heteronuclear single quantum coherence spectroscopy
Ile	Isoleucine
iPr	Isopropyl
L-Ala	L-Alanine
LAT1	L-type amino acid transporter-1
Leu	Leucine
LS	Ligand strain
Me	Methyl
MeOH	Methanol
MHz	Megahertz
MRI	Magnetic resonance imaging
MS	Multiple sclerosis
NA	Nucleoside analogue
NMI	1-methylimidazole
Pe	Pentyl
Ph	Phenyl
Phe	Phenylalanine
PK/PD	Pharmacokinetic/pharmacodynamic
Ppm	Parts per million
³¹ P NMR	Phosphorus nuclear magnetic resonance spectroscopy
PNS	Peripheral nervous system
PPMS	Primary progressive multiple sclerosis

PRMS	Progressive relapsing multiple sclerosis
Pro	Proline
PSA	Polar surface area
PTSD	Post traumatic stress disorder
RBF	Round bottom flask
RRMS	Relapsing-remitting multiple sclerosis
R.T.	Room temperature
S1P	Sphingosine 1-phosphate
SPMS	Secondary progressive multiple sclerosis
TEA	Triethylamine
THF	Tetrahydrofuran
TLC	Thin layer chromatography
UV	Ultraviolet
v/v	Volume-volume percent
VZV	Varicella-zoster virus

Contents

Chapter 1 - Introduction	1
1.1 Neurodegenerative Disease and Multiple Sclerosis	1
1.1.1 The Nervous System	1
1.1.1.1 The Central Nervous System	1
1.1.1.2 The Peripheral Nervous System	3
1.1.1.3 Neurodegenerative Disease	4
1.1.2 The Immune System	4
1.1.2.1 Innate Immune System	4
1.1.2.2 Adaptive Immune System	5
1.1.2.3 Autoimmune Disease	6
1.1.3 Multiple Sclerosis	7
1.1.3.1 Genetics	11
1.1.3.2 Vitamin D	12
1.1.3.3 Hygiene Hypothesis	14
1.1.3.4 Epstein-Barr Virus	14
1.1.3.5 Treatments for Multiple Sclerosis	15
1.2 Fingolimod and S1P Receptors	17
1.2.1 Development of FTY720 / Fingolimod / Gilenya	17
1.2.2 S1P Receptors	22
1.2.3 Mode of Action of Fingolimod	24
1.2.4 Potential Therapeutic Uses of Fingolimod	27
1.2.5 Side Effects and Dangers of Fingolimod	27
1.2.6 Fingolimod Analogues and Other S1P Receptor Modulators	28
1.3 The Pharmacology of Drug Action: Opportunities for Prodrugs	33
1.3.1 CNS Acting Drugs	33
1.3.2 Prodrugs	34
1.3.3 Phosphate Delivery Prodrugs	36
1.3.4 Phosphoramidate (ProTide) Prodrugs	39
1.3.5 Mode of Action of Phosphoramidates	41
1.4 Aim of Work: Phosphoramidate Fingolimod Analogues	43
1.5 References	45

Chapter 2 - Finding the Chemical Pathway to Synthesise “ProTide”	52
Fingolimod	
2.1 Discussion	52
2.1.1 The Synthetic Challenge	52
2.1.2 Phosphorochloridate Chemistry	54
2.1.3 Phosphoramidate Synthesis Using a NaH Base	58
2.1.4 Phosphoramidate Synthesis Using a NMI Base	61
2.1.5 Phosphoramidate Synthesis Using a NaOMe Base	63
2.1.6 Phosphoramidate Synthesis Using a tBuMgCl Base	65
2.2 References	73
 Chapter 3 - Synthesis of ProTide Fingolimod Analogues	 74
3.1 Phosphoramidate Fingolimod Synthesis	74
3.1.1 Fractions 16 – 20	77
3.1.2 Fractions 26 – 29	78
3.1.3 Fractions 32 – 40	80
3.1.4 NMR Analyses of Phenyl-(Methoxy-L-Alaninyl) Phosphoramidate Fingolimod	82
3.2 Further Syntheses	87
 Chapter 4 - Chiral Synthesis	 92
4.1 Discussion	92
4.1.1 Review of the Chiral Synthetic Challenge and Available Literature	92
4.1.2 Development of the Chiral Synthetic Procedure	97
4.1.3 The Final Chiral Synthesis	105
4.2 References	106

Chapter 5 - Biochemical Processing of ProTide Fingolimod Analogues	108
5.1 Stability Assays	108
5.1.1 Acid Stability Test	108
5.1.2 Base Stability Test	110
5.1.3 DMSO Freeze Thaw Stability Tests	111
5.2 Enzymatic and Human Serum Assays	114
5.2.1 Ph-LAla-OEt-F Carboxypeptidase Experiment	115
5.2.2 Ph-Gly-OBzl-F Carboxypeptidase Experiment	117
5.2.3 Ph-LAla-OEt-F Porcine Liver Esterase Experiment	121
5.2.4 Initial Conclusions	122
5.2.5 Ph-LAla-OBzl-F Carboxypeptidase Experiment	123
5.2.6 Ph-Leu-OBzl-F Porcine Liver Esterase Experiment	124
5.2.7 Naphth-LAla-OEt-F Porcine Liver Esterase Experiment	125
5.2.8 Controlled Ph-LAla-OBzl-F Carboxypeptidase Experiment	127
5.2.9 Ph-LAla-OBzl-F Human Serum Experiment	129
5.3 Final Conclusions	132
5.4 References	134
Chapter 6 - Benzyl Ether Derivative “Tsuji” Compounds	135
6.1 Rationale for Selection of BED Family of Compounds for ProTide Synthesis	135
6.2 Synthesis of BED Compounds	142
6.2.1 Synthesis of BED(a)	142
6.2.2 Synthesis of BED(h)	148
6.3 Synthesis of Phosphorus Prodrug BED Compounds	156
6.3.1 Synthesis of ProTide BED Analogues	156
6.3.2 CycloSal BED	164
6.3.3 HepDirect BED	165
6.3.4 Aryl SATE BED(a) and Fingolimod	167
6.4 References	170

Chapter 7 – Biochemical Processing and Analysis of ProTide BED	173
Compounds	
7.1 Enzymatic and Cell Lysate Assays	173
7.1.1 Ph-LAla-OMe-BED(a) Carboxypeptidase Experiment	173
7.1.2 Ph-LAla-OMe-BED(a) Neuronal Cell Lysate Experiment	176
7.1.3 Ph-LAla-OBzl-BED(a) Neuronal Cell Lysate Experiment	178
7.1.4 Ph-LAla-OMe-BED(h) Carboxypeptidase Experiment	180
7.2 Stability Assays Part 1	182
7.2.1 Ph-LAla-OMe-BED(h) Base Stability Experiment	182
7.2.2 Ph-LAla-OiPr-BED(a) Base Stability Experiment	184
7.2.3 Ph-LAla-OMe-BED(h) Acid Stability Experiment	186
7.3 HPLC	187
7.3.1 Analytical HPLC	187
7.3.2 Preparative HPLC	191
7.4 Stability Assays Part 2	193
7.4.1 Ph-LAla-OiPr-BED(h) Acid Stability Experiment	193
7.4.2 Ph-LAla-OMe-BED(a) Base Stability Experiment	194
7.4.3 Ph-LAla-OMe-BED(h) Base Stability Experiment	195
7.4.4 Ph-LAla-OMe-BED(a) Human Serum Experiment	196
7.4.5 Ph-LAla-OiPr-BED(a) Human Serum Experiment	198
7.4.6 Ph-LAla-OMe-BED(h) Human Serum Experiment	200
7.5 Potential for Therapeutic Viability and FDA Approval	202
7.5.1 ProTide Moiety Stability and Processing	202
7.5.2 CNS Transfer Properties	202
7.5.3 Discussion of ProTide Processing in Human Serum	205
7.5.4 Metabolic Stability	206
7.5.5 Toxicity	206
7.6 References	208

Chapter 8 - Molecular Modelling Studies	210
8.1 S1P₁ Selectivity	210
8.2 Homology Modelling	213
8.2.1 Molecular Docking	213
8.2.2 S1P ₁ Docking	219
8.2.3 S1P ₃ Docking	220
8.3 Conclusions	224
8.4 References	225
Chapter 9 - Experimental	226
9.1 General Experimental Details	226
9.2 Standard Procedures	228
9.3 Phosphorochloridate Syntheses	231
9.4 Non-S1P Receptor Modulator Phosphoramidate Syntheses	245
9.5 Syntheses of Fingolimod Derived Phosphoramidates	250
9.6 Chiral Phosphoramidate Fingolimod Synthesis and Intermediates	261
9.7 Syntheses of BED Compounds	270
9.8 Syntheses of BED Compound Derived Phosphoramidates	286
9.9 SATE Phosphorus Prodrugs	298
9.10 HepDirect Phosphorus Prodrugs	302

Chapter 1 - Introduction

1.1 Neurodegenerative Disease and Multiple Sclerosis

1.1.1 The Nervous System

The nervous system is the part of an animal's body responsible for coordinating voluntary and involuntary actions and transmitting signals from one region of the body to another. The nervous system is comprised of the sensory organs, nervous tissue, spinal cord and the brain. In the majority of animal species the nervous system is subdivided into two further systems: the central nervous system (CNS) and the peripheral nervous system (PNS). The CNS consists of the brain and spinal cord whereas the PNS consists predominantly of nerves.¹

1.1.1.1 The Central Nervous System

The central nervous system (CNS) is comprised of the brain and spinal cord and is responsible for processing information, regulation of systems, performing actions and storing memories. The CNS contains both white matter and grey matter. White matter consists predominantly of myelinated axons and grey matter consists mainly of neuronal cell bodies.¹ Both white matter and grey matter contain glial cells, often referred to as supporting cells, which serve a variety of different functions including providing scaffold support for neurogenesis (generation of neurons from neural stem cells) and immunoregulation.²

Axons are specialised projections from neurons (nerve cells). Their function is to conduct electrical impulses, also known as action potentials, from the neuron's larger cell body to other neurons, muscles and glands.¹ Oligodendrocytes act to support and insulate axons by producing the electrically insulating myelin sheath thus enabling electrical conduction of the action potential along the length of the axon.³

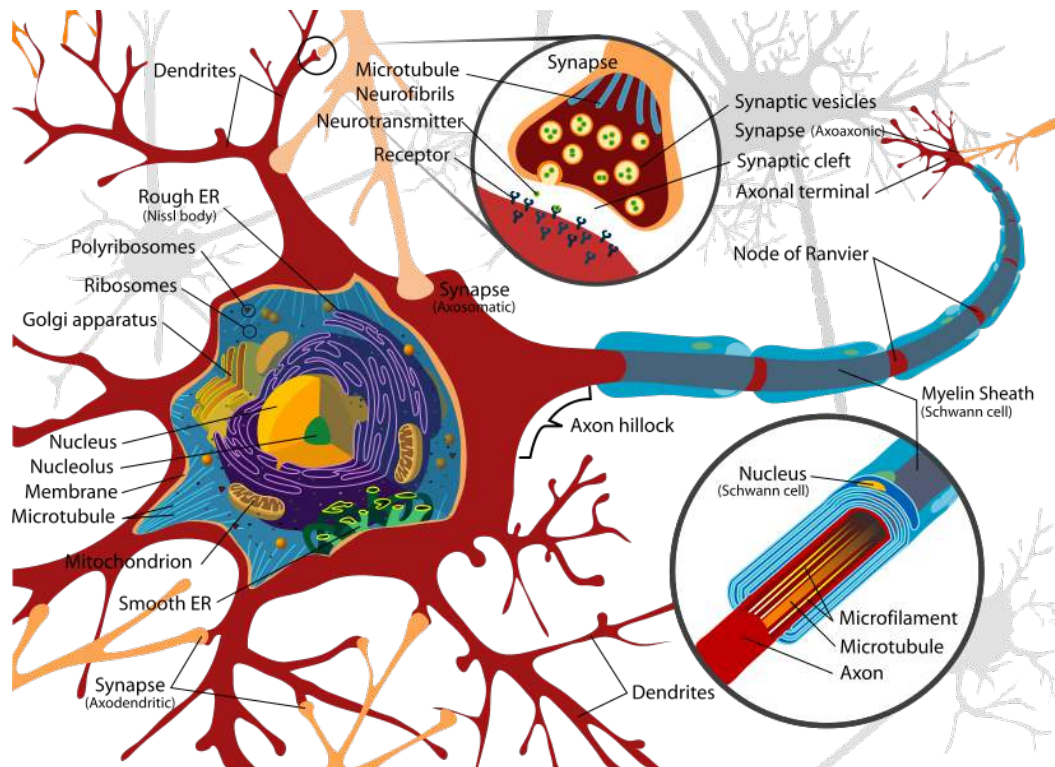


Figure 1.1 Neuron (Image: public domain. Produced by Mariana Ruiz Villarreal)

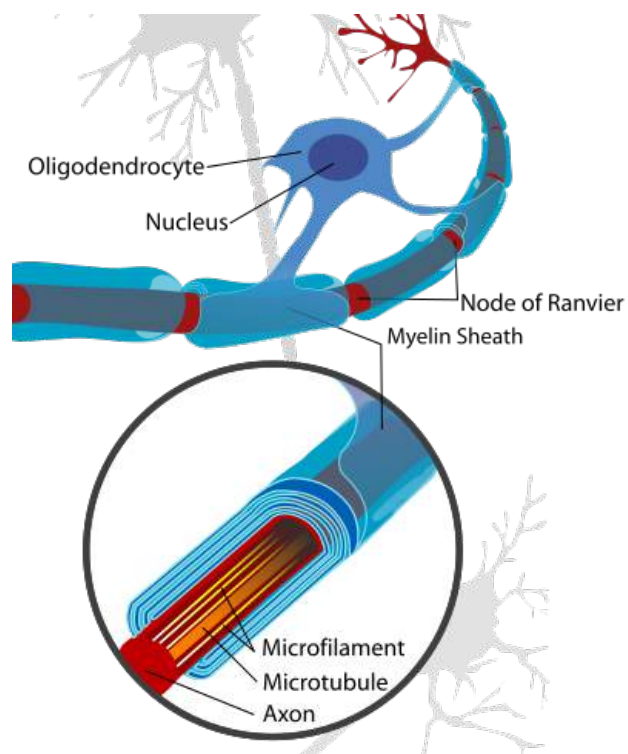


Figure 1.2 Neuron with oligodendrocyte and myelin sheath (Image: public domain. Produced by Mariana Ruiz Villarreal)

The human brain performs an enormous range of functions and has the capacity to consciously and unconsciously process information received from the PNS and take actions to ensure the continued survival of the organism. The brain is located in the head close to primary sensory organs responsible for vision (the eyes), taste (the tongue), smell (the nose), equilibrioception (the vestibular system) and hearing (the ears).¹ The brain is believed to be the organ of the body responsible for consciousness and the development of personality and character. It is considered to essentially define what makes a person who they are and any damage to the brain can cause considerable changes in character and personality.⁴

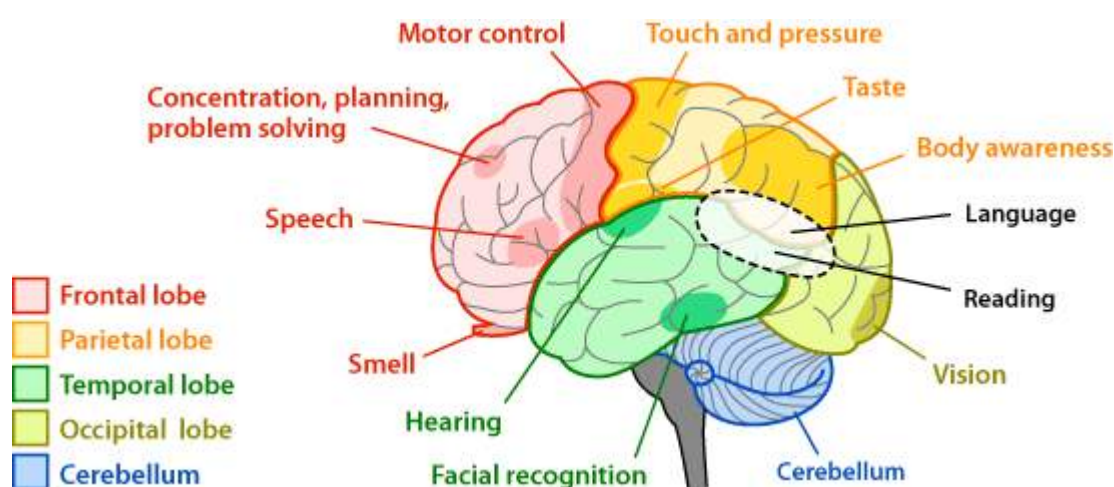


Figure 1.3 Simplified model of the brain. Different regions of the brain and their functions (Image: Arizona State University School of Life Sciences website)

1.1.1.2 The Peripheral Nervous System

The peripheral nervous system (PNS) comprises the nerves and ganglia outside the CNS organs of the brain and spinal cord. The PNS connects the CNS to the body's limbs and organs and acts to facilitate communication between the brain and the various non-CNS regions of the body.¹

1.1.1.3 Neurodegenerative Disease

Neurodegenerative diseases are illnesses in which neurodegeneration is observed to occur. Neurodegeneration can be defined as the progressive loss of function and structure of neurons (nerve cells) and includes the death of neurons. Three of arguably the most well-known neurodegenerative diseases include Alzheimer's disease (the most common form of dementia), Parkinson's disease and Huntington's disease.⁵

1.1.2 The Immune System

Organisms have their own systems to try to defend against infection and disease. In animals, such as humans, this system of defence is known as the immune system and is comprised of a complex network of defence mechanisms that work in a variety of ways. Unicellular organisms such as bacteria have their own versions of the immune system that typically include enzymes which protect against infection from viruses known as bacteriophages. In this document the human immune system will be the focus as it is relevant to the research described.

In humans the immune system can be described as being comprised of two subsystems: the innate immune system (also found in all animals and plants) and the adaptive immune system (found in all jawed vertebrates).^{6,7}

1.1.2.1 Innate Immune System

The innate immune system is an organism's first line of defence and is different to the adaptive immune system in that the innate immune system doesn't change with time and exposure to different pathogens. The innate immune system is non-specific and consists of a variety of defensive measures including:

- Physical barriers such as the skin
- Enzymatic defence mechanisms such as antimicrobial lysozyme
- Anatomical traps such as the nasal cavity
- Mechanical cleansing mechanisms such as cilia

- Phagocytes which ingest foreign entities such as bacteria and particles
- Reflexes such as coughing and sneezing⁶

1.1.2.2 Adaptive Immune System

The adaptive immune system is also known as the acquired immune system and consists of specialised cells that destroy invading pathogens. The specialised cells of the adaptive immune system are known as lymphocytes and are a subset of leukocytes (white blood cells). The two major types of lymphocyte are known as B cells and T cells. Lymphocytes are located predominantly in the tissues and in the lymphatic system but also to a lesser extent in the circulatory system.^{6,7}

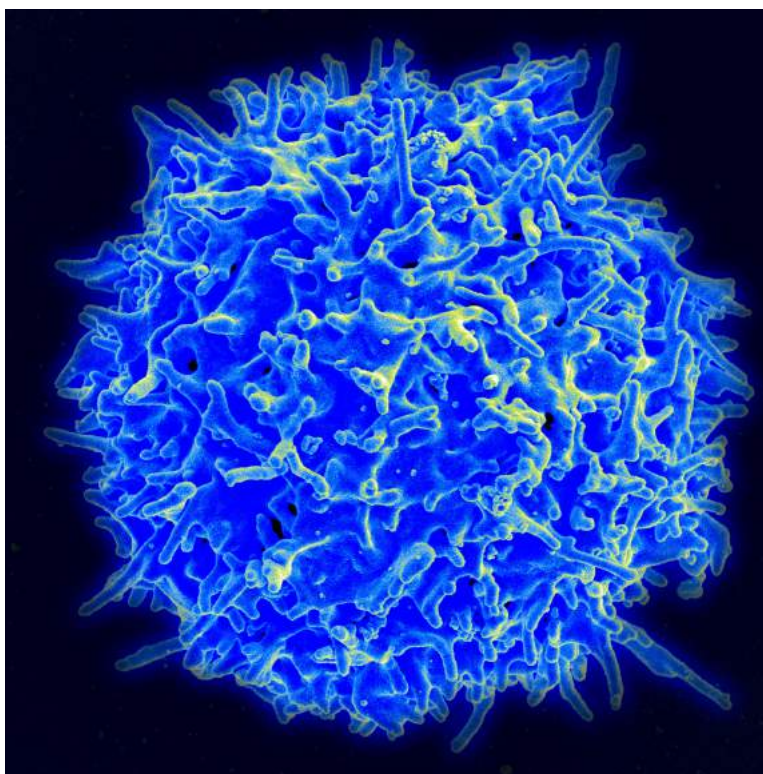


Figure 1.4 Scanning electron micrograph of a human T cell (Image courtesy of the National Institute of Allergy and Infectious Diseases)

The adaptive immune system begins to target a pathogen if the pathogen has successfully evaded the innate immune system. The adaptive immune system will begin the process of neutralising the threat to the organism if the pathogen

overcomes a threshold of accepted antigen concentration and activates antigen-presenting dendritic cells.^{6,7}

The process of acquired immunity includes: the recognition of non-self antigens during the dendritic process of antigen presentation, the generation of a specific response that has been adapted to the specific pathogen and the development of immunological memory. Immunological memory is the process of antibodies (also known as immunoglobulins) and memory cells developing ways to recognise a specific foreign antigen and then inducing an antigen-specific response whenever the antigen is detected again.^{6,7}

The adaptive immune response predominantly takes place in the lymphoid tissues of the spleen, lymph nodes and bone marrow. Antibodies are produced in all of these tissues although the rate of antibody production is greater in the lymph nodes and spleen. The overall mass of antibody production is, however, greater in the bone marrow due to the comparatively greater mass of this tissue within the body. The lymph nodes, bone marrow, spleen and other lymphatic tissues that are involved in antibody production are collectively known as a vascular filtration system.^{6,7}

1.1.2.3 Autoimmune Disease

Autoimmune diseases are caused by an abnormal immune response of the body to regions of the body normally present in a healthy organism. Autoimmune diseases occur when the body's own immune system doesn't recognise certain regions as native to the body and the immune system attacks these regions in the body it usually works to protect. Two of the more well known autoimmune disorders include rheumatoid arthritis and type I diabetes.⁸

1.1.3 Multiple Sclerosis

"...the chief curse of the illness... I must ask constant services of people I love most closely... it is an illness accompanied by frustration... it is an illness that inflicts awareness of loss... sporadically it is, in its manifestations, a disgusting disease."

- Brigid Antonia Brophy (1929-95) novelist and MS sufferer⁹

Multiple sclerosis can reasonably be defined as both an autoimmune disease and a neurodegenerative disease. In the case of multiple sclerosis the immune system attacks the central nervous system causing myelin sheaths to become damaged and thus negatively impact nervous transmission. This neurodegeneration leads to varying severities of symptoms that can include but are not limited to: pain, fatigue, temperature sensitivity, constipation, erectile dysfunction, bladder dysfunction, stiffness, spasms, weakness, impaired speech, impaired swallowing, vertigo (dizziness), clumsiness, poor balance, tremor, loss of vision, depression and cognitive impairment.^{9,10}

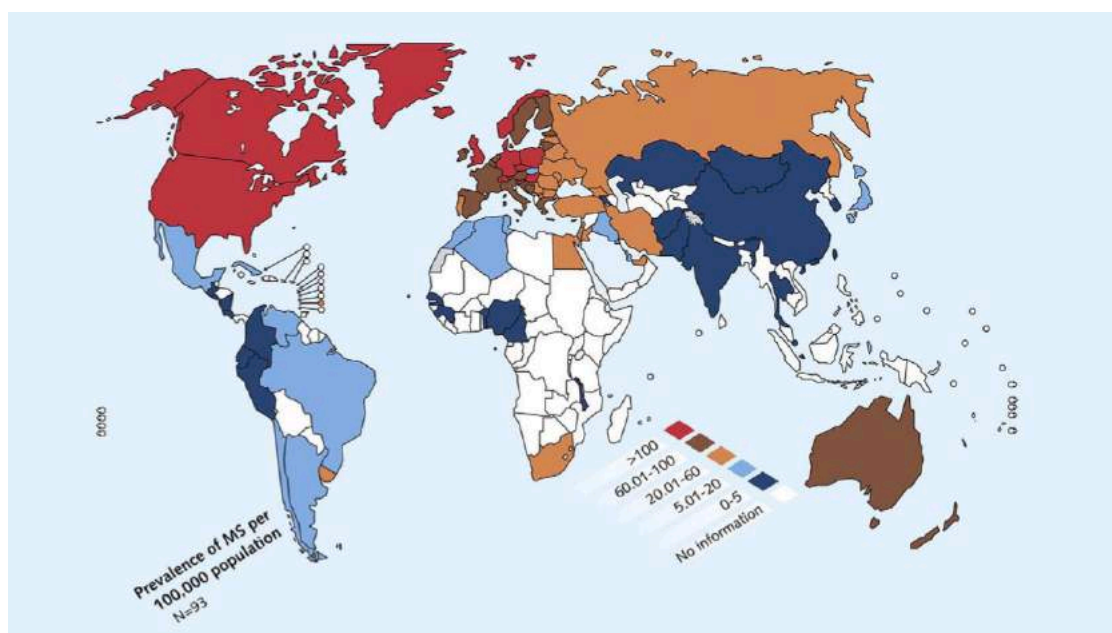


Figure 1.5 The geography of MS: prevalence per 100,000 of the population¹¹



Figure 1.6 Multiple sclerosis sufferer Debbie Purdy outside the Royal Courts of Justice in London, UK. Debbie Purdy has campaigned to find out if her husband would be prosecuted if he were to help her to travel abroad to commit suicide.

Multiple sclerosis is estimated to affect approximately 2.5 million people worldwide⁹ and predominantly affects Caucasians in the developed world. Multiple sclerosis is approximately twice as common in women as in men¹¹ and in fact more recent data show proportionately more females are developing MS than men than was observed in earlier periods.¹²

The disease appears to be caused by a variety of contributory environmental and genetic factors and follows four accepted clinical courses:

1. Relapsing remitting
2. Secondary progressive
3. Primary progressive
4. Progressive relapsing

Relapsing remitting multiple sclerosis (RRMS) is the most common form of the disease and is observed in around 85% of MS sufferers.¹¹ Relapsing remitting MS is characterised by attacks of neurological symptoms that are then followed by complete or incomplete recovery. These relapsing remitting symptoms typically last between a few days to several months and are experienced between phases of stable neurological condition without significant symptoms characteristic of the disease. Approximately 10 - 15% of MS sufferers exhibit symptoms of primary progressive multiple sclerosis (PPMS). PPMS is characterised by a progressive increase of neurological disability. A small number of patients exhibit symptoms of progressive relapsing multiple sclerosis (PRMS) and this disease course is characterised by superimposed relapses. After a number of years of RRMS many patients progress to secondary progressive multiple sclerosis (SPMS) and this clinical course features progressively accumulated neurological disability between or without additional relapses.¹¹

Multiple sclerosis is an inflammatory disease of the spinal cord and brain in which lymphocytes infiltrate the central nervous system and damage neuronal myelin sheaths and axons. The name *multiple sclerosis* refers to the scars (the sclerae) or lesions that are typically observed in regions of the central nervous system that are characteristic of the disease. It is widely held that these scars / lesions / plaques are caused by egress of T cells out of the lymph nodes which then cross the blood brain barrier and into the central nervous system; the T cells are believed to not recognise native neuronal antigens and begin to attack the myelin sheath as if it were a foreign entity. The damage caused to the neuronal axons by the demyelination leads to ineffectual saltatory conduction and a range of symptoms that get progressively worse over time.⁹

As well as the physical symptoms associated with MS, people who suffer from MS are at a greater risk of suicide. This reflects an increased likelihood of depression of up to around 50% according to some studies. The greater incidence of depression among MS sufferers is possibly due to cerebral inflammation or, as is probably more likely, it is a response to the uncertain future and physical restrictions that are symptomatic of steadily worsening disability.⁹

Magnetic resonance imaging (MRI) is often used to assist in the diagnosis of MS. In figure 1.7 abnormalities of the brain can be seen as shown by MRI. The white spots that can be seen on the scan of the brain are what are referred to as plaques or lesions. Anomalies of this type observed on an MRI scan of the brain are indicative of a brain that displays characteristics that are commonly seen in the brain of a person suffering from multiple sclerosis. Figure 1.8 shows three different brains and two of which are brains of MS sufferers. Brain C is the brain of a person suffering from SPMS and when compared to the healthy brain labelled A the stark difference can be seen as caused by the high levels of demyelination.



Figure 1.7 MRI scan showing lesions in the brain typical of MS¹⁰

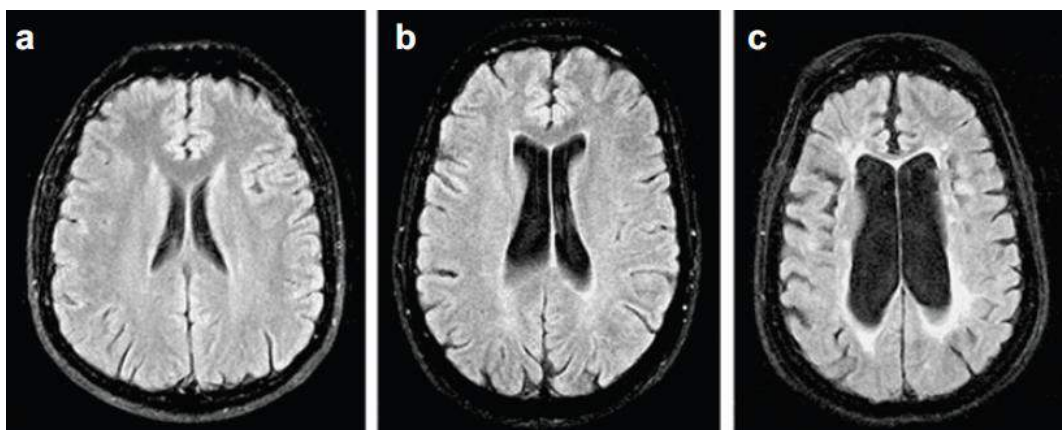


Figure 1.8 MRI scans of A- normal brain, B- RRMS brain and C- SPMS brain¹³

The exact causes of multiple sclerosis are complex and, at the time of writing, relatively poorly understood. Sunlight exposure, exposure to viruses and genetics are the most widely discussed causes of the disease but a myriad of other contributory factors such as dietary fat and cigarette smoking have been proposed.¹⁴ What follows are summaries of some of these proposed contributory factors.

1.1.3.1 Genetics

Looking at the distribution of multiple sclerosis around the world it has been suggested that MS is at least in part due to genetic defects of people who possess Scandinavian ancestry. The explanation for MS incidence in predominantly Caucasian populations is sometimes referred to as the “Viking Gene Hypothesis”. The theory claims that there was a mutation in the genetics of Scandinavian people that causes some of the population to develop multiple sclerosis. The Viking invasions of Great Britain and other places in Europe enabled these genes to spread and the later British Empire further caused these genes to be disseminated to the various places around the world where MS is most common. Nowadays MS is most highly prevalent in such countries as the United States, Canada, Australia, New Zealand, Norway, Iceland, Denmark and the United Kingdom. When taking these facts into account the Viking Gene Hypothesis is an attractive explanation for the occurrence of MS worldwide.

Trygve Holmøy, a researcher based in the neurology department at Ullevål University Hospital in Oslo, conducted an investigation of Norse literature to try to find descriptions of multiple sclerosis in Viking sagas, “however, most sagas are focused on feuds and struggles for power, and not so much is written about women’s health.”¹⁵ Holmøy did not find many reports of MS in Viking literature although in one publication he describes the miraculous curing of a woman called Halldora who suffered occasional paralysis between 1193 and 1198.¹⁵ While this piece of evidence is far from being particularly convincing proof of the validity of the Viking Gene Hypothesis it does show that medieval Viking populations were aware of the existence of diseases that exhibit symptoms reminiscent of MS.

However, while the Viking Gene Hypothesis is quite convincing, it can be said that, “genetic predisposition... cannot explain the remarkable differences in risk among people of common ancestry who migrate to areas of high or low MS prevalence.”¹² It therefore must be concluded that, while genetics probably do play a role in the development of MS, there must also be environmental factors that contribute to the likelihood of developing the disease.

1.1.3.2 Vitamin D

One of the major points of discussion with regard to the causes of the disease is vitamin D. Vitamin D is synthesised in the skin from 7-dehydrocholesterol in the presence of UV radiation. One of the most common sources of UV radiation for humans is the sun.

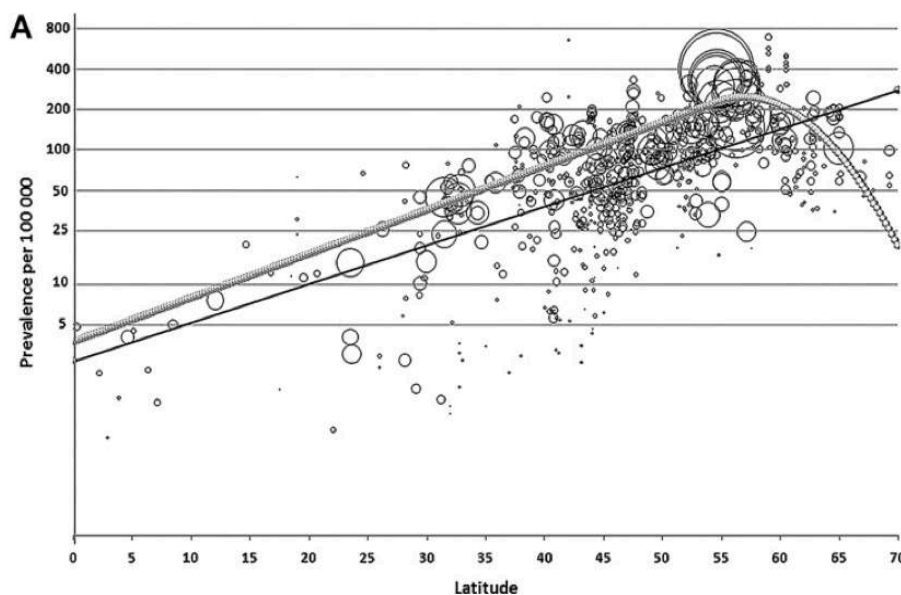


Figure 1.9 Prevalence of MS per every 100,000 people against latitude¹⁶

Studies, such as the one shown in figure 1.9, have found that people who are more frequently exposed to sunlight have a lower likelihood of developing multiple sclerosis.^{12,17} The general trend, as shown in figure 1.9, is that the further north the population is from the equator, the higher the incidence rate of MS. The total number of hours of darkness during the winter increases the further north a point on Earth is from the equator. Also at higher latitudes the temperatures are generally cooler than in more equatorial regions so people further north are more likely to wear more clothes in order to keep them warm which obscure their skin from the sun. This combination of cooler temperatures and longer nights during winter means that people living at higher latitudes have lower serum levels of vitamin D throughout the year than people living closer to the equator.¹⁴

An unfortunate observation is that with increasing exposure to sunlight there is both a decreased risk of developing MS and an increased risk of developing skin cancer. In practice it would be very difficult for anyone to realistically balance the risks and benefits of sunlight by receiving a carefully calculated daily dosage of UV radiation from the sun. An alternative method of elevating the daily intake of vitamin D is through diet and some studies have shown that a daily intake of vitamin D supplements can reduce the risk of developing MS.¹⁴

1.1.3.3 Hygiene Hypothesis

Another proposed contributory factor in the development of MS is personal hygiene. In fact, contrary to common wisdom, it has been proposed that an excessively hygienic childhood could lead to an increased likelihood of developing MS in later life. According to the hypothesis being exposed to a variety of viral pathogens in early development helps develop protection against developing MS in later life.¹² This idea does superficially seem to correspond with MS prevalence rates as MS is most prevalent in the developed world where cleanliness and personal hygiene is typically taken more seriously and is easier to achieve. In poorer parts of the world where high levels of personal hygiene are perhaps somewhat more difficult to maintain, such as subsaharan Africa, South East Asia and parts of Latin America, MS is far less prevalent; although, as previously highlighted, other factors appear to contribute to the lower prevalence rates in these parts of the world such as genetics and hours of sunlight per day.^{9,14}

1.1.3.4 Epstein-Barr Virus

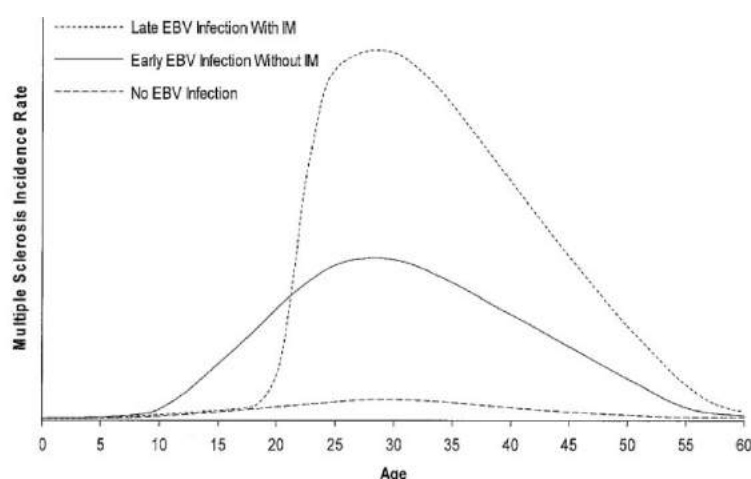


Figure 1.10 MS incidence rates against EBV infection and infectious mononucleosis^{12,18}

The Epstein-Barr virus (EBV) has been suggested as a pathogen that directly affects the likelihood of developing MS but the evidence regarding this virus appears to contradict the hygiene hypothesis. There is a very low likelihood of developing MS for individuals who are seronegative for EBV but a much higher chance of developing MS in people who have at some point been infected by EBV.

This apparent contradiction between the two hypotheses has been termed the Epstein-Barr virus paradox.⁷ There is a correlation between late EBV infection that exhibits infectious mononucleosis and the chances of developing MS as seen in figure 1.10.

1.1.3.5 Treatments for Multiple Sclerosis

Multiple sclerosis is a disease that does not currently have a particularly broad range of effective treatments and many of the treatments are used to alleviate the symptoms of the disease rather than treat the underlying causes. Table 1.1 is a table of typical symptoms and treatments for multiple sclerosis.

	Symptoms	Signs	Established or Equivocal Treatment	Speculative (Alternative) Treatment
Cerebrum	Cognitive impairment Hemisensory and motor Affective (depression) Epilepsy (rare) Focal cortical deficits (rare)	Deficits in attention, reasoning, and executive function (early); dementia (late) Upper motor neuron sign	 Antidepressant drugs Anticonvulsant drugs	Cognitive training
Optic nerve	Unilateral painful loss of vision	Scotoma, reduced visual acuity, colour vision and relative afferent pupillary defect	Low vision aids	
Cerebellum and cerebellar pathways	Tremor Clumsiness and poor balance	Postural and action tremor, dysarthria Limb incoordination and gait ataxia		Wrist weights, carbamazepine, isoniazid, β blockers, clonazepam, thalamotomy and thalamic stimulation
Brainstem	Diplopia, oscillopsia Vertigo Impaired swallowing Impaired speech and emotional lability	Nystagmus, internuclear and other complex ophthalmoplegias Dysarthria Pseudobulbar palsy	 Prochlorperazine, cinnarizine Anticholinergic drugs Tricyclic antidepressant drugs	Baclofen, gabapentin Speech therapy Speech therapy

	Paroxysmal symptoms		Carbamazepine, gabapentin	
Spinal cord	Weakness Stiffness and painful spasms Bladder dysfunction Erectile dysfunction Constipation	Upper motor neuron signs Spasticity	Tizanidine, baclofen, dantrolene, benzodiazepines, intrathecal baclofen, corticosteroids Anticholinergic drugs and/or intermittent self-catheterisation, subrapubic catheterisation Sildenafil (Viagra) Bulk laxatives, enemas	Cannabinoids Abdominal vibration, cranberry juice
Other	Pain Fatigue Temperature sensitivity and exercise intolerance		Carbamazepine, gabapentin Amantadine, modafanil	Premoline, fluoxetine Cooling suit, 4- aminopyridine

Table 1.1 Symptoms and treatments of MS by site^{9,10}

There are a number of treatments for multiple sclerosis that do aim to treat the underlying causes of the disease. Some of these treatments such as mitoxantrone, azathioprine, bone marrow transplantation, teriflunomide, campath (alemtuzumab), tysabri (natalizumab) and T cell vaccination have an action on peripheral autoreactive T-cell activation or migration, or both. Other treatments such as glatiramer acetate and beta interferons have an action on T cell microglial interactions with the CNS.¹⁰

1.2 Fingolimod and S1P Receptors

Fingolimod is the first FDA approved oral treatment for RRMS. It was marketed under the name Gilenya by Novartis and is currently a “blockbuster” drug with annual sales in excess of \$1 billion.

1.2.1 Development of FTY720 / Fingolimod / Gilenya

Fingolimod was originally developed in Japan by a team comprised of individuals such as Kunitomo Adachi, Kenji Chiba and Tetsuro Fujita. Their work was conducted in several institutions and companies such as the Faculty of Pharmaceutical Sciences at Kyoto University and Yoshitomi Pharmaceuticals Ltd. The team used the chemical structure of an immunosuppressive compound known as myriocin (ISP-I),^{19,20} found in a Chinese eternal youth nostrum, as the basis for its development.

The eternal youth elixir contains the fungus *Isaria sinclairii* and it is believed by some that ingesting a Chinese folk medicine containing this fungus can provide a wide range of health benefits. Modern analytical research techniques have indeed identified fungal metabolites such as cordycepin, an inhibitor of tumour growth, present in the fungus with beneficial biological properties in humans. *Isaria sinclairii* is a species of entomopathogenic (parasitic) fungus that thrives on insects including the larvae of cicadas. *Isaria sinclairii* is the anamorph stage of the phyla *Ascomycota* and belongs to the *Cordyceps* genus. *Cordyceps* fungi infect living insects and other arthropods, digest the internal organs of the host and eventually grow out of the dead host organism to form the fruiting body of the fungus.²¹



Figure 1.11 *Isaria sinclairii*²¹



Figure 1.12 The cordyceps genus of fungus forms the basis for the pathogen responsible for the fictitious 2013 outbreak of a devastating pandemic in the Playstation™ game The Last of Us²²

Another family of natural products with similar pharmacological effects and chemical structures to myriocin, known as the mycestericins, was isolated from *Mycelia sterilia*.^{23,24}

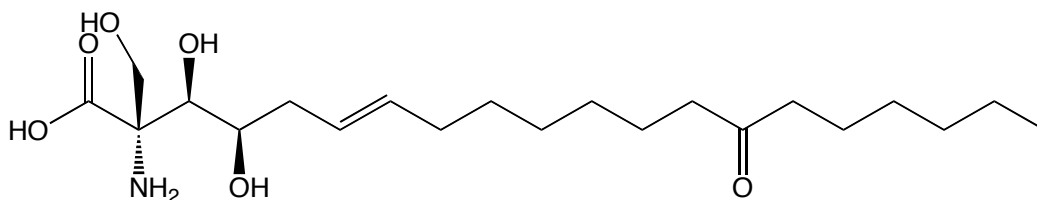


Figure 1.13 Myriocin (ISP-1)

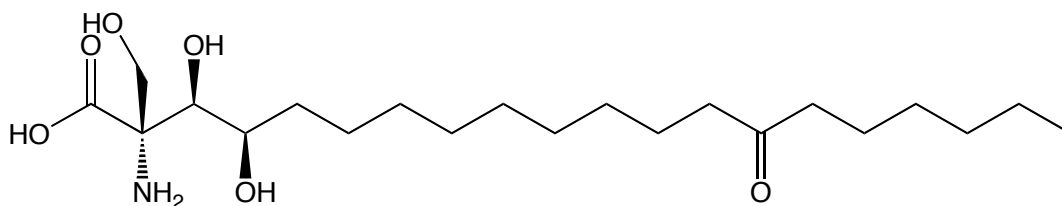


Figure 1.14 Mycestericin C

At nanomolar concentrations myriocin was observed to inhibit the proliferation of T cells in mouse allogeneic mixed lymphocyte reaction.²⁰ Chiba *et al* also showed that myriocin can be used to effectively prolong the survival of rat skin allograft although at higher doses myriocin was observed to induce significant toxicity *in vivo*. Based on these preliminary results with myriocin the Japanese team optimised their lead compounds by screening them using *in vitro* mouse allogeneic mixed lymphocyte reaction and *in vivo* rat skin allograft.

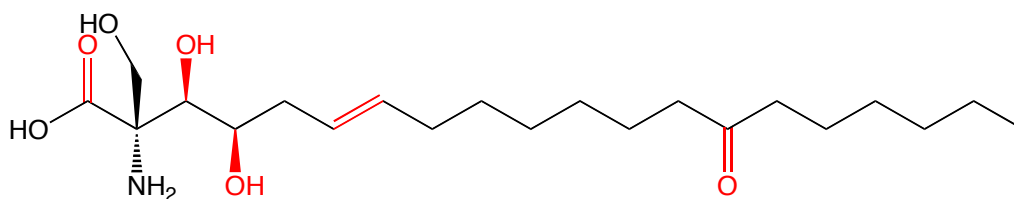
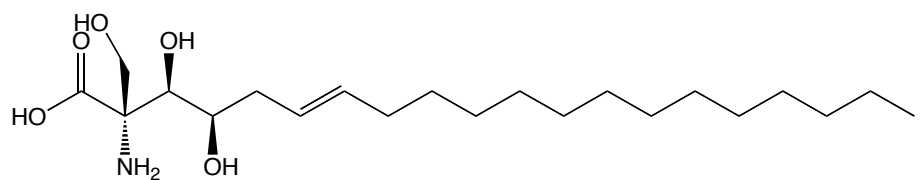


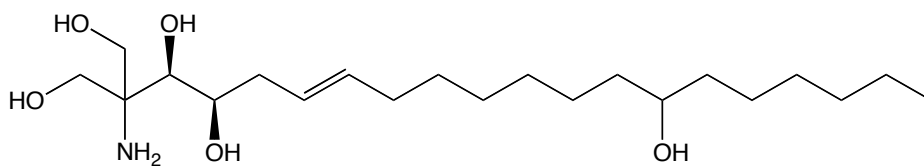
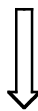
Figure 1.15 SAR studies found that the functional groups highlighted in red are not essential for biological activity

Structure activity relationship studies of myriocin and the mycestericins were used to demonstrate which of the functional groups present are essential for favourable biological activity and which are not. It was found that the hydroxyl group at position 4, the alkene group at position 6 and the configuration of the carbon bearing the 3-hydroxyl group are not essential in eliciting the desired

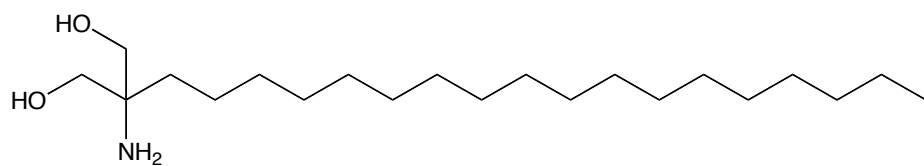
activity of myriocin. Changing the carboxylic acid group to a hydroxymethyl group was found to be favourable as this reduced toxicity, increased desired activity *in vivo* and presented less of a synthetic challenge by removing a chiral centre.²⁴ Further simplification eventually led to compounds such as ISP-I-36 and ISP-I-55 which have a 2-alkyl-2-aminopropane-1,3-diol framework.²⁵ Further modification of ISP-I-55 by introducing a benzene ring within the side chain led to the eventual synthesis of FTY720 (2-amino-2-[2-(4-octylphenyl)ethyl]propane-1,3-diol hydrochloride) (fingolimod.HCl).²⁵ The synthesis of FTY720 was first published in 1995 in a paper written by Adachi *et al.*²⁶ Fingolimod possesses a more potent immunosuppressive activity than ISP-I-55 *in vivo* and the significant alterations of myriocin to yield FTY720 effectively improved the immunosuppressive activity, toxicity and the physicochemical properties.



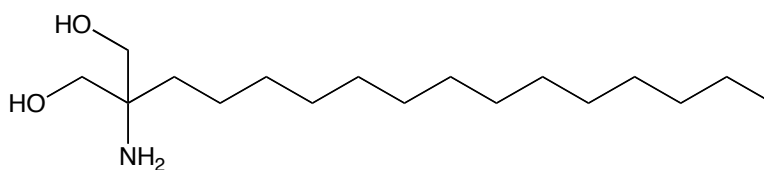
ISP-I-13



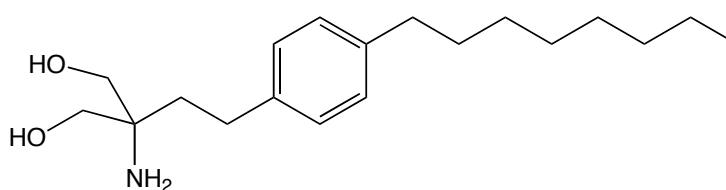
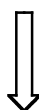
ISP-I-28



ISP-I-36



ISP-I-55

**Scheme 1.1** The development of fingolimod (FTY720)²⁵

The name FTY720 is derived from the names of its discoverers: **F**ujita and colleagues at Kyoto University, **T**aito Company and **Y**oshitomi Pharmaceutical Industries.¹⁷ The internationally recognised non-proprietary name “fingolimod” was created from two words: “sphingosine” and “immunomodulator”.²⁵

Fingolimod was found to be effective in treating multiple sclerosis and other ailments such as Huntington’s disease and can improve upon skin allograft rejection problems. The pharmaceutical company Novartis entered into a licensing agreement with the original Japanese developers and in 2010 Fingolimod became an FDA approved drug and sold under the name Gilenya. Fingolimod has been approved by the Food and Drug Administration to treat RRMS.

1.2.2 S1P Receptors

Sphingosine 1-phosphate (S1P) receptors are G protein-coupled receptors²⁷ expressed in a variety of tissues and cover a range of different functions. There are 5 types of S1P receptors referred to as the S1P₁, S1P₂, S1P₃, S1P₄ and S1P₅ receptors.²⁸ The natural ligand is sphingosine-1-phosphate as shown in figure 1.17 which is the phosphorylated analogue of sphingosine as shown in figure 1.16.²⁹

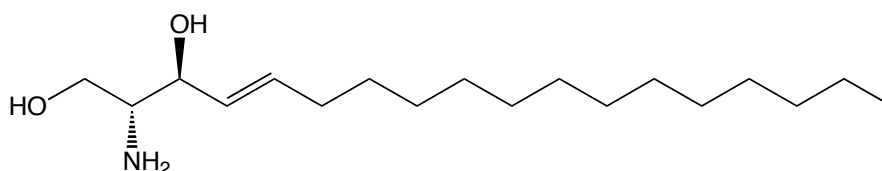


Figure 1.16 Sphingosine

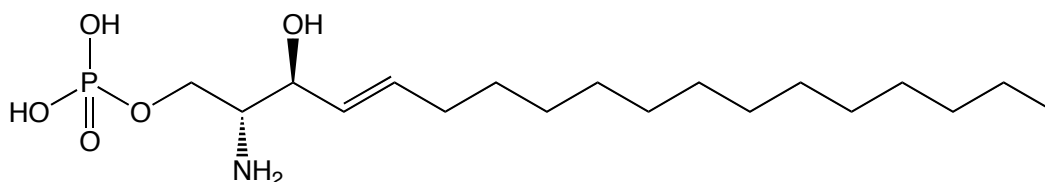


Figure 1.17 Sphingosine-1-phosphate

S1P receptors are implicated in a wide variety of physiological roles including cardiovascular development, neurogenesis, vasoregulation, regulating BBB integrity, endothelial cell function and lymphocyte migration.^{30,31,32} S1P receptors

are located in a broad range of different tissues including in the cardiovascular system, central nervous system and renal system.²⁷ The S1P₁ receptor has been implicated in lymphocyte egress from the lymph node and the down-regulation and possibly reversal of demyelination in oligodendrocytes as shown in figures 1.18 and 1.19.²⁸

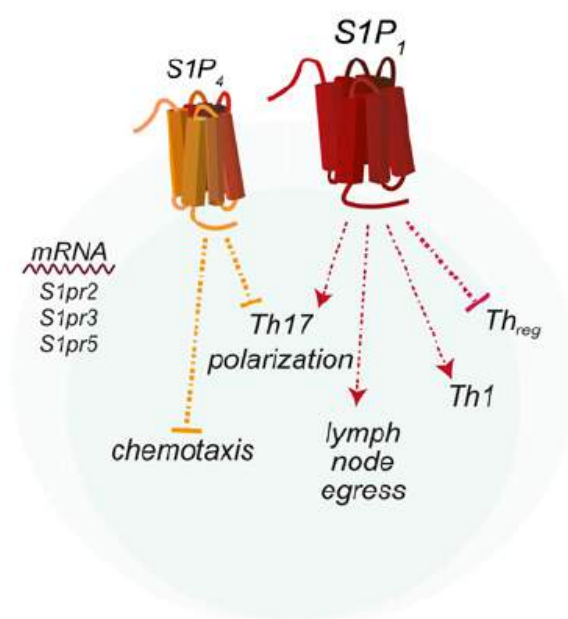


Figure 1.18 S1P₁ receptors affect T cell egress from the lymph node²⁸



Figure 1.19 Oligodendrocytes express S1P₅ and S1P₁ receptors and play a role in regulating myelination²⁸

1.2.3 Mode of Action of Fingolimod

When ingested orally, fingolimod is absorbed by the digestive tract and is disseminated to different regions of the body including the blood stream, lymphatic system and the central nervous system.²⁸ Fingolimod is phosphorylated by sphingosine kinase to form fingolimod-phosphate.²⁴ The active molecule fingolimod-phosphate binds to sphingosine receptors and induces a range of biological responses. Fingolimod is known as a sphingosine receptor modulator as it binds to these receptors. Fingolimod is also known as an immunomodulator because it has a functional antagonistic effect on the S1P receptors and causes T cells to be sequestered in the lymph nodes and thus decreases lymphocyte concentration in the blood.^{29,33,34}

Fingolimod-phosphate has similar effects to the naturally occurring sphingosine-1-phosphate and fingolimod-phosphate interferes with the normal relationship between sphingosine-1-phosphate and the sphingosine receptors.²⁹ Of the 5 types of S1P receptors fingolimod-phosphate is known to interact with the S1P₁, S1P₃, S1P₄ and S1P₅ receptors. Fingolimod in particular binds to the S1P₁ and S1P₃ receptors with high affinity.²⁸

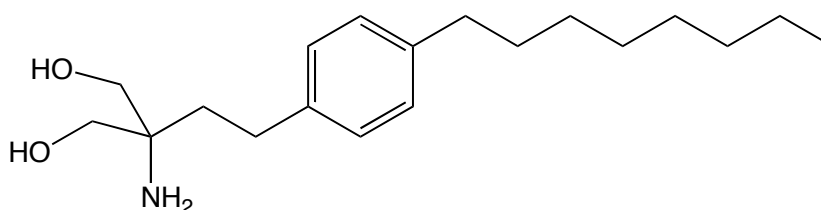


Figure 1.20 Fingolimod (FTY720)²⁹

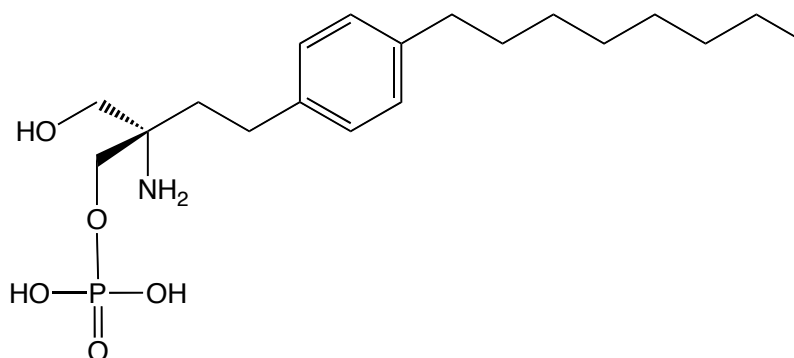


Figure 1.21 The pharmacologically active (*S*)-fingolimod-phosphate²⁹

One of the principle effects of phosphorylated fingolimod binding to the S1P receptors is the sequestration of lymphocytes in the lymph nodes and thymus.^{34,35} The sequestration of T cells causes fewer lymphocytes to cross the blood brain barrier and infiltrate the recently discovered³⁶ CNS lymphatic vessels. The reduced T cell entry to the central nervous system therefore leads to reduced degeneration of the myelin sheaths by the lymphocytes in individuals who suffer from MS and a reduction in the number of lesions detected by MRI.³⁷

Phosphorylated fingolimod has been referred to as a functional antagonist²⁹ of the S1P₁ receptor as binding to the S1P₁ receptor induces internalisation of the receptor.³⁸ The internalisation of the receptor reduces the probability of S1P binding to the S1P₁ receptors and inducing the usual biological responses such as T cell proliferation as shown in figures 1.22 and 1.23.³⁴

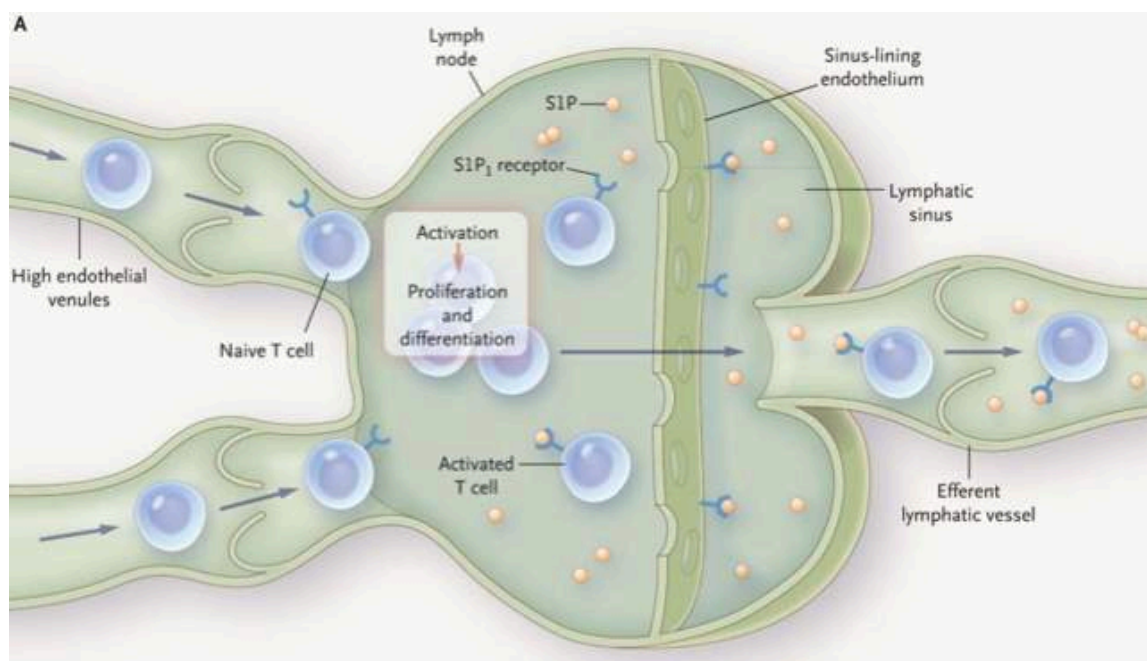


Figure 1.22 Normal functioning of lymph node. Activated T cells egress from the lymph node along a sphingosine 1-phosphate – S1P receptor gradient³⁴

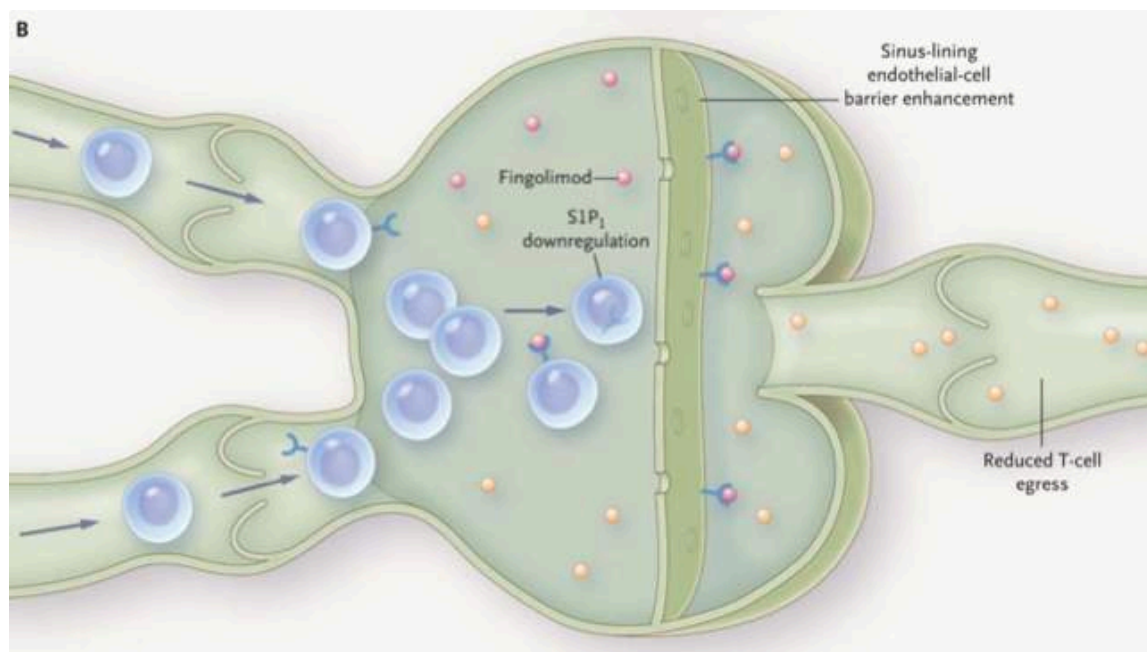


Figure 1.23 Phosphorylated fingolimod binds to and internalises S1P receptors causing lymphocyte sequestration³⁴

Additionally, fingolimod has been proposed to exhibit its neuroprotective effects by acting directly upon the CNS.³³ Some studies have suggested that in addition to reducing the rate of demyelination as observed in neurodegenerative disease, fingolimod is able to actively increase remyelination in CNS tissues.^{38,39,40} The direct mode of action of the neuroprotective effects proposed in a number of studies involves the increased expression of brain-derived neurotrophic factor (BDNF) in neurons.^{41,42,43} BDNF release has been observed to up-regulate neuronal generation and regeneration and deliberate modulation of this system could prove beneficial in ameliorating the symptoms of further neurological diseases such as Alzheimer's⁴² and Rett syndrome.⁴¹ If both the proposed BDNF and lymphocyte sequestration modes of action are correct then fingolimod is able to decrease neurodegeneration by inhibiting the release of lymphocytes from lymph nodes and increase neural regeneration by up-regulating BDNF release.

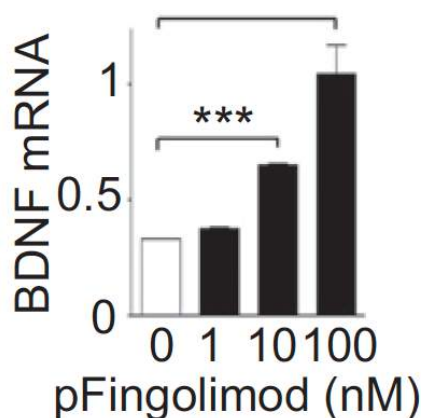


Figure 1.24 Phospho-fingolimod induces increased BDNF expression in cultured neurons⁴¹

The inhibition of histone deacetylases (HDACs) by phosphorylated fingolimod also has further implications for the CNS processes of memory and learning. There is perhaps potential for future therapeutic applications of fingolimod or other S1P receptor modulators for disorders of psychological functions modulated by HDACs.⁴⁴

1.2.4 Potential Therapeutic Uses of Fingolimod

Fingolimod has proven to be an effective treatment for RRMS and studies have shown potential uses in other diseases such as Huntington's disease,⁴⁵ Rett syndrome,⁴¹ PTSD,⁴⁴ cancer,⁴⁶ obesity,⁴⁷ ocular immune-mediated inflammation,⁴⁸ Alzheimer's disease,⁴⁹ diabetes,⁵⁰ autoimmune neuropathies,⁵¹ stroke⁵² and intracerebral hemorrhage.⁵³

1.2.5 Side Effects and Dangers of Fingolimod

A range of unwanted side effects have been observed in patients using fingolimod. Fingolimod is known to adversely affect the immune response to and clearance of enteric pathogen *C. rodentium*.⁵⁴ Fingolimod is known to induce transient bradycardia (decrease in heart rate) and other chronotropic effects⁵⁵ although a paper by Kovarik (of Novartis) published in 2008 states that atropine can reverse the chronotropic effect.⁵⁶ Fingolimod has also been observed to cause cancer in mice, increased likelihood of infection by viruses such as VZV, increased airway resistance, hepatotoxicity and macular edema.^{55,57,58}

1.2.6 Fingolimod Analogues and Other S1P Receptor Modulators

The S1P receptors have been the recipients of a great amount of attention as of late and the broad range of recently developed S1P receptor modulators is a reflection of this fact.

In order to try to reduce the bradycardia experienced by patients who take fingolimod, novel analogues have been developed which aim to reduce the amount of S1P₃ selectivity as S1P₃ receptors were found to have a greater influence over heart rate than S1P₁ receptors.⁵⁹ What follows are summaries of a few selected published S1P receptor modulators of which some may have the potential to replace fingolimod due to improved therapeutic profiles.

The compound shown in figure 1.25 has been named AAL(R) in a 2002 paper⁶⁰ and was developed in the 90s around the same time as fingolimod by the same Japanese team that developed FTY720. It has a similar pharmacological profile to FTY720 and similar selectivity towards S1P₁ and S1P₃ receptors. According to Brinkmann *et al* in their 2002 paper the phosphorylated version of the drug has EC₅₀ values of: S1P₁ 8.6 nM and S1P₃ 8.4 nM. It is likely that the original Japanese team chose to further develop FTY720 as AAL(R) has a chiral centre and large scale manufacture would presumably be more difficult and costly.

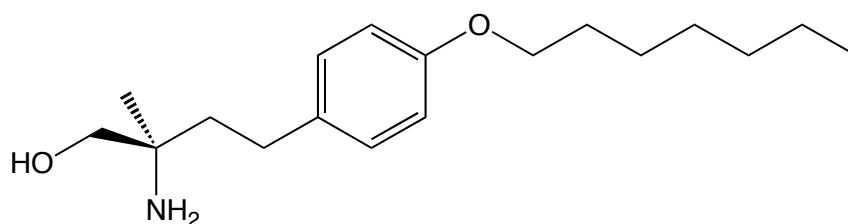


Figure 1.25 AAL(R)

KRP-203 as shown in figure 1.26 is currently in phase 2 clinical trials for the treatment of various diseases and phase 1 clinical trials for the treatment of RRMS.⁵⁹ The phosphorylated version of the drug is reported to have EC₅₀ values of: S1P₁ 0.84 nM and S1P₃ >1,000 nM. This improved selectivity of S1P₁ receptors over S1P₃ receptors means that transient bradycardia isn't such a prominent side effect of ingesting the drug. KRP-203 is the property of Novartis / Kyorin.

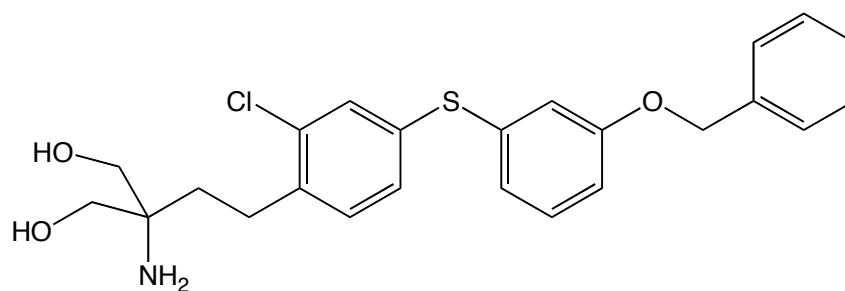


Figure 1.26 KRP-203

CS-0777 as shown in figure 1.27 is currently in phase 2 clinical trials for the treatment of MS.⁵⁹ The phosphorylated version of the drug is reported to have EC50 values of: S1P₁ 1.1 nM and S1P₃ 350 nM. CS-077 is the property of Daiichi Sankyo.

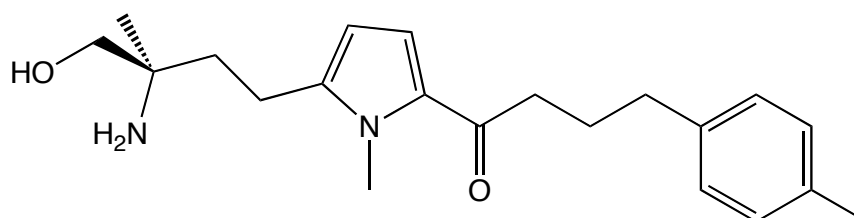


Figure 1.27 CS-0777

GSK1842799⁶¹ has been chosen as a clinical candidate due to favourable biological activity. Of the other similar analogues developed this analogue is phosphorylated more efficiently by sphingosine kinase *in vivo*. The phosphorylated version of the drug is reported to have EC50 values of: S1P₁ 0.52 nM and S1P₃ 1,898 nM. GSK1842799 is the property of Praecis Pharma and GlaxoSmithKline.

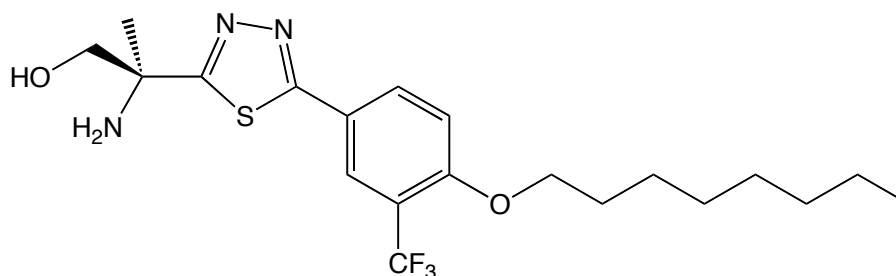


Figure 1.28 GSK184279

PPI-4955 (analogue 6)⁶¹ was not chosen for clinical trials because the phosphorylation step is slow *in vivo*. The phosphorylated version of the drug is

reported to have EC₅₀ values of: S1P₁ 1.1 nM and S1P₃ >10,000 nM. PPI-4955 (6) is the property of Praecis Pharma.

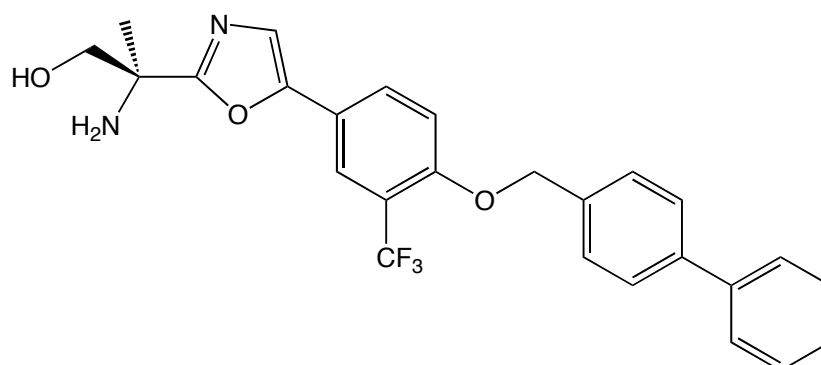


Figure 1.29 PPI-4955 (6)

PPI-4955⁶¹ was not chosen for clinical trials because the phosphorylation step is slow *in vivo*. The phosphorylated version of the drug is reported to have EC₅₀ values of: S1P₁ 0.83 nM and S1P₃ 7,352 nM which is an improvement of S1P₁ and S1P₃ selectivity when compared with GSK1842799. PPI-4955 is the property of Praecis Pharma.

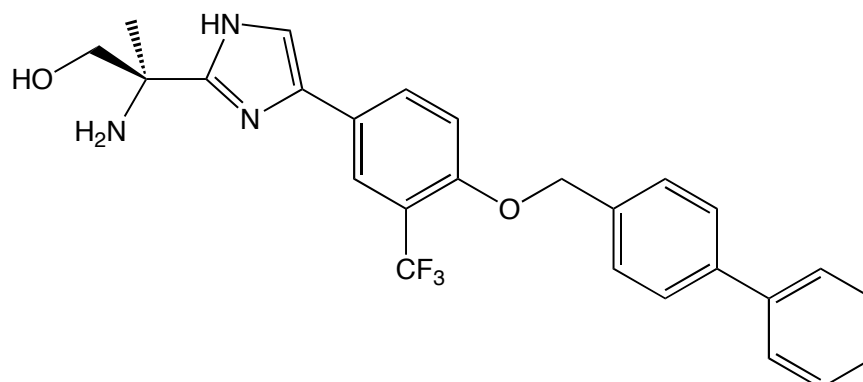


Figure 1.30 PPI-4955

The compound shown in figure 1.31 was labelled 2f in Takashi Tsuji *et al's* 2014 paper titled: "Synthesis and SAR studies of benzyl ether derivatives as potent orally active S1P₁ agonists".⁶² The phosphorylated version of the drug is reported to have EC₅₀ values of: S1P₁ 2.3 nM and S1P₃ 12,000 nM. The compound in question is presumably the property of Daiichi Sankyo and has excellent S1P₁ selectivity over S1P₃. The overall potency of the drug is greatly reduced by the rate of the *in vivo* phosphorylation step.

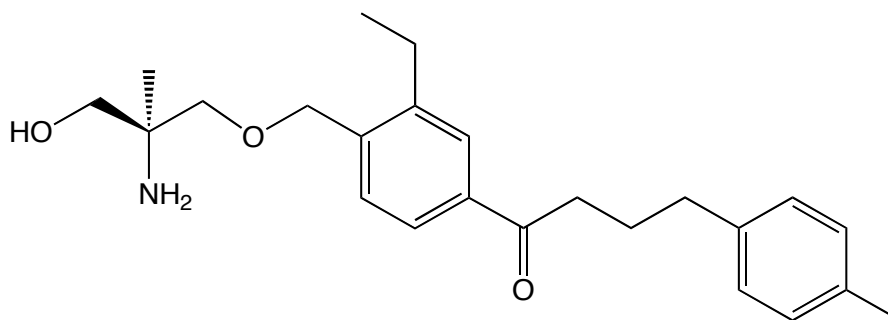


Figure 1.31 2f (Tsuji 2014)⁶²

The compound shown in figure 1.32 was labelled 2h in Takashi Tsuji *et al's* 2014 paper.⁶² The phosphorylated version of the drug is reported to have EC50 values of: S1P₁ 6.5 nM and S1P₃ >20,000 nM. The compound in question is presumably the property of Daiichi Sankyo and has excellent S1P₁ selectivity over S1P₃. The overall potency of the drug is greatly reduced by the rate of the *in vivo* phosphorylation step.

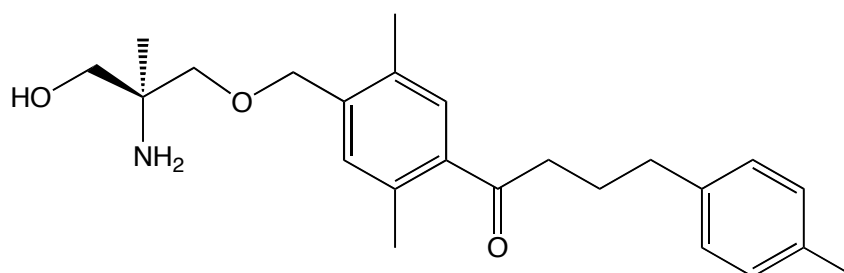


Figure 1.32 2h (Tsuji 2014)⁶²

The compound shown in figure 1.33 was labelled 6d in Maiko Hamada *et al's* 2010 paper titled: "Removal of sphingosine 1-phosphate receptor-3 (S1P₃) agonism is essential, but inadequate to obtain immunomodulating 2-aminopropane-1,3-diol S1P₁ agonists with reduced effect on heart rate".⁶³ The phosphorylated version of the drug is reported to have EC50 values of: S1P₁ 3.0 nM and S1P₃ >1,000 nM. The compound in question is the property of Mitsubishi Tanabe Pharma Corporation and has good S1P₁ selectivity over S1P₃. Testing with mice showed insignificant bradycardia induced by the drug.

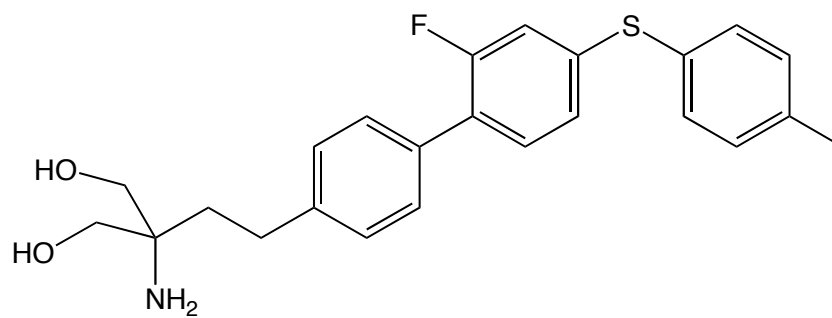


Figure 1.33 6d (Hamada 2010)⁶³

1.3 The Pharmacology of Drug Action: Opportunities for Prodrugs

Christopher Lipinski developed the 'rule of 5' and it is used as a general guide to determine whether a potential therapeutic compound will be orally active. "The rule of 5 states that: poor absorption or permeation are more likely when:

- There are more than 5 H-bond donors (expressed as the sum of OHs and NHs)
- The molecular weight is over 500
- The Log P is over 5 (or MLog P is over 4.15)
- There are more than 10 H-bond acceptors (expressed as the sum of Ns and Os)
- Compound classes that are substrates for biological transporters are exceptions to the rule"⁶⁴

When developing novel small molecule therapeutics it is prudent to keep these rules in mind however there are FDA approved drugs that do not meet the requirements of every one of the five rules. A number of antibiotics and antifungal compounds, in particular, are known to be orally active despite not adhering to the rule of 5.⁶⁴

1.3.1 CNS Acting Drugs

When developing therapeutics which are designed to be active in the central nervous system there is an even lower likelihood that any novel compound will effectively migrate to the desired CNS tissues. The blood-brain barrier (BBB) has evolved to protect the central nervous system from devastating invasion by unwanted toxins and pathogens. However, the BBB poses a serious obstacle to drug developers who wish to develop agents that are active in the CNS.

Lipinski developed another set of rules⁶⁵ which can be applied to a compound when considering its potential to cross the BBB:

- Molecular weight ≤ 400 g/mol
- LogP ≤ 5
- Hydrogen bond donors ≤ 3
- Hydrogen bond acceptors ≤ 7

The majority of drugs which cross the BBB do so *via* passive diffusion although some compounds such as gabapentin and L-DOPA are transported across the epithelial cell barrier *via* active transport. Gabapentin and L-DOPA are transported into the CNS by L-type amino acid transporter-1 (LAT1).⁶⁶

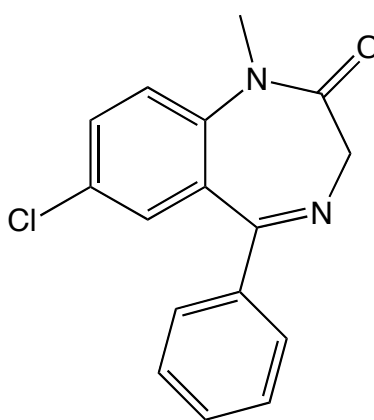


Figure 1.34 Diazepam (Valium)

Diazepam is a benzodiazepine CNS-acting pharmaceutical product and has a molecular weight of 284.7 g/mol, a logP of 2.74, 3 hydrogen bond acceptors and 0 hydrogen bond donors. Diazepam conforms to all of Lipinski's rules of the CNS.

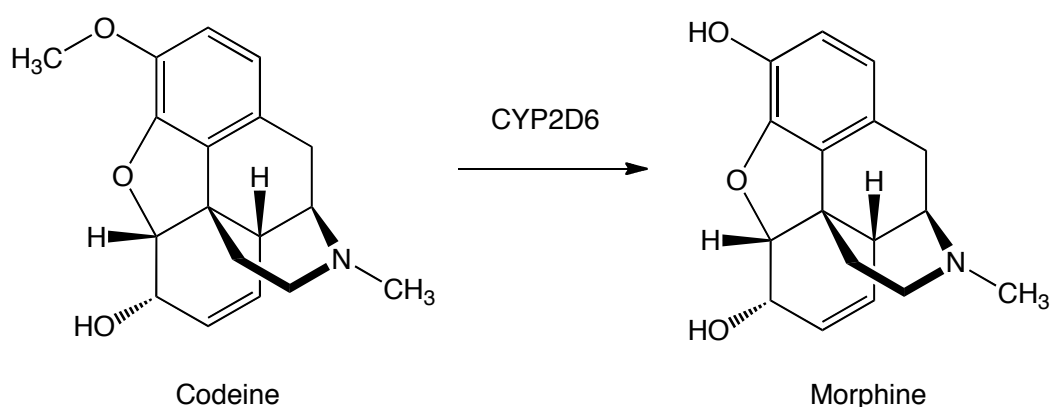
1.3.2 Prodrugs

Prodrugs can be described as pharmacologically inactive or less than fully active derivatives of active drugs that are converted into the active drug within the body *via* enzymatic or non-enzymatic metabolic processes.⁶⁷ Prodrugs act to maximise the amount of the active drug that reaches the site of action. This is achieved by manipulating various properties of the molecule including the physicochemical, biopharmaceutical and pharmacokinetic properties.⁶⁸

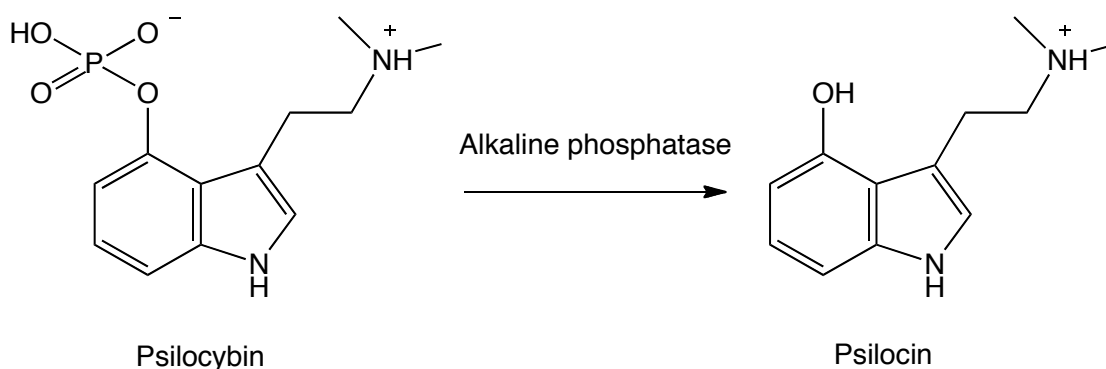
The prodrug approach can be preferable to administering the active molecule itself due to improvements in ADME properties (absorption, distribution, metabolism and excretion).⁶⁹ A fuller list of improvements the prodrug approach can provide includes improvements in:

- Patient acceptance i.e. taste/odour
- Selectivity and reduced toxicity
- Stability and/or prolonged release
- Absorption and distribution
- Physicochemical properties i.e. solubility and LogP
- Site-specific delivery^{68,69}

Two comparatively well-known prodrugs include the painkiller codeine and the psychopharmacologically active compound psilocybin. Codeine has a very close structural similarity to morphine but contains a methyl ether group rather than an alcohol group. The cytochrome P450 enzyme CYP2D6 converts the ether group to an alcohol group in the liver yielding morphine.⁶⁹ Psilocybin on the other hand is metabolised to the active molecule psilocin by dephosphorylating enzymes known as alkaline phosphatases.⁷⁰



Scheme 1.2 Metabolism of codeine to the active molecule⁶⁹



Scheme 1.3 Metabolism of psilocybin to the active molecule⁷⁰

Fingolimod is in fact a prodrug as fingolimod itself is not the pharmacologically active molecule. The phosphorylation step is essential to induce the desired biological activity as it is fingolimod-phosphate that binds to the S1P receptors and induces the immunomodulatory effects.³⁰

1.3.3 Phosphate Delivery Prodrugs

A large number of different types of phosphate prodrug have been developed and publicised. Some examples of phosphorus prodrug technologies include:^{71,72}

- Bis(pivaloyloxymethyl) (POM) prodrugs
- Bis(isopropylloxymethyl) carbonate (POC) prodrugs
- S-acyl-2-thioethyl (SATE) prodrugs
- Cyclosal prodrugs
- HepDirect prodrugs
- Ether lipid ester (Hostetler) prodrugs
- Phosphoramidate (ProTide) prodrugs

POM, HepDirect, lipid esters (Hostetler) and phosphoramidates have been in clinical trials and some POM and phosphoramidate compounds are FDA approved to treat certain health concerns.⁷¹

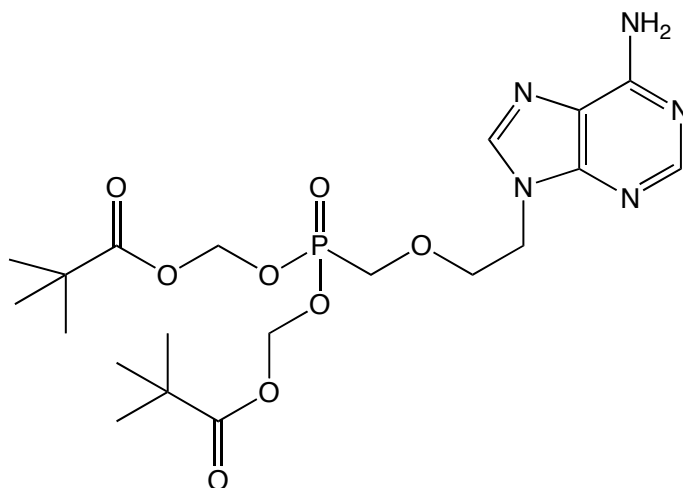


Figure 1.35 Adefovir dipivoxil contains a bis POM phosphate delivery motif⁷¹

Adefovir dipivoxil is FDA approved to treat infections of the hepatitis B virus. It was originally developed to treat HIV but it was found that kidney toxicity was too much of an issue for that application.⁷¹

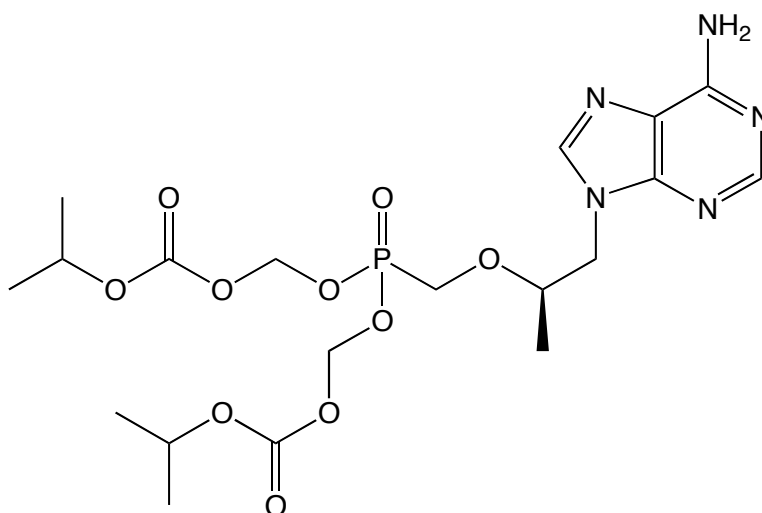


Figure 1.36 Tenofovir disoproxil fumarate contains a bis POC phosphate delivery motif⁷¹

Tenofovir disoproxil fumarate is FDA approved to treat HIV and hepatitis B infections.⁷¹ It has a molecular weight of 519.17 g/mol and so does not conform to all of Lipinski's rules. This example shows that Lipinski's rules should be used as a general guide as opposed to a definitive set of unbreakable rules. The version of the drug that is sold comes as a fumarate salt with fumaric acid (structure not shown) and this helps the drug's bioavailability.

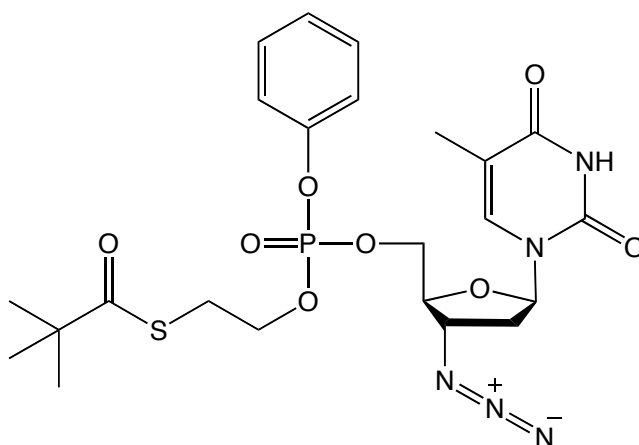


Figure 1.37 Analogue of azidothymidine containing aryl SATE phosphate delivery motif⁷¹

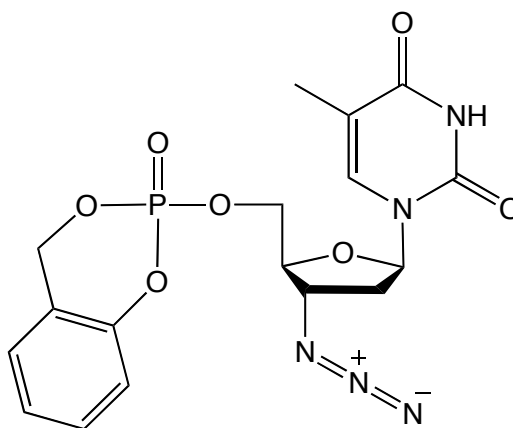


Figure 1.38 Analogue of azidothymidine containing CycloSal phosphate delivery motif⁷¹

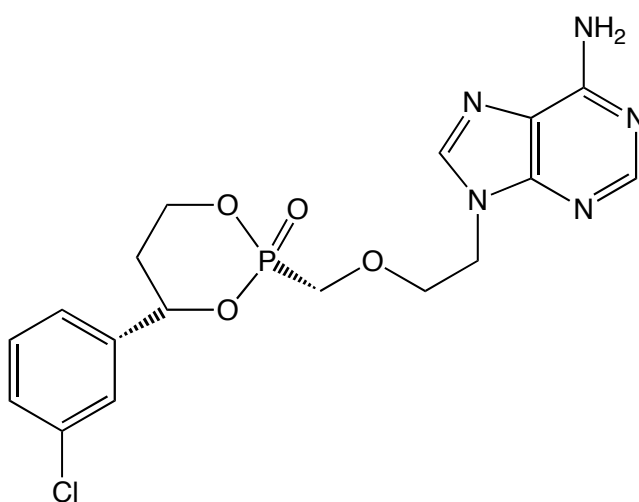


Figure 1.39 Pradefovir is an analogue of adefovir which possesses a HepDirect phosphate delivery motif and has been in clinical trials⁷¹

1.3.4 Phosphoramidate (ProTide) Prodrugs

Phosphoramidate “ProTides” have been developed, synthesised and patented by Prof. Chris McGuigan and his researchers for over a decade. They act as a form of prodrug that can have much greater potencies than the original drug molecule.⁷³ Typically the ProTide method is applied to nucleosides.⁷⁴

Nucleosides consist of a DNA-type base such as guanine or cytosine, or analogues thereof, and a sugar. The image below depicts gemcitabine. Gemcitabine is an FDA approved drug that is currently used to treat a range of types of cancer including breast cancer, pancreatic cancer and lung cancer.⁷⁵

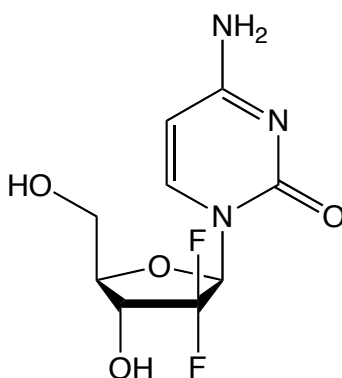


Figure 1.40 Gemcitabine⁷⁶

Prof. McGuigan and researchers applied the ProTide technology to gemcitabine to produce a compound now known as NUC-1031 / Acelarin (figure 1.41).⁷⁶ Acelarin is currently in phase III clinical trials (as of April 2016) and the drug may eventually become an FDA approved drug if there is an acceptable profile of efficacy and toxicity. The commercial and clinical future of Acelarin depends on the outcome of the clinical trials.

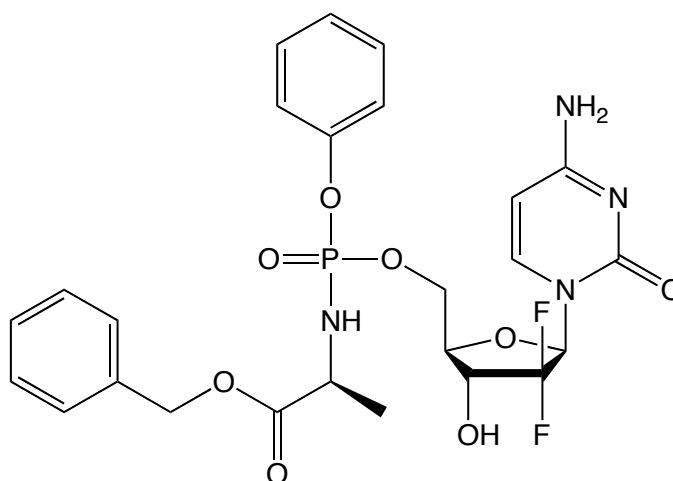


Figure 1.41 Acelarin based on gemcitabine⁷⁶

Another drug, developed by the pharmaceutical company Gilead, which makes use of phosphoramidate technology is sofosbuvir.⁷⁷ The FDA approved Sofosbuvir in 2013 for treatment of the hepatitis C virus in combination with ribavirin. Sofosbuvir's mode of action involves the inhibition of the RNA polymerase used by the virus to replicate the viral RNA. Sofosbuvir has generated in excess of \$1 billion in revenue since its approval and continues to be a very financially successful treatment for the hepatitis C virus.

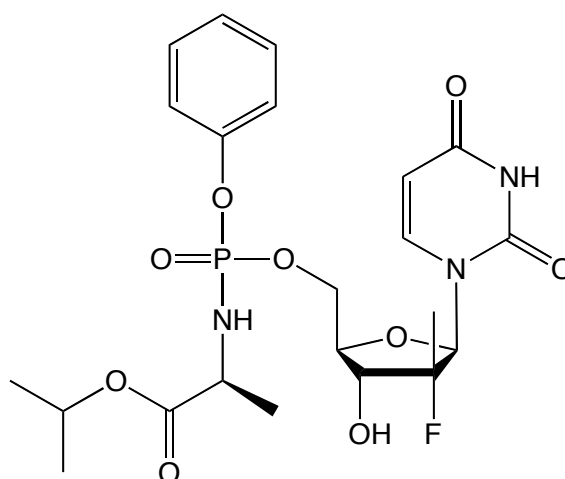


Figure 1.42 Sofosbuvir

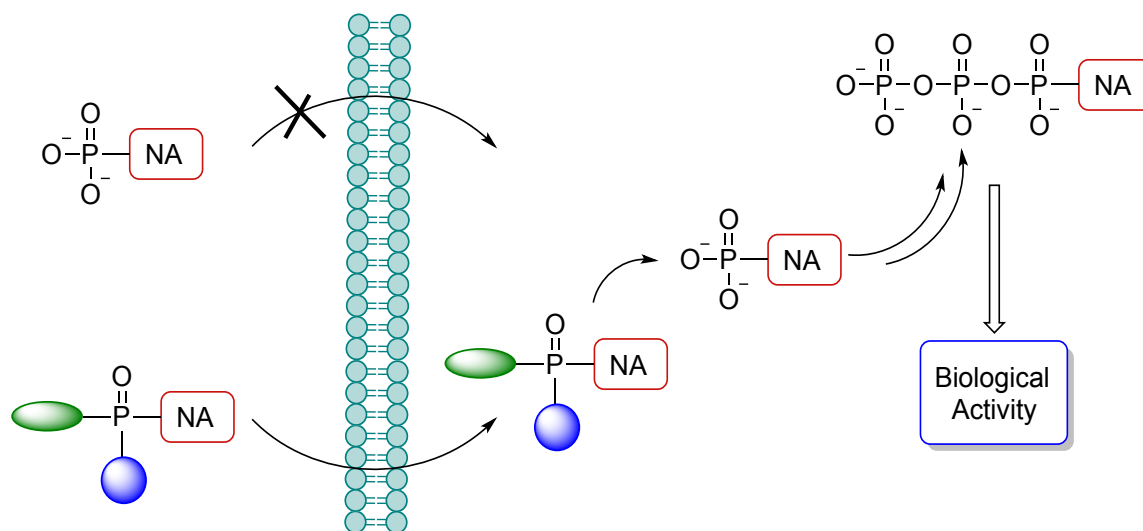
Other ProTide nucleosides which have been in clinical trials include:

- GS-7340, containing an L-alanyl isopropyl ester ProTide moiety, for HIV treatment⁷¹

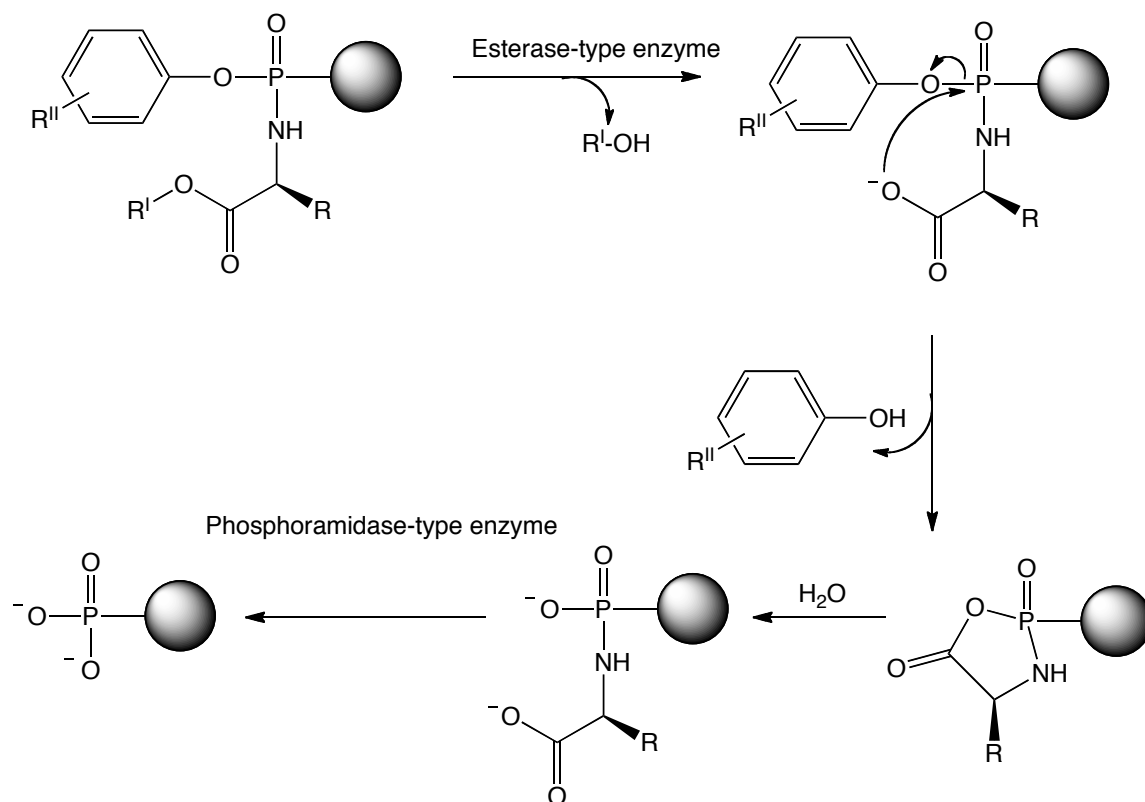
- GS-9131, containing an L-alaninyl ethyl ester ProTide moiety, for HIV treatment⁷¹
- INX-08189, containing an L-alaninyl neopentyl ester ProTide moiety, for HCV treatment⁷¹
- Thymectacin, containing an L-alaninyl methyl ester ProTide moiety, for cancer treatment⁷¹

1.3.5 Mode of Action of Phosphoramidates

Nucleosides possessing phosphoramidate structures are believed to diffuse through the cell membrane *via* passive diffusion. The lipophilic nature of the phosphoramidate moiety is believed to facilitate this process and in the case of nucleosides this is beneficial as the polar nature of the monophosphate nucleoside does not facilitate diffusion across the cell membrane (see scheme 1.4). When inside the cell the ProTide is processed by enzymes such as cathepsine A⁷⁸, carboxypeptidases and phosphoramidases such as Hint enzyme⁷⁹ to form the nucleoside-phosphate molecule (as shown in scheme 1.5).

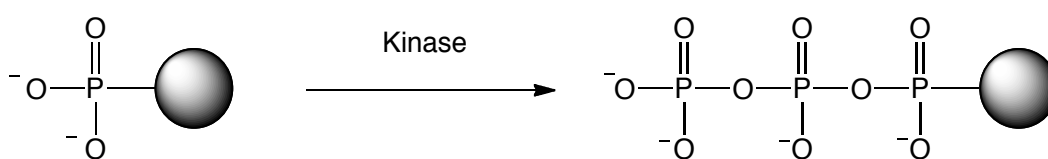


Scheme 1.4 Typical ProTide activity profile of nucleosides. The lipophilic ProTide moiety aids diffusion of the nucleoside analogue (NA) across the cell membrane and the ProTide moiety is processed by the intracellular enzymes to the monophosphate and then kinases to the triphosphate.



Scheme 1.5 Proposed intracellular enzymatic processing of ProTides⁷³

In the case of nucleosides the monophosphate is often further phosphorylated by kinases to form a triphosphate active molecule that is then processed and incorporated into the host DNA/RNA.



Scheme 1.6 Processing of free phosphate nucleoside drug to triphosphate by kinases⁷⁴

1.4 Aim of Work: Phosphoramidate Fingolimod Analogues

The original aim of the research project described was to produce kinase-independent second generation ProTide fingolimod analogues and to allow the project to evolve depending on experimental results and extensive searching of the available literature.

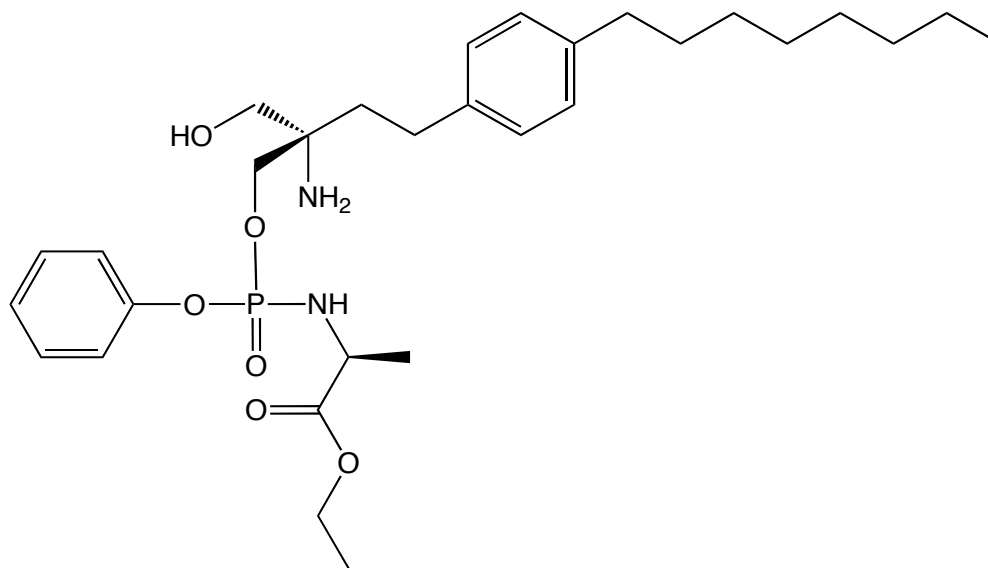


Figure 1.43 Example of a ProTide Fingolimod analogue that could have favourable biological activity

As fingolimod is phosphorylated *in vivo* by sphingosine kinase to form the active molecule it can be hypothesised that using phosphoramidate technology could give rise to an increase in potency and perhaps an improvement in ADME properties. The lipophilic phosphoramidate moiety in theory should help diffusion into the cell and the metabolism of the phosphoramidate to the fingolimod-phosphate could be a more efficient process than the phosphorylation step that takes place with standard fingolimod *in vivo*. An additional benefit of applying ProTide technology to fingolimod is that activity could also be retained in kinase-deficient environments.

Initially a synthetic pathway needs to be developed in order to produce the compounds. Once synthesis has been achieved, different analogues need to be tested for their biological activity and potential use as useful pharmacologically

active compounds. An original aim of the research was to conduct the project in collaboration with Prof. Yves-Alain Barde and his PhD student Katharina Säuberli who would use primary cultures of mouse embryonic stem cell derived neurons to determine if the application of ProTide fingolimod analogues can cause an increase in the expression of BDNF and thereby present an exciting therapeutic opportunity for the treatment of neurodegenerative diseases. Different types of *in vitro* testing such as cell lysate, carboxypeptidase and acid stability experiments were also planned as detailed later.

1.5 References

1. Carpenter M. *Human Neuroanatomy*. Seventh edition. 1976.
2. Villegas S, Poletta F, Carri N. GLIA: A reassessment based on novel data on the developing and mature central nervous system. *Cell Biol. Int.* **2003**, 27, 599-609.
3. Rosenberg S, Chan J. Modulating myelination: knowing when to say Wnt. *Genes Dev.* **2009**, 23, 1487-1493.
4. Brooks D, McKinlay W. Personality and behavioural change after severe blunt head injury- a relative's view. *J Neurol Neurosurg Psychiatry.* **1983**, 46, 336-344.
5. Friedlander R. Apoptosis and caspases in neurodegenerative diseases. *N. Engl. J. Med.* **2003**, 348, 1365-1375.
6. Weir D M. *Immunology*. Fifth edition. Churchill Livingstone Medical Text, 1983.
7. Chaplin D. Overview of the immune response. *J. Allergy Clin. Immunol.* **2010**, 125, 1-29.
8. Zhang Q, Vignali D. Co-stimulatory and co-inhibitory pathways in autoimmunity. *Immunity.* **2016**, 44, 1034-1051.
9. Compston A, Coles A. Multiple sclerosis. *Lancet.* **2008**, 372, 1502-17.
10. Compston A, Coles A. Multiple sclerosis. *Lancet.* **2002**, 359, 1221-31.
11. Milo R, Kahana E. Multiple sclerosis: Geoepidemiology, genetics and the environment. *Autoimmun. Rev.* **2010**, 9, A387-A394.
12. Ascherio A, Munger K. Environmental risk factors for multiple sclerosis. Part I: The role of infection. *Ann. Neurol.* **2007**, 61, 288-299.
13. Trapp B, Nave K. Multiple sclerosis: an immune or neurodegenerative disorder? *Annu. Rev. Neurosci.* **2008**, 31, 247-269.
14. Ascherio A, Munger K. Environmental risk factors for multiple sclerosis. Part II: Noninfectious factors. *Ann. Neurol.* **2007**, 61, 504-513.
15. Holmøy T. A Norse contribution to the history of neurological diseases. *Eur. Neurol.* **2006**, 55, 57-58.
16. Simpson S, Blizzard L, Otahal P, Van der Mei I, Taylor B. Latitude is significantly associated with the prevalence of multiple sclerosis: a meta-analysis. *J. Neurol. Neurosurg. Psychiatry.* **2011**, 82, 1132-1141.

17. Simpson S, Taylor B, Blizzard L, Ponsonby A, Pittas F, Tremlett H, Dwyer T, Gies P, Van der Mei I. Higher 25-hydroxyvitamin D is associated with lower relapse risk in multiple sclerosis. *Ann. Neurol.* **2010**, 68, 193-203.
18. Thacker E, Mirzaei F, Ascherio A. Infectious mononucleosis and risk for multiple sclerosis: a meta-analysis. *Ann. Neurol.* **2006**, 59, 499-503.
19. Fujita T, Inoue K, Yamamoto S, Ikumoto T, Sasaki S, Toyama R, Yoneta M, Chiba K, Hoshino Y, Okumoto T. Fungal metabolites. Part 11. A potent immunosuppressive activity found in *Isaria sinclairii* metabolite. *J. Antibiot.* **1994**, 47, 208-215.
20. Fujita T, Inoue K, Yamamoto S, Ikumoto T, Sasaki S, Toyama R, Yoneta M, Chiba K, Hoshino Y, Okumoto T. Fungal metabolites. Part 12. Potent immunosuppressant, 14-deoxomyriocin, (2S, 3R, 4R)-(E)-2-amino-3,4-dihydroxy-2-hydroxymethyleicos-6-enoic acid and structure-activity relationships of myriocin derivatives. *J. Antibiot.* **1994**, 47, 216-224.
21. Chun J, Brinkmann V. A mechanistically novel, first oral therapy for multiple sclerosis: the development of fingolimod (FTY720, Gilenya). *Discov. Med.* **2011**, 12, 213-228.
22. http://thelastofus.wikia.com/wiki/The_Infected
23. Sasaki S, Hashimoto R, Kiuchi M, Inoue K, Ikumoto T, Hirose R, Chiba K, Hoshino Y, Okumoto T, Fujita T. Fungal metabolites. Part 14. Novel potent immunosuppressants, mycestericins, produced by *Mycelia sterilia*. *J. Antibiot.* **1994**, 47, 420-433.
24. Fujita T, Hamamichi N, Kiuchi M, Matsuzaki T, Kitao Y, Inoue K, Hirose R, Yoneta M, Sasaki S, Chiba K. Determination of absolute configuration and biological activity of new immunosuppressants, mycestericins D, E, F and G. *J. Antibiot.* **1996**, 49, 846-853.
25. Chiba K, Adachi K. Discovery of fingolimod, the sphingosine 1-phosphate receptor modulator and its application for the therapy of multiple sclerosis. *Future Med. Chem.* **2012**, 4, 771-781.
26. Adachi K, Kohara T, Nakao N, Arita M, Chiba K, Mishina T, Sasaki S, Fujita T. Design, synthesis, and structure-activity relationships of 2-substituted-2-amino-1,3-propanediols: Discovery of a novel immunosuppressant, FTY720. *Bioorg. Med. Chem. Lett.* **1995**, 8, 853-856.

27. Oldstone M, Rosen H. Sphingosine-1-phosphate signalling in immunology and infectious diseases. *Microbiol. Immunol.* **2014**, 378, 1-183.
28. Blaho V, Hla T. An update on the biology of sphingosine 1-phosphate receptors. *J. Lipid Res.* **2014**, 55, 1596-1608.
29. Brinkmann V, Billich A, Baumruker T, Heining P, Schmouder R, Francis G, Aradhye S, Burtin P. Fingolimod (FTY720): discovery and development of an oral drug to treat multiple sclerosis. *Nat. Rev. Drug Discov.* **2010**, 9, 883-897.
30. Chun J, Hartung H. Mechanism of action of oral fingolimod (FTY720) in multiple sclerosis. *Clin. Neuropharmacol.* **2010**, 33, 91-101.
31. Massberg S, Andrian U. Fingolimod and sphingosine-1-phosphate – Modifiers of lymphocyte migration. *N. Engl. J. Med.* **2006**, 355, 1088-1091.
32. Prager B, Spampinato S, Ransohoff R. Sphingosine 1-phosphate signalling at the blood-brain barrier. *Trends Mol. Med.* **2015**, 21, 354-363.
33. Miron V, Schubart A, Antel J. Central nervous system-directed effects of FTY720 (fingolimod). *J. Neurol. Sci.* **2008**, 274, 13-17.
34. Pelletier D, Hafler D. Fingolimod for multiple sclerosis. *N. Engl. J. Med.* **2012**, 366, 339-47.
35. Sensken S, Bode C, Gräler M. Accumulation of fingolimod (FTY720) in lymphoid tissues contributes to prolonged efficacy. *J. Pharmacol. Exp. Ther.* **2008**, 328, 963-969.
36. Louveau A, Smirnov I, Keyes T, Eccles J, Rouhani S, Peske J, Derecki N, Castle D, Mandell J, Lee K, Harris T, Kipnis J. Structural and functional features of the central nervous lymphatic vessels. *Nature.* **2015**, 523, 337-341.
37. Kappos L, Antel J, Comi G, Montalban X, O'Connor P, Polman C, Haas T, Korn A, Karlsson G, Radue E. Oral fingolimod (FTY720) for relapsing multiple sclerosis. *N. Engl. J. Med.* **2006**, 355, 1124-1140.
38. Mullerhausen F, Zecri F, Cetin C, Billich A, Guerini D, Seuwen K. Persistence signalling induced by FTY720-phosphate is mediated by internalized S1P1 receptors. *Nat. Chem. Biol.* **2009**, 5, 428-434.
39. Miron V, Ludwin S, Darlington P, Jarjour A, Soliven B, Kennedy T, Antel J. Fingolimod (FTY720) enhances remyelination following demyelination of organotypic cerebellar slices. *Am. J. Pathol.* **2010**, 176, 2682-2694.
40. Jackson S, Giovannoni G, Baker D. Fingolimod modulates microglial activation to augment markers of remyelination. *J. Neuroinflammation.* **2011**, 8, 1-12.

41. Deogracias R, Yazdani M, Dekkers M, Guy J, Ionescu M, Vogt K, Barde Y. Fingolimod, a sphingosine-1 phosphate receptor modulator, increases BDNF levels and improves symptoms of a mouse model of Rett syndrome. *PNAS*. **2012**, 109, 14230-14235.
42. Fukumoto K, Mizoguchi H, Takeuchi H, Horiuchi H, Kawanokuchi J, Jin S, Mizuno T, Suzumura A. Fingolimod increases brain-derived neurotrophic factor levels and ameliorates amyloid β -induced memory impairment. *Behav. Brain Res*. **2014**, 268, 88-93.
43. Doi Y, Takeuchi H, Horiuchi H, Hanyu T, Kawanokuchi J, Jin S, Parajuli B, Sonobe Y, Mizuno T, Suzumura A. Fingolimod phosphate attenuates oligomeric amyloid β -induced neurotoxicity via increased brain-derived neurotrophic factor expression in neurons. *PLOS ONE*. **2013**, 8, 1-10.
44. Hait N, Wise L, Allegood J, O'Brien M, Avni D, Reeves T, Knapp P, Lu J, Luo C, Miles M, Milstien S, Lichtman A, Spiegel S. Active phosphorylated fingolimod inhibits histone deacetylases and facilitates fear extinction memory. *Nat. Neurosci*. **2014**, 17, 971-980.
45. Pardo A, Amico E, Favellato M, Castrataro R, Fucile S, Squitieri F, Maglione V. FTY720 (fingolimod) is a neuroprotective and disease-modifying agent in cellular and mouse models of Huntington disease. *Hum. Mol. Gen*. **2014**, 23, 2251-2265.
46. Liao A, Broeg K, Fox T, Tan S, Watters R, Shah M, Zhang L, Li Y, Ryland L, Yang J, Aliaga C, Dewey A, Rogers A, Loughran K, Hirsch L, Jarbadan N, Baab K, Liao J, Wang H, Kester M, Desal D, Amin S, Loughran T, Liu X. Therapeutic efficacy of FTY720 in a rat model of NK-cell leukemia. *Blood*. **2011**, 118, 2793-2800.
47. Moon M, Jeong J, Lee J, Park Y, Lee Y, Seol J, Park S. Antiobesity activity of a sphingosine 1-phosphate analogue FTY720 observed in adipocytes and obese mouse model. *Exp. Mol. Med*. **2012**, 44, 603-614.
48. Copland D, Liu J, Schewitz-Bowers L, Brinkmann V, Anderson K, Nicholson L, Dick A. Therapeutic dosing of fingolimod (FTY720) prevents cell infiltration, rapidly suppresses ocular inflammation, and maintains the blood-ocular barrier. *AJP*. **2012**, 180, 672-681.
49. Hemmati F, Dargahi L, Nasoohi S, Omidbaksh R, Mohamed Z, Chik Z, Naidu M, Ahmadiani A. Neurorestorative effect of FTY720 in a rat model of Alzheimer's disease: comparison with memantine. *Behav. Brain Res*. **2013**, 252, 415-421.

50. Moon H, Chon J, Joo J, Kim D, In J, Lee H, Park J, Choi J. FTY720 preserved islet β -cell mass by inhibiting apoptosis and increasing survival of β -cells in db/db mice. *Diabetes Metab. Res. Rev.* **2013**, 29, 19-24.
51. Kim H, Jung C, Dukala D, Bae H, Kakazu R, Wollmann R, Soliven B. Fingolimod and related compounds in a spontaneous autoimmune polyneuropathy. *J. Neuroimmunol.* **2009**, 214, 93-100.
52. Brunkhorst R, Kanaan N, Koch A, Ferreiros N, Mirceska A, Zeiner P, Mittelbronn M, Derouiche A, Steinmetz H, Foerch C, Pfeilschifter J, Pfeilschifter W. FTY720 treatment in the convalescence period improves functional recovery and reduces reactive astrogliosis in photothrombotic stroke. *PLOS ONE.* **2013**, 8, 1-9.
53. Rolland W, Lekic T, Krafft P, Hasegawa Y, Altay O, Hartman R, Ostrowski R, Manaenko A, Tang J, Zhang J. Fingolimod reduces cerebral lymphocyte infiltration in experimental models of rodent intracerebral hemorrhage. *Exp. Neurol.* **2013**, 241, 45-55.
54. Murphy C, Hall L, Huley G, Quinlan A, MacSharry J, Shanahan F, Nally K, Melgar S. The sphingosine-1-phosphate analogue FTY720 impairs mucosal immunity and clearance of enteric pathogen *Citrobacter rodentium*. *Infect. Immun.* **2012**, 80, 2712-2723.
55. Cohen J, Chun J. Mechanisms of fingolimod's efficacy and adverse effects in multiple sclerosis. *Ann. Neurol.* **2011**, 69, 759-777.
56. Kovarik J, Slade A, Riviere G, Neddermann D, Maton S, Hunt T, Schmouder R. The ability of atropine to prevent and reverse the negative chronotropic effect of fingolimod in healthy subjects. *Br. J. Clin. Pharmacol.* **2008**, 66, 199-206.
57. Gross C, Baumgartner A, Rauer S, Stich O. Multiple sclerosis rebound following herpes zoster infection and suspension of fingolimod. *Neurology.* **2012**, 79, 1942-1943.
58. Gasperini C, Ruggieri S. Development of oral agent in the treatment of multiple sclerosis: how the first available oral therapy, fingolimod will change therapeutic paradigm approach. *Drug Des. Dev. Ther.* **2012**, 6, 175-186.
59. Bigaud M, Guerini D, Billich A, Bassilana F, Brinkmann V. Second generation S1P pathway modulators: Research strategies and clinical developments. *Biochim. Biophys. Acta.* **2014**, 1841, 745-758.

60. Brinkmann V, Davis M, Heise C, Albert R, Cottens S, Hof R, Bruns C, Prieschl E, Baumruker T, Hiestand P, Foster C, Zollinger M, Lynch K. The immune modulator FTY720 targets sphingosine 1-phosphate receptors. *J. Biol. Chem.* **2002**, 277, 21453-21457.
61. Deng H, Bernier S, Doyle E, Lorusso J, Morgan B, Westlin W, Evindar G. Discovery of clinical candidate GSK1842799 as a selective S1P1 receptor agonist (prodrug) for multiple sclerosis. *ACS Med. Chem. Lett.* **2013**, 4, 942-947.
62. Tsuji T, Suzuki K, Nakamura T, Goto T, Sekiguchi Y, Ikeda T, Fukuda T, Takemoto T, Mizuno Y, Kimura T, Kawase Y, Nara F, Kagari T, Shimozato T, Yahara C, Inaba S, Honda T, Izumi T, Tamura M, Nishi T. Synthesis and SAR studies of benzyl ether derivatives as potent orally active S1P1 agonists. *Bioorg. Med. Chem.* **2014**, 22, 4246-4256.
63. Hamada M, Nakamura M, Kiuchi M, Marukawa K, Omatsu A, Shimano K, Sato N, Sugahara K, Asayama M, Takagi K, Adachi K. Removal of sphingosine 1-phosphate receptor-3 (S1P3) agonism is essential, but inadequate to obtain immunomodulating 2-aminopropane-1,3-diol S1P1 agonists with reduced effect on heart rate. *J. Med. Chem.* **2010**, 53, 3154-3168.
64. Lipinski C, Lombardo F, Dominy B, Feeney P. Experimental and computational approaches to estimate solubility and permeability in drug discovery and development settings. *Adv. Drug Deliv. Rev.* **2001**, 46, 3-26.
65. Pajouhesh H, Lenz G. Medicinal chemical properties of successful central nervous system drugs. *NeuroRx*. **2005**, 2, 541-553.
66. Rankovic Z. CNS drug design: balancing physicochemical properties for optimal brain exposure. *J. Med. Chem.* **2015**, 58, 2584-2608.
67. Rautio J, Kumpulainen H, Heimbach T, Oliyai R, Oh D, Järvinen T, Savolainen J. Prodrugs: design and clinical applications. *Nat. Rev. Drug Discov.* **2008**, 7, 255-270.
68. Stanczak A, Ferra A. Prodrugs and soft drugs. *Pharmacol. Rep.* **2006**, 58, 599-613.
69. Huttunen K, Raunio H, Rautio J. Prodrugs-from serendipity to rational design. *Pharmacol. Rev.* **2011**, 63, 750-771.
70. Passie T, Seifert J, Schneider U, Emrich H. The pharmacology of psilocybin. *Addict. Biol.* **2002**, 7, 357-364.

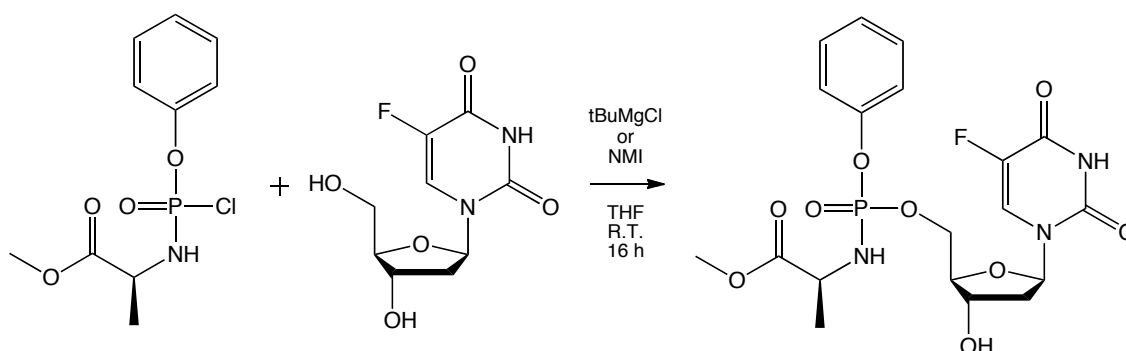
71. Pradere U, Garnier-Amblard E, Coats S, Amblard F, Schinazi R. Synthesis of nucleoside phosphate and phosphonate prodrugs. *Chem. Rev.* **2014**, 114, 9154-9218.
72. Hartline C, Gustin K, Wan W, Ciesla S, Beadle J, Hostetler K, Kern E. Ether lipid-ester prodrugs of acyclic nucleoside phosphonates: activity against adenovirus replication in vitro. *J. Infect. Dis.* **2005**, 191, 396-9.
73. McGuigan C, Murziani P, Slusarczyk M, Gonczy B, Voorde J, Liekens S, Balzarini J. Phosphoramidate ProTides of the anticancer agent FUDR successfully deliver the preformed bioactive monophosphate in cells and confer advantage over the parent nucleoside. *J. Med. Chem.* **2011**, 54, 7247-7258.
74. Mehellou Y, Balzarini J, McGuigan C. Aryloxy phosphoramidate triesters: a technology for delivering monophosphorylated nucleosides and sugars into cells. *ChemMedChem.* **2009**, 4, 1779-1791.
75. Toschi L, Finocchiaro G, Bartolini S, Gioia V, Cappuzzo F. The role of gemcitabine in cancer therapy. *Future Oncol.* **2005**, 1, 7-17.
76. Slusarczyk M, Lopez M, Balzarini J, Mason M, Jiang W, Blagden S, Thompson E, Ghazaly E, McGuigan C. Application of ProTide technology to gemcitabine: a successful approach to overcome the key cancer resistance mechanisms leads to a new agent (NUC-1031) in clinical development. *J. Med. Chem.* **2014**, 57, 1531-1542.
77. Sofia M, Bao D, Chang W, Du J, Nagarathnam D, Rachakonda S, Reddy P, Ross B, Wang P, Zhang H, Bansal S, Espiritu C, Keilman M, Lam A, Micolochick H, Niu C, Otto M, Furman P. Discovery of a β -D-2'-deoxy-2'- α -fluoro-2'- β -C-methyluridine nucleotide prodrug (PSI-7977) for the treatment of hepatitis C virus. *J. Med. Chem.* **2010**, 53, 7202-7218.
78. Birkus G, Wang R, Liu X, Kutty N, MacArthur H, Cohlar T, Gibbs C, Swaminathan S, Lee W, McDermott M. Cathepsin A Is the Major Hydrolase Catalyzing the Intracellular Hydrolysis of the Antiretroviral Nucleotide Phosphonoamidate Prodrugs GS-730 and GS-9131. *Antimicrob. Agents Chemother.* **2007**, 51, 543-550.
79. Zhou X, Chou T, Aubol B, Park C, Wolfenden R, Adams J, Wagner C. Kinetic Mechanism of Human Histidine Triad Nucleotide Binding Protein 1. *Biochemistry.* **2012**, 52, 3588-3600.

Chapter 2 - Finding the Chemical Pathway to Synthesise “ProTide” Fingolimod

2.1 Discussion

2.1.1 The Synthetic Challenge

In order to produce novel phosphoramidate prodrugs of fingolimod a synthesis route needs to be developed. As the synthesis of these compounds has never been previously performed, and literature searching provides no synthesis routes to produce the desired compounds, the method needs to be discovered.



Scheme 2.1 Phosphoramidate nucleoside synthesis¹

What is required for an expected S1P receptor modulator prodrug phosphoramidate fingolimod is a phosphoramidate moiety bound selectively to one of the alcohol groups on fingolimod. Potential problems of applying typical phosphorochloridate chemistry (binding a phosphorochloridate to one OH in a nucleoside: see scheme 2.1) to fingolimod include the formation of bis products where the phosphorochloridate is bound to both OH groups and the possible formation of the phosphorochloridates bound to the NH₂ group. There is the additional problem of only wanting *S*-isomers of ProTide fingolimod as *R*-isomers are unlikely to bind effectively to S1P receptors once the phosphoramidate has been processed to form *R*-fingolimod-phosphate.

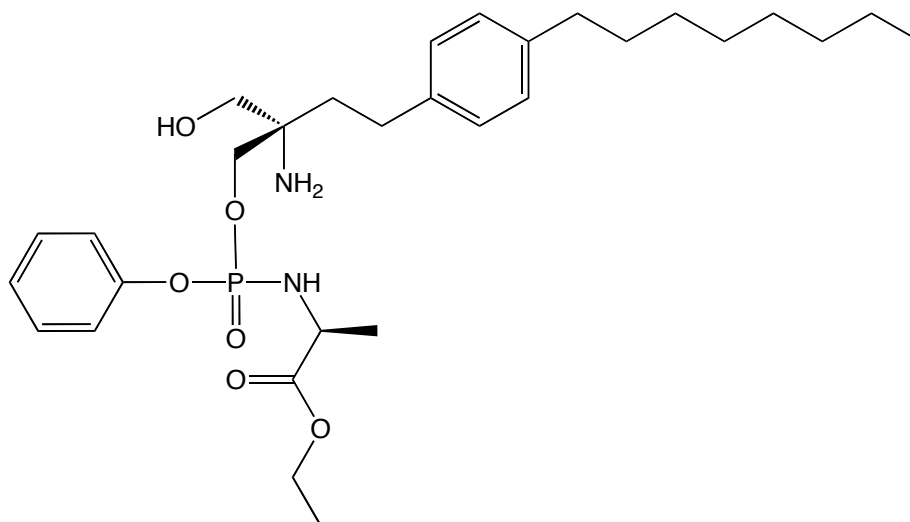


Figure 2.1 Desired *S*-isomer of ProTide Fingolimod

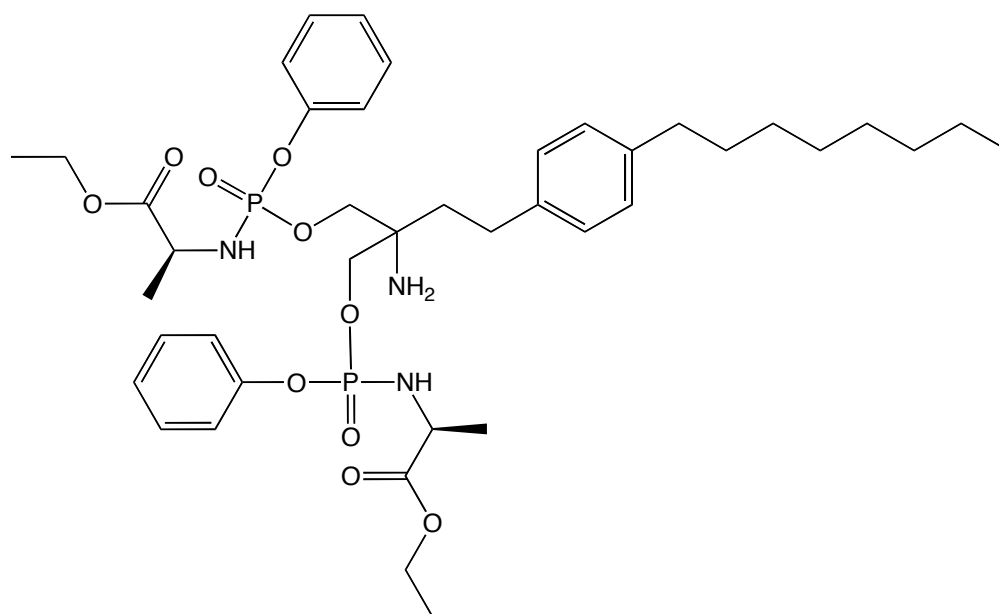


Figure 2.2 Likely bis-product which is not expected to have favourable biological activity

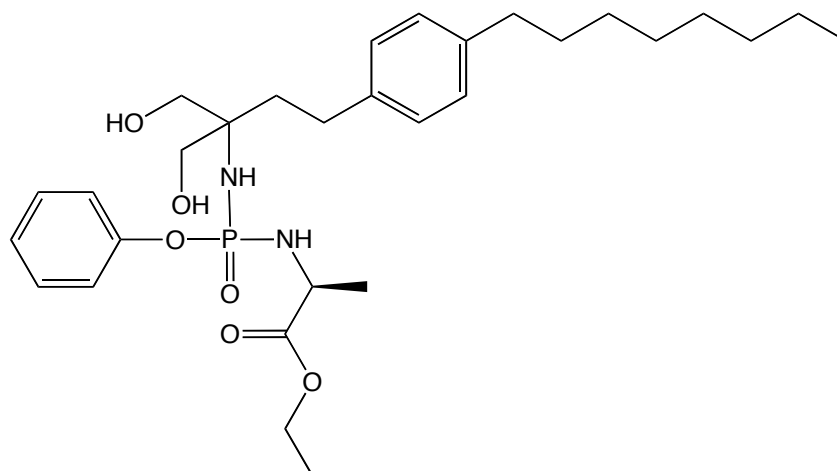


Figure 2.3 Likely unwanted *N*-bound side product

The first problem to tackle regarding this synthetic challenge was to try to find a reaction system that would cause a phosphorochloridate to selectively bind to the OH group rather than the NH₂ group. NH₂ groups are significantly more basic than OH groups and the OH groups on fingolimod have a pK_a value of approximately 16 whereas the amine has a pK_a value of around 30 and it is logical to expect that the NH₂ group will nucleophilically attack the phosphorus atom of the phosphorochloridate more readily than an OH group.² In order to find a method that would lead to *O*-bound phosphoramidate an alternative molecule that could act as a model for fingolimod was used. It was decided that 3-amino-1-propanol would make a good model as it possesses an OH group and a NH₂ group. The simplicity of the molecule should also make interpretation of the data easier than it would be if a more complex model were used.

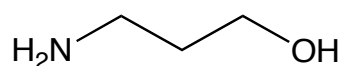
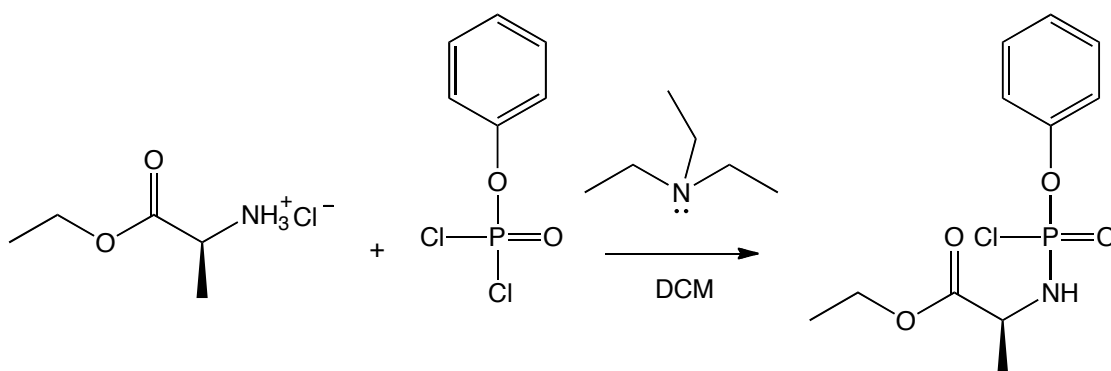


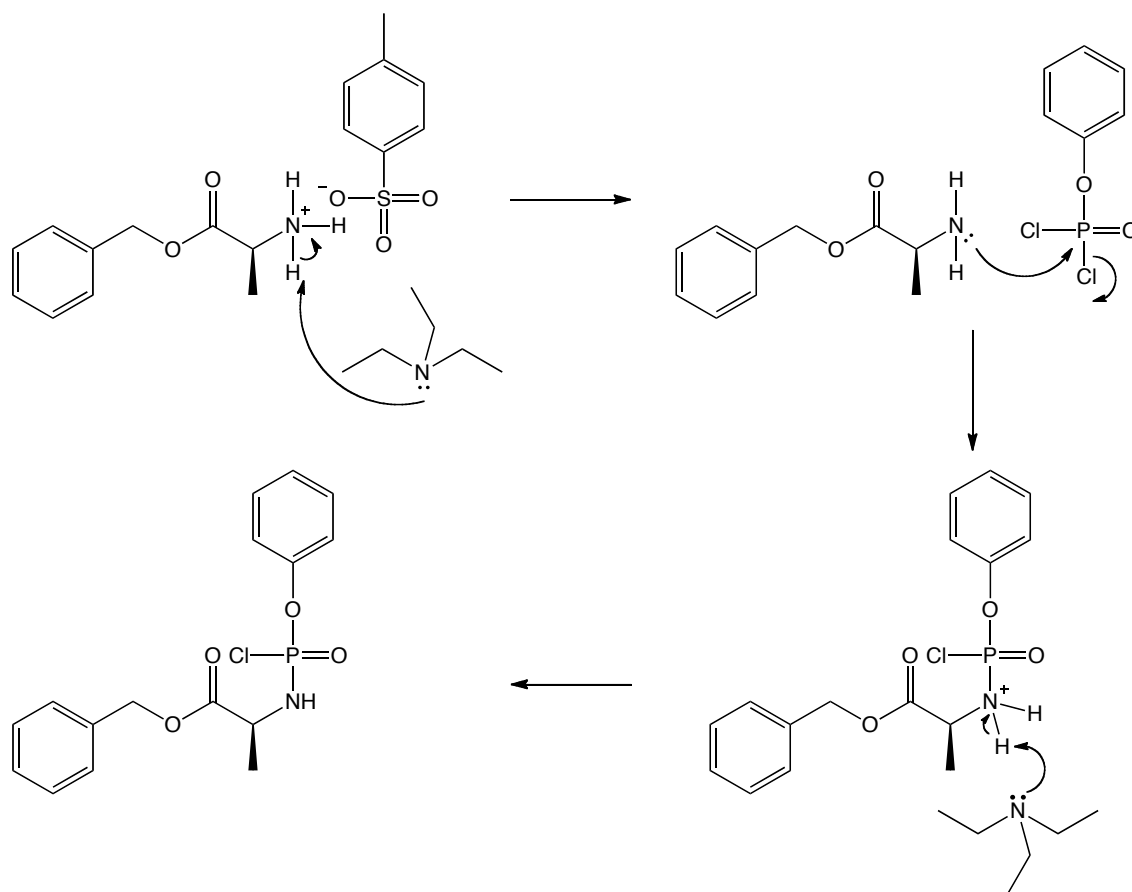
Figure 2.4 3-amino-1-propanol

2.1.2 Phosphorochloridate Chemistry

The first step of a standard phosphoramidate synthesis is to synthesise a phosphorochloridate.^{1,3,4} It was decided that phenyl-(benzyloxy-L-alaninyl) phosphorochloridate would be an adequate starting phosphorochloridate as ProTides synthesised with this phosphorochloridate are often found to have more favourable biological activity.



Scheme 2.2 Synthesis of phenyl-(ethyloxy-L-alaninyl) phosphorochloridate or Ph-LAla-OEt PCl



Scheme 2.3 Proposed mechanism of phenyl-(benzyloxy-L-alaninyl) phosphorochloridate synthesis reaction

One of the key pieces of evidence that can be used to determine whether or not a phosphorochloridate has been successfully synthesised is a spectrum obtained using phosphorus nuclear magnetic resonance spectroscopy (³¹P NMR). For a phosphorochloridate like phenyl-(benzyloxy-L-alaninyl) phosphorochloridate (shorthand: Ph-LAla-OBzl PCl) you would typically expect to see two peaks on the ³¹P NMR spectrum; these two peaks correspond to the presence of two chiral centres. The L-Alanine chiral centre is fixed, at the *S*-configuration, but the phosphorus centre can form both *S* and *R* configurations thus two different diastereoisomers are produced by the reaction: *S_CS_P* and *S_CR_P*. Because the molecules are not mirror images of each other they appear as two different peaks in the ³¹P NMR spectrum (as diastereoisomers).

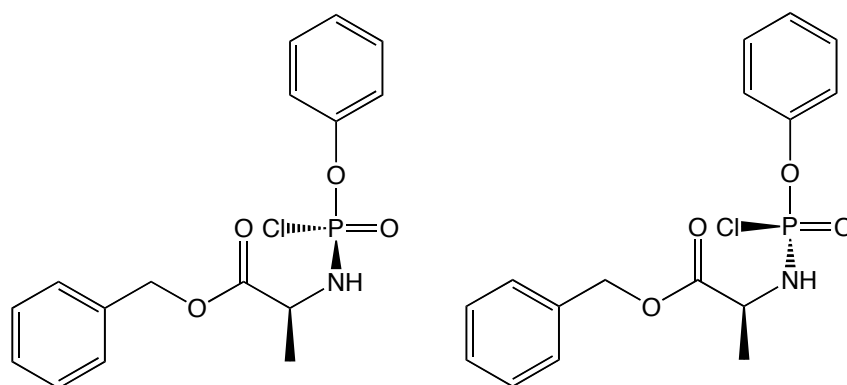


Figure 2.5 Here it can be seen that the two diastereoisomers produced by this reaction are non-superimposable

In figure 2.6 the ^{31}P NMR spectrum of one of the first phosphorochloridates synthesised during this project can be seen. There are two major peaks at 7.88 ppm and 7.53 ppm. These chemical shifts are indicative of a successfully synthesised phosphorochloridate.^{1,3} The very small peaks at -8.99 ppm and -9.05 ppm are unwanted side-products but one can see from the relative height that the amount of impurity is negligible and typically a ^{31}P NMR spectrum like this where only a very small amount of impurity is visible is used as an indication that the phosphorochloridate is of acceptable quality to be used in a phosphoramidate synthesis. Figure 2.7 shows a fairly clean ^1H NMR spectrum of Ph-Gly-OMe PCl and the relevant peaks with their corresponding integrations and assignments on the chemical structure.

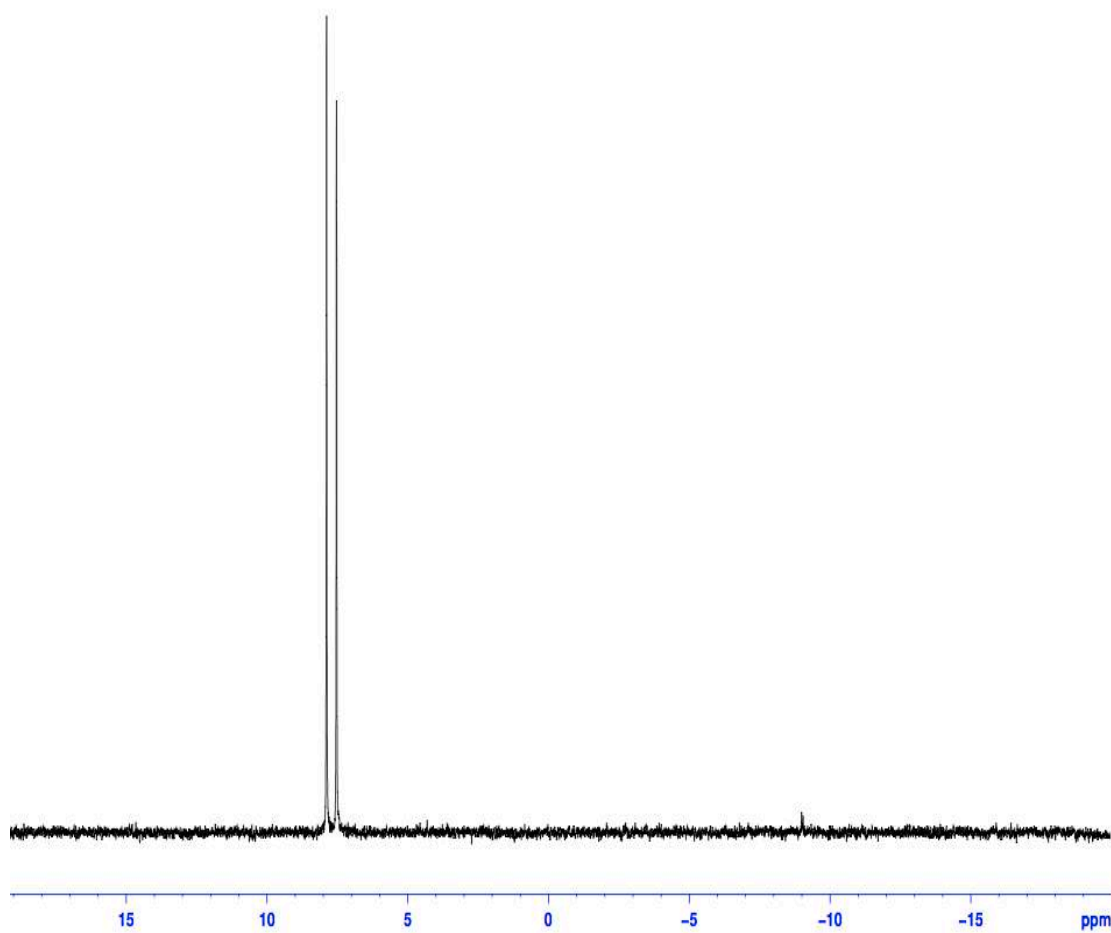


Figure 2.6 ^{31}P NMR of Ph-LAla-OBzl PCI

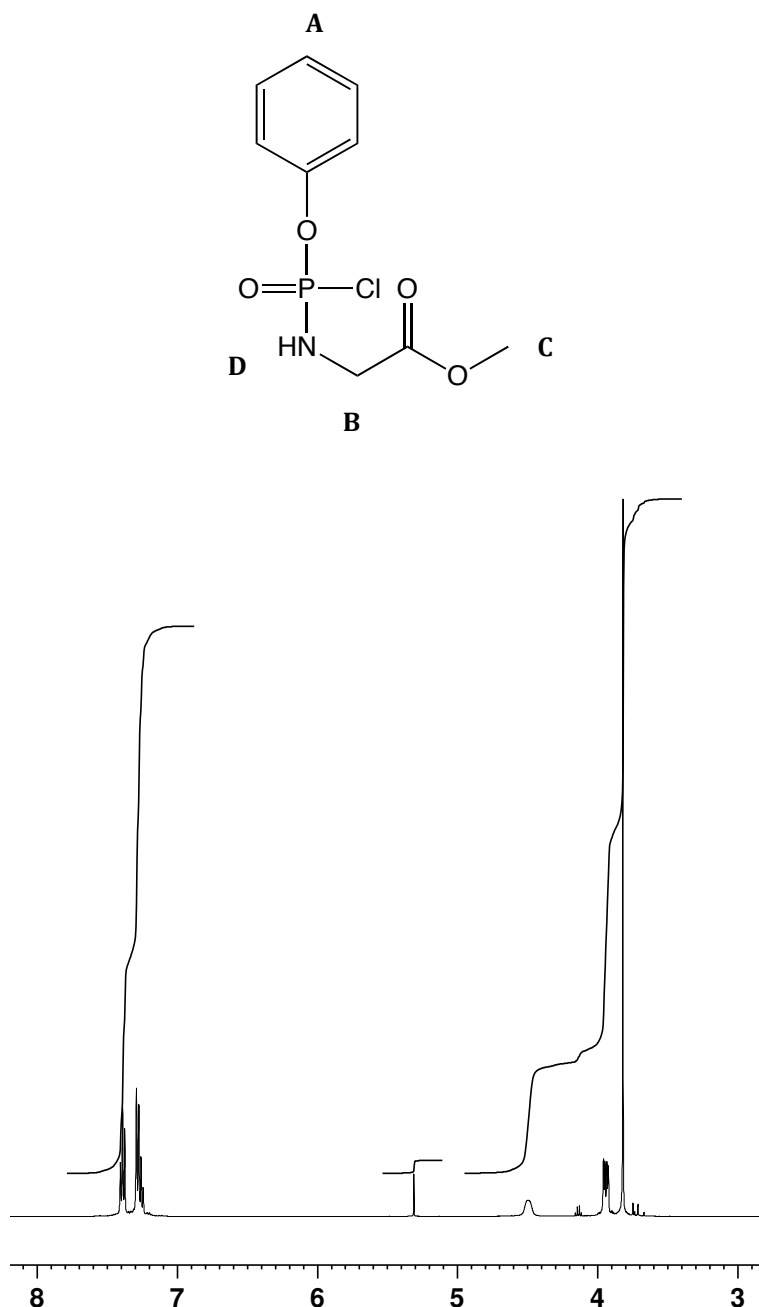


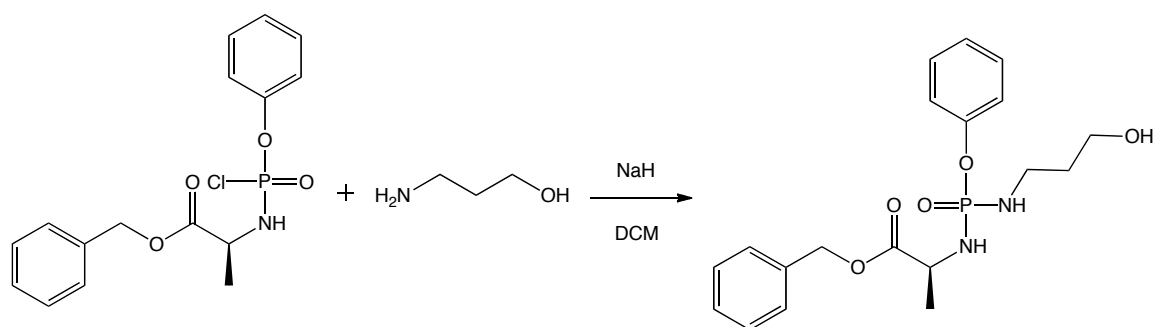
Figure 2.7 Structure and ^1H NMR spectrum of Ph-Gly-OMe PCl

A = 7.2 – 7.5 ppm (5H), **B** = 3.95 ppm (2H), **C** = 3.8 ppm (3H), **D** = 4.5 ppm (1H)

2.1.3 Phosphoramidate Synthesis Using a NaH Base

The first attempted phosphoramidate synthesis involved reacting a phosphorochloridate, 3-amino-1-propanol and sodium hydride base in anhydrous dichloromethane solvent at room temperature over the weekend. This base has previously been used to successfully synthesise novel phosphoramidates.⁵ The

product of this reaction was observed to be the unwanted *N*-bound phosphoramidate with no *O*-bound phosphoramidate observed.



Scheme 2.4 3-amino-1-propanol phosphoramidate synthesis using NaH

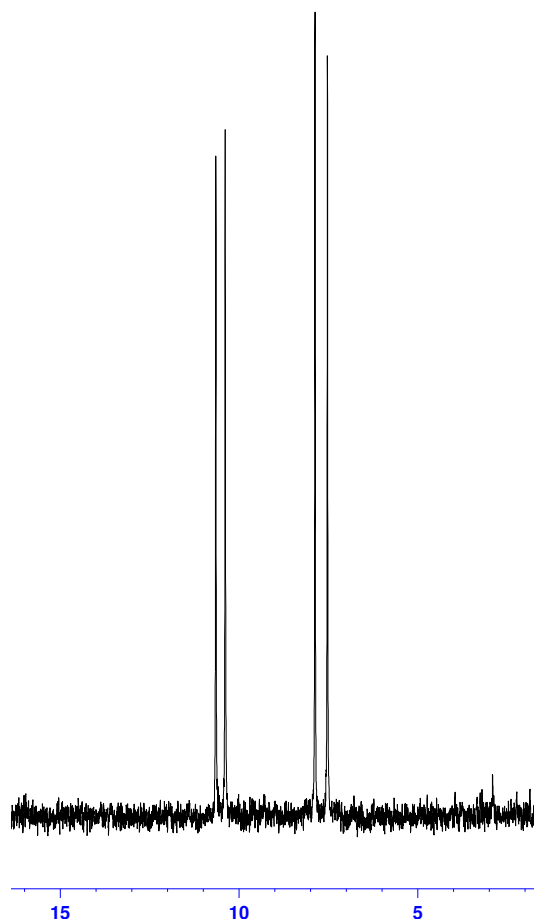


Figure 2.8 ^{31}P NMR of the product showing the unreacted PCl peaks at around 7.5 ppm and the *N*-bound product at around 10.5 ppm

When conducting this reaction 2 equivalents of phosphorochloridate were used and 1 equivalent of 3-amino-1-propanol was used. The peaks in figure 2.8 corresponding to the unreacted phosphorochloridate can be seen at 7.87 ppm and 7.52 ppm. The peaks corresponding to the *N*-bound 3-amino-1-propanol

phosphoramidate can be seen further downfield at 10.65 ppm and 10.38 ppm. These chemical shifts are indicative of the *N*-bound product as *N*-bound phosphoramidates usually have a chemical shift of between 10 and 11 ppm. The two peaks observed for the product correspond to the two expected diastereoisomers.

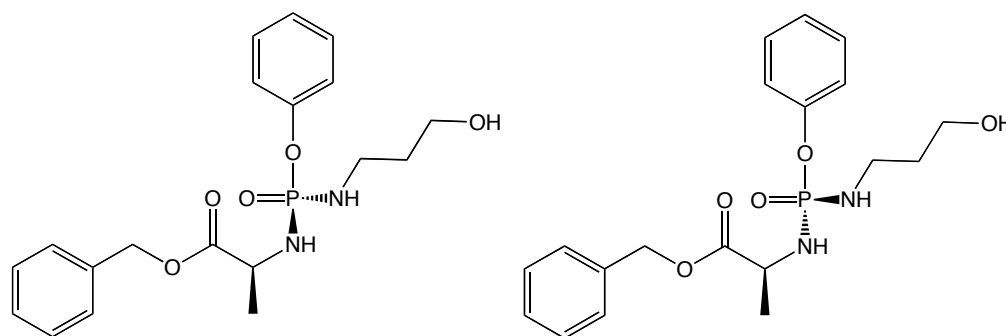
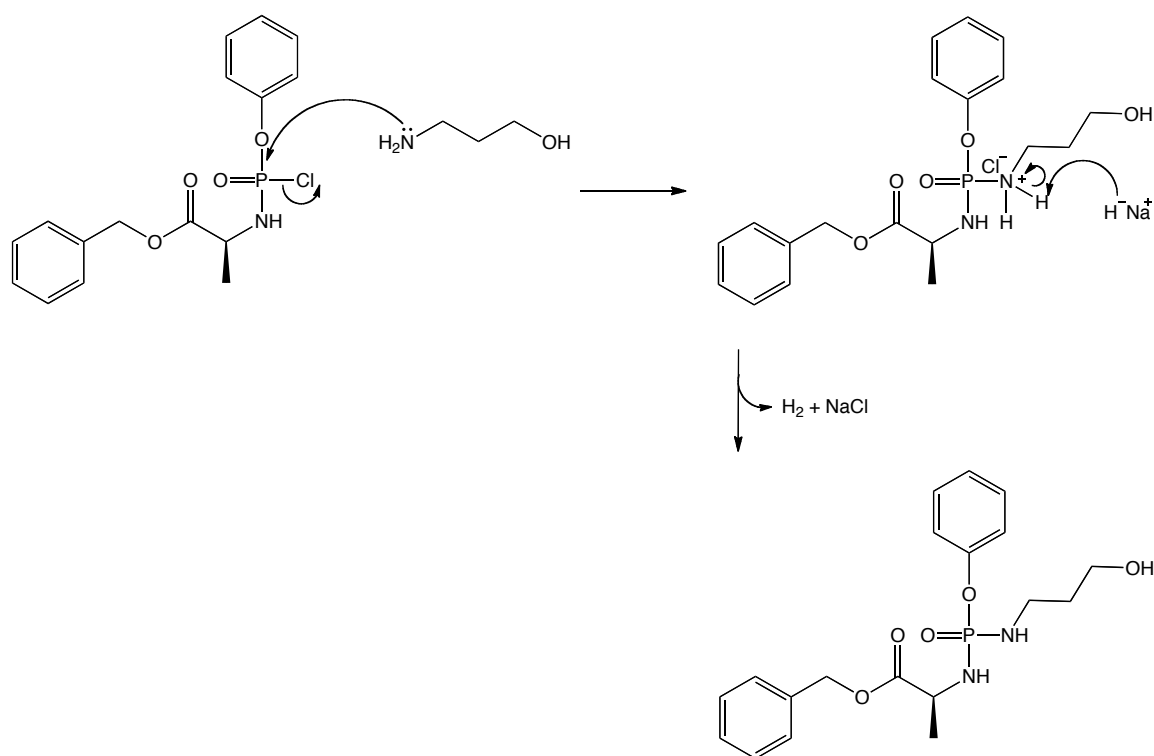


Figure 2.9 The two *N*-bound diastereoisomers formed

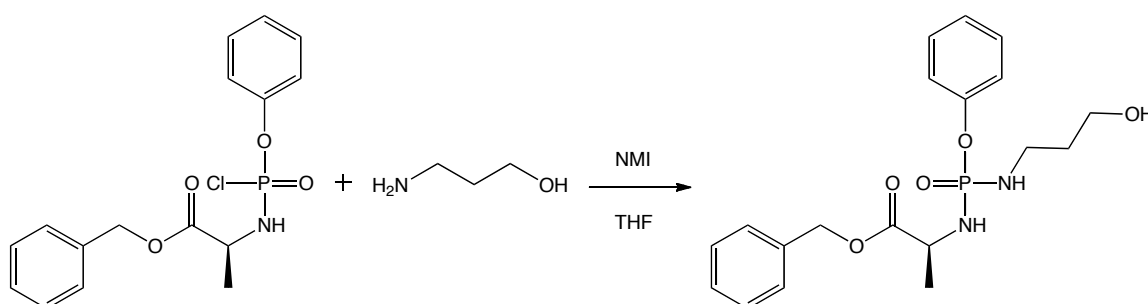


Scheme 2.5 Proposed mechanism of phosphoramidate synthesis using NaH

Scheme 2.5 shows the likely mechanism of the phosphoramidate formation. As the 3-amino-1-propanol and phosphorochloridate are mixed together before the NaH base is added and instant cloudiness is observed when mixing them together in DCM the formation of a salt is implied.

2.1.4 Phosphoramidate Synthesis Using a NMI Base

The next reaction conditions tested involved using *N*-methylimidazole base in anhydrous tetrahydrofuran solvent. The reaction was begun at 0 °C but then allowed to warm to room temperature. The reaction mixture was left to stir over the weekend. These reaction conditions have previously proven to be effective in synthesising novel phosphoramidates.^{1,4,6,7,8}



Scheme 2.6 3-amino-1-propanol phosphoramidate synthesis using NMI

As with the NaH experiment only the *N*-bound 3-amino-1-propanol product was produced by the reaction. Figure 2.10 shows the ³¹P NMR spectrum of the product of this reaction. It can be clearly seen that, while only the unwanted *N*-bound product was formed, the quality and purity are much greater than with the first phosphoramidate synthesis. For this reaction 1 equivalent was used of both the phosphorochloridate and 3-amino-1-propanol and as a result no additional peaks corresponding to unreacted phosphorochloridate were observed. The absence of peaks between 0 and -10 ppm implies an improvement in synthetic technique due to a more successful attempt at ensuring the reaction conditions are anhydrous.

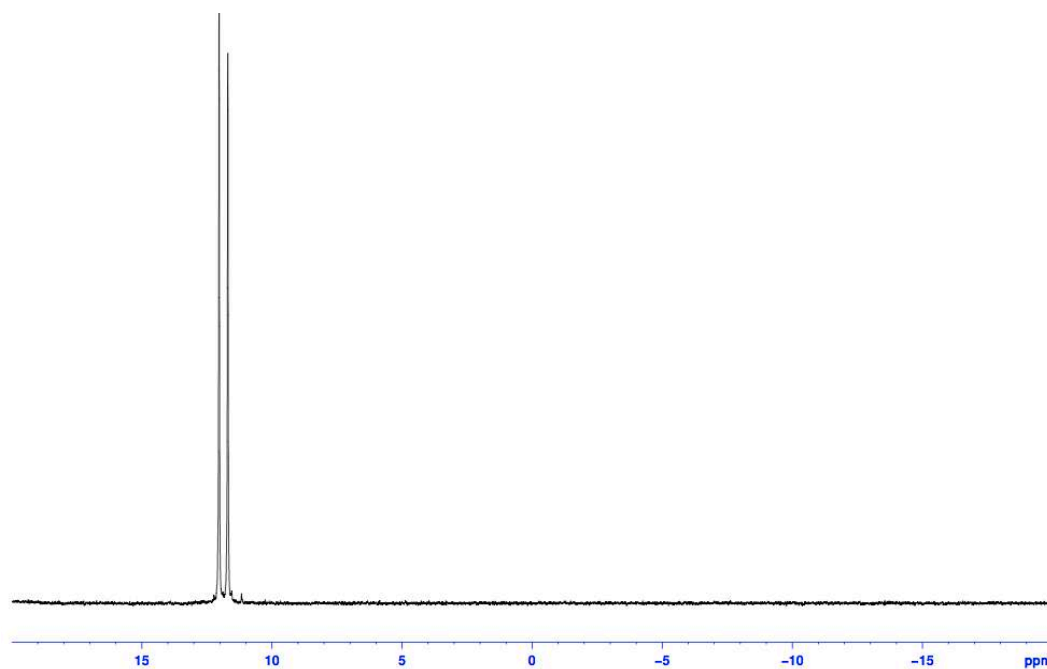
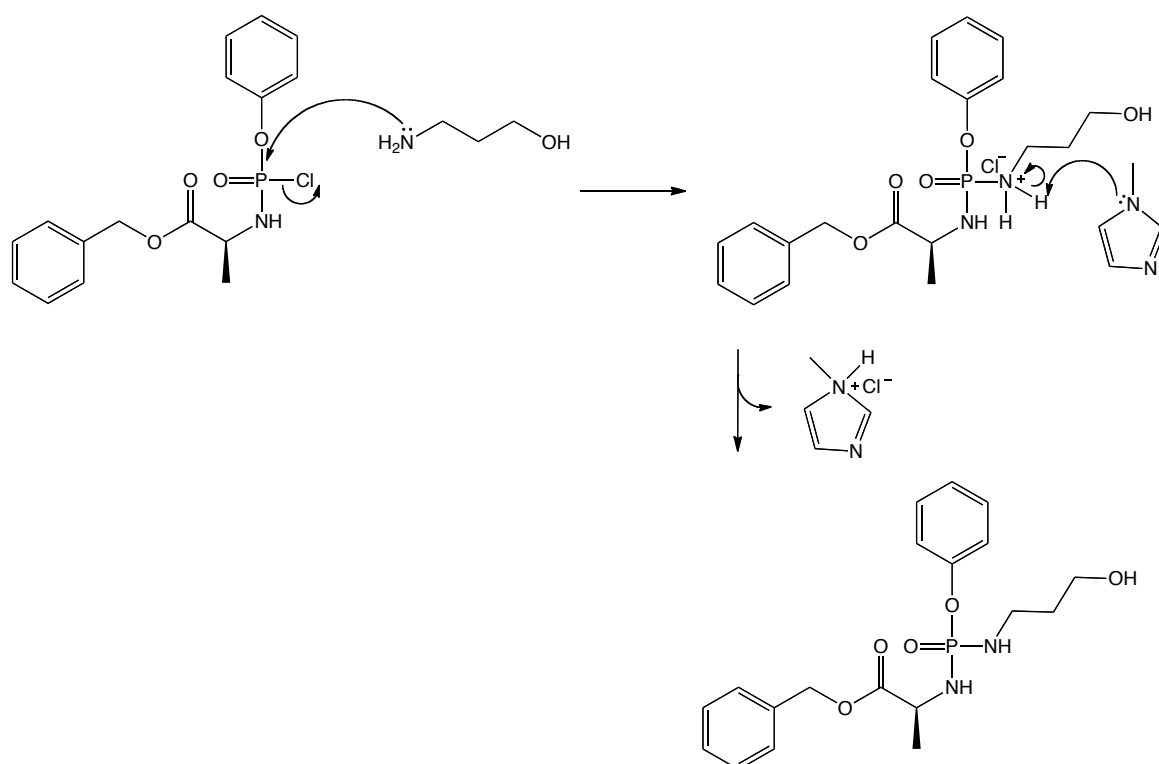


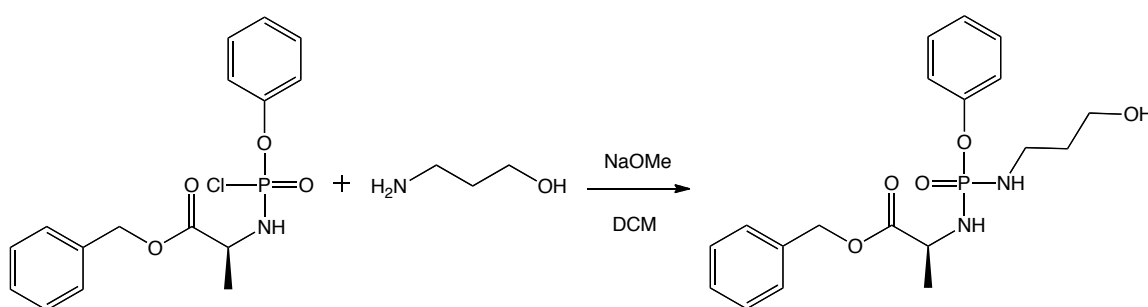
Figure 2.10 ^{31}P NMR of phosphoramidate product



Scheme 2.7 Proposed mechanism of phosphoramidate formation using NMI

2.1.5 Phosphoramidate Synthesis Using a NaOMe Base

Other reaction conditions tested involved using sodium methoxide base in anhydrous dichloromethane solvent. The reaction was begun at -78 °C and then allowed to warm to room temperature. The reaction mixture was left to stir for 1.5 hours. Again the major product of the reaction was the N-bound phosphoramidate and no *O*-bound product was observed.



Scheme 2.8 3-amino-1-propanol phosphoramidate synthesis using NaOMe

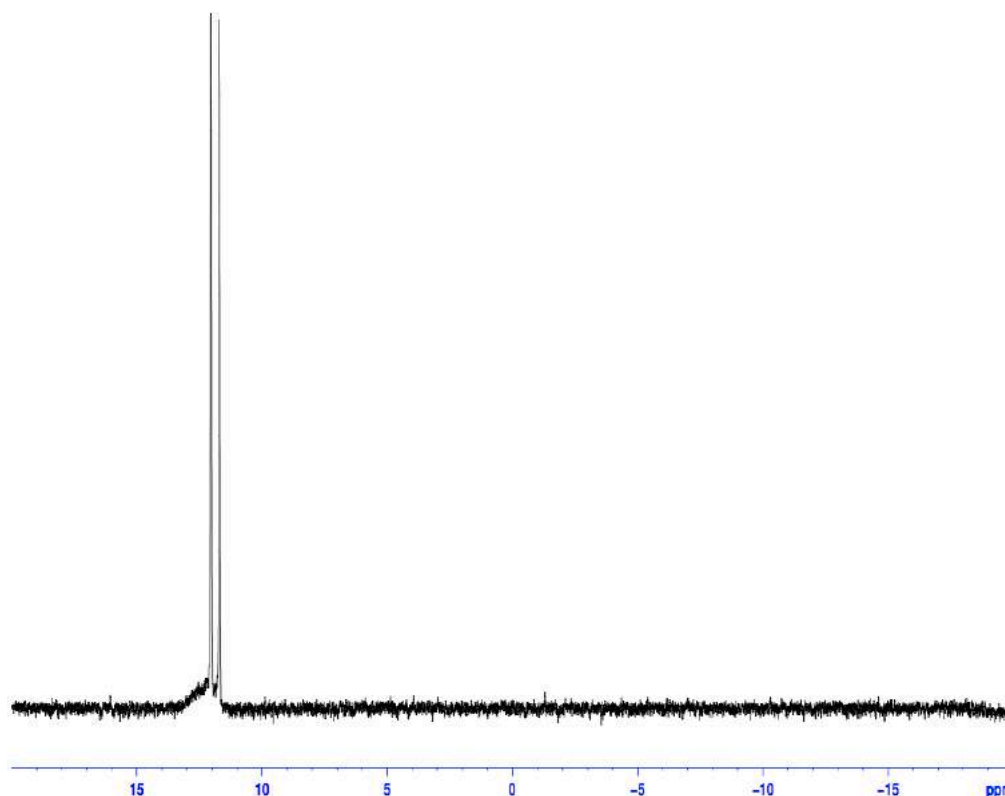
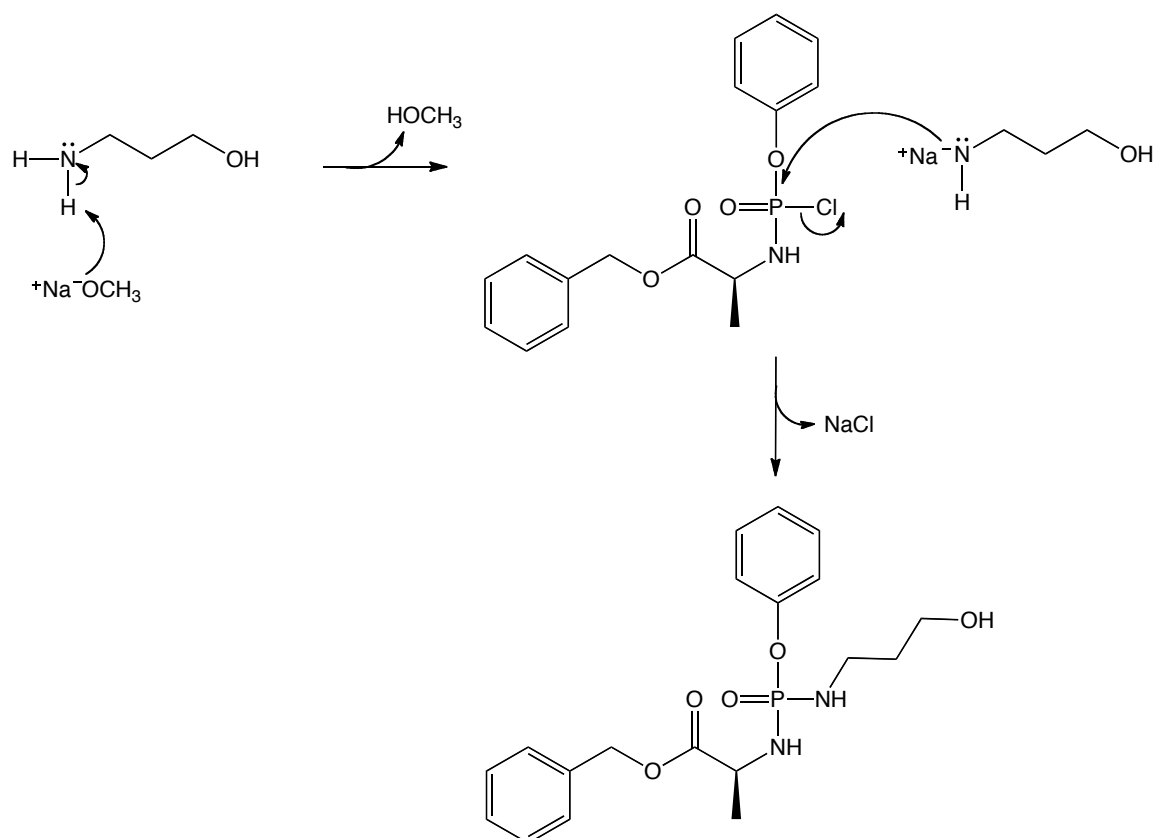


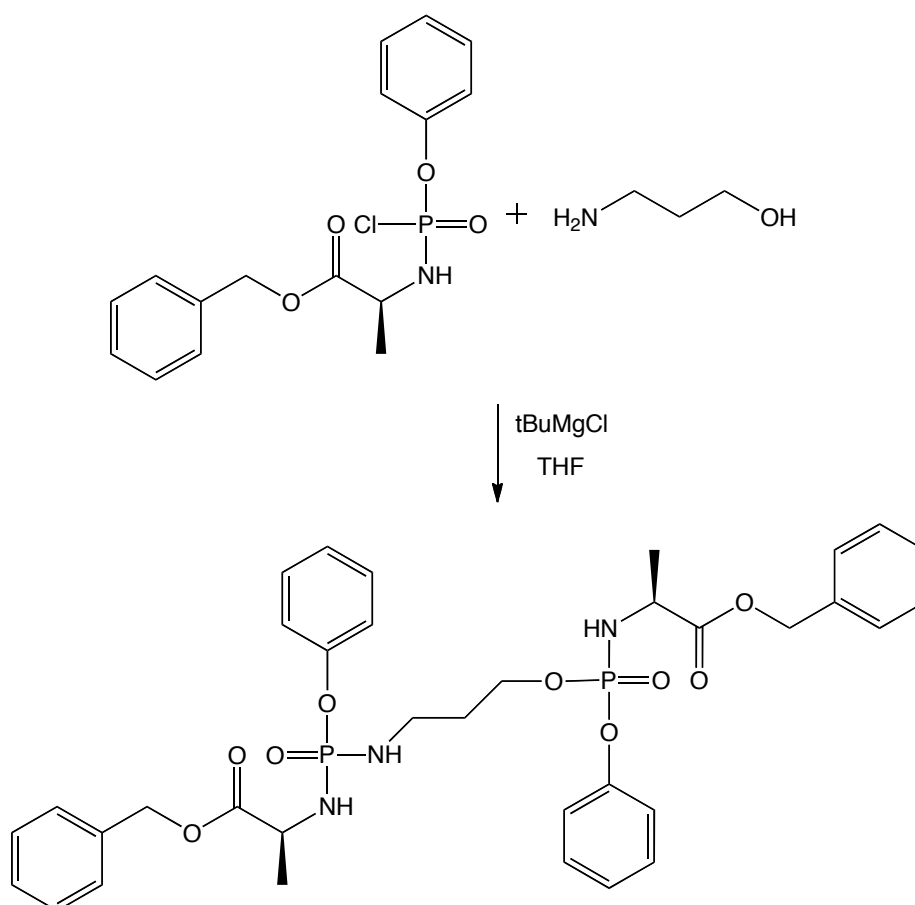
Figure 2.11 ^{31}P NMR of phosphoramidate product



Scheme 2.9 Proposed mechanism of phosphoramidate formation using NaOMe

2.1.6 Phosphoramidate Synthesis Using a tBuMgCl Base

However it was found that when using tertiary-butylmagnesium chloride (tBuMgCl) in anhydrous tetrahydrofuran solvent at room temperature^{1,3,4,5,6,7,9} for 24 hours the phosphorochloridate bound to both the OH group and the NH₂ group:



Scheme 2.10 3-amino-1-propanol bis phosphoramidate synthesis using tBuMgCl

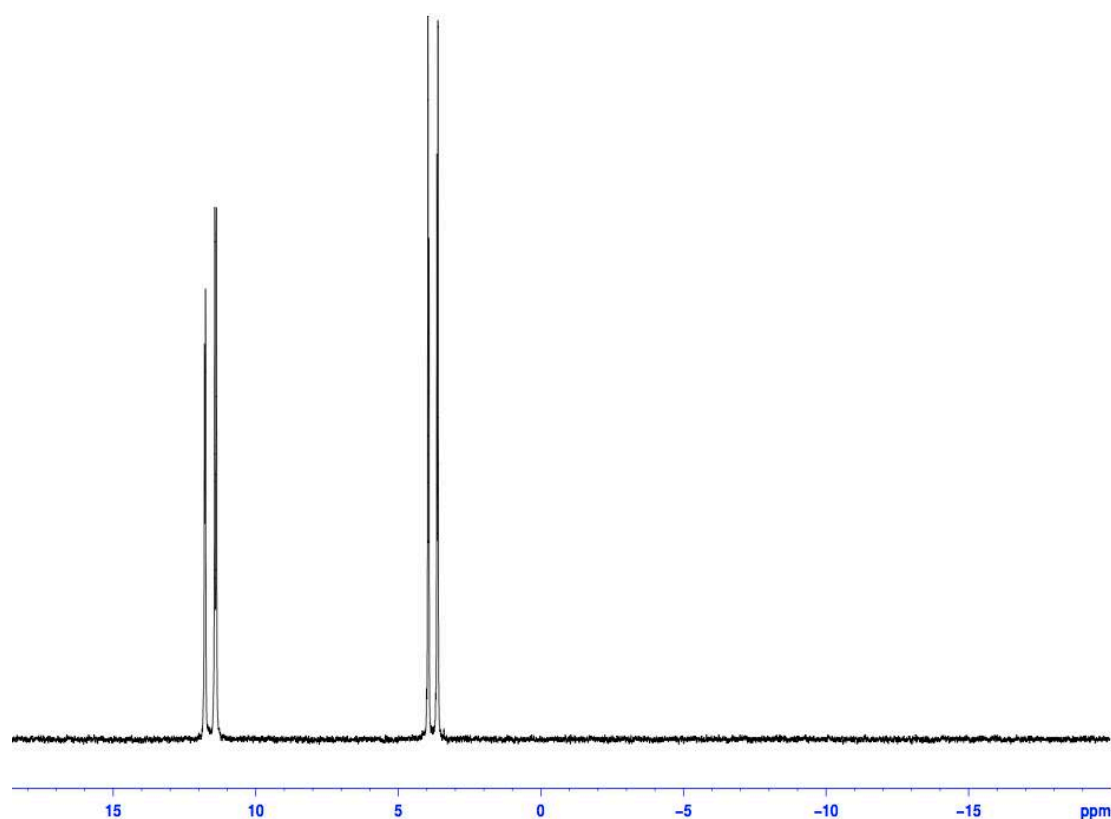


Figure 2.12 ^{31}P NMR of phosphoramidate product using tBuMgCl

The 4 major peaks observed at 3.96, 3.92, 3.64 and 3.61 ppm were considered to likely be indicative of an *O*-bound phosphoramidate. To be sure that the new peaks further upfield were not unreacted phosphorochloridate the product was “spiked” with phosphorochloridate starting material. Figure 2.13 shows the ^{31}P NMR spectrum obtained when the product of the tBuMgCl synthesis was spiked with the phosphorochloridate. The peaks which correspond to the N-bound phosphorus on the 3-amino-1-propanol can be seen at 11.75, 11.44 and 11.38 ppm. The peaks which correspond to the *O*-bound phosphorus on the 3-amino-1-propanol can be seen at 3.95, 3.92, 3.63 and 3.60 ppm. The spiked phosphorochloridate peaks can be seen at 5.04 and 4.81 ppm. The phosphorochloridate peaks are further upfield in this spectrum compared to the earlier spectra shown (figures 2.6 and 2.8) because this particular NMR experiment was conducted in MeOD as opposed to CDCl_3 and different solvents can cause the chemical shifts to be different when run in NMR.

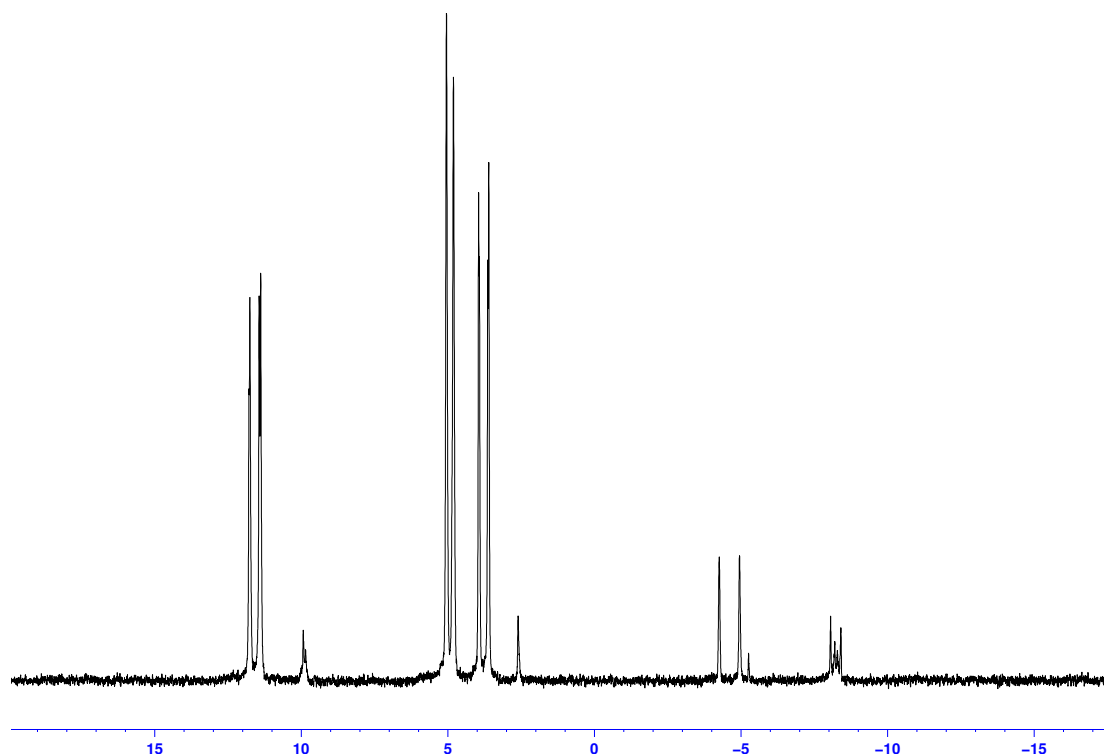


Figure 2.13 ^{31}P NMR of phosphoramidate product 'spiked' with phosphorochloridate starting material

After establishing that the new peaks seen between 3 – 4 ppm do correspond to *O*-bound phosphoramidate it was considered that the data may be spectra of a mixture of *O*-bound and *N*-bound phosphoramidates. Mass spectrometry showed that it is just one product: 3-amino-1-propanol with phosphoramidate moieties bound at both the *N*-terminal and the *O*-terminal. The predicted mass of this bis-product is 709.2 g/mol and the observed mass is 710.3 m/z ($\text{M}+\text{H}^+$). Further evidence to prove that it is just one compound rather than a mixture include the fact that the product was observed just as one spot on thin layer chromatography (TLC) and the presence of 4 peaks at both the O and N regions of the ^{31}P NMR spectrum. The 8 major peaks observed in the ^{31}P NMR spectrum are presumably due to the 4 different diastereoisomers that are formed by this synthesis as shown in figure 2.14.

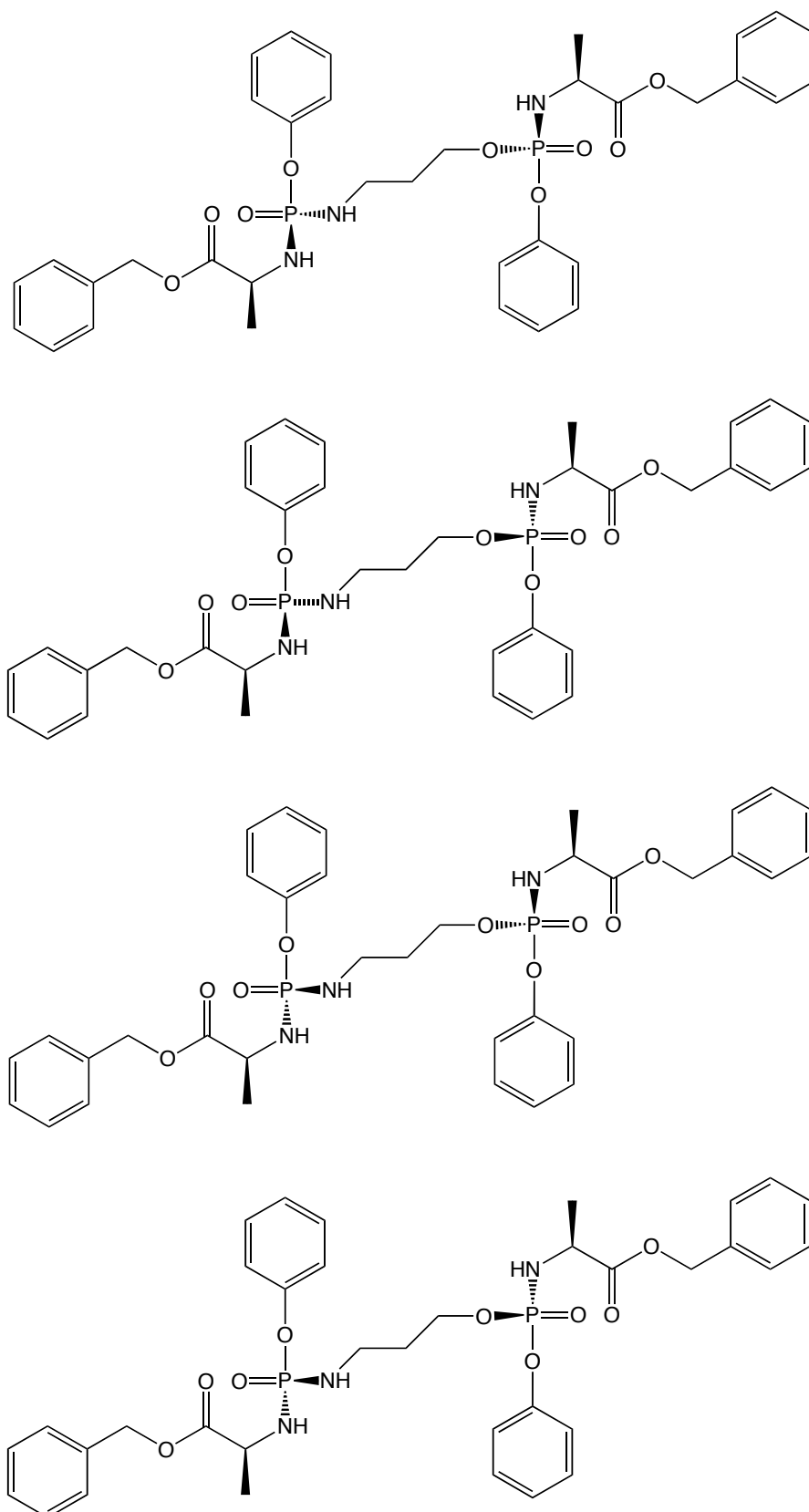
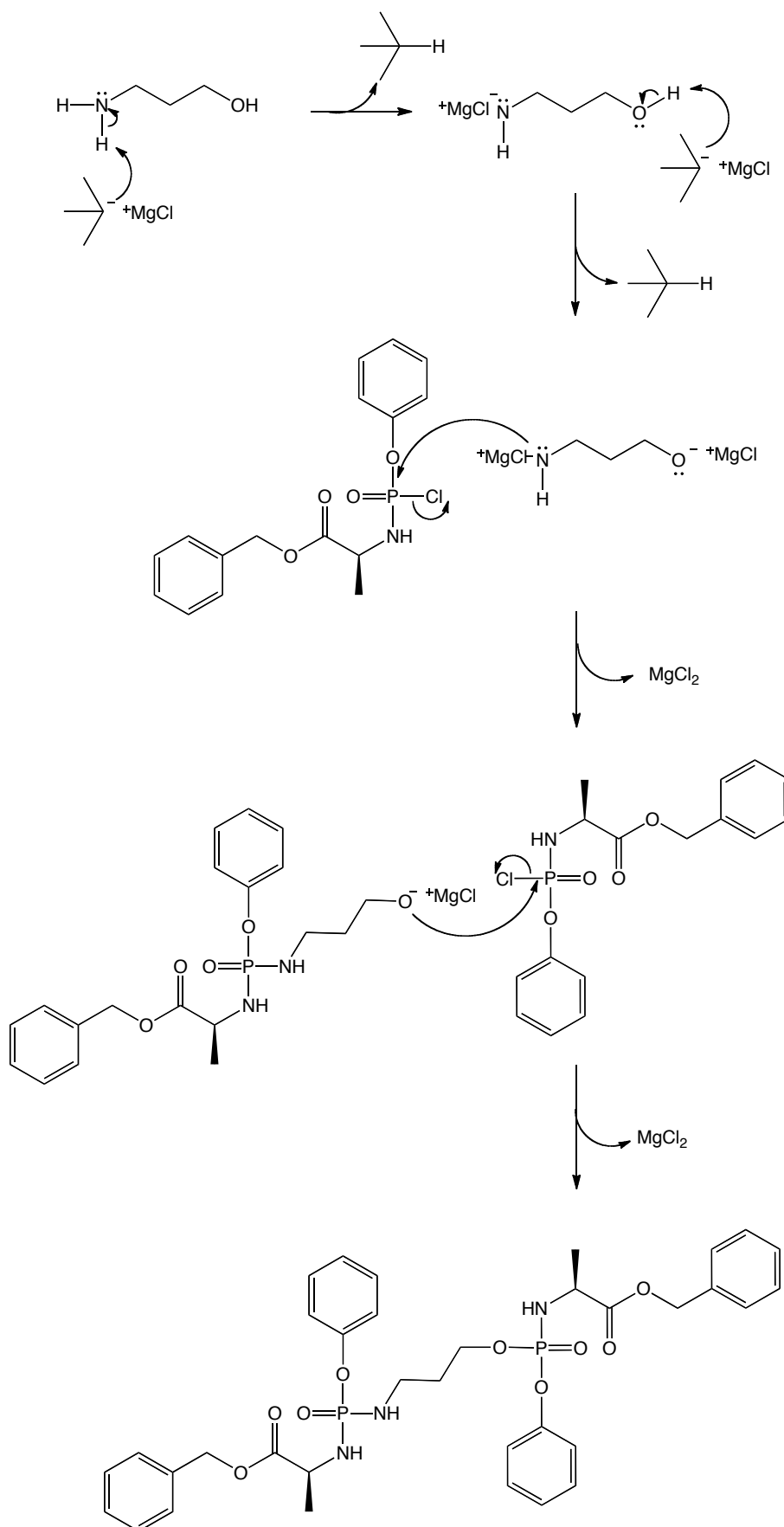
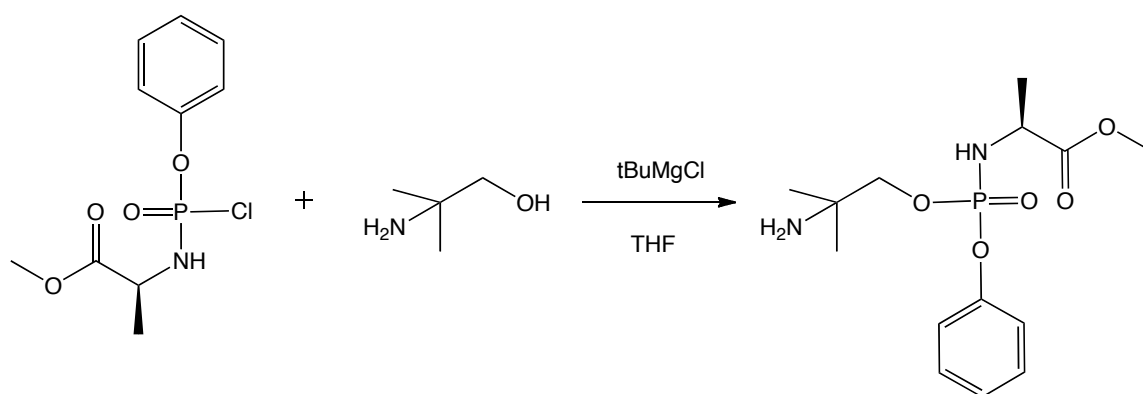


Figure 2.14 The four suggested phosphoramidate diastereoisomers formed using tBuMgCl

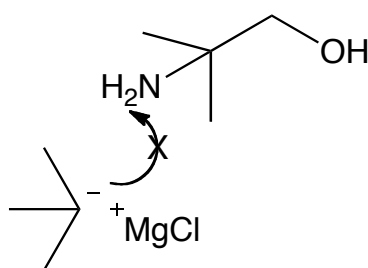


Scheme 2.11 Suggested mechanism for bis-phosphate formation. A salt is clearly formed before adding the phosphorochloridate and the mechanism is in part deduced from this observation.

As the NH_2 group in fingolimod is far more sterically hindered than the NH_2 present in 3-amino-1-propanol it was hypothesised that the bulky tertiary butyl group of tBuMgCl would not be able to easily deprotonate the amine group and thus the amine group would not bind to the phosphorochloridate. It was decided that another model would be used which more accurately represents the functional characteristics of fingolimod. This time 2-amino-2-methyl-1-propanol was used as it has a primary alcohol group and a NH_2 group attached to a quaternary carbon thus putting the NH_2 group in a much more sterically hindered position. For the purposes of the regioselective questions trying to be addressed this molecule is a more accurate model of fingolimod.



Scheme 2.12 Phosphoramidate formation using tBuMgCl and 2-amino-2-methyl-1-propanol



Scheme 2.13 The tBuMgCl cannot deprotonate the amine group due to the steric interactions between the bulky tertiary butyl group and the CH_3 groups adjacent to the free amine

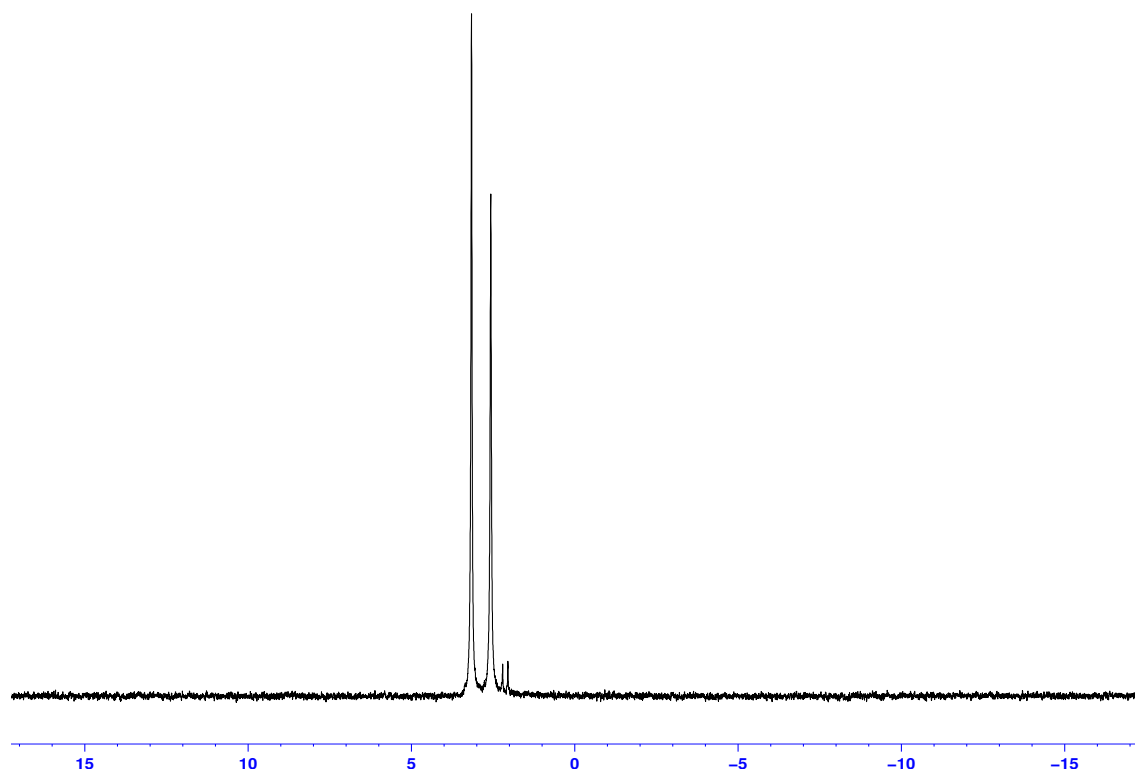


Figure 2.15 ^{31}P NMR of phosphoramidate product using tBuMgCl and 2-amino-2-methyl-1-propanol

The ^{31}P NMR spectrum of the yielded product shown in figure 2.15 clearly shows the desired 2 major peaks between 2 and 4 ppm that correspond to *O*-bound phosphoramidate and no peaks between 10 and 12 ppm that would imply the phosphoramidate bound to the NH_2 amine group. Mass spectrometry further confirmed the synthesis as the predicted mass is 330.1 g/mol and the observed mass is 331.1 m/z. This represented a breakthrough in this project and removed a significant synthetic hurdle.

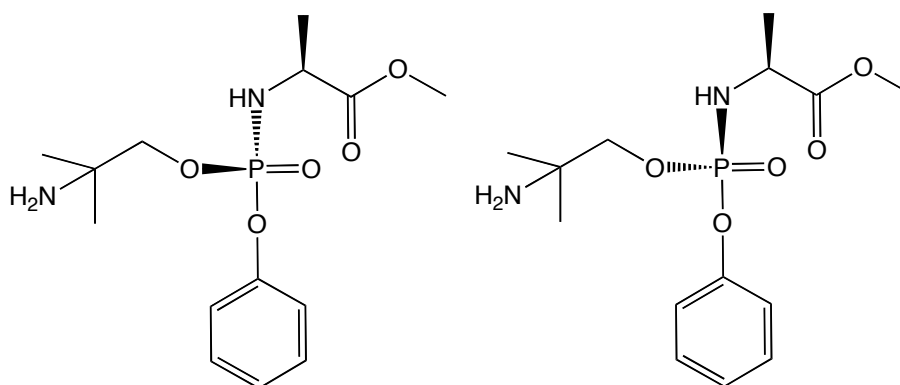


Figure 2.16 The two products of the reaction that give the two major peaks observed in the ^{31}P NMR spectrum

Following the success of the phosphoramidate 2-amino-2-methyl-1-propanol synthesis it was concluded that there was enough evidence to suggest that those reaction conditions used could be used to synthesise novel ProTide fingolimod analogues. The lead reaction conditions devised after conducting these experiments are:

tBuMgCl (1 equivalent) is added dropwise to a solution of primary alcohol (e.g. fingolimod hydrochloride) (1 equivalent) in anhydrous THF (7 ml) under anhydrous conditions. The mixture is stirred at room temperature for one hour. After one hour the phosphorochloridate (1 equivalent) in anhydrous THF (2 ml) is added dropwise to the stirring reaction mixture. The reaction is left to stir for 24 hours. After 24 hours the solvent is removed in vacuo and the desired product is isolated using flash chromatography.

2.2 References

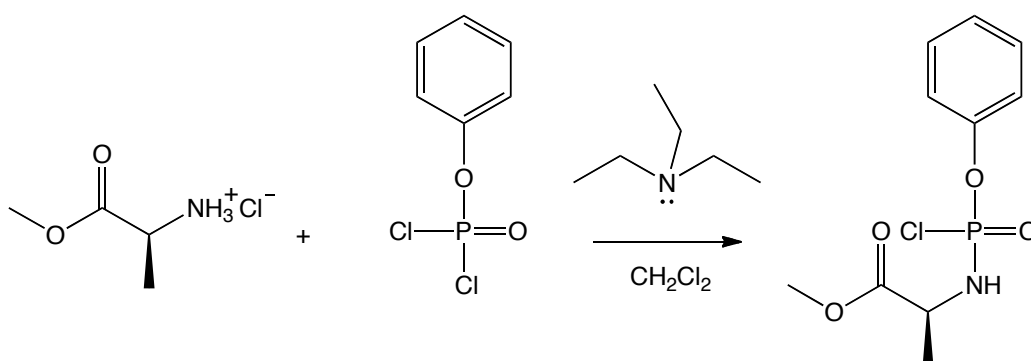
1. McGuigan C, Murziani P, Slusarczyk M, Gonczy B, Voorde J, Liekens S, Balzarini J. Phosphoramidate ProTides of the anticancer agent FUDR successfully deliver the preformed bioactive monophosphate in cells and confer advantage over the parent nucleoside. *J. Med. Chem.*, **2011**, 54, 7247-7258.
2. McMurry J. *Organic Chemistry*. Sixth edition. 2004.
3. Slusarczyk M, Lopez M, Balzarini J, Mason M, Jiang W, Blagden S, Thompson E, Ghazaly E, McGuigan C. Application of ProTide technology to gemcitabine: a successful approach to overcome the key cancer resistance mechanisms leads to a new agent (NUC-1031) in clinical development. *J. Med. Chem.* **2014**, 57, 1531-1542.
4. Serpi M, Madela K, Pertusati F, Slusarczyk M. Synthesis of phosphoramidate prodrugs: ProTide approach. *Curr. Protoc. Nucleic. Acid Chem.* **2013**, Chapter 15, Unit 15.5.
5. Balzarini J, Meier C. Diastereoselective synthesis of aryloxy phosphoramidate prodrugs of 3'-deoxy-2',3'-didehydrothymidine monophosphate. *J. Med. Chem.* **2010**, 53, 7675-7681.
6. Serpi M, Bibbo R, Rat S, Roberts H, Hughes C, Caterson B, Alcaraz M, Gibert A, Verson C, McGuigan C. Novel phosphoramidate prodrugs of *N*-acetyl-(D)-glucosamine with antidegenerative activity on bovine and human cartilage explants. *J. Med. Chem.* **2012**, 55, 4629-4639.
7. Pradere U, Garnier-Amblard E, Coats S, Amblard F, Schinazi R. Synthesis of nucleoside phosphate and phosphonate prodrugs. *Chem. Rev.* **2014**, 114, 9154-9218.
8. Mehellou Y, Valente R, Mottram H, Walsby E, Mills K, Balzarini J, McGuigan C. Phosphoramidates of 2'- β -d-arabinouridine (AraU) as phosphate prodrugs; design, synthesis, in vitro activity and metabolism. *Bioorg. Med. Chem.* **2010**, 18, 2439-2446.
9. Mehellou Y, McGuigan C, Brancale A, Balzarini J. Design, synthesis, and anti-HIV activity of 2',3'-didehydro-2',3'-dideoxyuridine (d4U), 2',3'-dideoxyuridine (ddU) phosphoramidate 'ProTide' derivatives. *Bioorg. Med. Chem. Lett.* **2007**, 17, 3666-3669.

Chapter 3 - Synthesis of ProTide Fingolimod Analogues

3.1 Phosphoramidate Fingolimod Synthesis

Using the reaction conditions that were developed to yield the bis 3-amino-1-propanol phosphoramidate and *O*-bound phosphoramidate 2-amino-2-methyl-1-propanol, a reaction with the aim of synthesising a phosphoramidate by reacting fingolimod hydrochloride with a phosphorochloridate was attempted.

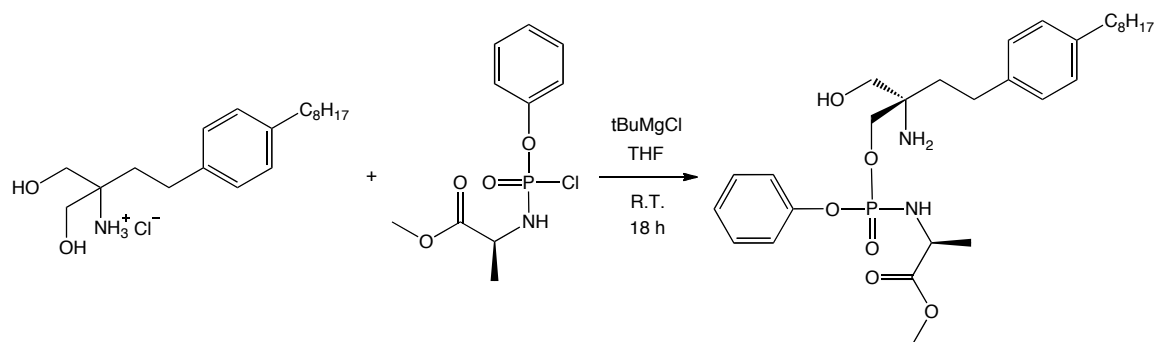
The phosphorochloridate that was initially synthesised in preparation for the reaction was phenyl-(methoxy-L-alaninyl) phosphorochloridate as shown in scheme 3.1.



Scheme 3.1 Synthesis of phenyl-(methoxy-L-alaninyl) phosphorochloridate

As suggested by the alcohol-selective phosphoramidate 2-amino-2-methyl-1-propanol synthesis it was hoped that an attempted phosphoramidate synthesis using fingolimod would only yield *O*-bound phosphoramidate fingolimod due to the steric hindrance caused by the 3 respective groups around the primary amine group. However, the two alcohol groups on fingolimod are chemically equivalent and it was therefore deduced that a phosphoramidate synthesis using the reaction conditions developed in the previous chapter would likely yield a mixture of fingolimod *O*-phosphoramidates. A highly predictable product is the unwanted bis phosphoramidate as shown in figure 2.3 in the previous chapter. What was not easily predictable when conducting the first attempted fingolimod phosphoramidate synthesis was whether the product would be purely the

unwanted bis product or a mixture of different products. Inevitably if this synthesis were to go as well as realistically possible, such as 100% yield of mono phosphoramidate fingolimod with the 4 likely diastereoisomers yielded in equal proportions of 25% of the overall yield, some form of separation would be necessary in order to isolate the desired *S*-isomer.



Scheme 3.2 Ideal (although highly improbable) result of the reaction yielding the *S*-isomer of fingolimod phosphoramidate

The reaction was conducted as described at the end of the Discussion section of Chapter 2. The reaction was left overnight and the process of analysing the reaction mixture and separating the products began the next day. TLC showed that there were more products or by-products from this reaction than were observed when conducting phosphoramidate syntheses with 3-amino-1-propanol or 2-amino-2-methyl-1-propanol.

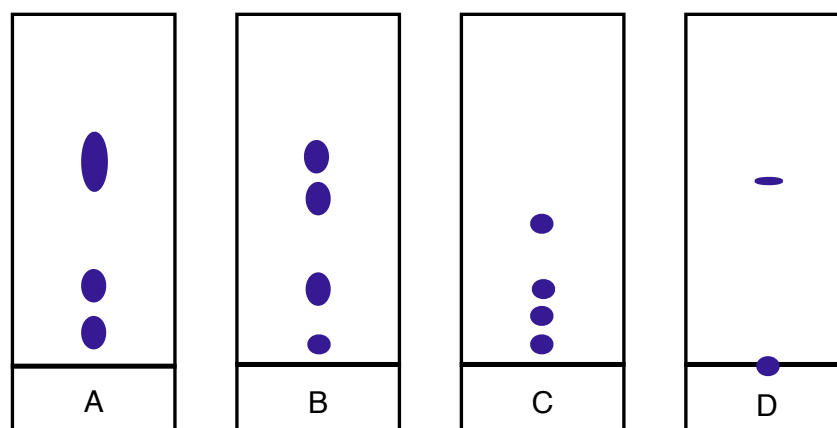


Figure 3.1 TLCs of the crude reaction mixture using eluent systems: **A** 10% MeOH + 90% AcOEt, **B** 10% MeOH + 90% DCM, **C** 5% MeOH + 95% DCM and **D** 100% DCM

The spots on the TLC were visible using UV light and were also visible when stained with KMnO_4 . It was decided that running column chromatography on the reaction mixture in an eluent system using dichloromethane and progressively increasing percentages of methanol would be a sensible method of trying to separate the different compounds observed using TLC.

After running the column a small sample of each of the fractions collected was spotted onto TLC paper and then held under UV light to see in which fractions the compounds of interest had eluted. UV activity was observed in:

- Fractions 16 – 20
- Fractions 26 – 29
- Fractions 32 – 40

It is believed that the UV activity observed in these fractions corresponds to the three areas of UV activity seen when conducting TLC on the crude reaction mixture in 10% MeOH and 90% AcOEt as shown in figures 3.1 and 3.2. The three groups of fractions were collected separately and the solvents were removed *in vacuo*.

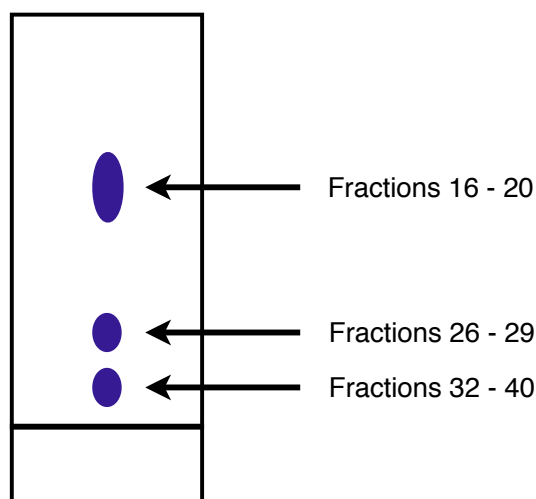


Figure 3.2 The spots observed *via* TLC (MeOH 10 % / AcOEt 90%) and the fractions to which they correspond

3.1.1 Fractions 16 - 20

The product of fractions 16 - 20 was observed to be a clear oil with a mass of 290 mg after commencing the experiment with 500 mg fingolimod HCl and 403 mg phosphorichloridate. ^{31}P NMR (as shown in figure 3.3) and ^1H NMR were conducted. Analysis of these spectra and later mass spectroscopic analysis showed that the mixture of compounds yielded in fractions 16 - 20 are 4 different isomers (figures 3.3 and 3.4) of the expected bis fingolimod phosphoramidate. Eight major peaks are seen in the ^{31}P NMR spectrum (as shown in figure 3.3) as there are 4 different isomers and 2 phosphorus atoms thus making the number of peaks $4 \times 2 = 8$ peaks. The predicted mass of the bis product is 789.4 g/mol and the main peak observed using mass spectrometry has a mass of 790.4 m/z. The integrations of the peaks in the aromatic region of the ^1H NMR spectrum are also highly indicative of the expected bis product.

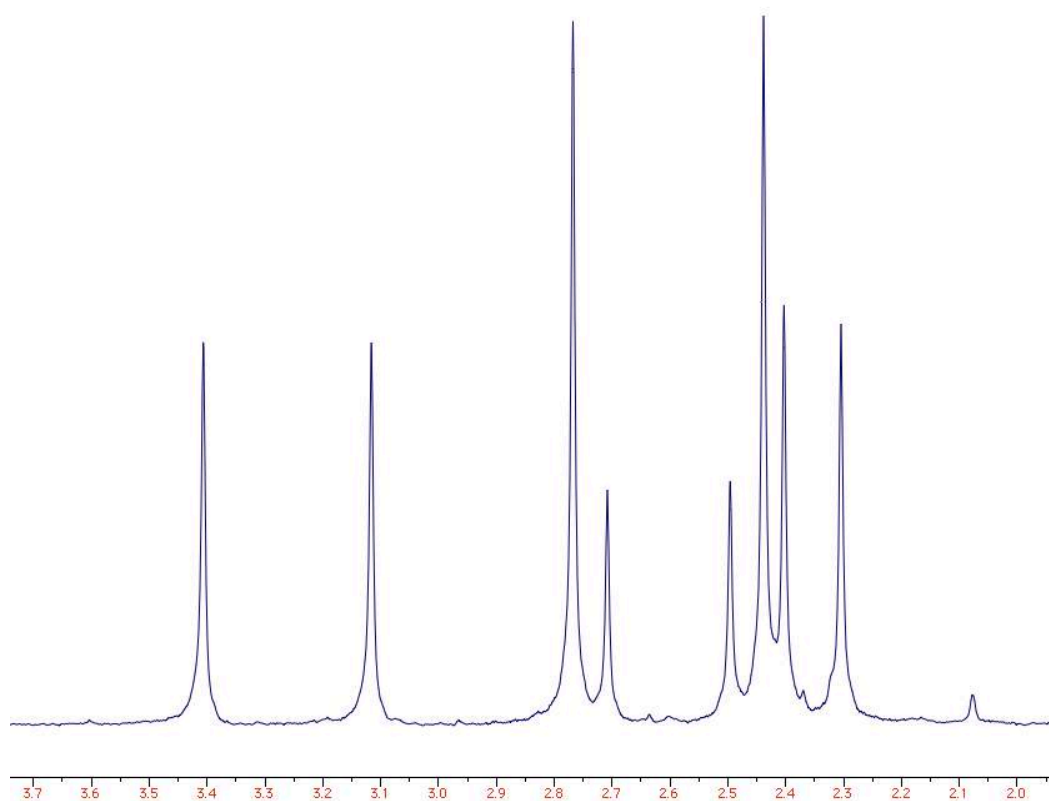


Figure 3.3 ^{31}P NMR of the product yielded in fractions 16 – 20

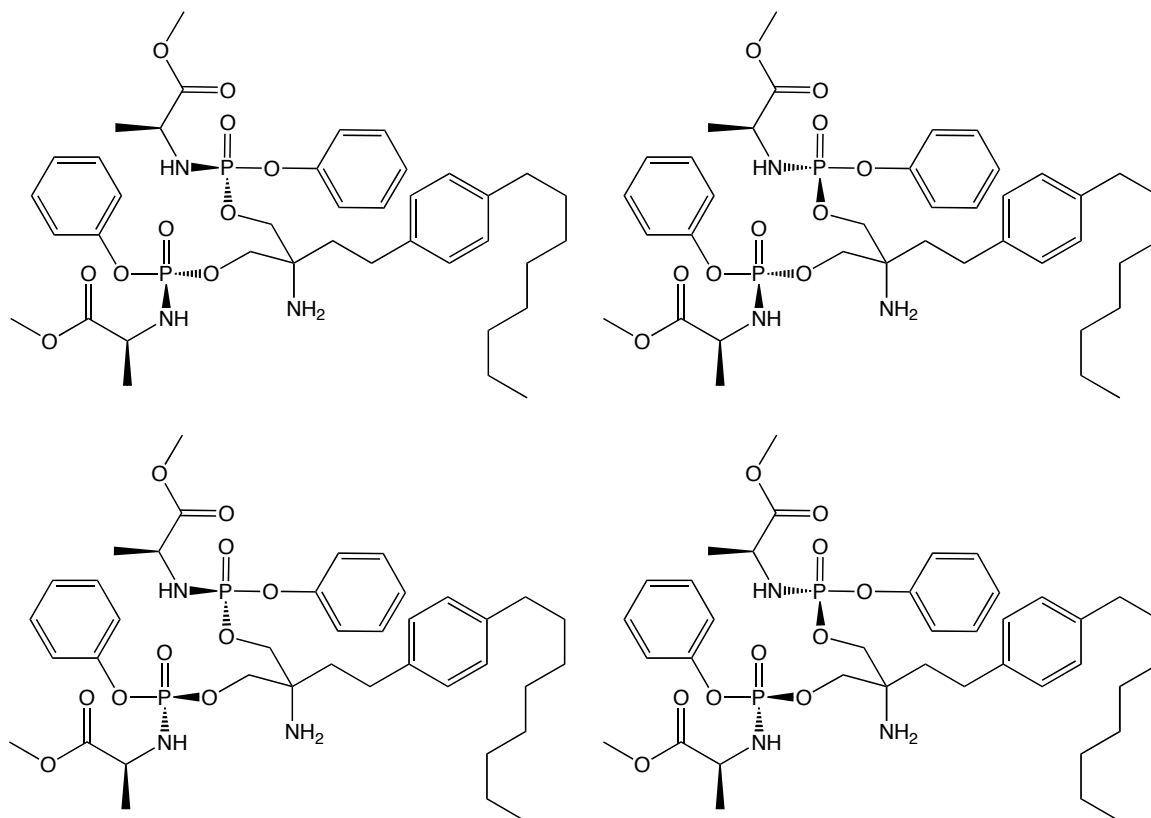


Figure 3.4 The suggested products collected in fractions 16 – 20

3.1.2 Fractions 26 - 29

The same series of analytical experiments were conducted on the product that eluted in fractions 26 – 29. As with the product of fractions 16 – 20 the product was a clear oil and had a mass of 350 mg. Analysis of the ³¹P NMR spectrum, the ¹H NMR spectrum and the data collected using mass spectrometry showed that the eluted product is in fact a mixture of four mono phosphoramidate fingolimod isomers (figure 3.6) of ratios around 35/15/15/35 (figure 3.5) and two of those isomers should be the desired *S*-ProTide fingolimod. From the 0.5 ppm phosphorus splitting and the 0.1 ppm carbon splitting of the ³¹P NMR it is also possible to suggest that around 70% (35 + 35) of the mass of the product is the *S* or *R* conformation on the carbon and 30% (15 + 15) is the other *S* or *R* on the carbon (see figure 3.6). This means that the oil product should contain either around 70% of the desired pharmacologically active compound or around 30%.

The predicted mass of freebase mono ProTide fingolimod synthesised using phenyl-(methoxy-L-alaninyl) phosphorochloridate is 548.3 g/mol and the

observed mass was 549.3 m/z. A yield of 350 mg of the desired product (ignoring isomer issues) is a satisfying yield of 44%. It was concluded that, barring the issues of having to still separate the different diastereoisomers, the synthesis and purification route devised is perfectly acceptable for small scale laboratory synthesis of ProTide fingolimod analogues.

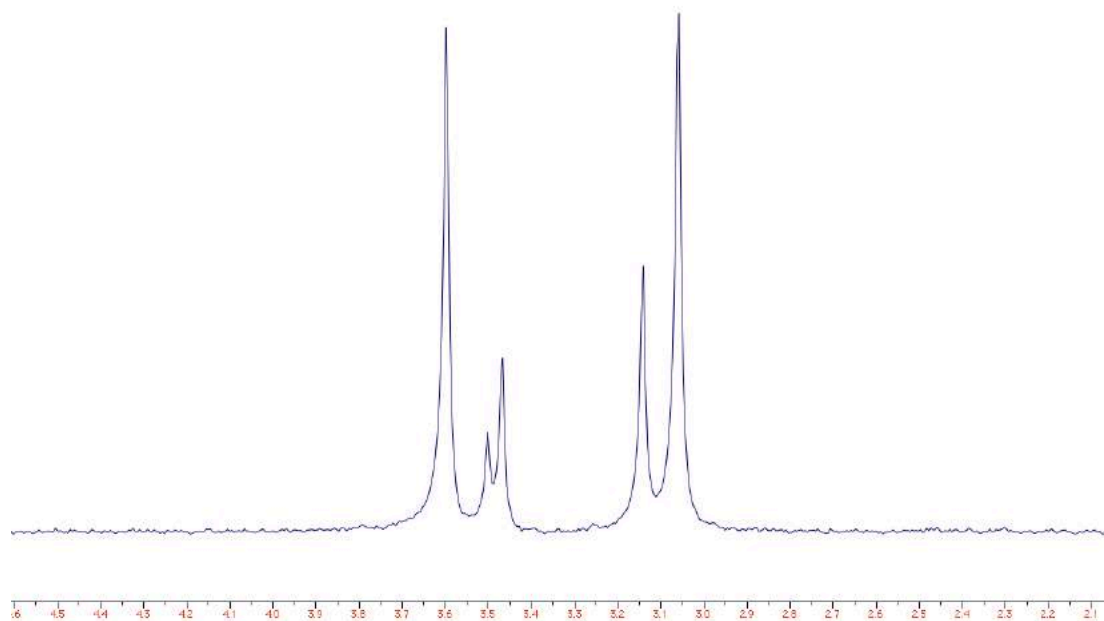


Figure 3.5 ^{31}P NMR of the product yielded in fractions 26 – 29

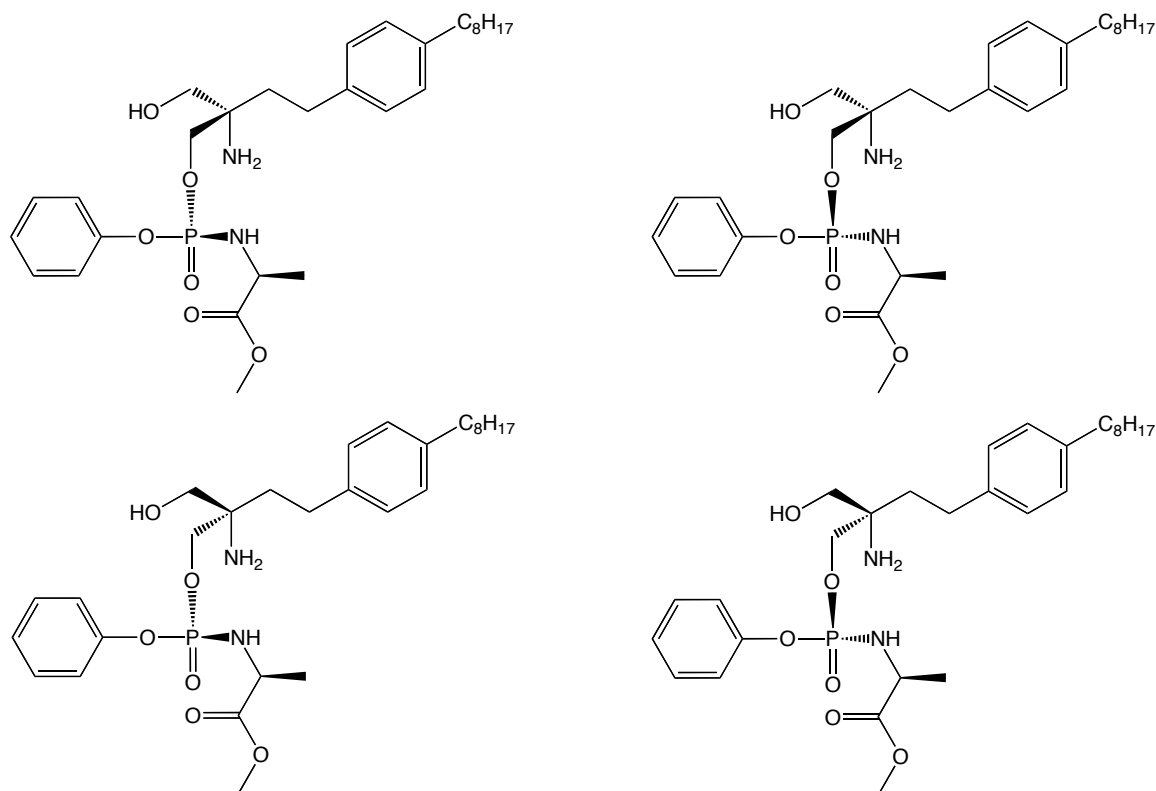


Figure 3.6 The four different diastereoisomers of mono ProTide fingolimod formed by the reaction with the desired *S*-Ph-LAla-OMe-F analogues above and the undesired *R*-Ph-LAla-OMe-F analogues below

3.1.3 Fractions 32 - 40

The product collected from fractions 32 – 40 was a mixture of a white solid powder with some oil. After analysing the initial data obtained from the NMR investigations and the mass spectrometry experiments, the third collected product obtained from fractions 32 – 40 was discarded.

The NMR data imply that the contents of these collected fractions are a mixture of unreacted fingolimod and unwanted by-products such as the structure shown in figure 3.7. The chemical shift of the broad peak in the ^{31}P NMR spectrum at -2.5 ppm (figure 3.8) is indicative of a phosphorochloridate that has reacted with water to hydrolyse the water and form an *O*-bound phosphorochloridate in which the chlorine atom has been exchanged for an OH group (as shown in figure 3.7). The broad nature of the peak visible around -2.5 ppm in the ^{31}P NMR spectrum (figure 3.8) may be due to a variety of different charged species such as Na^+ ionising the phosphate group.

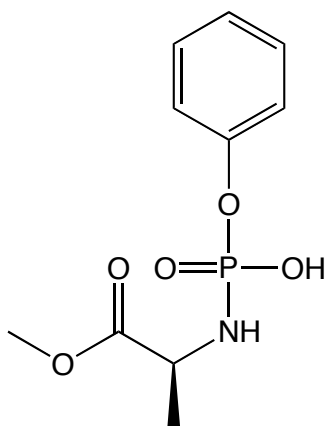


Figure 3.7 An unwanted by-product of the reaction that is possibly responsible for the peak observed in the PNMR spectrum of the product obtained in fractions 32 – 40

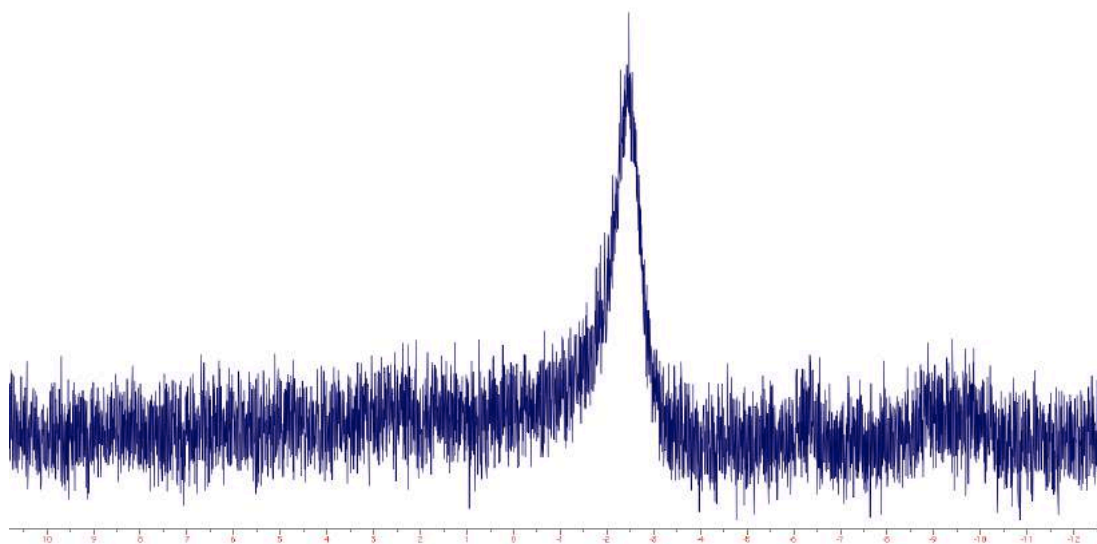


Figure 3.8 ^{31}P NMR of the product yielded in fractions 32 – 40

3.1.4 NMR Analyses of Phenyl-(Methoxy-L-Alaninyl) Phosphoramidate Fingolimod

The mixture of bis isomers obtained from fractions 16 – 20 and the mixture of mono isomers obtained from fractions 26 – 29 were placed under high vacuum to try to remove remaining solvents such as dichloromethane and methanol. Solvent peaks are easily visible in the original ^1H NMR spectra and removal of remaining solvent from the product leads to improved ^1H NMR results. After placing the mono ProTide fingolimod (named unofficially as Ph-LAla-OMe-F) mixture under high vacuum ^{31}P NMR, ^1H NMR, ^{13}C NMR, COSY and HSQC nuclear magnetic resonance experiments were conducted.

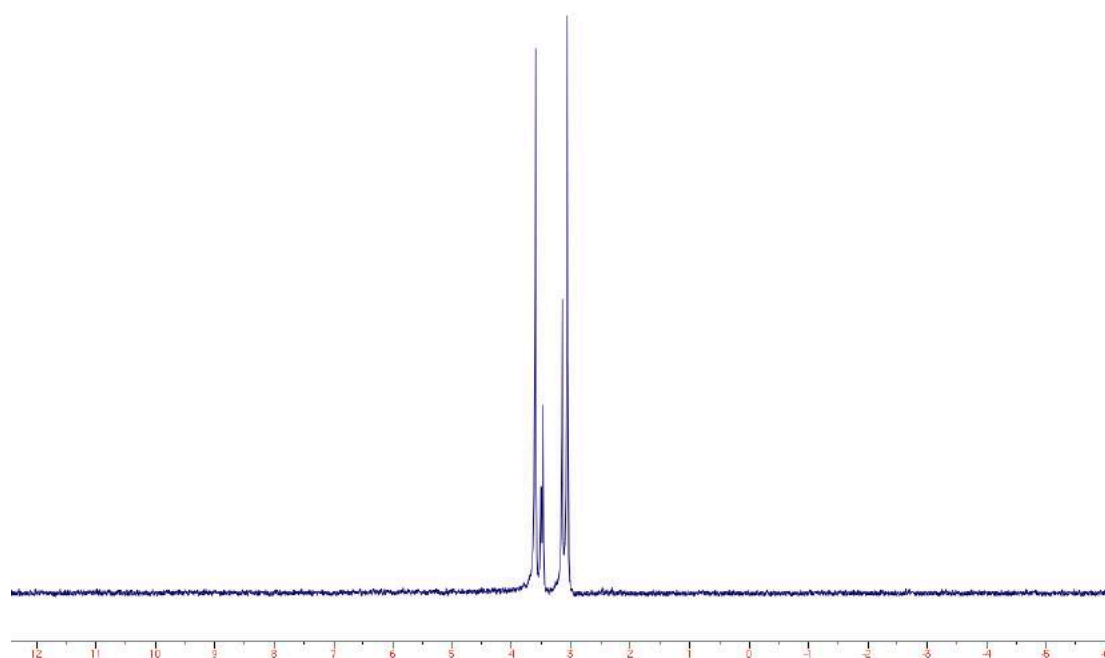


Figure 3.9 ^{31}P NMR spectrum of Ph-LAla-OMe-F showing no unwanted impurities or N-bound phosphoramidate moiety as would be seen at around 11 ppm

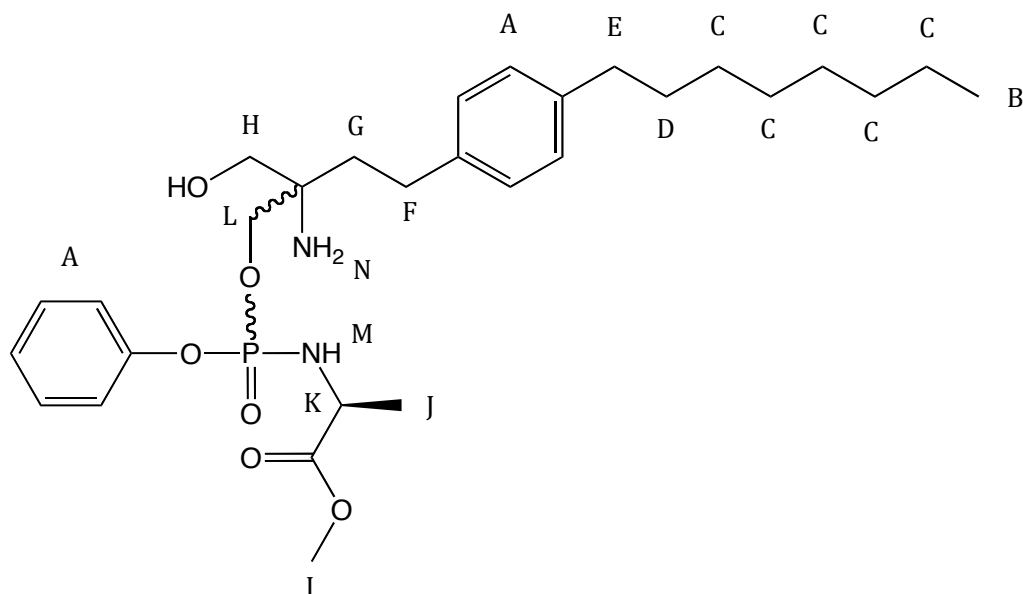


Figure 3.10 Ph-LAla-OMe-F (1), letters A – N correspond to the peaks labelled in the ^1H NMR spectrum in figure 3.11

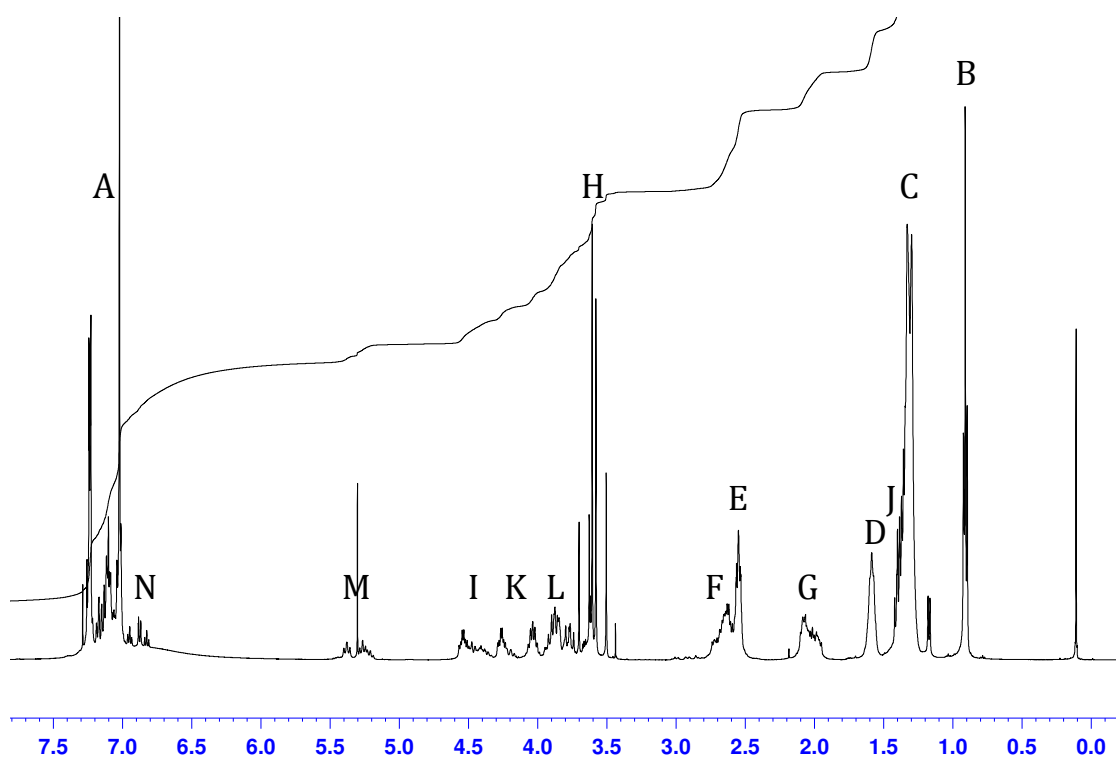


Figure 3.11 ^1H NMR of the mono ProTide fingolimod (Ph-LAla-OMe-F) mixture after high vacuum. The letters A – N correspond to the regions of the structure labelled in figure 3.10

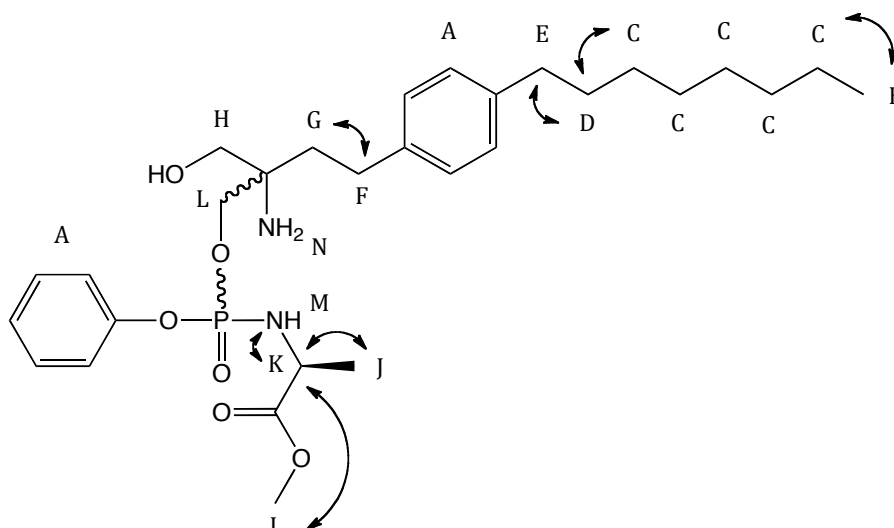


Figure 3.12 The doubled-headed arrows signify regions on the chemical structure and ^1H NMR spectrum which correspond as shown in the COSY experiment (figure 3.13) and are therefore close to each other in 3D space.

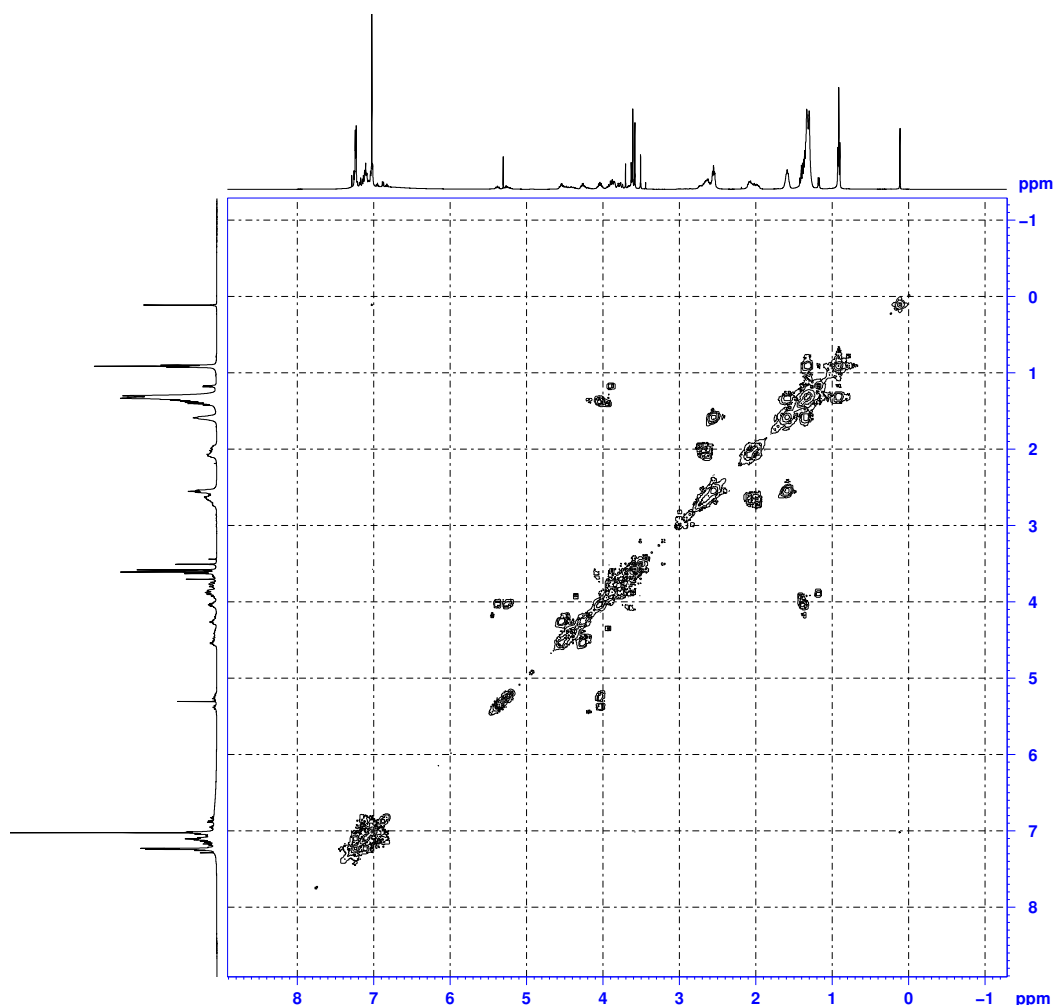


Figure 3.13 COSY experiment of Ph-LAla-OMe-F (1) The aromatic regions labelled A show spins which are coupled to each other. The regions labelled B & C, C & D, E & D, F & G, I & K, J & K and K & M can also be seen to be close to each other in 3D space due to the correlations with each other as seen in the spectrum above.

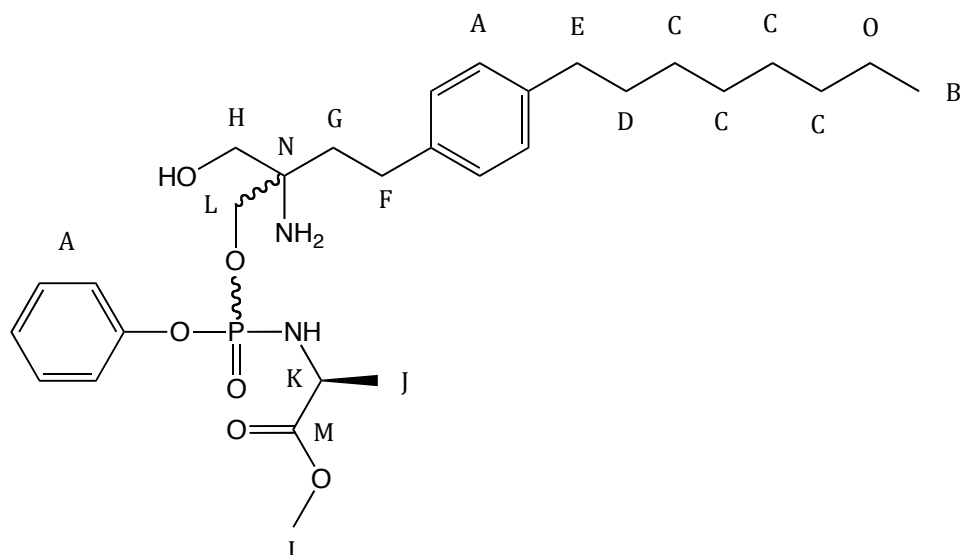


Figure 3.14 Ph-LAla-OMe-F (1), letters A – O correspond to the peaks labelled in the ¹³C NMR spectrum (figure 3.15)

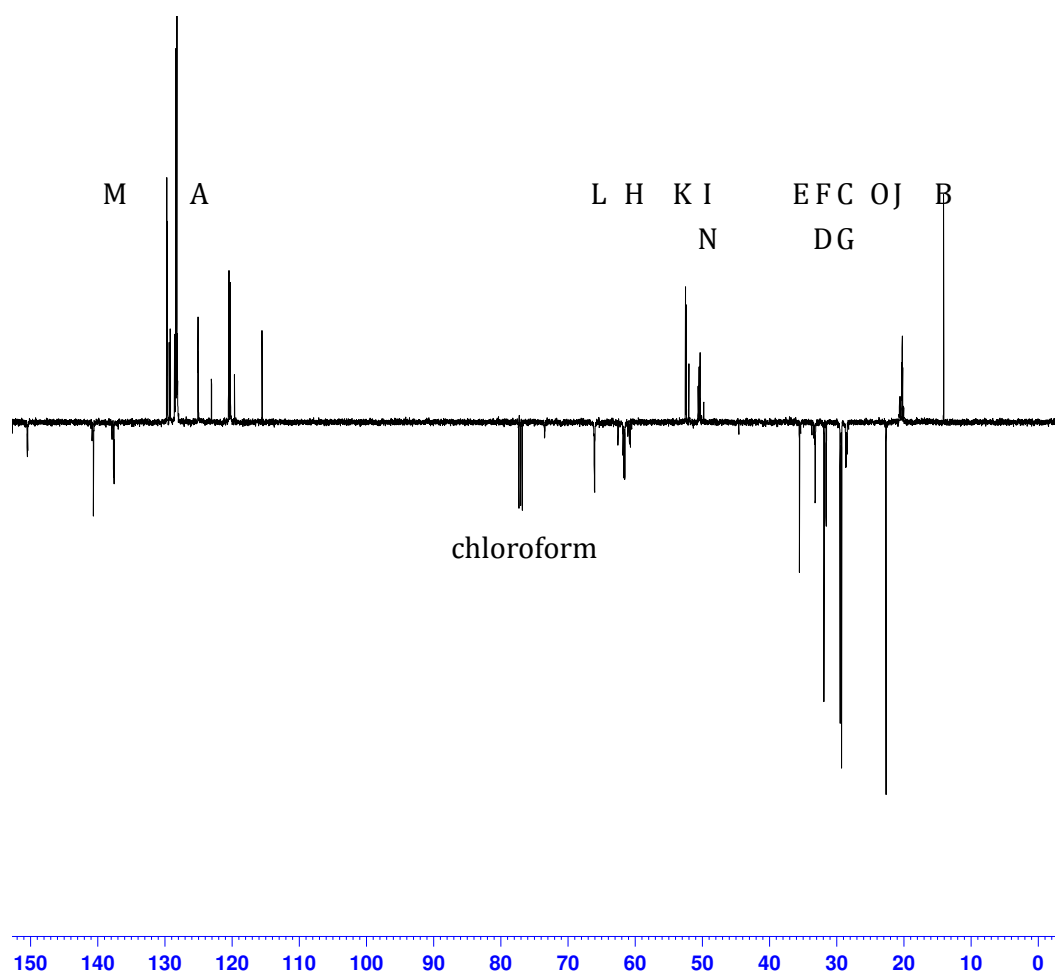


Figure 3.15 ¹³C NMR (pendant) of the mono ProTide fingolimod 1 mixture after high vacuum treatment. Letters A – O correspond to the regions of the structure labelled in figure 3.14

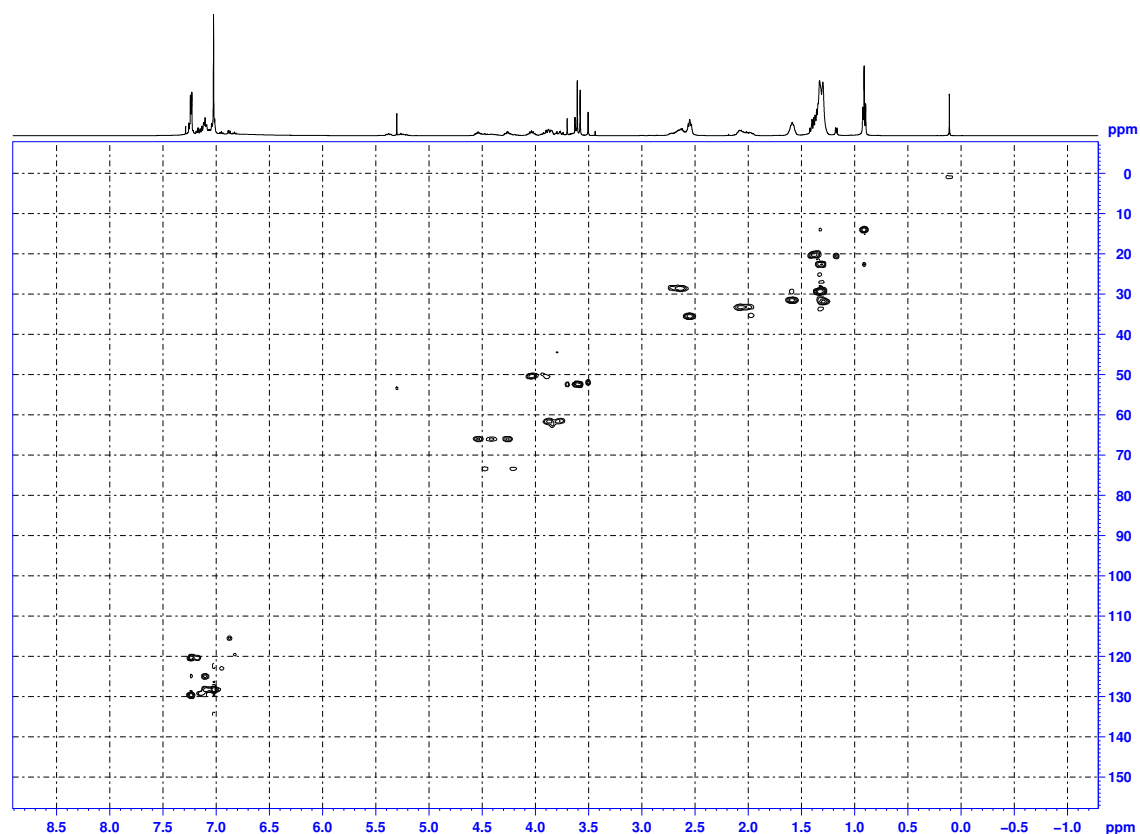


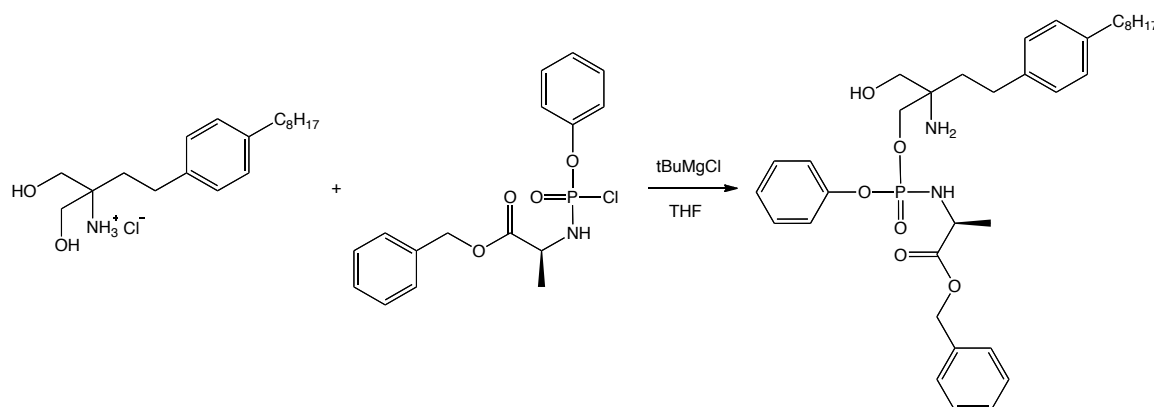
Figure 3.16 HSQC experiment of Ph-LAla-OMe-F (1) that shows how the peaks in the ^1H NMR and ^{13}C NMR spectra correlate with each other

A comparison of the ^1H NMR and ^{13}C NMR spectra with the HSQC experiment above (figure 3.16) confirms that the protons and carbons of the molecule have been correctly correlated with each other.

3.2 Further Syntheses

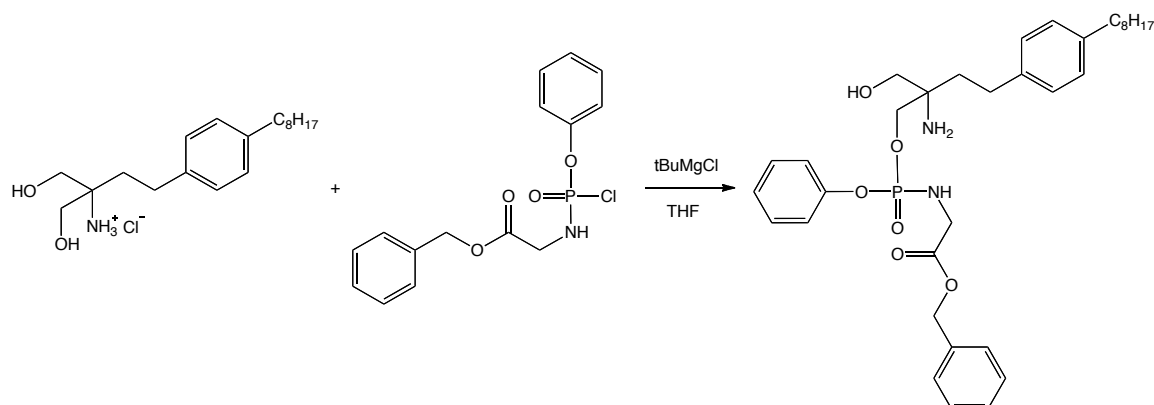
After the confirmed successful synthesis of phenyl-(methoxy-L-alaninyl) phosphoramidate fingolimod (1) an additional ten analogues were synthesised. The syntheses generally followed the same pattern of products and by-products as described in similar ratios and therefore the obtained data for these experiments will not be discussed in detail.

Phenyl-(benzyloxy-L-alaninyl) phosphoramidate fingolimod (2)

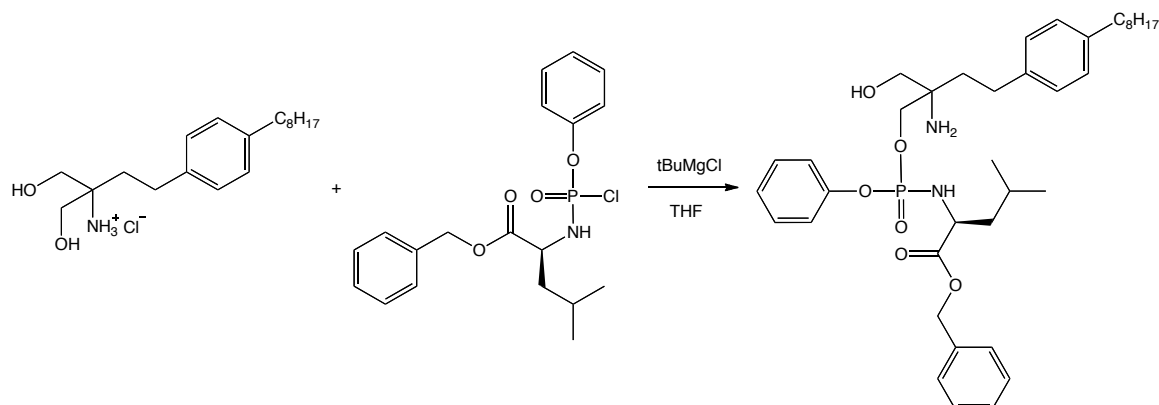


Scheme 3.3 Ph-LAla-OBzl-F was successfully synthesised as a mixture of 4 diastereoisomers with a yield of 22%

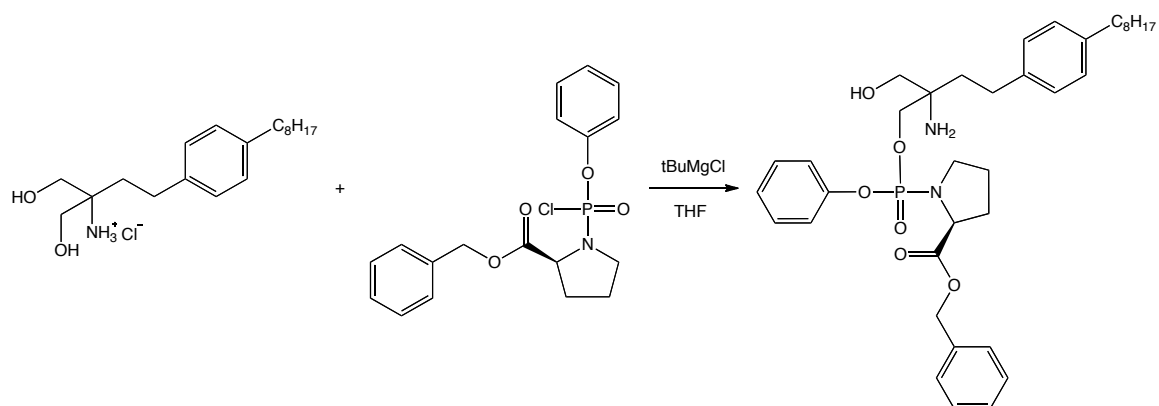
Phenyl-(benzyloxy-glycinyl) phosphoramidate fingolimod (3)



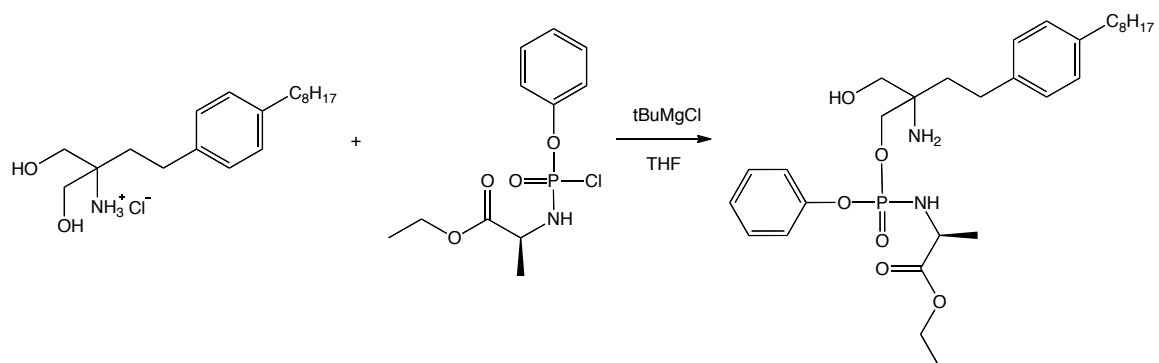
Scheme 3.4 Ph-Gly-OBzl-F was successfully synthesised as a mixture of 4 diastereoisomers with a yield of 17%

Phenyl-(benzyloxy-L-leucinyl) phosphoramidate fingolimod (4)

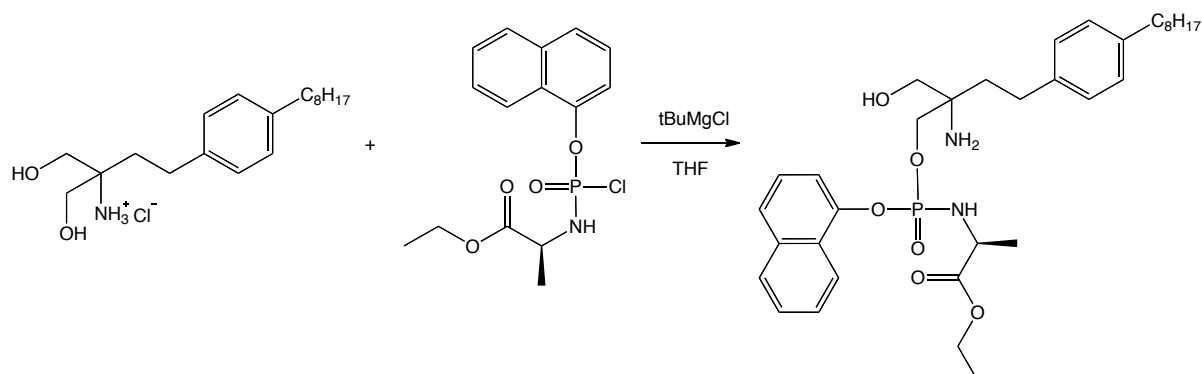
Scheme 3.5 Ph-Leu-OBzl-F was successfully synthesised as a mixture of 4 diastereoisomers with a yield of 23%

Phenyl-(benzyloxy-L-prolinyl) phosphoramidate fingolimod (5)

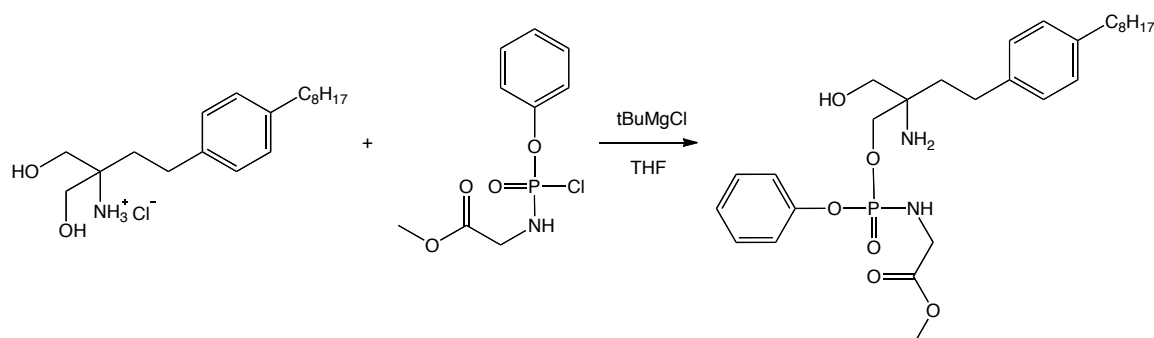
Scheme 3.6 Ph-Pro-OBzl-F was successfully synthesised as a mixture of diastereoisomers with a yield of 20%

Phenyl-(ethoxy-L-alaninyl) phosphoramidate fingolimod (6)

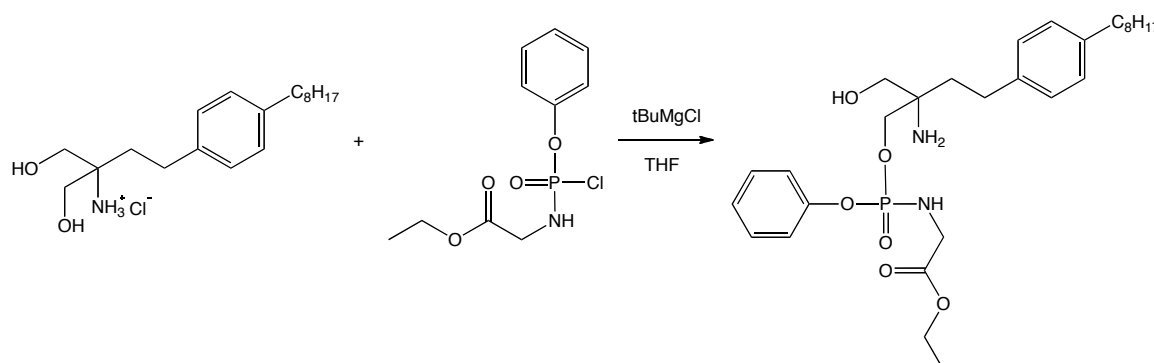
Scheme 3.7 Ph-LAla-OEt-F was successfully synthesised as a mixture of 4 diastereoisomers with a yield of 20%

Naphthyl-(ethoxy-L-alaninyl) phosphoramidate fingolimod (7)

Scheme 3.8 Naphth-LAla-OEt-F was successfully synthesised as a mixture of 4 diastereoisomers with a yield of 23%

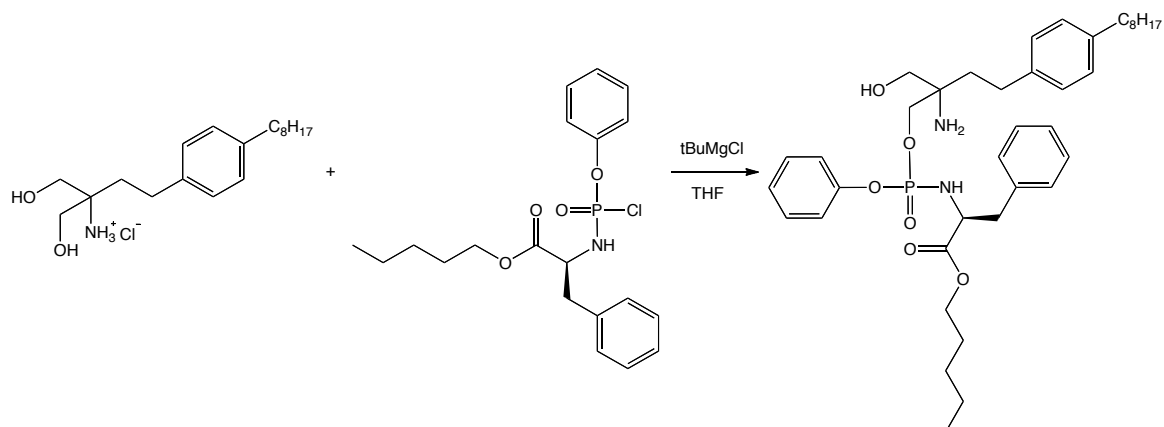
Phenyl-(methoxy-glycinyl) phosphoramidate fingolimod (8)

Scheme 3.9 Ph-Gly-OMe-F was successfully synthesised as a mixture of 4 diastereoisomers with a yield of 33%

Phenyl-(ethoxy-glycinyl) phosphoramidate fingolimod (9)

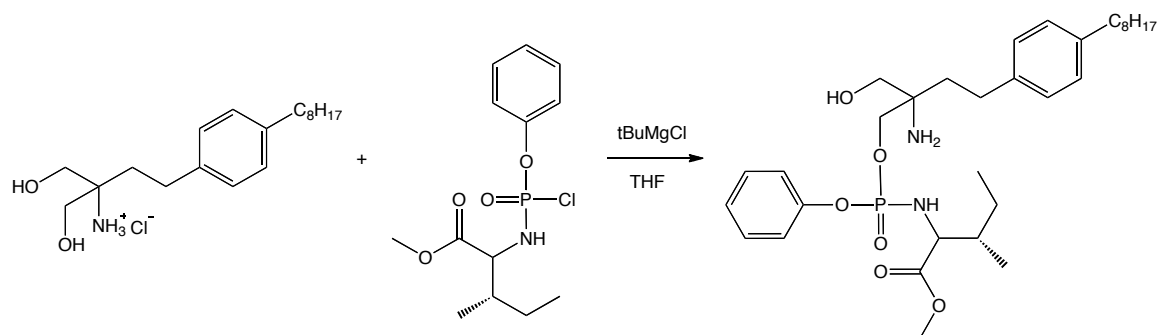
Scheme 3.10 Ph-Gly-OEt-F was successfully synthesised as a mixture of 4 diastereoisomers with a yield of 39%

Phenyl-(pentoxo-L-phenylalanyl) phosphoramidate fingolimod (10)



Scheme 3.11 Ph-Phe-O_{Pe}-F was successfully synthesised as a mixture of 4 diastereoisomers with a yield of 10%

Phenyl-(methoxy-L-isoleucinyl) phosphoramidate fingolimod (11)



Scheme 3.12 Ph-Ile-OMe-F was successfully synthesised as a mixture of 4 diastereoisomers with a yield of 38%

Compound	Ar	AA	R	% Yield	³¹ P NMR δ (ppm)
1	Ph	L-Ala	Me	44	3.60, 3.47, 3.14, 3.06
2	Ph	L-Ala	Bzl	22	3.58, 3.22, 3.11
3	Ph	Gly	Bzl	17	4.27, 3.99
4	Ph	Leu	Bzl	23	4.66, 4.46, 4.20, 3.95
5	Ph	Pro	Bzl	20	2.99, 2.94
6	Ph	L-Ala	Et	20	4.05, 3.84, 3.73, 3.59
7	Naphth	L-Ala	Et	23	4.90, 4.70, 4.42, 3.55
8	Ph	Gly	Me	33	3.62, 3.00
9	Ph	Gly	Et	39	4.48
10	Ph	Phe	Pe	10	4.11, 3.95, 3.11
11	Ph	Ile	Me	38	4.30, 4.25, 3.65, 3.60

Table 3.1 ProTide Fingolimod analogues synthesised

Chapter 4 - Chiral Synthesis

4.1 Discussion

4.1.1 Review of the Chiral Synthetic Challenge and Available Literature

The synthetic procedure developed and detailed in chapters 2 and 3 overcomes all but one of the primary synthetic challenges involved in the production of ProTide fingolimod analogues. The final problem is the issue of chirality. As previously explained, it is *S*-monophosphate fingolimod which is the active compound. The syntheses detailed in the previous chapters yield a mixture of *S* and *R* ProTide fingolimod as shown in figures 4.1 and 4.2 below.

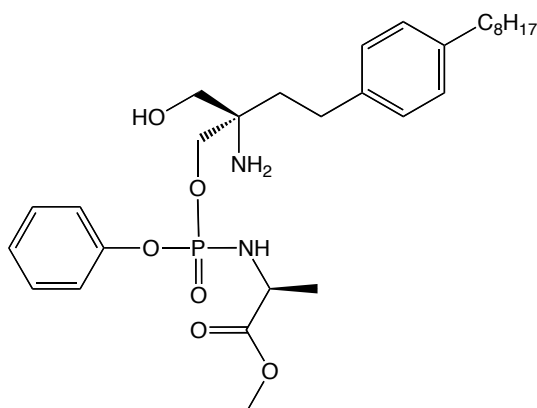


Figure 4.1 Undesired *R*-isomer of ProTide Fingolimod

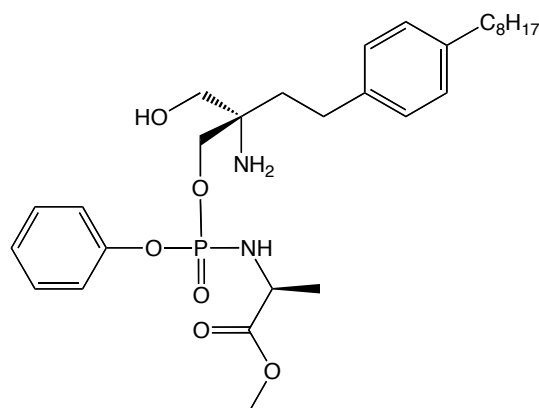


Figure 4.2 *S*-isomer of ProTide Fingolimod

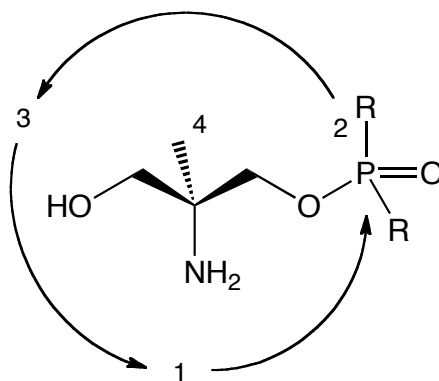
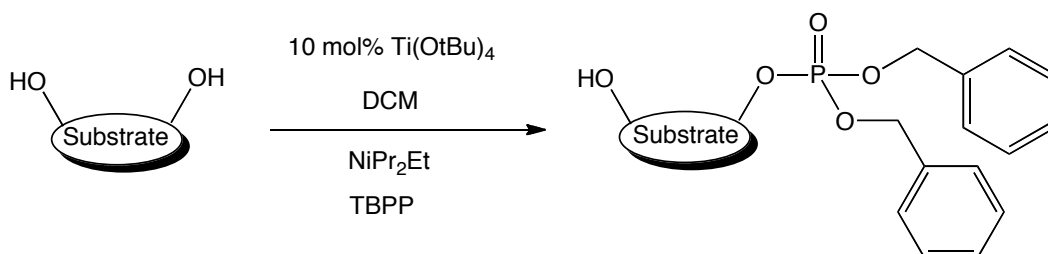


Figure 4.3 *S* configuration of the chiral carbon centre¹

After several attempts to separate the different diastereoisomers using HPLC were attempted (data not shown), but showed no potential for being a viable method of isolating the desired *S*-isomers, a paper was chosen which details the chiral synthesis of *S*-monophosphate fingolimod as a basis for developing the chiral synthesis of ProTide fingolimod.² The general method detailed in Kiuchi's paper² showed potential as being relatively simple, cheap and high yielding when compared with the other papers reviewed.

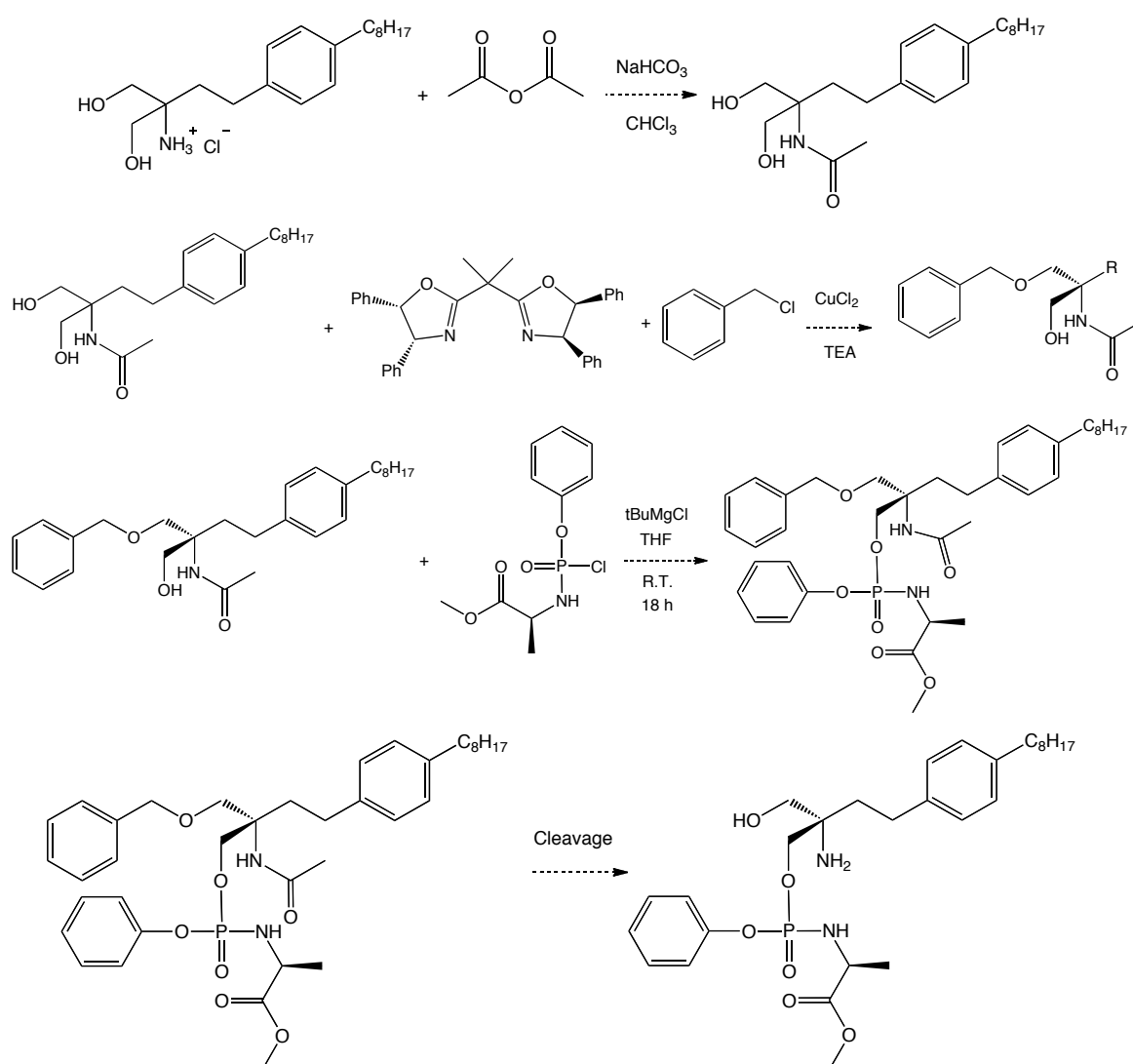
Kyle Coppola's 2014 paper³ details a method devised to synthesise phosphorylated diols using titanium alkoxide catalysts as shown in scheme 4.1. In their paper they state that the aim of their work is to design a method that can be used for the phosphorylation of fingolimod but when looking at their results it seems unlikely that their method could be used to achieve enantioselectivity. Another detracting factor was that they had not tested their method on fingolimod itself. Certainly when compared with the other literature available the application of their work to the chiral synthetic problem was inevitably going to be far more experimental and potentially difficult than the other applicable routes. If one were to use their method then the use of chiral HPLC to separate the *S* and *R* enantiomers would probably be essential. It is also highly unlikely that one could replace the tetrabenzyl pyrophosphate used in their reaction for a phosphorochloridate or any other phosphorus compound that could be converted into a ProTide post-phosphorylation. For numerous reasons this route was considered a poor choice for chiral ProTide fingolimod synthesis.



Scheme 4.1 The chemistry detailed was considered a poor starting point for chiral ProTide fingolimod synthesis³

Another paper⁴, which showed more potential as a starting point, involves the use of copper complexes to form *N* and *O*-protected fingolimod using benzyl and acetyl

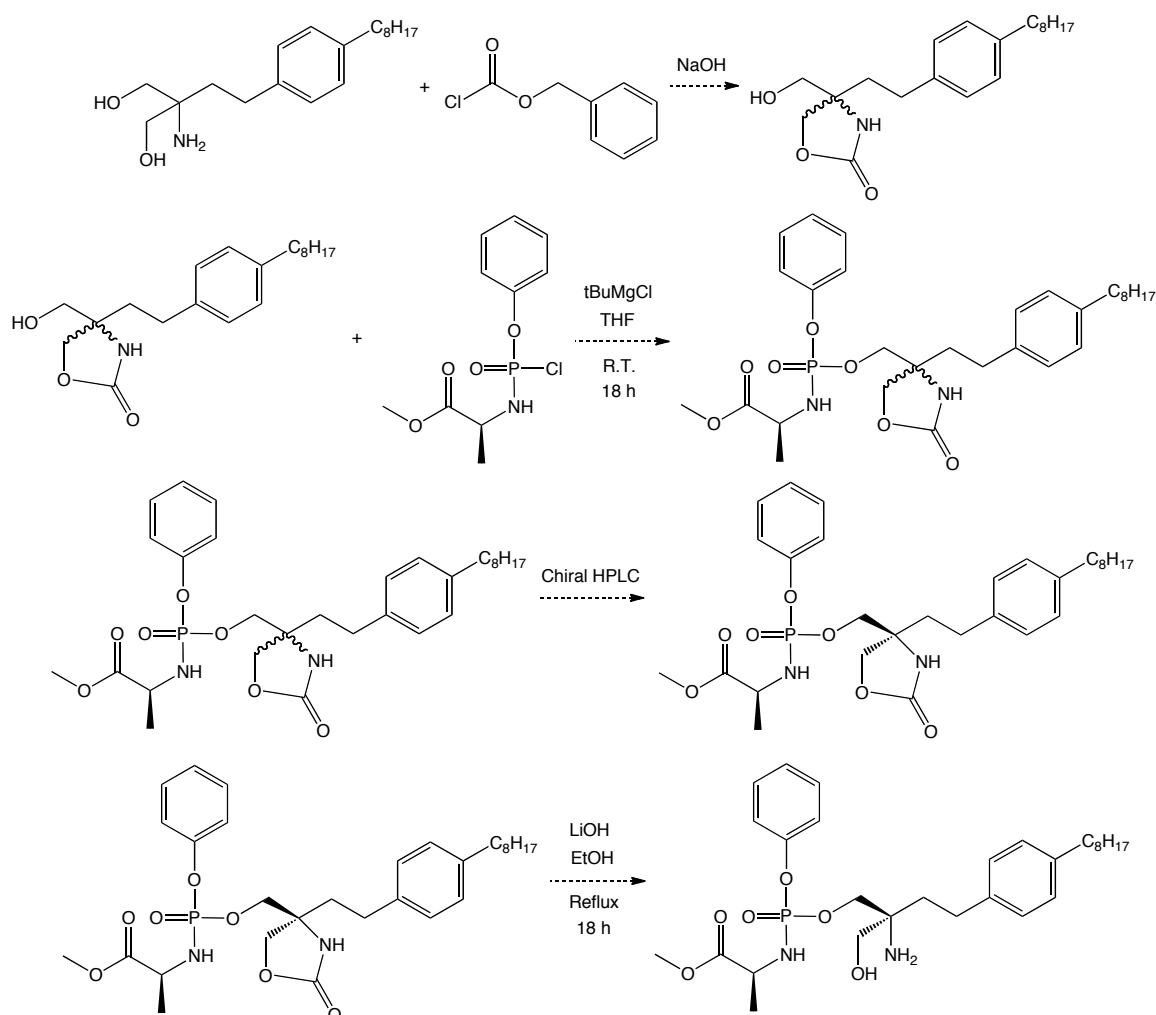
groups. In theory, as shown in scheme 4.2, after protecting the amine and then selectively protecting one OH the free OH could then bind to a phosphorochloridate and then the benzyl and acetyl protecting groups could be removed. However, the best enantioselectivity of any reaction in their paper is 64% which is poor in comparison with the 99% enantioselectivity reported in the paper chosen.² Another detracting factor is that benzyl and acetyl protecting groups would presumably be much harder to remove from ProTide fingolimod, than the benzyloxycarbonyl groups reported in the lead paper, without inadvertently also decomposing the ester moiety of the ProTide.



Scheme 4.2 Possible chiral synthesis route⁴

Two other papers reviewed^{5,6} showed more potential as a basis for the chiral synthesis but both require the use of chiral HPLC. Chiral HPLC requires a chiral

column, which was not immediately available, and is generally only applicable to smaller laboratory scales. For the purposes of the research described preparative chiral HPLC can be done on an acceptable scale but if ever the chiral synthesis were to be scaled up for industrial applications then an alternative route would need to be devised. A further likely problem of relying on chiral HPLC is that all ProTide fingolimod analogues contain at least 2 chiral centres (a carbon chiral centre and a phosphorus chiral centre). The potential synthetic strategy shown in scheme 4.3 requires the separation of compounds containing 3 chiral centres as opposed to one. This would almost certainly lead to an even greater challenge in obtaining the desired compounds *via* the use of a chiral column. It was decided that a route that does not require the use of chiral HPLC would be preferable.



Scheme 4.3 Possible chiral synthesis route⁶

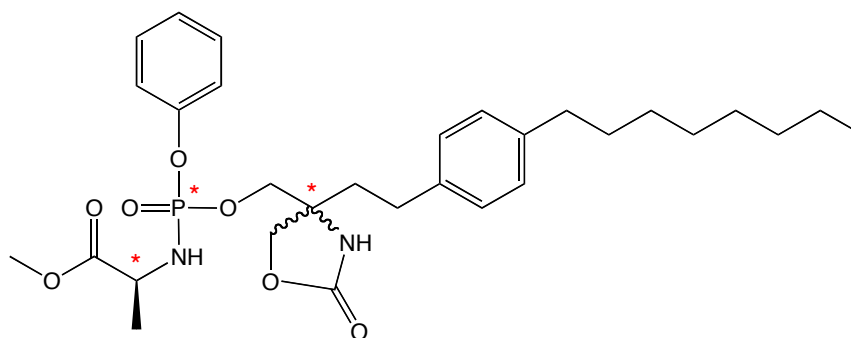
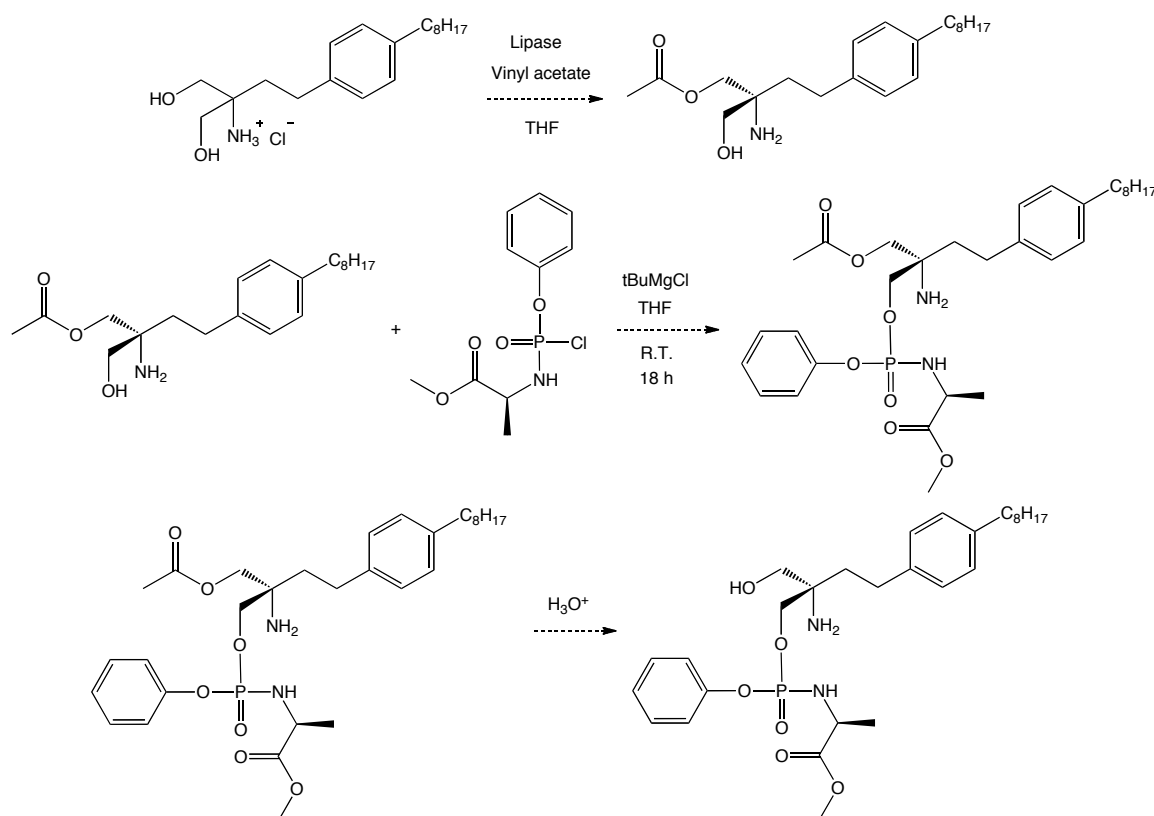


Figure 4.4 The three chiral centres which would likely make any attempted chiral HPLC separation extremely challenging if not impossible

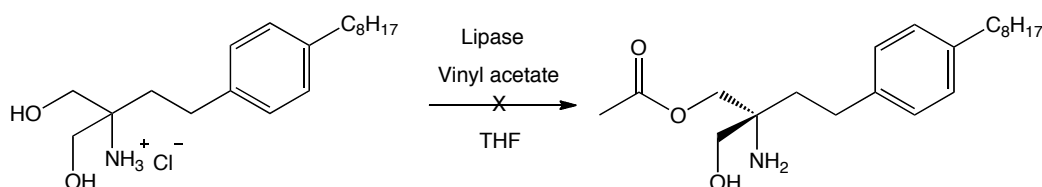
The paper which appeared to show the most promise² reports the use of lipase enzymes to selectively protect one OH group with a reported enantiomeric purity of 99%. No chiral HPLC separation is necessary and the chemistry involved, for the most part, is already established as being reliable, effective and cheap. The paper describes the enantioselective synthesis of fingolimod phosphate and it was considered that the chemistry described could be applied to the chiral synthesis of phosphoramidate fingolimod. An initial best-case scenario synthesis was devised as shown in scheme 4.4.



Scheme 4.4 Initially devised potential chiral synthesis route which was chosen for experimental investigation²

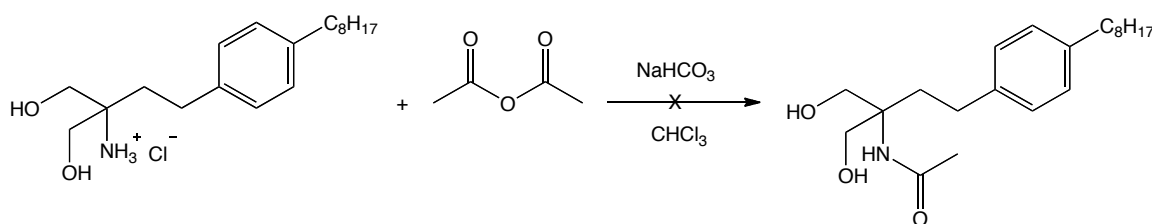
4.1.2 Development of the Chiral Synthetic Procedure

The first attempted experiment, as shown in scheme 4.5, was ineffective. The experimental procedure as described in the relevant paper¹ was followed carefully. The lipase used, *Lipase from Porcine Pancreas Type II*, was cheap and easily obtained from Sigma Aldrich. However, the paper clearly states that a number of different enzymes were trialled and that, “...some other lipases (*Lipase AS, PS, AK, M10, F-AP15, AYS, and G50*) and *PPL (porcine pancreas lipase)* were ineffective like *Lipase SL*, our successive screening of lipase revealed that immobilized lipase (*Toyobo Co.*) and *Novozyme 435* had excellent catalytic activities.”² It therefore came as little surprise that the first experiment as shown in scheme 4.5 was not successful.



Scheme 4.5 First attempted enzymatic enantioselective protection of fingolimod hydrochloride

Following section 5.3 of the paper, protection of the free amine was attempted using acetic anhydride and sodium bicarbonate as shown in scheme 4.6. However, unexpectedly, after initially assuming that the yielded compound was the desired product (mass of 350.3 m/z observed) after further analysis it became apparent that the primary product was actually *O*-protected fingolimod with an assumed 0% of enantioselectivity. The broad peak at around 4.4 ppm in figure 4.5 has an integration of 2 and is typical of a free amine.



Scheme 4.6 Attempted protection of the free amine

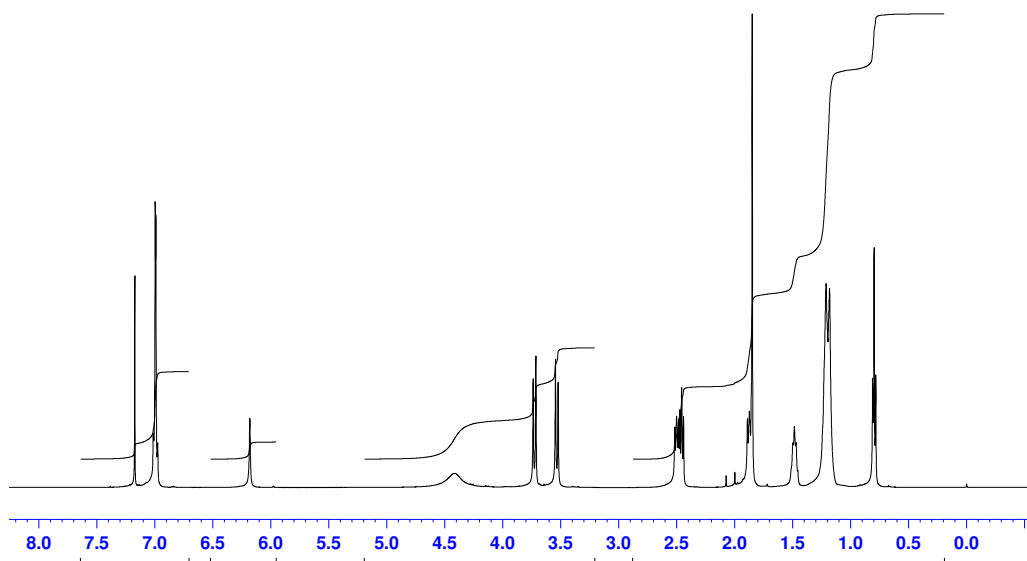


Figure 4.5 ^1H NMR spectrum of product with clear broad free amine peak at around 4.4 ppm

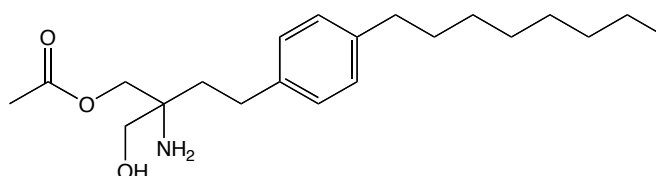
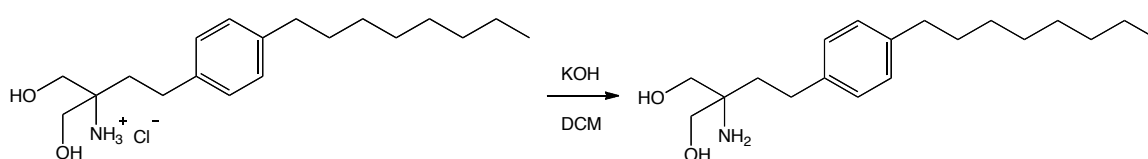


Figure 4.6 Main product of reaction described in scheme 4.6

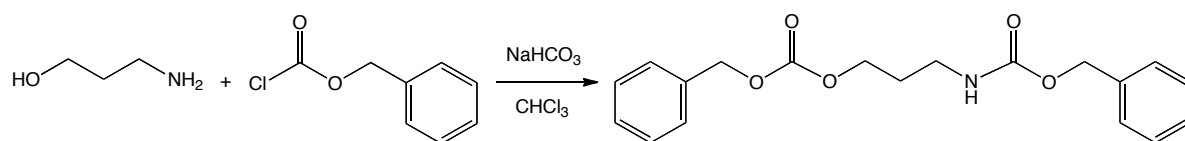
In order to improve the likelihood of effective *N*-protection a simple yet effective procedure to form the freebase was developed as described in scheme 4.7. The procedure, after a little experimentation, gives a yield of around 100%.



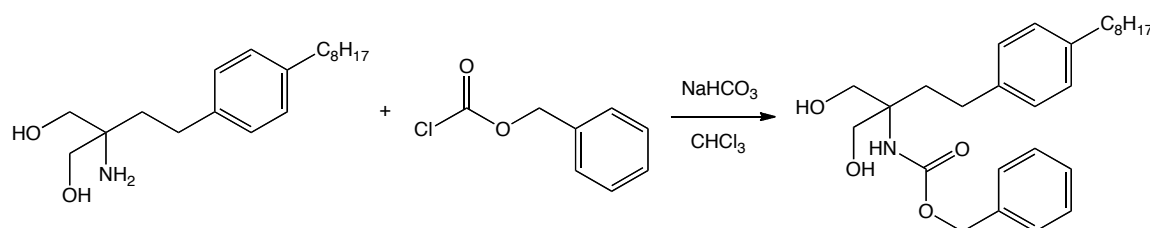
Scheme 4.7 Synthesis of freebase fingolimod from fingolimod hydrochloride (100% yield)

As described in the paper² the use of benzyl chloroformate as an *N*-protecting agent was investigated as it was considered possible that it would be more *N*-selective than acetic anhydride. A test reaction was attempted as shown in scheme 4.8 and then the conditions were applied to freebase fingolimod as shown in scheme 4.9. The products of both reactions contained a mixture of *N*-protected and *O*-protected compounds but these were separable *via* column chromatography to the desired compound as shown in scheme 4.9 with an initial yield of 78%. The

second attempt of the reaction described in scheme 4.9 gave the product with a satisfying yield of 95%.

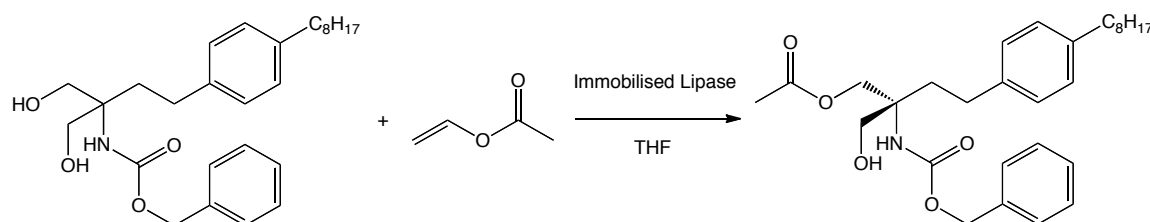


Scheme 4.8 Test of the reaction conditions was conducted using 3-amino-1-propanol



Scheme 4.9 *N*-protection of freebase fingolimod using benzyl chloroformate and sodium bicarbonate (95% yield)

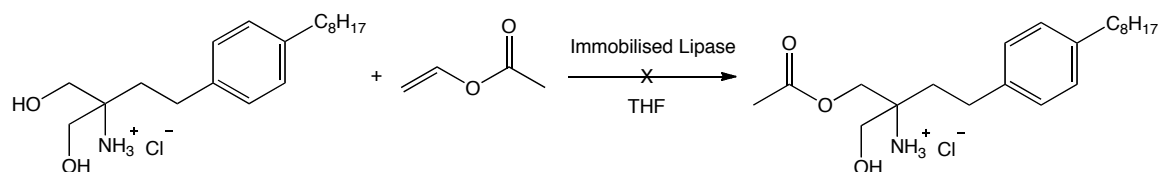
Once the lipase enzyme, derived from gram-negative pseudomonas bacteria⁷, described as being the most effective and enantioselective in the lead paper² arrived from the Japanese producers an *O*-protection experiment was conducted on *N*-protected fingolimod, as shown in scheme 4.10. The reaction gave the desired product with a yield of 78%.



Scheme 4.10 Successful enantioselective *O*-protection of *N*-protected fingolimod using Immobilized Lipase (LIP-301) (78% yield)

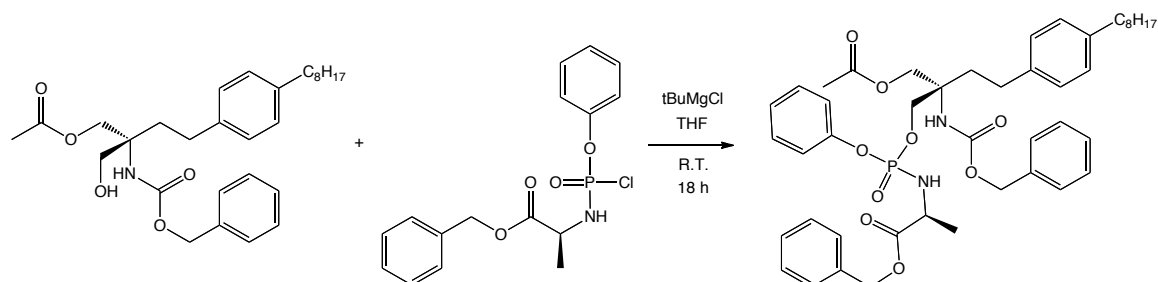
It had been questioned whether protection of the free amine was necessary for effective enantioselective protection of fingolimod hydrochloride and so the experiment described in scheme 4.10 was attempted on unmodified fingolimod HCl as shown in scheme 4.11. Surprisingly, and somewhat unfortunately, no reaction took place. The reasons for this remain purely speculative and the current

hypothesis is that the NH_3^+Cl^- or free NH_2 interact with the enzyme in a way as to prevent ease of access of the free OH to the active site of the enzyme.



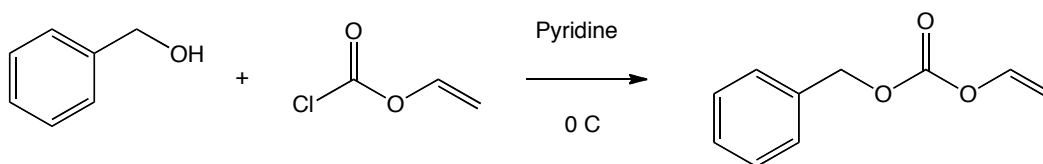
Scheme 4.11 Unsuccessful enantioselective *O*-protection of fingolimod HCl

Scheme 4.12 shows the successful synthesis of a phosphoramidate of the product of the reaction shown in scheme 4.10. However, when considering that the harsh conditions that would be required to deprotect the alcohol (such as pH 2 conditions) would likely cause an unwanted decomposition of the ester component of the phosphoramidate (by acid catalysed ester hydrolysis¹), it was decided that a more labile OH protecting group would be used.



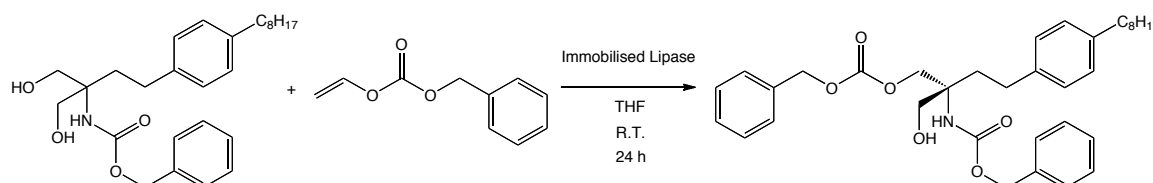
Scheme 4.12 Phosphoramidate synthesis of *N* and *O* protected fingolimod (77% yield)

The alternative to an acetyl protecting group described in the lead paper² is a benzyloxycarbonyl protecting group derived from benzyl vinyl carbonate. Benzyl vinyl carbonate is not readily commercially available and was therefore synthesised following a published procedure.⁸



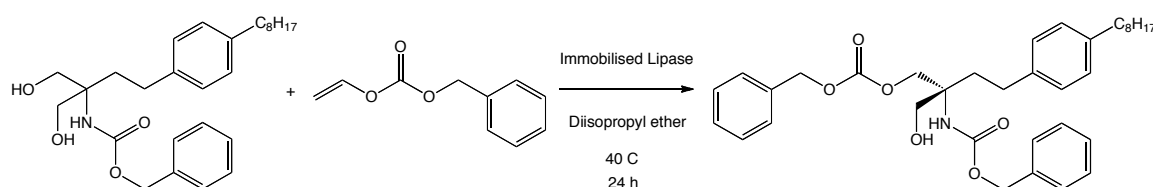
Scheme 4.13 Benzyl vinyl carbonate synthesis⁸ (81% yield)

The first attempted *O*-protection of *N*-protected fingolimod using benzyl vinyl carbonate, as shown in scheme 4.14, was successful but the product was only obtained in a disappointing 141 mg yield of 18%. This is in contrast to the same reaction conducted using vinyl acetate as shown in scheme 4.10 that gave a yield of 78% and in stark contrast to the reported yield of 99%. The reaction was attempted again this time at a higher temperature of 35 °C for 2 days but this time the yield was an even more disappointing 7%.



Scheme 4.14 Enantioselective *O*-protection of *N*-protected fingolimod (18% yield)

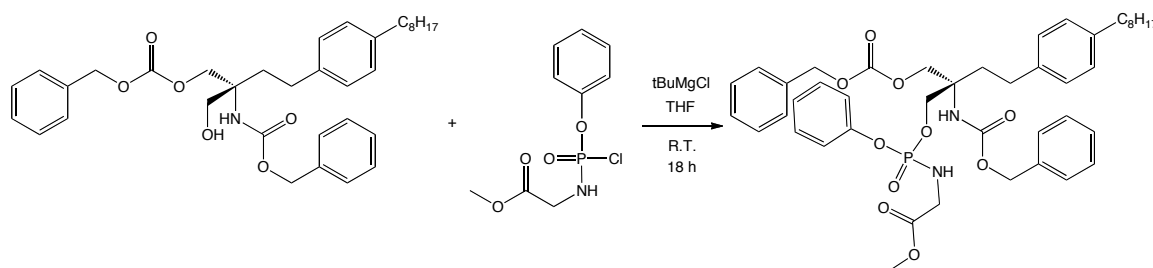
A search of the relevant literature provided two papers which suggested that changing the solvent from THF to diisopropyl ether and increasing the temperature to 40 °C could give more favourable results.^{9,10} Fortunately changing the reaction conditions as previously described gave an improved 583 mg yield of 54%. A polarimetry experiment was run on the product giving an optical rotation value of $[\alpha] = -56.59$ ($[\alpha]_{D^{24}} = -1.2$) suggesting a non-racemic mixture. Enantiomeric excess would need to be determined by further work such as by chiral HPLC.



Scheme 4.15 Enantioselective benzyloxycarbonyl *O*-protection of *N*-protected fingolimod (54% yield)

Now a phosphoramidate synthesis was attempted with benzyloxycarbonyl *N* and *O*-protected fingolimod as shown in scheme 4.16. A parent phosphorochloridate with a methyl ester moiety as opposed to the previously used benzyl ester moiety, as shown in scheme 4.12, was used as it was predicted that the methyl ester would

be less likely to be cleaved when removal of the benzyloxycarbonyl protecting groups was attempted. The ^{31}P NMR spectrum of the product of the reaction shown in scheme 4.16 can be seen in figure 4.7. There are clearly 2 peaks at 3.67 ppm and 3.53 ppm which correspond to the 2 diastereoisomers shown in figure 4.8. Enantiomeric excess would need to be determined *via* chiral HPLC.



Scheme 4.16 Phosphoramidate synthesis of benzyloxycarbonyl *N* and *O*-protected fingolimod (23% yield)

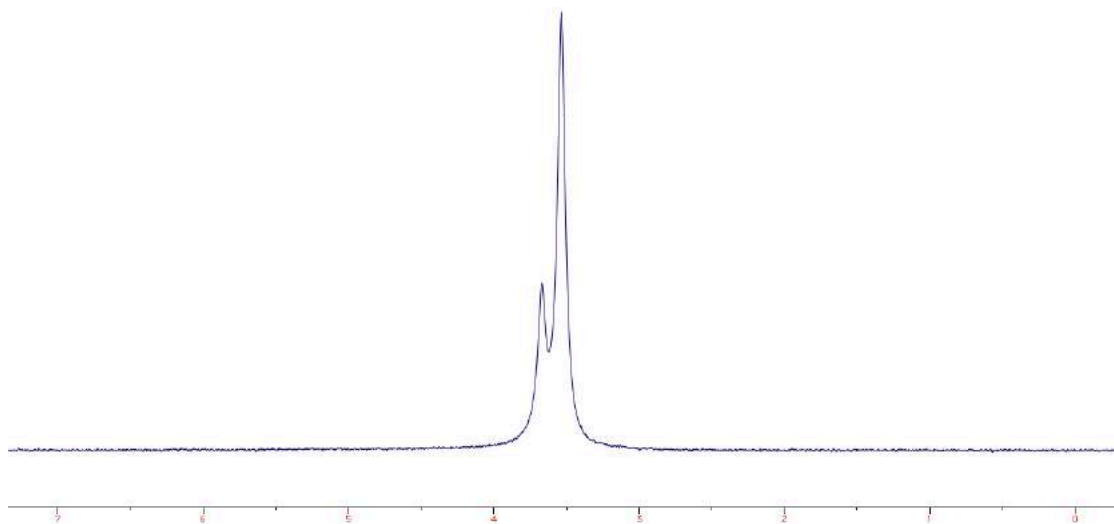


Figure 4.7 ^{31}P NMR spectrum of product of reaction shown in scheme 4.16

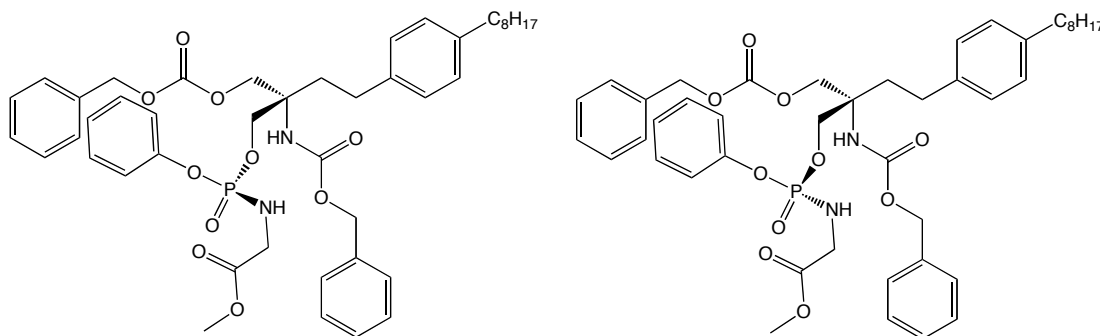
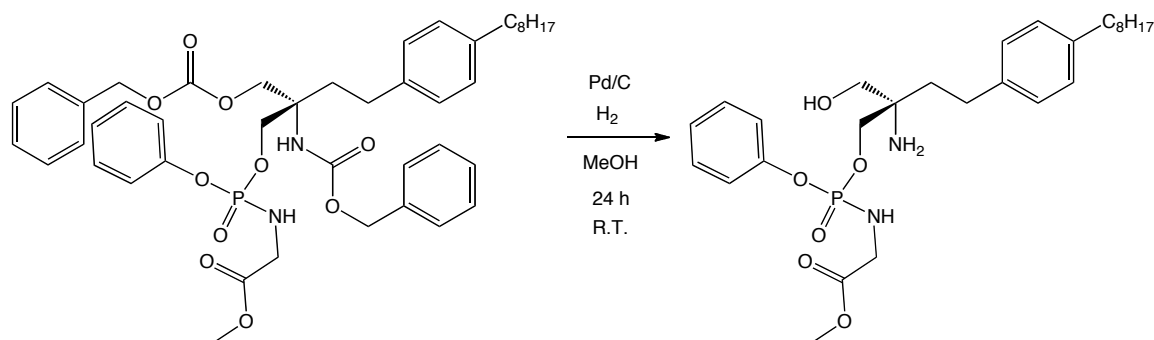
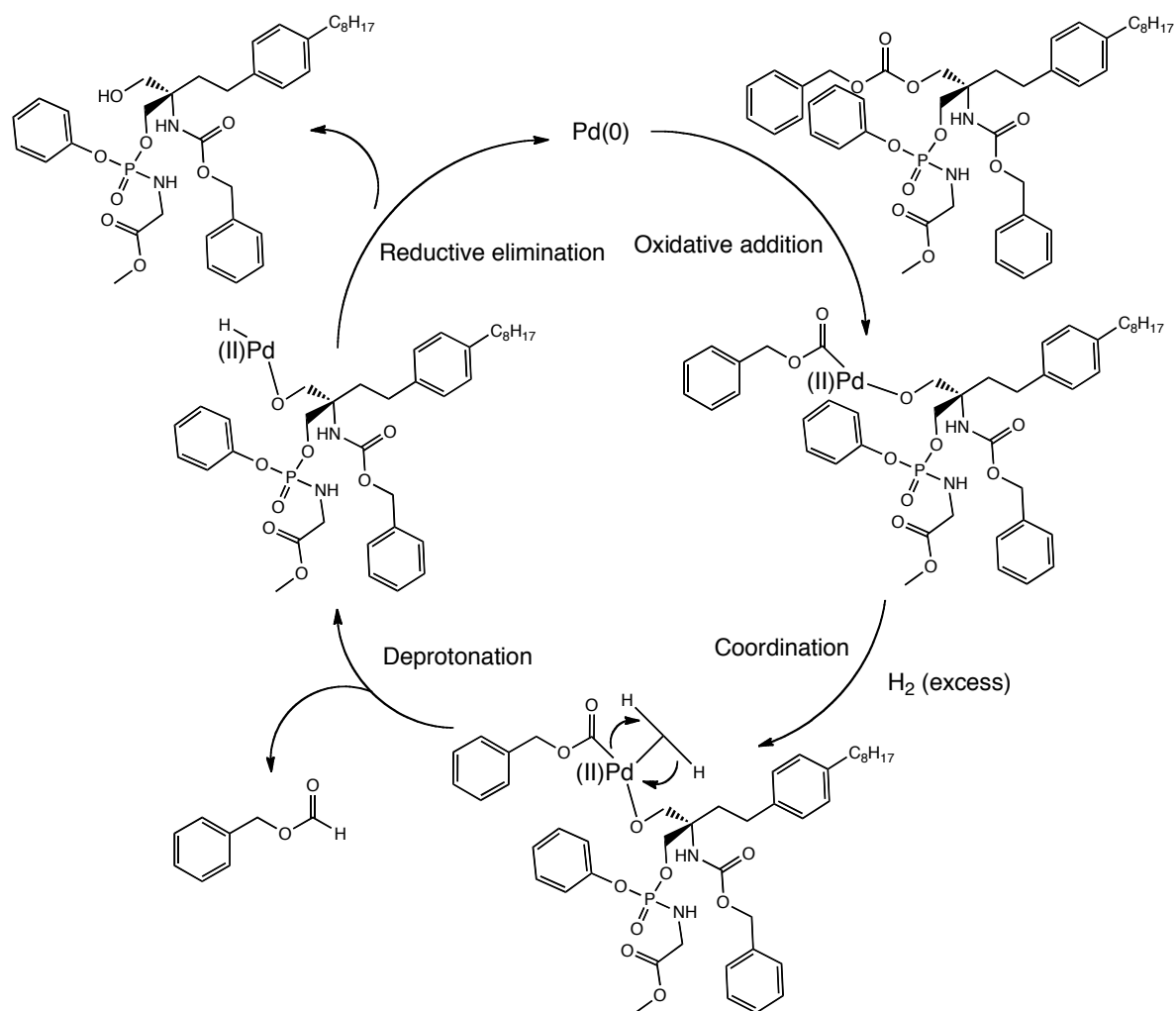


Figure 4.8 The 2 diastereoisomers responsible for the peaks at 3.67 ppm and 3.53 ppm in the ^{31}P NMR spectrum shown in figure 4.7

Finally, cleavage of the protecting groups was successfully achieved on the first attempt following a procedure described in the lead paper.² The use of a palladium catalyst was employed in a hydrogen rich environment as shown in schemes 4.17 and 4.18.



Scheme 4.17 Successful cleavage of the protecting groups yielding the final target compound (59% yield)



Scheme 4.18 Putative protecting group cleavage mechanism¹¹

Unfortunately, however, a major by-product of the reaction was the cyclised structure shown in figure 4.9. The exact mass of the cyclised compound is 440.24 g/mol and a mass of 441.2 m/z was detected in the mass spectrometric analysis which almost certainly corresponds to the unwanted cyclised product shown below.

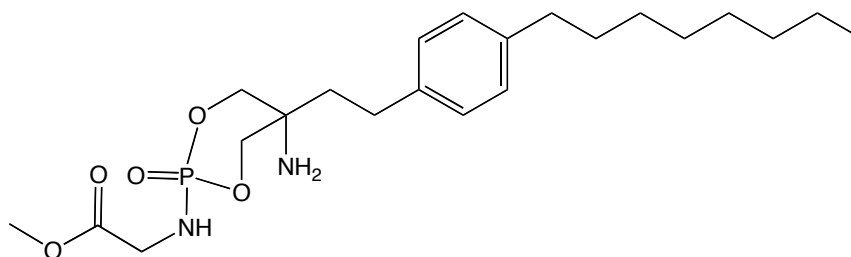
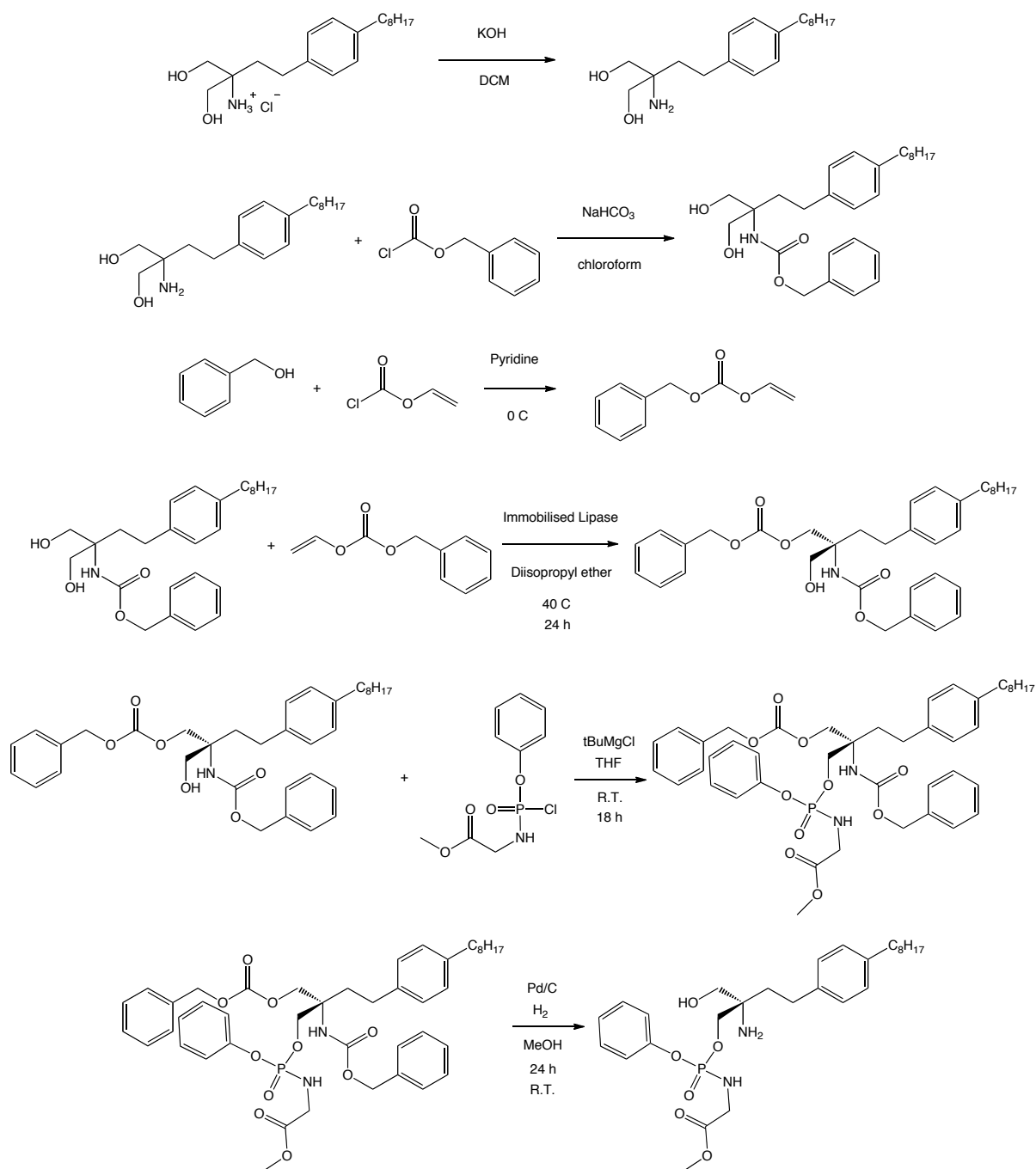


Figure 4.9 Unwanted side product of the final protecting group cleavage reaction

As more fully explained in Chapter 5 unwanted cyclisations of the type shown in figure 4.9 are a major unwanted feature of the whole family of ProTide fingolimod compounds. Therefore, while the chiral synthesis of ProTide fingolimod was successfully achieved, the extreme ease with which ProTide fingolimod decomposes to the cyclised structure shown in figure 4.9 renders the greater effort, expense and consumption of time dedicated to the chiral synthesis of little value as the high level of chirality achieved is very quickly lost due to the unwanted cyclisation.

4.1.3 The Final Chiral Synthesis



Scheme 4.19 The final chiral synthesis

4.2 References

1. McMurry J. *Organic Chemistry*. Sixth edition. 2004.
2. Kiuchi M, Adachi K, Tomatsu A, Chino M, Takeda S, Tanaka Y, Maeda Y, Sato N, Mitsutomi N, Sugahara, Chiba K. Asymmetric synthesis and biological evaluation of the enantiomeric isomers of the immunosuppressive FTY720-phosphate. *Bioorg. Med. Chem.* **2005**, 13, 425-432.
3. Coppola K, Testa J, Allen E, Sculimbrenne B. Selective phosphorylation of diols with a Lewis acid catalyst. *Tetrahedron Lett.* **2014**, 55, 4203-4206.
4. Hikawa H, Hamada M, Uchida Y, Kikkawa S, Yokoyama Y, Azumaya I. Enantioselective desymmetrization of FTY720. *Chem. Pharm. Bull.* **2014**, 62, 1041-1044.
5. Hale J, Yan L, Neway W, Hajdu R, Bergstrom J, Milligan J, Shei G, Chrebet G, Thornton R, Card D, Rosenbach M, Rosen H, Mandala S. Synthesis, stereochemical determination and biochemical characterization of the enantiomeric phosphate esters of the novel immunosuppressive agent FTY720. *Bioorg. Med. Chem.* **2004**, 12, 4803-4807.
6. Albert R, Hinterding K, Brinkmann V, Guerini D, Muller-Hartweig C, Knecht H, Simeon C, Streiff M, Wagner T, Welzenbach K, Zecri F, Zollinger M, Cooke N, Francotte E. Novel immunomodulator FTY720 is phosphorylated in rats and humans to form a single stereoisomer. Identification, chemical proof, and biological characterization of the biologically active species and its enantiomer. *J. Med. Chem.* **2005**, 48, 5373-5377.
7. http://www.toyobo-global.com/seihin/xr/enzyme/pdf_files/283_286LIP_301.pdf
8. Pozo M, Pulido R, Gotor V. Vinyl carbonates as novel alkoxycarbonylation reagents in enzymatic synthesis of carbonates. *Tetrahedron.* **1992**, 48, 6477-6484.
9. Nakai K, Hiratake J, Oda J. Kinetic resolution of racemic α -aminonitriles via stereoselective *N*-acetylation catalyzed by lipase in organic solvent. *Bull. Inst. Chem. Res., Kyoto Univ.* **1992**, 70, 333-337.

10. Inagaki M, Hiratake J, Nishioka T, Oda J. Lipase catalyzed stereoselective acylation of [1,1'-binaphthyl]-2,2'-diol and deacylation of its esters in an organic solvent. *Agric. Biol. Chem.* **1989**, 53, 1879-1884.
11. Johnstone R, Wilby A. Heterogenous catalytic transfer hydrogenation and its relation to other methods for reduction of organic compounds. *Chem. Rev.* **1985**, 85, 129-170.

Chapter 5 – Biochemical Processing of ProTide Fingolimod Analogues

In order to assess the viability of ProTide fingolimod analogues as potentially efficacious therapeutics different types of *in vitro* testing such as stability assays and enzymatic processing experiments need to be conducted.

5.1 Stability Assays

It is important to find out if the ProTide fingolimod analogues are stable and do not decompose when exposed to environmental conditions typical of an effective orally-acting medication.

5.1.1 Acid Stability Test

Oral medication (medicine taken as a pill) needs to be stable in the acidic conditions of the stomach for at least an hour before it is transferred to the digestive tract where it can be absorbed by the lumen and enter the bloodstream. The stomach is a highly acidic environment of between pH 1 - 2.

In order to determine the viability of ProTide fingolimod analogues as orally active drugs capable of withstanding the conditions of the stomach Ph-Gly-OBzl-F was subjected to a pH 1.5 buffer for 12 hours. Figure 5.1 shows the change in the ^{31}P NMR spectrum of the pH 1.5 Ph-Gly-OBzl-F solution over 12 hours.

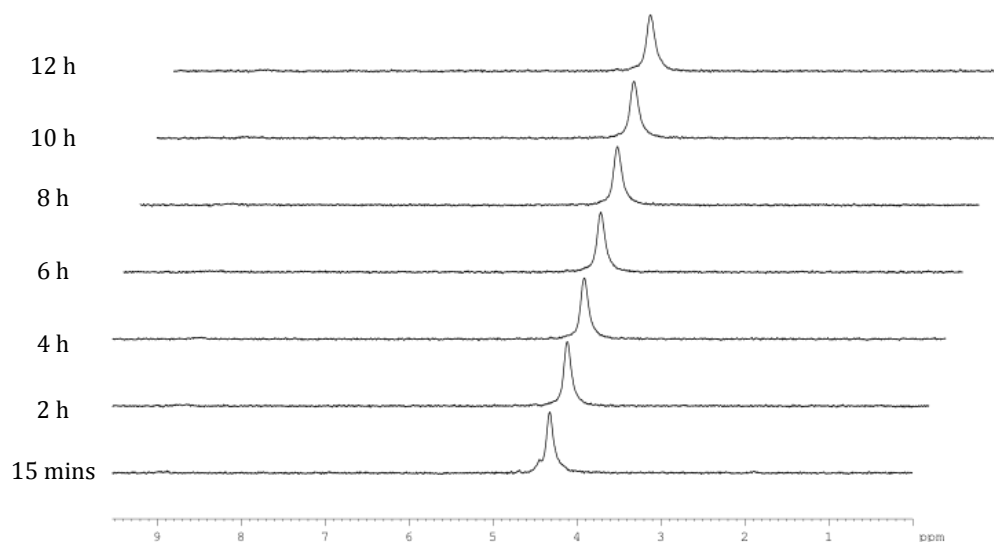
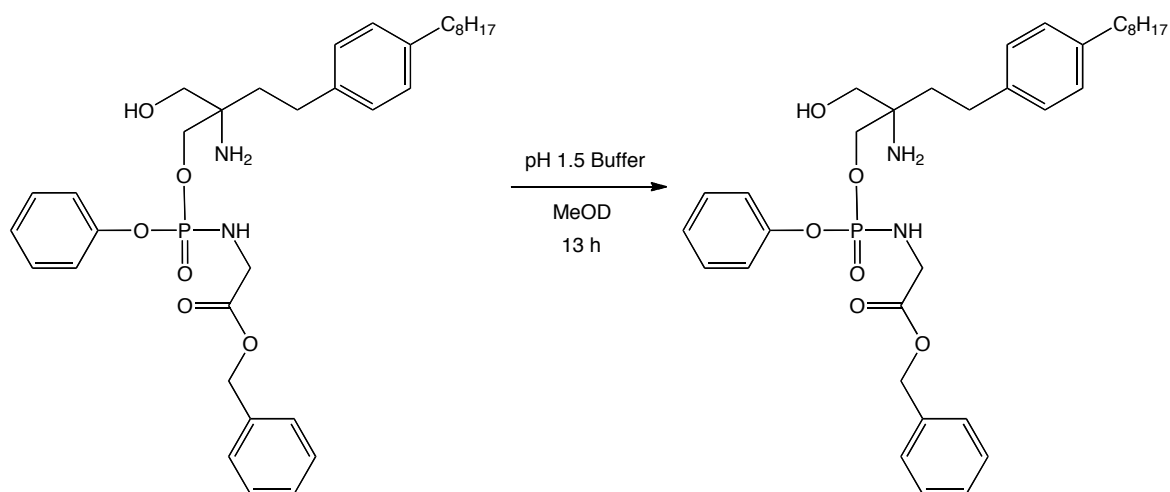


Figure 5.1 Stacked ^{31}P NMR spectra of Ph-Gly-OBzl-F stability test over 12 hours in the presence of pH 1.5 buffer

It can be clearly seen that the peak indicative of Ph-Gly-OBzl-F does not decrease in height and that no new peaks are formed. This is a favourable result as it implies that ProTide fingolimod analogues will not be degraded in the stomach and will be intact by the time they reach the small intestine.



Scheme 5.1 No degradation of ProTide fingolimod observed over 13h in highly acidic conditions

5.1.2 Base Stability Test

A pH 8 buffer was made using carefully measured amounts of HCl and tris (hydroxymethyl) aminomethane. Ph-Gly-OBzl-F was subjected to pH 8 conditions for 13 hours at room temperature. Figure 5.2 shows the change in the ^{31}P NMR spectra of the pH 8 Ph-Gly-OBzl-F solution over 13 hours. Significant levels of degradation can be seen. The half-life of Ph-Gly-OBzl-F has been calculated to be approximately 13 hours as during a period of around 13 hours the parent peak was reduced to a relative integration of 50%.

Although the stomach does reach pH between 1 - 2 and the acid stability test is very relevant to determining if a compound could be an effective oral medication, no area of the human body reaches a basicity equal to or greater than pH 8. The results of the pH 8 base test prove that additional chemical reactions or analysis should not be conducted in pH 8 or above as degradation is a likely consequence.

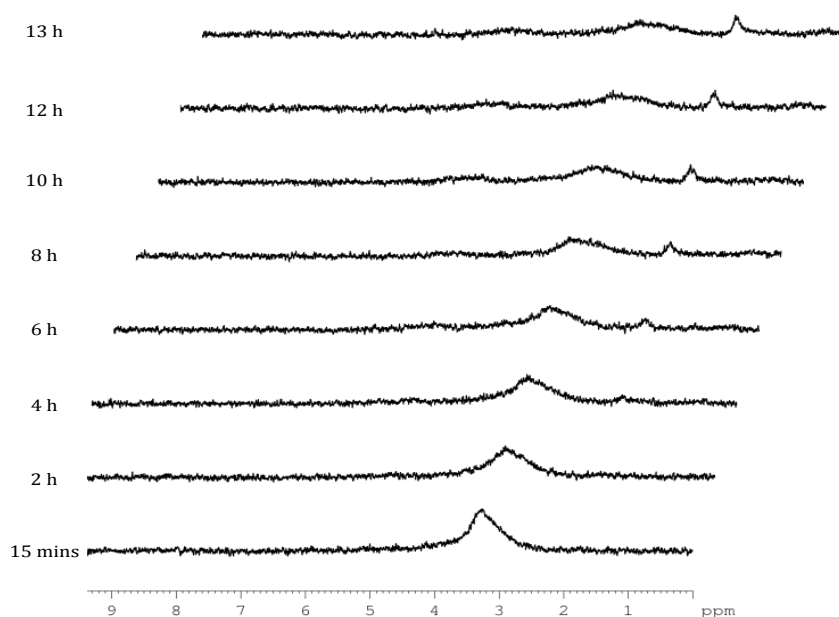
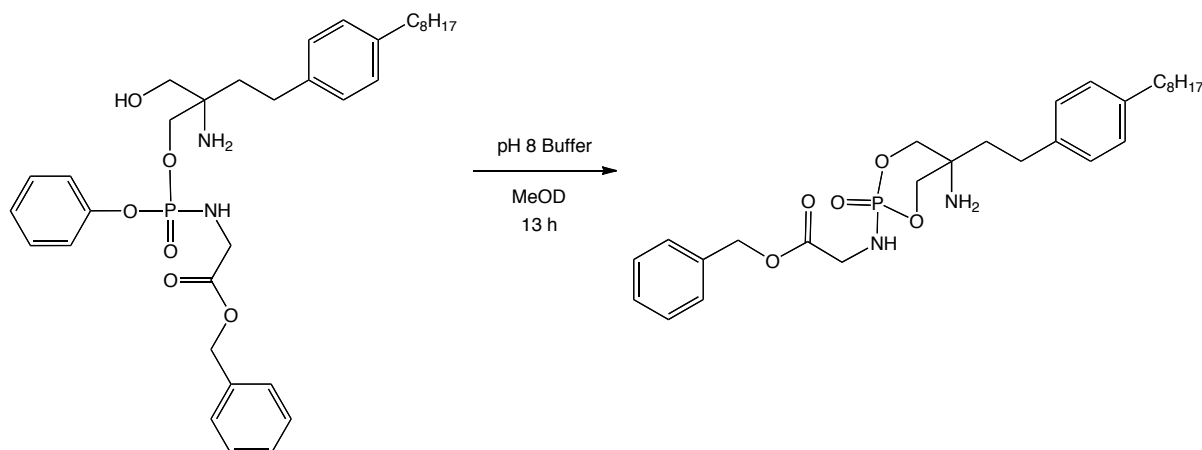


Figure 5.2 Stacked ^{31}P NMR spectra of Ph-Gly-OBzl-F stability test over 13 hours in the presence of pH 8 buffer

In light of the later carboxypeptidase experiments (see section 5.2) it seems highly probable that the product of the pH 8 stability experiment is the unwanted cyclised compound as shown in scheme 5.2.



Scheme 5.2 Probable base-induced degradation of ProTide fingolimod to unwanted cyclised product

5.1.3 DMSO Freeze Thaw Stability Tests

Katharina Säuberli conducted biological *in vitro* testing on the novel ProTide fingolimod analogues to determine if they are able to up-regulate BDNF production in mouse ES cell-derived neurons using techniques such as western blot and ELISA. The compounds were frozen in DMSO then thawed when a sample is taken and then refrozen and placed back in the freezer. It was decided that it should be determined whether or not ProTide fingolimod analogues are degraded by subjecting them to these conditions.

Four ProTide fingolimod analogues were subjected to a freeze-thaw experiment conducted over 5 days. 5 mg of each ProTide was placed in a NMR tube in 0.8 ml DMSO and then analysed using ^{31}P NMR. The solutions were then frozen for 18 hours then thawed and analysed again using ^{31}P NMR.

Figures 5.3 – 5.6 show the results of the DMSO freeze-thaw experiments. It can be seen that no significant level of degradation is observed. It should be noted that the day 2 and day 3 peaks are generally smaller due to insufficient time left to thaw thus leading to spectra of less than preferable definition. Arguably the experiments could be conducted again with sufficient length of time of thawing for each of the days ^{31}P NMR analysis is conducted.

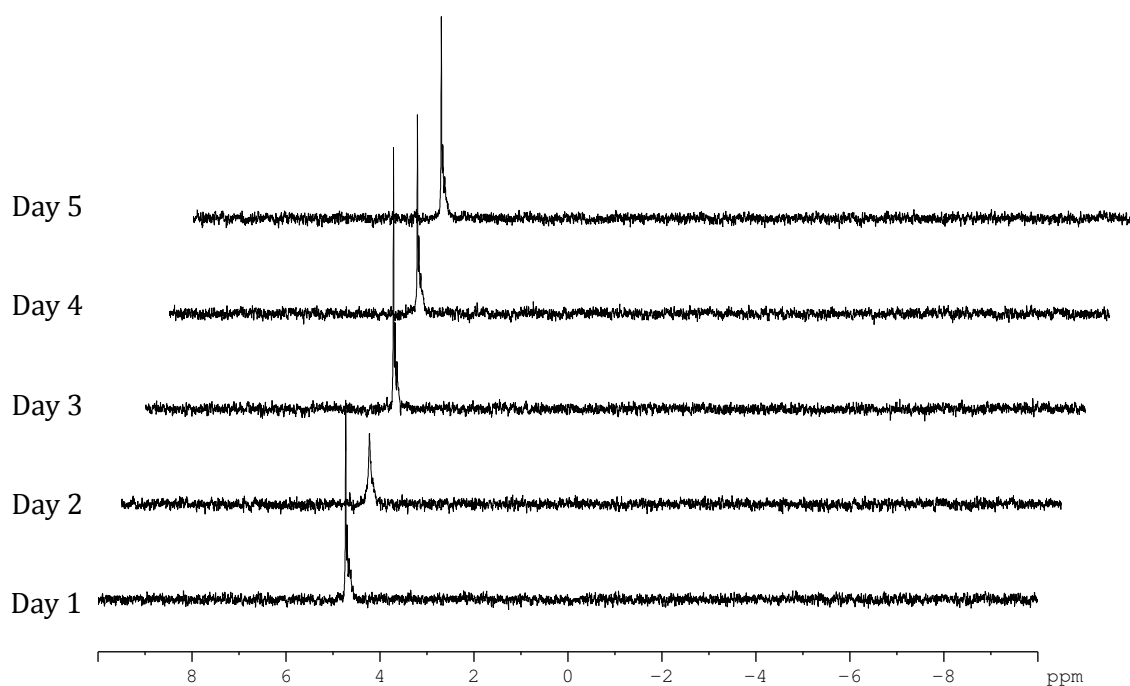


Figure 5.3 Stacked ^{31}P NMR spectra of freeze-thaw experiment of Ph-Gly-OBzl-F in DMSO over 5 days

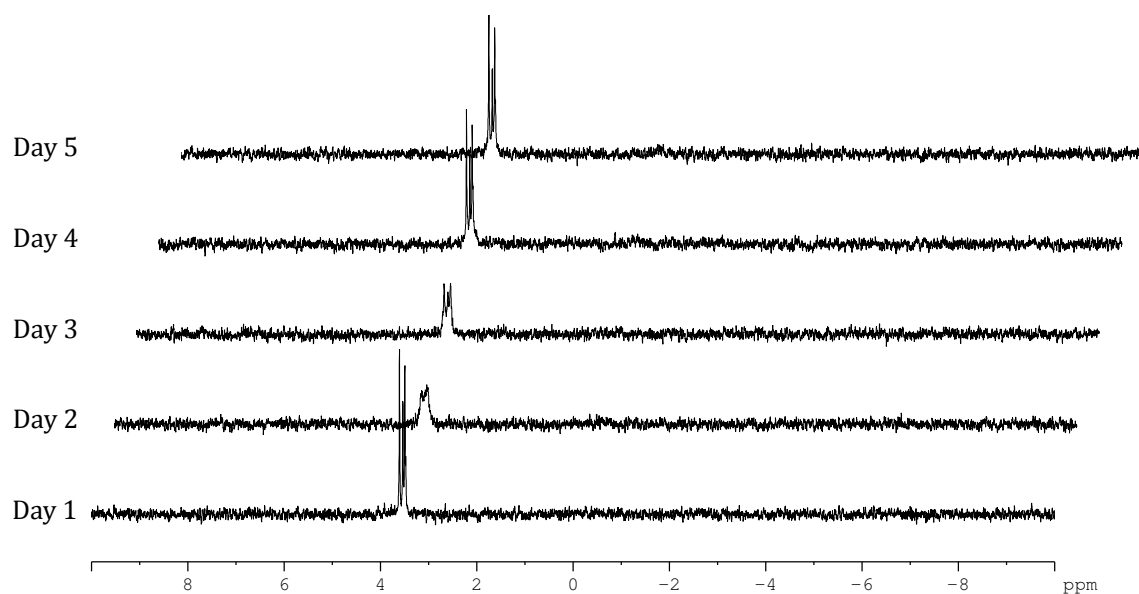


Figure 5.4 Stacked ^{31}P NMR spectra of freeze-thaw experiment of Ph-LAla-OBzl-F in DMSO over 5 days

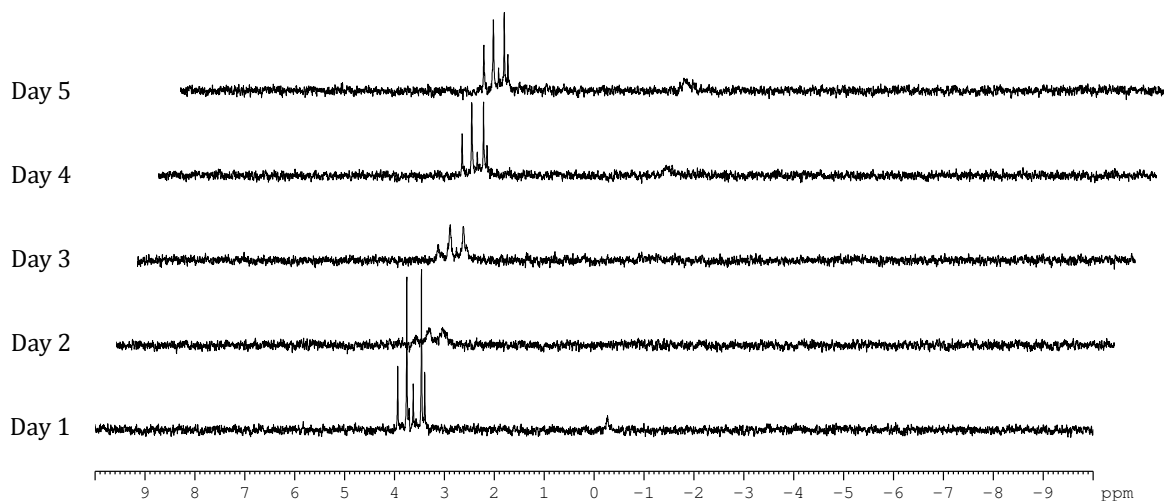


Figure 5.5 Stacked ^{31}P NMR spectra of freeze-thaw experiment of Ph-LAla-OMe-F in DMSO over 5 days

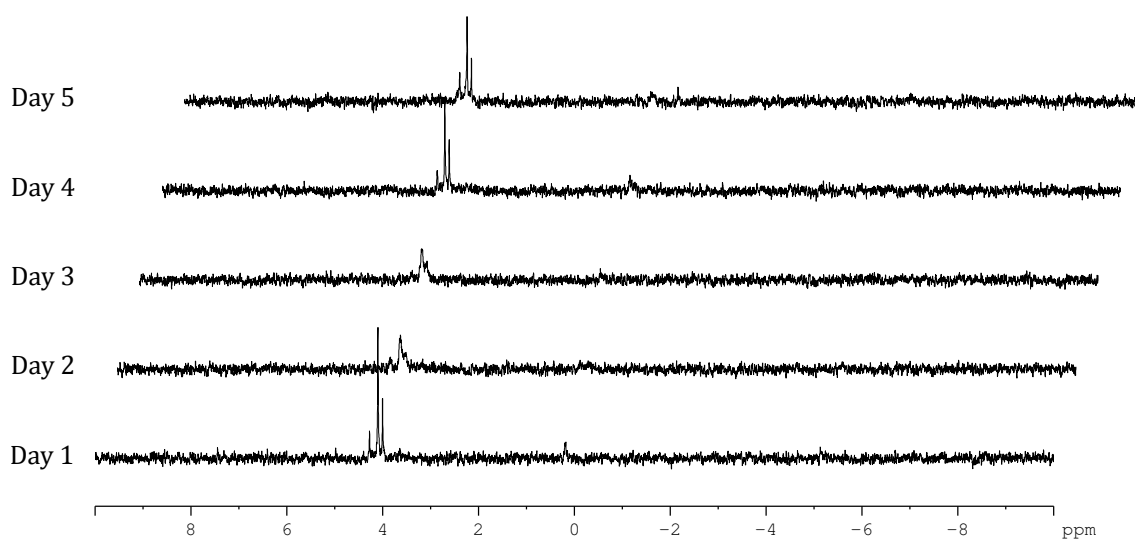
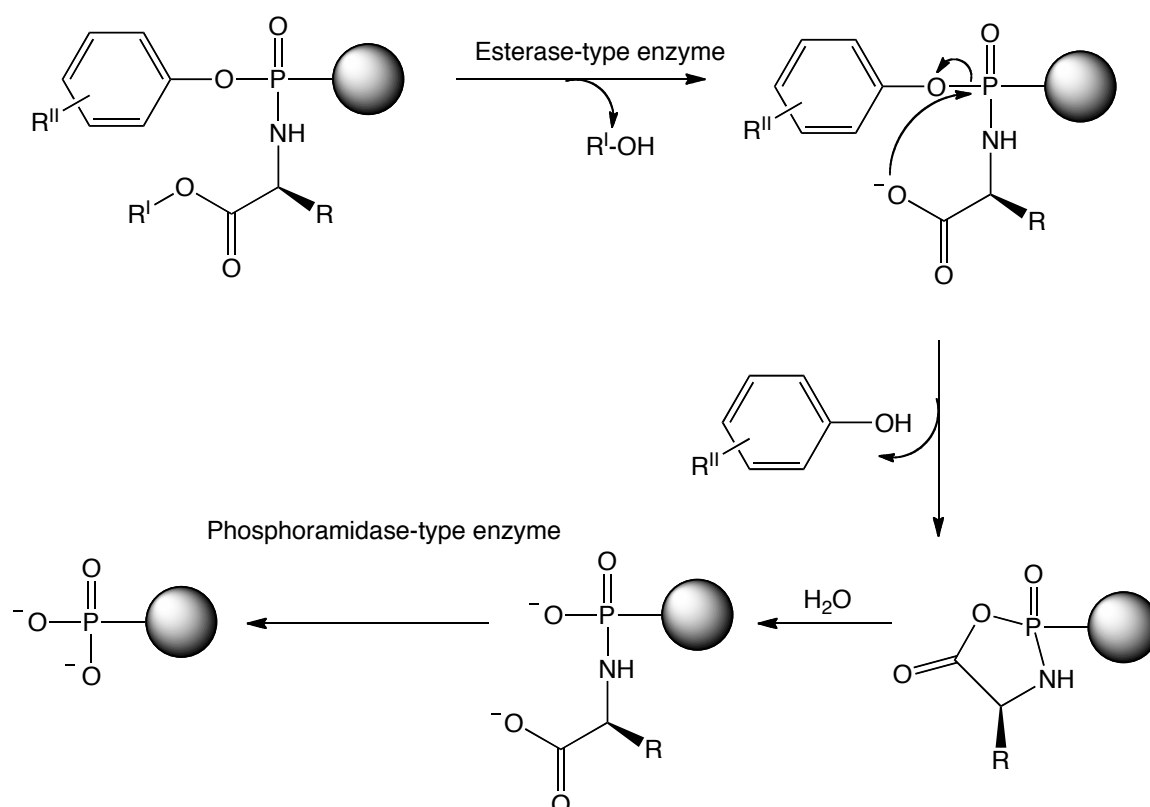


Figure 5.6 Stacked ^{31}P NMR spectra of freeze-thaw experiment of Ph-Leu-OBzl-F in DMSO over 5 days

5.2 Enzymatic and Human Serum Assays

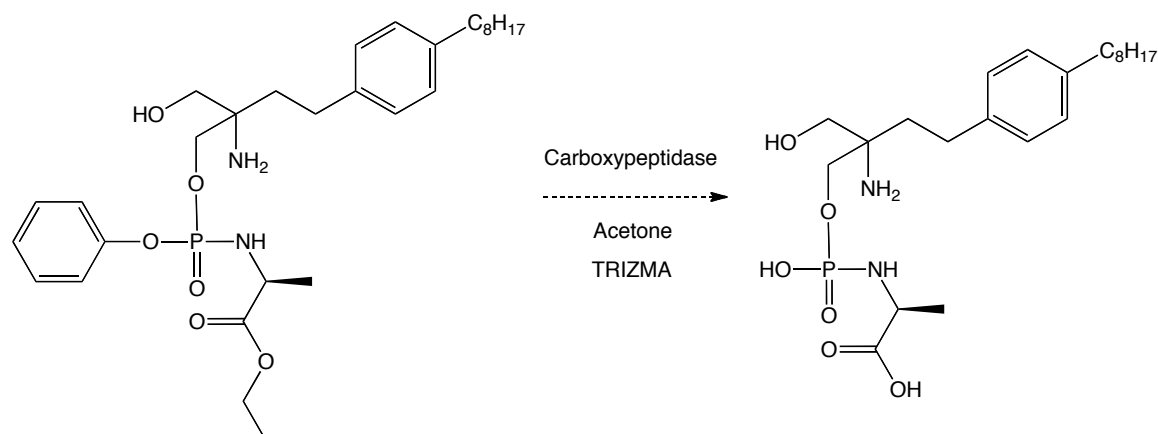
Established ProTides, such as sofosbuvir, are processed by naturally occurring enzymes in the human body to the monophosphate form (as shown in scheme 5.3 below). ^{31}P NMR enzymatic assays have been developed to assess previously synthesised ProTides for their capacity to be processed by enzymes such as carboxypeptidase and porcine liver esterase.



Scheme 5.3 Intracellular enzymatic processing of ProTides¹

Following a previously published experimental procedure¹ enzymatic experiments were conducted. The enzyme used was carboxypeptidase Y purchased from Sigma Aldrich and the experiments were conducted over a 12 - 13 hour period inside an NMR tube while the NMR machine conducted ^{31}P NMR experiments.

5.2.1 Ph-LAla-OEt-F Carboxypeptidase Experiment



Scheme 5.4 Expected carboxypeptidase processing reaction

Figure 5.7 shows the change in the chemical shifts of the peaks when Ph-LAla-OEt-F was exposed to carboxypeptidase in acetone- d_6 and Trizma buffer (pH 7.6) over 12 hours. A drawback of the experimental procedure is that you cannot run the whole experiment from before you add the enzyme. The result of this is that one can see degradation of the major peaks in the first scan by noting the small peak at around 1.7 ppm which progressively increases in size over the 12 hour period. The progressive loss of the peaks visible between 3 – 4 ppm and the appearance of the new peak seen at approximately 1.7 ppm demonstrates that the phosphoramidate fingolimod analogue assayed is processed/degraded during the experiment.

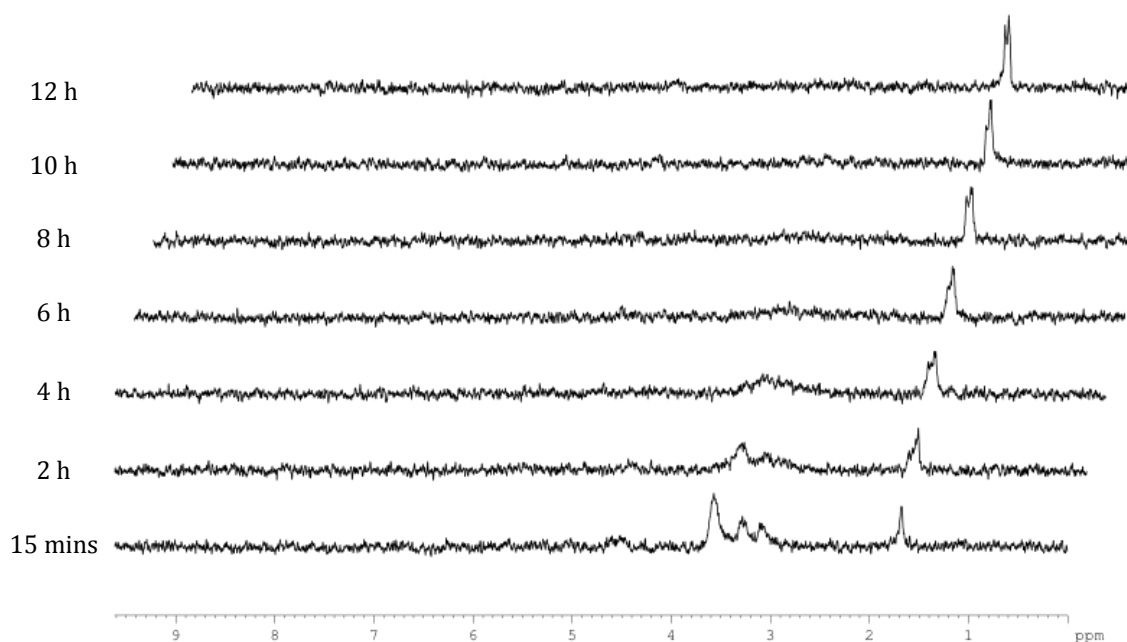


Figure 5.7 Stacked ^{31}P NMR spectra of Ph-LAla-OEt-F processing by carboxypeptidase over 12 hours

Mass spectrometric analysis of the products of the Ph-LAla-OEt-F experiment did not show the presence of a product that would typically be expected to be seen after conducting an enzymatic experiment. The most significant observed masses in positive mode after conducting the experiment were:

- 336.3 m/z
- 395.2 m/z
- 469.3 m/z
- 563.3 m/z

The mass of the unprocessed Ph-LAla-OEt-F analogue is 562.3 g/mol so it can be concluded that the mass observed of 563.3 m/z is unreacted phosphoramidate fingolimod $[\text{M}+\text{H}^+]$. What follow are the structures of the parent compound and compounds that were expected to be observed after processing by carboxypeptidase and their predicted masses.

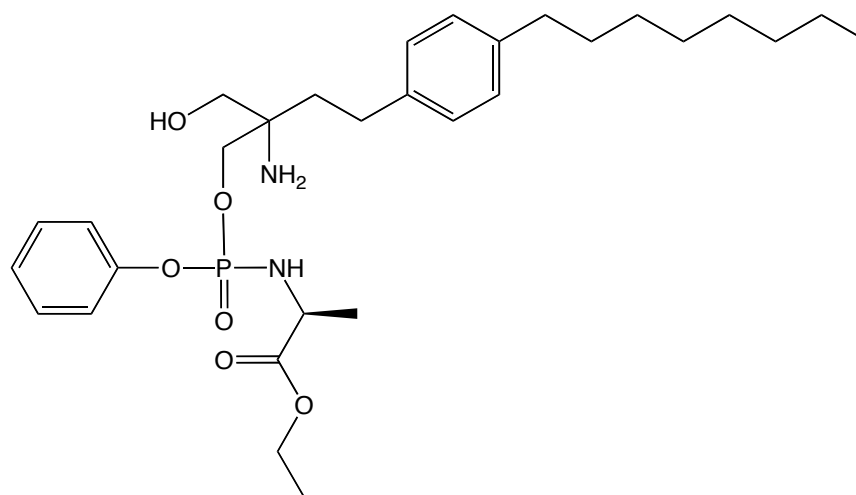


Figure 5.8 Parent compound Ph-LAla-OEt-F (562.3 g/mol)

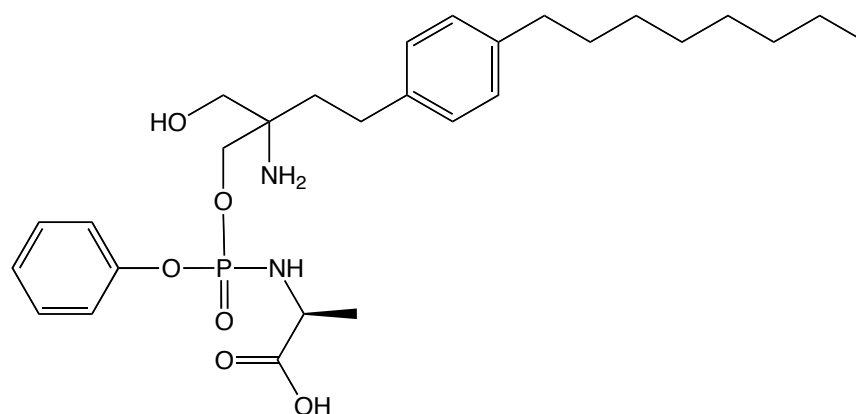


Figure 5.9 Possible initial product of processing of Ph-LAla-OEt-F by carboxypeptidase (534.3 g/mol)

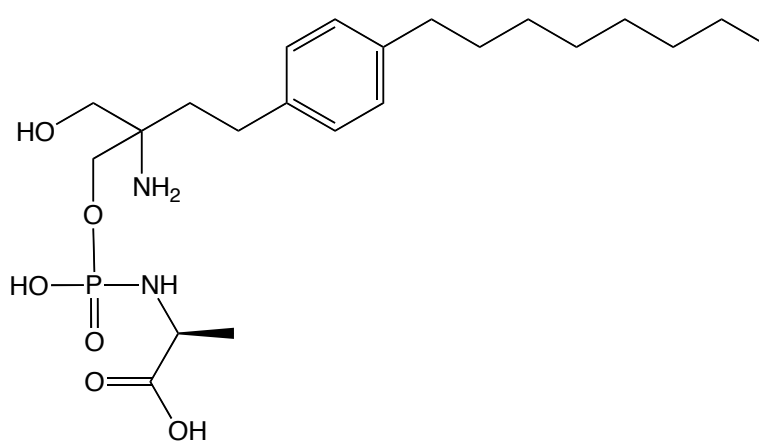


Figure 5.10 Possible product of processing of Ph-LAla-OEt-F by carboxypeptidase (458.3 g/mol)

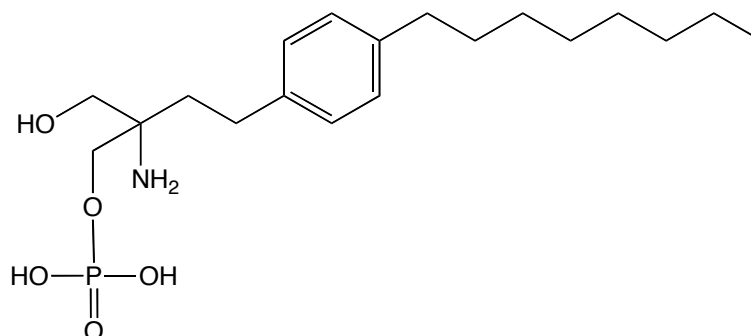


Figure 5.11 Possible product of processing of Ph-LAla-OEt-F by carboxypeptidase (387.2 g/mol)

No masses corresponding to the expected products of carboxypeptidase processing were observed. The most significant non-parent peak in the mass spectrum is the peak of 469.3 m/z. It is currently understood that this is the primary degradation product of the enzymatic experiment and it is the mildly basic conditions (pH 7.6) that catalyse an unwanted cyclisation of the parent compound to the product shown in figure 5.12. The predicted mass of the cyclisation product is 468.28 g/mol so it therefore appears highly likely that the mass peak observed as 469.3 m/z corresponds to this unwanted cyclised compound.

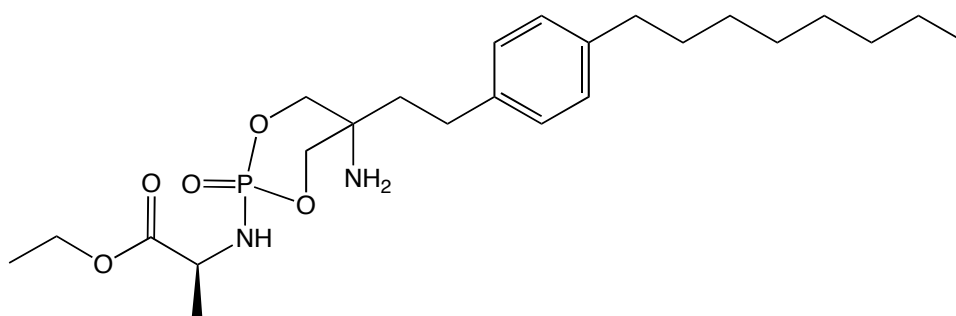
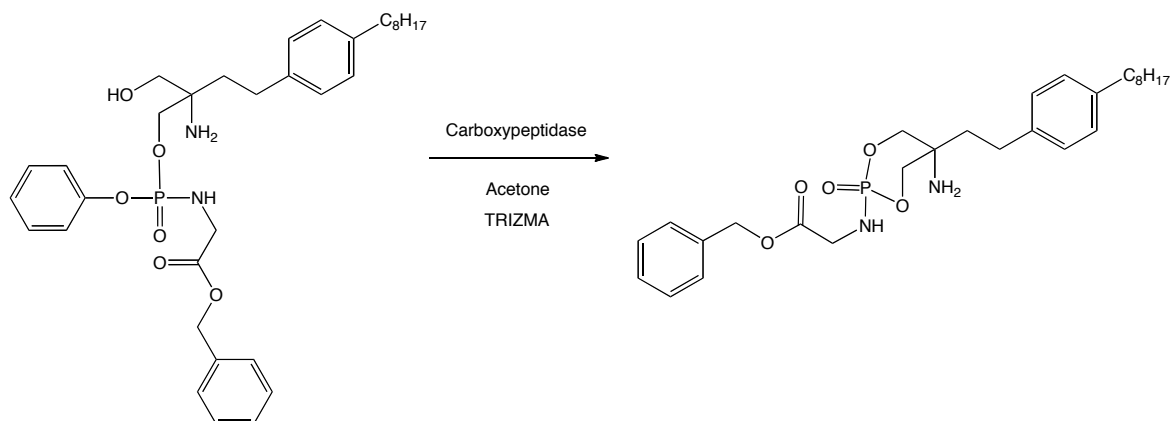


Figure 5.12 Major degradation product of enzymatic experiment (468.28 g/mol)

5.2.2 Ph-Gly-OBzl-F Carboxypeptidase Experiment



Scheme 5.5 Ph-Gly-OBzl-F carboxypeptidase processing experiment

An identical experiment (ignoring unintentional differences in the amount of enzyme used) was conducted with Ph-Gly-OBzl-F. The results of this experiment can be seen in figure 5.13. There was an apparently slightly slower processing/degradation of this phosphoramidate fingolimod analogue than was observed with Ph-LAla-OEt-F.

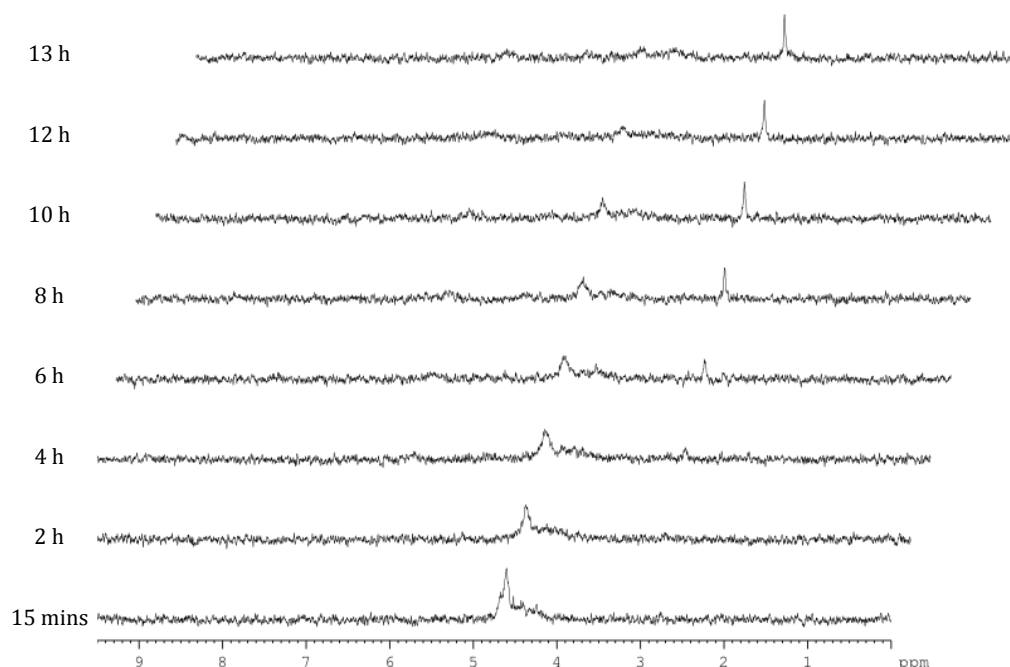


Figure 5.13 Stacked ^{31}P NMR spectra of Ph-Gly-OBzl-F processing by carboxypeptidase over 13 hours

In this case another NMR tube containing the same ratios of acetone, starting material and Trizma buffer but without the enzyme was used as a control experiment and the phosphorus NMR spectrum run the next day can be seen in figure 5.14. It can be clearly seen that the degradation pattern observed in the control experiment without the enzyme is very similar to the degradation observed in the presence of enzyme so it can be concluded that the environmental conditions of the enzymatic experiment e.g. pH and solvent system are partly or perhaps completely responsible for the degradation observed. No mass spectrometric analysis was conducted on the products of this experiment but considering the results of the Ph-LAla-OEt-F experiment it seems likely that the major product as seen at 2.8 ppm in figure 5.13 is another cyclised product as shown in scheme 5.5. The slightly different chemical shifts observed in figures 5.13 and 5.14 are due to the incorrect input of the solvent being MeOD as opposed to deuterated acetone.

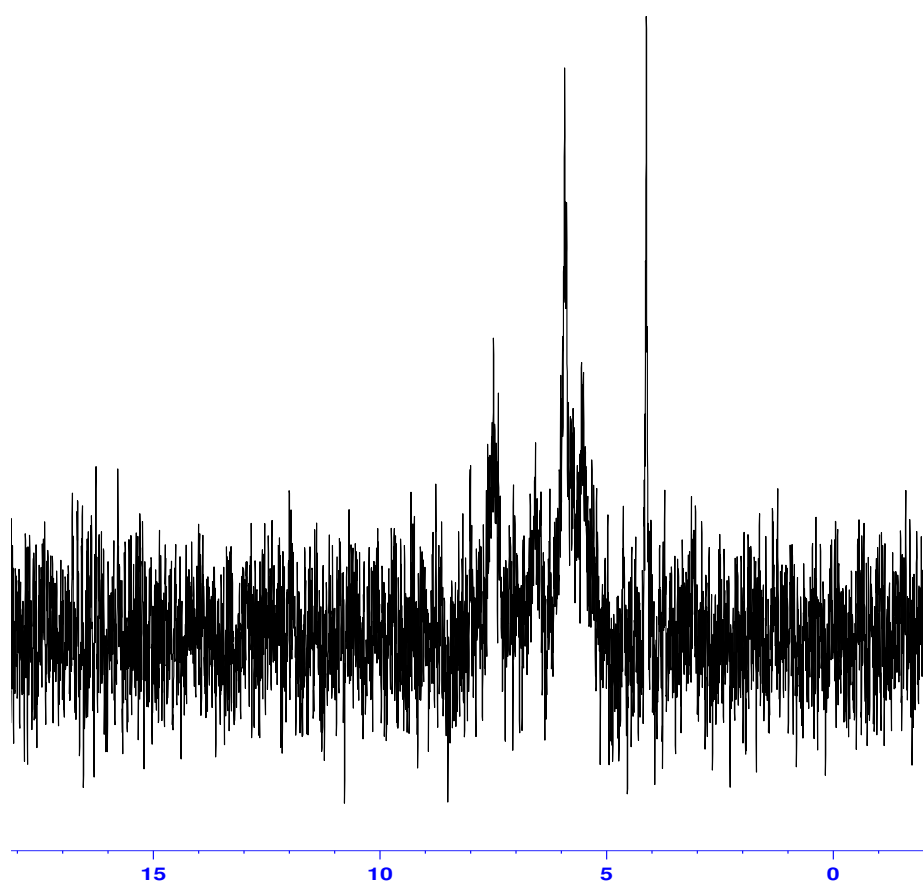
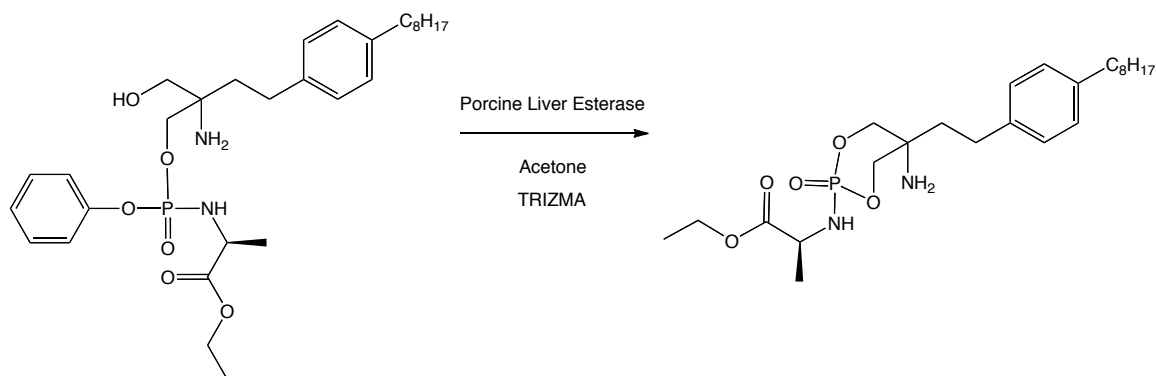


Figure 5.14 ^{31}P NMR Ph-Gly-OBzl-F control experiment (all the same reagents and reaction conditions but without the carboxypeptidase enzyme) spectrum at 11am the next day

5.2.3 Ph-LAla-OEt-F Porcine Liver Esterase Experiment



Scheme 5.6 Ph-LAla-OEt-F porcine liver esterase processing experiment

A larger scale enzymatic experiment, this time using porcine liver esterase as opposed to carboxypeptidase, was conducted on Ph-LAla-OEt-F using a method adapted from a published paper.² In this experiment 30 mg starting material was stirred in 1 ml Trizma buffer and 2 ml acetone and was monitored *via* TLC over 2 days.

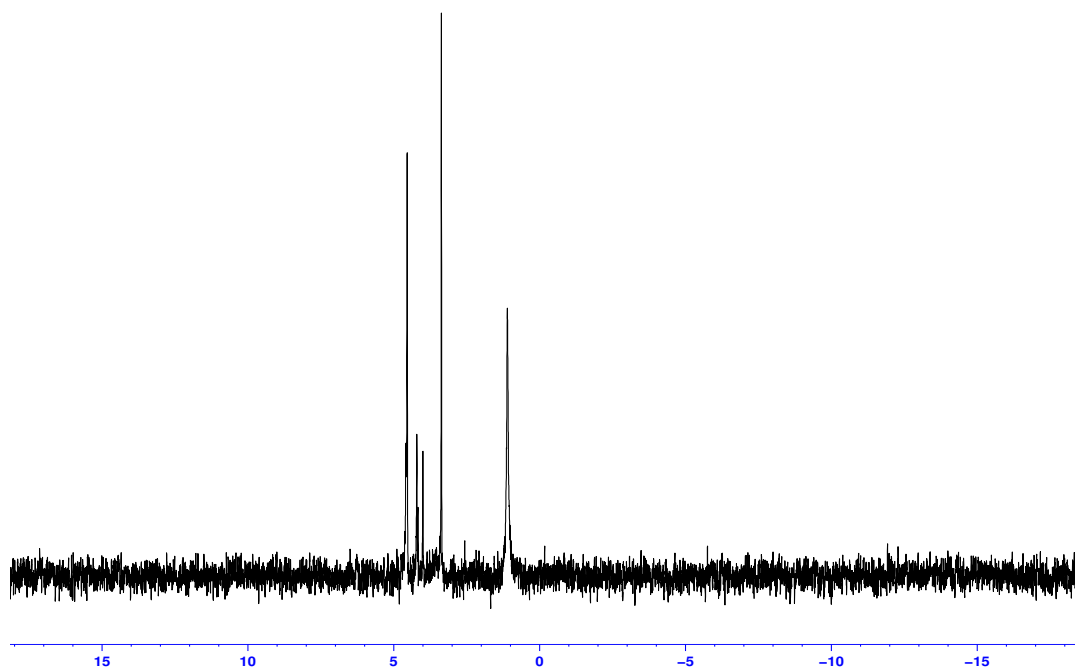


Figure 5.15 ³¹P NMR spectrum of the organic extract after Ph-LAla-OEt-F was stirred with porcine liver esterase, Trizma buffer and acetone for 2 days at 37 °C for 2 days

The major peaks observed in the mass spectrum of the organic extract were:

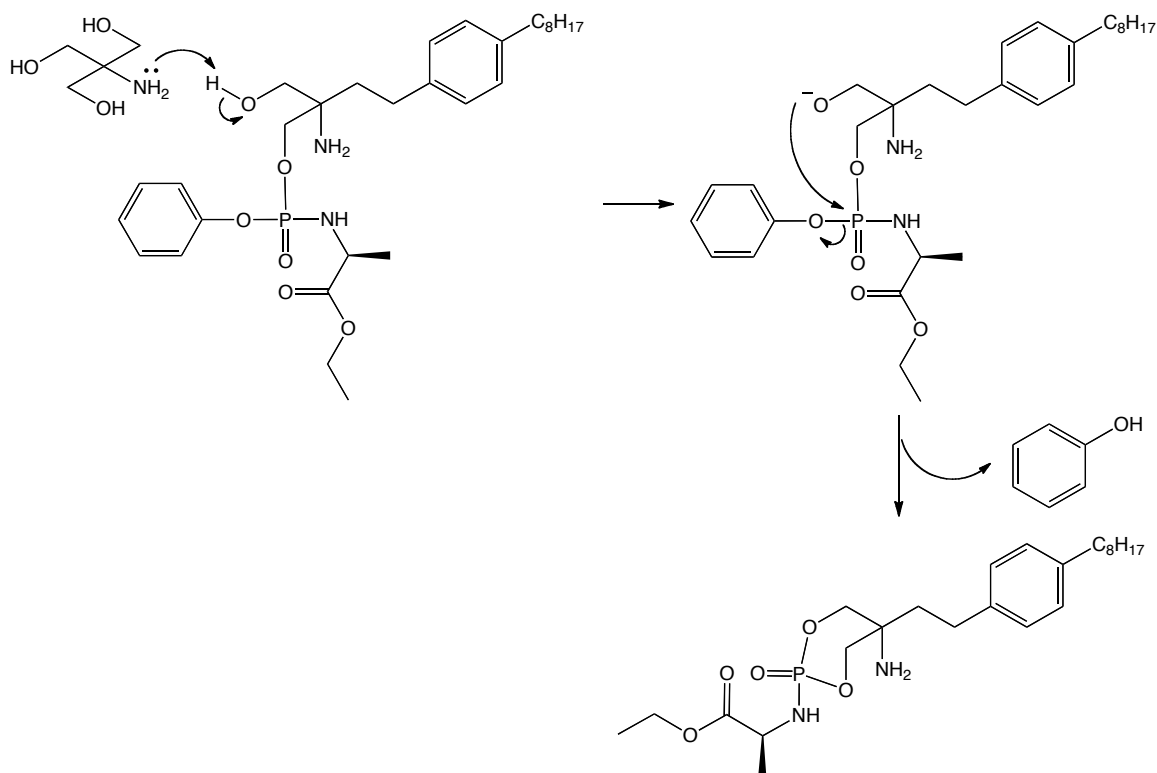
- 330.3 m/z
- 469.3 m/z
- 563.3 m/z

All three of these peaks can be assigned. The peak of 330.3 m/z corresponds to fingolimod+Na, 469.3 m/z corresponds to the same unwanted cyclisation product as shown in figure 5.12 and scheme 5.6 and 563.3 m/z is the unreacted parent ProTide fingolimod compound.

5.2.4 Initial Conclusions

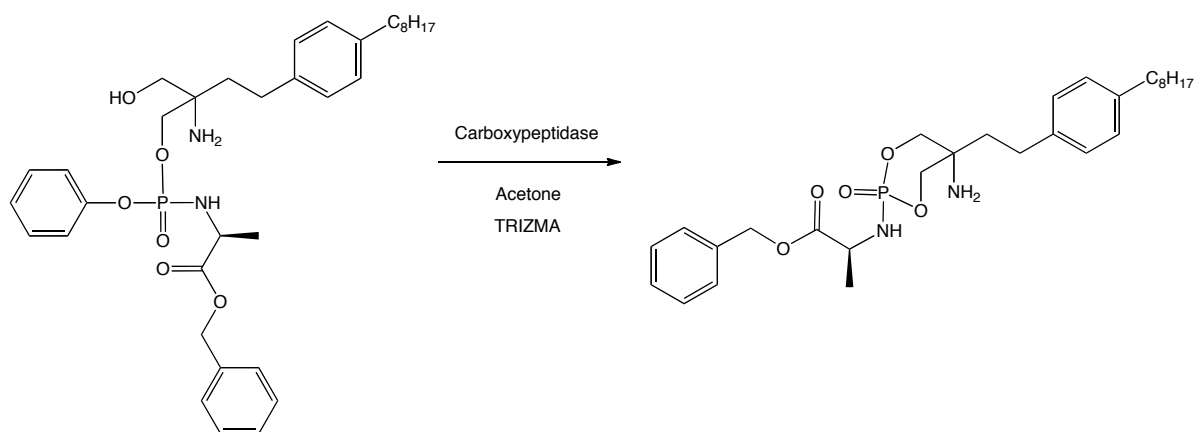
In both the carboxypeptidase experiment and the porcine liver esterase experiment with Ph-LAla-OEt-F none of the desired products of enzymatic processing were observed. The human small intestine has been measured to reach pH 7.5,³ a pH that is essentially identical to Trizma buffer (published to be pH 7.6), so it appears likely that Ph-LAla-OEt-F is not a viable fingolimod phosphorus prodrug to be used in humans as a therapeutically active compound. Base catalysed degradation to the unwanted cyclised product was experimentally observed to occur and enzymatic processing was not.

After analysis of the data obtained from the basic and enzymatic experiments previously described it was concluded that ***all ProTide fingolimod analogues are likely to be too unstable to be therapeutically viable compounds***. The base-induced degradation pattern of Ph-Gly-OBzl-F as shown in figure 5.2 is almost identical to the degradation pattern observed in the carboxypeptidase experiment of the same compound as shown in figure 5.13. When compared with the spectra obtained for the Ph-LAla-OEt-F experiments it seems that it is the mildly basic environment that is responsible for the degradation rather than the enzyme. A putative mechanism of degradation is shown in scheme 5.7. Further experiments were conducted to ascertain whether this is indeed the case.



Scheme 5.7 Proposed mechanism of Trizma catalysed cyclisation of ProTide fingolimod

5.2.5 Ph-LAla-OBzl-F Carboxypeptidase Experiment



Scheme 5.8 Ph-LAla-OBzl-F carboxypeptidase processing experiment

A carboxypeptidase experiment was conducted on Ph-LAla-OBzl-F following the previously used procedure¹ and the compound degraded in a similar fashion to other ProTide fingolimod analogues as shown in figure 5.16. A mass of 531.3 m/z corresponding to the relevant unwanted cyclisation product with a mass of 530.29 g/mol as shown in scheme 5.8 was detected.

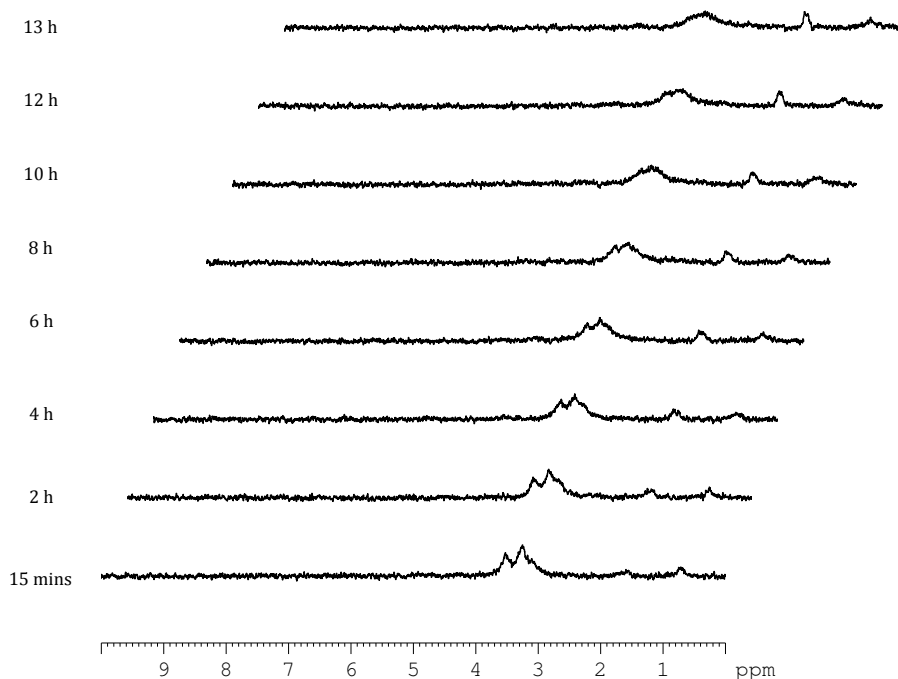
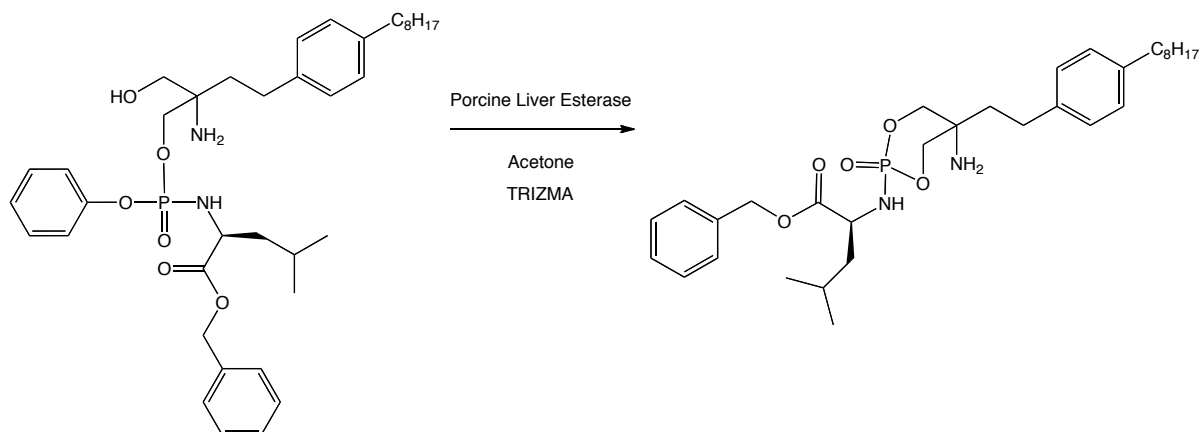


Figure 5.16 Stacked ^{31}P NMR spectra of Ph-LAla-OBzl-F processing by carboxypeptidase over 13 hours

5.2.6 Ph-Leu-OBzl-F Porcine Liver Esterase Experiment



Scheme 5.9 Ph-Leu-OBzl-F carboxypeptidase processing experiment

A larger scale porcine liver esterase experiment was conducted on Ph-Leu-OBzl-F and monitored *via* TLC as previously described.² Again the main product of the reaction was the, now expected, cyclisation product as shown in scheme 5.9. The predicted mass is 572.34 g/mol and the observed mass of the product of the reaction is 573.35 m/z.

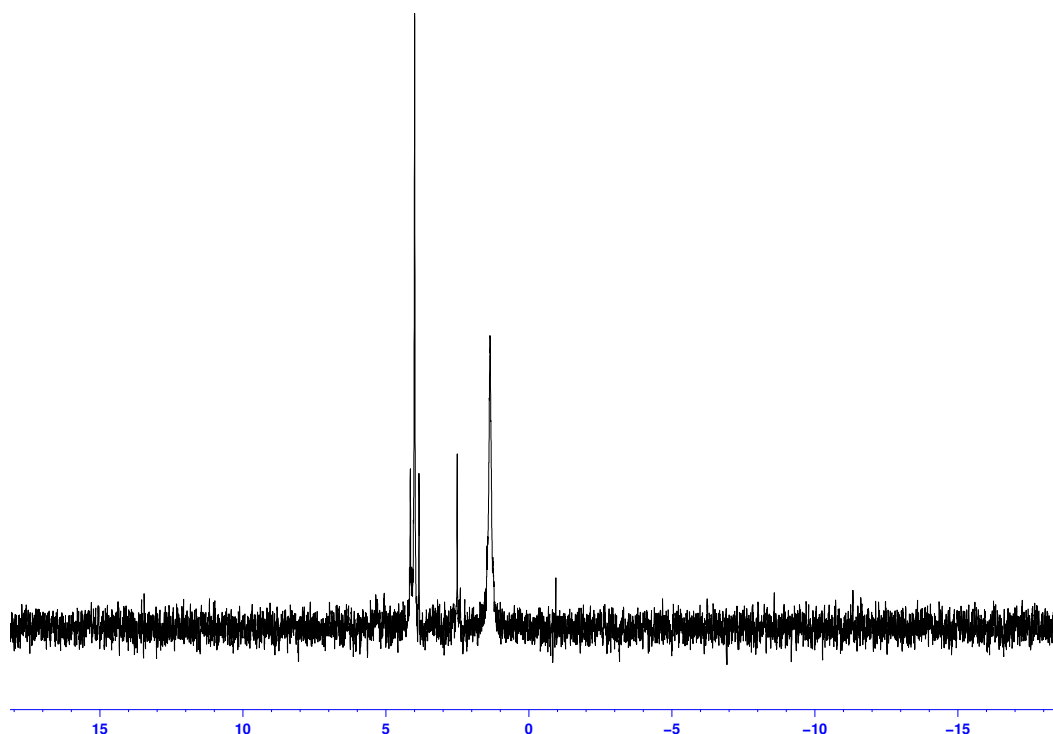
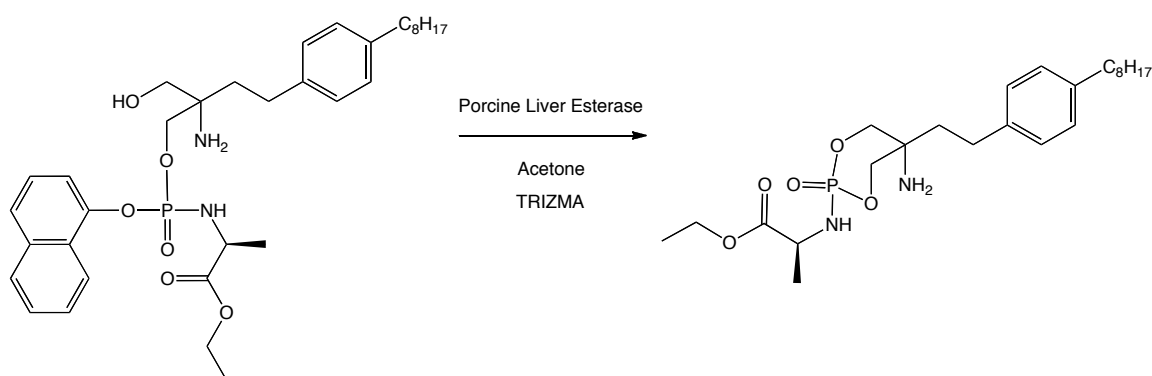


Figure 5.17 ^{31}P NMR spectrum of organic extract of Ph-Leu-OBzl-F large scale enzymatic experiment with porcine liver esterase

5.2.7 Naphth-LAla-OEt-F Porcine Liver Esterase Experiment



Scheme 5.10 Unwanted cyclisation of Naphth-LAla-OEt-F to compound of observed mass of 469.3 m/z

Another porcine liver esterase experiment was conducted on Naphth-LAla-OEt-F. This experiment is an adequate test of the hypothesis that the major product of these enzymatic reactions is the cyclisation product as previously described. The only difference between Ph-LAla-OEt-F and Naphth-LAla-OEt-F is that one

compound contains a phenol attached to the phosphorus and the other compound contains a naphthol attached to the phosphorus. If the cyclisation hypothesis is correct then the major degradation product of both Ph-LAla-OEt-F and Naphth-LAla-OEt-F should be the same compound with an identical chemical shift as observed by ^{31}P NMR and identical mass as observed by mass spectrometry. Indeed the major degradation product has a mass peak ion of 469.3 m/z which is identical to the mass observed for both porcine liver esterase and carboxypeptidase processing experiments with Ph-LAla-OEt-F.

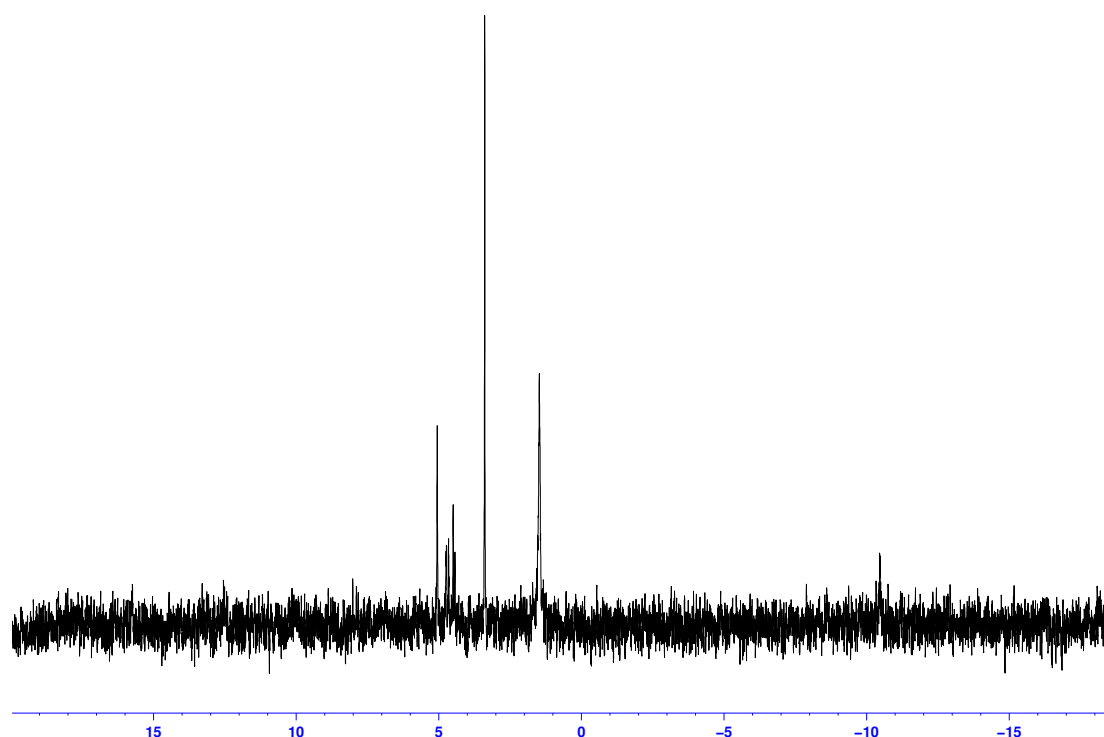
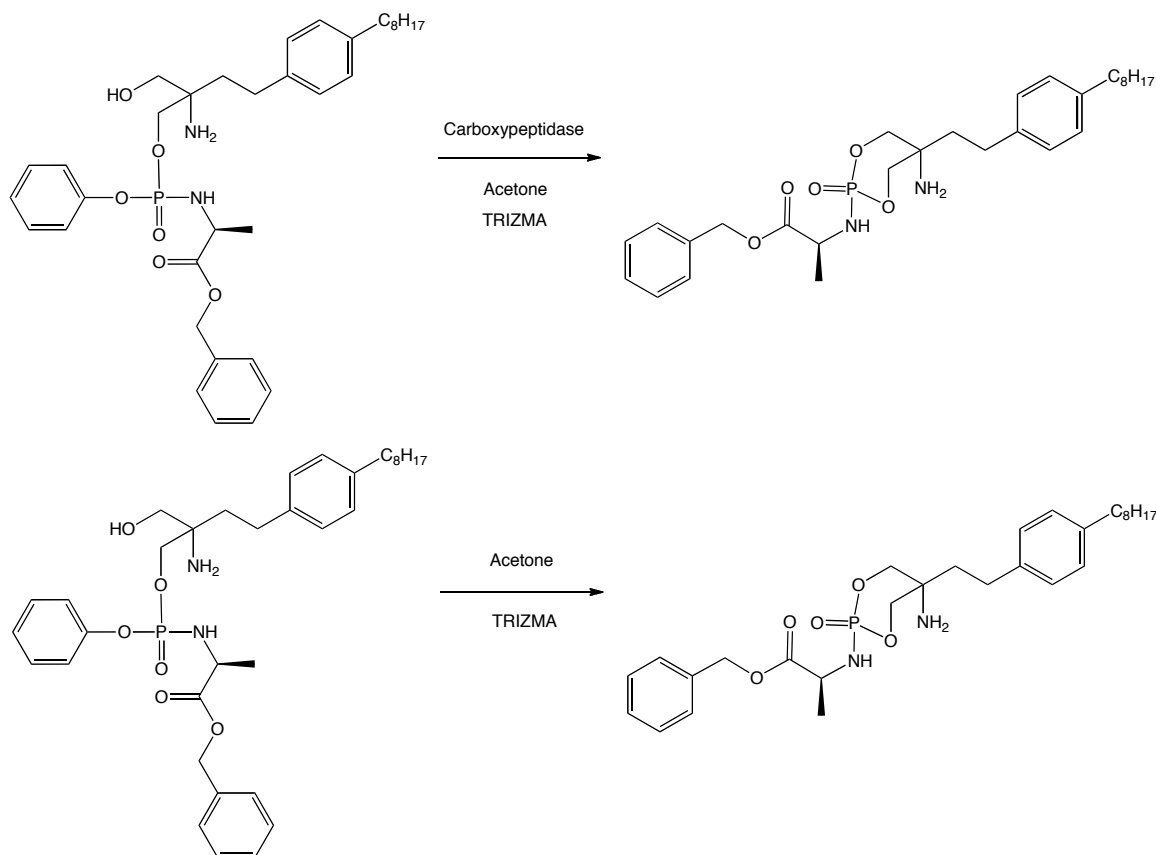


Figure 5.18 ^{31}P NMR spectrum of organic extract of Naphth-LAla-OEt-F large scale enzymatic experiment with porcine liver esterase

5.2.8 Controlled Ph-LAla-OBzl-F Carboxypeptidase Experiment



Scheme 5.11 Controlled Ph-LAla-OBzl-F carboxypeptidase processing experiment

In an effective, and somewhat elegant, final test of the cyclisation hypothesis another controlled carboxypeptidase experiment was conducted on Ph-LAla-OBzl-F. This time great care was taken to ensure that the contents of both NMR tubes were identical apart from one contained carboxypeptidase and one tube did not. In this experiment both the final control ³¹P NMR data and enzymatic ³¹P NMR data are identical and so were the fragmentation patterns observed *via* mass spectrometry. These data confirm beyond any reasonable doubt that the basic environment catalyses the observed cyclisation and the enzyme has no opportunity to process the phosphoramidate moiety before it is quickly decomposed by the adjacent free OH of the fingolimod parent molecule. The major ion observed in the mass spectrometry data in both the control and enzyme experiments has a mass of 531.31m/z which corresponds exactly to the predicted mass of the cyclised compound of 530.29 g/mol.

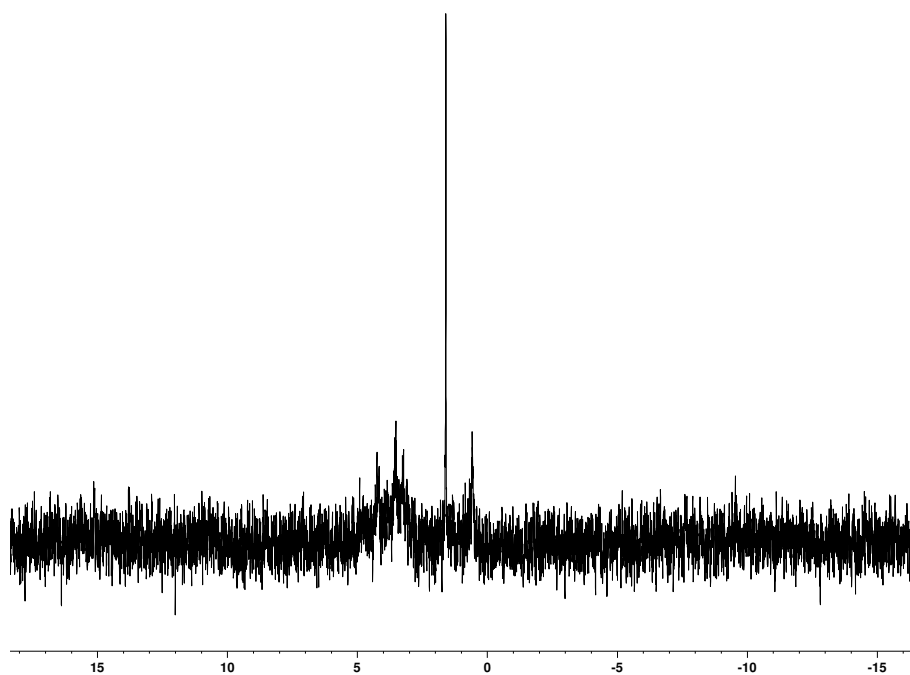


Figure 5.19 ^{31}P NMR spectrum of Ph-LAla-OBzl-F control with no enzyme in acetone and Trizma after 24 h

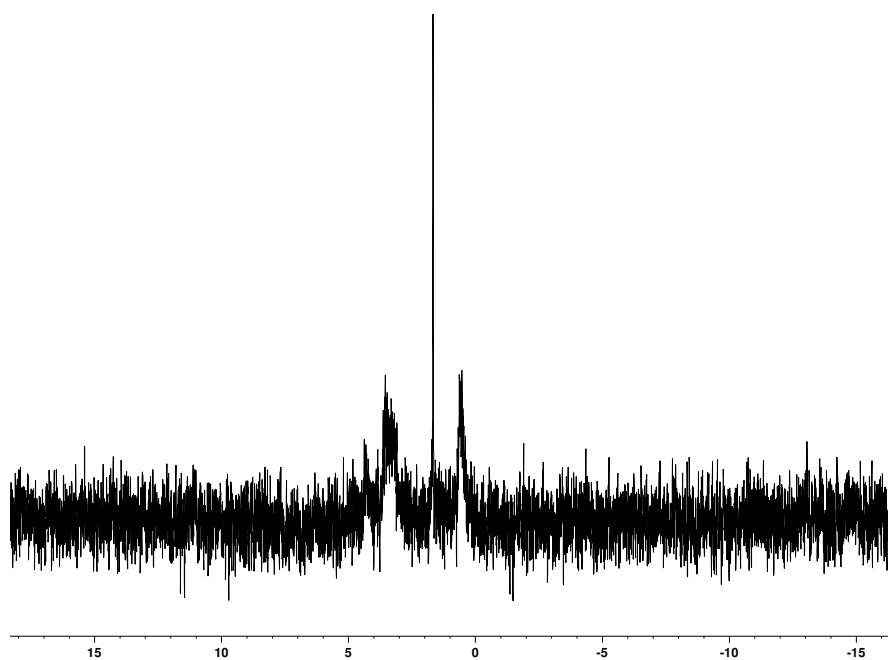
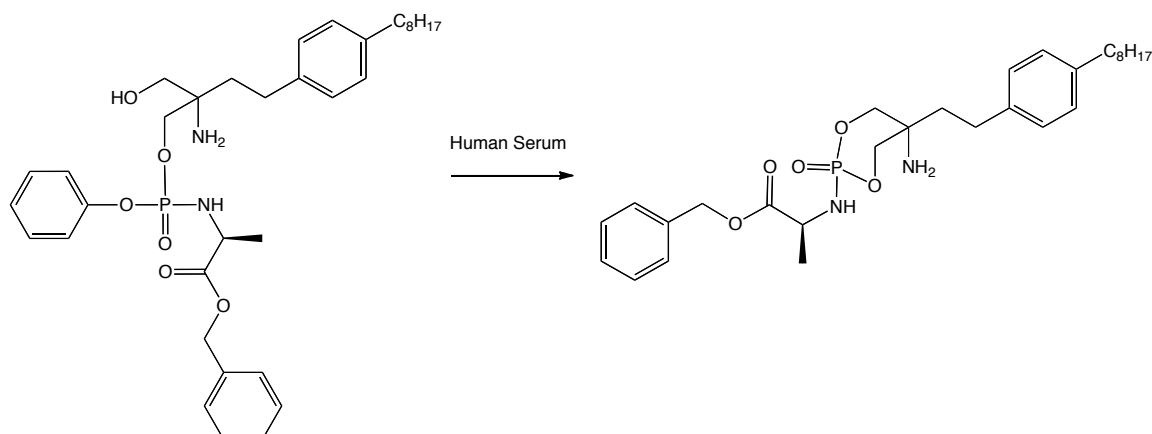


Figure 5.20 ^{31}P NMR spectrum of Ph-LAla-OBzl-F with carboxypeptidase in acetone and Trizma after 24 h

5.2.9 Ph-LAla-OBzl-F Human Serum Experiment



Scheme 5.12 Ph-LAla-OBzl-F human serum processing experiment

A stability study of Ph-LAla-OBzl-F in human serum was also conducted following a previously reported procedure.¹ It appears that, as with the enzymatic experiments, the major product is likely to be the same unwanted cyclised product. The parent peak in this case is not observed as it is not significantly soluble in the D₂O, serum and DMSO environment.

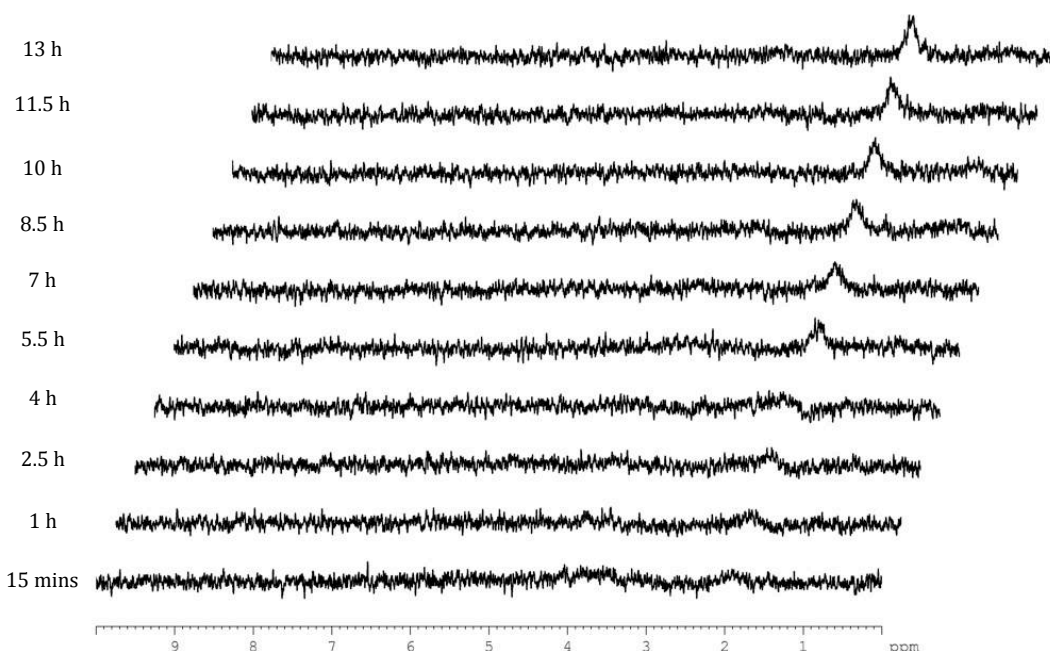


Figure 5.21 Stacked ³¹P NMR spectra of Ph-LAla-OBzl-F decomposition in human serum over 13 hours

The major peaks observed in the positive mode mass spectrum were:

- 380.07 m/z
- 438.03 m/z
- 464.12 m/z
- 532.28 m/z

The exact mass of the cyclised structure is 530.29 g/mol so in this case none of the observed peaks correspond exactly to the cyclised compound. The peak with a mass of 532.28 m/z is clearly very similar to the mass of the cyclised product but unlike with the carboxypeptidase experiments no peak that corresponds exactly to the $[M+H^+]$ cyclised compound peak is observed. During the time in which this mass spectrometric analysis was conducted the MS device used repeatedly gave results in which the peak corresponding to the expected product had a mass +1 that would be expected. This occurred with numerous samples and so the most likely explanation for the 532.28 m/z peak is that it is in fact the cyclised structure expected and the +1 mass observed is an artefact of a slightly malfunctioning mass spectrometer.

The major peaks observed in the negative mode mass spectrum were:

- 334.07 m/z
- 392.04 m/z
- 450.01 m/z
- 507.98 m/z
- 565.95 m/z
- 567.94 m/z
- 623.91 m/z

The exact mass of the parent Ph-LAla-OBzl-F molecule is 624.33 g/mol so possibly the peak of 623.91 m/z $[M-H]$ corresponds to that. The mass of the desired monophosphate is 387.22 g/mol and none of the peaks observed correspond to that. The peak at 334.07 m/z in the negative mode analysis is perhaps due to the cleaved ProTide moiety as shown in figure 5.22 $[M-H]$. The mass data obtained was

thoroughly compared with published fingolimod degradation mass data⁴, with modifications of the structures to include likely ProTide degradation products but no other proposed structures appear to correlate with the mass data observed for the human serum degradation products.

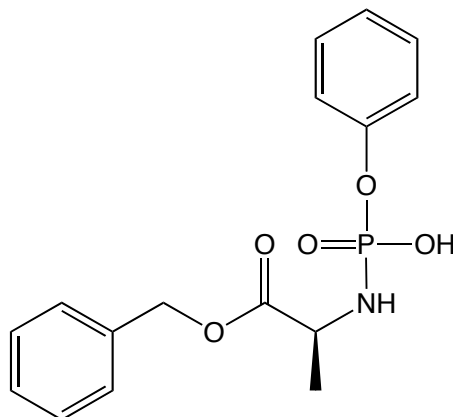


Figure 5.22 Likely human serum degradation product with exact mass of 335.09 g/mol

5.3 Final Conclusions

The enzymatic processing experimental data have repeatedly shown that all ProTide fingolimod analogues tested are not processed as initially expected to any of the desired compounds as shown in scheme 5.3. It seems that the adjacent free OH on the fingolimod parent molecule gives rise to an unacceptable level of instability and lack of effective processing to the final pharmacologically active monophosphate or expected intermediates. The logical conclusion to mitigate this problem, if one still wishes to develop novel phosphoramidate S1P receptor modulator compounds, is to synthesise S1P receptor modulator parent molecules which only contain one OH group and convert them to phosphoramidates as shown in figure 5.23.

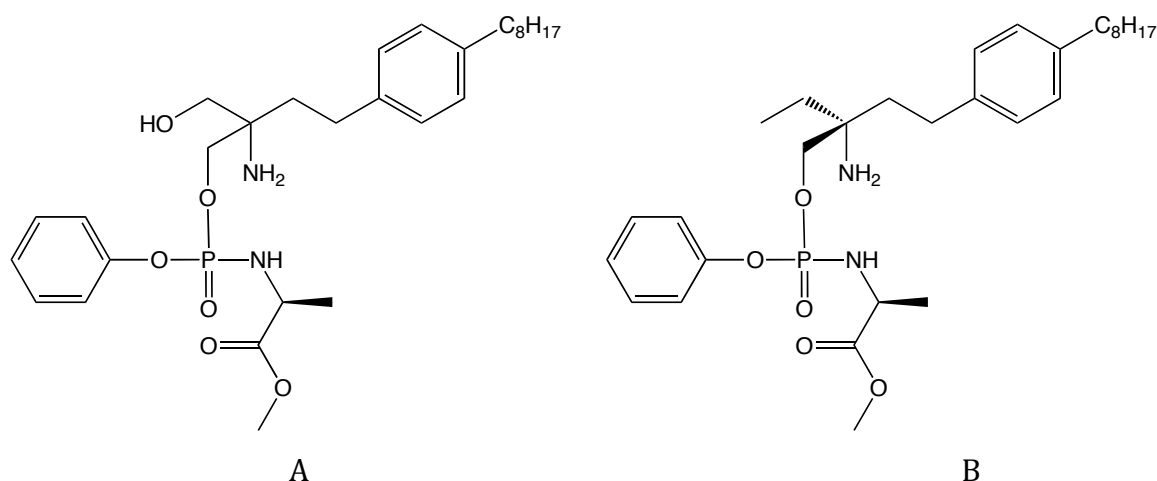


Figure 5.23 The enzymatic and stability studies of ProTide fingolimod analogues yielded data which suggest that compound B above is likely to be far more stable than compound A

While later biological data obtained by our collaborators in the School of Biosciences (data not shown) suggest that ProTide fingolimod analogues do have favourable biological activity on neurons, the processing experiments described have repeatedly demonstrated poor levels of stability. ProTide fingolimod analogues have been found to degrade quite rapidly when stored at room temperature and even in the freezer (data not shown). One cannot be sure that during storage over a period of weeks or months that no ProTide fingolimod has degraded over time. In order for a drug to be approved by the FDA typically it needs to be stable under normal ambient conditions. Storage of ProTide

fingolimod analogues at room temperature has led to degradation and therefore it appears unlikely that ProTide fingolimod analogues present a realistic therapeutic opportunity.

A method of mitigating the unwanted cyclisation issue was investigated by Dr Fabrizio Pertusati. The structure shown in figure 5.24 possesses a *p*-methoxy group on the phenyl component of the phosphoramidate. While this structure may improve stability (unpublished results) it is unlikely to completely mitigate the unwanted cyclisation issue and the cyclisation will presumably just proceed at a slower rate. The synthesis of the *p*-methoxy analogue still leaves the unwanted diastereoisomer issue unaddressed and stability is likely to be too much of an issue for FDA approval.

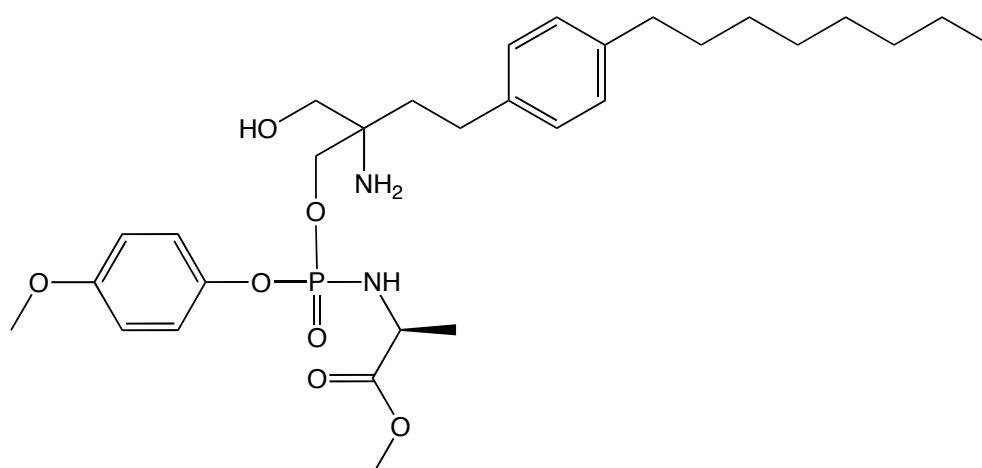


Figure 5.24 Alternative structure designed to improve upon ProTide fingolimod stability. Not chosen for detailed synthesis and analysis as the structure still leaves other synthetic and purification challenges unmitigated.

5.4 References

1. McGuigan C, Murziani P, Slusarczyk M, Gonczy B, Voorde J, Liekens S, Balzarini J. Phosphoramidate ProTides of the anticancer agent FUDR successfully deliver the preformed bioactive monophosphate in cells and confer advantage over the parent nucleoside. *J. Med. Chem.*, **2011**, 54, 7247-7258.
2. McGuigan C, Tsang H, Sutton P, Clercq E, Balzarini J. Synthesis and anti-HIV activity of some novel chain-extended phosphoramidate derivatives of d4T (stavudine): esterase hydrolysis as a rapid predictive test for antiviral potency. *Antivir. Chem.*, **1998**, 9, 109-115.
3. Evans D, Pye G, Bramley R, Clark A, Dyson T, Hardcastle J. Measurement of gastrointestinal pH profiles in normal ambulant human subjects. *Gut*. **1988**, 29, 1035-1041.
4. Patel P, Kalariya P, Gananadhamu S, Srinivas R. Forced degradation of fingolimod: Effect of co-solvent and characterization of degradation products by UHPLC-Q-TOF-MS/MS. *J. Pharm. Biomed. Anal.* **2015**, 115, 388-394.

Chapter 6 – Benzyl Ether Derivative “Tsuji” Compounds

6.1 Rationale for Selection of BED Family of Compounds for Phosphorus Prodrug Synthesis

After the initial stability and enzymatic studies on ProTide fingolimod did not appear to give favourable results it was decided that it would be better to synthesise phosphorus prodrugs of chiral parent molecules which only contain one OH group. The rationale for this can be summarised as follows:

1. Improved stability (removes possibility of cyclisation by the free adjacent OH group)
2. Removes issues of unwanted diastereoisomers of the final product

As shown in section 1.4.5 of the introduction there are a large number of candidates which meet the requirements. In fact before beginning any experimental work the fingolimod analogue shown in figure 6.1 below was considered an excellent candidate for ProTide synthesis as it does not possess the free OH and the predicted problems of having a racemic mixture of the final product.

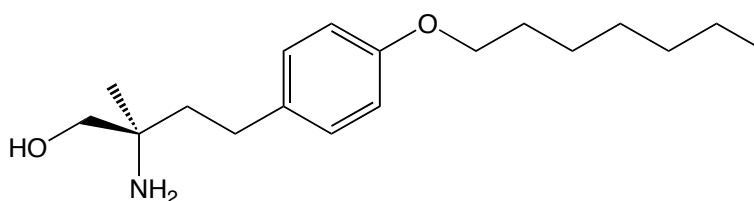


Figure 6.1 This compound, AAL(R), was initially considered an excellent candidate for ProTide synthesis

While the compound above is the published compound¹ by far the most analogous to fingolimod that has the desired single OH it was decided that it would perhaps be more worthwhile to investigate other S1P receptor modulators. AAL(R) has a very similar S1P₁ to S1P₃ selectivity to fingolimod² and as previously explained it is the unwanted modulation of the S1P₃ receptor which is believed be responsible for a number of fingolimod's unwanted side effects such as bradycardia³,

hypertension⁴ and unwanted thickening of the heart valves known as cardiac fibrosis.⁵ The available literature was extensively searched to find S1P receptor modulators which possess favourable S1P₁ to S1P₃ selectivity, a synthesis of relative feasibility and, importantly, a mono alcohol functionality.

Due to the commercial success of FTY720 a large amount of interest has arisen regarding the development of novel S1P receptor modulators. The result is that there are a large number of papers that detail the synthesis and biological evaluation of novel S1P receptor modulators developed in many academic research groups and private companies globally. A large proportion of these analogues are diols and, as previously explained in chapter 5, these are not of interest to the research described herein due to the inevitable unwanted cyclisation of phosphoramidate prodrugs. Some examples of S1P receptor modulator diols which were not of interest include the structures shown in figures 6.2 – 6.4.

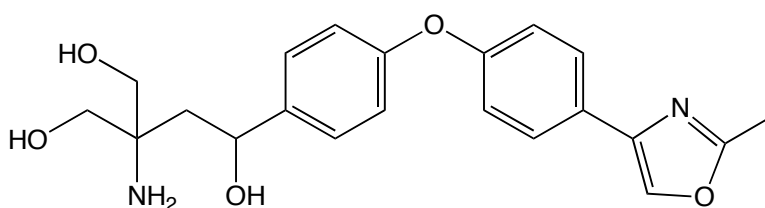


Figure 6.2 This compound has reported favourable biological activity⁶ but was not selected for phosphoramidate synthesis due to expected unwanted cyclisation issues

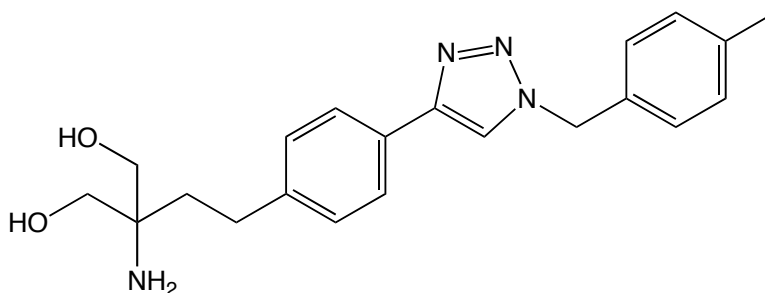


Figure 6.3 This compound has reported favourable biological activity⁷ but was not selected for phosphoramidate synthesis due to expected unwanted cyclisation issues

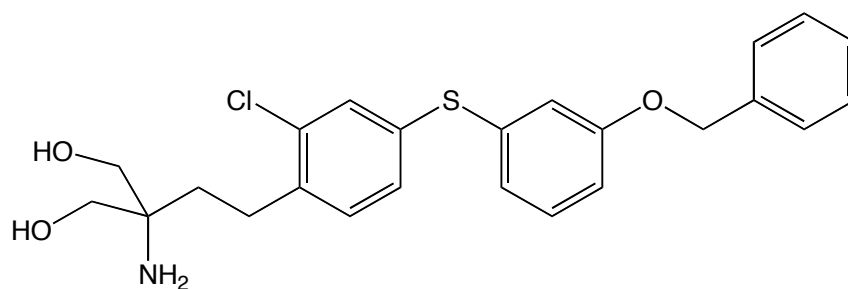


Figure 6.4 This compound, KRP-203, has reported favourable biological activity^{8,3} but was not selected for phosphoramidate synthesis due to expected unwanted cyclisation issues

Some novel S1P receptor modulators do not need to be phosphorylated *in vivo* in order to be pharmacologically active. The application of ProTide technology to S1P receptor modulators which do not need to be phosphorylated *in vivo* is not, at least based on current understanding, likely to yield therapeutically useful novel compounds. The compound shown in figure 6.5 is one such example. The compound shown in figure 6.5 contains only one alcohol group so the cyclisation problem should not arise but it is reported that phosphorylation is not required for favourable therapeutic activity and therefore the application of phosphoramidate technology was not seriously considered.

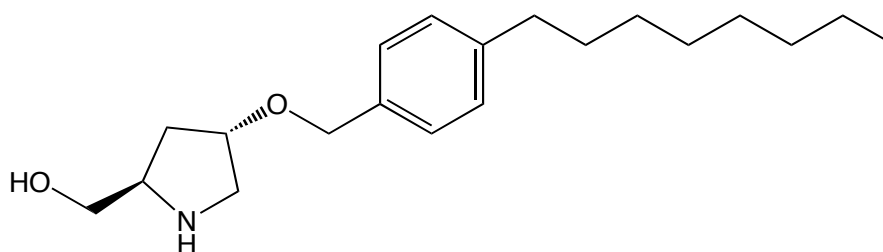


Figure 6.5 This compound has reported favourable biological activity⁹ but was not selected for phosphoramidate synthesis due to it being reported that phosphorylation is not necessary for therapeutic viability

A number of papers have been published which detail the organic synthesis of potentially effective S1P receptor modulators that satisfy the criterion of being a mono alcohol but no biological data are reported. Due to the fact that no biological data are reported these potentially interesting compounds were not selected for phosphoramidate synthesis as there is no published evidence to suggest that these compounds could be potentially useful therapeutics. Two examples of such compounds are shown in figures 6.6 and 6.7.

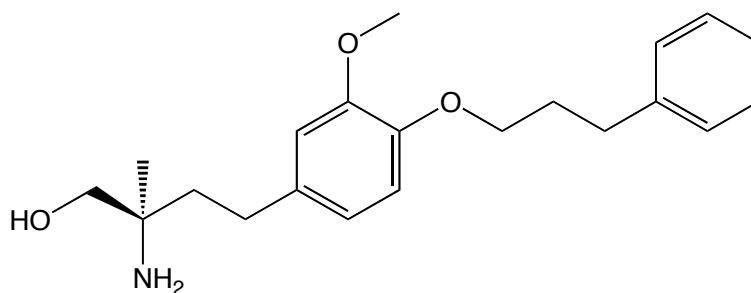


Figure 6.6 This compound has no reported favourable biological activity¹⁰ and was therefore was not selected for phosphoramidate synthesis

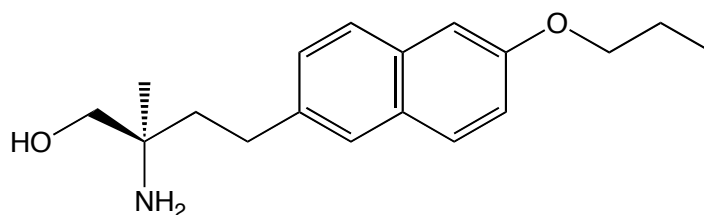


Figure 6.7 This compound has no reported favourable biological activity¹¹ and was therefore was not selected for phosphoramidate synthesis

Some papers have published detailed syntheses and biological evaluation of S1P receptor modulators which could potentially benefit from phosphoramidate technology but S1P₁ to S1P₃ selectivity is not reported.¹² Compounds which have no reported S1P₁ to S1P₃ selectivity were not selected for phosphoramidate synthesis as unwanted side effects are somewhat more difficult to predict.

A number of papers report the synthesis of mono alcohol S1P receptor modulators with favourable S1P₁ to S1P₃ selectivity but the experimental sections of the papers are not as comprehensive as in the paper eventually chosen. These compounds^{13,14,15,16} were not chosen for the first application of phosphoramidate technology to mono alcohol S1P receptor modulators as it was expected that there would be a potentially very lengthy period of experimentation to finally yield the desired parent compounds.

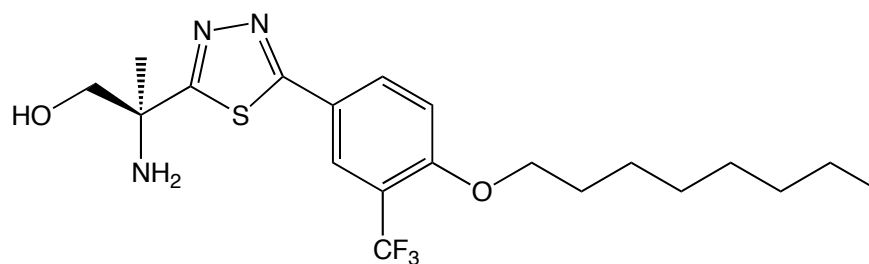


Figure 6.8 This compound, GSK1842799, has reported favourable biological activity and possesses the desired mono alcohol moiety; however the synthesis is not explained in great detail and was therefore was not selected for the first phosphoramidate synthesis of a mono alcohol S1P receptor modulator¹³

The first family of non-FTY720 compounds that was selected for phosphoramidate modification was published by Takashi Tsuji *et al* in 2014.¹⁷ The family of structures reported in their paper are colloquially referred to as *Tsuji compounds* and are referred to formally as *benzyl ether derivative (BED) compounds*. The BED family was selected for the following reasons:

1. Detailed organic syntheses reported
2. Excellent S1P₁ to S1P₃ selectivity of some analogues
3. Mono alcohol functional group of parent compounds
4. Chiral HPLC not required
5. Poor *in vivo* phosphorylation rate of the most S1P₁ to S1P₃ selective analogues making them ideal candidates for the application of phosphorus prodrug technology

The compound shown in figure 6.9 is the simplest analogue in the BED family and the phosphorylated version is reported to have far greater S1P₁ to S1P₃ selectivity than phosphorylated fingolimod as shown in table 6.1.¹⁷

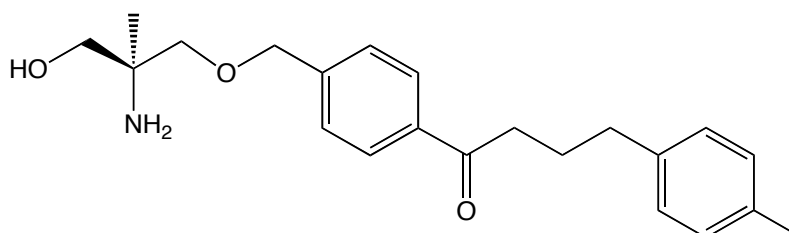
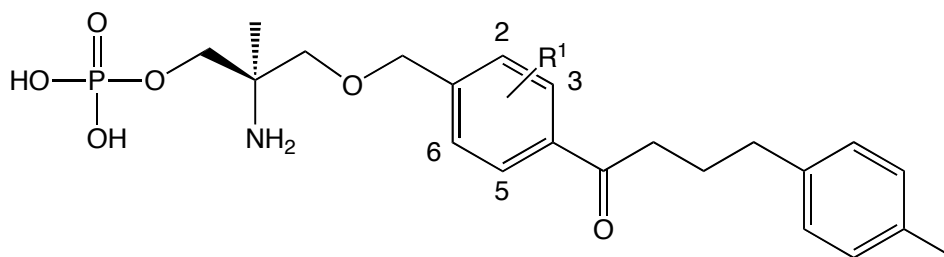


Figure 6.9 Simplest "Tsuji compound", BED(a)



Compound	R ¹	S1P ₁	S1P ₃	Selectivity (S1P ₁ / S1P ₃)
		γGTP EC ₅₀ (nM)	γGTP EC ₅₀ (nM)	
FTY720-p	N/A	7.0	2.0	0.29
BED(a)-p	H	7.0	200	29
BED(b)-p	2-Me	3.0	180	60
BED(c)-p	3-Me	19.0	>20,000	>1052
BED(d)-p	2-F	2.8	60	21
BED(e)-p	2-Cl	4.0	220	55
BED(f)-p	2-Et	2.3	12,000	5217
BED(g)-p	2,6-Me ₂	2.2	340	155
BED(h)-p	2,5-Me ₂	6.5	>20,000	>3077

Table 6.1 SAR information about the biological activity and S1P₁ to S1P₃ selectivity of fingolimod phosphate and the phosphates of different BED analogues¹⁷

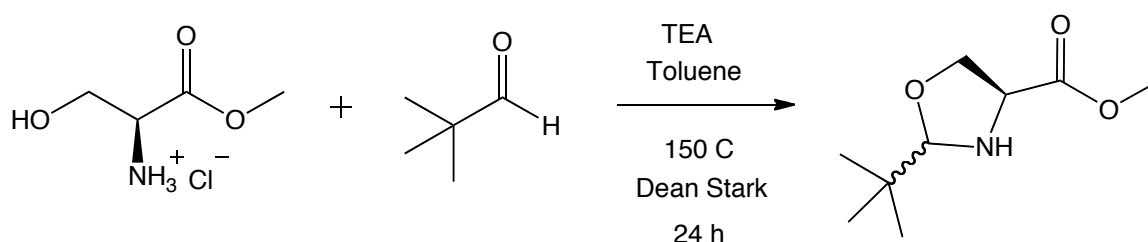
Their paper states that, "...compounds **2f** and **2h** (BED(f) and BED(h) in table 6.1), of which phosphates showed high selectivity to S1P₁, unfortunately demonstrated almost no efficacy in rat HvGR, inhibiting only 10% and 11% of immunoreactions compared with the vehicle controlled group. To investigate the reason for this drastic deactivation, we measured the phosphorylation rate of each compound in rat whole blood. Through this analysis, it was revealed that efficacious compounds **2a**, **2b** and **2e** were properly converted to their phosphate after three hours of being added to rat whole blood, resulting in 39.5%, 83.8% and 38.4% conversion from parental alcohol to phosphate, respectively, while ineffective compounds **2f** and **2h** were transformed in only 13.9% and 6.0% of the total compounds. With this result it is reasonable to speculate that the bulkiness of the central benzene ring moiety of **2a** largely affected the substrate recognition of the responsible kinases which convert our compounds to their phosphates in whole blood, and thereby, the phosphorylation

6.2 Synthesis of BED Compounds

6.2.1 Synthesis of BED(a)

The synthesis of the compounds in the early stages of the total synthesis are not adequately described in the paper¹⁷ and some further literature searching and repeated experimentation was required in order to synthesise the desired compounds with an acceptable yield.

After multiple attempts at using different solvents (toluene, pentane and methanol), temperatures, glassware, reaction times and purification methods an amalgamation of synthetic procedures found in 3 papers^{17,18,19} was eventually developed to yield the compound shown in scheme 6.1 in acceptable yields (>80%). It was found that thorough grinding of the L-serine methyl ester HCl starting material improved the yield. As the starting material is not soluble in toluene, thorough grinding increases the surface area of the amino acid ester when in suspension in toluene. The description in Seebach's 1984 paper that the experiment was conducted with "continuous removal of water"¹⁸ was deciphered to mean that the use of a Dean Stark trap was employed as shown in figure 6.11. The use of Dean Stark apparatus allows the selective removal of water but without the unwanted excessive loss of toluene solvent. The continuous loss of water from the reaction system may help to drive the reaction further to completion.



Scheme 6.1 Synthesis of (4S)-methyl 2-(tert-butyl)oxazolidine-4-carboxylate

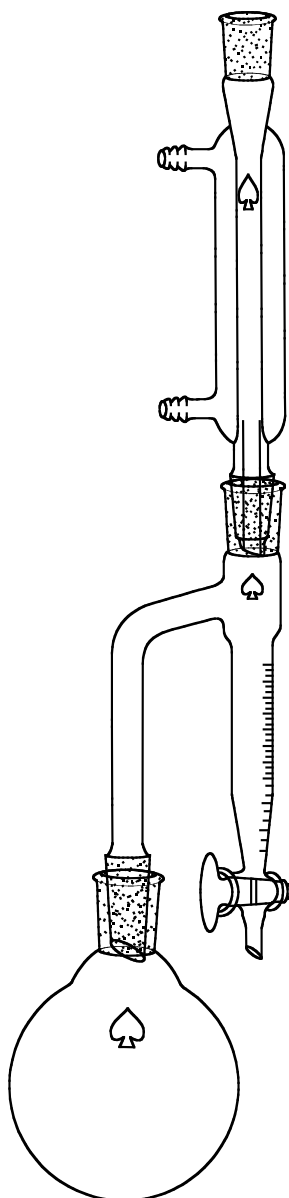
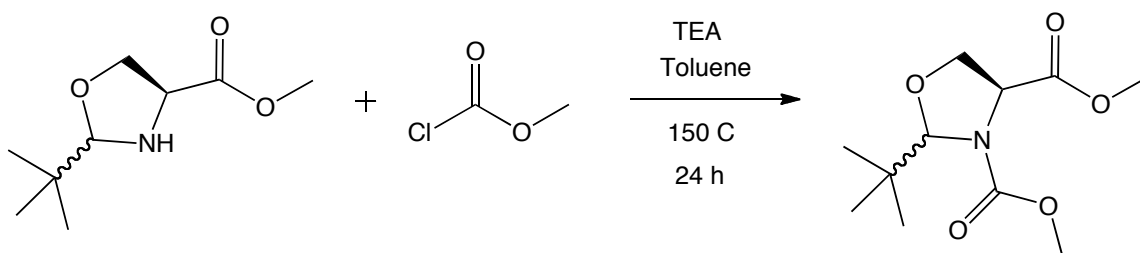


Figure 6.11 Diagram of Dean Stark apparatus set up in a fashion similar to that used to successfully synthesise the compounds described in schemes 6.1 and 6.2

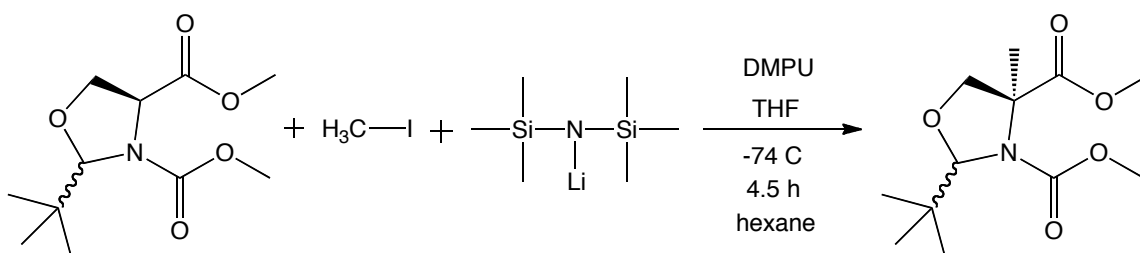
The synthesis of the following intermediate, as shown in scheme 6.2, was eventually tuned after a similar process of experimentation using different solvents (toluene, THF and DCM), temperatures (from $-78\text{ }^{\circ}\text{C}$ to $150\text{ }^{\circ}\text{C}$), glassware, reaction times (2 h to 72 h) and purification methods and a combination of different experimental procedures from different papers.^{17,19,20} In one paper¹⁹ it is recommended that the reaction is done below $5\text{ }^{\circ}\text{C}$, however after many variations of the synthetic procedure it was found that in order to obtain yields greater than 80% the reaction should be heated in toluene at $150\text{ }^{\circ}\text{C}$ using Dean Stark apparatus as in the first reaction shown in scheme 6.1. A fortunate feature of the syntheses of

the first two intermediates is that the reaction conditions required for both reactions are very similar and that the purification simply requires an extraction, vacuum filtration and removal of solvent under vacuum. Column chromatography is not required for the first two stages of BED compound synthesis which helps to improve the speed and ease with which the synthesis can be achieved.



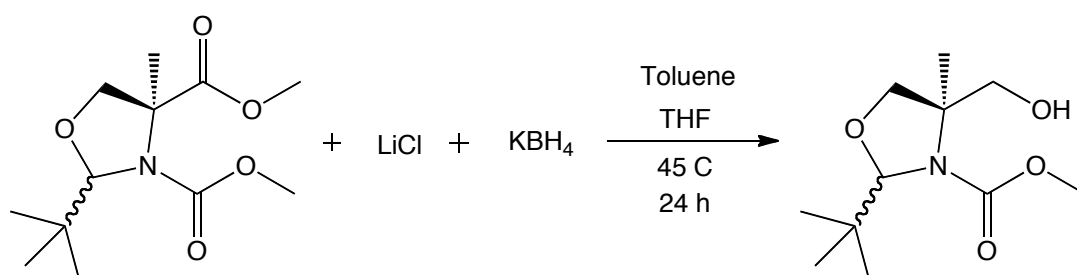
Scheme 6.2 Synthesis of (4S)-dimethyl 2-(tert-butyl)oxazolidine-3,4-dicarboxylate

The synthesis of the third intermediate in BED compound synthesis also underwent a number of variations in reagents (potassium *t*-butoxide and lithium bis(trimethylsilyl)amide), reaction time, temperature and purification methods and the final procedure was also devised from a combination of procedures from different papers^{17,21,22} and fine tuning of the experimental technique. An unusual quirk of the synthesis, as shown in scheme 6.3, is that if the reaction is done at -78 °C the whole mixture congeals and forms a hard solid but if the mixture is kept at -74 °C the reaction is very effective. At temperatures much warmer than -74 °C the yield is compromised. Achieving this delicate balance in temperature was eventually accomplished by simply conducting the reaction in a dry ice bath with no added acetone. The mixture is quenched using saturated ammonium chloride solution and care needs to be taken to add it slowly as excessive effervescence and loss of product can occur if the ammonium chloride solution is added too rapidly.



Scheme 6.3 Synthesis of (4S)-dimethyl 2-(tert-butyl)-4-methyloxazolidine-3,4-dicarboxylate

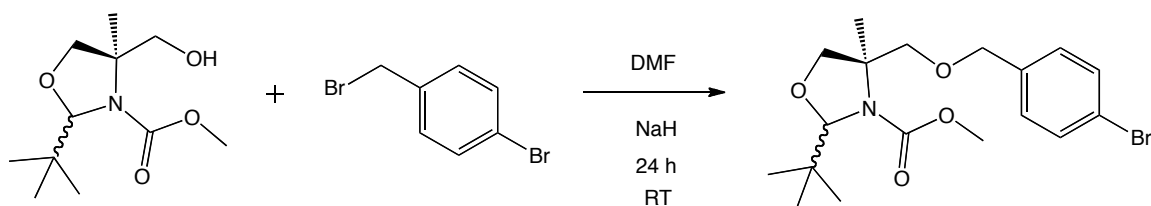
Synthesis of the fourth intermediate of BED compound synthesis, of which no practical experimental procedure is detailed in the lead paper, underwent fewer variations than the preceding three compounds. The synthesis was developed principally using two papers.^{17,22} The key modifications made to the original procedure devised were an increase in temperature to 45 °C from room temperature, addition of toluene to the reaction mixture and the use of LiCl and KBH₄ as opposed to the more costly moisture sensitive LiBH₄.



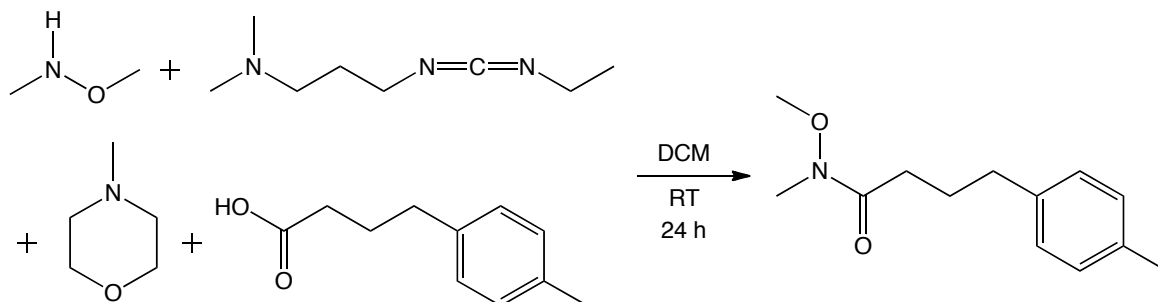
Scheme 6.4 Synthesis of (4*R*)-methyl 2-(*tert*-butyl)-4-(hydroxymethyl)-4-methyloxazolidine-3-carboxylate

The first time the product shown in scheme 6.4 above was successfully synthesised the overall yield was a mere 2.5% (187 mg) after initially starting with 5 g L-serine methyl ester HCl as in scheme 6.1. However, after a period of experimentation and streamlining of the synthetic process, much more acceptable overall yields were achieved. An example of a greatly improved overall yield of (4*R*)-methyl 2-(*tert*-butyl)-4-(hydroxymethyl)-4-methyloxazolidine-3-carboxylate as shown in scheme 6.4 from the initial 5 g L-serine methyl ester HCl is an overall yield of 46% (3.432 g).

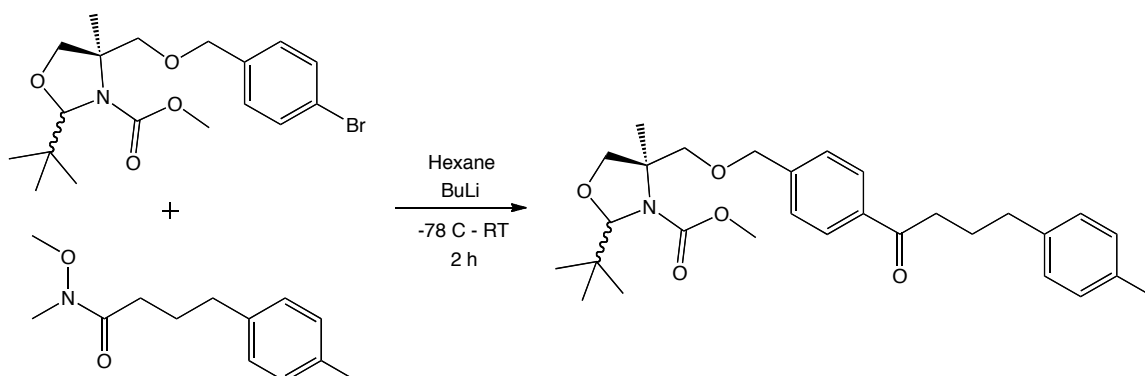
Once achieving satisfactory yields of the initial 4 intermediates of the BED(a) synthesis was attained the rest of the synthetic process was more straightforward to accomplish as the later stages are detailed in the experimental section of the lead paper.¹⁷



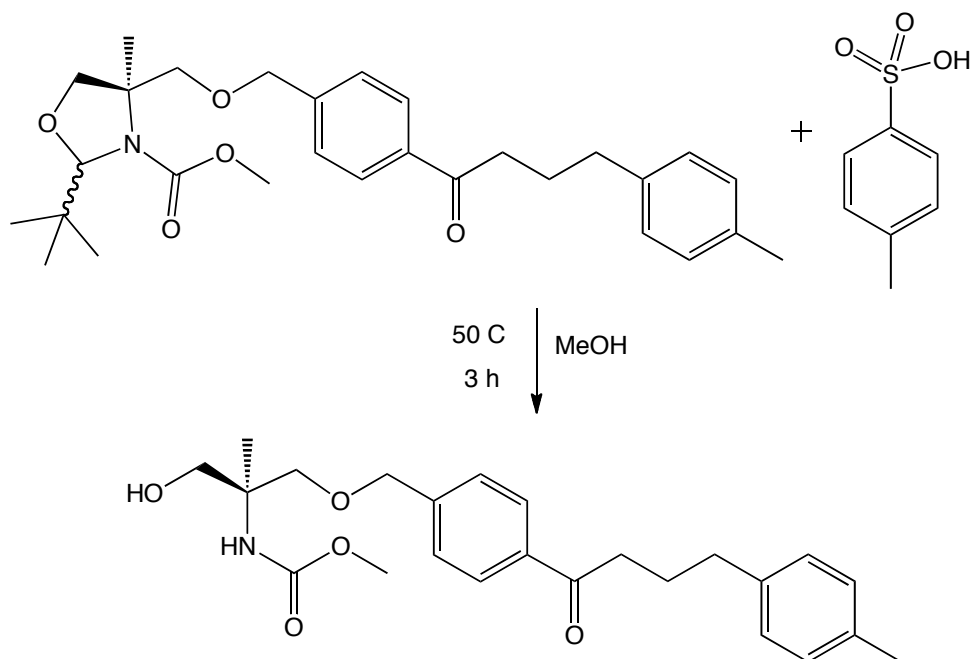
Scheme 6.5 Synthesis of (4R)-methyl 4-(((4-bromobenzyl)oxy)methyl)-2-(tert-butyl)-4-methyloxazolidine-3-carboxylate has been achieved with a yield of 70% (3.415 g)



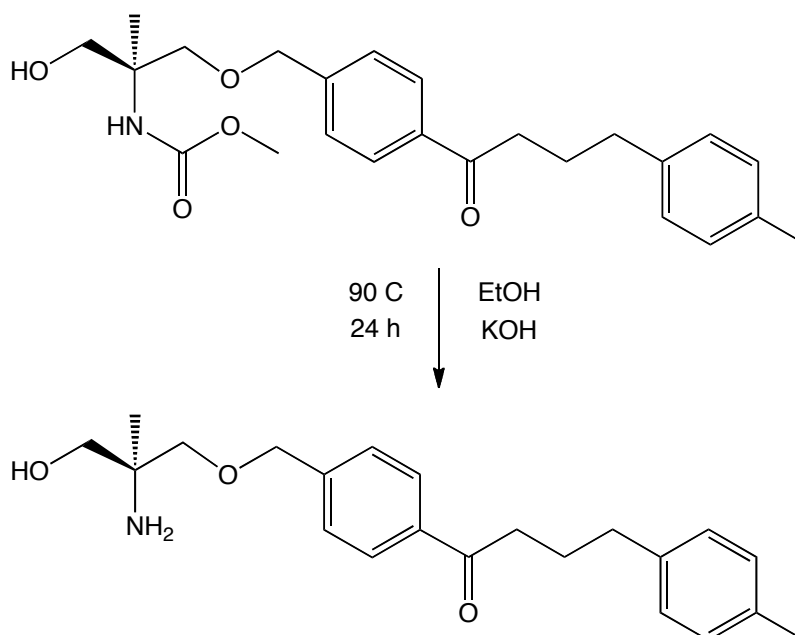
Scheme 6.6 Synthesis of the Weinreb amide N-methoxy-N-methyl-4-(p-tolyl)butanamide has been achieved with a yield of 82% (5.084 g)



Scheme 6.7 Synthesis of (4R)-methyl 2-(tert-butyl)-4-methyl-4-(((4-(4-(p-tolyl)butanoyl)benzyl)oxy)methyl) oxazolidine-3-carboxylate remains the step with the lowest highest yield achieved for any one step in the total synthesis of BED(a) with a greatest yield of 38% (3.518 g)



Scheme 6.8 Synthesis of (*S*)-methyl (1-hydroxy-2-methyl-3-((4-(4-(*p*-tolyl)butanoyl) benzyl) oxy) propan-2-yl)carbamate has been achieved with a yield of 89% (2.691 g)



Scheme 6.9 Synthesis of (*S*)-1-(4-((2-amino-3-hydroxy-2-methylpropoxy)methyl)phenyl)-4-(*p*-tolyl)butan-1-one or BED(a) has been achieved with a yield of 73% (1.69 g)

Some alterations were made to the final stages of the synthesis. The final two steps as shown previously in schemes 6.8 and 6.9 are reported in the same experimental and no column is reportedly used to purify the product of the reaction shown in scheme 6.8. These stages were conducted separately and a column was used. In the

paper¹⁷ they report converting the final compound into a hydrochloride salt but this was not attempted as it was deemed unnecessary. The final BED(a) compound synthesised was analysed using polarimetry to measure the optical rotation giving an optical rotation value of $[\alpha] = 25.12$ ($[\alpha]_{\text{D}}^{24} = 0.5$) suggesting that the enantioselective chirality of the starting amino acid ester was retained and the final product is not a 50/50 racemic mixture.

6.2.2 Synthesis of BED(h)

In order to make the more S1P₁ selective analogues, as described in table 6.1, more complex compounds than 4-bromobenzyl bromide, as shown in scheme 6.5, need to be used. In the lead paper¹⁷ the syntheses of BED(h) and BED(f) are very poorly described, referring to experimental procedures in the paper which in fact do not exist. Even if one were to correct their procedural numbers to ones which do exist (e.g. taking procedure 4.1.4 to mean procedure 5.1.4) the explanation is still extremely limited and does not appear to be an approach which has a particularly high chance of success. In light of the insufficient information provided by the authors with regard to synthesising these lead compounds, and no relevant references being provided, novel experimentation and research was required. Based on the successful synthesis of BED(a) the logical reagents needed for the syntheses of BED(f) and BED(h) are shown in figure 6.12. Unfortunately the reagents which can potentially be used to synthesise the optimal target compounds BED(f) and BED(h) cannot be readily purchased at an acceptable price and must therefore be synthesised in the lab.

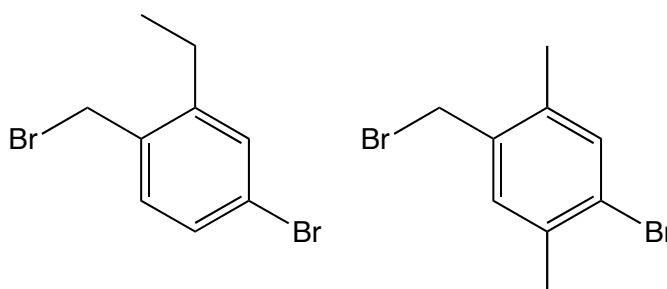
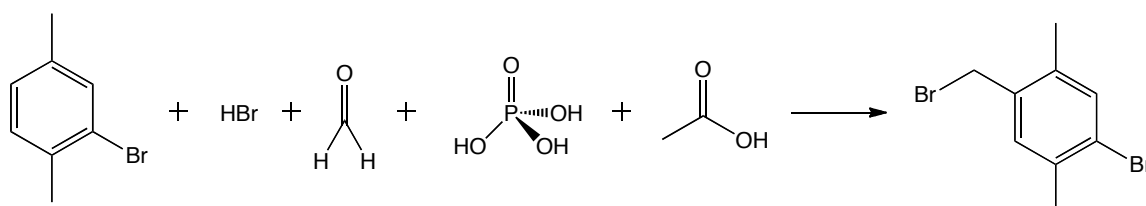


Figure 6.12 The reagents potentially needed to successfully synthesise optimal target compounds BED(f) and BED(h)

While superficially appearing to be relatively simple compounds the syntheses of the two structures shown in figure 6.12 pose a significant synthetic challenge. The synthesis of either compound is not explained in the lead paper¹⁷ and after an extensive literature search it was decided that the structure that can be used to synthesise BED(h), 1-bromo-4-(bromomethyl)-2,5-dimethylbenzene, would probably be the easiest of the two compounds to synthesise.²³ A synthesis as shown in scheme 6.10 was attempted and successfully achieved, however it appears that an unwanted inseparable (due to identical solubility) side product of the reaction is 2-bromo-3-(bromomethyl)-1,4-dimethylbenzene as shown in figure 6.13. After looking at the relative integrations of the main product and side product in the proton NMR spectrum, as shown in figure 6.14, it appears that the desired product and undesired product are synthesised in a ratio of approximately 2.5 : 1 respectively.



Scheme 6.10 Synthesis of 1-bromo-4-(bromomethyl)-2,5-dimethylbenzene²³

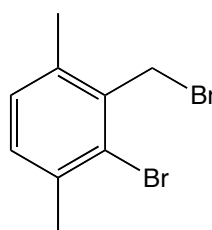


Figure 6.13 Unwanted 2-bromo-3-(bromomethyl)-1,4-dimethylbenzene side product

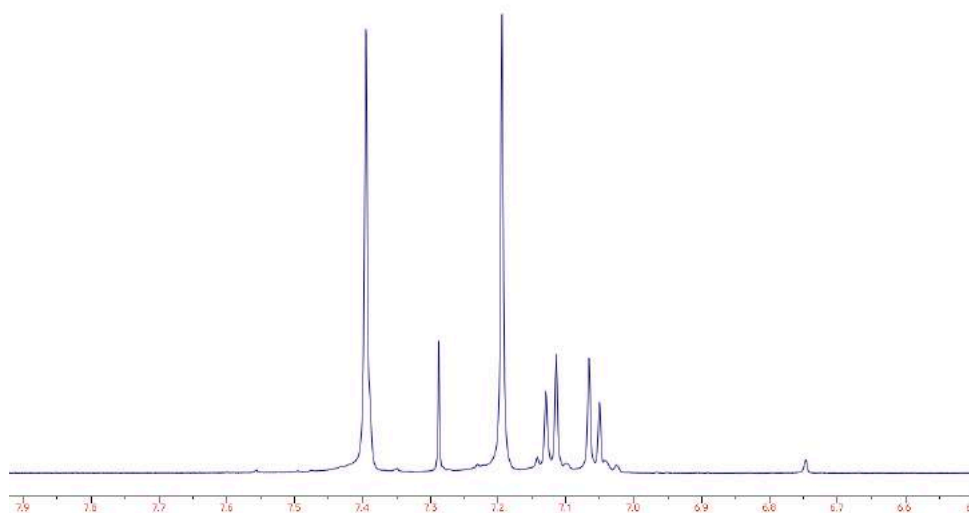
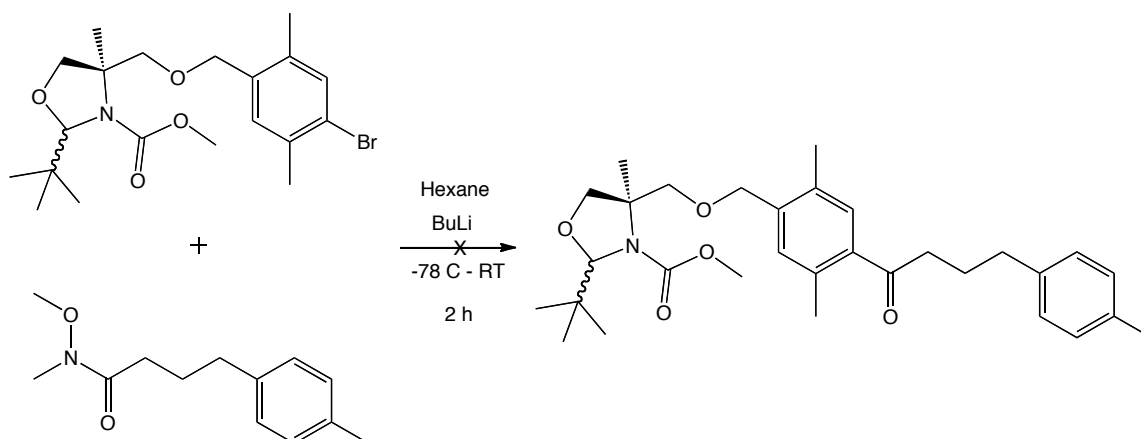
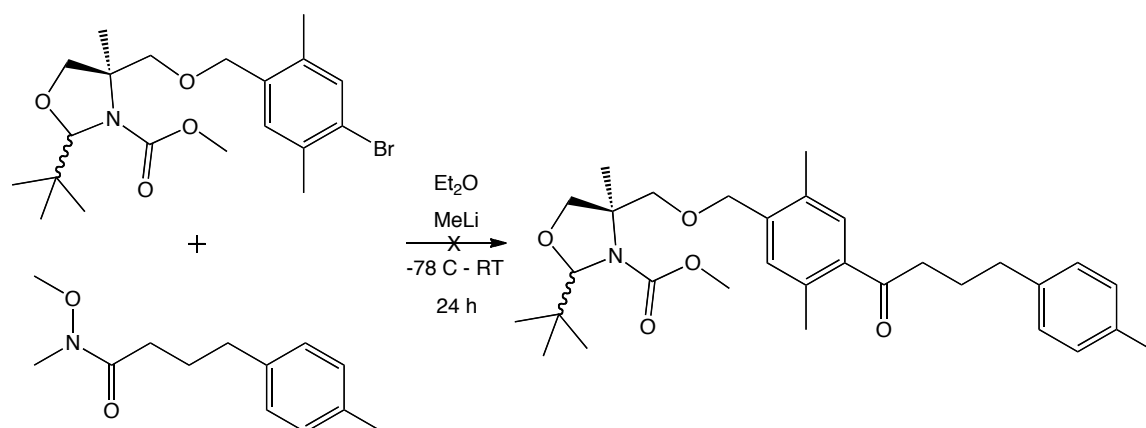


Figure 6.14 The area of the ¹H NMR spectrum of the product of the synthesis of 1-bromo-4-(bromomethyl)-2,5-dimethylbenzene which suggests the presence of the unwanted by-product 2-bromo-3-(bromomethyl)-1,4-dimethylbenzene (the peak at around 7.3 ppm is the CDCl₃ solvent peak)

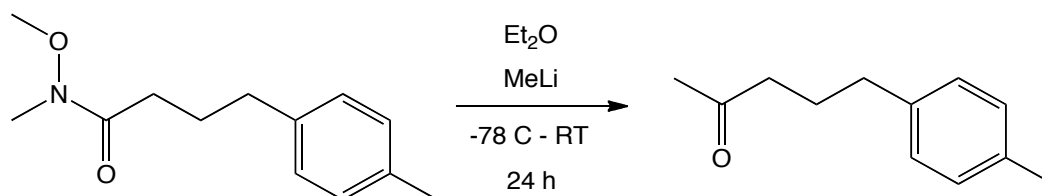
A further complication was encountered in the synthesis of BED(h) when the Weinreb amide coupling was unsuccessfully attempted as shown in scheme 6.11. After some discussion it was suggested that the butyl lithium reagent may be deprotonating the adjacent ortho methyl group on the bromo benzene ring and that perhaps a weaker base such as methyl lithium may yield better results. The same reaction was attempted using methyl lithium and it appears that that attempt was also unsuccessful as shown in scheme 6.12. Initially it was thought that the synthesis was successful but the product was challenging to separate from the starting reagent due to similar solubility, leading to a similar R_f value. But after some further analysis and experimentation it became apparent that the reaction had not been successful and an unwanted adduct was the principal product as shown in scheme 6.13. There is precedent for this type of unwanted by-product in Weinreb amide coupling reactions as previous publications suggest.²⁴



Scheme 6.11 Unsuccessful synthesis of (4*R*)-methyl 2-(*tert*-butyl)-4-(((2,5-dimethyl-4-(4-(*p*-tolyl)butanoyl)benzyl)oxy)methyl)-4-methyloxazolidine-3-carboxylate using BuLi



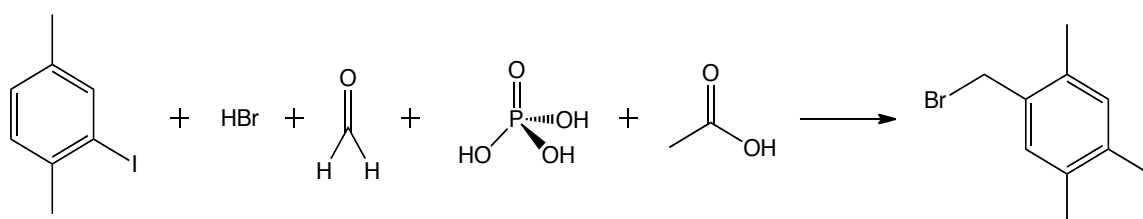
Scheme 6.12 Unsuccessful synthesis of (4*R*)-methyl 2-(*tert*-butyl)-4-(((2,5-dimethyl-4-(4-(*p*-tolyl)butanoyl)benzyl)oxy)methyl)-4-methyloxazolidine-3-carboxylate using MeLi



Scheme 6.13 This unwanted adduct appears to be the primary product of the reactions shown in this scheme and scheme 6.12

As iodine has been reported as being a much more reactive leaving group than bromine in Weinreb amide coupling reactions,²⁴ the synthesis of 1-iodo-4-(bromomethyl)-2,5-dimethylbenzene was attempted in the same fashion as 1-bromo-4-(bromomethyl)-2,5-dimethylbenzene as shown in scheme 6.14. The Weinreb amide coupling was re-attempted using the conditions that were initially successful, as shown in scheme 6.15, but unfortunately the desired product was not yielded. However, a repetition of the reaction shown in scheme 6.7 gave a

surprisingly poor results suggesting that the BuLi reagent may have degraded over time.



Scheme 6.14 Successful synthesis of 1-iodo-4-(bromomethyl)-2,5-dimethylbenzene

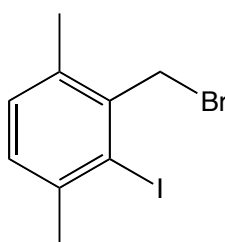
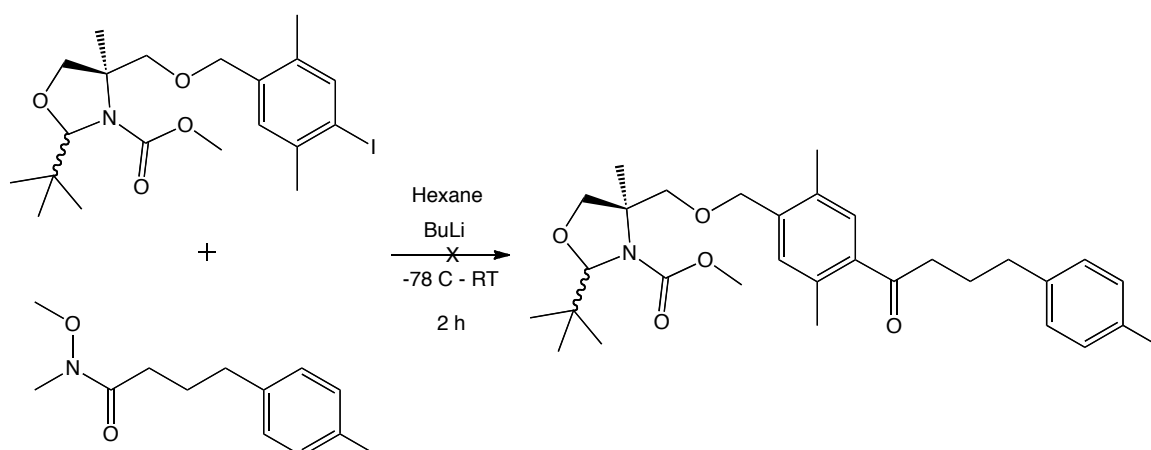
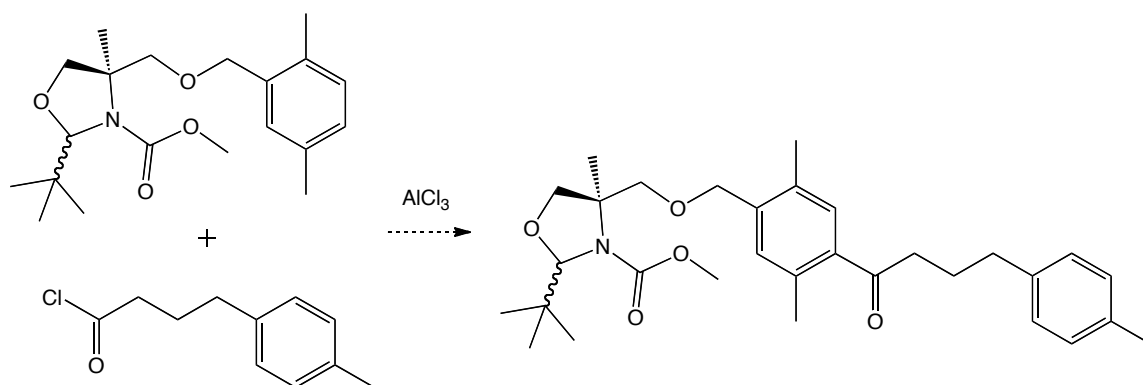


Figure 6.15 This unwanted by-product is present in a similar ratio to that seen in figure 6.14



Scheme 6.15 Unsuccessful synthesis of (4*R*)-methyl 2-(*tert*-butyl)-4-(((2,5-dimethyl-4-(4-(*p*-tolyl)butanoyl)benzyl)oxy)methyl)-4-methyloxazolidine-3-carboxylate using BuLi

After numerous failed attempts to synthesise the desired intermediate for BED(h) synthesis, an alternative strategy using Friedel-Crafts acylation was considered as shown in scheme 6.16. The route was not attempted, however, as it was considered extremely probable that unwanted side-products would result which would be inseparable due to identical solubility properties. A predicted unwanted side-product is shown in figure 6.16.



Scheme 6.16 A possible route for the synthesis of (4*R*)-methyl 2-(*tert*-butyl)-4-(((2,5-dimethyl-4-(4-(*p*-tolyl)butanoyl)benzyl)oxy)methyl)-4-methyloxazolidine-3-carboxylate using Friedel-Crafts acylation

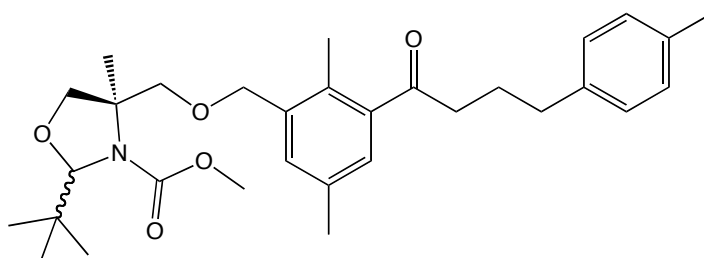
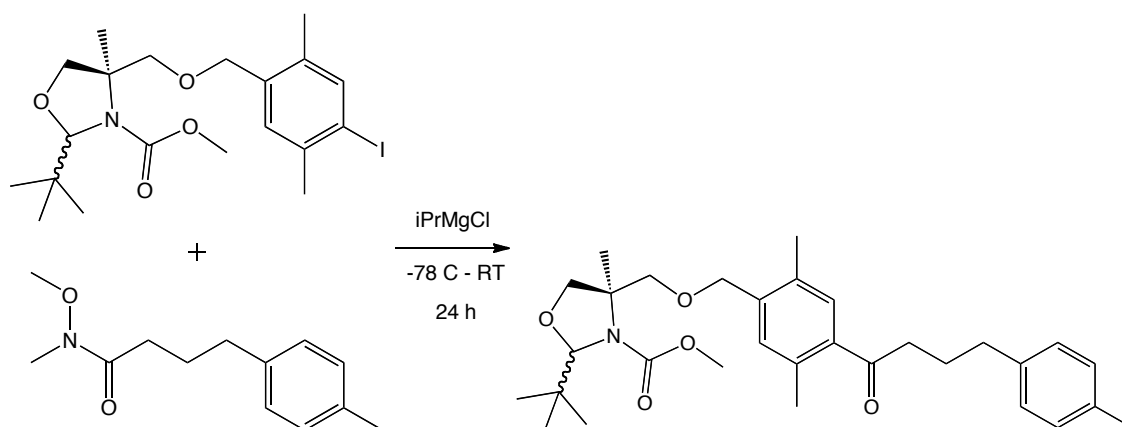


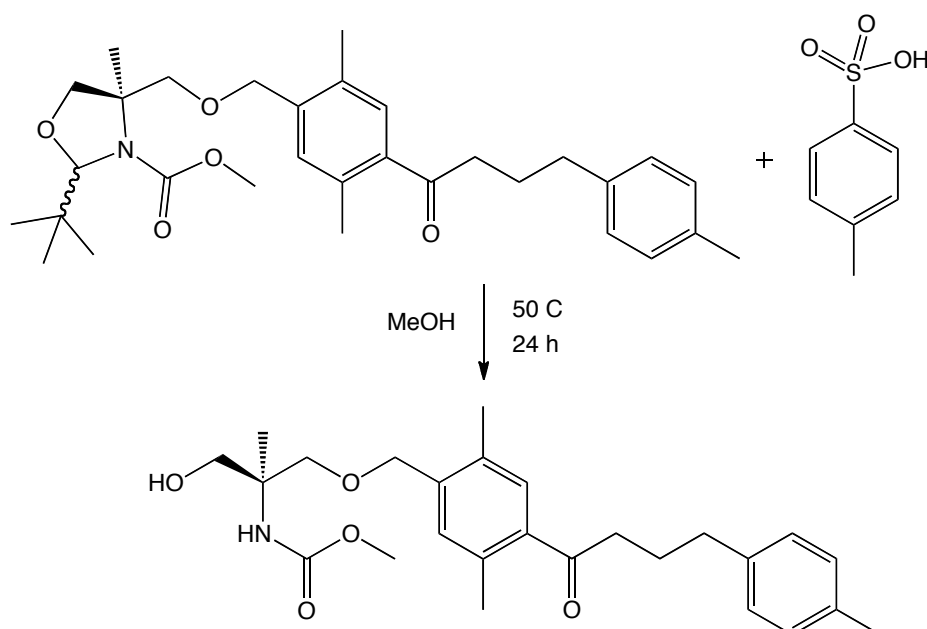
Figure 6.16 Example of a likely unwanted side-product if Friedel-Crafts acylation were attempted as shown in scheme 6.16

Using a reported synthetic strategy as a basis for trying an alternative isopropylmagnesium chloride base for the Weinreb amide coupling step finally proved to be an effective way of forming the bond.²⁴ The first time the *i*PrMgCl reagent was used the procedure used in the paper was followed as precisely as possible but this led to a poor 18 mg yield of 3%. The second time the coupling was attempted the procedure used was modelled on the procedure used as shown in scheme 6.7 and this method gave a yield of 42% (5.855 g). The whole process of developing a synthetic procedure to form the desired intermediate as shown in figure 6.17 took approximately 2.5 months due to the fact that it takes roughly 1.5 – 2 weeks to prepare all the necessary reagents and more variations of the coupling procedures were attempted than shown here.



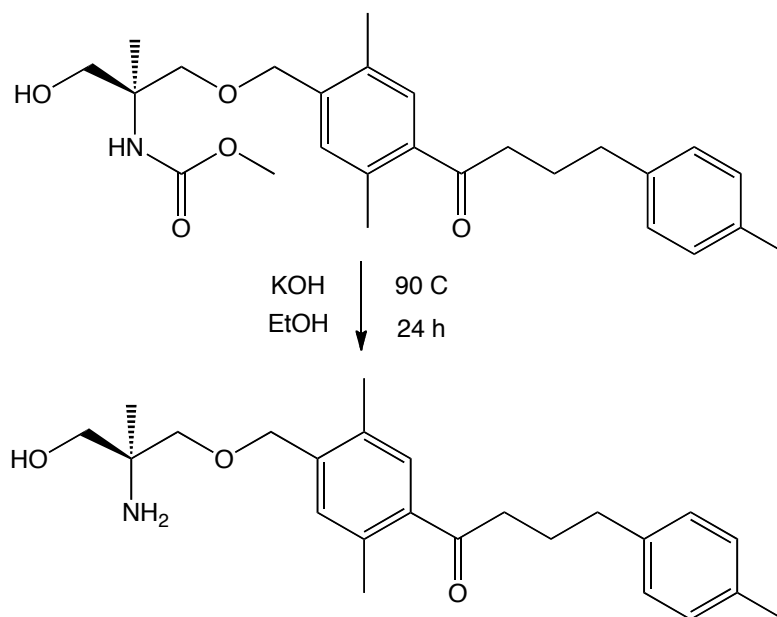
Scheme 6.17 Successful synthesis of (4*R*)-methyl 2-(*tert*-butyl)-4-(((2,5-dimethyl-4-(4-(*p*-tolyl)butanoyl)benzyl)oxy)methyl)-4-methyloxazolidine-3-carboxylate using $i\text{PrMgCl}$ with a yield of 42% (5.855 g)

The next stage of the BED(h) synthesis was successfully achieved on the first attempt and the same procedure was used as for the equivalent step in the BED(a) synthesis as shown in scheme 6.8. The only difference was that the reaction was conducted over 24 h to try to maximise the yield. The yield was a very satisfying yield of 97% (271 mg) on the first attempt.



Scheme 6.18 Successful synthesis of (S)-methyl (1-((2,5-dimethyl-4-(4-(*p*-tolyl)butanoyl)benzyl)oxy)-3-hydroxy-2-methylpropan-2-yl)carbamate has been achieved with a yield of 85% (4.32 g)

Finally, the synthesis of BED(h) was successfully accomplished as shown in scheme 6.19. The first time the BED(h) synthesis was conducted the yield was a low yield of just a few milligrams and purification proved challenging. The desired product was detected by mass spectrometry with a peak in positive mode detected as 384.17 m/z [M+H⁺]. The second time the total synthesis of BED(h) was attempted a satisfying yield of 2.09 g was achieved.

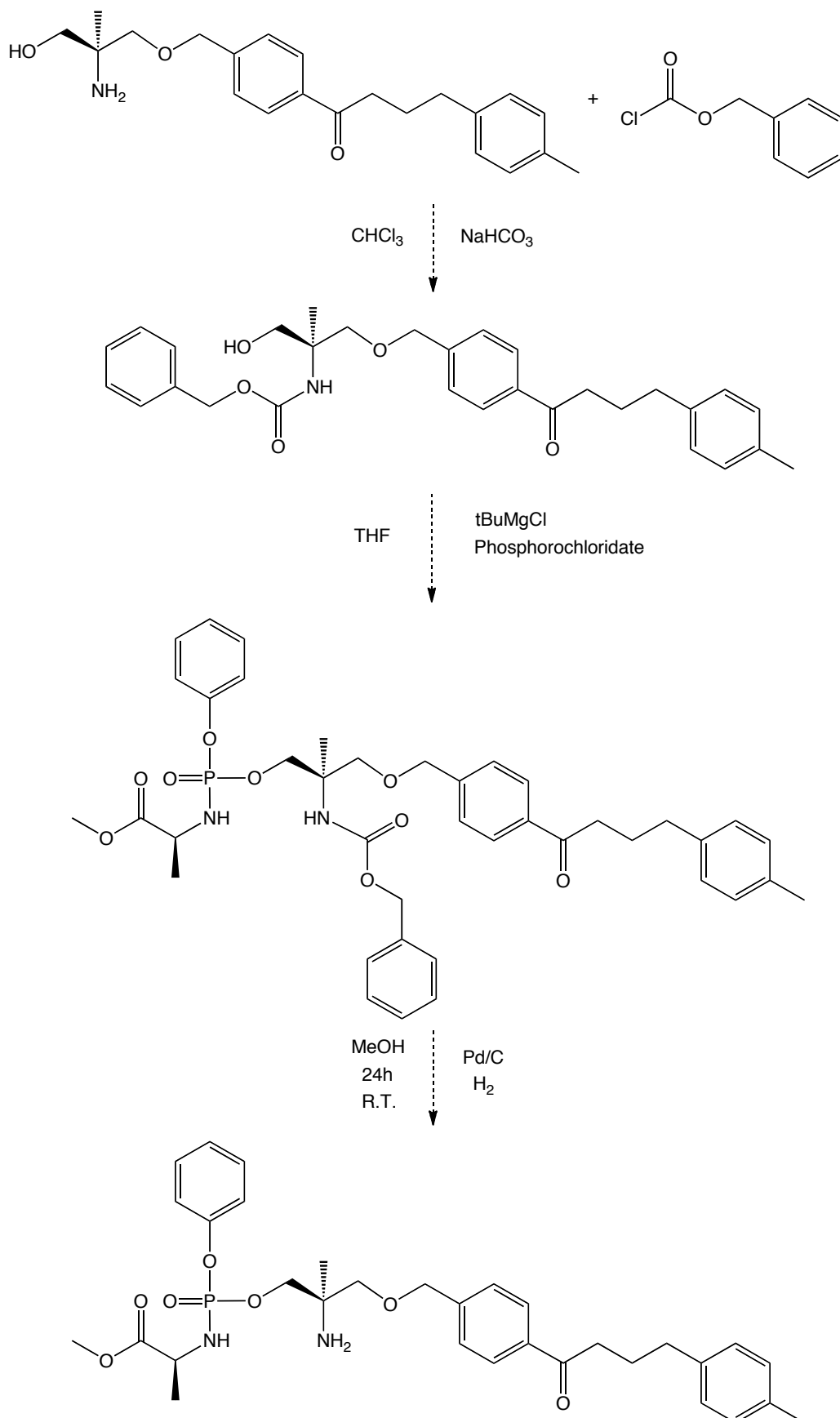


Scheme 6.19 Successful synthesis of (*S*)-1-(4-((2-amino-3-hydroxy-2-methylpropoxy)methyl)-2,5-dimethylphenyl)-4-(*p*-tolyl)butan-1-one has been achieved with a yield of 56% (2.09 g)

6.3.1 Synthesis of ProTide BED Analogues

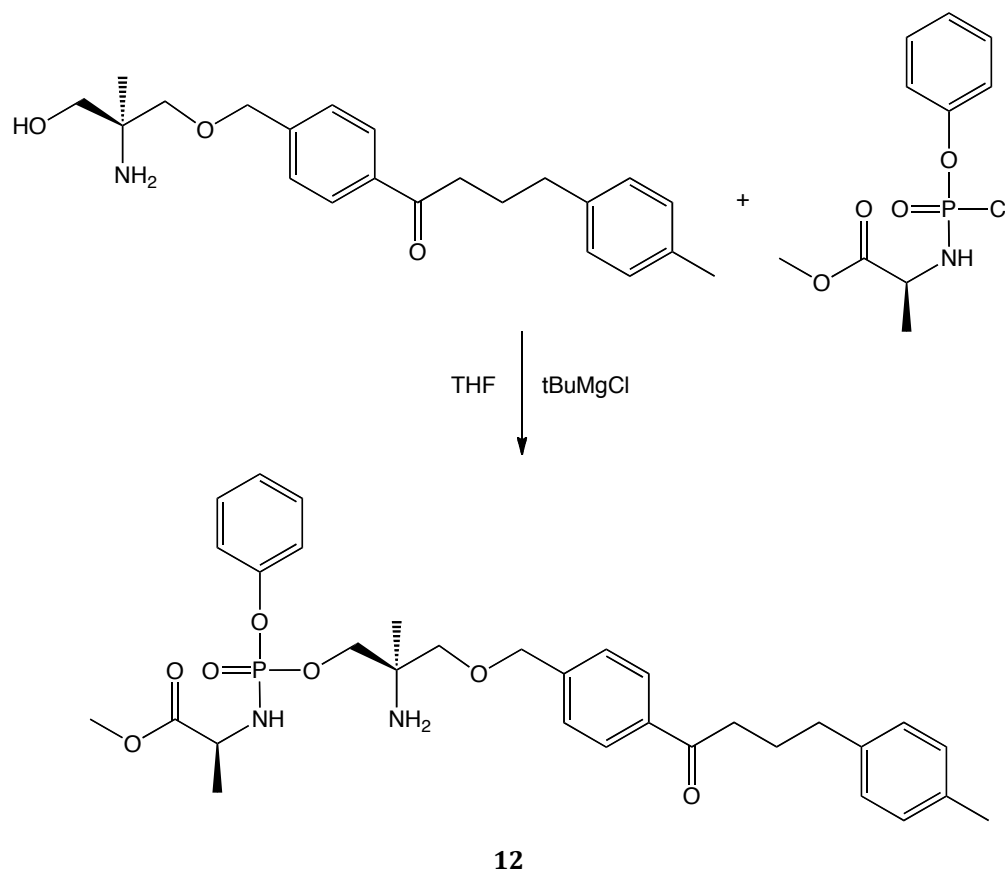
Chemical structure of a complex phosphonate derivative. The molecule features a central phosphorus atom double-bonded to an oxygen and single-bonded to three other groups: a phenyl group, a methoxy-substituted chiral carbon, and a chiral carbon with a methyl group and a phosphonate group. This phosphonate group is further substituted with a benzyl group and a 4-(4-methylphenyl)butyryl group. Stereochemistry is indicated with wedges and dashes.

Confidential



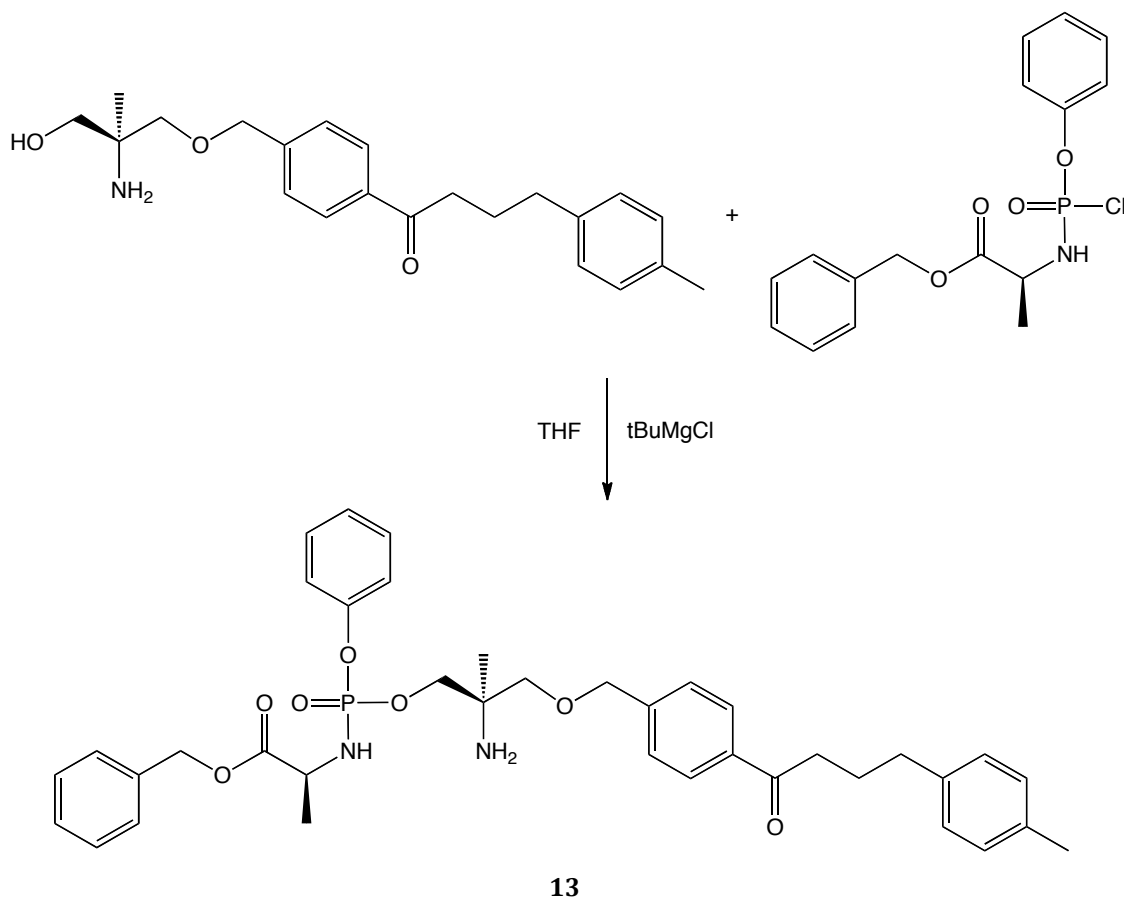
Scheme 6.20 Possible synthetic procedure which was *not required* for successful ProTide BED(a) synthesis

The simple synthetic procedure shown in scheme 6.21 was all that was required for successful ProTide BED(a) synthesis in an acceptable 44% yield (188 mg). The synthetic scheme shown in scheme 6.21 appears to be the world's first successful total synthesis of ProTide BED compounds and even the world's first total synthesis of any phosphorus prodrug of a mono alcohol S1P receptor modulator.

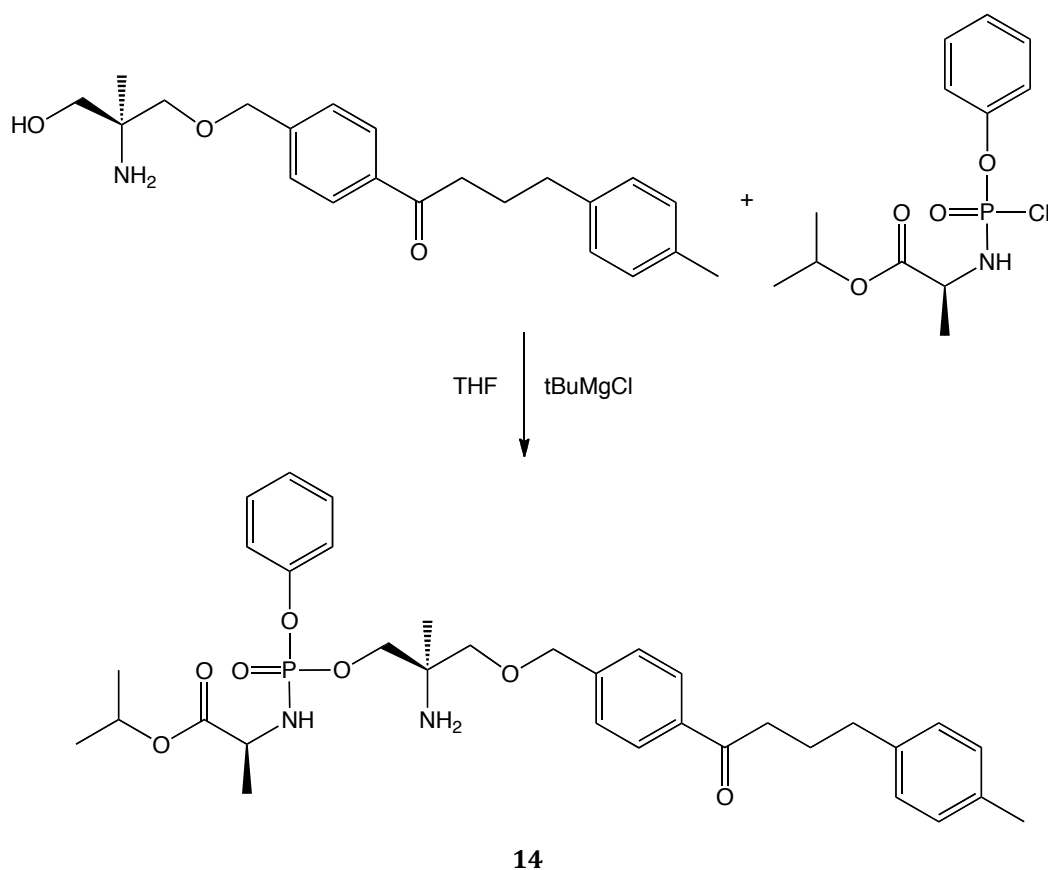


Scheme 6.21 Successful application of the ProTide fingolimod synthesis procedure to the BED family of compounds to yield (2*S*)- methyl 2-(((*R*)-2-amino-2-methyl-3-((4-(4-(*p*-tolyl) butanoyl) benzyl)oxy)propoxy)(phenoxy) phosphoryl) amino) propanoate (**12**) or Ph-LAla-OMe-BED(a) with a yield of 44% (188 mg)

The same synthetic procedure was also applied to Ph-LAla-OBzl PCl and BED(a) to successfully synthesise Ph-LAla-OBzl BED(a) as shown in scheme 6.22 with a 65% yield of 365 mg. The synthetic procedure was also applied to synthesise 4 more ProTide BED analogues as detailed in schemes 6.23 – 6.26 and summarised in tables 6.2 and 6.3.



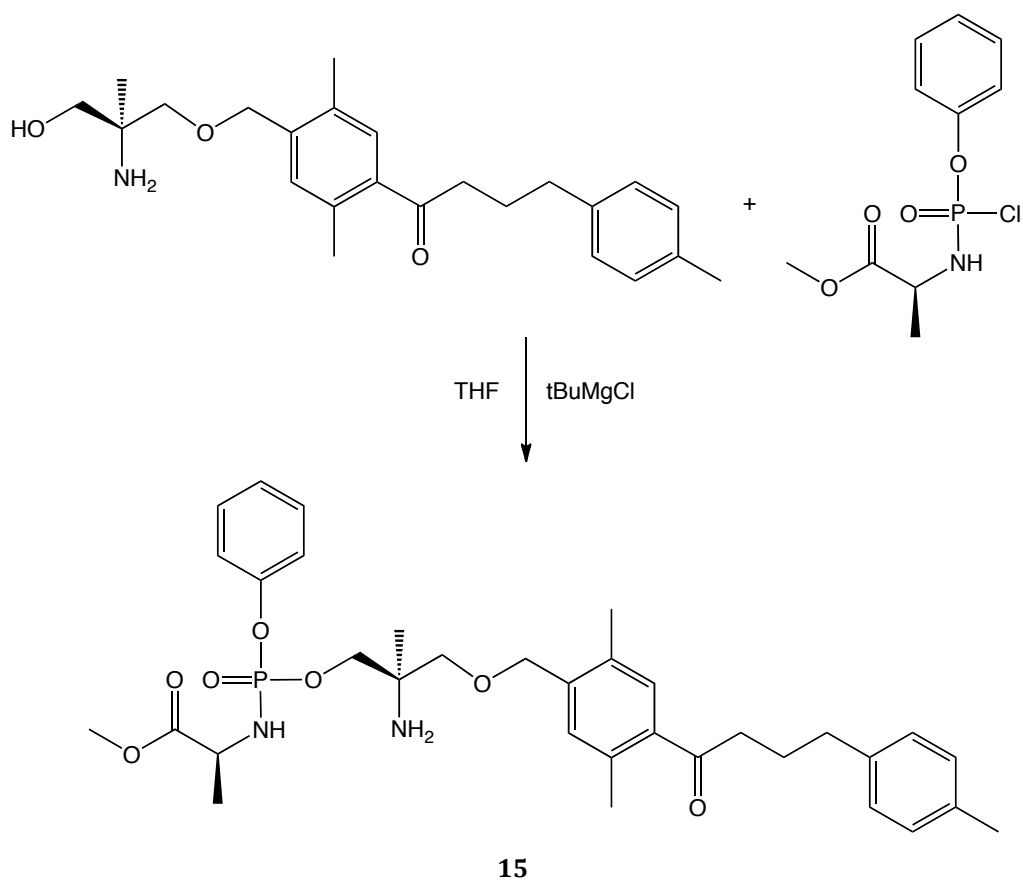
Scheme 6.22 Successful application of the ProTide fingolimod synthesis procedure to the BED family of compounds to yield (2*S*)- benzyl 2-((((*R*)-2-amino-2-methyl-3-((4-(4-(*p*-tolyl) butanoyl) benzyl) oxy) propoxy)(phenoxy) phosphoryl) amino) propanoate (**13**) or Ph-LAla-OBzl-BED(a) with a yield of 65% (365 mg)



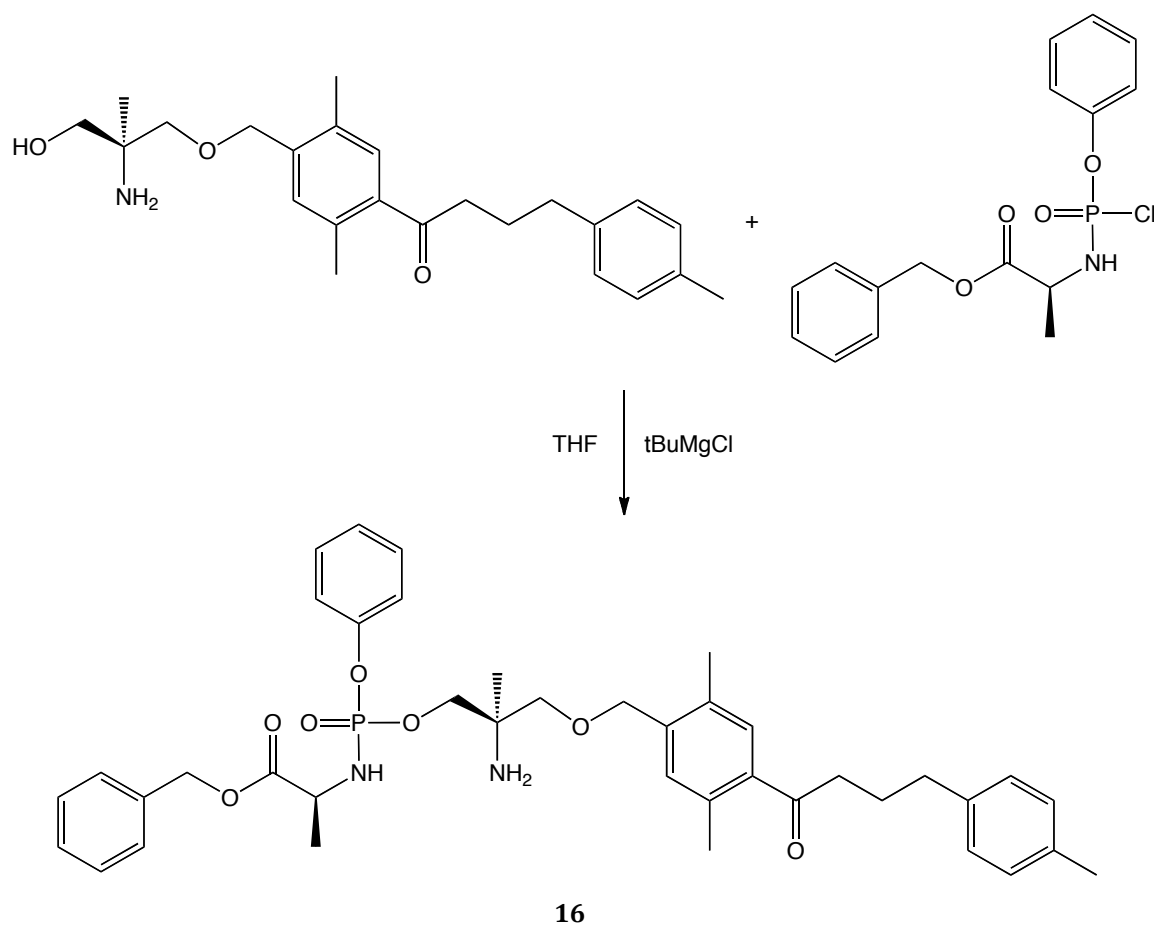
Scheme 6.23 Successful application of the ProTide fingolimod synthesis procedure to the BED family of compounds to yield (2*S*)-isopropyl 2-((((*R*)-2-amino-2-methyl-3-((4-(4-(*p*-tolyl) butanoyl) benzyl) oxy) propoxy) (phenoxy) phosphoryl) amino) propanoate (**14**) or Ph-LAla-OiPr-BED(a) with a yield of 50% (234 mg)

Compound	Ar	AA	R	% Yield	³¹ P NMR δ (ppm)
12	Ph	L-Ala	Me	44%	2.55, 2.52, 2.47, 2.17
13	Ph	L-Ala	Bzl	65%	3.14, 2.67, 2.26
14	Ph	L-Ala	iPr	50%	3.13, 2.77, 2.41

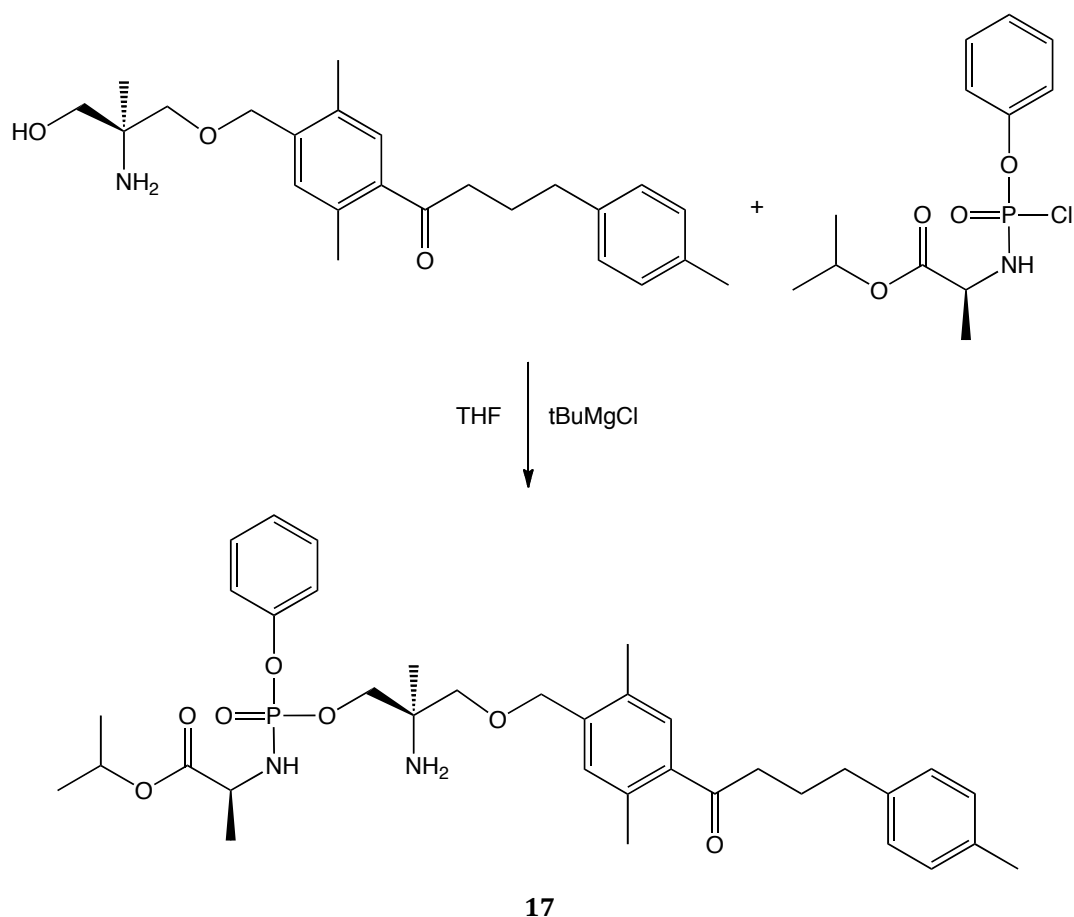
Table 6.2 ProTide BED(a) analogues synthesised



Scheme 6.24 Successful application of the ProTide fingolimod synthesis procedure to the BED family of compounds to yield (2S)-methyl 2-((((R)-2-amino-3-((2,5-dimethyl-4-(4-(p-tolyl) butanoyl) benzyl) oxy)-2-methylpropoxy) (phenoxy) phosphoryl) amino) propanoate (**15**) or Ph-LAla-OMe-BED(h) with a yield of 99% (803 mg)



Scheme 6.25 Successful application of the ProTide fingolimod synthesis procedure to the BED family of compounds to yield (2*S*)-benzyl 2-(((*R*)-2-amino-3-((2,5-dimethyl-4-(4-(*p*-tolyl)butanoyl) benzyl) oxy)-2-methylpropoxy) (phenoxy) phosphoryl) amino) propanoate (**16**) or Ph-LAla-OBzl-BED(h) with a yield of 87% (791 mg)



Scheme 6.26 Successful application of the ProTide fingolimod synthesis procedure to the BED family of compounds to yield (2*S*)-isopropyl 2-((((*R*)-2-amino-3-((2,5-dimethyl-4-(4-(*p*-tolyl)butanoyl)benzyl)oxy)-2-methylpropoxy) (phenoxy) phosphoryl) amino) propanoate (**17**) or Ph-LAla-OiPr-BED(h) with a yield of 15% (129 mg)

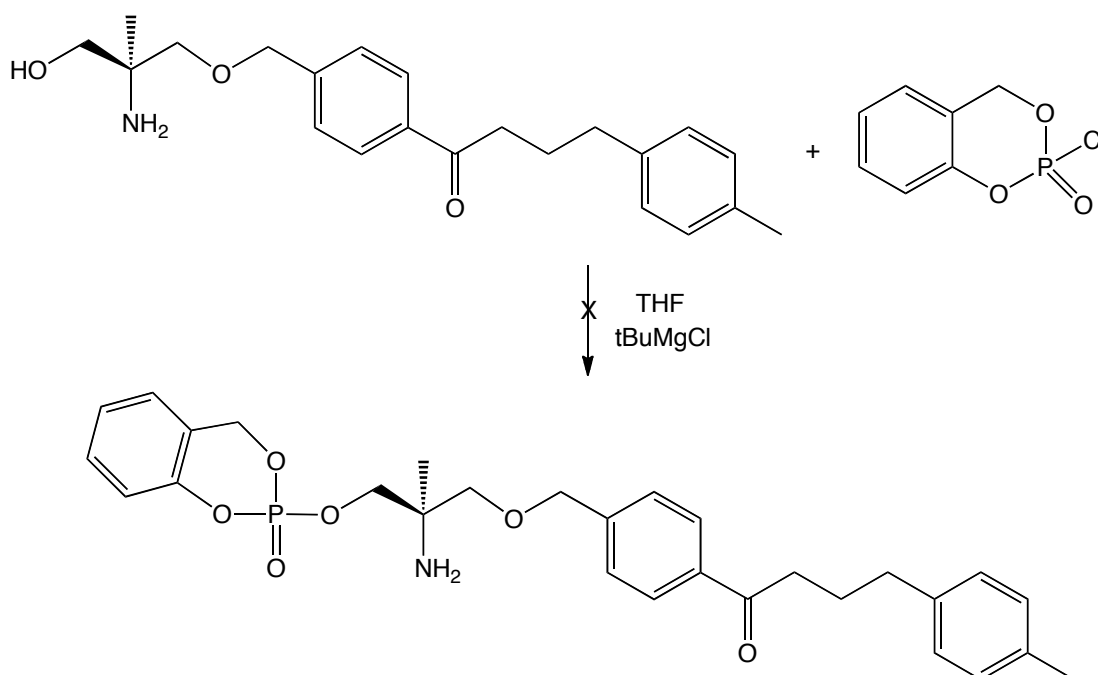
Compound	Ar	AA	R	% Yield	³¹ P NMR δ (ppm)
15	Ph	L-Ala	Me	99%	3.72, 3.37, 3.30
16	Ph	L-Ala	Bzl	87%	3.60, 3.51, 3.08, 3.05
17	Ph	L-Ala	iPr	15%	2.58, 2.52, 2.29, 2.27

Table 6.3 ProTideBED(h) analogues synthesised

6.3.2 CycloSal BED

The synthesis of CycloSal BED(a) was attempted as shown in scheme 6.27 but was not successfully achieved.^{25,26} It appears that the main product of the reaction is the unwanted salt as shown in figure 6.18. The ¹H NMR of the product appears to have the right chemical shifts and relative integrations, however the key pieces of evidence which suggest that the unwanted salt was formed include:

1. No mass peak corresponding to the desired product. The major peak being that which corresponds to the parent BED(a)
2. No obvious coupling in the ¹³C NMR spectrum of the carbon adjacent to the alcohol group with a phosphorus atom
3. Poor solubility in CHCl₃ and other conventional solvents apart from methanol
4. Solid salt-like appearance unlike the usual oil type appearance of previously synthesised phosphorus prodrugs
5. Very large NH₃⁺ peak in the ¹H NMR similar to that of fingolimod HCl



Scheme 6.27 Unsuccessful synthesis of CycloSal BED(a)

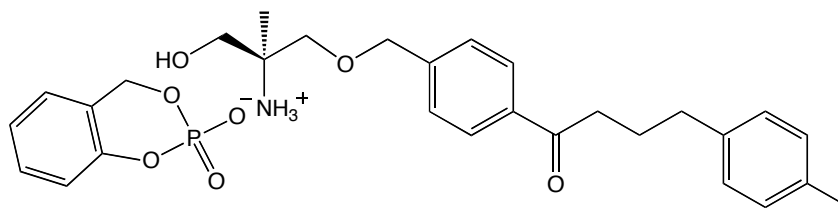
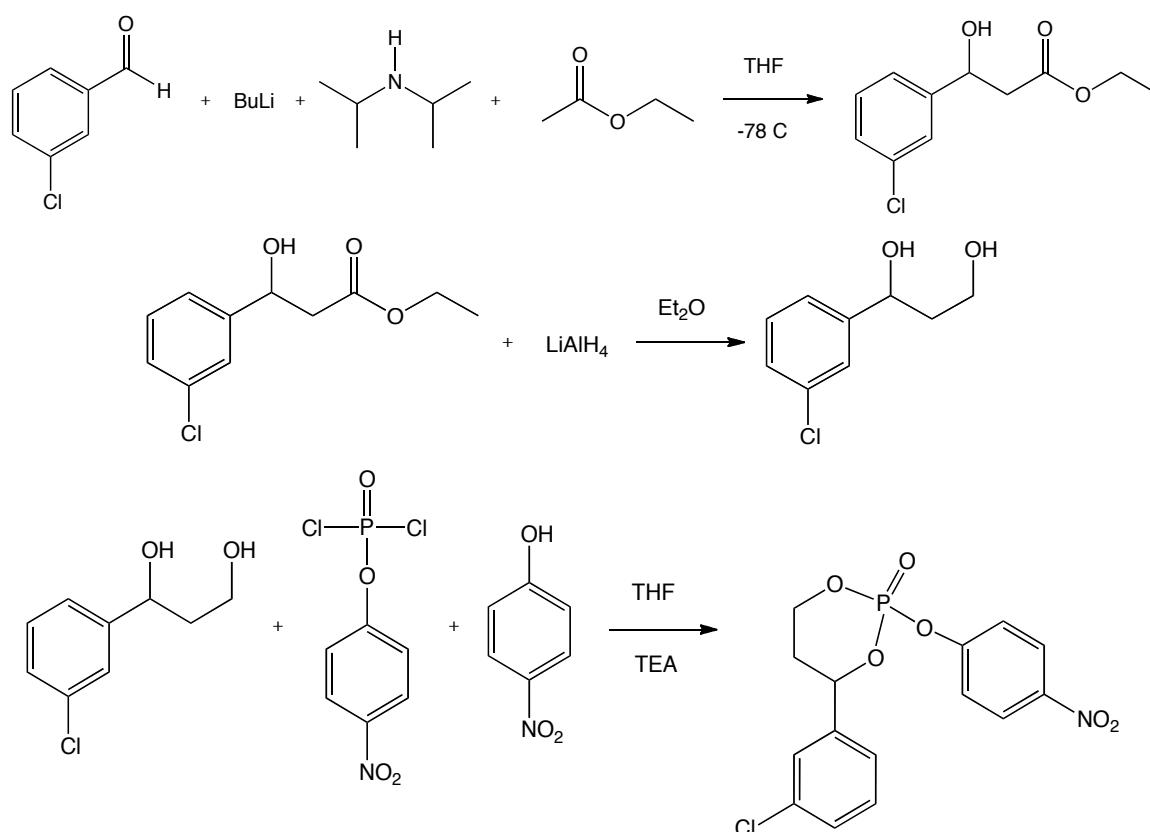


Figure 6.18 Likely undesired product of the attempted CycloSal BED(a) synthesis

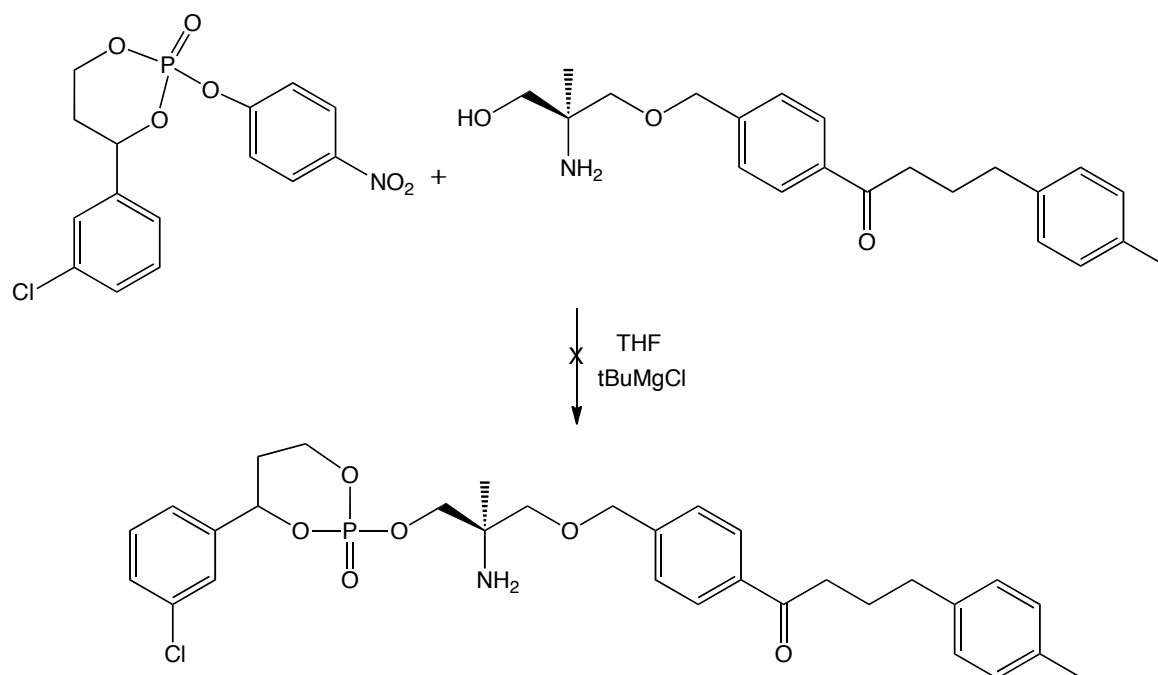
The unsuccessful synthesis of CycloSal BED(a) is not a great cause for concern as no CycloSal analogue has reached clinical trials and there is little precedent for CycloSal phosphate delivery prodrugs to be particularly effective therapeutic agents.²⁵

6.3.3 HepDirect BED

The synthesis of HepDirect BED(a) was attempted as shown in schemes 6.28 and 6.29.^{25,27} The synthesis of the prodrug reagent was successful but the final step of the synthesis was unsuccessful.



Scheme 6.28 Successful synthesis of HepDirect prodrug reagent

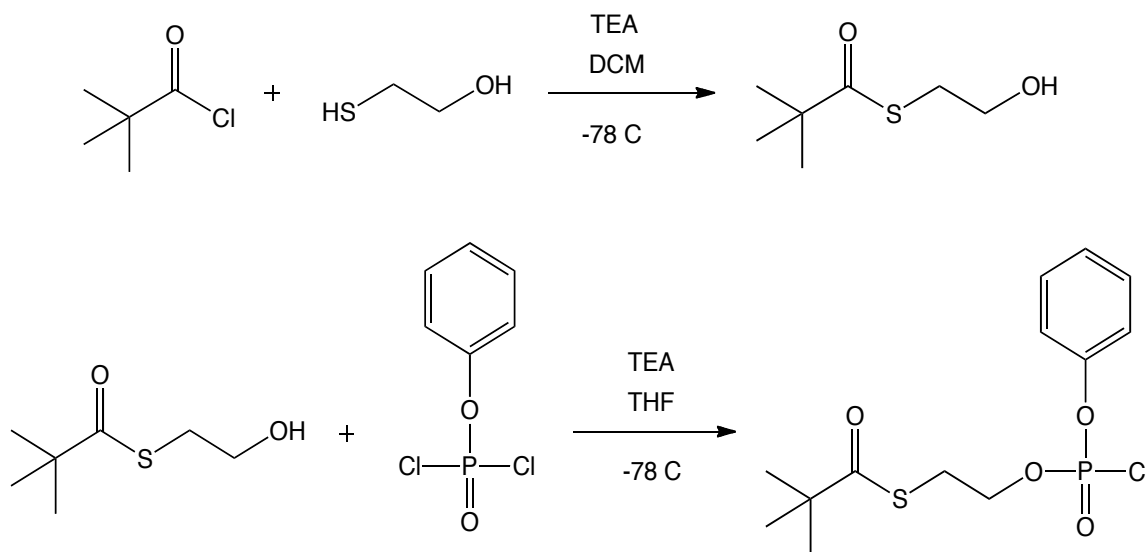


Scheme 6.29 Unsuccessful synthesis HepDirect BED(a)

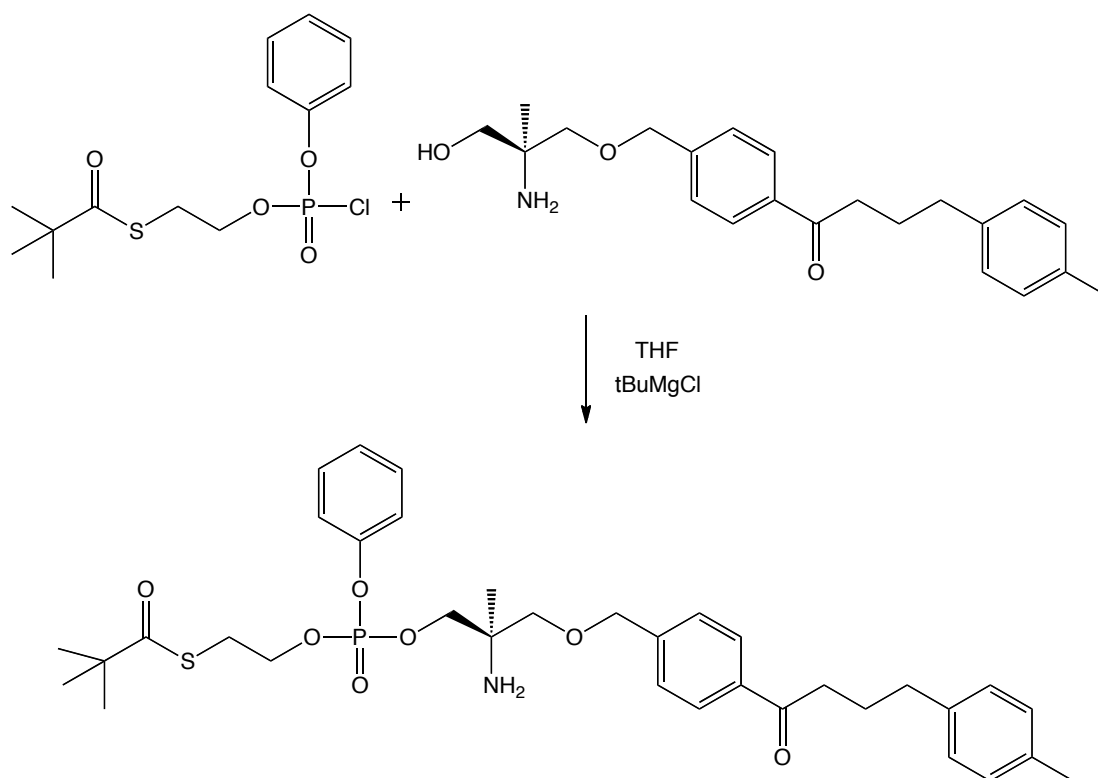
The unsuccessful synthesis of HepDirect BED(a) is not necessarily a great cause for concern as HepDirect prodrugs have been reported as being activated in the liver by cytochrome P450.²⁷ As the compounds being developed in this research are designed to be therapeutically-active in the central nervous system, and ideally cross the blood-brain barrier, the formation of the monophosphate in the liver may lead to poor delivery to the target tissues due to increased hydrophilicity. However, it is possible that formation of the monophosphate in the liver may increase delivery of the therapeutically-active compounds to the central nervous system as logP prediction programs suggest that monophosphate BED(a) has a logP value closer to the range (logP 1.5-2.7) typical of FDA approved CNS-acting drugs.²⁸ At this stage one can merely hypothesise and PK/PD studies would have to be conducted in order to reach a definitive conclusion.

6.3.4 Aryl SATE BED(a) and Fingolimod

The synthesis of aryl SATE BED(a) was attempted and appears to have been successfully achieved.^{25,29,30} The purification of the final step (scheme 6.31) was unusually challenging, taking 2 days, and the final yield was a very poor 3% (14 mg). The ¹H NMR, ¹³C NMR and ³¹P NMR data suggest that the synthesis was successful although a mass fragment ion corresponding to the desired product was not detected using mass spectrometry. However, masses of 674.29 m/z and 696.28 m/z were detected in the positive mode which are likely to correspond to [M+H₂O+H⁺] and [M+H₂O+Na⁺] respectively. Likewise a mass of 672.39 m/z was detected in negative mode which is likely to correspond to [M+H₂O-H]. The +18 masses detected in both positive and negative mode are very likely due to H₂O being added to the parent mass and it can be argued that this is most likely to be an artifact of the mass spectrometric analysis rather than the aryl SATE BED(a) has gained 2 hydrogen atoms and an oxygen during the synthetic procedure.

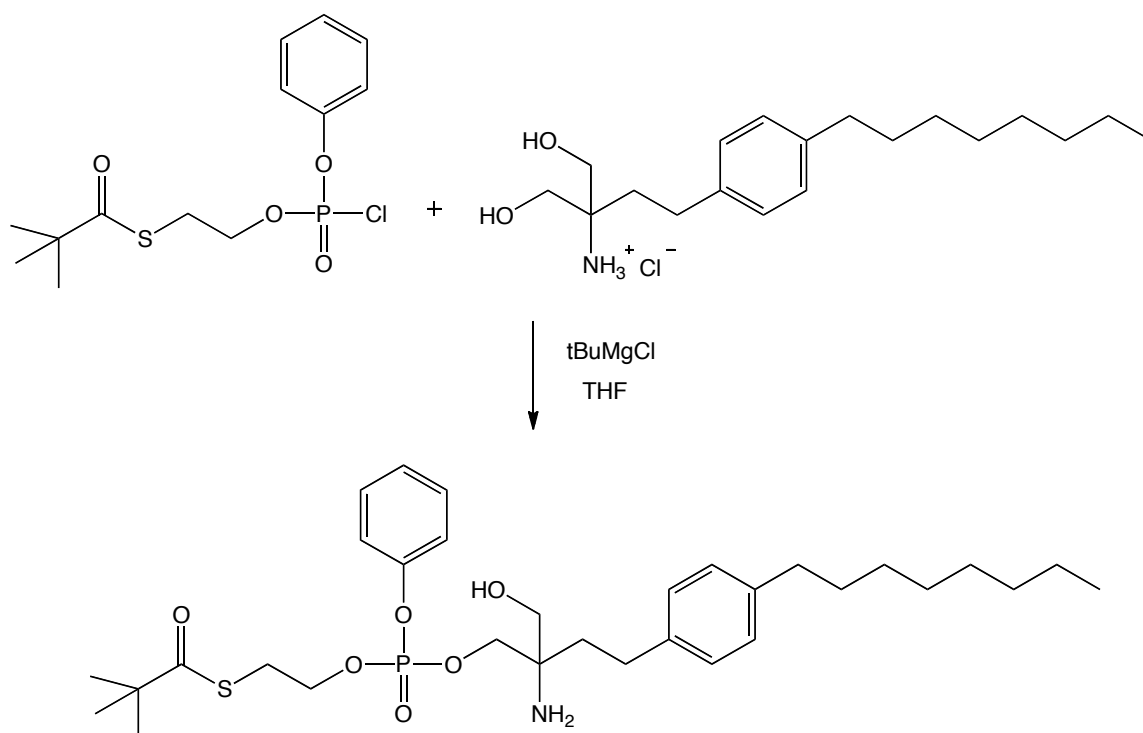


Scheme 6.30 Successful synthesis Aryl SATE prodrug reagent



Scheme 6.31 Successful synthesis Aryl SATE BED(a) with a poor yield of 3% (14 mg)

The synthesis of SATE fingolimod was attempted and successfully achieved as shown in schemes 6.30 and 6.32.^{25,29,30} As with aryl SATE BED(a) the purification of the final step (scheme 6.32) was unusually challenging, taking 2 days, and the final yield was a poor 9% (76 mg). The ^1H NMR, ^{13}C NMR and ^{31}P NMR data suggest that the synthesis was successful although a mass fragment ion corresponding to the desired product was not detected using mass spectrometry. However, a mass of 648.28 m/z was detected in the positive mode which may correspond to $[\text{M}+\text{H}_2+\text{K}^+]$. Masses of 624.8 m/z and 660.81 m/z were detected in negative mode which are likely to correspond to $[\text{M}+\text{H}_2\text{O}-\text{H}]$ and $[\text{M}+\text{H}_2\text{O}+\text{Cl}^-]$ respectively. The +18 masses detected in negative mode are very likely due to H_2O being added to the parent mass and it can be argued that this is most likely to be an artifact of the mass spectrometric analysis rather than the aryl SATE fingolimod has gained 2 hydrogen atoms and an oxygen during the synthetic procedure.



Scheme 6.32 Synthesis of SATE fingolimod giving a poor yield of 9% (76 mg)

As the synthesis of aryl SATE phosphate delivery prodrugs of S1P receptor modulators was comparatively challenging and there is little precedent for SATE compounds to be particularly effective therapeutics the synthesis of further SATE analogues was not seriously considered.²⁵ The synthesis of SATE analogues of fingolimod still has the same problem of unwanted diastereoisomers as previously encountered with the synthesis of ProTide fingolimod analogues.

6.4 References

1. Kiuchi M, Adachi K, Kohara T, Teshima K, Masubuchi Y, Mishina T, Fujita T. Synthesis and biological evaluation of 2,2-disubstituted 2-aminoethanols: analogues of FTY720. *Bioorg. Med. Chem. Lett.* **1998**, 8, 101-106.
2. Brinkmann V, Davis M, Heise C, Albert R, Cottens S, Hof R, Bruns C, Prieschl E, Baumruker T, Hiestand P, Foster C, Zollinger M, Lynch K. The immune modulator FTY720 targets sphingosine 1-phosphate receptors. *J. Biol. Chem.* **2002**, 277, 21453-21457.
3. Bigaud M, Guerini D, Billich A, Bassilana F, Brinkmann V. Second generation S1P pathway modulators: Research strategies and clinical developments. *Biochim. Biophys. Acta.* **2014**, 1841, 745-758.
4. Blaho V, Hla T. An update on the biology of sphingosine 1-phosphate receptors. *J. Lipid Res.* **2014**, 55, 1596-1608.
5. Buzard D *et al.* (7-Benzyloxy-2,3-dihydro-1H-pyrrolo[1,2-a]indol-1-yl)acetic acids as S1P₁ functional antagonists. *Med. Chem. Lett.* **2014**, 5, 1334-1339.
6. Li G, Han W, Jin J, Wang X, Xiao Q. Design, synthesis and biological evaluation of fingolimod analogues containing diphenyl ether moiety. *Acta Pharm. Sinic.* **2014**, 49, 896-904.
7. Tian Y, Jin J, Wang X, Hu J, Xiao Q, Zhou W, Chen X, Yin D. Discovery of oxazole and triazole derivatives as potent and selective S1P₁ agonists through pharmacophore-guided design. *Eur. J. Med. Chem.* **2014**, 85, 1-15.
8. Chiba K, Adachi K. Discovery of fingolimod, the sphingosine 1-phosphate receptor modulator and its application for the therapy of multiple sclerosis. *Future Med. Chem.* **2012**, 4, 771-781.
9. Fransson R, McCracken A, Chen B, McGonigle R, Edinger A, Hanessian S. Design, synthesis, and antileukemic activity of stereochemically defined constrained analogues of FTY720 (Gilenya). *Med. Chem. Lett.* **2013**, 4, 969-973.0
10. Hinterding K, Cottens S, Albert R, Zecri F, Buehlmayer P, Spanka C, Brinkmann V, Nussbaumer P, Ettmayer P, Hoegenauer K, Gray N, Pan S. Synthesis of chiral analogues of FTY720 and its phosphate. *Synthesis.* **2003**, 11, 1667-1670.
11. Jiang X, Gong B, Prasad K, Repic O. A practical synthesis of a chiral analogue of FTY720. *Org. Process Res. Dev.* **2008**, 12, 1164-1169.

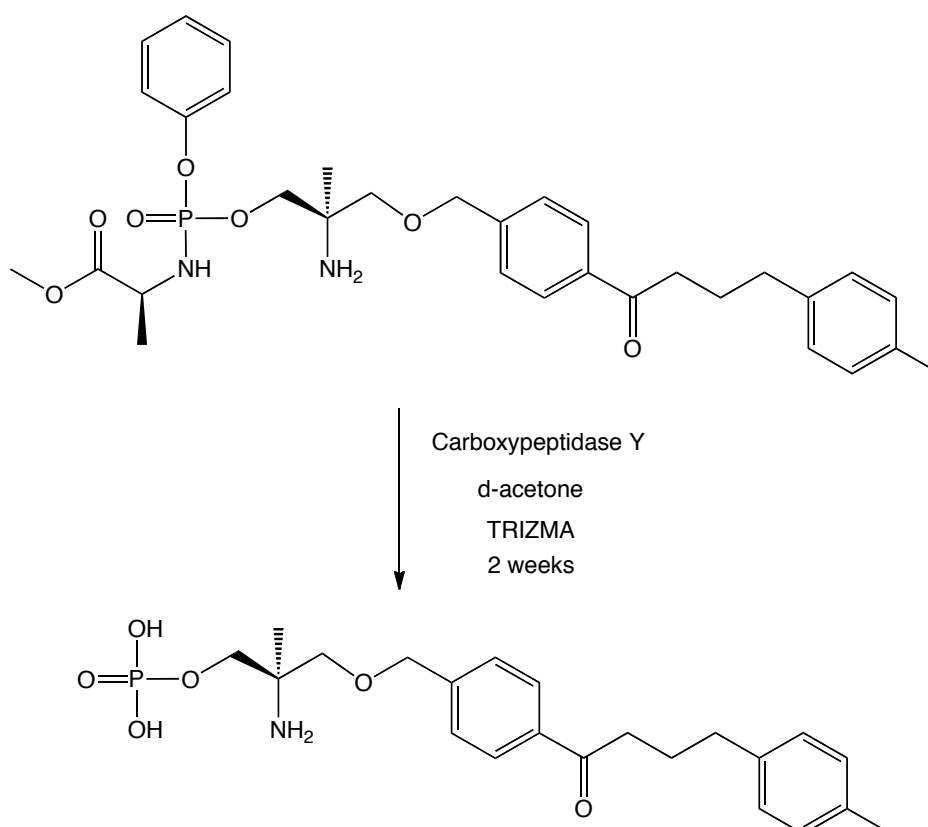
12. Kiuchi M, Adachi K, Kohara T, Minoguchi M, Hanano T, Aoki Y, Mishina T, Arita M, Nakao N, Ohtsuki M, Hoshino Y, Teshima K, Chiba K, Sasaki S, Fujita T. Synthesis and immunosuppressive activity of 2-substituted 2-aminopropane-1,3-diols and 2-aminoethanols. *J. Med. Chem.* **2000**, 43, 2946-2961.
13. Deng H, Bernier S, Doyle E, Lorusso J, Morgan B, Westlin W, Evindar G. Discovery of clinical candidate GSK1842799 as a selective S1P₁ receptor agonist (prodrug) for multiple sclerosis. *Med. Chem. Lett.* **2013**, 4, 942-947.
14. Nishi T *et al.* Discovery of CS-0777: A potent, selective, and orally active S1P₁ agonist. *Med. Chem. Lett.* **2010**, 2, 368-372.
15. Clemens J, Davis M, Lynch K, Macdonald T. Synthesis of 4(5)-phenylimidazole-based analogues of sphingosine-1-phosphate and FTY720: Discovery of potent S1P₁ receptor agonists. *Bioorg. Med. Chem. Lett.* **2005**, 15, 3568-3572.
16. Horan J *et al.* Piperazinyl-oxadiazoles as selective sphingosine-1-phosphate receptor agonists. *Bioorg. Med. Chem. Lett.* **2014**, 24, 4807-4811.
17. Tsuji T, Suzuki K, Nakamura T, Goto T, Sekiguchi Y, Ikeda T, Fukuda T, Takemoto T, Mizuno Y, Kimura T, Kawase Y, Nara F, Kagari T, Shimoizato T, Yahara C, Inaba S, Honda T, Izumi T, Tamura M, Nishi T. Synthesis and SAR studies of benzyl ether derivatives as potent orally active S1P₁ agonists. *Bioorg. Med. Chem.* **2014**, 22, 4246-4256.
18. Seebach D, Aebi J. α -Alkylation of serine with self-reproduction of the center of chirality. *Tetrahedron Lett.* **1984**, 25, 2545-2548.
19. Seebach D, Stucky G, Renaud P. Chirale synthesebausteine aus aminosäuren über einen elektrochemischen schüsselschritt: Herstellung von (*R*)-2-*tert*-butyl-3-methoxycarbonyl-1,3-oxazolinen aus (*S*)-serin und (*S*)-threonin. *Chimia.* **1988**, 42, 176-178.
20. Ghosez L, Yang G, Cagnon J, Bideau F, Marchand-Brynaert J. Synthesis of enantiomerically pure α -amino- β -hydroxy-cyclobutanone derivatives and their transformations into polyfunctional three- and five-membered ring compounds. *Tetrahedron.* **2004**, 60, 7591-7606.
21. Giacomo M, Vinci V, Serra M, Colombo L. New fast and practical method for the enantioselective synthesis of α -vinyl, α -alkyl quaternary α -amino acids. *Tetrahedron: Asymmetry.* **2008**, 19, 247-257.
22. Iio Y, Jin M, Nakamura Y, Nishi T. Asymmetric synthesis of α,α -disubstituted α -amino alcohol derivatives. *Tetrahedron: Asymmetry.* **2011**, 22, 323-328.

23. Yamamoto K, Ikeda T, Kitsuki T, Okamoto Y, Chikamatsu H, Nakazaki M. Synthesis and chiral recognition of optically active crown ethers incorporating a helicene moiety as the chiral centre. *J. Chem. Soc. Perkin Trans. 1.* **1990**, 2, 271-276.
24. Conrad K, Hsiao Y, Miller R. A practical one-pot process for a α -amino aryl ketone synthesis. *Tetrahedron Lett.* **2005**, 46, 8587-8589.
25. Pradere U, Garnier-Amblard E, Coats S, Amblard F, Schiazi R. Synthesis of nucleoside phosphate and phosphonate prodrugs. *Chem. Rev.* **2014**, 114, 9154-9218.
26. Ludek O, Kramer T, Balzarini J, Meier C. Divergent synthesis and biological evaluation of carbocyclic α -, *iso*- and 3'-*epi*-nucleosides and their lipophilic nucleotide prodrugs. *Synthesis.* **2006**, 8, 1313-1324.
27. Erion M, Reddy K, Boyer S, Matelich M, Gomez-Galeno J, Lemus R, Ugarkar B, Colby T, Schanzer J, Van Poelje P. Design, synthesis and characterization of a series of cytochrome P450 3A-activated prodrugs (HepDirect prodrugs) useful for targeting phosph(on)ate-based drugs to the liver. *J. Am. Chem. Soc.* **2004**, 126, 5154-5163.
28. Pajouhesh H, Lenz G. Medicinal chemical properties of successful central nervous system drugs. *NeuroRx.* **2005**, 2, 541-553.
29. Ruda G, Alibu V, Mitsos C, Bidet O, Kaiser M, Brun R, Barrett M, Gilbert I. Synthesis and biological evaluation of phosphate prodrugs of 4-phospho-D-erythronohydroxamic acid, an inhibitor of 6-phosphogluconate dehydrogenase. *Chem. Med. Chem.* **2007**, 2, 1169-1180.
30. Schlienger N, Beltran T, Perigaud C, Lefebvre I, Pompon A, Aubertin A, Gosselin G, Imbach J. Rational design of a new series of mixed anti-HIV pronucleotides. *Bioorg. Med. Chem. Lett.* **1998**, 8, 3003-3006.

Chapter 7 – Biochemical Processing and Analysis of ProTide BED Compounds

7.1 Enzymatic and Cell Lysate Assays

7.1.1 Ph-LAla-OMe-BED(a) Carboxypeptidase Experiment



Scheme 7.1 Processing of Ph-LAla-OMe-BED(a) to the monophosphate by carboxypeptidase

After successfully synthesising ProTide BED(a) the crucial question of whether the loss of the adjacent free alcohol group from ProTide fingolimod would lead to improved stability and the desired enzymatic processing could now be addressed. An enzymatic processing reaction was set up in an identical manner to the ProTide fingolimod carboxypeptidase experiments discussed in Chapter 5.¹ After the initial 12 hours very little had changed in the ³¹P NMR spectra of the mixture. While this did not suggest any significant enzymatic processing, it did suggest greatly improved stability in the mildly basic conditions of the experiment. More carboxypeptidase was added and ³¹P NMR was run on the sample over a period of

2 weeks with occasional shaking of the NMR tube to ensure effective mixing of the reagents.

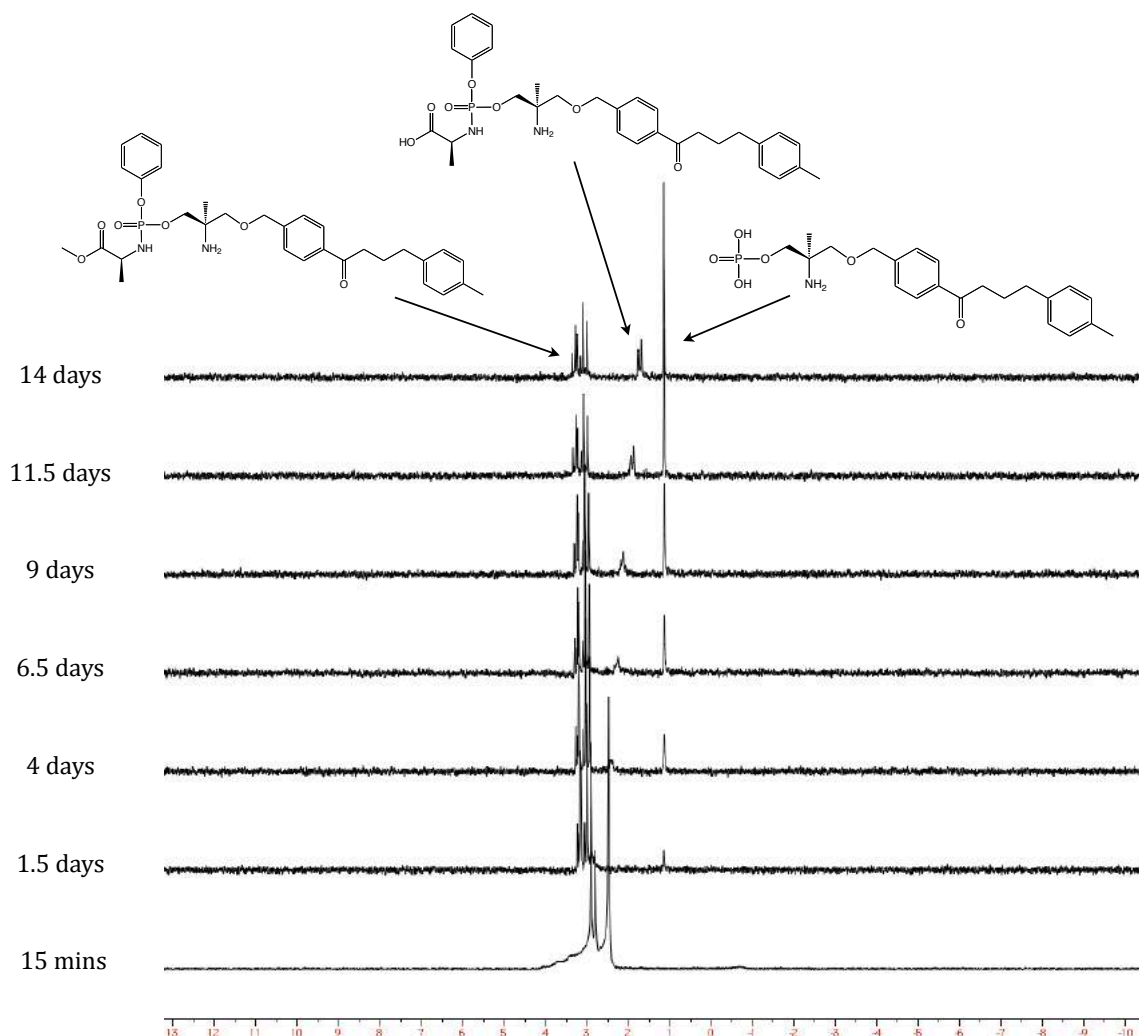


Figure 7.1 Stacked ^{31}P NMR spectra showing carboxypeptidase processing of Ph-LAla-OMe-BED(a) over 2 weeks

The intermediary compound shown in figure 7.1 in which the ester has been cleaved leaving a free carboxylic acid group is likely to be the structure shown as the peak has clearly 2 signals, which suggests that the chirality of the molecule has been maintained.

Mass spectrometric analysis was conducted on the mixture after 2 weeks and the 3 most significant mass signals in the negative mode analysis were:

- 631.25 m/z

- 595.27 m/z
- 434.16 m/z

The peaks of 631.25 m/z [M+Cl⁻] and 595.27 m/z [M-H⁻] correspond to the starting material whereas the peak of 434.16 m/z [M-H] is likely to correspond to the desired monophosphate as it has a predicted mass of 435.18 g/mol. The positive mode analysis also provided a significant peak of 437.17 m/z which very likely corresponds to the monophosphate. It is probable that the 437.17 m/z signal has a mass +1 than would be typically expected due to the fact that the sample submitted for mass spectrometric analysis was highly concentrated and it is the C¹³ isotope that is detected. The mass spectrometer used had also consistently been giving results in the positive mode analysis of mass +1 than would be expected for a range of compounds.

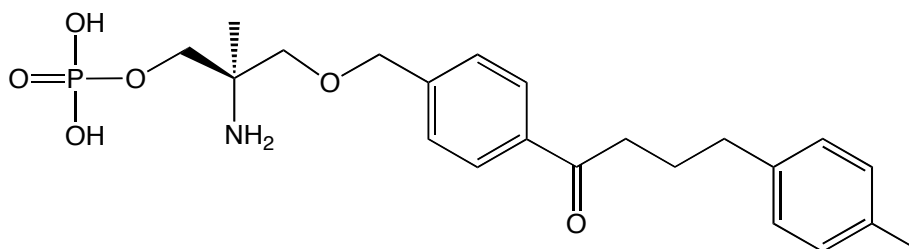
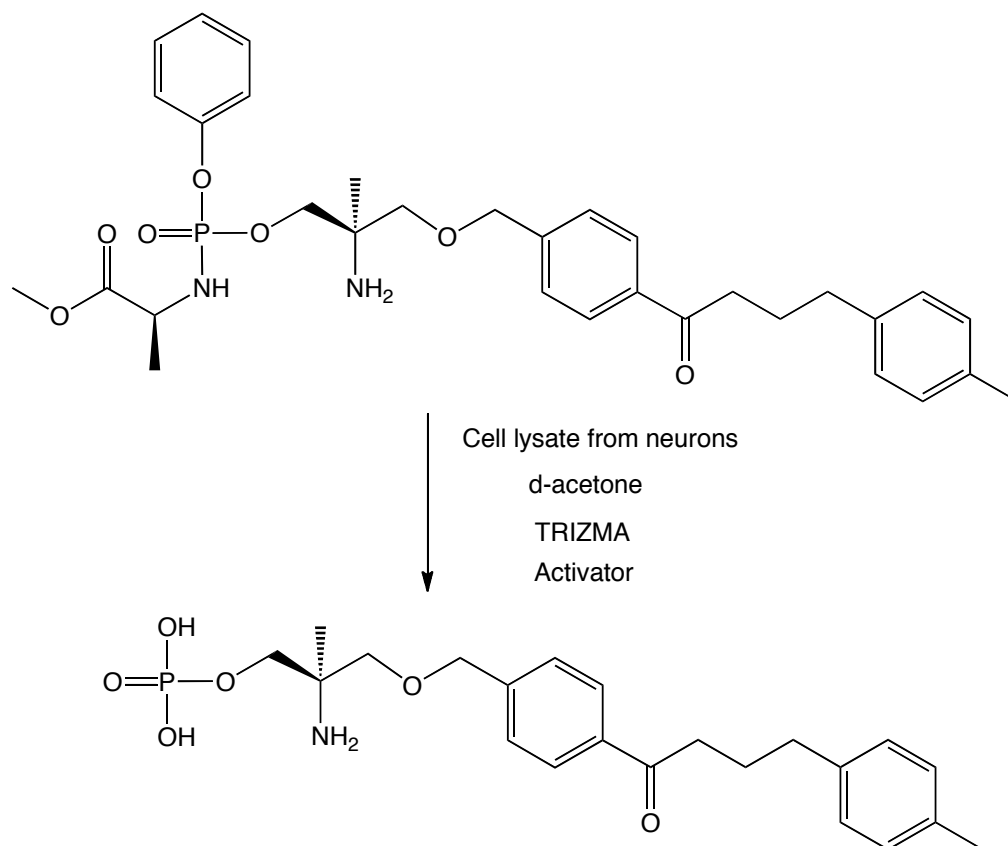


Figure 7.2 Monophosphate BED(a) has a predicted mass of 435.18 g/mol

It can be concluded that: **removal of the adjacent free alcohol from ProTide analogues of S1P receptor modulators such as fingolimod and KRP-203 leads to:**

1. **Greatly improved stability**
2. **Desired enzymatic processing by carboxypeptidase to the pharmacologically active monophosphate**

7.1.2 Ph-LAla-OMe-BED(a) Neuronal Cell Lysate Experiment



Scheme 7.2 Processing of Ph-LAla-OMe-BED(a) to the monophosphate in neuronal cell lysate

Our collaborators in the School of Biosciences prepared neuronal cell lysate and activator which was used to conduct a cell lysate experiment following previously described experimental procedures² (see experimental section). It appears that the main product of the processing is the desired monophosphate. Mass spectrometric analysis in positive mode gave peaks of 436.20 m/z and 459.30 m/z which are likely to correspond to monophosphate peaks of [M+H] and [M+Na⁺] respectively.

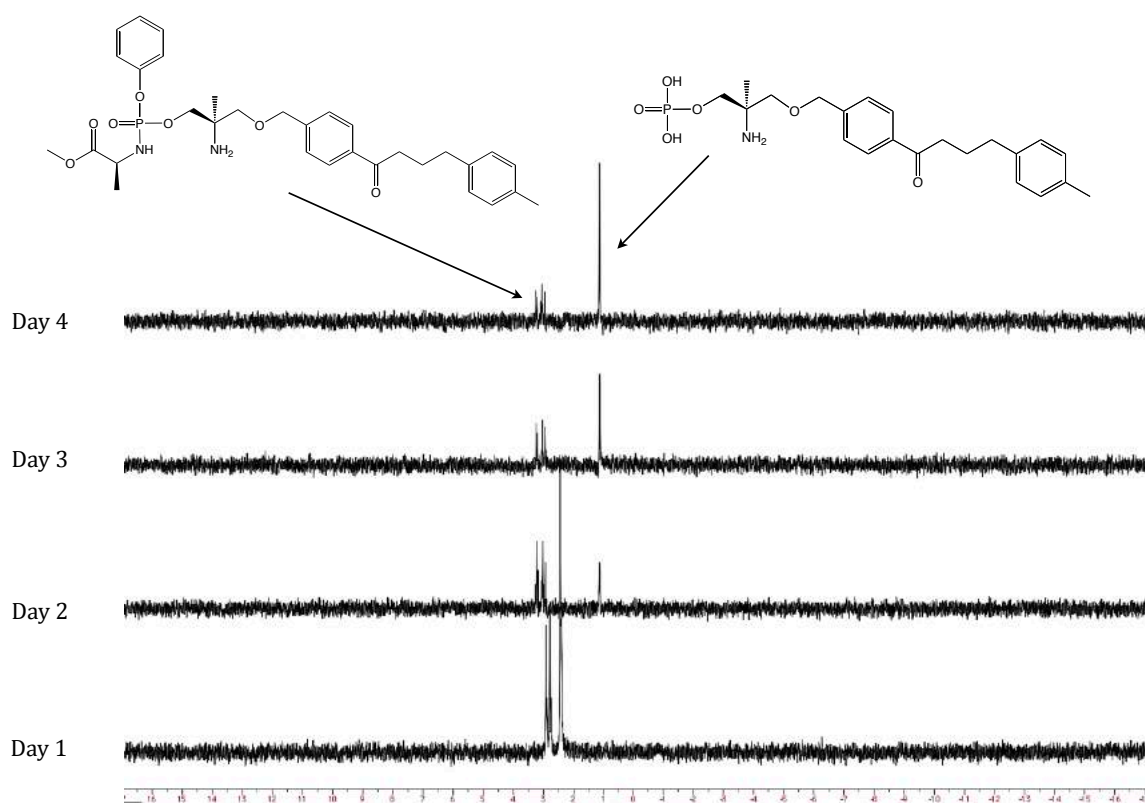
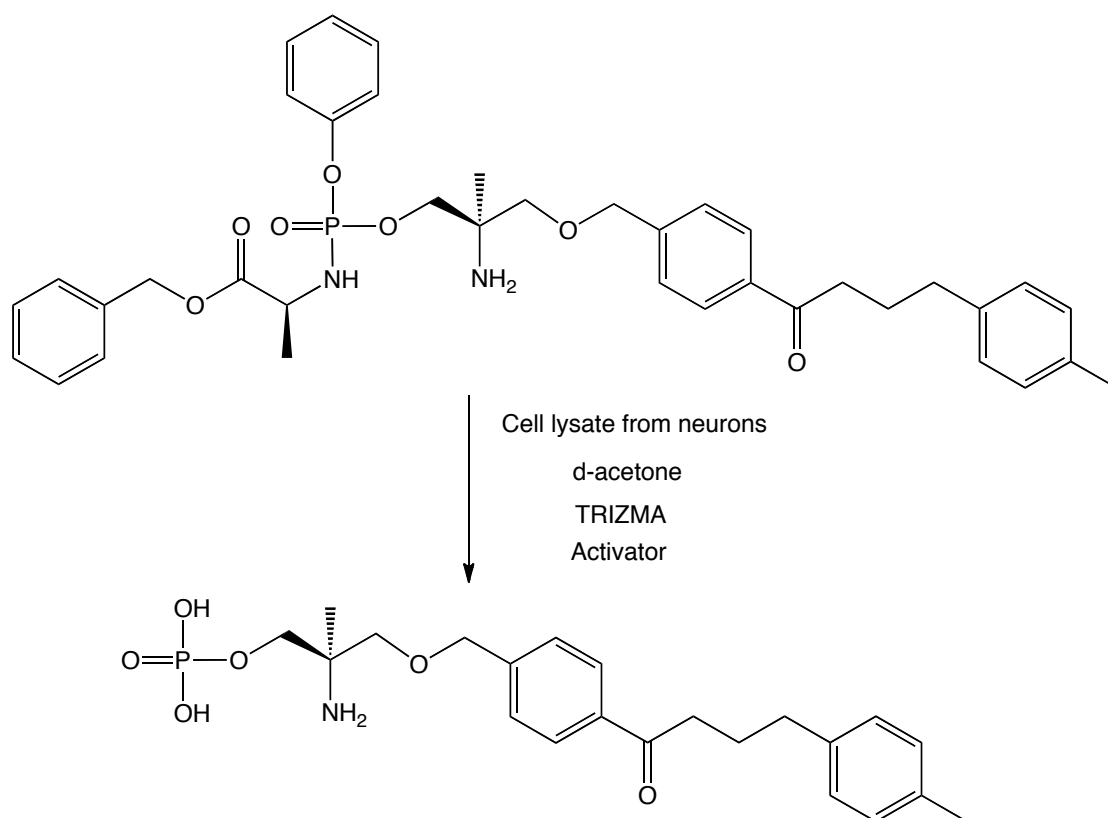


Figure 7.3 Stacked ^{31}P NMR spectra of Ph-LAla-OMe-BED(a) processing in cell lysate over 4 days

7.1.3 Ph-LAla-OBzl-BED(a) Neuronal Cell Lysate Experiment



Scheme 7.3 Processing of Ph-LAla-OBzl-BED(a) to the monophosphate in neuronal cell lysate

An identical experiment was conducted on Ph-LAla-OBzl-BED(a) which gave very similar results to those obtained in the previous experiment. A peak which is highly indicative of the monophosphate was observed in the ^{31}P NMR data, as shown in figure 7.4, and peaks corresponding to the first two products of the reported ProTide processing steps were observed in the mass spectrometric analysis as shown in figures 7.5 and 7.6.

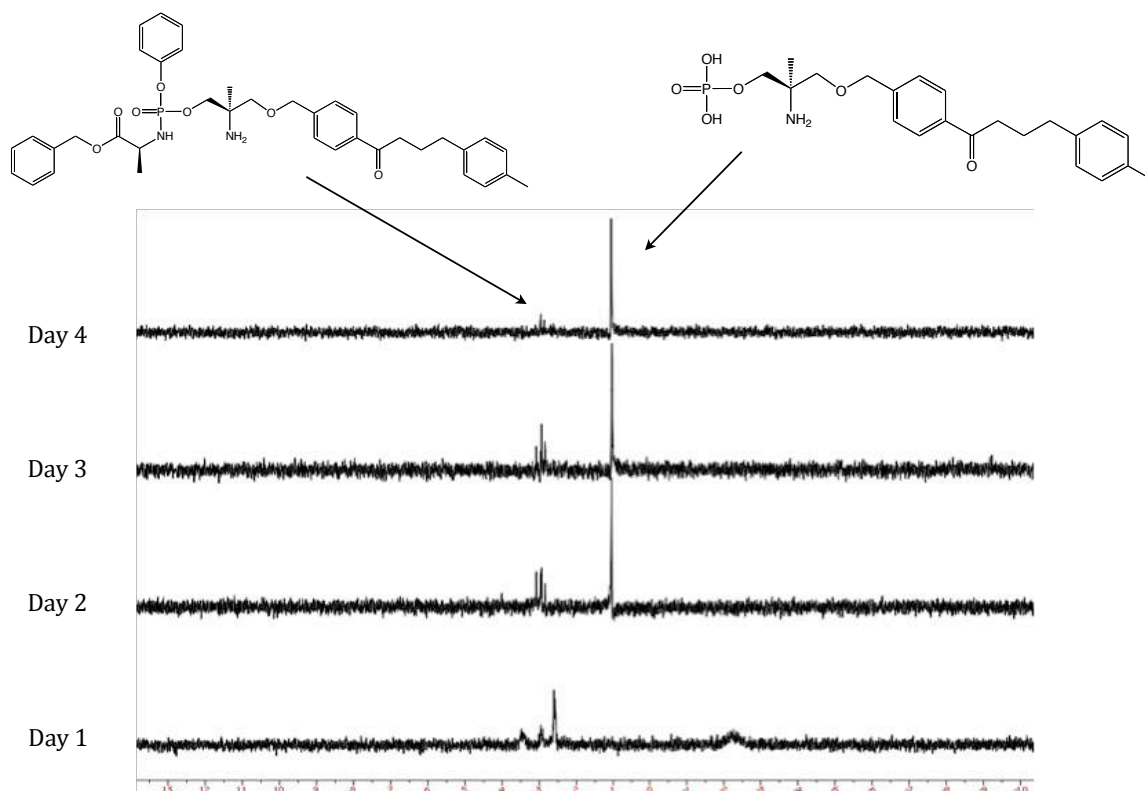


Figure 7.4 Stacked ^{31}P NMR spectra of Ph-LAla-OBzl-BED(a) processing in cell lysate over 4 days

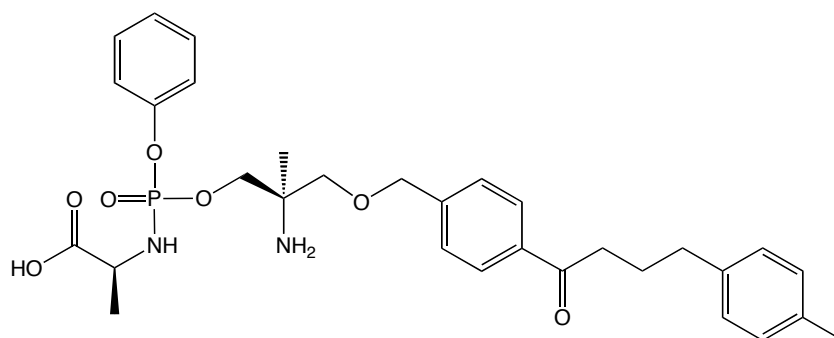


Figure 7.5 Exact mass: 582.25 g/mol, observed mass in negative mode: 581.46 m/z [M-H]

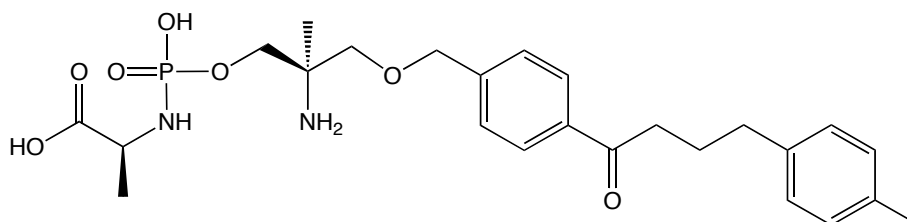
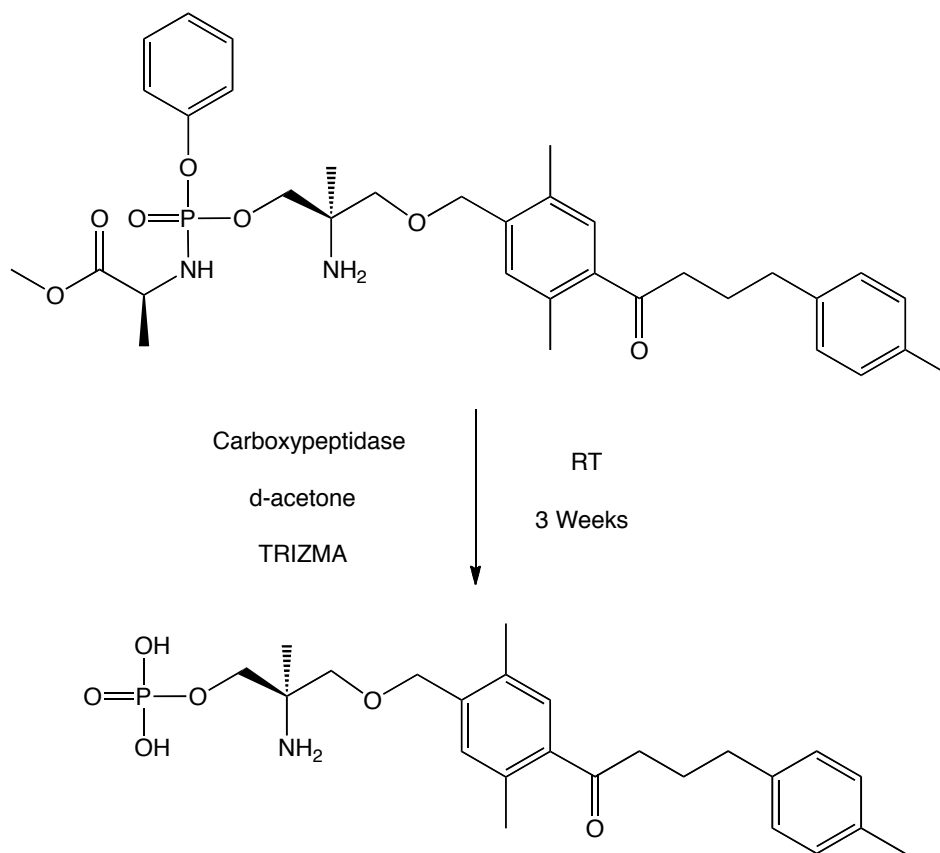


Figure 7.6 Exact mass: 506.22 g/mol, observed mass in negative mode: 541.51 m/z [M+Cl⁻]

7.1.4 Ph-LAla-OMe-BED(h) Carboxypeptidase Experiment



Scheme 7.4 Processing of Ph-LAla-OMe-BED(h) to the monophosphate by carboxypeptidase

A carboxypeptidase processing experiment of Ph-LAla-OMe-BED(h) was conducted over 3 weeks at room temperature. Processing was especially slow but MS analysis shows that the parent molecule was processed to the pharmacologically active monophosphate. A peak of 464.23 m/z [M+H⁺] was observed which corresponds to the monophosphate (predicted mass of 463.21 g/mol) and 625.31 m/z which corresponds to the parent molecule.

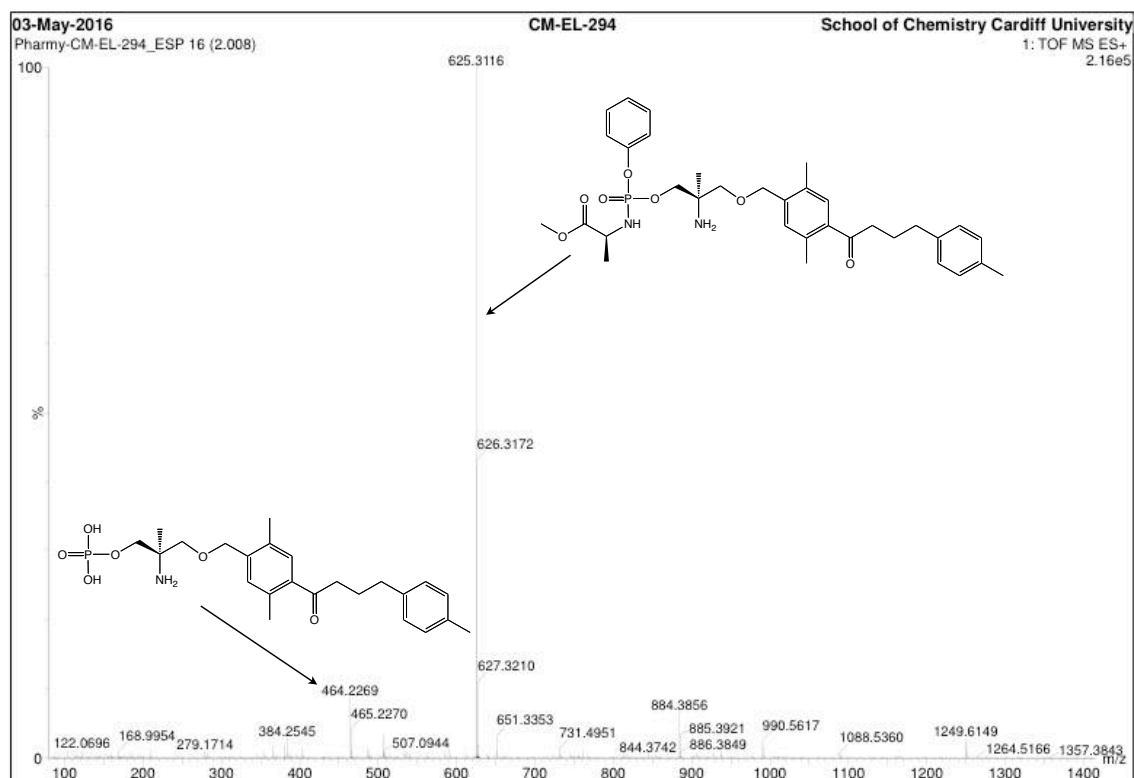


Figure 7.7 Mass spectrometry experiment of Ph-LAla-OMe-BED(h) carboxypeptidase processing experiment with a small peak at 464.23 m/z corresponding to the desired monophosphate

7.2 Stability Assays Part 1

7.2.1 Ph-LAla-OMe-BED(h) Base Stability Experiment

Ph-LAla-OMe-BED(h) was subjected to a pH 8 stability experiment as described in section 5.1.2. Interestingly there appears to have been some instant degradation on adding the base but then the compound was not degraded further over 13 hours. What may have happened is that some impurity in the starting material may have degraded in the presence of base but the parent Ph-LAla-OMe-BED(h) compound has not degraded. Certainly it appears that ProTide BED analogues are more stable in basic conditions than ProTide fingolimod analogues.

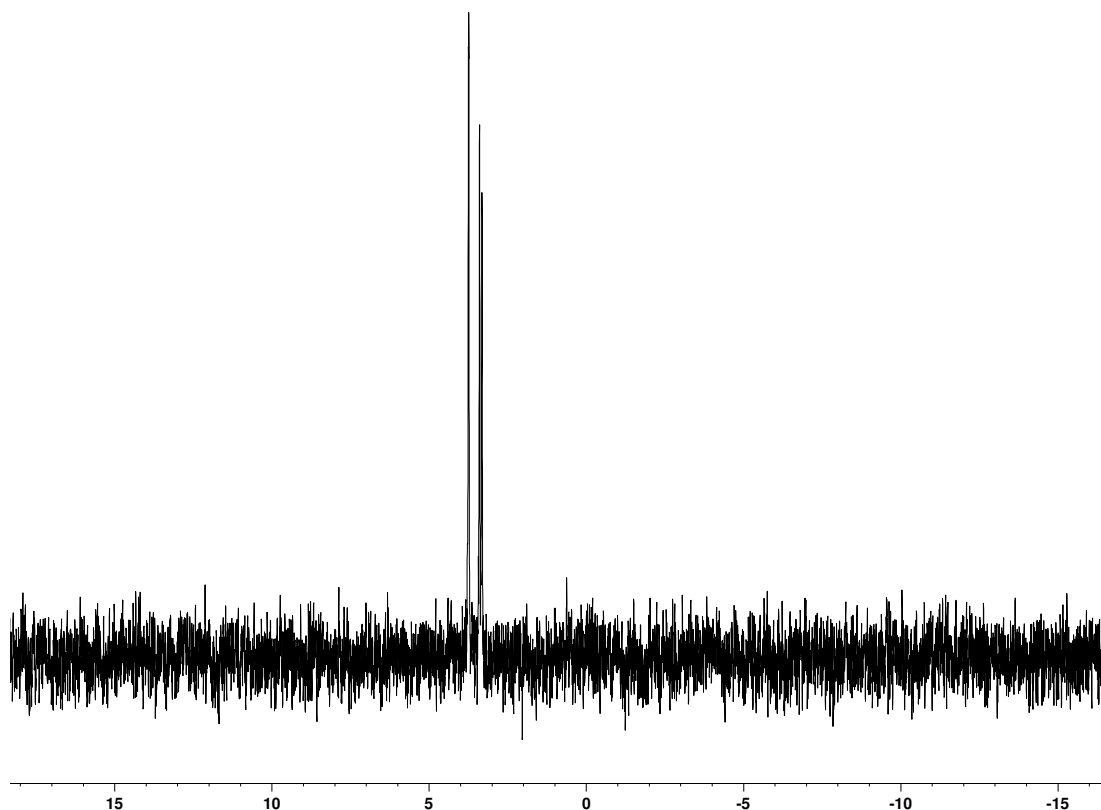


Figure 7.8 ^{31}P NMR spectrum of blank containing Ph-LAla-OMe-BED(h) dissolved in MeOD

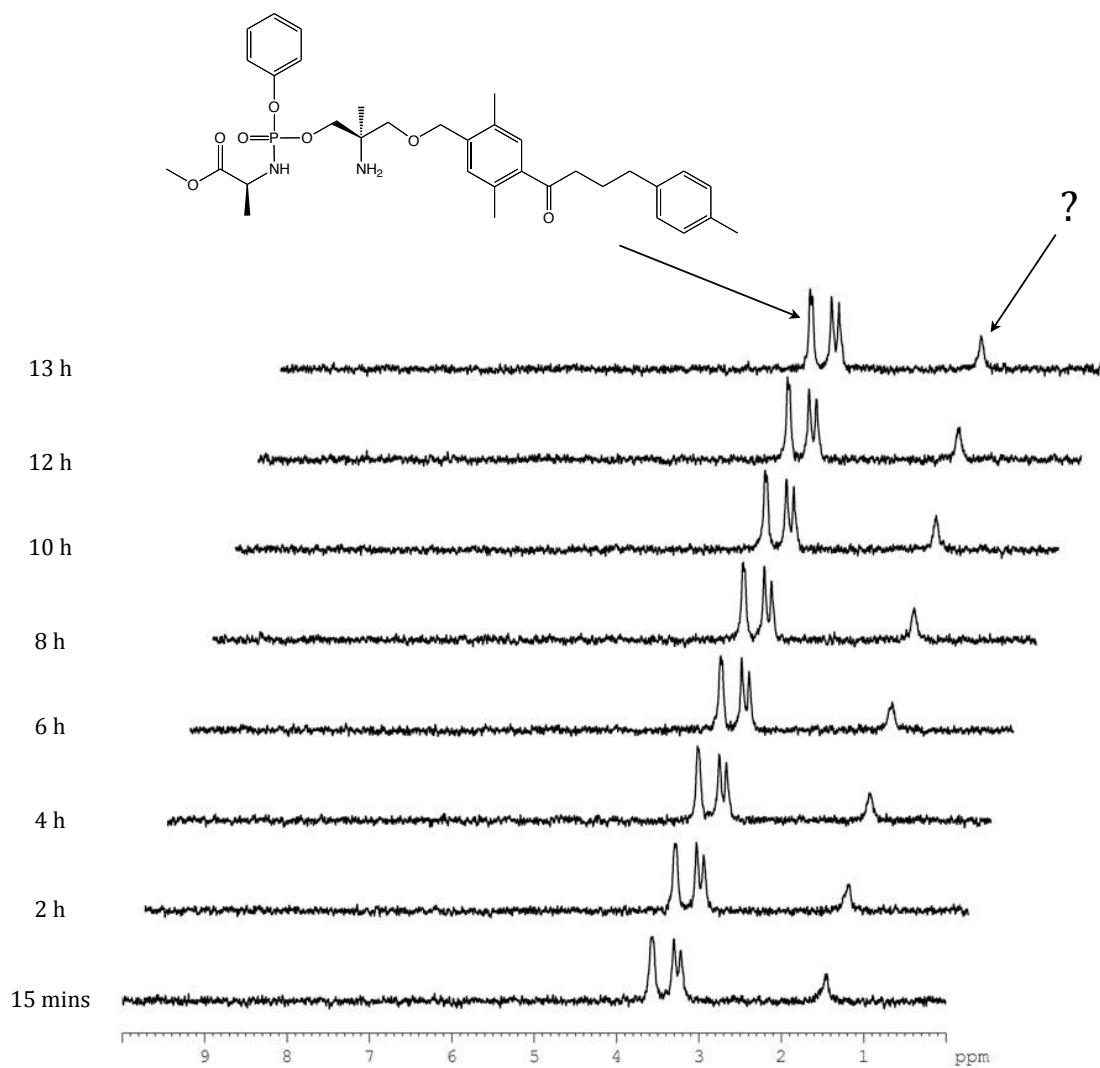


Figure 7.9 Stacked ^{31}P NMR spectra of Ph-LAla-OMe-BED(h) in pH 8 buffer over 13 hours

7.2.2 Ph-LAla-OiPr-BED(a) Base Stability Experiment

Ph-LAla-OiPr-BED(a) was subjected to a pH 8 stability experiment as described in section 5.1.2. Interestingly it appears to have rapidly degraded in part and then remained constant as with the same experiment conducted with Ph-LAla-OMe-BED(h) as shown in figure 7.10.

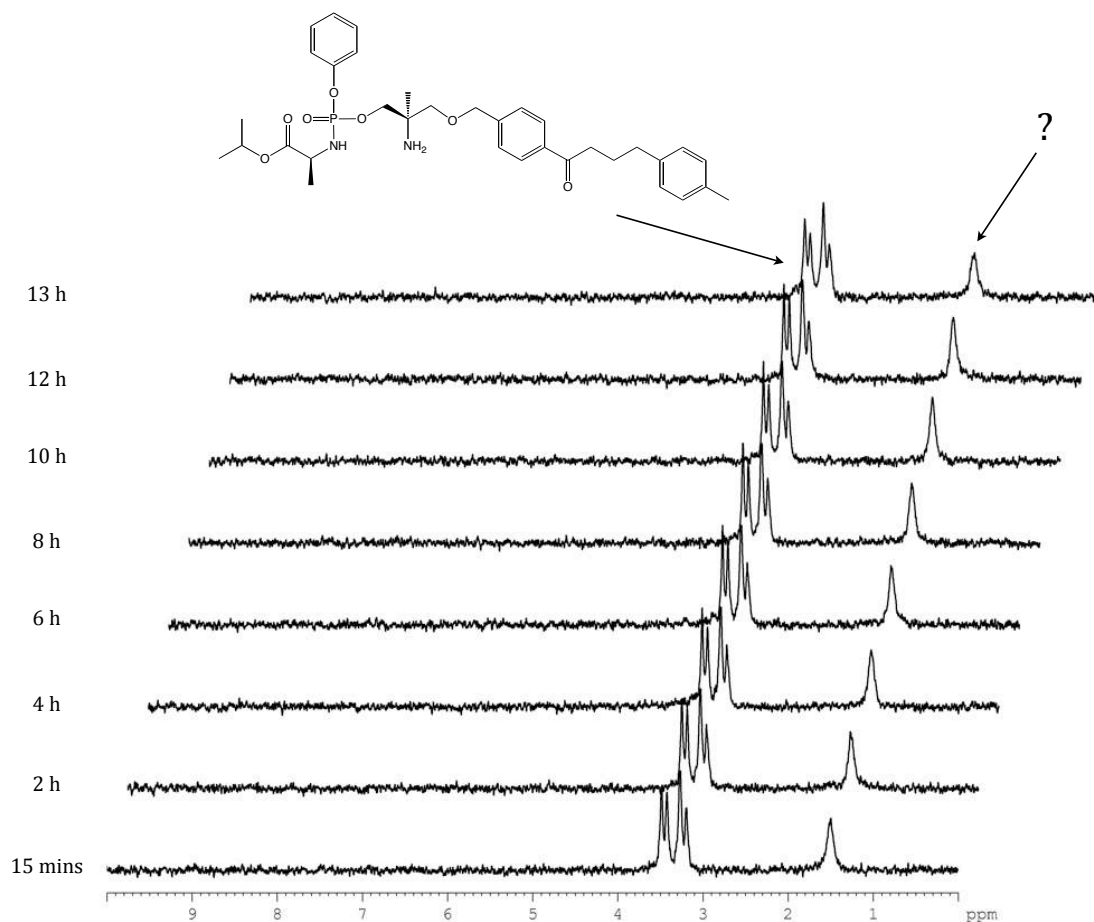


Figure 7.10 Stacked ^{31}P NMR spectra of Ph-LAla-OiPr-BED(a) in pH 8 buffer over 13 hours

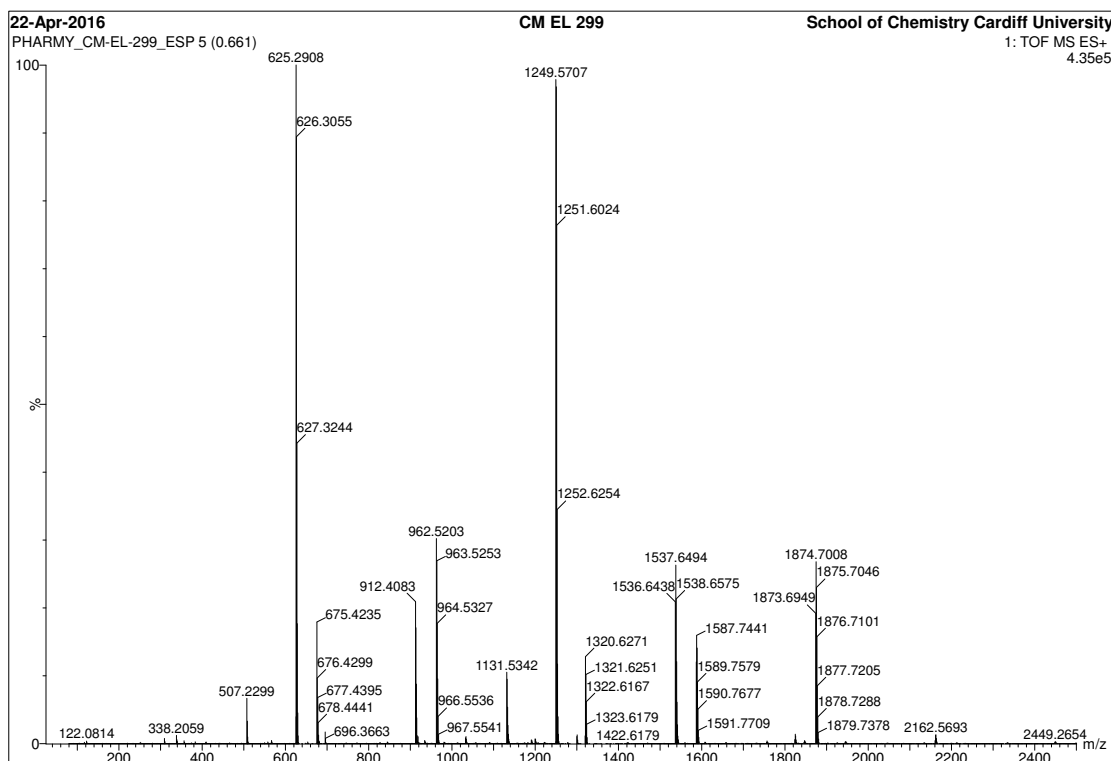


Figure 7.11 Mass spectrometry experiment of base induced Ph-LAla-OiPr-BED(h) degradation

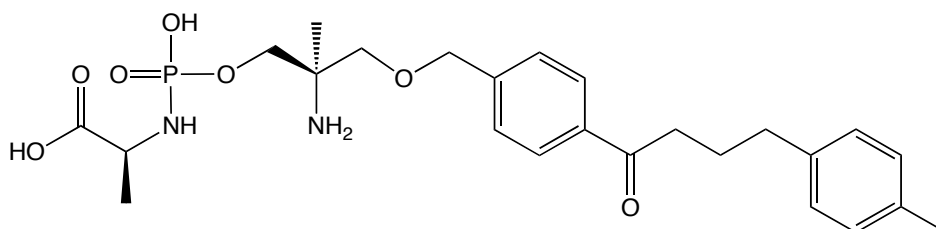


Figure 7.12 Exact mass: 506.22 g/mol, observed mass in positive mode 507.23 m/z [M+H]

The small peak observed in figure 7.10 may correspond to the “X-compound” shown above. This is based on the MS data as shown in figure 7.11. There is no precedent for this degradation in base and certainly there is no simple explanation as to how it may form instantaneously on adding the base and then not continue to degrade over time so it is unknown if the 507.23 m/z peak corresponds to the small peak at around 1.5 ppm in figure 7.10 or whether those two data correspond to the compound shown in figure 7.12.

7.2.3 Ph-LAla-OMe-BED(h) Acid Stability Experiment

The acid stability experiment involving Ph-LAla-OMe-BED(h) in pH 1.5 buffer over 13 h gave similar results to the base stability experiments. Small new peaks appear but the main parent peaks did not decrease in intensity. It appears likely that in the base experiments figures 7.9 and 7.10 and the acid stability experiment shown in figure 7.13 impurities have been degraded but the compound being tested has not degraded.

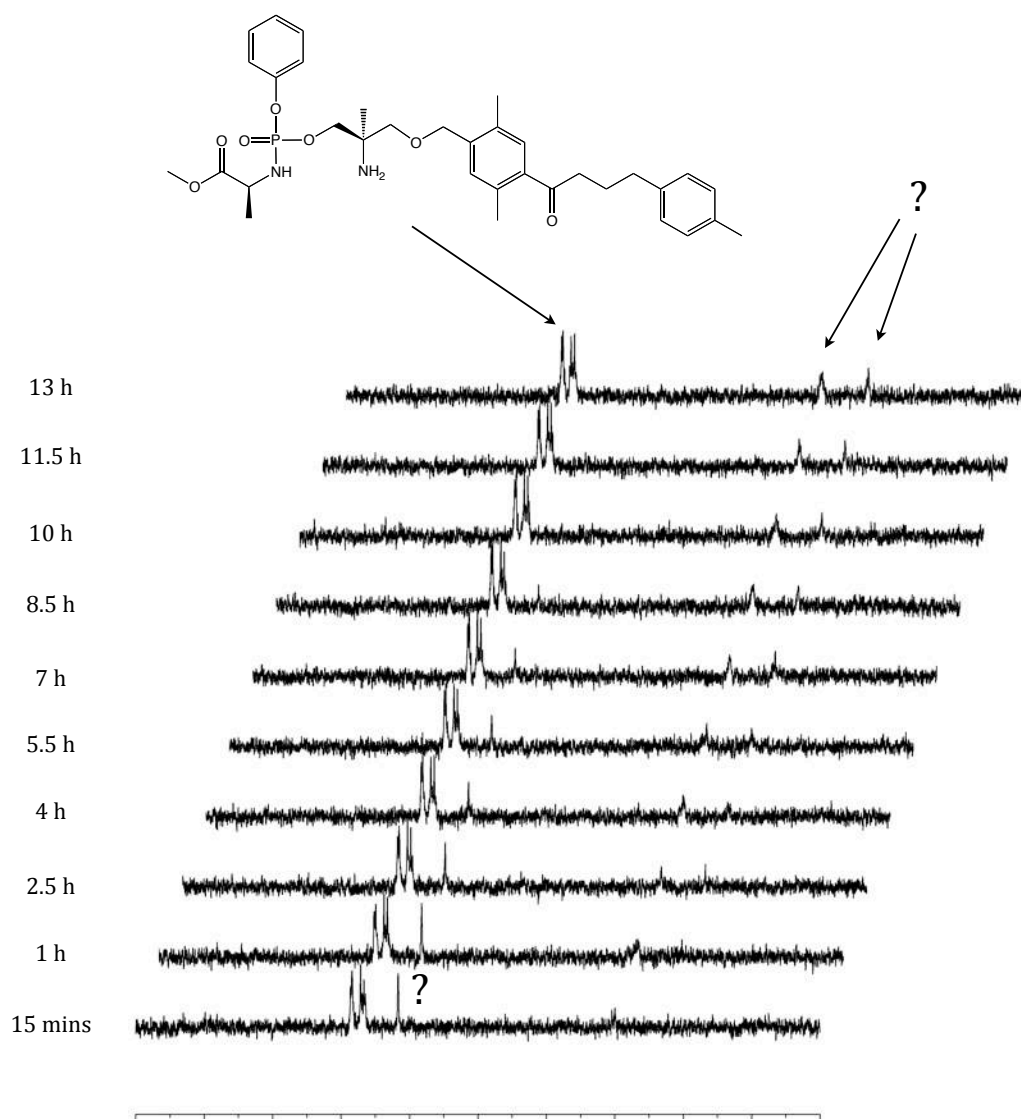


Figure 7.13 Stacked ^{31}P NMR spectra of Ph-LAla-OMe-BED(h) acid stability experiment over 13 h at pH 1.5

7.3 HPLC

7.3.1 Analytical HPLC

In order to confirm the hypothesis that the compounds being tested were not sufficiently pure and that it is impurities that are being degraded and detected by phosphorus NMR, analytical HPLC was conducted on the ProTide BED analogues.

The HPLC method used 20% ACN and 80% 0.1% TFA in H₂O increasing to ACN 100% over 34 minutes.³ The UV detector was set to 220 nm and 263 nm.

	Time (min)	Methanol (%)	ACN (%)	Water (%)	W (%)	Flow (mL/min)
1	0.0		20.0	80.0		1.00
2	30.0		100.0			1.00
3	34.0		100.0			1.00
4	37.0		20.0	80.0		1.00
5						

Figure 7.14 Analytical HPLC method information for BED analogues

	Time (min)	Wavelength 1 (nm)	Wavelength 2 (nm)
1	0.0	220	263
2	35.0	220	263
3			

Figure 7.15 Analytical HPLC method information for BED analogues

Figures 7.17 and 7.18 show the data for the analytical HPLC experiments for the two ProTide BED analogues previously tested in base and acid stability experiments. As can be seen, the analogues tested are not sufficiently pure to rule

out the possibility that the new peaks seen in the base and acid stability experiments are degraded impurities. With purities of around:

- 87% for Ph-LAla-OMe-BED(h)
- 82% for Ph-LAla-OiPr-BED(a)

It was decided that, in order to be able to progress with the stability experiments, preparative HPLC needed to be conducted on the ProTide BED analogues in order to be able to rule out impurities as an explanation for any further data of the type previously seen in the base and acid stability experiments for BED analogues. Typically purities of around 95% or more are more acceptable for biological testing and publication standard data.

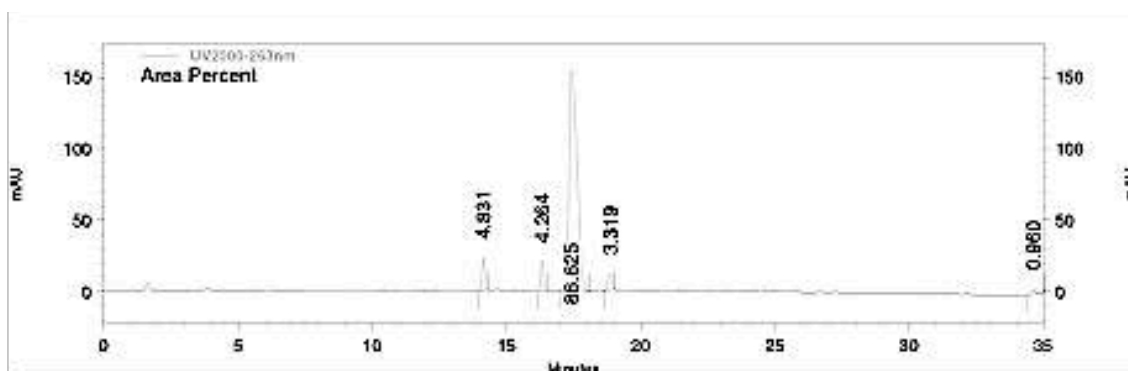


Figure 7.16 Analytical HPLC chromatograph of Ph-LAla-OMe-BED(h)

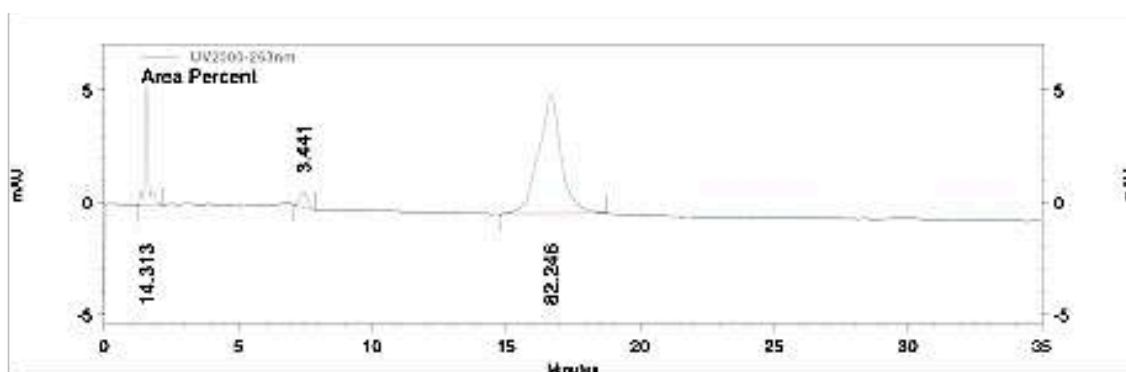


Figure 7.17 Analytical HPLC chromatograph of Ph-LAla-OiPr-BED(a)

A similar level of purity was observed in all 6 ProTide BED analogues synthesised and purified by column chromatography. Parent BED(a) and BED(h) were both a

more acceptable 94% and 95% pure respectively after column chromatography as shown in figures 7.19 and 7.20.

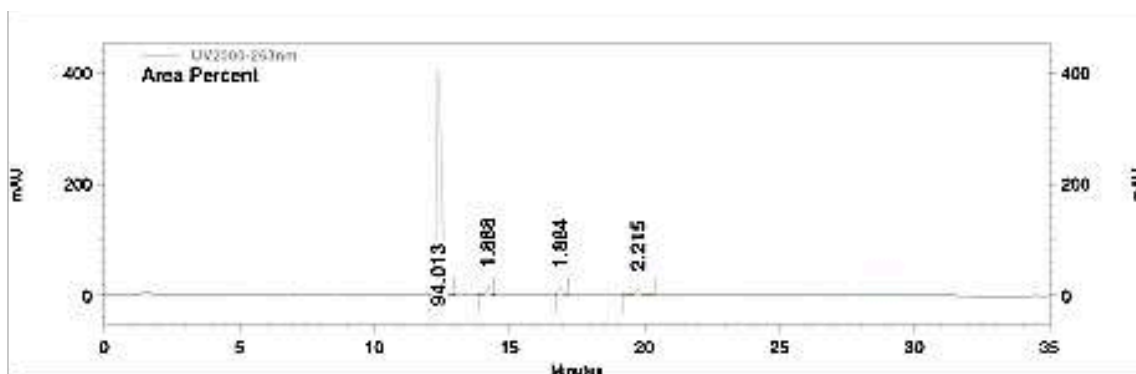


Figure 7.18 Analytical HPLC chromatograph of BED(a)

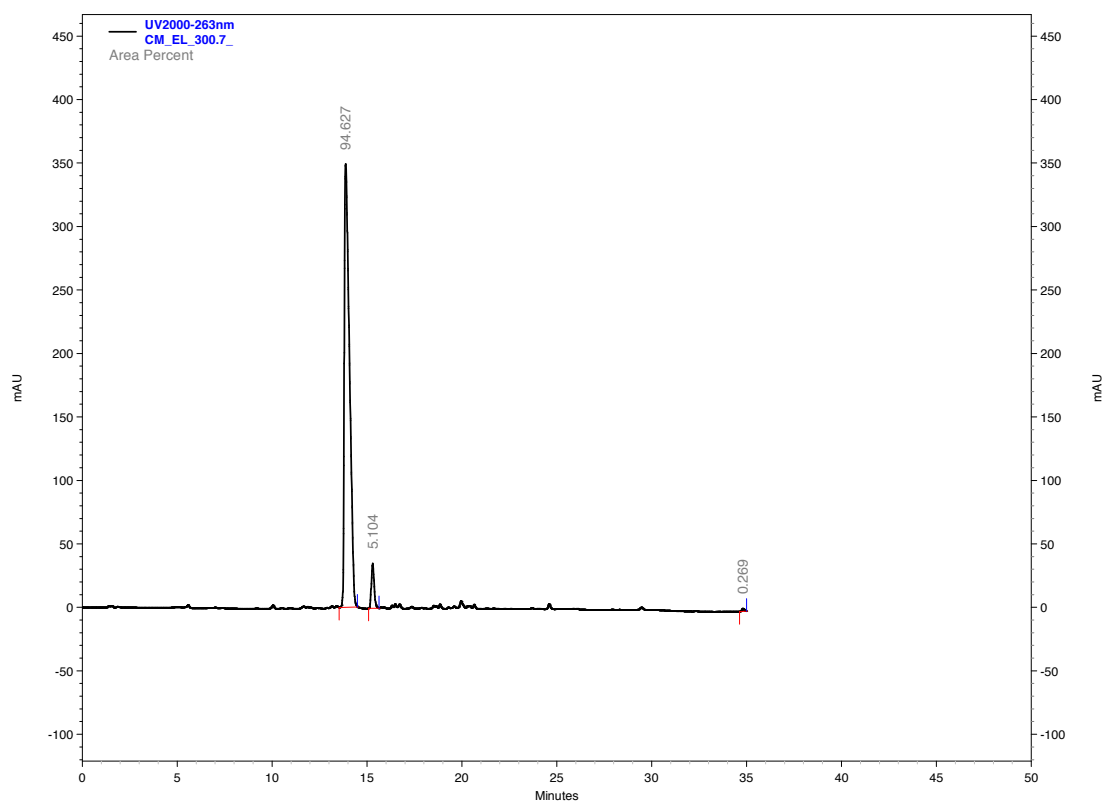


Figure 7.19 Analytical HPLC chromatograph of BED(h)

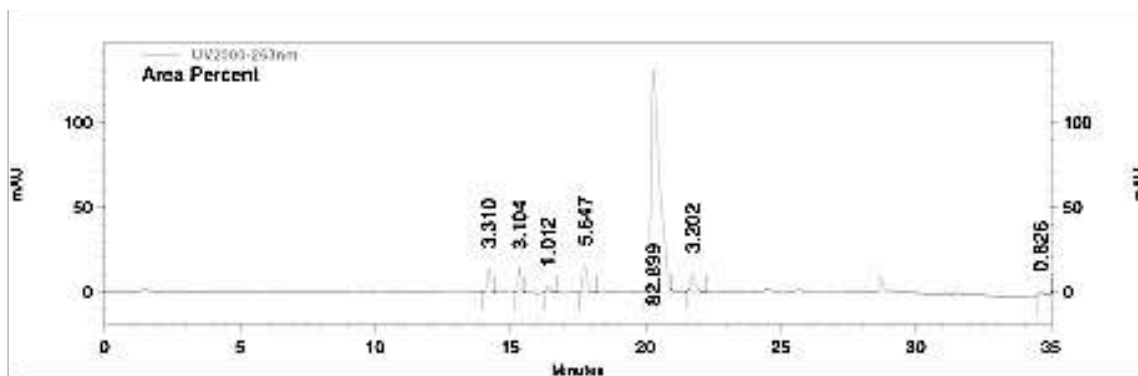


Figure 7.20 Analytical HPLC chromatograph of Ph-LAla-OBzl-BED(h)

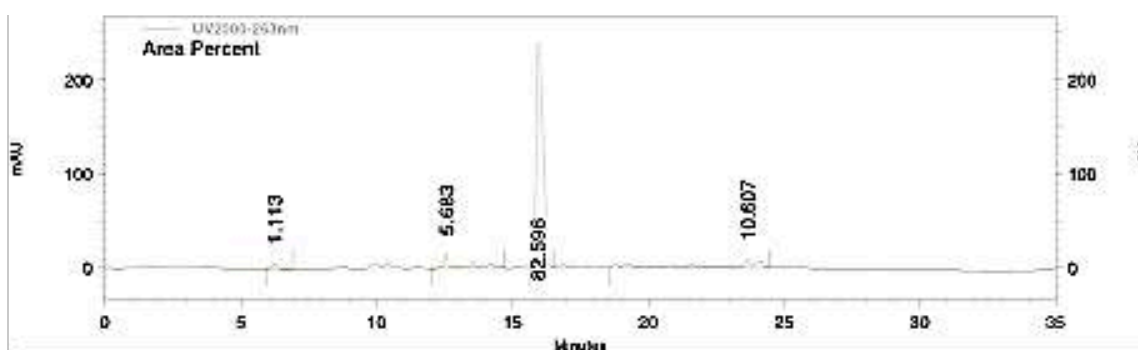


Figure 7.21 Analytical HPLC chromatograph of Ph-LAla-OMe-BED(a)

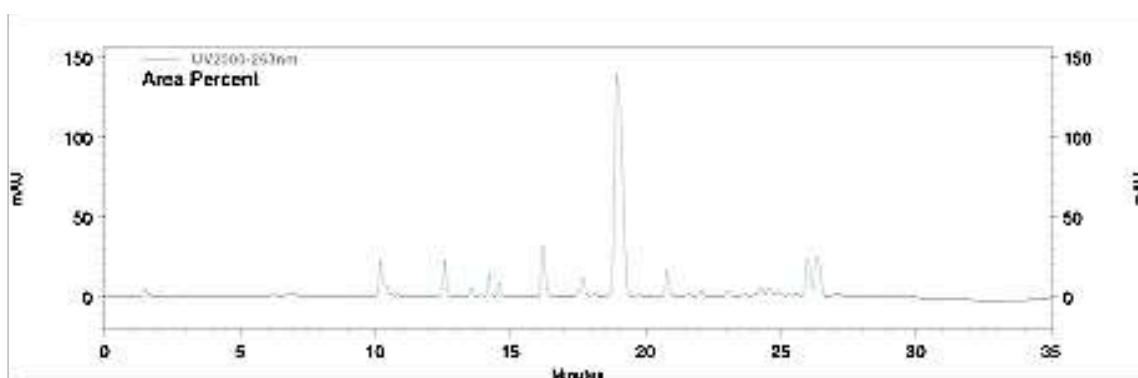


Figure 7.22 Analytical HPLC chromatograph of Ph-LAla-OBzl-BED(a)

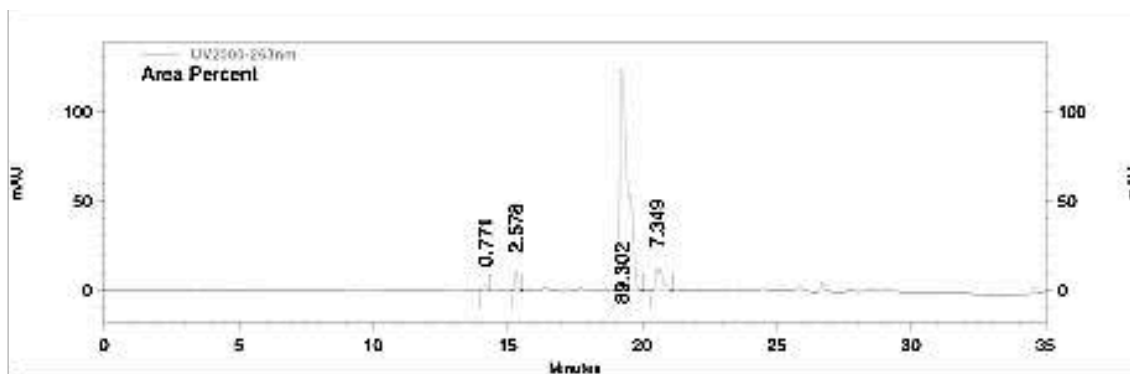


Figure 7.23 Analytical HPLC chromatograph of Ph-LAla-OiPr-BED(h)

7.3.2 Preparative HPLC

Preparative HPLC was conducted on the ProTide BED analogues and then the purified compounds were checked for purity again using analytical HPLC. The solvent system used for the preparative method was the same as the analytical but on a larger scale. The UV detector was set to 220 nm and 245 nm / 263 nm.

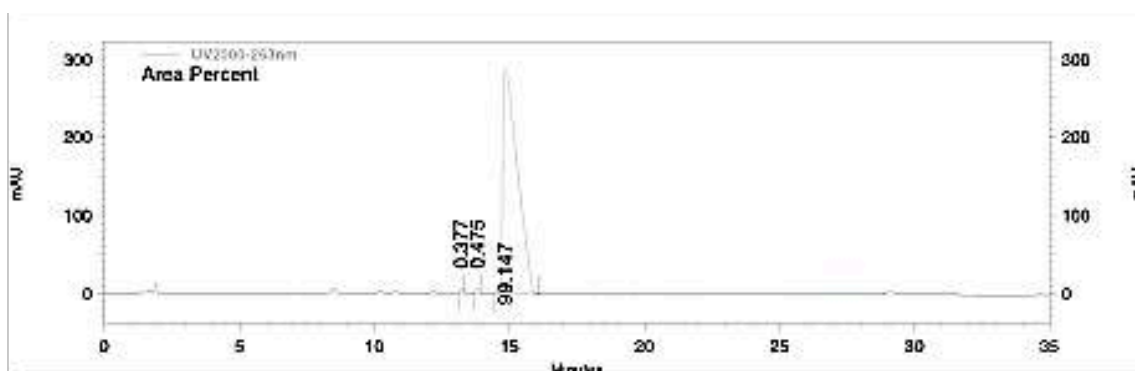


Figure 7.24 Analytical HPLC chromatograph of Ph-LAla-OMe-BED(a) after preparative HPLC

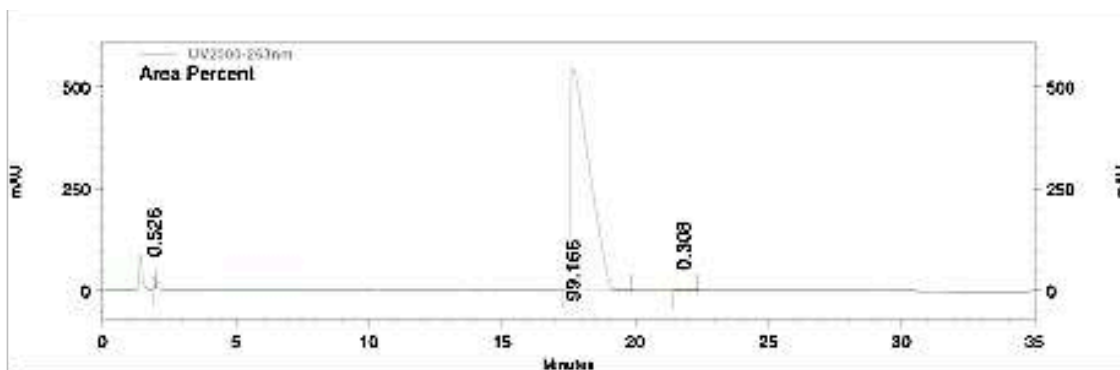


Figure 7.25 Analytical HPLC chromatograph of Ph-LAla-OBzl-BED(a) after preparative HPLC

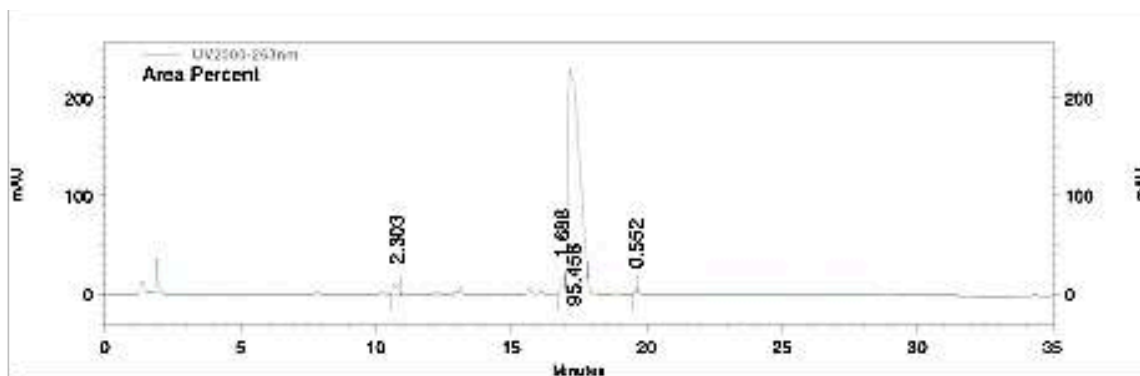


Figure 7.26 Analytical HPLC chromatograph of Ph-LAla-OiPr-BED(a) after preparative HPLC

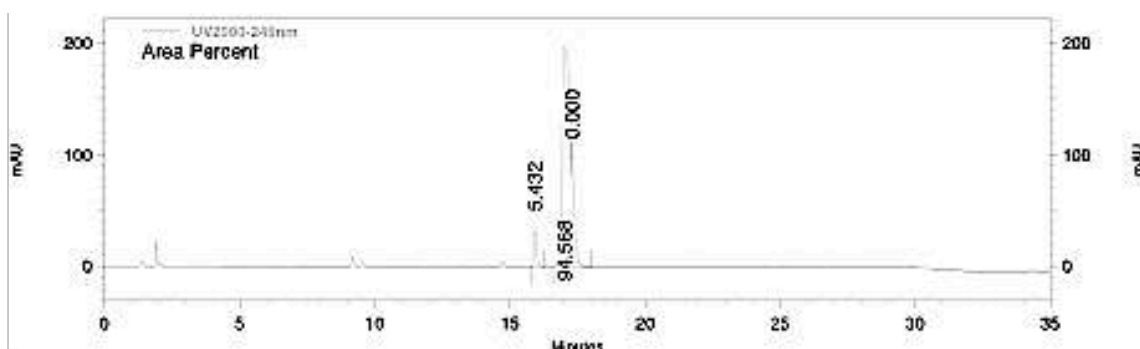


Figure 7.27 Analytical HPLC chromatograph of Ph-LAla-OMe-BED(h) after preparative HPLC

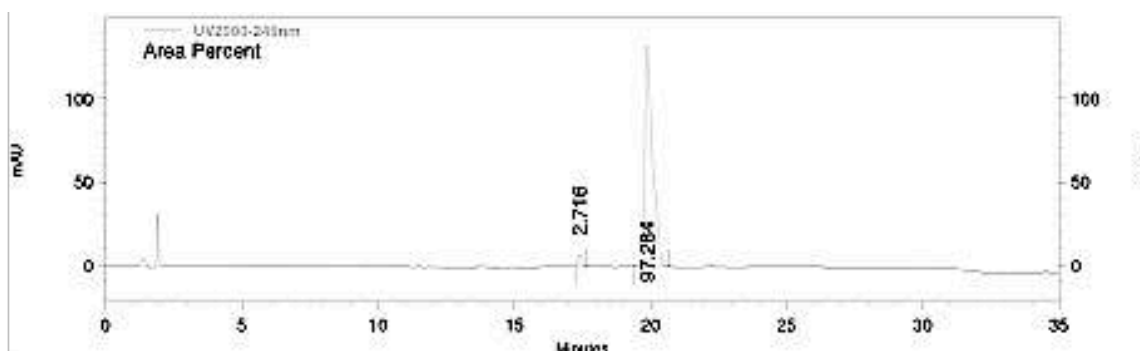


Figure 7.28 Analytical HPLC chromatograph of Ph-LAla-OBzl-BED(h) after preparative HPLC

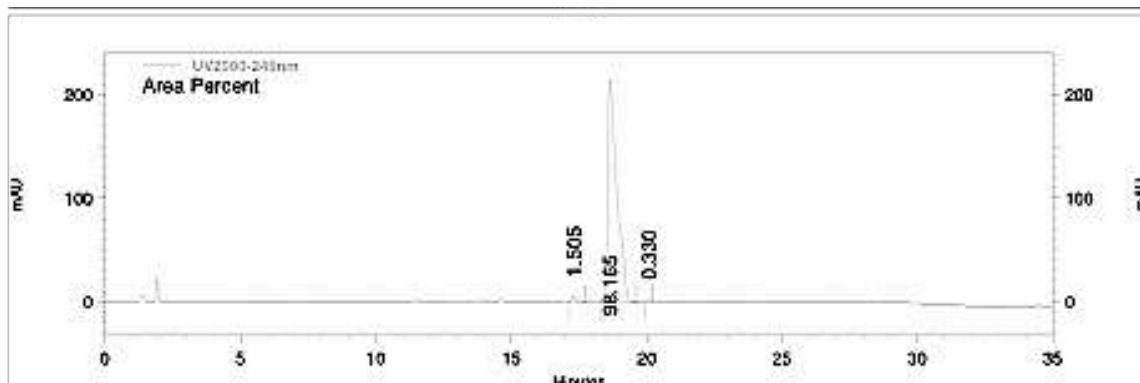


Figure 7.29 Analytical HPLC chromatograph of Ph-LAla-OiPr-BED(h) after preparative HPLC

7.4 Stability Assays Part 2

7.4.1 Ph-LAla-OiPr-BED(h) Acid Stability Experiment

An acid stability experiment involving preparative HPLC purified Ph-LAla-OiPr-BED(h) in pH 1.5 buffer over 13 h gave much better results than in figure 7.13. As can be seen below in figure 7.30 there was no discernable change over 13 hours at pH 1.5 suggesting that ProTide BED analogues are able to withstand the acidic conditions of the stomach and that the previously observed peaks seen in figure 7.13 are in fact degraded compounds of impurities.

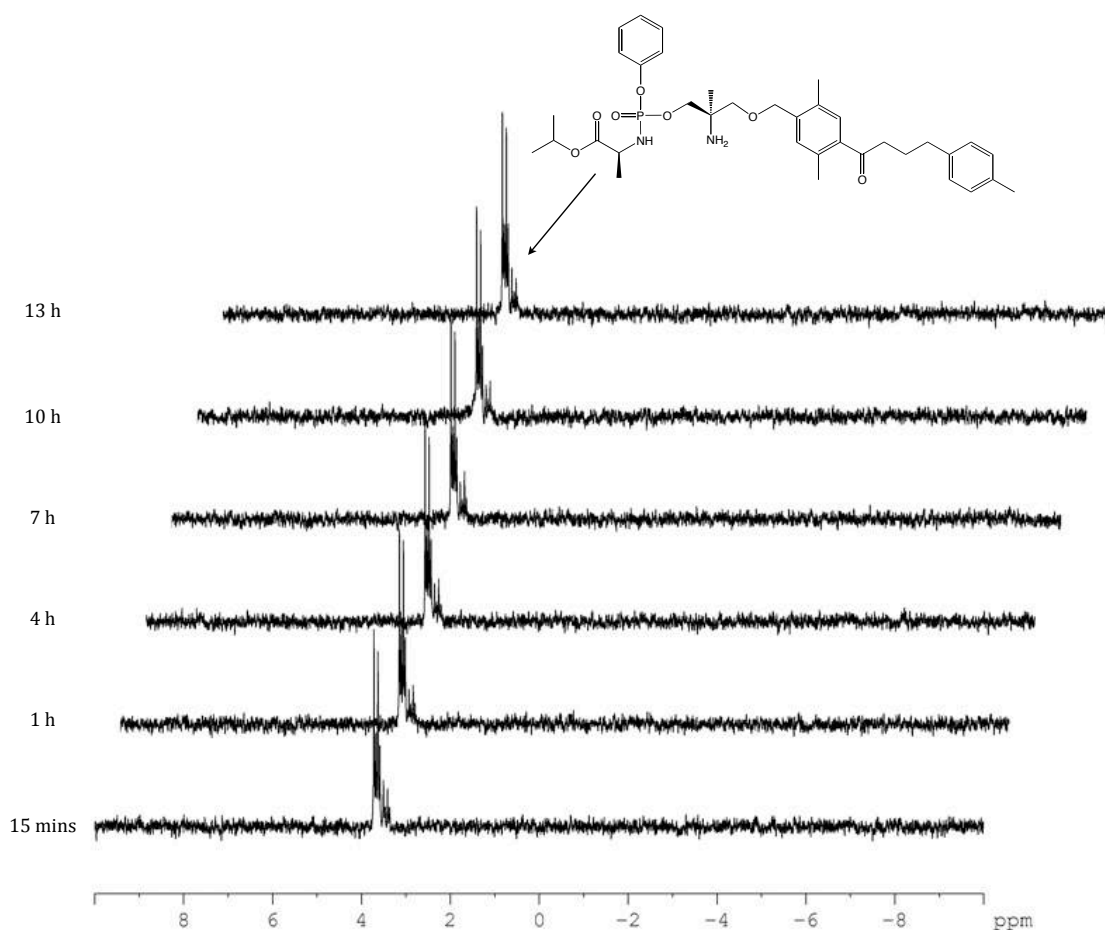


Figure 7.30 Ph-LAla-OiPr-BED(h) acid stability experiment over 13 h at pH 1.5

7.4.2 Ph-LAla-OMe-BED(a) Base Stability Experiment

Ph-LAla-OMe-BED(a) was subjected to a pH 8 stability experiment as described in sections 7.2.1 and 7.2.2. This time, however, the expected results were observed. No degradation is discernable in the NMR spectra confirming that:

- ProTide BED analogues are more stable in basic conditions than ProTide fingolimod analogues
- The previously observed unexpected degradations seen in figures 7.9 and 7.10 are the result of impurities in the compound degrading as opposed to the desired ProTide BED analogues themselves

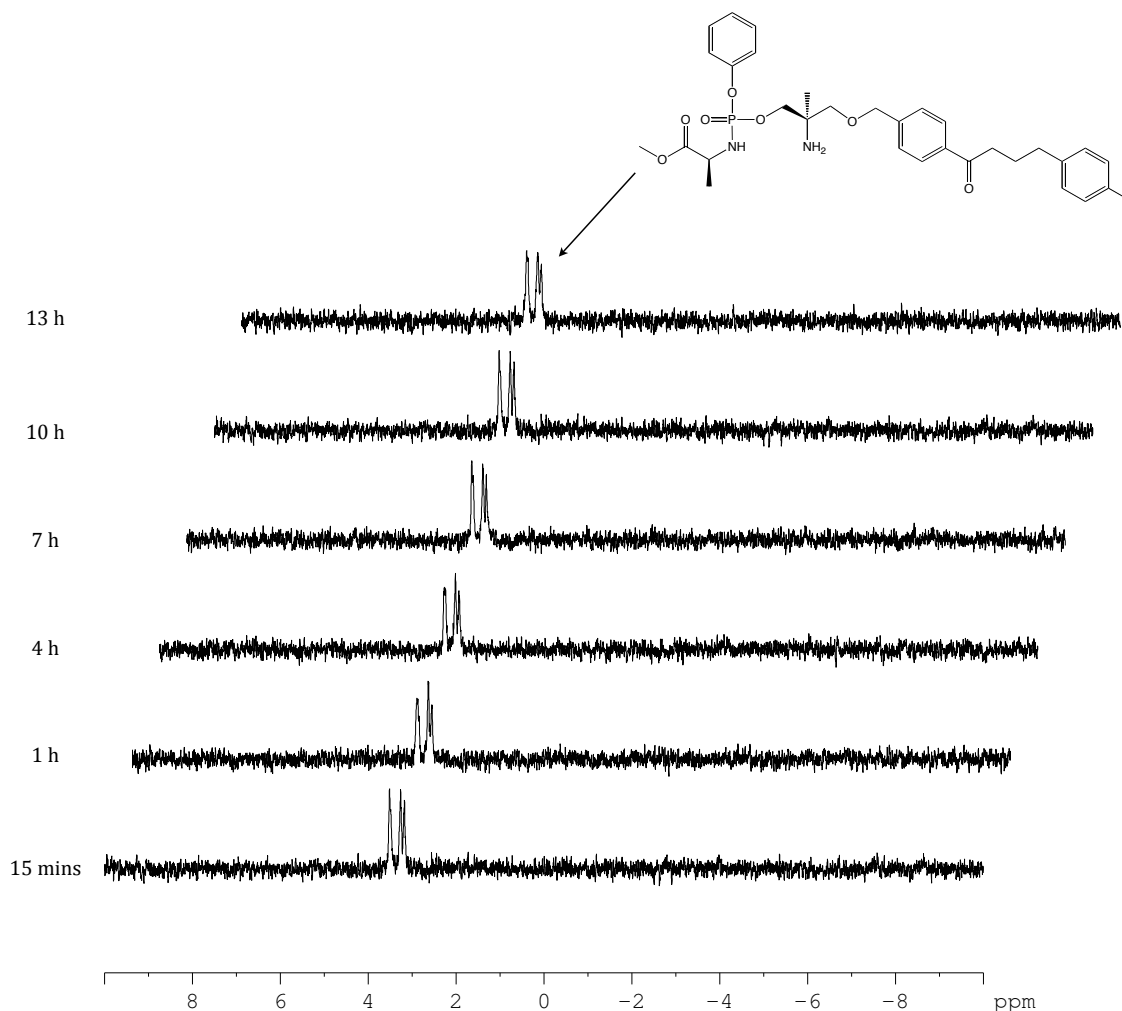


Figure 7.31 Ph-LAla-OMe-BED(a) base stability experiment over 13 h at pH 8

7.4.3 Ph-LAla-OMe-BED(h) Base Stability Experiment

Ph-LAla-OMe-BED(h) was subjected to a pH 8 stability experiment of the same type as described in section 7.2.1. This time, however, no small peak appeared. This confirms beyond any reasonable doubt that the previously seen small peak that was observed was due to an impurity rather than degradation of the parent compound itself.

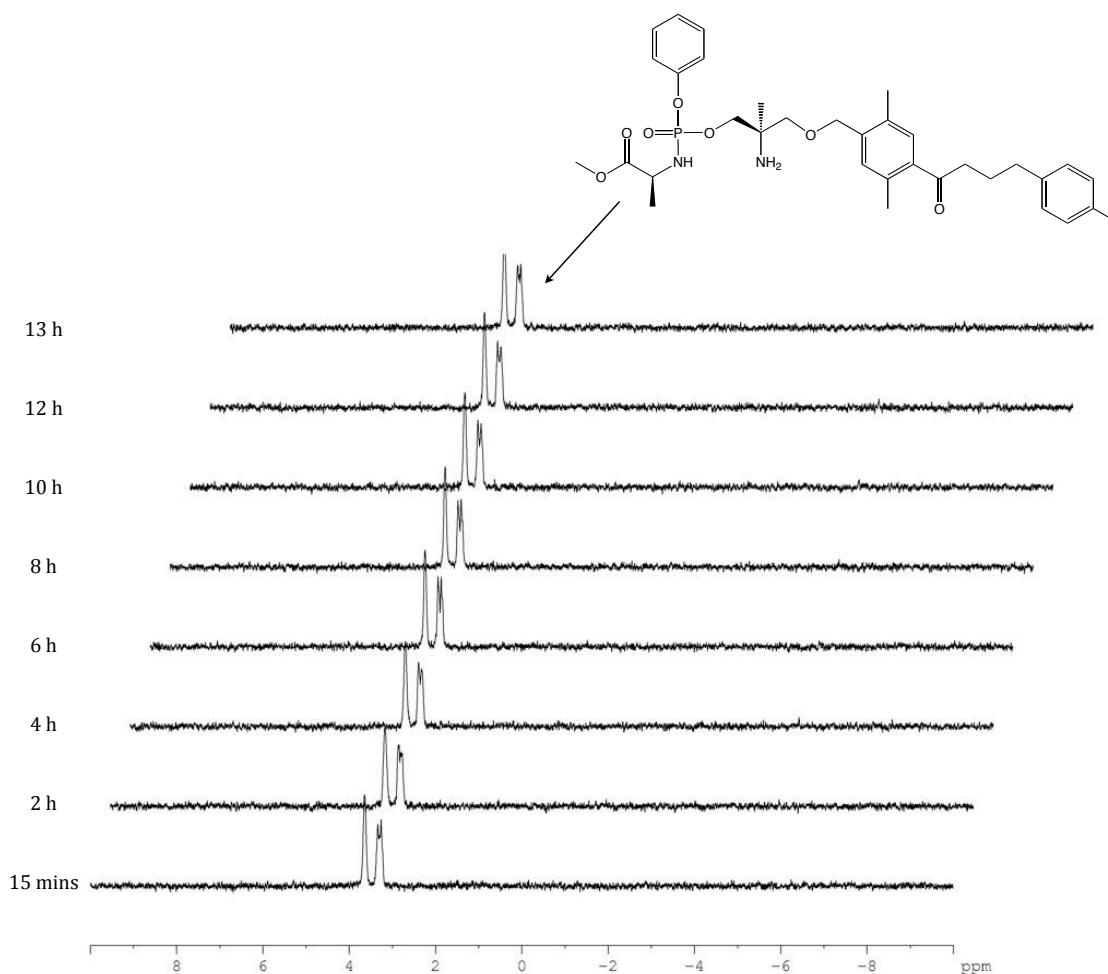
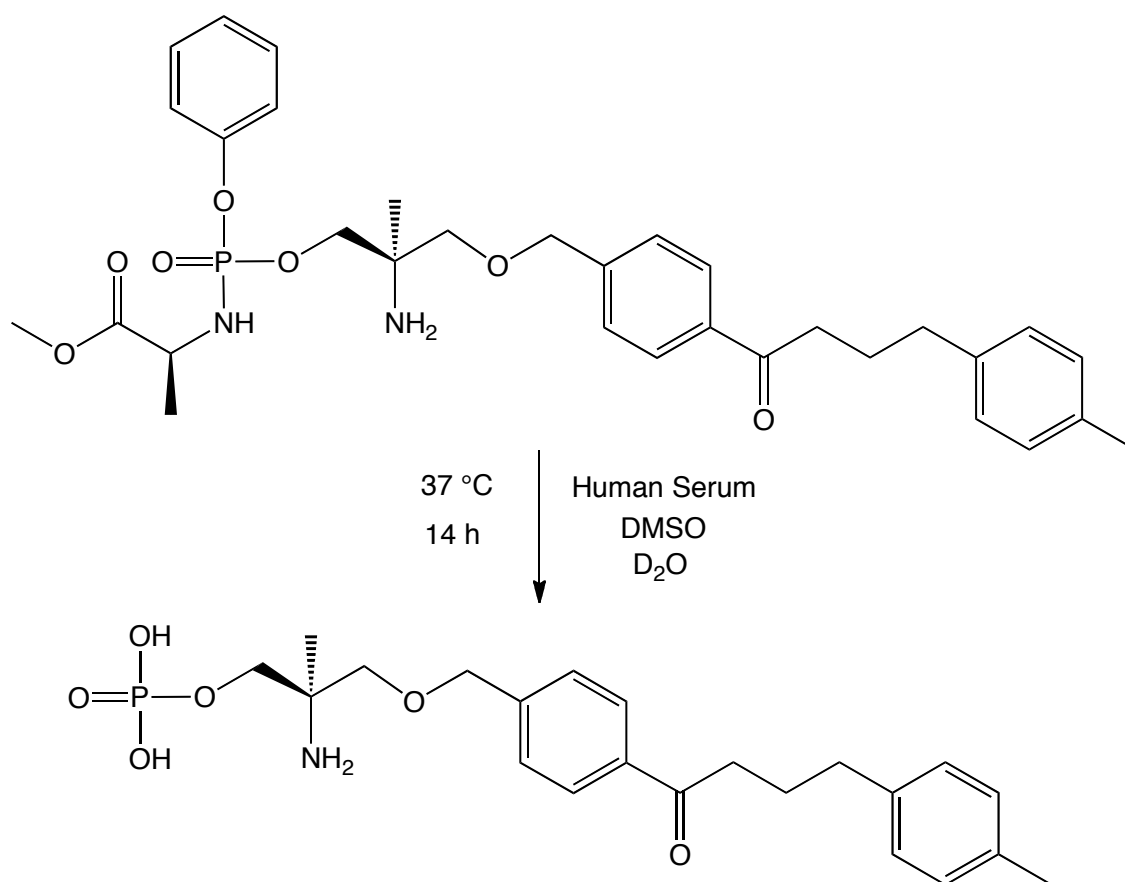


Figure 7.32 Ph-LAla-OMe-BED(h) base stability experiment over 13 h at pH 8

7.4.4 Ph-LAla-OMe-BED(a) Human Serum Experiment



Scheme 7.5 Degradation of Ph-LAla-OMe-BED(a) to the monophosphate in human serum

A stability study of Ph-LAla-OMe-BED(a) in human serum was also conducted following a previously reported procedure.¹ Unlike the human serum experiment conducted on ProTide fingolimod (section 5.2.9) it appears that the primary product is not any unwanted cyclised product but the therapeutically relevant monophosphate. The mass spectrometer used to determine different masses had been giving a few anomalous results and the mass spectrometric analysis of this experiment appears to be an example of this. In the positive mode analysis the masses observed include 437.19 m/z and 459.17 m/z which both have a mass +1 of that expected of the peaks are [M+H] and [M+Na⁺] respectively. In light of the fact that the phosphorus chemical shift is what has been previously shown to be indicative of the monophosphate and there is precedent for the mass spectrometer used to give anomalous +1 than expected masses it seems highly likely that the ProTide BED(a) analogue tested has degraded to the monophosphate.

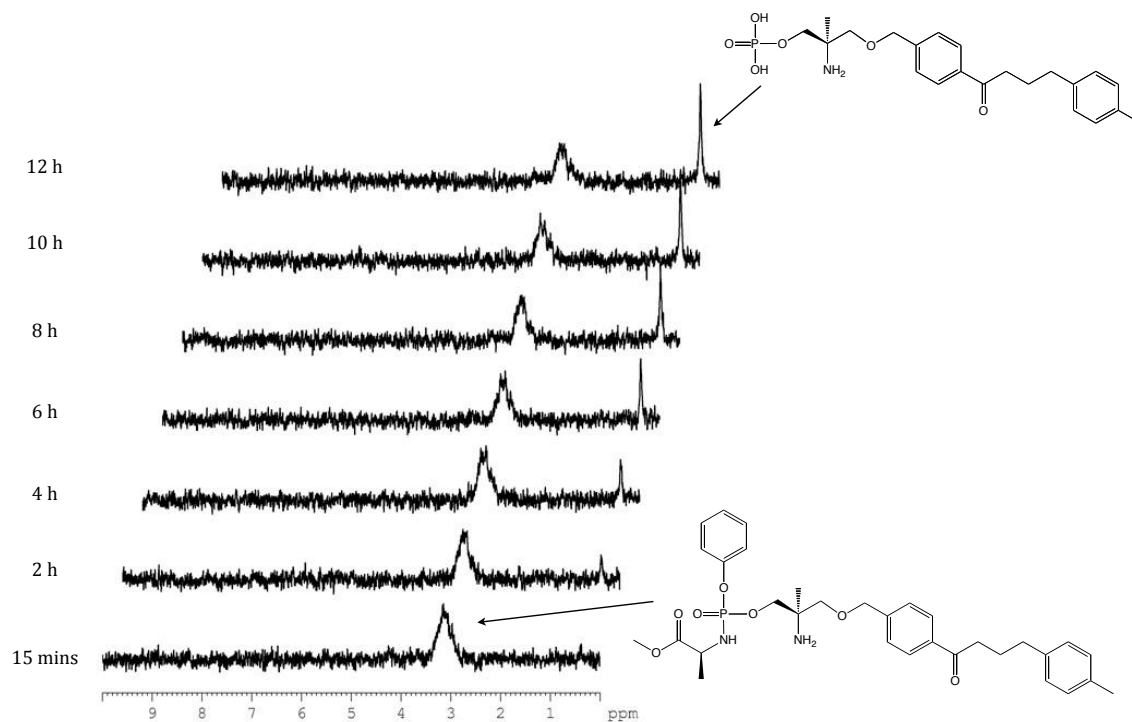
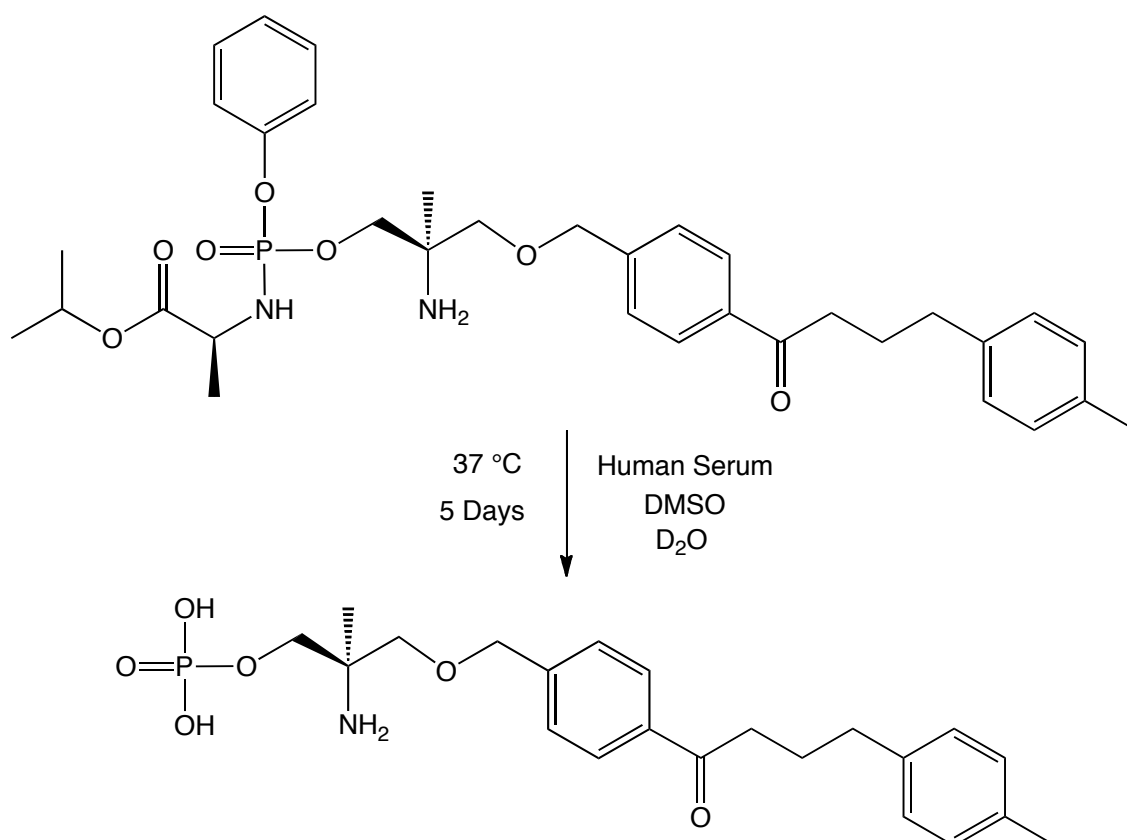


Figure 7.33 Stacked ^{31}P NMR spectra of Ph-LAla-OMe-BED(a) processing in human serum over 12 hours at 37 °C

The estimated half-life for this reaction is around 14 hours. This figure was calculated from the change of the integrations of the two peaks over time.

7.4.5 Ph-LAla-OiPr-BED(a) Human Serum Experiment

A stability study of Ph-LAla-OiPr-BED(a) in human serum at 37 °C was conducted over 5 days. The sample tube was kept warm during the 5 day experiment time period using a water bath set to 37°C.



Scheme 7.6 Degradation of Ph-LAla-OiPr-BED(a) to the monophosphate in human serum

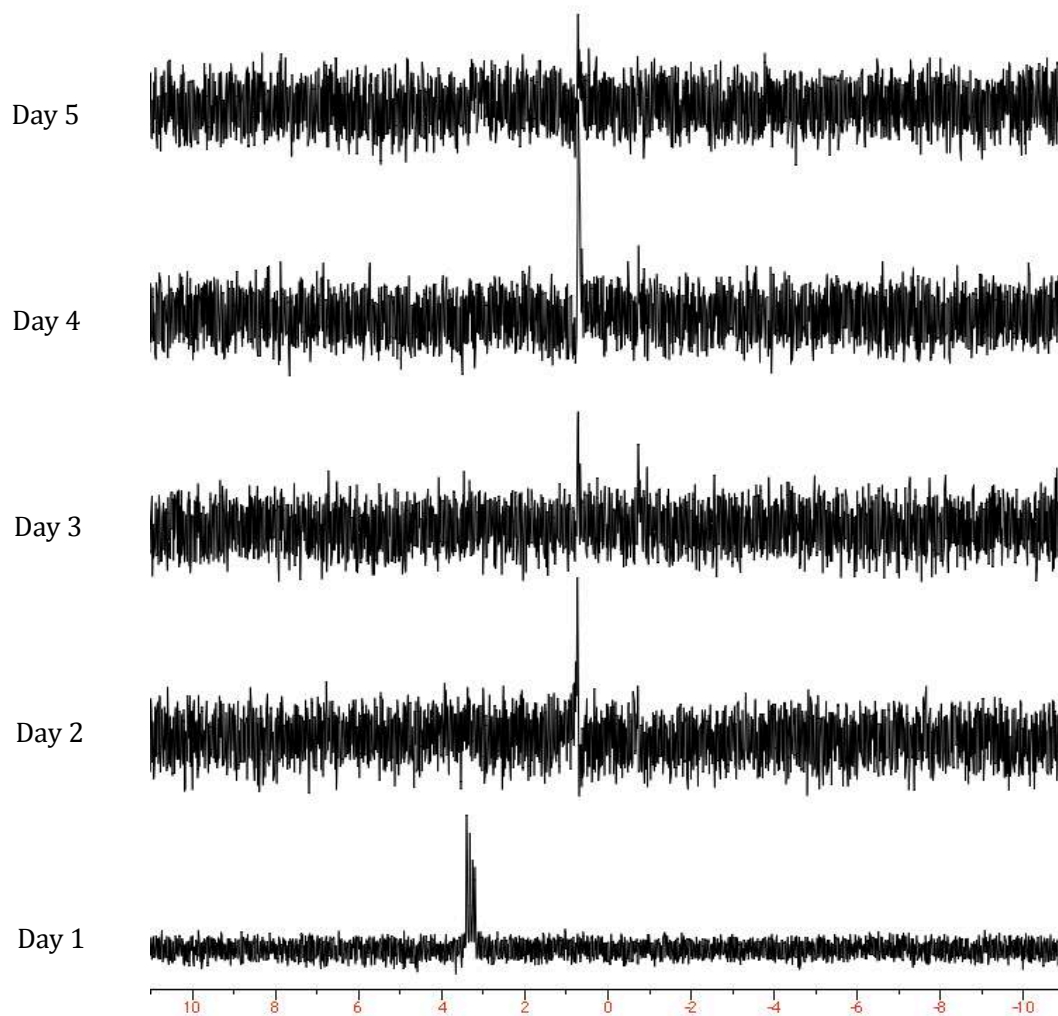
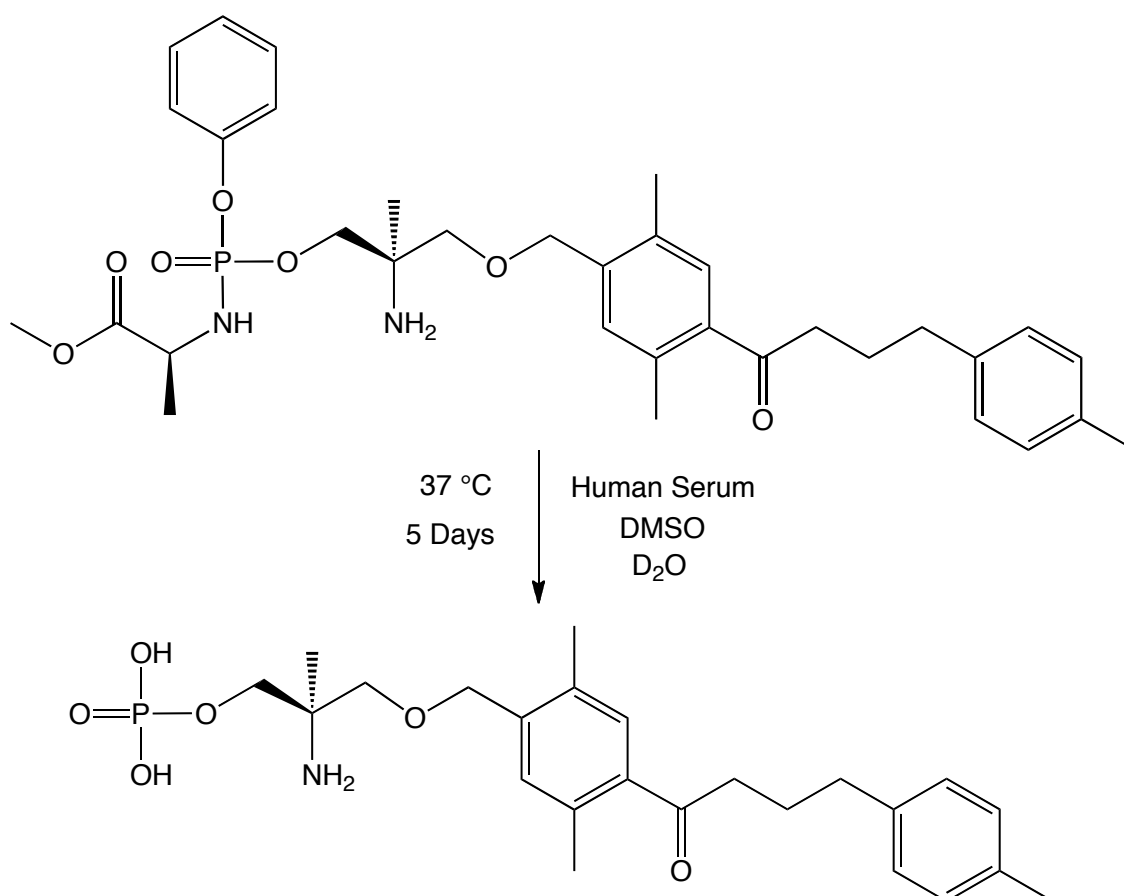


Figure 7.34 Stacked ^{31}P NMR spectra of Ph-LAla-OiPr-BED(a) processing in human serum over 5 days at 37 °C

7.4.6 Ph-LAla-OMe-BED(h) Human Serum Experiment

A stability study of Ph-LAla-OMe-BED(h) in human serum at 37 °C was conducted over 5 days. The sample tube was kept warm during the 5 day experiment time period using a water bath set to 37°C.



Scheme 7.7 Degradation of Ph-LAla-OMe-BED(h) to the monophosphate in human serum

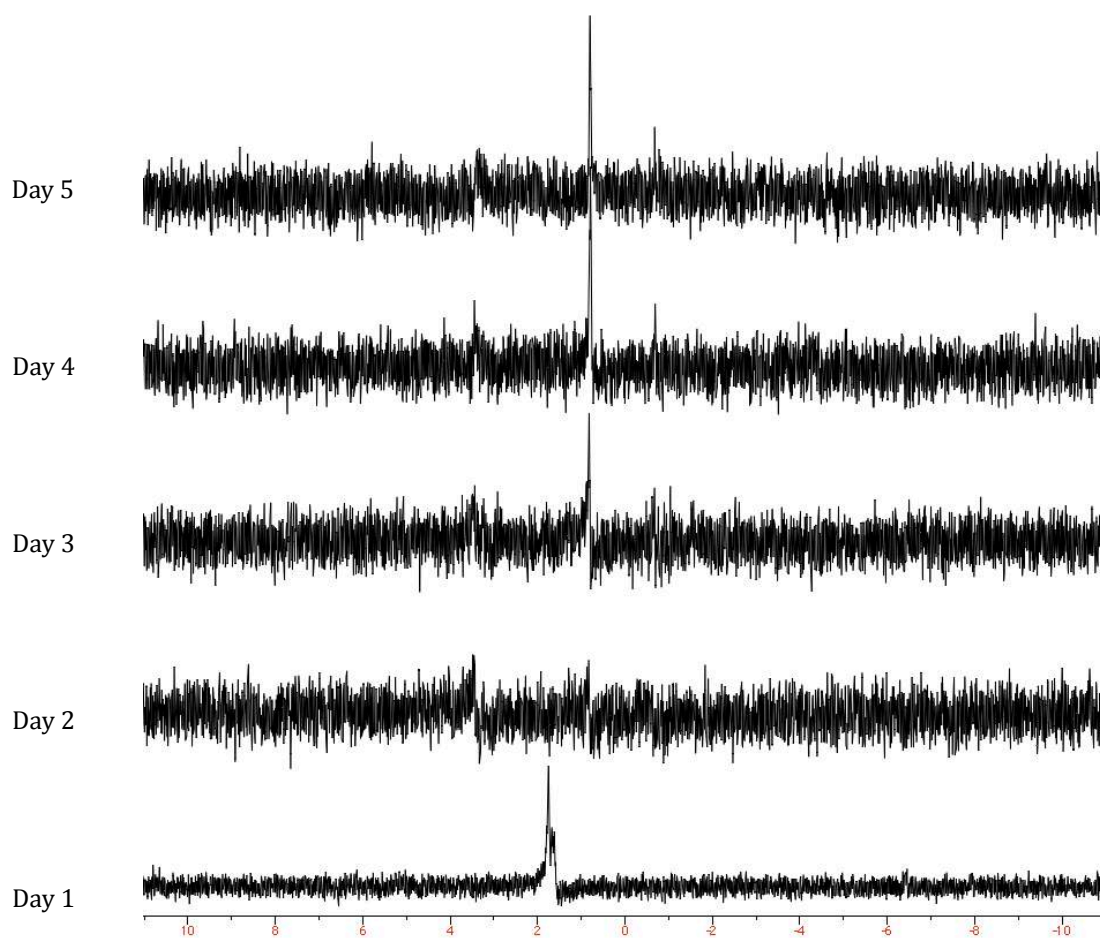


Figure 7.35 Stacked ^{31}P NMR spectra of Ph-LAla-OMe-BED(h) processing in human serum over 5 days at 37 °C

7.5 Potential for Therapeutic Viability and FDA Approval

7.5.1 ProTide Moiety Stability and Processing

ProTide BED analogues have proven to be far more stable than ProTide fingolimod analogues and have been observed to be processed to the desired monophosphate in various processing experiments. Certainly with regards to stability and proof-of-concept experiments these compounds appear to show more potential as viable therapeutics when compared with ProTide fingolimod. However, there are a vast range of other key factors which influence a compound's oral bioavailability, CNS penetration properties and ultimate chances of being approved by the FDA and EMA.

7.5.2 CNS Transfer Properties

A paper published by Pajouhesh *et al* suggests that the ideal logP range for CNS acting drugs is 1.5-2.7.⁴ ProTide BED compounds have much higher lipophilicity e.g. 5.24 for Ph-LAla-OMe-BED(a) (calculated using a website⁵). A possible way of mediating this unwanted lipophilicity could be to change the amino acid of the ProTide to tune the polarity to help CNS absorption. However, fingolimod has a logP of 4.72, according to the same site, suggesting that it is possible for a compound to have a higher logP than the published ideal 1.5-2.7 range and still cross the BBB.

The same paper says the polar surface area (PSA) of CNS therapeutics is typically 60-70 Å with an upper limit of 90 Å. Another website⁶ has been used to calculate that Ph-LAla-OMe-BED(a) has a PSA of 126.18 Å, further suggesting that ProTide BED analogues are not likely to cross the BBB.⁴ The monophosphate of BED(a) has a calculated PSA of 119.08 Å which again is too large according to Pajouhesh *et al*'s paper. Fingolimod has a calculated PSA of 66.48 Å which fits with the reported range of appropriate values.

The Pajouhesh paper also reports that the mean value of molecular weight for CNS active therapeutics is 310 g/mol. Fingolimod has a molecular weight of 307.5

g/mol which correlates very well with the published value for ideal molecular weight. ProTide BED compounds have a much larger molecular weight (e.g. 596.3 g/mol for Ph-LAla-OMe-BED(a)) which further suggests that ProTide BED analogues are less likely to cross the BBB than fingolimod.⁴

A possible way around the likely inability for ProTide BED compounds to cross the BBB *via* passive diffusion is to use an amino acid moiety similar to one used in the commercially successful drug gabapentin (figure 7.39) or the natural endogenously occurring dopamine precursor L-DOPA (figure 7.37). Potentially this would increase the likelihood of active transport across the BBB by the LAT1 transporter⁷ although this would dramatically increase the molecular weight even further and potentially reduce the efficacy of ProTide activation by the host enzymes. A cursory look at a paper⁸ detailing approaches for CNS delivery suggests that the possible CNS infiltration moiety suggested in figure 7.40 is arguably unlikely to be effective as it lacks the reportedly essential components for LAT1 transport of a negatively charged carboxyl group and positively charged amino group as present in the CNS-acting drugs melphalan (figure 7.38) and gabapentin. Interestingly the amino and alcohol functionalities of fingolimod are very reminiscent of the carboxyl and amino functional groups in melphalan and gabapentin and this may aid fingolimod's transport across the BBB.

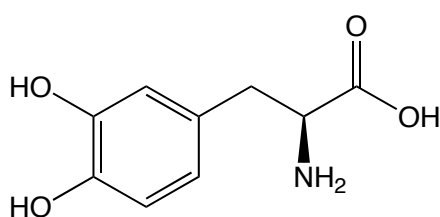


Figure 7.37 Naturally occurring endogenous metabolic precursor of dopamine- L-DOPA

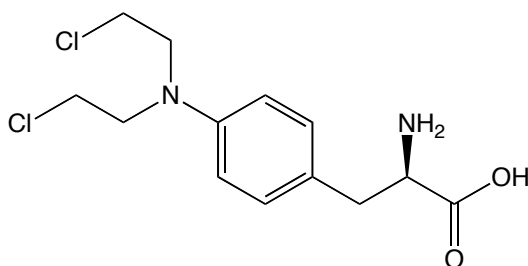


Figure 7.38 Melphalan

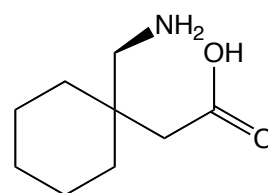


Figure 7.39 Gabapentin

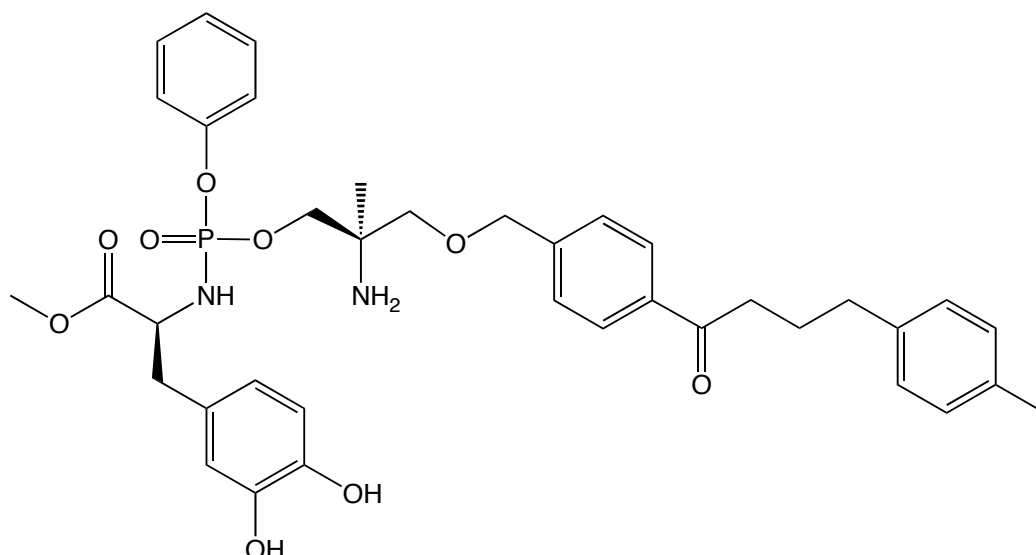


Figure 7.40 ProTide BED(a) analogue containing the same amino acid moiety present in L-DOPA which could possibly lead to enhanced penetration of the BBB *via* active transport by the LAT1 transporter⁵

An alternative possibility to aid transport across the BBB could be to synthesise analogues which possess a C6-glucose functional group to aid transport *via* the GLUT1 transporter. This has been previously performed⁸ as with *D*-glucose conjugates of 7-chlorokynurenic acid.⁹ However, the synthesis of *D*-glucose ProTide analogues would increase the molecular mass of the compound even further and it is unknown whether *D*-glucose ProTide analogues are capable of being processed to the monophosphate. It is possible that an unwanted cyclisation would result of a type similar to that as previously described in Chapter 5.

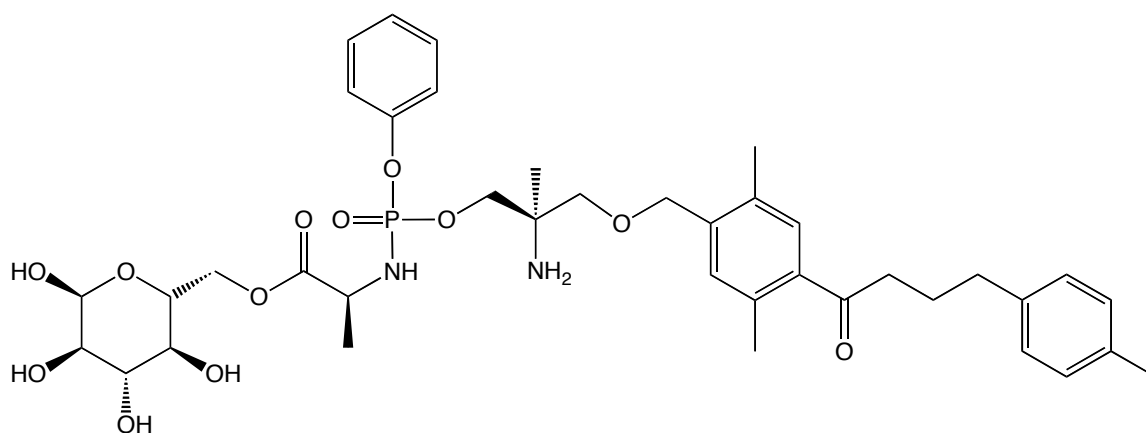


Figure 7.41 Possible BED(h) analogue containing a C6-glucose ester group which may help active transport across the BBB *via* the GLUT-1 transporter

7.5.3 Discussion of ProTide Processing in Human Serum

Human serum experiments, such as in section 7.4.4, suggest that ProTide BED analogues can be processed to the monophosphate in the blood with Ph-LAla-OMe-BED(a) having a half-life of around 14 h. Typically with ProTide therapeutics this would be considered as a negative outcome as the monophosphate does not readily transfer across the cell membrane and the monophosphate is only active intracellularly. However, it is possible that in the case of S1P receptor modulators this may not be such negative result. There are potentially 2 reasons as to why processing of ProTide S1P receptor modulators to the monophosphate in the serum may not be such an unwanted result as with typical ProTide nucleoside drugs:

- Possible diffusion across the BBB in the style of psilocybin which also possesses a phosphate and amine group
- S1P receptors are reported as being on the outside of the cell membrane as opposed to in the intracellular matrix^{10,11}

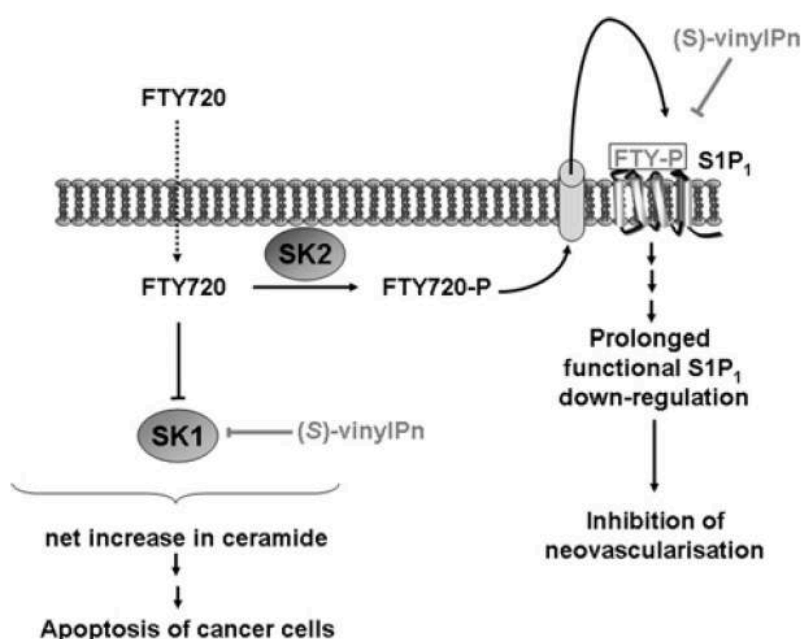


Figure 7.42 Putative mode of activation of fingolimod *in vivo*¹¹

The mode of activation of fingolimod, as shown in figure 7.42, suggests that processing of ProTide S1P receptor modulators to the monophosphate in human

serum may not be as negative a consequence as is typical for ProTide nucleoside analogues. ProTide nucleosides are typically incorporated into the host DNA or RNA and therefore need to be activated intracellularly.¹² However, as S1P receptors are G protein-coupled receptors¹⁰ and are therefore located on the outside of the cell¹¹ processing of ProTide BED analogues to the monophosphate may in fact be a positive outcome.

7.5.4 Metabolic Stability

According to Tsuji *et al*'s paper¹³ the compounds they produced have a poorer metabolic stability profile than fingolimod and phospho-fingolimod. For example, fingolimod has a metabolic stability percentage (of the remaining compounds after 30 min incubation at 37 °C with rat hepatic microsomes) of 97% and phospho-fingolimod has a metabolic stability of >100%- this is in contrast to 51% for BED(a) and 92% for phospho-BED(a). The ether functional group present in all the BED compounds is potentially the region of the molecule which is most liable to metabolism catalysed degradation. This poorer metabolic stability is also another contributory factor which leads to the conclusion that phosphorus prodrugs of BED compounds are not likely to be preferable to parent fingolimod.

7.5.5 Toxicity

ProTide BED analogues were exposed to mouse embryonic stem cell-derived neurons at 10 nM, 100 nM and 1 µM concentrations for 3 weeks. ProTide BED analogues were found to not be toxic at 10 nM and 100 nM but were toxic at 1 µM concentration. Crucially, phospho-fingolimod was also found to be toxic at 1 µM concentration, suggesting that ProTide BED analogues are not more toxic to neurons than the pharmacologically active monophosphate of the commercially available fingolimod. The toxicity testing was conducted by Katharina Säuberli in the School of Biosciences.

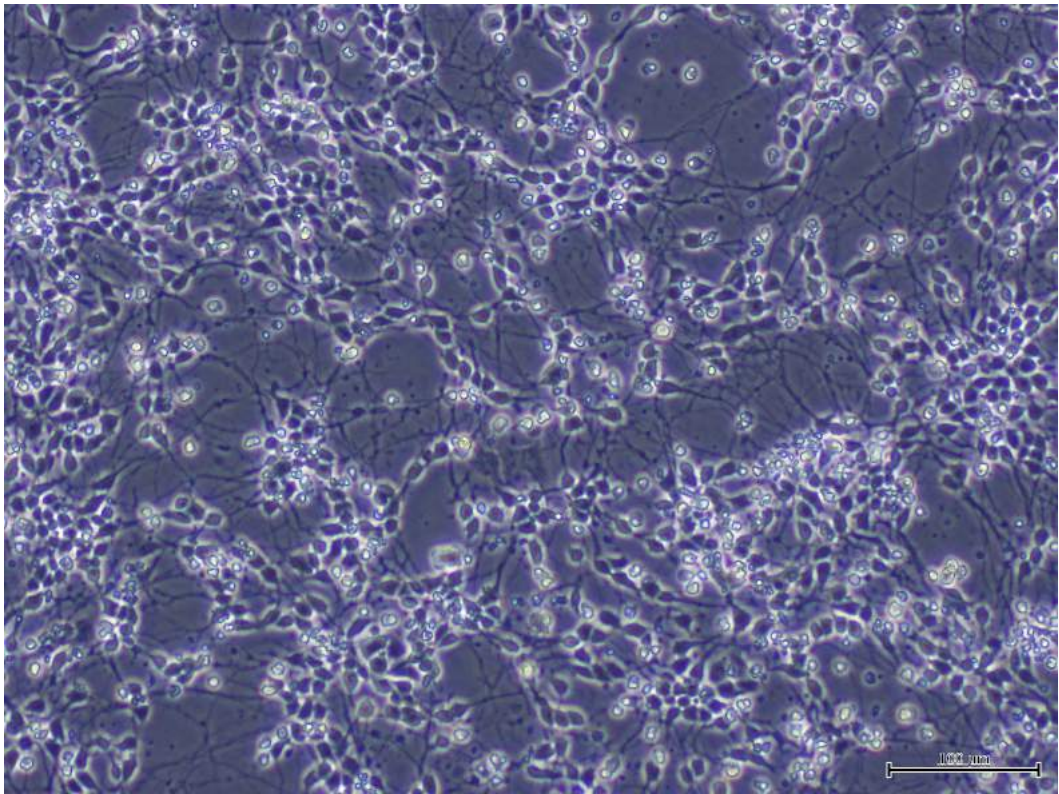


Figure 7.43 Day 2 culture of neurons derived from mouse embryonic stem cells (Image courtesy of Katharina Säuberli)

7.6 References

1. McGuigan C, Murziani P, Slusarczyk M, Gonczy B, Voorde J, Liekens S, Balzarini J. Phosphoramidate ProTides of the anticancer agent FUDR successfully deliver the preformed bioactive monophosphate in cells and confer advantage over the parent nucleoside. *J. Med. Chem.* **2011**, 54, 7247-7258.
2. Madela K. Design, synthesis and biological evaluation of novel anti-HCV nucleosides and nucleotides: From bench to clinical trials. **2012**. PhD thesis. Cardiff University.
3. Chhabda P, Balaji M, Srinivasarao V. Development and validation of a stability indicating RP-HPLC method for quantification of fingolimod in bulk and pharmaceutical dosage form. *Pharmanest.* **2013**, 4, 1206-1218.
4. Pajouhesh H, Lenz G. Medicinal chemical properties of successful central nervous system drugs. *NeuroRx.* **2005**, 2, 541-553.
5. <http://www.molinspiration.com/cgi-bin/properties>
6. <http://www.daylight.com/meetings/emug00/Ertl/tpsa.html>
7. Rankovic Z. CNS drug design: balancing physicochemical properties for optimal brain exposure. *J. Med. Chem.* **2015**, 58, 2584-2608.
8. Rautio J, Laine K, Savolainen J. Prodrug approaches for CNS delivery. *AAPS*, **2008**, 10, 92-102.
9. Battaglia G, La Russa M, Bruno V, Arenare L, Ippolito R, Copani A, Bonina F, Nicoletti F. Systemically administered D-glucose conjugates of 7-chlorokynurenic acid are centrally available and exert anticonvulsant activity in rodents. *Brain Res.* **2000**, 860, 149-156.
10. Hanson M, Roth C, Jo E, Griffith M, Scott F, Reinhart G, Desale H, Clemons B, Cahalan S, Schuerer S, Sanna M, Han G, Kuhn P, Rosen H, Stevens R. Crystal Structure of a Lipid G protein-Coupled Receptor. *Science.* **2012**, 335, 851-855.
11. Pyne N, Tonelli F, Lim K, Long J, Edwards J, Pyne S. Sphingosine 1-phosphate signalling in cancer. *Biochem. Soc. Trans.* **2012**, 40, 94-100.
12. Mehellou Y. The ProTides Boom. *ChemMedChem.* **2016**, 11, 1-4.
13. Tsuji T, Suzuki K, Nakamura T, Goto T, Sekiguchi Y, Ikeda T, Fukuda T, Takemoto T, Mizuno Y, Kimura T, Kawase Y, Nara F, Kagari T, Shimoizato T, Yahara C, Inaba S, Honda T, Izumi T, Tamura M, Nishi T. Synthesis and SAR

studies of benzyl ether derivatives as potent orally active S1P₁ agonists. *Bioorg. Med. Chem.* **2014**, 22, 4246-4256.

Chapter 8 – Molecular Modelling Studies

8.1 S1P₁ Selectivity

While the improved stability and biochemical processing of ProTide BED compounds over ProTide fingolimod is indicative that making phosphorus prodrugs of mono alcohol S1P receptor modulators is more likely to lead to a viable therapeutic, some of the other characteristics of ProTide BED compounds such as published metabolic stability,¹ logP and polar surface area suggest that ProTide BED analogues are not likely to be more effective therapeutics than fingolimod. The next logical stage in the development of the project is arguably to try to incorporate the most favourable aspects of the BED compounds and fingolimod while eliminating the less favourable aspects of both.

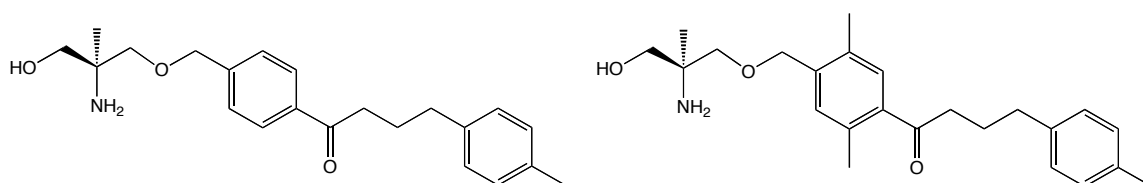


Figure 8.1 BED(a) and BED(h)

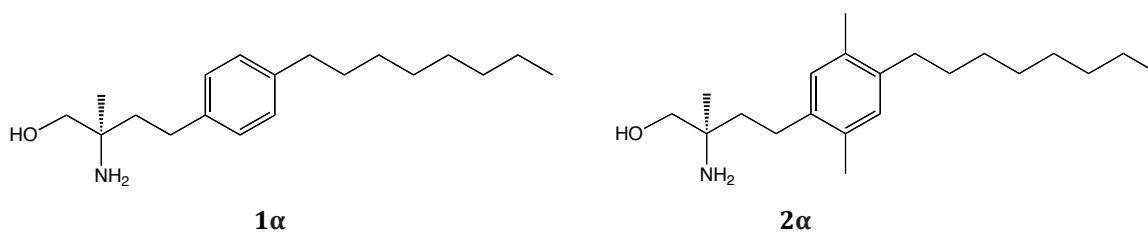


Figure 8.2 Mono-alcohol fingolimod analogue (**1α**) and hypothetically more S1P₁ selective analogue (*R*)-2-amino-4-(2,5-dimethyl-4-octylphenyl)-2-methylbutan-1-ol (**2α**)

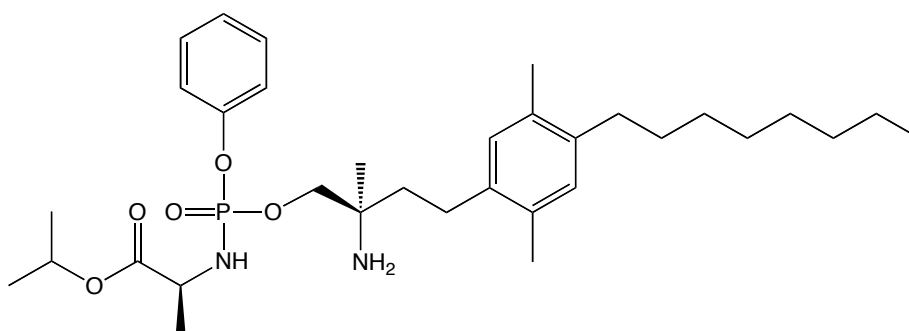


Figure 8.3 Potential new target molecule containing sofosbuvir ProTide moiety

According to Tsuji *et al* BED(h), as shown in figure 8.1, is more S1P₁ selective over S1P₃ than BED(a) and this selectivity seems a consequence of the 2,5-dimethyl groups in the central aromatic ring. Starting from this finding, the 2,5-dimethyl groups could be added to the aryl moiety of the mono-alcohol analogues of fingolimod, potentially leading to greater S1P₁ selectivity compared to fingolimod. Greater S1P₁ selectivity could potentially lead to fewer unwanted side effects.

Different molecular modelling techniques were to be exploited in order to verify the potential selectivity of the newly designed molecules. Initially the structure of the S1P₁ receptor was deduced by a comparison of computational models with other receptors such as the X-ray crystal structure of bovine rhodopsin.² In 2012 the crystal structure of the S1P₁ receptor fused to T4-lysozyme in complex with the antagonist sphingolipid mimic ML056 was published.³ X-ray crystallography was used to determine the 3D structure of the transmembrane GPCR S1P₁ receptor as shown in figures 8.4 and 8.5.⁴

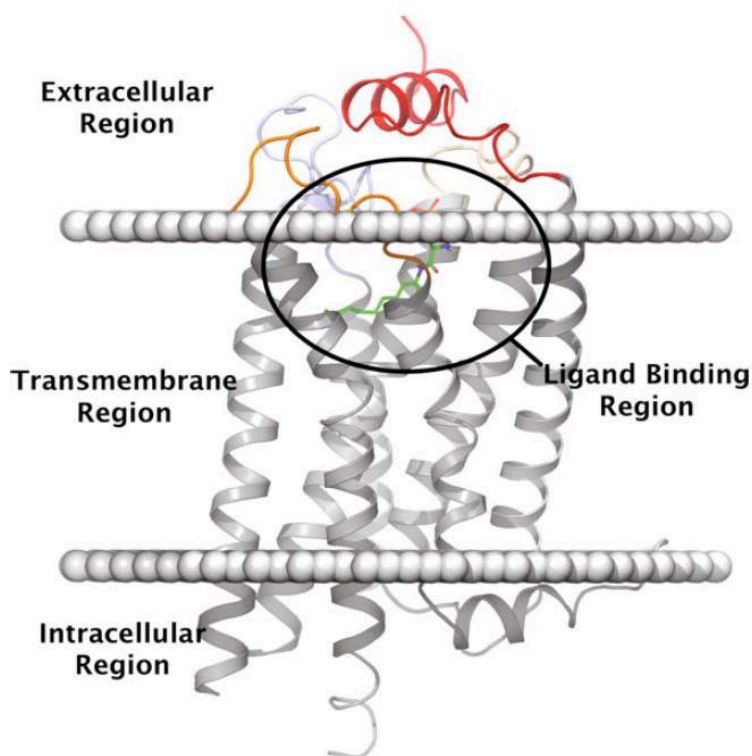


Figure 8.4 Structure of the S1P₁ receptor and its 4 primary regions with the position of the cell membrane shown with white spheres⁴

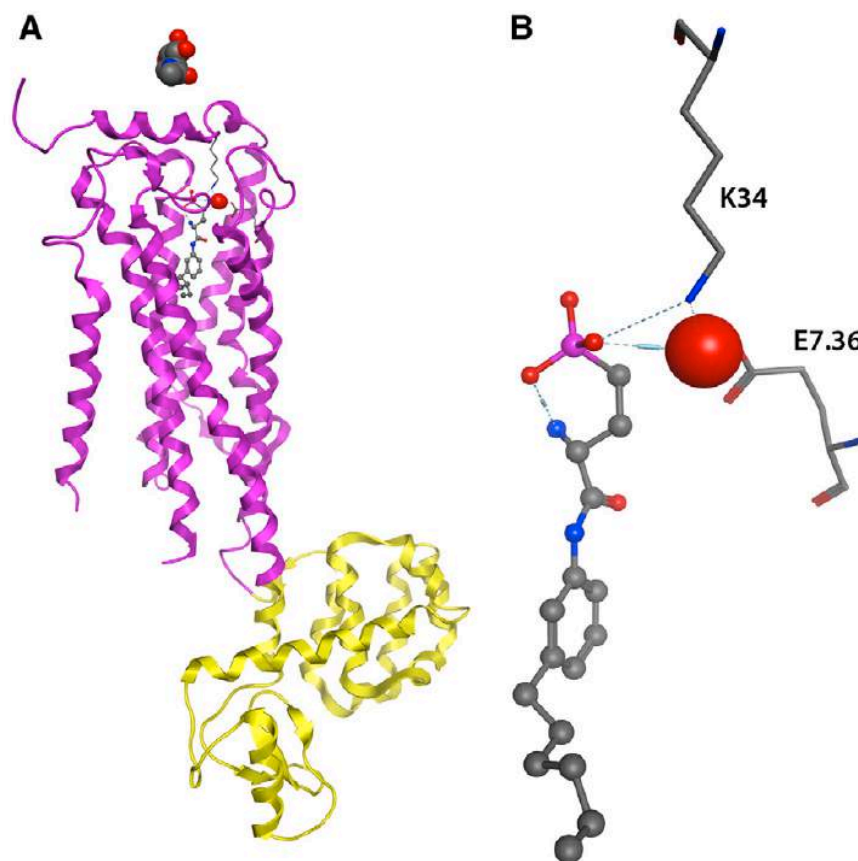


Figure 8.5 A: S1P₁ receptor in magenta fused to the T4 lysozyme in yellow with ML056 antagonist in complex with the active site. B: Water-mediated ligand-receptor interactions⁵

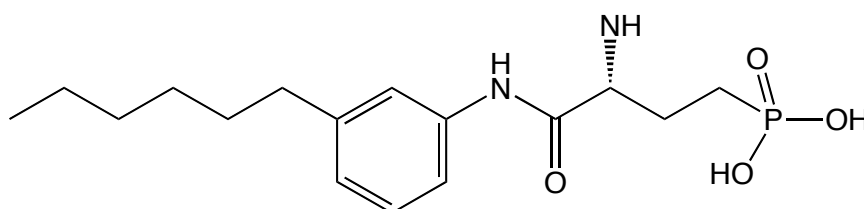


Figure 8.6 ML056

8.2 Homology Modelling

As no human S1P₃ protein crystal structure is available a homology model was prepared using the crystal structure of the human sphingosine 1-phosphate receptor 1 (S1P₁) fused to T4-lysozyme (PDB ID: 3V2Y) in complex with an antagonist sphingolipid mimic (ML056), having a sequence similarity of 53% with S1P₃. After removing the T4-lysozyme portion, the model was prepared using MOE2015.10 homology tool using a previously reported procedure.⁶ The antagonist's atoms were included in the environment for induced fit in order to shape the active site of the new model. The final model was energy minimised using AMBER99 force field.

8.2.1 Molecular Docking

According to Hanson *et al.*^{3,4} the antagonist conformation of the available S1P₁ crystal structure cannot accommodate a long lateral chain, which is a common feature in the fingolimod, the natural substrate sphingosine-1-phosphate and other S1P₁ agonists. The necessary space to accommodate a lateral chain of an agonist could be obtained by performing an induced fit docking of an agonist in the S1P₁ antagonist conformation. Induced fit docking is a technique that takes in account the potential side-chain or backbone movements of a protein upon ligand binding, whereas standard virtual docking studies consider the ligand free to move but the protein is held rigid. Following previously published work,^{3,4} induced fit docking of the natural substrate sphingosine-1-phosphate and phospho-fingolimod was performed on the S1P₁ crystal structure. As reported, the induced fit docking allows a better accommodation of the lateral chain in the hydrophobic pocket, inducing residue conformation changes in that area of the protein. Moreover, $\Delta G_{\text{binding}}$ energy and ligand strain (LS) energy calculations of the ligand-protein complex after standard docking and induced fit docking show a drop in both values in the case of the induced fit, confirming that the induced agonist conformation is the optimal protein conformation for a potential agonist molecular modelling evaluation. The study was performed in both S1P₁ crystal and S1P₃ homology

models. The results are shown in tables 8.1 and 8.2 and are in accordance with the work reported for other agonists by Hanson *et al.*^{3,4}

Sphingosine-1-phosphate

	S1P₁		S1P₃	
	Docking	Induced Fit	Docking	Induced Fit
$\Delta G =$	-86.95	-122.428	-66.783	-149.51
LS =	24.427	7.204	13.917	10.458

Table 8.1 Docking study data of sphingosine-1-phosphate in the S1P₁ and S1P₃ receptors. The $\Delta G_{\text{binding}}$ energy and ligand strain (LS) energy values are in (kcal/mol).

Phospho-fingolimod

	S1P₁		S1P₃	
	Docking	Induced Fit	Docking	Induced Fit
$\Delta G =$	-94.383	-109.154	-76.028	-135.124
LS =	22.065	12.960	20.591	12.424

Table 8.2 Docking study data of phospho-fingolimod in the S1P₁ and S1P₃ receptors. The $\Delta G_{\text{binding}}$ energy and ligand strain (LS) energy values are in (kcal/mol).

Considering these data, the proteins obtained from induced fit docking were therefore selected to be used in the following standard docking studies. According to the data above, phospho-fingolimod fits slightly more comfortably in the S1P₃ receptor than the S1P₁ receptor. This correlates well with much of the published data which suggest that phospho-fingolimod has a comparable or slightly higher affinity for the S1P₃ receptor than the S1P₁ receptor.^{1,7}

In the case of S1P₁, the protein coming from the induced fit docking of BED(h), the most active S1P₁ agonist according to Tsuji *et al.*¹ was chosen, whereas in the case of S1P₃ the protein obtained after the phospho-fingolimod, the most active S1P₃ agonist according to Tsuji *et al.*¹ induced docking was selected. The two proteins

were used to perform a Glide SP docking of the proposed new agonists together with the reported BED(a) and BED(h) derivatives as controls.

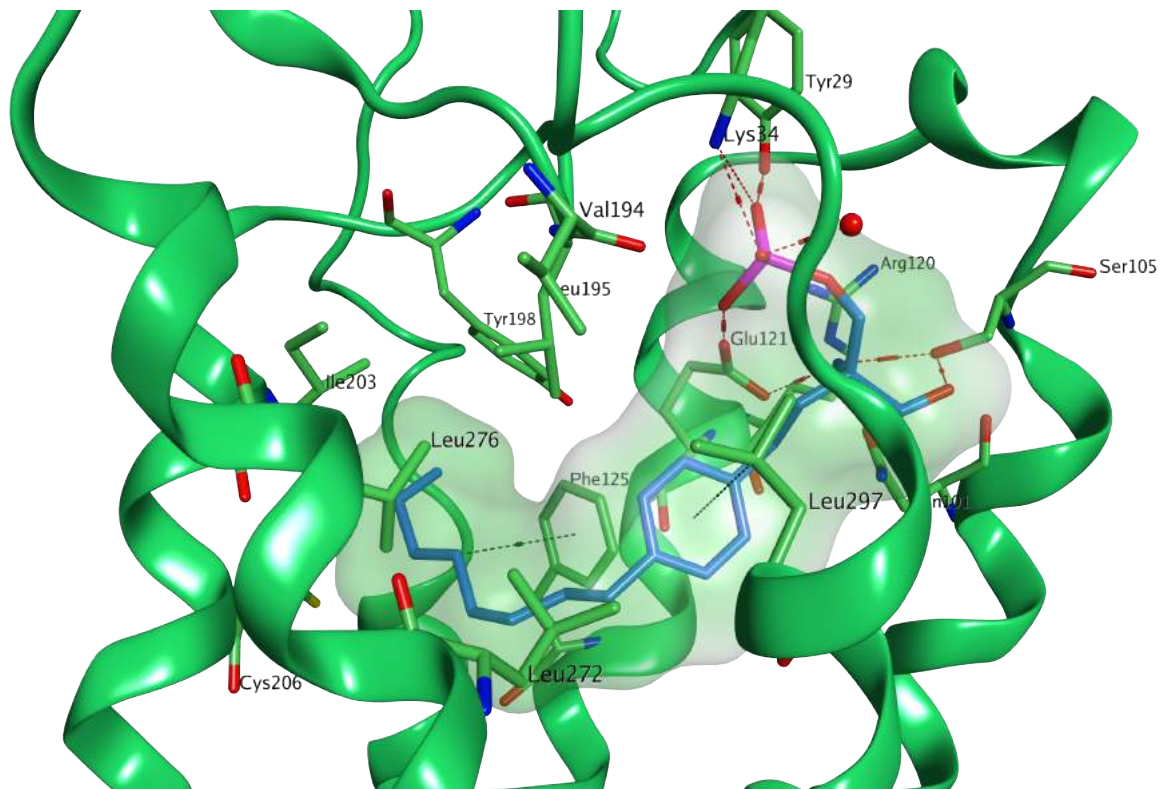


Figure 8.7 Phospho-fingolimod in S1P₁

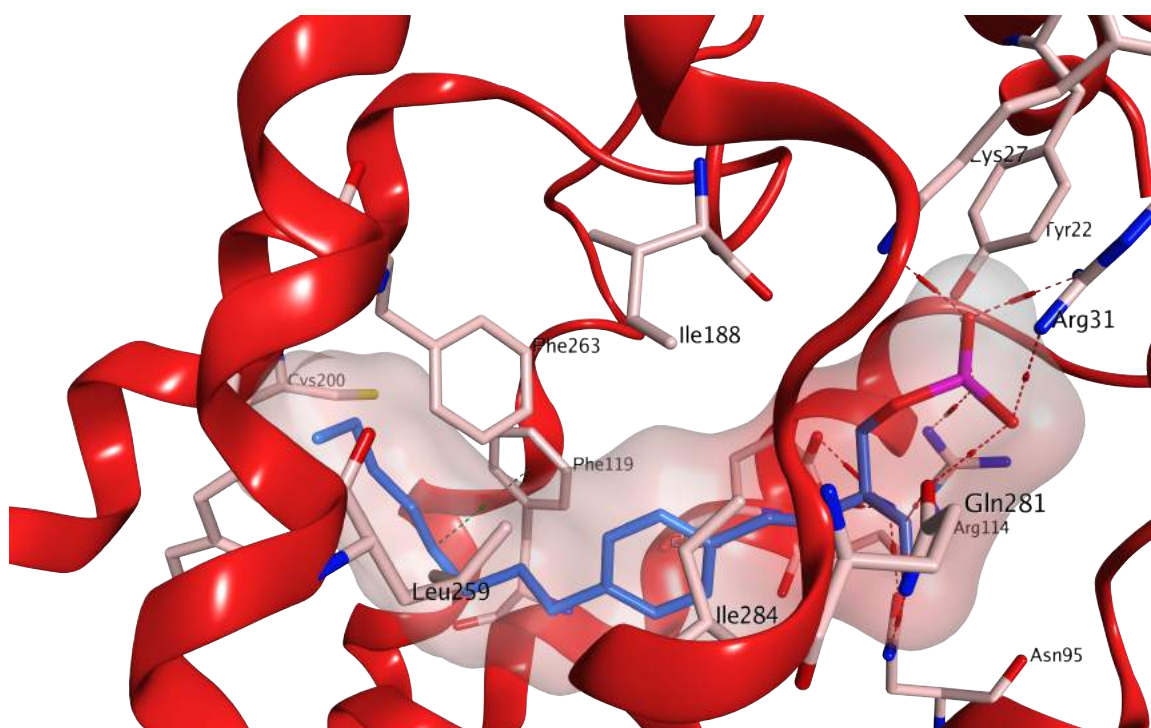


Figure 8.8 Phospho-fingolimod in S1P₃

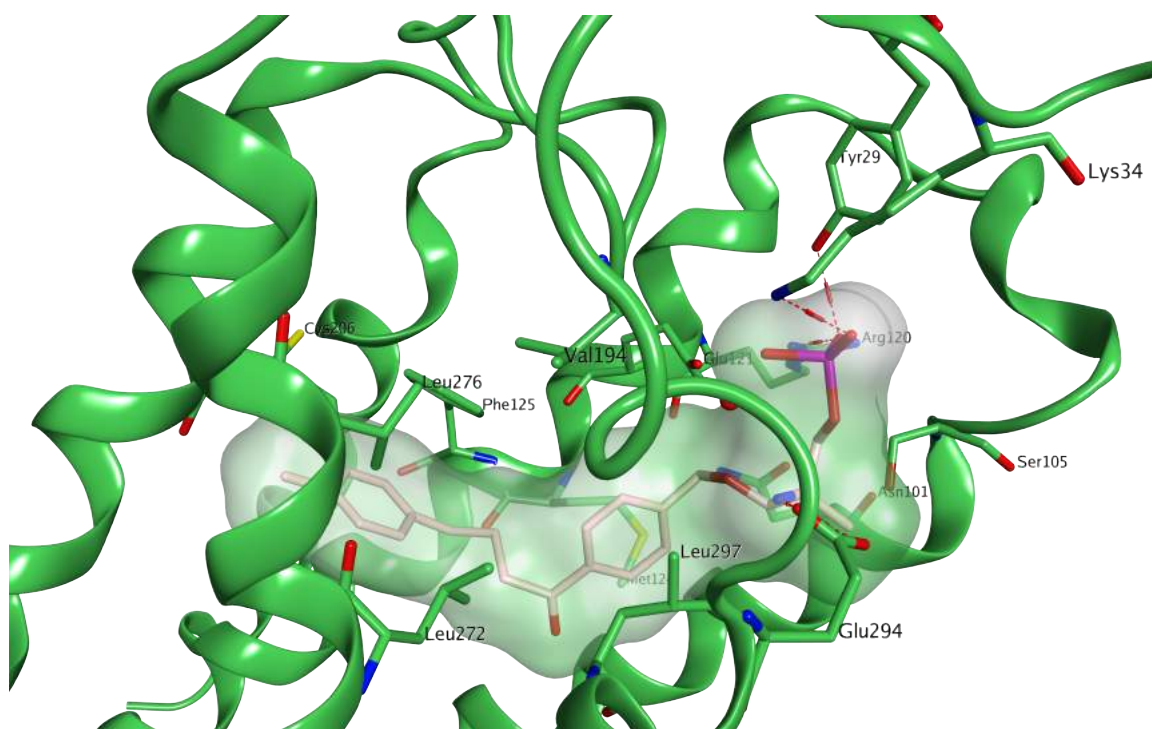


Figure 8.9 Phospho-BED(a) in S1P₁

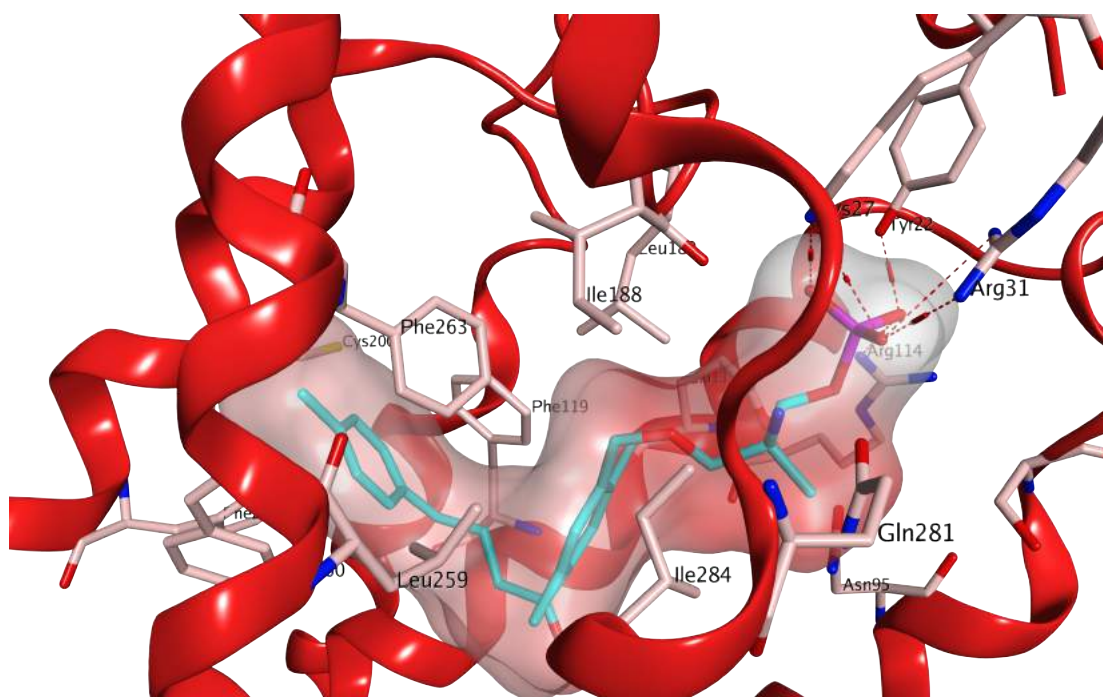


Figure 8.10 Phospho-BED(h) in S1P₃

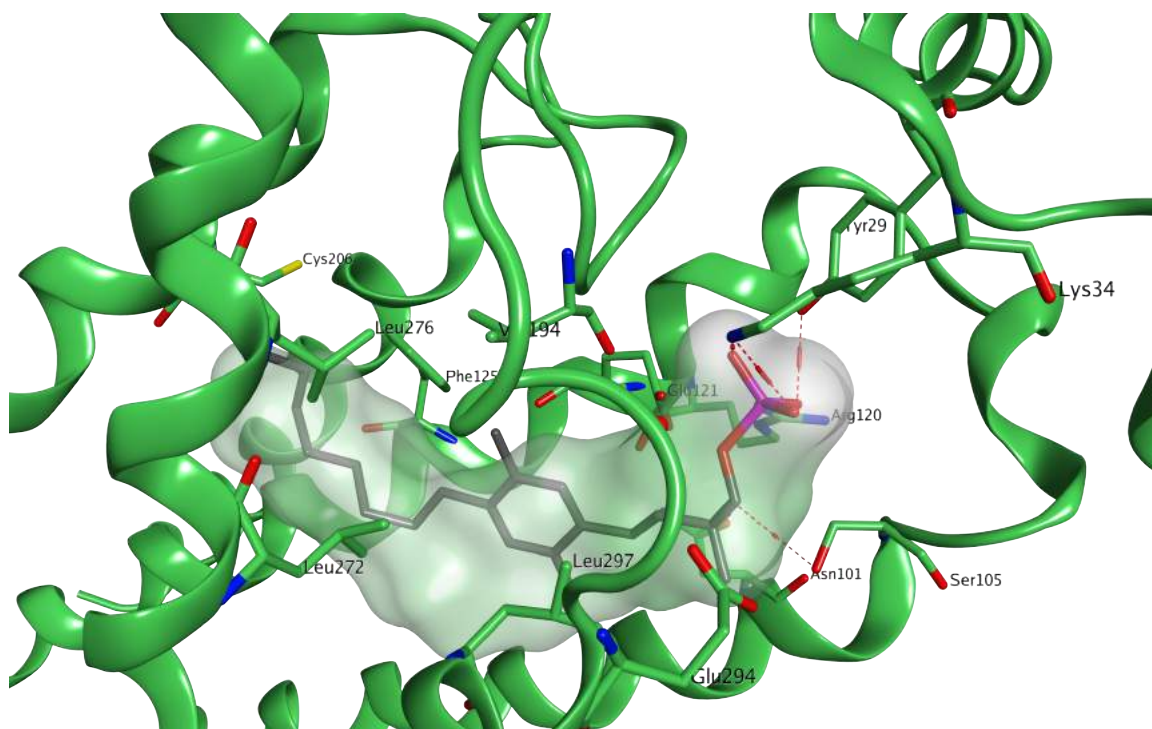


Figure 8.11 Proposed phospho-dimethyl fingolimod (**2α**) in S1P₁

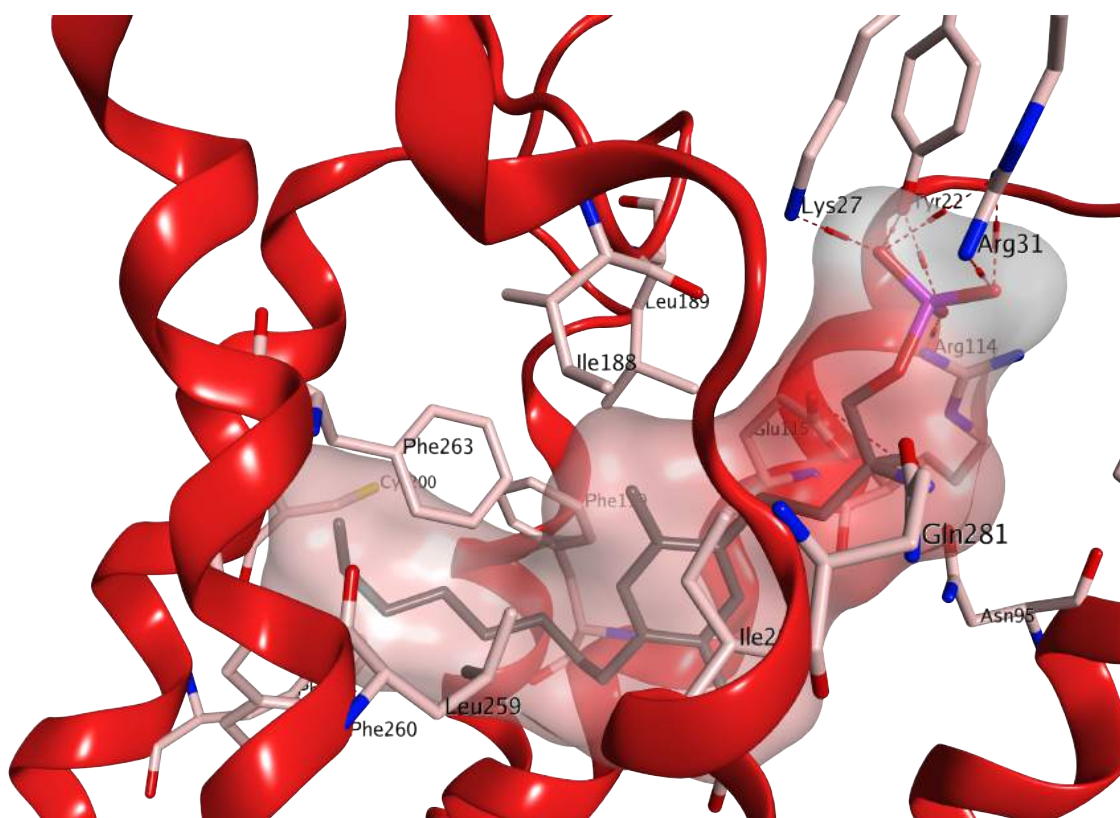


Figure 8.12 Proposed phospho-dimethyl fingolimod (**2α**) in S1P₃

After the homology modelling induced fit docking studies provided data which suggest that the initially proposed aryl dimethyl fingolimod analogue **2α** shown in figure 8.2 was unlikely to be particularly more S1P₁ selective than fingolimod (see section 8.2.3) the structures shown in figures 8.13 and 8.14 were chosen for investigation.

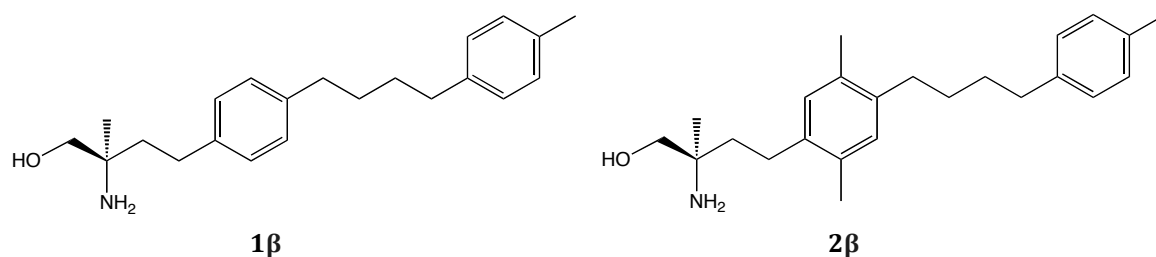


Figure 8.13 (*R*)-2-amino-2-methyl-4-(4-(4-(*p*-tolyl)butyl)phenyl)butan-1-ol (**1β**) and (*R*)-2-amino-4-(2,5-dimethyl-4-(4-(*p*-tolyl)butyl)phenyl)-2-methylbutan-1-ol (**2β**) structures for S1P₁ and S1P₃ receptor selectivity investigation

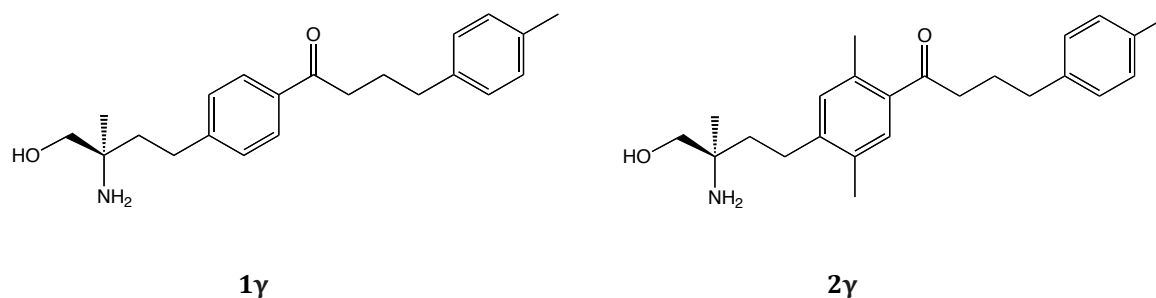


Figure 8.14 (*R*)-1-(4-(3-amino-4-hydroxy-3-methylbutyl)phenyl)-4-(*p*-tolyl)butan-1-one (**1γ**) and (*R*)-1-(4-(3-amino-4-hydroxy-3-methylbutyl)-2,5-dimethylphenyl)-4-(*p*-tolyl)butan-1-one (**2γ**) structures for S1P₁ and S1P₃ receptor selectivity investigation

The benzene ring in the lateral chain of BED(h) appears to have a significant influence on S1P₁ selectivity so this feature was incorporated into the structures. The ether group of the BED analogues was chosen for removal as it was deemed probable that the ether group is likely to be a major contributing factor to the relative ease of metabolism of BED analogues in comparison to fingolimod as reported in the lead paper by Tsuji *et al.*¹ The significance of the ketone group in the BED compounds was also chosen for investigation as it is not present in parent fingolimod but is present in the BED compounds. Any role in the S1P₁ selectivity of BED(h) was unknown.

8.2.2 S1P₁ Docking

All the derivatives, including sphingosine-1-phosphate and phospho-fingolimod, occupy the S1P₁ binding site in a similar manner with the phosphate head mainly interacting with Tyr29, Lys34 and Arg120, all amino acids reported to be important for the interaction with the phosphate head^{1,3,4} and the rest of the molecule points to the active site towards the area defined by Val194, Phe125, Cys206, Leu276. An example of the interaction with the active site is shown in figure 8.15. The results suggest that the phosphates of all the novel structures in figures 8.2, 8.12 and 8.13, can bind as effectively as phospho-fingolimod.

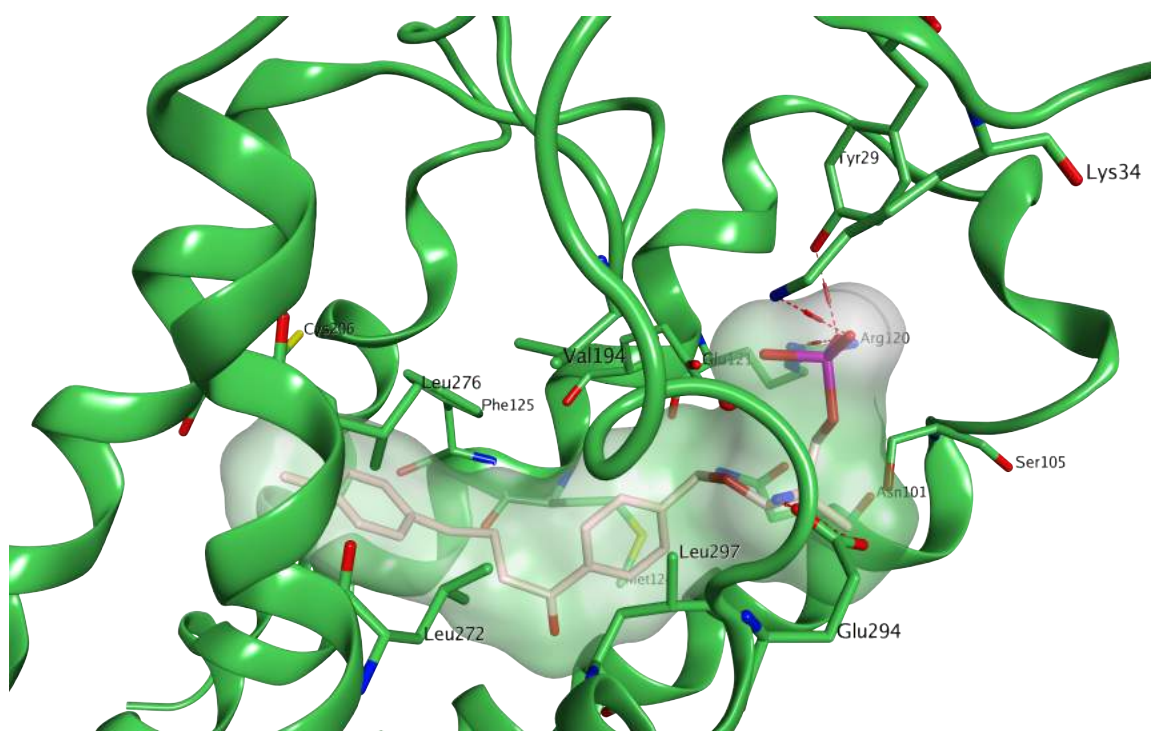


Figure 8.15 Phospho-(*R*)-1-(4-(3-amino-4-hydroxy-3-methylbutyl)phenyl)-4-(*p*-tolyl)butan-1-one (**1y**) in S1P₁

8.2.3 S1P₃ Docking

Sphingosine-1-phosphate and phospho-fingolimod occupy the S1P₃ binding site with the phosphate head interacting with Tyr22, Lys27, Arg31 and Arg114 (see figure 8.15). The rest of the molecule is inserted in the active pocket pointing to the area delimited by Phe119, Ile188 (corresponding to the Val194 in S1P₁), Cys200 and Phe263 (corresponding to the Leu276 in S1P₁).

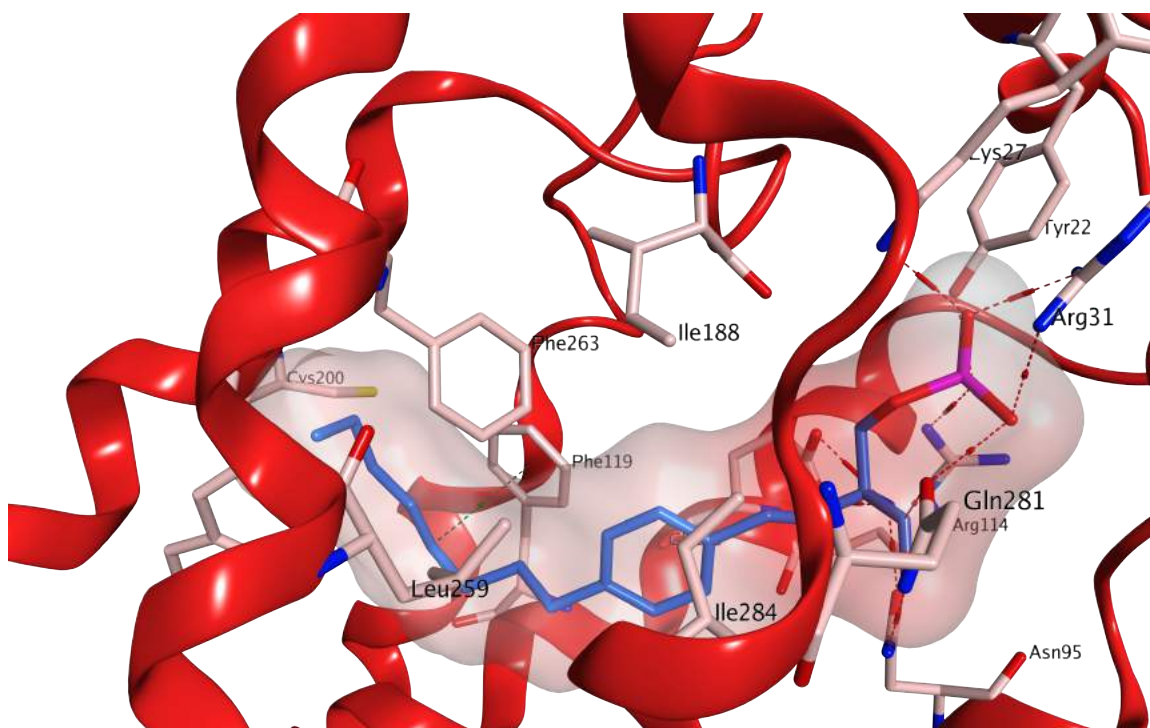


Figure 8.16 Phospho-fingolimod in S1P₃

It is evident that the presence of Ile188 (Val194 in S1P₁) and Phe263 (Leu276 in S1P₁) narrows the S1P₃ binding site when compared to S1P₁. Particularly, Phe263 in the S1P₃ receptor together with Phe119 and Phe260 form a phenylalanine area which can easily accommodate the linear lateral chain of the phospho-fingolimod but it does not easily allow the positioning of the extra benzene ring present in the lateral chain of BED(h). Figure 8.17 shows the docking of phospho-BED(h) in S1P₃ and the potential clashes, represented as surface contacts, between the aromatic ring in the lateral chain and the phenylalanine area.

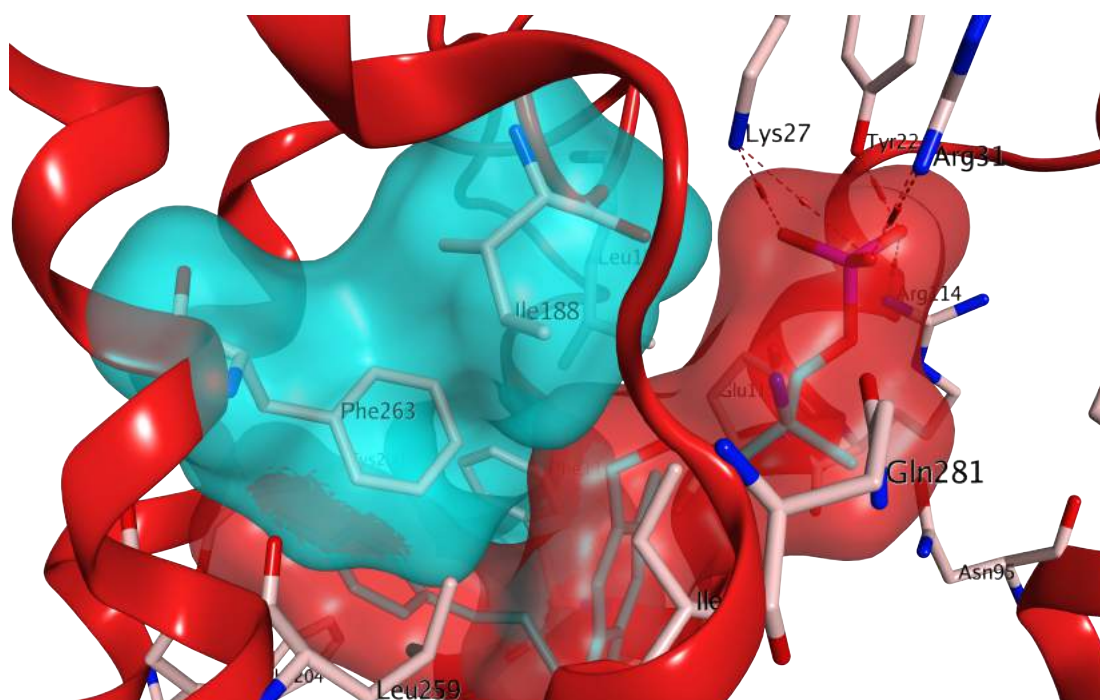


Figure 8.17 Phospho-BED(h) in S1P₃ showing clashes between Phe263 and the benzene ring in the lateral chain

The presence of the rigid ketone group in phospho-BED(h) and the 2,5-dimethyl substituent in the central benzene ring in phospho-BED(h) (figure 8.17) seem to force the lateral chain into a conformation that is not optimal for the interaction with the receptor, due to the presence of additional steric hindrance induced by Ile188. These findings, together with the clashes with Phe263, could justify the large loss of S1P₃ activity reported for BED(h) and BED(a) when compared with fingolimod, making these two molecules unlikely to have a high affinity for the S1P₃ receptor.

Docking studies of the newly designed derivatives were in line with these results. The structure of the monophosphate of **2α**, shown in figure 8.2, obtained by combining the structure of BED(h) and fingolimod, perfectly occupies the binding site, with the phosphate head interacting with the relevant amino acids, the linear lateral chain pointing toward the inner part of the active site with no clashes observed. In this case, it seems that the presence of the 2,5-dimethyl substituent does not influence in a negative manner the binding of the molecule, making this compound a potential agonist for S1P₃ (see figure 8.18).

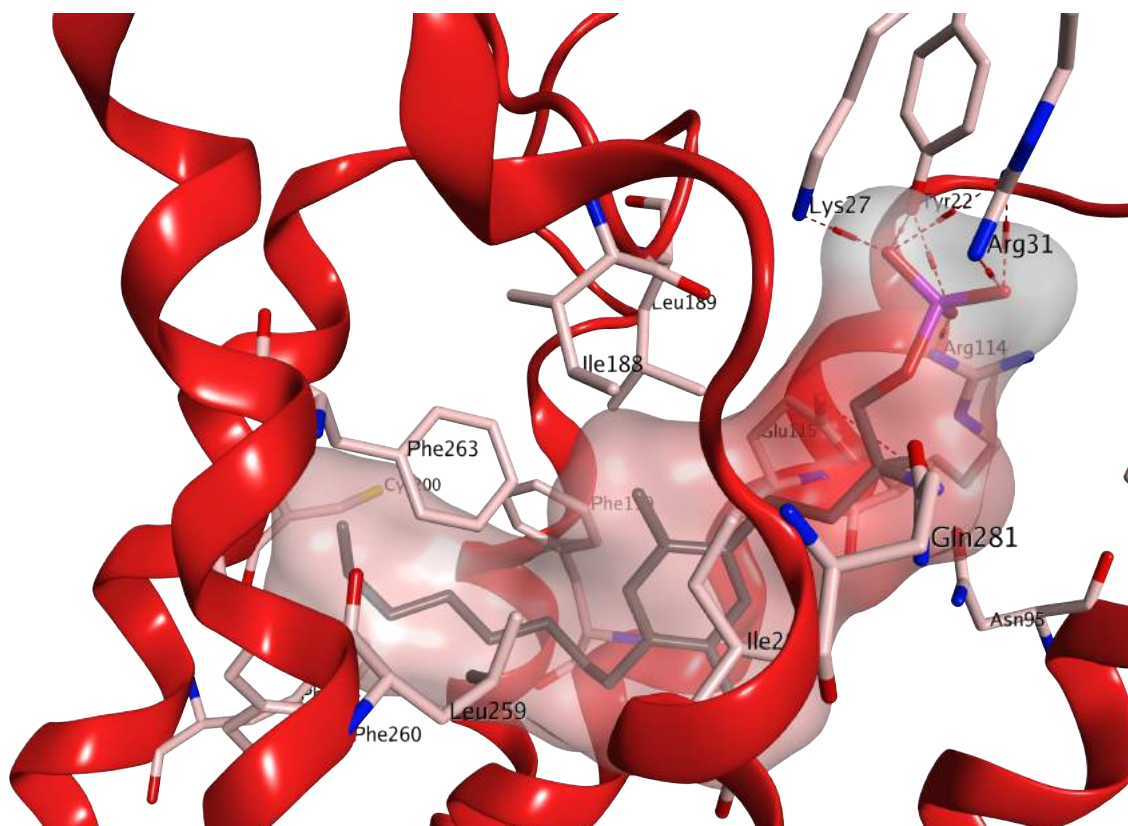


Figure 8.18 Proposed phospho-dimethyl fingolimod (**2α**) in S1P₃

However, compounds **1β**, **2β**, **1γ** and **2γ** in figures 8.13 and 8.14, with much greater structural similarity to parent BED compounds, give similar results to BED(h) with the extra aromatic portion leading to clashes with the phenylalanine area influencing in a negative way the interaction with the receptor. Moreover, the combination of the extra aromatic ring, together with the 2,5-dimethyl substituent and the lateral ketone in **2γ** (as shown in figure 8.19) causes a completely unfavourable binding of the molecule, especially in the phosphate head area.

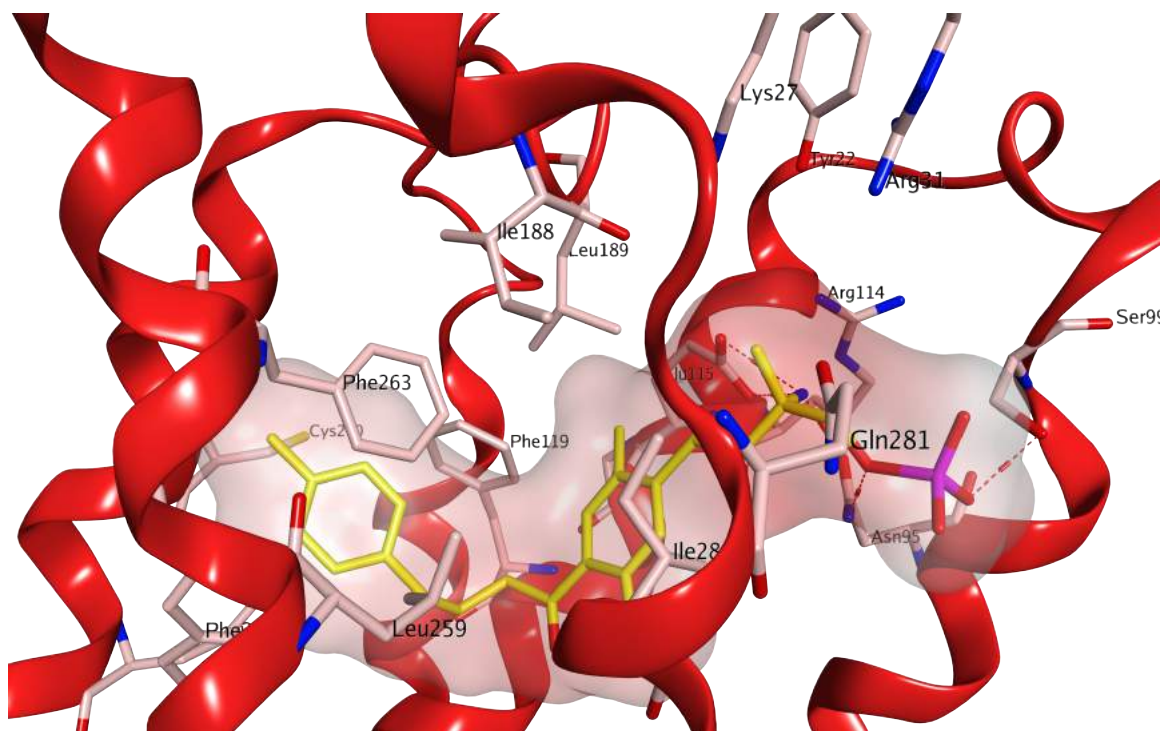


Figure 8.19 Phospho-(*R*)-1-(4-(3-amino-4-hydroxy-3-methylbutyl)-2,5-dimethylphenyl)-4-(*p*-tolyl)butan-1-one (**2γ**) in S1P₃

8.3 Conclusions

After preparing a reliable S1P₃ homology model, a series of molecular modelling studies were performed in order to predict the potential selectivity of the newly designed compounds. All the new derivatives bind to the S1P₁ receptor in a similar manner to phospho-fingolimod and they can be considered potential agonists of this receptor.

Different results were obtained for the S1P₃ protein. The compounds **1α** and **2α**, reported in figure 8.2, seem to perfectly dock in the binding pocket and therefore they are potential S1P₃ agonists lacking the desired S1P₁ selectivity. On the other hand, the binding of derivatives **1β**, **2β**, **1γ**, and **2γ**, reported in figures 8.13 and 8.14, due to the addition of an extra aromatic ring and the combination of the 2,5-dimethyl substituent in **2β** and **2γ** and the lateral ketone in **1γ** and **2γ**, is characterised by different clashes with the protein amino acids. It can be speculated that this unfavourable binding could lead to an absence of S1P₃ activity and therefore can lead to potential S1P₁ selectivity over S1P₃.

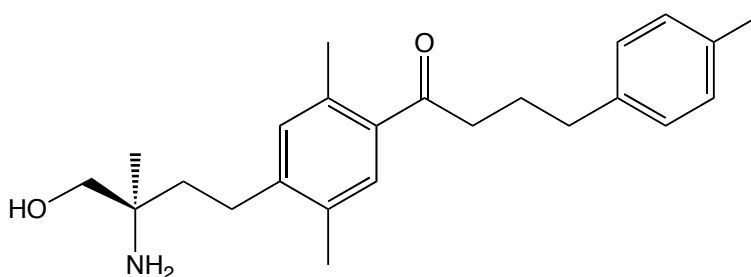


Figure 8.20 (*R*)-1-(4-(3-amino-4-hydroxy-3-methylbutyl)-2,5-dimethylphenyl)-4-(*p*-tolyl)butan-1-one (**2γ**)

8.4 References

1. Tsuji T, Suzuki K, Nakamura T, Goto T, Sekiguchi Y, Ikeda T, Fukuda T, Takemoto T, Mizuno Y, Kimura T, Kawase Y, Nara F, Kagari T, Shimozato T, Yahara C, Inaba S, Honda T, Izumi T, Tamura M, Nishi T. Synthesis and SAR studies of benzyl ether derivatives as potent orally active S1P₁ agonists. *Bioorg. Med. Chem.* **2014**, 22, 4246-4256.
2. Deng Q, Clemas J, Chrebet G, Fischer P, Hale J, Li Z, Mills S, Bergstrom J, Mandala S, Mosley R, Parent S. Identification of Leu276 of the S1P₁ Receptor and Phe263 of the S1P₃ Receptor in Interaction with Receptor Specific Agonists by Molecular Modeling, Site-Directed Mutagenesis, and Affinity Studies. *Mol. Pharmacol.* **2007**, 71, 724-735.
3. Hanson M, Roth C, Jo E, Griffith M, Scott F, Reinhart G, Desale H, Clemons B, Cahalan S, Schuerer S, Sanna M, Han G, Kuhn P, Rosen H, Stevens R. Crystal Structure of a Lipid G protein-Coupled Receptor. *Science.* **2012**, 335, 851-855.
4. Hanson M, Peach R. Structural Biology of the S1P₁ Receptor. *Curr. Top. Microbiol. Immunol.* **2014**, 378, 23-53.
5. Parrill A, Tigyi G. Integrating the puzzle pieces: The current atomistic picture of phospholipid-G protein coupled receptor interactions. *Biochim. Biophys. Acta.* **2013**, 1831, 2-12.
6. Gomaa M, Simons C, Brancale A. Homology model of 1 α ,25-dihydroxyvitamin D₃ 24-hydroxylase cytochrome P450 24A1 (CYP24A1): Active site architecture and ligand binding. *J. Steroid Biochem. Mol. Biol.* **2007**, 104, 53-60
7. Nishi T *et al.* Discovery of CS-0777: A potent, selective, and orally active S1P₁ agonist. *Med. Chem. Lett.* **2010**, 2, 368-372.

Chapter 9 – Experimental

9.1 General Experimental Details

Solvents and Reagents

The following anhydrous solvents and reagents were bought from Sigma-Aldrich with a suba-seal stopper: dichloromethane (DCM), N,N-dimethyl-formamide (DMF), tetrahydrofuran (THF), triethylamine (TEA) and N-methylimidazole (NMI). All commercially available reagents and solvents were used without further purification.

Thin Layer Chromatography

Pre-coated, aluminium backed plates supplied by Merck (60 F₂₅₄, 0.2 mm thickness) were visualised under both short and long wave ultraviolet light (254 nm and 366 nm), or by burning using TLC indicators such as vanillin and potassium permanganate solution.

Flash Column Chromatography

Column chromatography was carried out using silica gel supplied by Fisher (60A, 35-70 μ m). Glass columns were slurry packed using the appropriate eluent with the sample being loaded pre-adsorbed onto silica gel. Fractions containing the desired product were identified by TLC, combined and the solvent removed *in vacuo*.

High Performance Liquid Chromatography

Analytical and preparative HPLC were conducted by Varian Prostar (LC Work Station- Varian Prostar 335 LC detector, Varian fraction collector (model 701), Prostar 210 solvent delivery system, using Agilent Eclipse Plus C18 (5 μ m) as an

analytical column and a Varian Pursuit XRs 5 C18 (150 x 21.2 mm) model as a preparative column. The software used was Galaxie Chromatography Data System.

Nuclear Magnetic Resonance Spectroscopy

^1H NMR (500 MHz), ^{13}C NMR (125 MHz), ^{31}P NMR (202 MHz) were recorded on a Bruker Avance 500 MHz spectrometer at 25 °C. Spectra were calibrated to the deuterated solvent used. Chemical shifts are detailed in parts per million (ppm) downfield from tetramethylsilane. For ^{31}P NMR experiments, chemical shifts are quoted in parts per million relative to an external phosphoric acid standard. Coupling constants are described in Hertz (J).

The following abbreviations are used in the assignment of NMR signals: s (singlet), d (doublet), t (triplet), q (quartet), quin (quintet), sep (septet), b (broad), m (multiplet) and dd (doublet of doublets). The ratio of diastereoisomers was based on ^{31}P NMR. The assignment of signals in ^1H NMR and ^{13}C NMR was done based on the analysis of coupling constants and additional two-dimensional experiments (COSY, HSQC, PENDANT).

Mass Spectrometry

Low resolution mass spectrometry was performed using a Bruker Daltonics device (atmospheric pressure ionisation, electrospray mass spectrometer) in either positive and/or negative mode.

Purity of Final Compounds

The $\geq 95\%$ purity of the final ProTide BED compounds was confirmed by HPLC analysis.

9.2 Standard Procedures

Phosphorochloridate Synthesis Standard Procedure

To a stirred solution of the appropriate amino acid ester salt (1 eq) and the appropriate aryl dichlorophosphate (1 eq) in anhydrous DCM was added dropwise at -78 °C anhydrous TEA (2 eq). Following the addition, the reaction mixture was stirred at -78 °C for 30 min and then at room temperature for 1 h. Formation of the desired compound was monitored by ^{31}P NMR. After this period the solvent was removed under reduced pressure to give an oil. Most of the aryl phosphorochloridates synthesised were purified by flash column chromatography (eluting with hexane - ethyl acetate 70:30 v/v).

Phosphoramidate Synthesis Using tBuMgCl Standard Procedure

tBuMgCl (1 eq) was added dropwise to a solution of primary alcohol (e.g. fingolimod hydrochloride / (S)-1-(4-((2-amino-3-hydroxy-2-methylpropoxy)methyl)phenyl)-4-(p-tolyl)butan-1-one) (1 eq) in anhydrous THF (7 ml) under anhydrous conditions. The mixture was stirred at room temperature for one hour. After one hour the phosphorochloridate (1 eq) in anhydrous THF (2 ml) was added dropwise to the stirring reaction mixture. The reaction was left to stir for 24 hours. After 24 hours the solvent was removed *in vacuo* and the desired product was dry-loaded to a column and isolated using flash chromatography (eluting with methanol – dichloromethane 0:100 v/v increasing to 10:90 v/v).

Carboxypeptidase Y Enzymatic Processing Experiment Standard Procedure

The experiment was carried out by dissolving phosphoramidate compound (3 mg) in acetone- d_6 (0.15 ml) and adding 0.3 ml of Trizma buffer (pH 7.6). After the ^{31}P NMR data were recorded at 25 °C as a control, a previously defrosted carboxypeptidase Y (0.1 mg dissolved in 0.15 ml of Trizma) was added to the sample. Next, the sample was submitted to ^{31}P NMR experiments (at 25 °C) and the

spectra were recorded every 7 min over 13 h. ^{31}P NMR recorded data were processed and analysed with the Bruker Topspin 2.1 program.¹

pH 1.5 Stability Assay Standard Procedure

The stability assay toward hydrolysis by aqueous buffer at pH 1.5 was conducted using *in situ* ^{31}P NMR (202 MHz). The experiment was carried out by dissolving test compound (e.g. phosphoramidate fingolimod) (3 mg) in methanol- d_4 (0.1 ml) and then adding buffer of pH 1.5 (prepared from HCl and KCl). Next, the sample was subjected to ^{31}P NMR experiments at 25 °C and the spectra were recorded every 12 min over 13 h.

pH 8 Stability Assay Standard Procedure

The stability assay toward hydrolysis by aqueous buffer at pH 8 was conducted using *in situ* ^{31}P NMR (202 MHz). The experiment was carried out by dissolving test compound (e.g. phosphoramidate fingolimod) (3 mg) in methanol- d_4 (0.1 ml) and then adding buffer, pH 8 (prepared from tris(hydroxymethyl)aminomethane and HCl). Next, the sample was subjected to ^{31}P NMR experiments at 25 °C and the spectra were recorded every 12 min over 13 h.

Human Serum Assay Standard Procedure

The experiment was carried out by dissolving test compound (e.g. phosphoramidate fingolimod) in DMSO (0.05 ml) and D_2O (0.15 ml). After the ^{31}P NMR data were recorded at 37 °C as a control, a previously defrosted human serum (0.3 ml dissolved) was added to the sample. Next, the sample was submitted to ^{31}P NMR experiments (at 37 °C) and the spectra were recorded every 15 min over 13 h. ^{31}P NMR recorded data were processed and analysed with the Bruker Topspin 2.1 program.

Porcine Liver Esterase Processing Experiment Standard Procedure

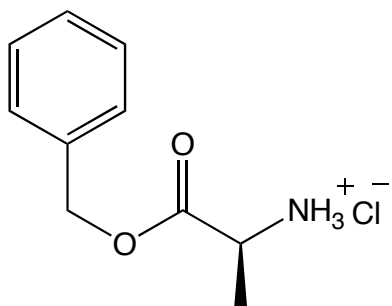
Test compound (e.g. phosphoramidate fingolimod) (30 mg) was added to Trizma solution (1 ml) and acetone (2 ml) and stirred at 37 °C for 24 h with monitoring by TLC. After 24 h the acetone was removed *in vacuo* and the remaining aqueous mixture was extracted with DCM. The organic layer was collected and the solvent removed under vacuum yielding the mixture of products and starting material which was then analysed by NMR and mass spectrometry.

Cell Lysate Processing Experiment Standard Procedure

The experiment was carried out by dissolving phosphoramidate compound (e.g. phosphoramidate BED(a)) (5 mg) in acetone- d_6 (0.3 ml) and adding 0.1 ml of Trizma buffer (pH 7.6). After the ^{31}P NMR data were recorded at 25 °C as a control, 0.125 ml cell lysate and 0.02 ml activator was added to the sample. Next, the sample was shaken and submitted to ^{31}P NMR experiments (at 37 °C) and the spectra were recorded every 7 min over 13 h. ^{31}P NMR recorded data were processed and analysed with the Bruker Topspin 2.1 program.

9.3 Phosphorochloridate Syntheses

Synthesis of (*S*)-1-(benzyloxy)-1-oxopropan-2-aminium chloride

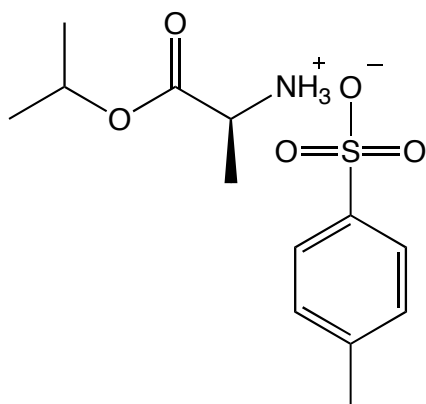


C₁₀H₁₄ClNO₂
MW: 215.07

To a stirred solution of benzyl alcohol (12.14 g, 112.25 mmol) at 0 °C under an argon atmosphere, thionyl chloride (3.27 ml, 45 mmol) was added. The reaction mixture was stirred at 0 °C for 30 minutes and after that time allowed to warm to ambient temperature. L-alanine (2 g, 22.5 mmol) was added and the mixture heated at 80 °C under reflux conditions overnight. The following day the solvent was removed *in vacuo*. Pure product was obtained by precipitation from diethyl ether as a white hydrochloride salt (57%, 2.74 g).

¹H NMR (CDCl₃, 500 MHz): δ 8.79 (3H, b, NH₃), 7.38-7.23 (5H, m, ArH), 5.20 (2H, m, OCH₂Ph), 4.23 (1H, q, *J* = 7 Hz, CH₃CH), 1.72 (3H, d, *J* = 7.5, CHCH₃).

Synthesis of (S)-1-isopropoxy-1-oxopropan-2-aminium 4-methylbenzenesulfonate

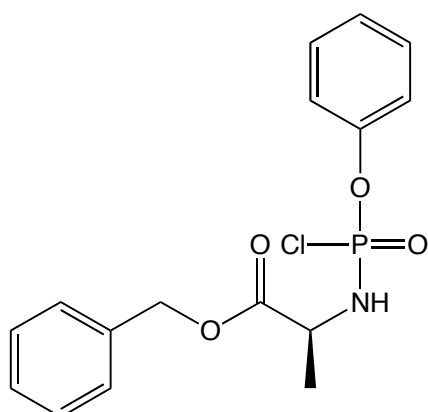


C₁₃H₂₁NO₅S
MW: 303.11

To a stirred solution of L-alanine (10 g, 112.25 mmol) in toluene (160 ml) was added propan-2-ol (129 ml, 1.684 moles) and p-toluenesulfonic acid (21.352 g, 112.25 mmol). The mixture was attached to Dean Stark apparatus and stirred at 120 °C overnight. After 24 h the solvent was removed *in vacuo*. The remaining white solid was subjected to vacuum filtration and washed with Et₂O yielding the pure product (88%, 29.938 g).

¹H NMR (CDCl₃, 500 MHz): δ 8.07 (3H, b, NH₃), 7.68 (2H, d, *J* = 8 Hz, ArH), 7.06 (2H, d, *J* = 8 Hz, ArH), 4.89 (1H, sep, *J* = 6 Hz, OCH), 3.86 (1H, q, *J* = 7 Hz, NH₃CHCH₃), 2.27 (3H, s, PhCH₃), 1.35 (3H, d, *J* = 7 Hz, CHCH₃), 1.09 (6H, d, *J* = 6.5 Hz, CHCH₃).

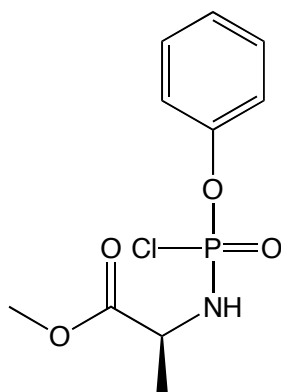
Synthesis of Phenyl-(benzyloxy-L-alaninyl) phosphorochloridate



C₁₆H₁₇ClNO₄P
MW: 353.1

To a stirred solution of H-LAla-OBzl.p-tosylate (3 g, 8.5 mmol) and phenyl dichlorophosphate (1.27 ml, 8.5 mmol) in anhydrous DCM (20 ml) was added dropwise at -78 °C anhydrous TEA (2.37 ml, 17 mmol). Following the addition, the reaction mixture was stirred at -78 °C for 30 min and then at room temperature for 1 h. Formation of the desired compound was monitored by ³¹P NMR. After this period the solvent was removed under reduced pressure to give an oil. The product was then purified by flash column chromatography (eluting with hexane - ethyl acetate 70:30 v/v) giving the desired oil product as mixture of 2 diastereoisomers (77%, 2.31 g).

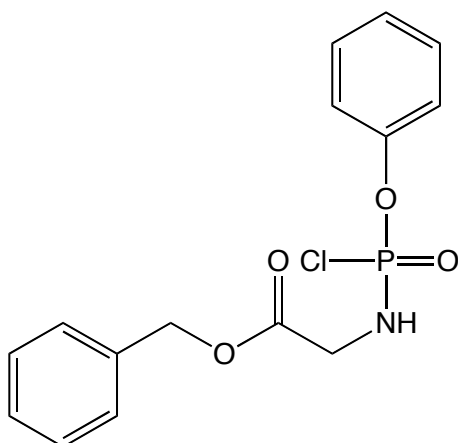
³¹P NMR (CDCl₃, 202 MHz): δ 8.15, 7.70. ¹H NMR (CDCl₃, 500 MHz): δ 7.29 (7H, m, ArH), 7.17 (3H, m, ArH), 5.14 (1H, s, OCH₂Ph), 5.13 (1H, s, OCH₂Ph), 4.28 (1H, m, CHNH), 4.17 (1H, m, CHCH₃), 1.46 (1.5H, d, *J* = 7 Hz, CHCH₃), 1.44 (1.5H, d, *J* = 7 Hz, CHCH₃). MS (ES+) *m/z* 354.1 (MH⁺).

Synthesis of Phenyl-(methoxy-L-alaninyl) phosphorochloridate

$C_{10}H_{13}ClNO_4P$
MW: 277.0

To a stirred solution of H-LAla-OMe.HCl (1.19 g, 8.5 mmol) and phenyl dichlorophosphate (1.27 ml, 8.5 mmol) in anhydrous DCM (20 ml) was added dropwise at -78 °C anhydrous TEA (2.37 ml, 17 mmol). Following the addition, the reaction mixture was stirred at -78 °C for 30 min and then at room temperature for 1 h. Formation of the desired compound was monitored by ^{31}P NMR. After this period the solvent was removed under reduced pressure to give an oil. The product was then purified by flash column chromatography (eluting with hexane - ethyl acetate 70:30 v/v) giving the desired oil product as mixture of 2 diastereoisomers (56%, 1.31 g).

^{31}P NMR ($CDCl_3$, 202 MHz): δ 8.16, 7.67. 1H NMR ($CDCl_3$, 500 MHz): δ 7.41 (2H, m, ArH), 7.29 (3H, m, ArH), 4.32 (1H, m, CHNH), 4.23 (1H, m, CHCH₃), 3.83 (1.5H, s, CHCH₃), 3.82 (1.5H, s, CHCH₃), 1.55 (3H, m, OCH₃).

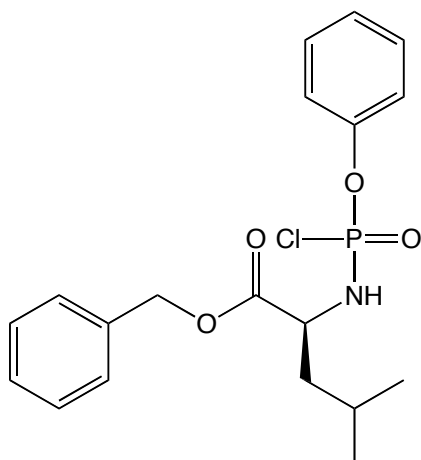
Synthesis of Phenyl-(benzyloxy-glyciny) phosphorochloridate

C₁₅H₁₅ClNO₄P
MW: 339.0

To a stirred solution of H-Gly-OBzl.p-tosylate (2.87 g, 8.5 mmol) and phenyl dichlorophosphate (1.27 ml, 8.5 mmol) in anhydrous DCM (20 ml) was added dropwise at -78 °C anhydrous TEA (2.37 ml, 17 mmol). Following the addition, the reaction mixture was stirred at -78 °C for 30 min and then at room temperature for 1 h. Formation of the desired compound was monitored by ³¹P NMR. After this period the solvent was removed under reduced pressure to give an oil. The product was then purified by flash column chromatography (eluting with hexane - ethyl acetate 70:30 v/v) giving the desired oil product as a mixture of 2 enantiomers (43%, 1.24 g).

³¹P NMR (CDCl₃, 202 MHz): δ 8.82. ¹H NMR (CDCl₃, 500 MHz): δ 7.42-7.27 (10H, m, ArH), 5.26 (1H, s, OCH₂Ph), 5.22 (1H, s, OCH₂Ph), 4.38 (1H, m, CH₂NH), 3.92 (2H, m, CH₂NH).

Synthesis of Phenyl-(benzyloxy-L-leucinyl) phosphorochloridate

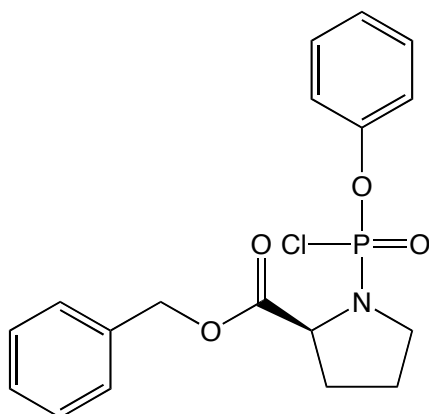


$C_{19}H_{23}ClNO_4P$
MW: 395.1

To a stirred solution of H-Leu-OBzl.p-tosylate (3.34 g, 8.5 mmol) and phenyl dichlorophosphate (1.27 ml, 8.5 mmol) in anhydrous DCM (20 ml) was added dropwise at $-78^{\circ}C$ anhydrous TEA (2.37 ml, 17 mmol). Following the addition, the reaction mixture was stirred at $-78^{\circ}C$ for 30 min and then at room temperature for 1 h. Formation of the desired compound was monitored by ^{31}P NMR. After this period the solvent was removed under reduced pressure to give an oil. The product was then purified by flash column chromatography (eluting with hexane - ethyl acetate 70:30 v/v) giving the desired oil product as mixture of 2 diastereoisomers (42%, 1.41 g).

^{31}P NMR ($CDCl_3$, 202 MHz): δ 8.45, 8.15. 1H NMR ($CDCl_3$, 500 MHz): δ 7.78-7.76 (0.5H, m, ArH), 7.25-7.05 (9.5H, m, ArH), 5.06 (2H, m, OCH_2Ph), 4.97 (1H, m, CHNP), 4.05 (1H, m, $CHCH_3$), 1.74 (0.5H, m, $CH(CH_3)_2$), 1.66 (0.5H, m, $CH(CH_3)_2$), 1.53 (2H, m, $CH_2CH(CH_3)_2$), 0.80 (6H, m, $CH(CH_3)_2$).

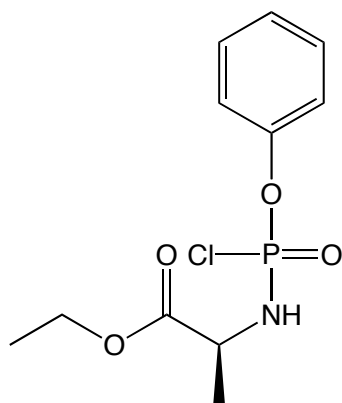
Synthesis of Phenyl-(benzyloxy-L-prolinyl) phosphorochloridate



C₁₈H₁₉ClNO₄P
MW: 379.1

To a stirred solution of L-Pro-OBzl.HCl (2.05 g, 8.5 mmol) and phenyl dichlorophosphate (1.27 ml, 8.5 mmol) in anhydrous DCM (20 ml) was added dropwise at -78 °C anhydrous TEA (2.37 ml, 17 mmol). Following the addition, the reaction mixture was stirred at -78 °C for 30 min and then at room temperature for 1 h. Formation of the desired compound was monitored by ³¹P NMR. After this period the solvent was removed under reduced pressure to give an oil. The product was then purified by flash column chromatography (eluting with hexane - ethyl acetate 70:30 v/v) giving the desired oil product as mixture of 2 diastereoisomers (72%, 2.33 g).

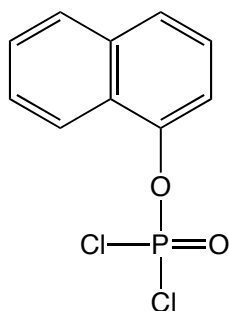
³¹P NMR (CDCl₃, 202 MHz): δ 7.74, 7.67. ¹H NMR (CDCl₃, 500 MHz): δ 7.38-7.16 (10H, m, ArH), 5.16 (2H, m, OCH₂Ph), 4.55 (1H, m, CHNP), 3.51 (2H, m, CH₂NP), 2.21 (2H, m, CHCH₂CH₂), 1.96 (2H, m, CHCH₂CH₂).

Synthesis of Phenyl-(ethoxy-L-alaninyl) phosphorochloridate

$C_{11}H_{15}ClNO_4P$
MW: 291.0

To a stirred solution of H-LAla-OEt.HCl (1.31 g, 8.5 mmol) and phenyl dichlorophosphate (1.27 ml, 8.5 mmol) in anhydrous DCM (20 ml) was added dropwise at -78 °C anhydrous TEA (2.37 ml, 17 mmol). Following the addition, the reaction mixture was stirred at -78 °C for 30 min and then at room temperature for 1 h. Formation of the desired compound was monitored by ^{31}P NMR. After this period the solvent was removed under reduced pressure to give an oil. The product was then purified by flash column chromatography (eluting with hexane - ethyl acetate 70:30 v/v) giving the desired oil product as mixture of 2 diastereoisomers (84%, 2.1 g).

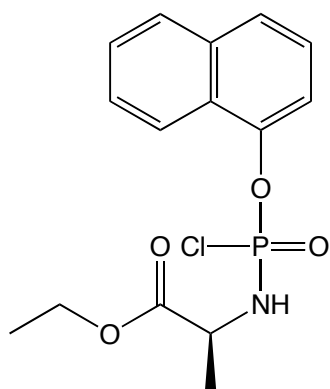
^{31}P NMR ($CDCl_3$, 202 MHz): δ 8.02, 7.70. 1H NMR ($CDCl_3$, 500 MHz): δ 7.39 (2H, m, ArH), 7.29 (3H, m, ArH), 4.41 (1H, m, PNH), 4.26 (2H, m, OCH_2CH_3), 4.19 (1H, m, $CHCH_3$), 1.55 (1.5H, d, J = 7 Hz, $CHCH_3$), 1.53 (1.5H, d, J = 7 Hz, $CHCH_3$), 1.33 (3H, t, J = 7 Hz, CH_2CH_3).

Synthesis of 1-Naphthyl dichlorophosphate

$\text{C}_{10}\text{H}_7\text{Cl}_2\text{O}_2\text{P}$
MW: 260.0

Phosphorus oxychloride (2.59 ml, 27.74 mmol) and 1-naphthol (4 g, 27.74 mmol) were stirred in anhydrous Et_2O under an argon atmosphere. Anhydrous TEA was added (3.87 ml, 27.74 mmol) at -78°C . After 30 minutes the solution was allowed to warm to room temperature. After 3.5 hours and ^{31}P NMR, the mixture was subjected to vacuum filtration. The solid salt mixture was discarded and Et_2O solvent was removed from the solution *in vacuo* yielding the yellow oil product (72%, 5.18 g).

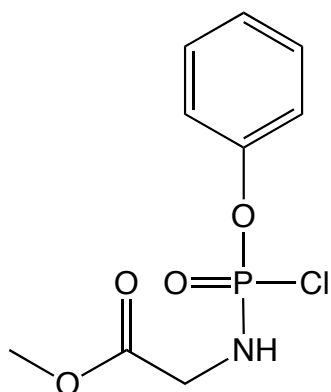
^{31}P NMR (CDCl_3 , 202 MHz): δ 3.73. ^1H NMR (CDCl_3 , 500 MHz): δ 8.13-7.37 (7H, m, ArH).

Synthesis of 1-Naphthyl-(ethoxy-L-alaninyl) phosphorochloridate

C₁₅H₁₇ClNO₄P
MW: 341.0

To a stirred solution of H-LAla-OEt.HCl (1.31 g, 8.5 mmol) and 1-naphthyl dichlorophosphate (1.51 ml, 8.5 mmol,) in anhydrous DCM (20 ml) was added dropwise at -78 °C anhydrous TEA (2.37 ml, 17 mmol). Following the addition, the reaction mixture was stirred at -78 °C for 30 min and then at room temperature for 1 h. Formation of the desired compound was monitored by ³¹P NMR. After this period the solvent was removed under reduced pressure to give an oil. The product was then purified by flash column chromatography (eluting with hexane - ethyl acetate 70:30 v/v) giving the desired oil product as mixture of 2 diastereoisomers (64.5%, 1.87 g).

³¹P NMR (CDCl₃, 202 MHz): δ 8.28, 8.00. ¹H NMR (CDCl₃, 500 MHz): δ 8.08 (1H, t, *J* = 7.5 Hz, *ArH*), 7.86 (1H, d, *J* = 7.5 Hz, *ArH*), 7.72 (1H, d, *J* = 8 Hz, *ArH*), 7.60 (3H, m, *ArH*), 7.43 (1H, t, *J* = 8 Hz, *ArH*), 4.52 (1H, m, *CHCH*₃), 4.27 (1H, m, *PNH*), 4.22 (2H, m, *OCH*₂*CH*₃), 1.56 (1.5H, d, *J* = 7.5 Hz, *CHCH*₃), 1.54 (1.5H, d, *J* = 7.5 Hz, *CHCH*₃), 1.29 (3H, m, *CH*₂*CH*₃).

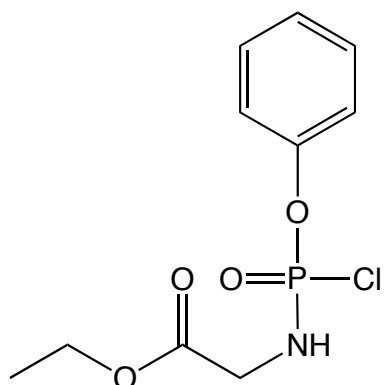
Synthesis of Phenyl-(methoxy-glyciny) phosphorochloridate

$C_9H_{11}ClNO_4P$
MW: 263.09

To a stirred solution of H-Gly-OMe.HCl (1.067 g, 8.5 mmol) and phenyl dichlorophosphate (1.27 ml, 8.5 mmol) in anhydrous DCM (20 ml) was added dropwise at -78 °C anhydrous TEA (2.37 ml, 17 mmol). Following the addition, the reaction mixture was stirred at -78 °C for 30 min and then at room temperature for 1 h. Formation of the desired compound was monitored by ^{31}P NMR. After this period the solvent was removed under reduced pressure to give an oil. The product was then purified by flash column chromatography (eluting with hexane - ethyl acetate 70:30 v/v) giving the desired oil product as mixture of 2 enantiomers (53%, 1.184 g).

^{31}P NMR ($CDCl_3$, 202 MHz): δ 9.02. 1H NMR ($CDCl_3$, 500 MHz): δ 7.45-7.21 (5H, m, ArH), 4.50 (1H, m, CH_2NH), 3.92 (2H, m, CH_2NH), 3.82 (3H, s, OCH_3).

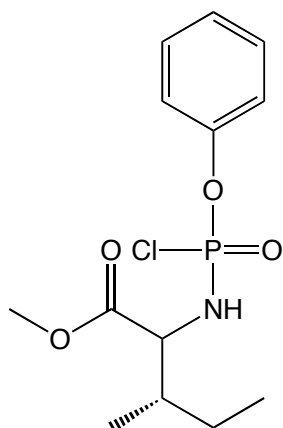
Synthesis of Phenyl-(ethoxy-glyciny) phosphorochloridate



C₁₀H₁₃ClNO₄P
MW: 277.03

To a stirred solution of H-Gly-OEt.HCl (1.186 g, 8.5 mmol) and phenyl dichlorophosphate (1.27 ml, 8.5 mmol) in anhydrous DCM (20 ml) was added dropwise at -78 °C anhydrous TEA (2.37 ml, 17 mmol). Following the addition, the reaction mixture was stirred at -78 °C for 30 min and then at room temperature for 1 h. Formation of the desired compound was monitored by ³¹P NMR. After this period the solvent was removed under reduced pressure to give an oil. The product was then purified by flash column chromatography (eluting with hexane - ethyl acetate 70:30 v/v) giving the desired oil product as mixture of 2 enantiomers (69%, 1.619 g).

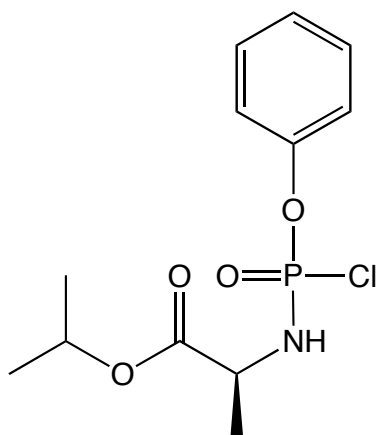
³¹P NMR (CDCl₃, 202 MHz): δ 9.23. ¹H NMR (CDCl₃, 500 MHz): δ 7.45-7.19 (5H, m, ArH), 4.67 (1H, b, CHNH), 4.25 (1H, d, *J* = 7 Hz, CH₂NH), 4.23 (1H, d, *J* = 7 Hz, CH₂NH), 3.89 (1H, q, *J* = 6 Hz, CH₂CH₃), 3.88 (1H, q, *J* = 6 Hz, CH₂CH₃), 1.27 (3H, t, *J* = 7 Hz, CH₂CH₃).

Synthesis of Phenyl-(methoxy-L-isoleuciny) phosphorochloridate

$C_{13}H_{19}ClNO_4P$
MW: 319.07

To a stirred solution of H-Ile-OMe.HCl (1.544 g, 8.5 mmol) and phenyl dichlorophosphate (1.27 ml, 8.5 mmol) in anhydrous DCM (20 ml) was added dropwise at -78 °C anhydrous TEA (2.37 ml, 17 mmol). Following the addition, the reaction mixture was stirred at -78 °C for 30 min and then at room temperature for 1 h. Formation of the desired compound was monitored by ^{31}P NMR. After this period the solvent was removed under reduced pressure to give an oil. The product was then purified by flash column chromatography (eluting with hexane - ethyl acetate 70:30 v/v) giving the desired oil product as mixture of 2 diastereoisomers (69%, 1.86 g).

^{31}P NMR ($CDCl_3$, 202 MHz): δ 9.20, 9.00. 1H NMR ($CDCl_3$, 500 MHz): δ 7.30 (2H, m, ArH), 7.19 (3H, m, ArH), 4.14 (1H, m, CHNH), 3.95 (1H, m, CHNH), 3.72 (1.5H, s, OCH_3), 3.70 (1.5H, s, OCH_3), 1.82 (1H, m, CH_3CHCH_2), 1.41 (1H, m, CH_3CH_2), 1.15 (1H, m, CH_3CH_2), 0.91 (3H, m, CH_3CH), 0.87 (3H, m, CH_3CH_2).

Synthesis of Phenyl-(isopropoxy-L-alaninyl) phosphorochloridate

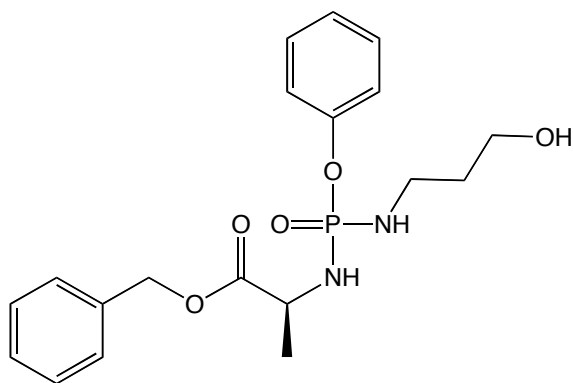
$C_{12}H_{17}ClNO_4P$
MW: 305.06

To a stirred solution of (*S*)-1-isopropoxy-1-oxopropan-2-aminium 4-methylbenzenesulfonate (6 g, 19.79 mmol) and phenyl dichlorophosphate (2.96 ml, 19.79 mmol) in anhydrous DCM (50 ml) was added dropwise at -78 °C anhydrous TEA (5.51 ml, 39.54 mmol). Following the addition, the reaction mixture was stirred at -78 °C for 1 h and then at room temperature for 2.5 h. Formation of the desired compound was monitored by ^{31}P NMR. After this period the solvent was removed under reduced pressure to give an oil. The product was then purified by flash column chromatography (eluting with hexane - ethyl acetate 50:50 v/v) giving the desired oil product as mixture of 2 diastereoisomers (55%, 3.297 g).

^{31}P NMR ($CDCl_3$, 202 MHz): δ 8.16, 7.77. 1H NMR ($CDCl_3$, 500 MHz): δ 7.35-7.14 (5H, m, ArH), 5.02 (1H, m, OCHCH₃), 4.27 (1H, m, NHCHCH₃), 2.42 (1H, s, CHNH), 1.43 (3H, m, NHCHCH₃), 1.21 (6H, m, CHCH₃).

9.4 Non-S1P Receptor Modulator Phosphoramidate Syntheses

Synthesis of (2*S*)-benzyl 2-((((3-hydroxypropyl) amino) (phenoxy) phosphoryl) amino) propanoate using NaH

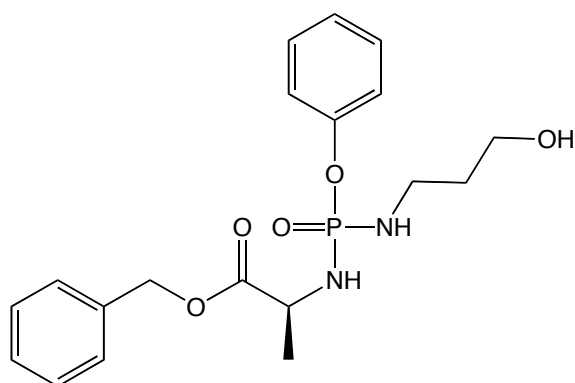


C₁₉H₂₅N₂O₅P
MW: 392.1

3-amino-1-propanol (0.3 ml, 4 mmol, 1 eq) was added dropwise to a solution of phosphorochloridate (2.89 g, 8.5 mmol, 2.25 eq) in anhydrous DCM (20 ml) under anhydrous conditions. The mixture was stirred at room temperature for one hour. After one hour NaH (96 mg, 4 mmol, 1 eq) was added and the mixture was left to stir for 3 days. After 3 days the solvent was removed *in vacuo* and the desired product was isolated using flash chromatography (petroleum ether – ethyl acetate 90:10 v/v increasing to 70:30 v/v) giving the desired oil product as mixture of 2 diastereoisomers.

³¹P NMR (MeOD, 202 MHz): δ 12.04, 11.70. ¹H NMR (MeOD, 500 MHz): δ 7.36 (7H, m, ArH), 7.20 (3H, m, ArH), 5.17 (1H, s, OCH₂Ph), 5.16 (1H, s, OCH₂Ph), 4.02 (1H, q, *J* = 7.5 Hz, CHCH₃), 3.60 (2H, t, *J* = 6 Hz, CH₂CH₂OH), 3.04 (2H, m, CH₂CH₂NH), 1.68 (2H, quin, *J* = 6.5 Hz, CH₂CH₂CH), 1.40 (1.5H, d, *J* = 7 Hz, CHCH₃), 1.38 (1.5H, d, *J* = 7 Hz, CHCH₃). ¹³C NMR (MeOD, 125 MHz): δ 175.39 (C=O), 152.75 (d, ²*J*_{C-P} = 5 Hz, POC-Ar), 152.69 (d, ²*J*_{C-P} = 5 Hz, POC-Ar), 137.37 (C-Ar), 130.62 (CH-Ar), 129.64 (CH-Ar), 129.37 (CH-Ar), 125.61 (CH-Ar), 125.54 (CH-Ar), 121.84 (CH-Ar), 121.80 (CH-Ar), 121.71 (CH-Ar), 121.67 (CH-Ar), 67.93 (PhCH₂), 60.45 (CH₂OH), 51.48 (CHCH₃), 39.17 (d, ²*J*_{C-P} = 7 Hz, CH₂NHP), 35.31 (CH₂CH₂CH₂), 20.78 (CHCH₃), 20.73 (CHCH₃). MS (ES+) *m/z* 393.1 (MH⁺) and 415.1 (MNa⁺).

Synthesis of (2S)-benzyl 2-((((3-hydroxypropyl) amino) (phenoxy) phosphoryl) amino) propanoate using NMI

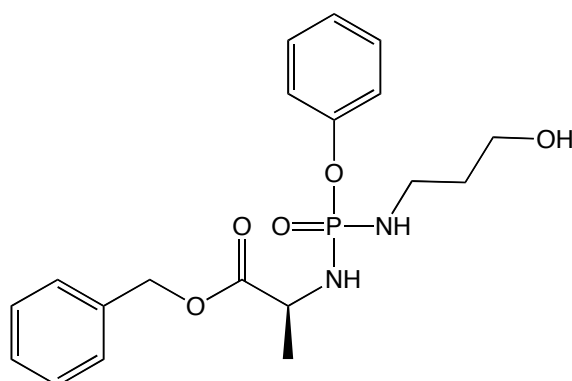


C₁₉H₂₅N₂O₅P
MW: 392.1

1-methylimidazole (0.39 ml, 4.9 mmol, 4.9 eq) was added dropwise to a solution of 3-amino-1-propanol (0.075 ml, 1 mmol, 1 eq) in anhydrous THF (10 ml) under anhydrous conditions at 0 °C. The mixture was stirred at 0 °C for 30 min. After 30 min the phosphorochloridate (500 mg, 1.4 mmol, 1.4 eq) in anhydrous THF (8 ml) was added dropwise to the stirring reaction mixture. Following the addition, the reaction mixture was stirred at 0 °C for a further 30 min and then at room temperature for 3 days. After 3 days the solvent was removed *in vacuo* to give a residue that was redissolved in DCM and washed twice with 0.5 M HCl (2 x 5 ml). The organic phase was purified by column chromatography (methanol – dichloromethane 2:98 v/v) giving the desired oil product as mixture of 2 diastereoisomers (62%, 0.23 g).

³¹P NMR (CDCl₃, 202 MHz): δ 10.86, 10.63. ¹H NMR (MeOD, 500 MHz): δ 7.36 (7H, m, ArH), 7.20 (3H, m, ArH), 5.17 (1H, s, OCH₂Ph), 5.16 (1H, s, OCH₂Ph), 4.02 (1H, q, *J* = 7.5 Hz, CHCH₃), 3.60 (2H, t, *J* = 6 Hz, CH₂CH₂OH), 3.04 (2H, m, CH₂CH₂NH), 1.68 (2H, quin, *J* = 6.5 Hz, CH₂CH₂CH), 1.40 (1.5H, d, *J* = 7 Hz, CHCH₃), 1.38 (1.5H, d, *J* = 7 Hz, CHCH₃). ¹³C NMR (MeOD, 125 MHz): δ 175.39 (C=O), 152.75 (d, ²*J*_{C-P} = 5 Hz, POC-Ar), 152.69 (d, ²*J*_{C-P} = 5 Hz, POC-Ar), 137.37 (C-Ar), 130.62 (CH-Ar), 129.64 (CH-Ar), 129.37 (CH-Ar), 125.61 (CH-Ar), 125.54 (CH-Ar), 121.84 (CH-Ar), 121.80 (CH-Ar), 121.71 (CH-Ar), 121.67 (CH-Ar), 67.93 (PhCH₂), 60.45 (CH₂OH), 51.48 (CHCH₃), 39.17 (d, ²*J*_{C-P} = 7 Hz, CH₂NHP), 35.31 (CH₂CH₂CH₂), 20.78 (CHCH₃), 20.73 (CHCH₃). MS (ES⁺) *m/z* 393.1 (MH⁺) and 415.1 (MNa⁺).

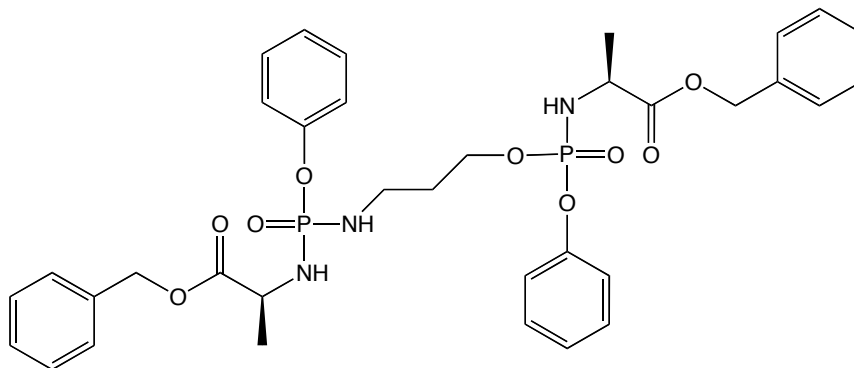
Synthesis of (2S)-benzyl 2-((((3-hydroxypropyl) amino) (phenoxy) phosphoryl) amino) propanoate using NaOMe



C₁₉H₂₅N₂O₅P
MW: 392.1

Phosphorochloridate (500 mg, 1.41 mmol) was added dropwise to a solution of 3-amino-1-propanol (0.11 ml, 1.41 mmol) in anhydrous DCM (5 ml) under anhydrous conditions. The temperature of the mixture was then lowered to -78 °C. After one hour NaOMe (25% in MeOH) (0.32 ml, 1.41 mmol) was added. Following the addition, the reaction mixture was stirred at -78 °C for 30 min and then at room temperature for 1 h. After 1 h the solvent was removed *in vacuo* and the desired product was isolated using flash chromatography (methanol – ethyl acetate 2:98 v/v) giving the desired oil product as mixture of 2 diastereoisomers (56%, 0.31 g). ³¹P NMR (MeOD, 202 MHz): δ 12.04, 11.70. ¹H NMR (MeOD, 500 MHz): δ 7.36 (7H, m, ArH), 7.20 (3H, m, ArH), 5.17 (1H, s, OCH₂Ph), 5.16 (1H, s, OCH₂Ph), 4.02 (1H, q, *J* = 7.5 Hz, CHCH₃), 3.60 (2H, t, *J* = 6 Hz, CH₂CH₂OH), 3.04 (2H, m, CH₂CH₂NH), 1.68 (2H, quin, *J* = 6.5 Hz, CH₂CH₂CH), 1.40 (1.5H, d, *J* = 7 Hz, CHCH₃), 1.38 (1.5H, d, *J* = 7 Hz, CHCH₃). ¹³C NMR (MeOD, 125 MHz): δ 175.39 (C=O), 152.75 (d, ²*J*_{C-P} = 5 Hz, POC-Ar), 152.69 (d, ²*J*_{C-P} = 5 Hz, POC-Ar), 137.37 (C-Ar), 130.62 (CH-Ar), 129.64 (CH-Ar), 129.37 (CH-Ar), 125.61 (CH-Ar), 125.54 (CH-Ar), 121.84 (CH-Ar), 121.80 (CH-Ar), 121.71 (CH-Ar), 121.67 (CH-Ar), 67.93 (PhCH₂), 60.45 (CH₂OH), 51.48 (CHCH₃), 39.17 (d, ²*J*_{C-P} = 7 Hz, CH₂NHP), 35.31 (CH₂CH₂CH₂), 20.78 (CHCH₃), 20.73 (CHCH₃). MS (ES+) *m/z* 393.1 (MH⁺) and 415.1 (MNa⁺).

Synthesis of (2S)-benzyl 2-(((3-((((S)-1-(benzyloxy)-1-oxopropan-2-yl) amino) (phenoxy) phosphoryl) amino) propoxy) (phenoxy) phosphoryl) amino) propanoate using tBuMgCl



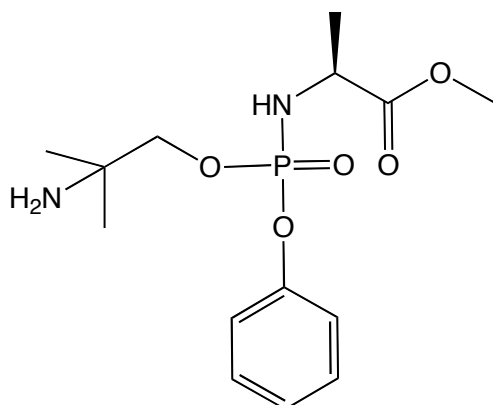
C₃₅H₄₁N₃O₉P₂
MW: 709.3

tBuMgCl (1.41 ml, 1.41 mmol) was added dropwise to a solution of 3-amino-1-propanol (0.11 ml, 1.41 mmol) in anhydrous THF (4 ml) under anhydrous conditions. The mixture was stirred at room temperature for one hour. After one hour the phosphorochloridate (500 mg, 1.41 mmol) in anhydrous THF (2 ml) was added dropwise to the stirring reaction mixture. The reaction was left to stir for 24 hours. After 24 hours the solvent was removed *in vacuo* and the desired product was isolated using flash chromatography (methanol – ethyl acetate 2:98 v/v) giving the desired oil product as mixture of 4 diastereoisomers (31%, 0.169 g).

³¹P NMR (MeOD, 202 MHz): δ 11.79, 11.76, 11.44, 11.38, 3.96, 3.92, 3.64, 3.61. ¹H NMR (MeOD, 500 MHz): δ 7.38-7.27 (14H, m, ArH), 7.22-7.11 (6H, m, ArH), 5.15 (2H, m, OCH₂Ph), 5.14 (2H, m, OCH₂Ph), 4.11 (2H, m, CHCH₃), 4.02 (2H, m, CH₂CH₂OP), 3.02 (2H, m, CH₂CH₂NH), 1.78 (2H, m, CH₂CH₂CH₂), 1.37 (3H, m, CHCH₃), 1.35 (3H, m, CHCH₃). ¹³C NMR (MeOD, 125 MHz): δ 175.34 (C=O), 175.02 (C=O), 174.73 (C=O), 173.00 (C=O), 152.69 (d, ²J_{C-P} = 6.9 Hz, POC-Ar), 152.66 (d, ²J_{C-P} = 6.9 Hz, POC-Ar), 152.34 (d, ²J_{C-P} = 6.9 Hz, POC-Ar), 152.32 (d, ²J_{C-P} = 6.9 Hz, POC-Ar), 137.36 (C-Ar), 137.32 (C-Ar), 137.30 (C-Ar), 130.79 (CH-Ar), 130.66 (CH-Ar), 129.41 (CH-Ar), 129.39 (CH-Ar), 129.38 (CH-Ar), 129.35 (CH-Ar), 126.10 (CH-Ar), 126.06 (CH-Ar), 125.65 (CH-Ar), 125.58 (CH-Ar), 121.87 (CH-Ar), 121.83 (CH-Ar), 121.73 (CH-Ar), 121.72 (CH-Ar), 121.69 (CH-Ar), 121.68 (CH-Ar), 121.62 (CH-Ar), 121.58 (CH-Ar), 121.56 (CH-Ar), 121.53 (CH-Ar), 121.49 (CH-Ar), 67.99 (PhCH₂), 67.97 (PhCH₂), 67.95 (PhCH₂), 67.93 (PhCH₂), 65.94 (d, ²J_{C-P} = 5.6 Hz, CH₂OP), 65.88 (d, ²J_{C-P} = 5.6 Hz, CH₂OP), 51.80 (CHCH₃), 51.68 (CHCH₃), 51.49 (CHCH₃),

38.51 (d, $^2J_{\text{C-P}} = 4.9$ Hz, CH_2NHP), 38.43 (d, $^2J_{\text{C-P}} = 5.6$ Hz, CH_2NHP), 33.28 ($\text{CH}_2\text{CH}_2\text{CH}_2$), 33.24 ($\text{CH}_2\text{CH}_2\text{CH}_2$), 33.18 ($\text{CH}_2\text{CH}_2\text{CH}_2$), 20.97 (CHCH_3), 20.81 (CHCH_3), 20.77 (CHCH_3), 20.57 (CHCH_3), 20.51 (CHCH_3). MS MS (ES+) m/z 710.3 (MH^+).

Synthesis of (2S)-methyl 2-(((2-amino-2-methylpropoxy) (phenoxy) phosphoryl) amino) propanoate



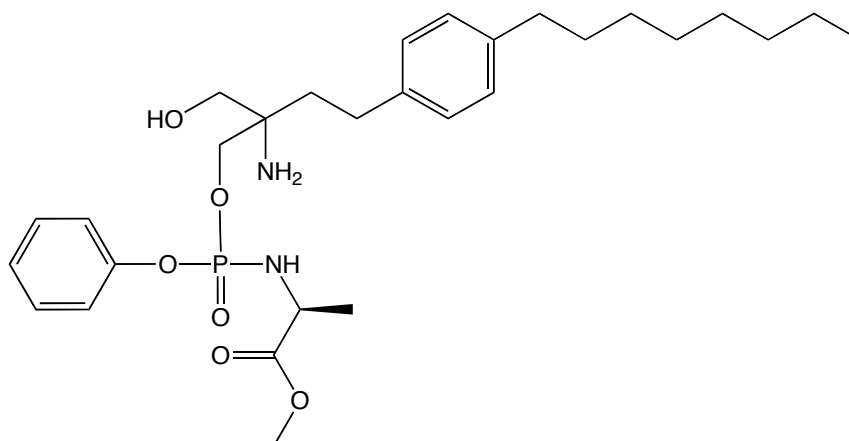
$\text{C}_{14}\text{H}_{23}\text{N}_2\text{O}_5\text{P}$
MW: 330.1

tBuMgCl (1.41 ml, 1.41 mmol) was added dropwise to a solution of 2-amino-2-methyl-1-propanol (0.13 ml, 1.41 mmol) in anhydrous THF (3 ml) under anhydrous conditions. The mixture was stirred at room temperature for one hour. After one hour the phosphorochloridate (390 mg, 1.41 mmol) in anhydrous THF (4.3 ml) was added dropwise to the stirring reaction mixture. The reaction was left to stir for 24 hours. After 24 hours the solvent was removed *in vacuo* and the desired product was isolated using flash chromatography (methanol – ethyl acetate 10:90 v/v) giving the desired oil product as mixture of 2 diastereoisomers (34%, 0.16 g).

^{31}P NMR (CDCl_3 , 202 MHz): δ 2.62, 2.16. ^1H NMR (CDCl_3 , 500 MHz): δ 7.32-7.13 (5H, m, ArH), 5.12 (1H, m, CHNH), 4.25 (1H, m, CHCH₃), 4.07 (2H, m, NH₂), 3.68 (2H, s, POCH₂), 2.17 (3H, s, OCH₃), 1.46 (3H, m, CHCH₃), 1.43 (3H, m, CCH₃), 1.37 (3H, m, CCH₃). MS (ES+) m/z 331.1 (MH^+).

9.5 Syntheses of Fingolimod Derived Phosphoramidates

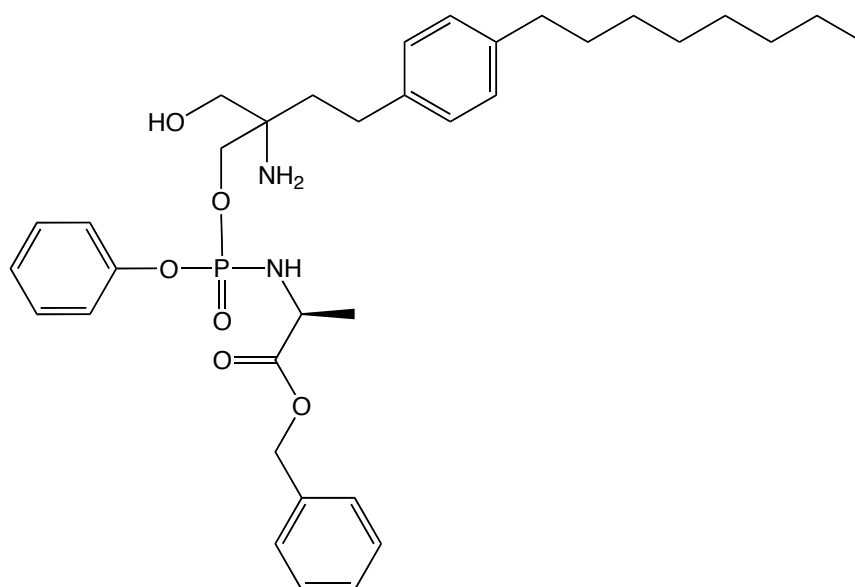
Synthesis of Phenyl-(methoxy-L-alaninyl) phosphoramidate fingolimod (1)



C₂₅H₄₅N₂O₆P
MW: 548.3

tBuMgCl (1.45 ml, 1.45 mmol) was added dropwise to a solution of fingolimod hydrochloride (500 mg, 1.45 mmol) in anhydrous THF (7 ml) under anhydrous conditions. The mixture was stirred at room temperature for one hour. After one hour phenyl-(methoxy-L-alaninyl) phosphorochloridate (403 mg, 1.45 mmol) in anhydrous THF (2.6 ml) was added dropwise to the stirring reaction mixture. The reaction was left to stir for 24 hours. After 24 hours the solvent was removed *in vacuo* and the desired product was isolated using flash chromatography (methanol – dichloromethane 0:100 v/v increasing to 10:90 v/v) giving the desired colourless oil compound as a mixture of 4 diastereoisomers (44%, 0.35 g).

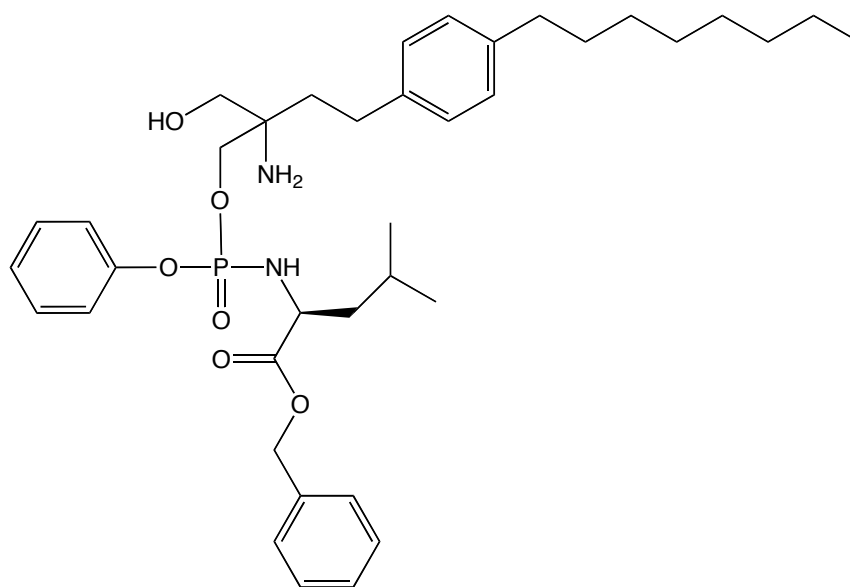
³¹P NMR (CDCl₃, 202 MHz): δ 3.60 (35%), 3.47 (15%), 3.14 (15%), 3.06 (35%). ¹H NMR (CDCl₃, 500 MHz): δ 7.29-7.02 (9H, m, ArH), 6.82 (2H, b, NH₂), 5.19 (1H, m, CHNH), 4.39 (3H, m, OCH₃), 4.18 (1H, m, CHCH₃), 3.81 (2H, m, POCH₂C), 3.61 (2H, m, HOCH₂C), 2.64 (2H, m, CH₂CH₂Ph), 2.54 (2H, m, CH₂CH₂Ph), 2.05 (2H, m, CCH₂CH₂), 1.61 (2H, m, CH₂CH₂CH₂), 1.42 (3H, m, CHCH₃), 1.33-1.27 (10H, m, CH₂CH₂CH₂), 0.91 (3H, m, CH₂CH₃). MS (ES⁺) *m/z* 549.3 (MH⁺).

Synthesis of Phenyl-(benzyloxy-L-alaninyl) phosphoramidate fingolimod (2)

C₃₅H₄₉N₂O₆P
MW: 624.3

tBuMgCl (1.45 ml, 1.45 mmol) was added dropwise to a solution of fingolimod hydrochloride (500 mg, 1.45 mmol) in anhydrous THF (7 ml) under anhydrous conditions. The mixture was stirred at room temperature for one hour. After one hour phenyl-(benzyloxy-L-alaninyl) phosphorochloridate (513 mg, 1.45 mmol) in anhydrous THF (1.5 ml) was added dropwise to the stirring reaction mixture. The reaction was left to stir for 24 hours. After 24 hours the solvent was removed *in vacuo* and the desired product was isolated using flash chromatography (methanol – dichloromethane 0:100 v/v increasing to 10:90 v/v) giving the desired colourless oil compound as a mixture of 4 diastereoisomers (22%, 0.2 g).

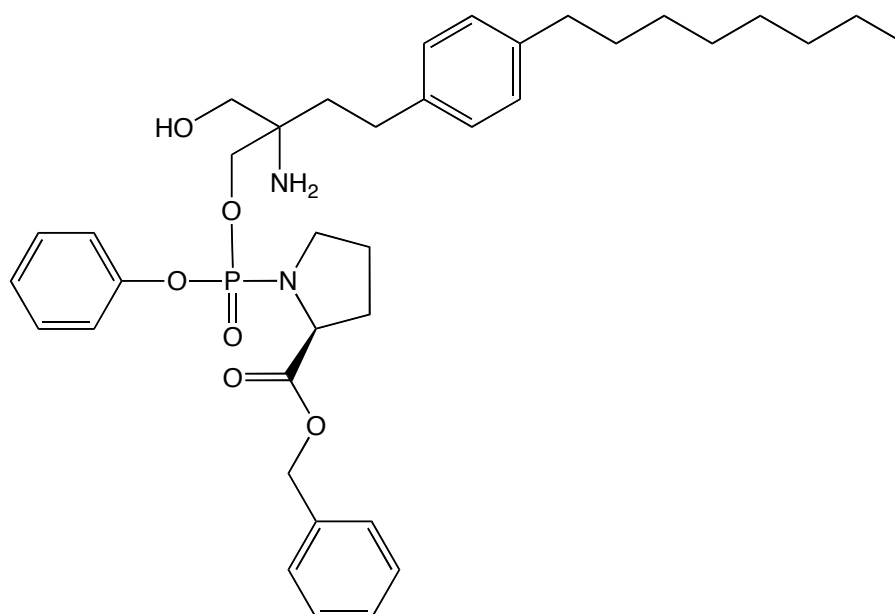
³¹P NMR (CDCl₃, 202 MHz): δ 3.58 (35%), 3.22 (30%), 3.11 (35%). ¹H NMR (CDCl₃, 500 MHz): δ 7.32-6.98 (14H, m, ArH), 6.72 (2H, b, NH₂), 5.23 (1H, m, CHNH), 5.06 (2H, m, OCH₂Ph), 4.38 (1H, m, CHCH₃), 4.08 (2H, m, POCH₂C), 3.78 (2H, m, HOCH₂C), 2.61 (2H, m, CH₂CH₂Ph), 2.54 (2H, m, CH₂CH₂Ph), 2.02 (2H, m, CCH₂CH₂), 1.58 (2H, m, CH₂CH₂CH₂), 1.39 (3H, m, CHCH₃), 1.32-1.30 (10H, m, CH₂CH₂CH₂), 0.92 (3H, m, CH₂CH₃). MS (ES⁺) *m/z* 625.3 (MH⁺).

Synthesis of Phenyl-(benzyloxy-L-leucinyl) phosphoramidate fingolimod (4)

C₃₈H₅₅N₂O₆P
MW: 666.4

tBuMgCl (1.45 ml, 1.45 mmol) was added dropwise to a solution of fingolimod hydrochloride (500 mg, 1.45 mmol) in anhydrous THF (5 ml) under anhydrous conditions. The mixture was stirred at room temperature for one hour. After one hour phenyl-(benzyloxy-L-leucinyl) phosphorochloridate (574 mg, 1.45 mmol) in anhydrous THF (3.2 ml) was added dropwise to the stirring reaction mixture. The reaction was left to stir for 24 hours. After 24 hours the solvent was removed *in vacuo* and the desired product was isolated using flash chromatography (methanol – dichloromethane 0:100 v/v increasing to 10:90 v/v) giving the desired colourless oil compound as a mixture of 4 diastereoisomers (23%, 0.22 g).

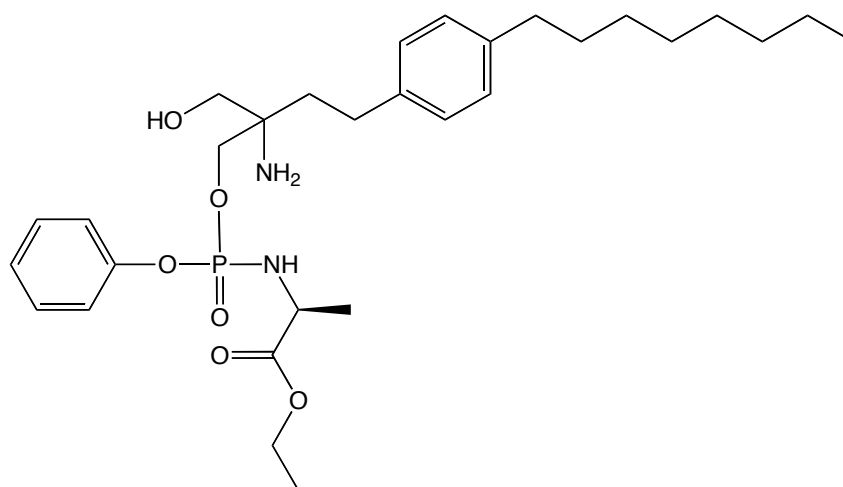
³¹P NMR (CDCl₃, 202 MHz): δ 4.66 (50%), 4.46 (30%), 4.20 (15%), 3.95 (5%). ¹H NMR (CDCl₃, 500 MHz): δ 7.26-6.74 (14H, m, ArH), 4.97 (2H, m, OCH₂Ph), 4.48 (1H, b, HOCH₂), 4.43 (1H, m, CHNH), 4.37 (2H, m, CNH₂), 4.07 (2H, m, POCH₂C), 3.92 (1H, m, CHCH₂), 3.57 (2H, m, HOCH₂C), 2.48 (2H, m, CH₂CH₂Ph), 2.45 (2H, m, CH₂CH₂Ph), 1.70 (2H, m, CCH₂CH₂), 1.48 (2H, m, CHCH₂CH), 1.43 (2H, m, CH(CH₃)₂), 1.41 (2H, m, CH₂CH₂CH₂), 1.22-1.19 (10H, m, CH₂CH₂CH₂), 0.80 (3H, m, CHCH₃), 0.73 (3H, m, CHCH₃), 0.70 (3H, m, CH₂CH₃). MS (ES⁺) *m/z* 667.4 (MH⁺).

Synthesis of Phenyl-(benzyloxy-L-prolinyl) phosphoramidate fingolimod (5)

$C_{37}H_{51}N_2O_6P$
MW: 650.4

tBuMgCl (1.45 ml, 1.45 mmol) was added dropwise to a solution of fingolimod hydrochloride (500 mg, 1.45 mmol) in anhydrous THF (5 ml) under anhydrous conditions. The mixture was stirred at room temperature for one hour. After one hour phenyl-(benzyloxy-L-prolinyl) phosphorochloridate (551 mg, 1.45 mmol) in anhydrous THF (4.5 ml) was added dropwise to the stirring reaction mixture. The reaction was left to stir for 24 hours. After 24 hours the solvent was removed *in vacuo* and the desired product was isolated using flash chromatography (methanol – dichloromethane 0:100 v/v increasing to 10:90 v/v) giving the desired colourless oil compound as a mixture of 4 diastereoisomers (20%, 0.19 g).

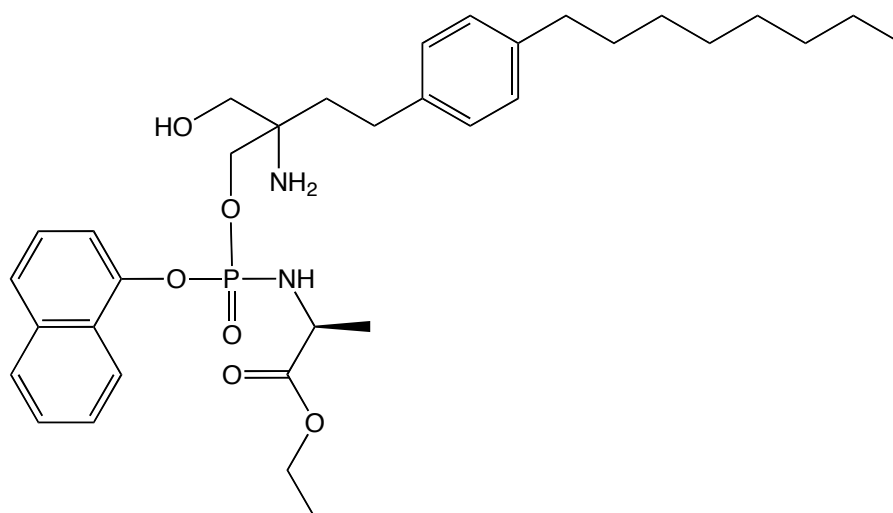
^{31}P NMR ($CDCl_3$, 202 MHz): δ 2.99 (92%), 2.94 (8%). 1H NMR ($CDCl_3$, 500 MHz): δ 7.32-6.98 (14H, m, ArH), 5.04 (2H, m, OCH_2Ph), 4.30 (1H, m, $CHNP$), 4.00 (2H, m, $POCH_2C$), 3.49 (2H, m, $HOCH_2C$), 3.30 (2H, m, CH_2NP), 2.52 (2H, m, CH_2CH_2Ph), 2.47 (2H, m, CH_2CH_2Ph), 1.92 (2H, m, CCH_2CH_2), 1.80 (2H, m, $CHCH_2CH_2$), 1.70 (2H, m, $CHCH_2CH_2$), 1.50 (2H, m, $CH_2CH_2CH_2$), 1.22-1.17 (10H, m, $CH_2CH_2CH_2$), 0.80 (3H, t, J = 7 Hz, CH_2CH_3). MS (ES+) m/z 651.4 (MH^+).

Synthesis of Phenyl-(ethoxy-L-alaninyl) phosphoramidate fingolimod (6)

C₃₀H₄₇N₂O₆P
MW: 562.3

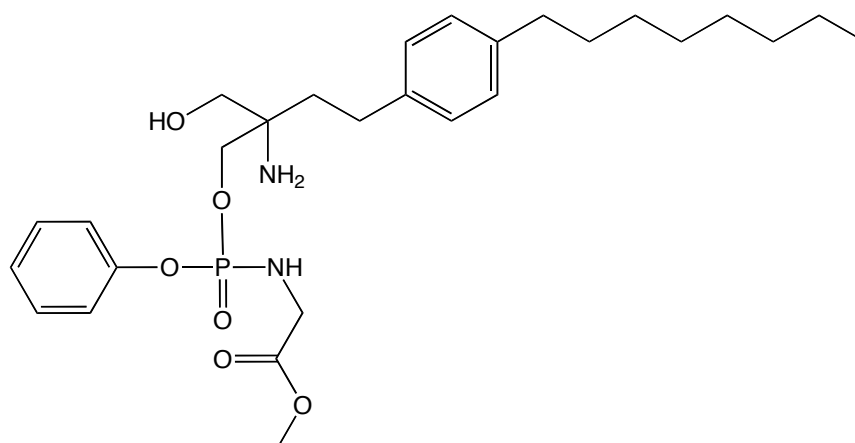
tBuMgCl (1.45 ml, 1.45 mmol) was added dropwise to a solution of fingolimod hydrochloride (500 mg, 1.45 mmol) in anhydrous THF (5 ml) under anhydrous conditions. The mixture was stirred at room temperature for one hour. After one hour phenyl-(ethoxy-L-alaninyl) phosphorochloridate (423 mg, 1.45 mmol) in anhydrous THF (2.8 ml) was added dropwise to the stirring reaction mixture. The reaction was left to stir for 24 hours. After 24 hours the solvent was removed *in vacuo* and the desired product was isolated using flash chromatography (methanol – dichloromethane 0:100 v/v increasing to 10:90 v/v) giving the desired colourless oil compound as a mixture of 4 diastereoisomers (20%, 0.16 g).

³¹P NMR (CDCl₃, 202 MHz): δ 4.05 (75%), 3.84 (8%), 3.73 (3%), 3.59 (14%). ¹H NMR (CDCl₃, 500 MHz): δ 7.36-7.06 (9H, m, ArH), 4.19 (2H, m, OCH₂CH₃), 4.06 (2H, m, POCH₂C), 4.01 (1H, m, CHCH₃), 3.47 (2H, m, HOCH₂C), 2.72 (1H, m, CHNH), 2.63 (2H, b, CH₂CH₂Ph), 2.58 (2H, m, CH₂CH₂Ph), 1.70 (2H, m, CCH₂CH₂), 1.61 (2H, m, CH₂CH₂CH₂), 1.42 (3H, m, CHCH₃), 1.33 (3H, m, CH₂CH₃), 1.30-1.22 (10H, m, CH₂CH₂CH₂), 0.98 (3H, t, *J* = 7 Hz, CH₂CH₃). MS (ES⁺) *m/z* 563.3 (MH⁺).

Synthesis of Naphthyl-(ethoxy-L-alaninyl) phosphoramidate fingolimod (7)

tBuMgCl (1.45 ml, 1.45 mmol) was added dropwise to a solution of fingolimod hydrochloride (500 mg, 1.45 mmol) in anhydrous THF (5 ml) under anhydrous conditions. The mixture was stirred at room temperature for one hour. After one hour naphthyl-(ethoxy-L-alaninyl) phosphorochloridate (496 mg, 1.45 mmol) in anhydrous THF (2.2 ml) was added dropwise to the stirring reaction mixture. The reaction was left to stir for 24 hours. After 24 hours the solvent was removed *in vacuo* and the desired product was isolated using flash chromatography (methanol – dichloromethane 0:100 v/v increasing to 10:90 v/v) giving the desired colourless oil compound as a mixture of 4 diastereoisomers (22.5%, 0.2 g).

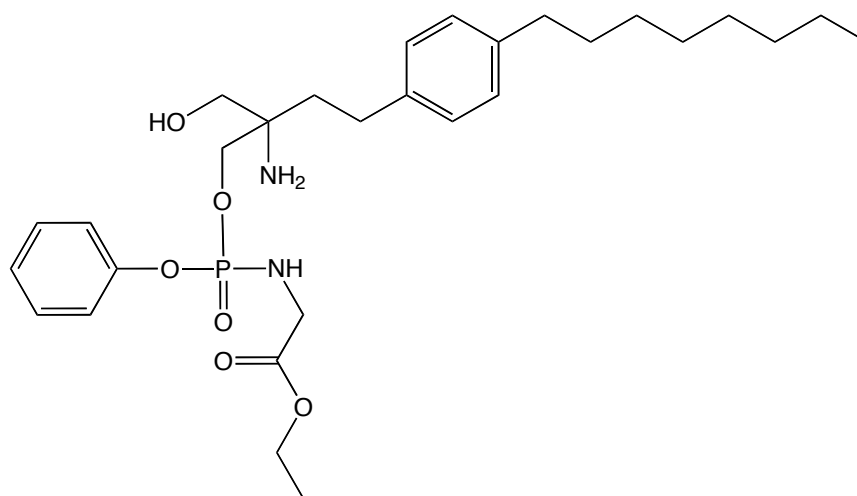
³¹P NMR (CDCl₃, 202 MHz): δ 4.90 (35%), 4.70 (35%), 4.42 (28%), 3.55 (2%). ¹H NMR (CDCl₃, 500 MHz): δ 8.25-6.82 (11H, m, ArH), 4.59 (1H, m, CHNP), 4.07 (2H, m, POCH₂C), 4.04 (2H, m, OCH₂CH₃), 3.78 (2H, b, NH₂), 3.66 (2H, m, HOCH₂C), 3.34 (1H, m, CHCH₃), 2.53 (2H, m, CH₂CH₂Ph), 2.46 (2H, m, CH₂CH₂Ph), 1.61 (2H, m, CCH₂CH₂), 1.54 (2H, m, CH₂CH₂CH₂), 1.41 (3H, m, CHCH₃), 1.33 (3H, m, CH₂CH₃), 1.33-1.09 (10H, m, CH₂CH₂CH₂), 0.88 (3H, m, CH₂CH₃). MS (ES⁺) *m/z* 613.3 (MH⁺).

Synthesis of Phenyl-(methoxy-glyciny) phosphoramidate fingolimod (8)

C₂₈H₄₃N₂O₆P
MW: 534.3

tBuMgCl (1.76 ml, 1.76 mmol) was added dropwise to a solution of fingolimod hydrochloride (607 mg, 1.76 mmol) in anhydrous THF (10 ml) under anhydrous conditions. The mixture was stirred at room temperature for one hour. After one hour phenyl-(methoxy-glyciny) phosphorochloridate (516 mg, 1.76 mmol) in anhydrous THF (7 ml) was added dropwise to the stirring reaction mixture. The reaction was left to stir for 24 hours. After 24 hours the solvent was removed *in vacuo* and the desired product was isolated using flash chromatography (methanol – dichloromethane 0:100 v/v increasing to 10:90 v/v) giving the desired colourless oil compound as a mixture of 4 diastereoisomers (33%, 0.308 g).

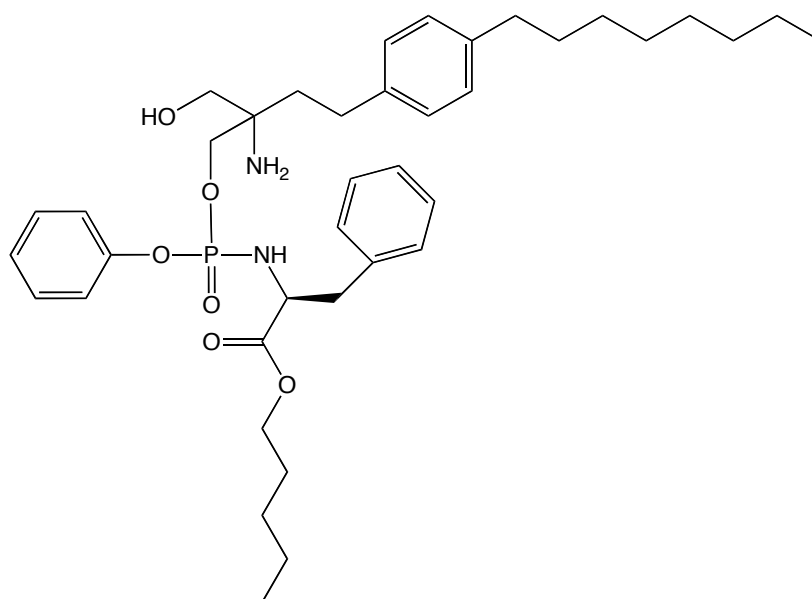
³¹P NMR (CDCl₃, 202 MHz): δ 4.50. ¹H NMR (CDCl₃, 500 MHz): δ 7.20-6.91 (9H, m, ArH), 5.51 (2H, b, NH₂), 5.29 (1H, m, CHNH), 4.16 (1H, m, HOCH₂C), 3.76 (2H, m, POCH₂C), 3.70 (2H, m, HOCH₂C), 3.50 (2H, m, CH₂NH), 3.29 (3H, s, OCH₃), 2.52 (2H, m, CH₂CH₂Ph), 2.43 (2H, m, CH₂CH₂Ph), 1.90 (2H, m, CCH₂CH₂), 1.46 (2H, m, CH₂CH₂CH₂), 1.25-1.15 (10H, m, CH₂CH₂CH₂), 0.79 (3H, t, *J* = 6.5 Hz, CH₂CH₃). MS (ES+) *m/z* 535.3 (MH⁺).



tBuMgCl (1.45 ml, 1.45 mmol) was added dropwise to a solution of fingolimod hydrochloride (500 mg, 1.45 mmol) in anhydrous THF (20 ml) under anhydrous conditions. The mixture was stirred at room temperature for one hour. After one hour phenyl-(ethoxy-glyciny) phosphorochloridate (403 mg, 1.45 mmol) in anhydrous THF (4 ml) was added dropwise to the stirring reaction mixture. The reaction was left to stir for 24 hours. After 24 hours the solvent was removed *in vacuo* and the desired product was isolated using flash chromatography (methanol – dichloromethane 0:100 v/v increasing to 10:90 v/v) giving the desired colourless oil compound as a mixture of 4 diastereoisomers (39%, 0.313 g).

³¹P NMR (CDCl₃, 202 MHz): δ 4.48. ¹H NMR (CDCl₃, 500 MHz): δ 8.37 (2H, b, CNH₂), 7.17-6.89 (9H, m, ArH), 5.29 (1H, m, CHNH), 4.48 (0.5H, m, HOCH₂C), 4.34 (0.5H, m, HOCH₂C), 4.16 (2H, m, POCH₂C), 3.93 (2H, m, CH₃CH₂O), 3.79 (2H, m, CH₂NH), 3.68 (2H, m, HOCH₂C), 2.50 (2H, m, CH₂CH₂Ph), 2.43 (2H, m, CH₂CH₂Ph), 1.94 (2H, m, CCH₂CH₂), 1.46 (2H, m, CH₂CH₂CH₂), 1.21-1.18 (10H, m, CH₂CH₂CH₂), 1.03 (3H, m, CH₂CH₃), 0.80 (3H, t, *J* = 7 Hz, CH₂CH₃). MS (ES+) *m/z* 549.3 (MH⁺).

Synthesis of Phenyl-(pentoxo-L-phenylalanyl) phosphoramidate fingolimod (10)

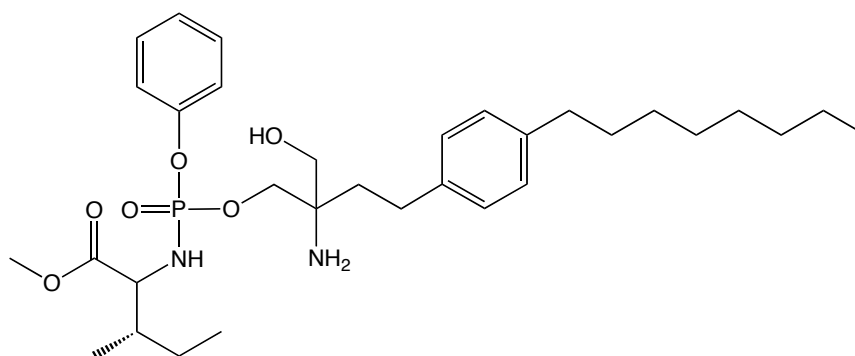


C₃₉H₅₇N₂O₆P
MW: 680.4

tBuMgCl (1.45 ml, 1.45 mmol) was added dropwise to a solution of fingolimod hydrochloride (500 mg, 1.45 mmol) in anhydrous THF (20 ml) under anhydrous conditions. The mixture was stirred at room temperature for one hour. After one hour phenyl-(pentoxo-L-phenylalanyl) phosphorochloridate (593 mg, 1.45 mmol) in anhydrous THF (5 ml) was added dropwise to the stirring reaction mixture. The reaction was left to stir for 24 hours. After 24 hours the solvent was removed *in vacuo* and the desired product was isolated using flash chromatography (methanol – dichloromethane 0:100 v/v increasing to 10:90 v/v) giving the desired colourless oil compound as a mixture of 4 diastereoisomers (10%, 0.102 g).

³¹P NMR (CDCl₃, 202 MHz): δ 4.17, 4.11, 3.95. ¹H NMR (CDCl₃, 500 MHz): δ 7.19-6.94 (14H, m, ArH), 4.11 (2H, m, POCH₂C), 3.94 (2H, m, OCH₂CH₂), 3.75 (2H, m, HOCH₂C), 3.49 (1H, m, CHNH), 3.34 (1H, m, CHNH), 2.92 (1H, m, CH₂OH), 2.75 (2H, m, CHCH₂Ph), 2.47 (2H, m, CH₂CH₂Ph), 2.44 (2H, m, CH₂CH₂Ph), 1.52 (2H, m, OCH₂CH₂), 1.49 (2H, m, CCH₂CH₂), 1.47 (2H, m, CH₂CH₂CH₂), 1.22-1.15 (14H, m, CH₂CH₂CH₂), 0.80 (3H, m, CH₂CH₃), 0.79 (3H, m, CH₂CH₃). MS (ES⁺) *m/z* 681.4 (MH⁺).

Synthesis of Phenyl-(methoxy-L-isoleuciny) phosphoramidate fingolimod (11)



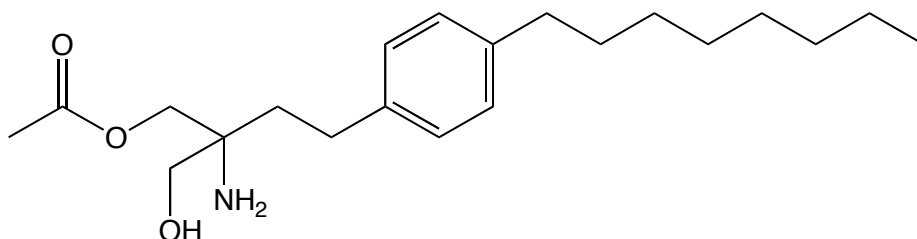
C₃₂H₅₁N₂O₆P
MW: 590.4

tBuMgCl (1.45 ml, 1.45 mmol) was added dropwise to a solution of fingolimod hydrochloride (500 mg, 1.45 mmol) in anhydrous THF (20 ml) under anhydrous conditions. The mixture was stirred at room temperature for one hour. After one hour phenyl-(methoxy-L-isoleuciny) phosphorochloridate (464 mg, 1.45 mmol) in anhydrous THF (4 ml) was added dropwise to the stirring reaction mixture. The reaction was left to stir for 24 hours. After 24 hours the solvent was removed *in vacuo* and the desired product was isolated using flash chromatography (methanol – dichloromethane 0:100 v/v increasing to 10:90 v/v) giving the desired colourless oil compound as a mixture of 4 diastereoisomers (38%, 0.322 g).

³¹P NMR (CDCl₃, 202 MHz): δ 4.30 (35%), 4.25 (15%), 3.65 (20%), 3.60 (30%). ¹H NMR (CDCl₃, 500 MHz): δ 8.34 (2H, b, CNH₂), 7.19-6.86 (9H, m, ArH), 5.08 (2H, m, POCH₂C), 4.32 (2H, m, HOCH₂C), 3.79 (1H, m, CH₂OH), 3.68 (1H, m, CHNH), 3.62 (1H, m, CHNH), 3.48 (3H, m, OCH₃), 2.54 (2H, m, CH₂CH₂Ph), 2.43 (2H, m, CH₂CH₂Ph), 1.91 (2H, m, CCH₂CH₂), 1.68 (1H, m, CHCHCH₃), 1.47 (2H, m, CH₂CH₂CH₂), 1.31 (1H, m, CHCH₂CH₃), 1.25-1.16 (10H, m, CH₂CH₂CH₂), 1.06 (1H, m, CHCH₂CH₃), 0.88 (3H, m, CHCH₃), 0.73 (3H, m, CH₂CH₃), 0.68 (3H, m, CH₂CH₃).

9.6 Chiral Phosphoramidate Fingolimod Synthesis and Intermediates

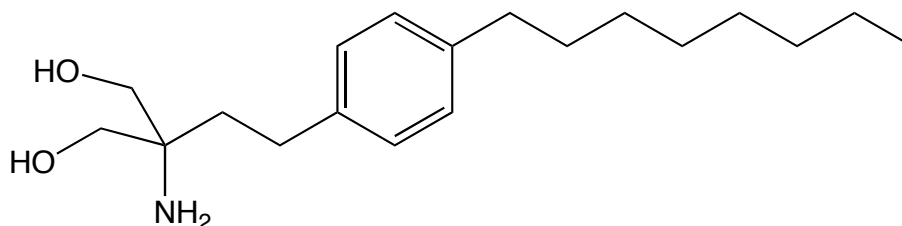
Synthesis of 2-amino-2-(hydroxymethyl)-4-(4-octylphenyl)butyl acetate



C₂₁H₃₅NO₃
MW: 349.26

A mixture of fingolimod HCl (500 ml, 1.454 mmol) and acetic anhydride (0.165 ml, 1.744 mmol) in CHCl₃ (40 ml) and saturated NaHCO₃ (25 ml) was stirred at room temperature for 3 h. After 3 h the mixture was extracted with brine and CHCl₃. The organic layer was dried over MgSO₄, vacuum filtered and the remaining solvent was removed *in vacuo* yielding a white residue (49%, 0.24 g).

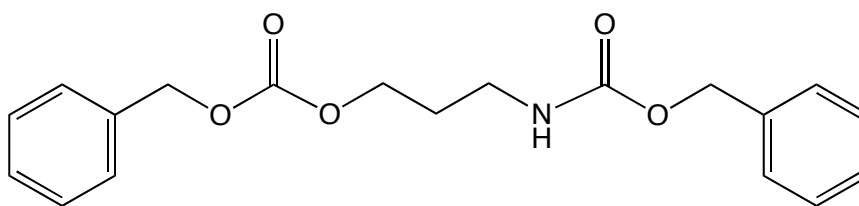
¹H NMR (CDCl₃, 500 MHz): δ 7.03 (4H, s, ArH), 6.18 (1H, s, OH), 4.43 (2H, b, NH₂), 3.71 (2H, d, *J* = 10.5 Hz, HOCH₂), 3.51 (2H, d, *J* = 10.5 Hz, HOCH₂), 2.55 (2H, m, CH₂CH₂Ph), 2.49 (2H, m, CH₂CH₂Ph), 1.86 (3H, s, COCH₃), 1.85 (2H, m, CCH₂CH₂), 1.51 (2H, quin, *J* = 7.5 Hz, CH₂CH₂CH₂), 1.25-1.16 (10H, m, CH₂CH₂CH₂), 0.81 (3H, t, *J* = 7 Hz, CH₂CH₃). MS (ES⁺) *m/z* 350.3 (MH⁺).

Synthesis of Freebase Fingolimod from Fingolimod HCl

$C_{19}H_{33}NO_2$
MW: 307.3

KOH solution (226 mg in 25 ml H_2O) was added to fingolimod HCl (500 mg, 1.45 mmol) in DCM (25 ml). The mixture was thoroughly stirred for 24 h. After 24 h the mixture was extracted with additional water and DCM. The organic layer was collected and solvent removed *in vacuo* yielding freebase fingolimod (100%, 0.46 g).

1H NMR ($CDCl_3$, 500 MHz): δ 7.03 (4H, s, ArH), 3.54 (2H, d, J = 11 Hz, $HOCH_2$), 3.44 (2H, d, J = 11 Hz, $HOCH_2$), 2.55 (2H, m, CH_2CH_2Ph), 2.49 (2H, t, J = 7.5 Hz, CH_2CH_2Ph), 1.87 (2H, b, NH_2), 1.62 (2H, m, CCH_2CH_2), 1.51 (2H, quin, J = 8 Hz, $CH_2CH_2CH_2$), 1.25-1.16 (10H, m, $CH_2CH_2CH_2$), 0.81 (3H, t, J = 7 Hz, CH_2CH_3).

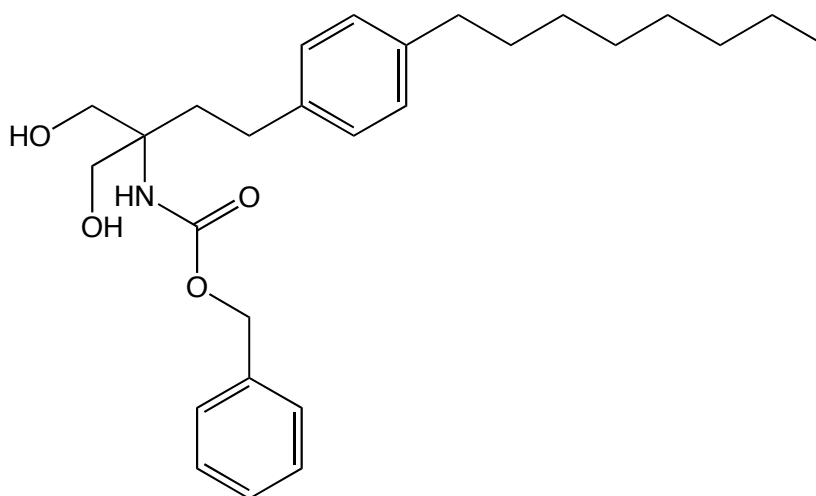
Synthesis of benzyl (3-(((benzyloxy)carbonyl)oxy)propyl)carbamate

$C_{19}H_{21}NO_5$
MW: 343.14

To 3-amino-1-propanol (0.11 ml) in $CHCl_3$ (65 ml) was added benzyl chloroformate (0.75 ml). After mixing thoroughly saturated $NaHCO_3$ solution (35 ml) was added and the mixture was left to stir at ambient temperature for 24 h. After 24 h the mixture was extracted with brine and $CHCl_3$. The organic layer was dried over $MgSO_4$, vacuum filtered and the solvent was removed *in vacuo* yielding a mixture of N, O and N & O bound product.

MS (ES+) m/z 344.2 (MH^+) and 366.2 (MNa^+).

Synthesis of benzyl (1-hydroxy-2-(hydroxymethyl)-4-(4-octylphenyl) butan-2-yl) carbamate

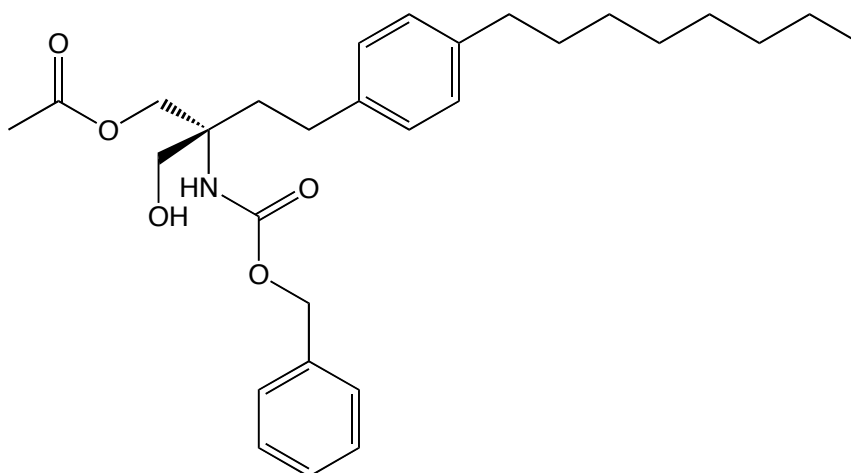


$C_{27}H_{39}NO_4$
MW: 441.3

A mixture of freebase fingolimod (470 mg, 1.53 mmol) and benzyl chloroformate (0.22 ml, 1.53 mmol) in $CHCl_3$ (67 ml) and saturated $NaHCO_3$ (40 ml) was stirred at room temperature for 24 h. The organic layer was separated, washed with brine and dried over $MgSO_4$. The desired product was isolated using flash chromatography (methanol – dichloromethane 5:95 v/v) giving the desired compound (95%, 0.638 g).

1H NMR ($CDCl_3$, 500 MHz): δ 7.39 (5H, m, ArH), 7.12 (4H, s, ArH), 5.44 (1H, s, CNH), 5.12 (2H, s, OCH_2Ph), 3.92 (2H, d, J = 10.5 Hz, $HOCH_2$), 3.75 (2H, d, J = 11.5 Hz, $HOCH_2$), 3.62 (2H, b, $HOCH_2$), 2.61 (2H, m, CH_2CH_2Ph), 2.58 (2H, m, CH_2CH_2Ph), 2.93 (2H, m, CCH_2CH_2), 1.62 (2H, quin, J = 7.5 Hz, $CH_2CH_2CH_2$), 1.46-1.39 (10H, m, $CH_2CH_2CH_2$), 0.93 (3H, t, J = 7 Hz, CH_2CH_3). MS (ES+) m/z 442.3 (MH^+) and 464.3 (MNa^+).

Synthesis of (R)-2-(((benzyloxy)carbonyl) amino)-2-(hydroxymethyl)-4-(4-octylphenyl) butyl acetate

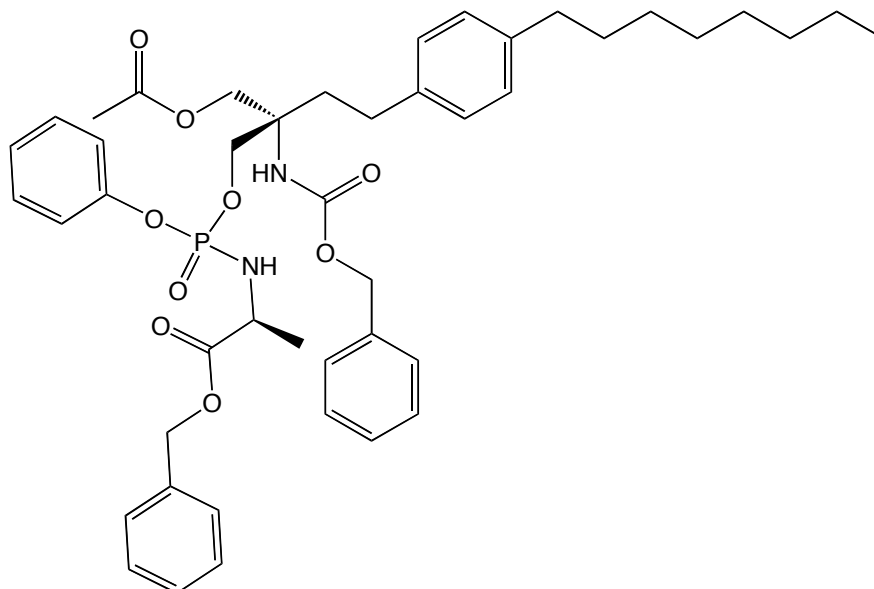


C₂₉H₄₁NO₅
MW: 483.3

To benzyl (1-hydroxy-2-(hydroxymethyl)-4-(4-octylphenyl)butan-2-yl)carbamate (638 mg, 1.45 mmol) in anhydrous THF (36 ml) was added vinyl acetate (1.34 ml, 14.5 mmol) and Immobilized Lipase (640 mg) and then stirred at 25 °C for 24 h. After 24 h the mixture was vacuum filtered to remove the enzyme and the desired product was isolated by removing the solvent *in vacuo* giving the desired oil product (78%, 0.561 g).

¹H NMR (CDCl₃, 500 MHz): δ 7.25 (5H, m, ArH), 6.98 (4H, m, ArH), 5.14 (1H, s, CNH), 4.98 (2H, s, PhCH₂), 4.24 (1H, d, *J* = 11.5 Hz, CO₂CH₂C), 4.10 (1H, d, *J* = 11.5 Hz, CO₂CH₂C), 3.65 (2H, m, HOCH₂C), 3.61 (1H, s, HOCH₂C), 2.46 (2H, m, CH₂CH₂Ph), 2.45 (2H, m, CH₂CH₂Ph), 2.02 (2H, m, CCH₂CH₂), 1.96 (3H, s, CH₃CO₂), 1.49 (2H, quin, *J* = 7.5 Hz, CH₂CH₂CH₂), 1.21-1.18 (10H, m, CH₂CH₂CH₂), 0.80 (3H, t, *J* = 6.5 Hz, CH₂CH₃). MS (ES⁺) *m/z* 484.3 (MH⁺) and 506.3 (MNa⁺).

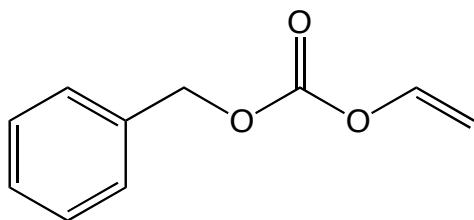
Synthesis of (2*S*)-benzyl 2-((((*S*)-2-(acetoxymethyl)- 2-(((benzyloxy) carbonyl) amino)-4-(4-octylphenyl) butoxy) (phenoxy) phosphoryl) amino) propanoate



C₄₅H₅₇N₂O₉P
MW: 800.38

tBuMgCl (1.13 ml, 1.13 mmol) was added dropwise to a solution of (*R*)-2-(((benzyloxy)carbonyl) amino)-2-(hydroxymethyl)-4-(4-octylphenyl) butyl acetate (544 mg, 1.13 mmol) in anhydrous THF (10 ml) under anhydrous conditions. The mixture was stirred at room temperature for one hour. After one hour phenyl-(benzyloxy-L-alaninyl) phosphorochloridate (399 mg, 1.13 mmol) in anhydrous THF (6 ml) was added dropwise to the stirring reaction mixture. The reaction was left to stir for 24 hours. After 24 hours the solvent was removed *in vacuo* and the desired product was isolated using flash chromatography (hexane – AcOEt 70:30 v/v increasing to 60:40 v/v) giving the desired oil product (77%, 0.699 g).

³¹P NMR (CDCl₃, 202 MHz): δ 2.76, 2.70, 2.57, 2.50. ¹H NMR (CDCl₃, 500 MHz): δ 7.23-6.88 (19H, m, ArH), 5.36 (1H, m, PNH), 5.00 (2H, m, PhCH₂O), 4.95 (2H, m, PhCH₂O), 4.17 (2H, m, POCH₂C), 4.07 (1H, m, CNH), 3.99 (2H, m, CO₂CH₂C), 3.90 (1H, m, CHCH₃), 2.46 (2H, m, CH₂CH₂Ph), 2.43 (2H, m, CH₂CH₂Ph), 1.90 (3H, m, CO₂CH₃), 1.88 (2H, m, CCH₂CH₂), 1.48 (2H, quin, *J* = 7 Hz, CH₂CH₂CH₂), 1.26 (3H, d, *J* = 6.5 Hz, CHCH₃), 1.20-1.14 (10H, m, CH₂CH₂CH₂), 0.78 (3H, t, *J* = 6.5 Hz, CH₂CH₃). MS (ES⁺) *m/z* 801.4 (MH⁺) and 823.4 (MNa⁺).

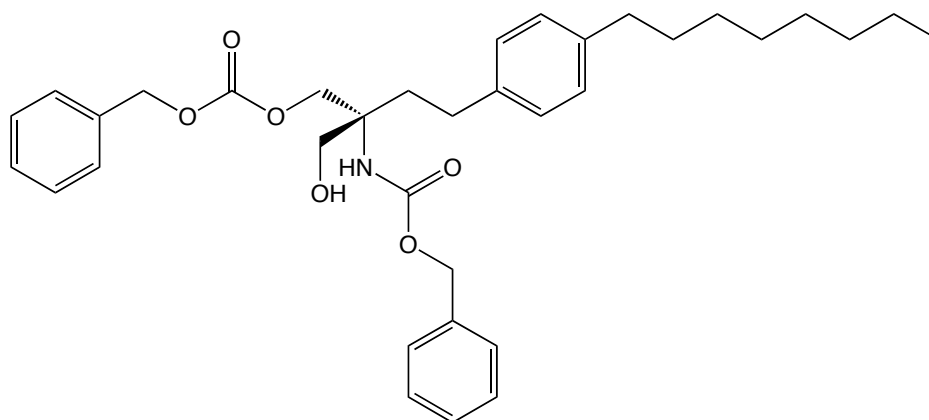
Synthesis of benzyl vinyl carbonate

C₁₀H₁₀O₃
MW: 178.1

To a solution of benzyl alcohol (3.62 ml, 35 mmol) in pyridine (4 ml) was added vinyl chloroformate (4.57 ml, 50 mmol) slowly under argon at 0 °C. After stirring for 40 min the solution was acidified with HCl (100 ml, 3 M) and extracted with DCM. The organic layer was collected and dried over MgSO₄ and the solvent was removed *in vacuo*. The desired product was isolated using flash chromatography (ethyl acetate – hexane 5:95 v/v) giving the desired oil product (81%, 5.06 g).

¹H NMR (CDCl₃, 500 MHz): δ 7.33-7.25 (5H, m, ArH), 7.02 (1H, dd, *J* = 6.5 Hz, OCHCH₂), 5.13 (2H, s, PhCH₂O), 4.84 (1H, dd, *J* = 2 Hz, OCHCH₂), 4.50 (1H, dd, *J* = 2 Hz, OCHCH₂).

Synthesis of (*R*)-benzyl (1-(((benzyloxy)carbonyl)oxy)-2-(hydroxymethyl)-4-(4-octylphenyl) butan-2-yl) carbamate

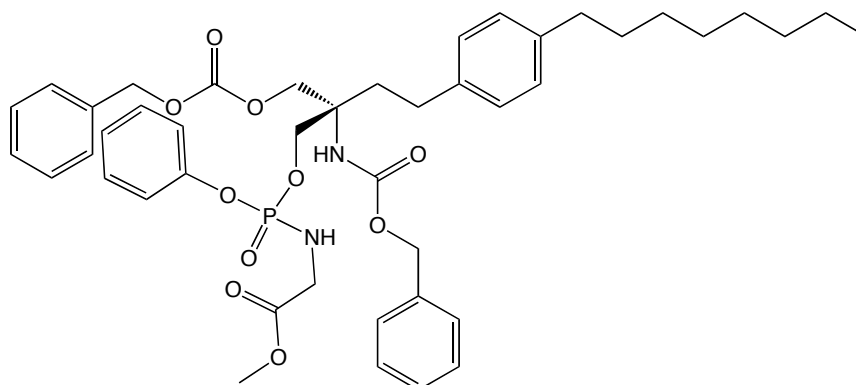


C₃₅H₄₅NO₆
MW: 575.3

To benzyl (1-hydroxy-2-(hydroxymethyl)-4-(4-octylphenyl)butan-2-yl)carbamate (834 mg, 1.89 mmol) in diisopropyl ether (50 ml) was added benzyl vinyl carbonate (3.413 g, 18.9 mmol) and Immobilized Lipase (1.447 g) and then stirred at 40 °C for 24 h. After 24 h the mixture was vacuum filtered to remove the enzyme and the desired product was isolated using flash chromatography (ethyl acetate – hexane 50:50 v/v) giving the desired compound (54%, 0.583 g).

¹H NMR (CDCl₃, 500 MHz): δ 7.24 (10H, m, ArH), 6.96 (5H, m, ArH), 5.23 (1H, s, CNH), 5.04 (2H, s, OCH₂Ph), 4.97 (2H, s, OCH₂Ph), 4.32 (1H, m, COCH₂), 4.24 (1H, m, COCH₂), 3.68 (1H, m, HOCH₂), 3.63 (2H, m, HOCH₂), 2.47 (2H, m, CH₂CH₂Ph), 2.44 (2H, m, CH₂CH₂Ph), 2.01 (1H, m, CCH₂CH₂), 1.80 (1H, m, CCH₂CH₂), 1.46 (2H, quin, *J* = 7 Hz, CH₂CH₂CH₂), 1.26-1.17 (10H, m, CH₂CH₂CH₂), 0.77 (3H, t, *J* = 7 Hz, CH₂CH₃).
¹³C NMR (CDCl₃, 125 MHz): δ 155.91 (C=O), 155.28 (C=O), 140.66 (C-Ar), 138.66 (C-Ar), 136.36 (C-Ar), 135.05 (C-Ar), 129.03 (CH-Ar), 128.85 (CH-Ar), 128.77 (CH-Ar), 128.74 (CH-Ar), 128.65 (CH-Ar), 128.56 (CH-Ar), 128.54 (CH-Ar), 128.30 (CH-Ar), 128.23 (CH-Ar), 127.58 (CH-Ar), 127.05 (CH-Ar), 70.23 (PhCH₂O), 68.60 (PhCH₂O), 66.92 (CCH₂OH), 65.20 (CCH₂O), 58.86 (NHC), 35.68 (PhCH₂), 34.47 (CH₂CH₂CH₂), 32.04 (CH₂CH₂CH₂), 31.71 (PhCH₂), 29.63 (CH₂CH₂CH₂), 29.49 (CH₂CH₂CH₂), 29.41 (CCH₂CH₂), 29.11 (CH₂CH₂CH₂), 21.08 (CH₂CH₂CH₂), 14.28 (CH₂CH₂CH₃). MS (ES⁺) *m/z* 576.3 (MH⁺). [α]_D²⁴ = -1.2 (*c* = 3.3, CHCl₃).

Synthesis of methyl 2-((((S)-2-(((benzyloxy) carbonyl) amino)-2-(((benzyloxy) carbonyl) oxy) methyl)-4-(4-octylphenyl) butoxy)(phenoxy) phosphoryl) amino) acetate

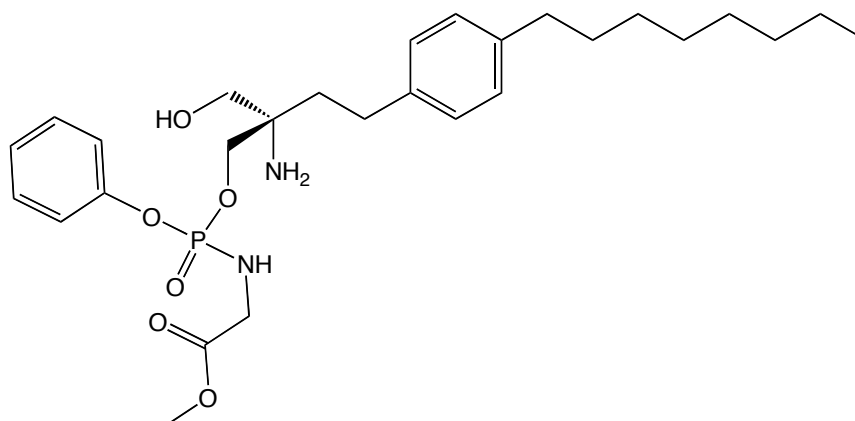


C₄₄H₅₅N₂O₁₀P
MW: 802.4

tBuMgCl (1.01 ml, 1.01 mmol) was added dropwise to a solution of (*R*)-benzyl (1-(((benzyloxy)carbonyl)oxy)-2-(hydroxymethyl)-4-(4-octylphenyl) butan-2-yl) carbamate (583 mg, 1.01 mmol) in anhydrous THF (40 ml) under anhydrous conditions. The mixture was stirred at room temperature for one hour. After one hour phenyl-(methoxy-glyciny) phosphorochloridate (296 mg, 1.01 mmol) in anhydrous THF (6 ml) was added dropwise to the stirring reaction mixture. The reaction was left to stir for 24 hours. After 24 hours the solvent was removed *in vacuo* and the desired product was isolated using flash chromatography (ethyl acetate – hexane 30:70 v/v increasing to 70:30 v/v) giving the desired oil product (23%, 0.176 g).

³¹P NMR (CDCl₃, 202 MHz): δ 3.69 (30%), 3.56 (70%). ¹H NMR (CDCl₃, 500 MHz): δ 7.29-6.87 (19H, m, ArH), 5.44 (1H, s, CNH), 5.01 (2H, s, OCH₂Ph), 4.95 (2H, s, OCH₂Ph), 4.30 (2H, m, POCH₂), 4.20 (2H, m, COCH₂), 3.83 (1H, m, CNH), 3.61 (2H, m, CH₂NH), 3.52 (3H, s, OCH₃), 2.44 (2H, m, CH₂CH₂Ph), 2.43 (2H, m, CH₂CH₂Ph), 2.03 (1H, m, CCH₂CH₂), 1.90 (1H, m, CCH₂CH₂), 1.48 (2H, quin, *J* = 7 Hz, CH₂CH₂CH₂), 1.25-1.13 (10H, m, CH₂CH₂CH₂), 0.79 (3H, t, *J* = 7 Hz, CH₂CH₃). MS (ES+) *m/z* 803.3 (MH⁺) and 825.3 (MNa⁺).

Synthesis of Phenyl-(methoxy-glyciny) phosphoramidate fingolimod



C₂₈H₄₃N₂O₆P
MW: 534.3

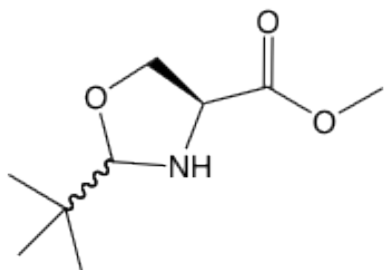
A mixture of methyl 2-((((*S*)-2-(((benzyloxy)carbonyl) amino)-2-((((benzyloxy)carbonyl) oxy)methyl)-4-(4-octylphenyl)butoxy)(phenoxy)phosphoryl)amino) acetate (176 mg, 0.22 mmol) and 10% Pd/C (0.5 g) in anhydrous MeOH (20 ml) was stirred under hydrogen atmosphere for 24 h. After 24 h the mixture was vacuum filtered to remove the catalyst and the desired product was isolated using flash chromatography (methanol– ethyl acetate 0:100 v/v increasing to 10:90 v/v) giving the desired oil product (59%, 0.077 g).

³¹P NMR (CDCl₃, 202 MHz): δ 4.50. ¹H NMR (CDCl₃, 500 MHz): δ 7.20-6.91 (9H, m, ArH), 5.51 (2H, b, NH₂), 5.29 (1H, m, CHNH), 4.16 (1H, m, HOCH₂C), 3.76 (2H, m, POCH₂C), 3.70 (2H, m, HOCH₂C), 3.50 (2H, m, CH₂NH), 3.29 (3H, s, OCH₃), 2.52 (2H, m, CH₂CH₂Ph), 2.43 (2H, m, CH₂CH₂Ph), 1.90 (2H, m, CCH₂CH₂), 1.46 (2H, m, CH₂CH₂CH₂), 1.25-1.15 (10H, m, CH₂CH₂CH₂), 0.79 (3H, t, *J* = 6.5 Hz, CH₂CH₃). * MS (ES+) *m/z* 535.3 (MH⁺) and 441.2 (CyclisedH⁺).

* Not easy to obtain pure chiral compound due to rapid cyclisation. Would need to re-purify possibly using preparative HPLC. Was deemed unnecessary as rapid cyclisation results in chiral synthesis being of little value.

9.7 Syntheses of BED Compounds

Synthesis of (4S)-methyl 2-(*tert*-butyl)oxazolidine-4-carboxylate

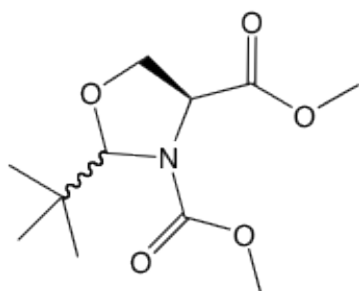


C₉H₁₇NO₃
MW: 187.21

Trimethyl acetaldehyde (6.98 ml, 64.28 mmol) was added to a mixture of TEA (17.92 ml, 128.56 mmol) and L-serine methyl ester hydrochloride (10 g, 64.28 mmol) in toluene (250 ml). The reaction mixture was attached to a Dean Stark trap and stirred at 150 °C for 24 h. After 24 h the mixture was vacuum filtered and washed with Et₂O. The solvent was removed *in vacuo* giving the desired dark brown oil product (83%, 9.951 g).

¹H NMR (CDCl₃, 500 MHz): δ 4.27 (0.5H, s, OCHC), 4.05 (0.5H, m, OCH₂), 4.02 (0.5H, s, OCHC), 3.89 (0.5H, m, OCH₂), 3.85 (1H, m, OCH₂), 3.70 (1.5H, s, OCH₃), 3.68 (1.5H, s, OCH₃), 3.65 (1H, m, NHCH), 2.52 (1H, b, NH), 0.93 (5H, s, CCH₃), 0.85 (4H, s, CCH₃). ¹³C NMR (CDCl₃, 125 MHz): δ 173.10 (C=O), 172.87 (C=O), 99.95 (NHCH), 99.23 (NHCH), 68.97 (CHCH₂O), 68.30 (CHCH₂O), 59.60 (NHCH), 59.40 (NHCH), 52.51 (OCH₃), 52.36 (OCH₃), 34.57 (C(CH₃)₃), 33.19 (C(CH₃)₃), 25.24 (C(CH₃)₃), 24.89 (C(CH₃)₃).

Synthesis of (4S)-dimethyl 2-(tert-butyl)oxazolidine-3,4-dicarboxylate

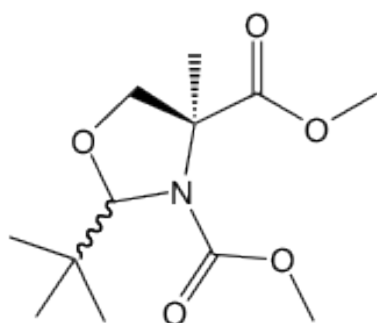


C₁₁H₁₉NO₅
MW: 245.13

Triethylamine (13.35 ml, 95.78 mmol) was added slowly to a mixture of methyl chloroformate (7.4 ml, 95.78 mmol) and (4S)-methyl 2-(tert-butyl)oxazolidine-4-carboxylate (8.961 g, 47.89 mmol) in toluene (200 ml). The reaction mixture was attached to a Dean Stark trap and stirred at 150 °C for 24 h. After 24 h the mixture extracted with 1M HCl and AcOEt and washed with brine. The organic layer was dried over MgSO₄ and vacuum filtered. The solvent was removed *in vacuo* giving the desired dark brown oil product (77%, 9.025 g).

¹H NMR (CDCl₃, 500 MHz): δ 5.01 (1H, s, OCH), 4.68 (1H, m, CHCH₂O), 4.29 (1H, m, CHCH₂O), 4.02 (1H, t, *J* = 8 Hz, CH₂CHCO), 3.70 (3H, s, OCH₃), 3.68 (3H, s, OCH₃), 0.86 (9H, s, CCH₃). ¹³C NMR (CDCl₃, 125 MHz): δ 170.67 (C=O), 156.65 (C=O), 97.89 (NCHC), 68.21 (NCHCH₂O), 59.65 (NCHCH₂O), 53.18 (OCH₃), 52.50 (OCH₃), 37.48 (C(CH₃)₃), 25.57 (C(CH₃)₃).

Synthesis of (4S)-dimethyl 2-(tert-butyl)-4-methyloxazolidine-3,4-dicarboxylate

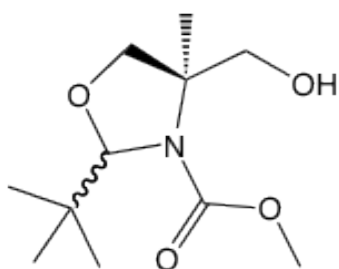


C₁₂H₂₁NO₅
MW: 259.14

Lithium bis(trimethylsilyl) amide solution (73.64 ml, 73.64 mmol, 1M in THF) was added to a mixture of (4S)-dimethyl 2-(tert-butyl)oxazolidine-3,4-dicarboxylate (9.025 g, 36.82 mmol), methyl iodide (9.17 ml, 147.28 mmol) and 1,3-dimethyl-3,4,5,6-tetrahydro-2(1H)-pyrimidinone (15 ml) in a THF (30 ml) and hexane (15 ml) mixture stirring at -74 °C. After 1 h the reaction mixture was quenched with saturated ammonium chloride solution and extracted with AcOEt and brine. The organic layer was dried over MgSO₄ and vacuum filtered. The solvent was removed *in vacuo* and the desired product was isolated using flash chromatography (hexane – ethyl acetate 80:20 v/v increasing to 60:40 v/v) giving the desired oil product (85.5%, 8.153 g).

¹H NMR (CDCl₃, 500 MHz): δ 5.00 (1H, s, OCH), 4.14 (1H, d, *J* = 8 Hz, CCH₂O), 3.68 (1H, d, *J* = 8.5 Hz, CCH₂O), 3.62 (3H, s, OCH₃), 3.54 (3H, s, OCH₃), 1.48 (3H, s, CCH₃), 0.84 (9H, s, CCH₃). ¹³C NMR (CDCl₃, 125 MHz): δ 172.7 (C=O), 105.84 (C=O), 97.56 (NCHC), 66.48 (CH₂O), 60.39 (NCCH₃), 52.65 (OCH₃), 52.44 (OCH₃), 39.41 (C(CH₃)₃), 26.32 (C(CH₃)₃), 21.19 (NCCH₃).

Synthesis of (4R)-methyl 2-(tert-butyl)-4-(hydroxymethyl)-4-methyloxazolidine-3-carboxylate

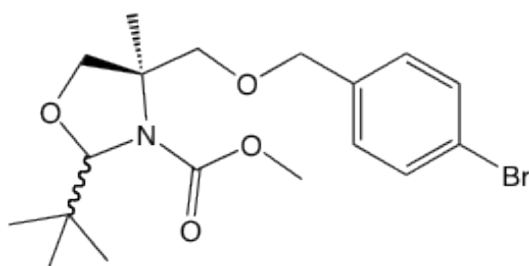


$C_{11}H_{21}NO_4$
MW: 231.15

(4S)-dimethyl 2-(tert-butyl)-4-methyloxazolidine-3,4-dicarboxylate (8.153 g, 31.46 mmol) dissolved in 35 ml toluene was added to a mixture of potassium borohydride (3.394 g, 62.92 mmol) and lithium chloride (2.667 g, 62.92 mmol) in THF (100 ml). The mixture was heated at 45 °C for 24 h. After 24 h the reaction mixture was slowly quenched with saturated ammonium chloride solution and extracted with AcOEt and water. The organic layer was dried over $MgSO_4$ and vacuum filtered. The solvent was removed *in vacuo* and the desired product was isolated using flash chromatography (hexane – ethyl acetate 60:40 v/v increasing to 50:50 v/v) giving the desired white solid product (80%, 5.802 g).

1H NMR ($CDCl_3$, 500 MHz): δ 5.15 (1H, s, OCH), 4.54 (1H, b, OH), 3.90 (1H, d, J = 8 Hz, CH_2OH), 3.84 (1H, m, CCH₂O), 3.76 (1H, d, J = 8.5 Hz, CH_2OH), 3.73 (3H, s, OCH₃), 3.57 (1H, m, CCH₂O), 1.44 (3H, s, CCH₃), 0.95 (9H, s, CCH₃). ^{13}C NMR ($CDCl_3$, 125 MHz): δ 156.94 (C=O), 97.39 (NCHC), 75.85 (CH_2O), 67.26 (NCCH₃), 60.42 (CH_2OH), 52.63 (OCH₃), 38.70 (C(CH₃)₃), 26.52 (C(CH₃)₃), 19.56 (NCCH₃).

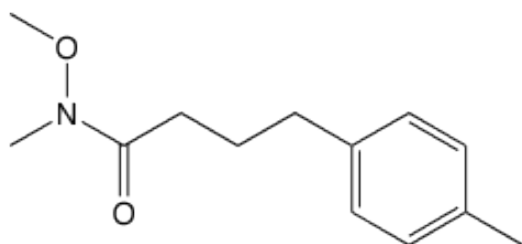
Synthesis of (4R)-methyl 4-(((4-bromobenzyl) oxy) methyl)-2-(tert-butyl)-4-methyloxazolidine-3-carboxylate



$C_{18}H_{26}BrNO_4$
MW: 399.10

Sodium hydride (60%, 0.752 g, 18.8 mmol) was added to a solution of (4R)-methyl 2-(tert-butyl)-4-(hydroxymethyl)-4-methyloxazolidine-3-carboxylate (2.822 g, 12.21 mmol) in DMF (30 ml) at 0 °C. The reaction mixture was stirred for 10 min, at which time 4-bromobenzyl bromide (4.699 g, 18.8 mmol) was added. The resultant mixture was warmed to ambient temperature and then stirred for 2 h. After 2 h the reaction mixture was quenched with saturated ammonium chloride solution and extracted with AcOEt and water and washed with brine. The organic layer was dried over $MgSO_4$ and vacuum filtered. The solvent was removed *in vacuo* and the desired product was isolated using flash chromatography (hexane – ethyl acetate 70:30 v/v increasing to 60:40 v/v) giving the desired oil product (70%, 3.415 g).

1H NMR ($CDCl_3$, 500 MHz): δ 7.28 (2H, d, J = 8.5 Hz, ArH), 7.03 (2H, d, J = 8 Hz, ArH), 5.01 (1H, s, OCH), 4.32 (2H, m, $PhCH_2O$), 4.04 (1H, d, J = 9 Hz, CCH_2O), 3.73 (1H, d, J = 9 Hz, CCH_2O), 3.60 (1H, d, J = 8.5 Hz, CCH_2O), 3.55 (1H, d, J = 8.5 Hz, CCH_2O), 3.51 (3H, s, OCH_3), 1.28 (3H, s, CCH_3), 0.80 (9H, s, CCH_3). ^{13}C NMR ($CDCl_3$, 125 MHz): δ 137.28 ($C=O$), 131.29 (CH-Ar), 129.01 (CH-Ar), 129.01 (C-Ar), 97.03 ($OCHC(CH_3)_3$), 76.78 (OCH_2C), 74.57 (OCH_2C), 72.46 (OCH_2Ph), 63.18 ($NCCH_3$), 51.76 (OCH_3), 38.43 ($C(CH_3)_3$), 26.48 ($C(CH_3)_3$), 20.43 ($NCCH_3$). MS (ES+) m/z 400.1 (MH^+) and 422.1 (MNa^+).

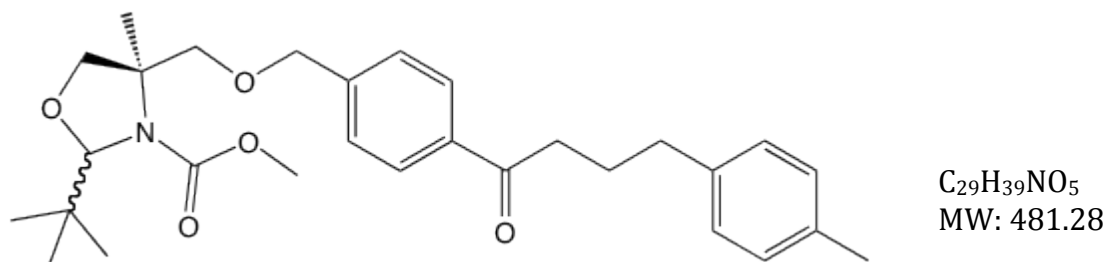
Synthesis of *N*-methoxy-*N*-methyl-4-(*p*-tolyl) butanamide

$C_{13}H_{19}NO_2$
MW: 221.14

To a solution of 4-(*p*-tolyl)butanoic acid (5 g, 28 mmol) in DCM (130 ml) were added *N,O*-dimethylhydroxylamine hydrochloride (3.3 g, 34 mmol) and 1-(3-dimethylaminopropyl)-3-ethyl-carbodiimide hydrochloride (6.5 g, 34 mmol). The solution was stirred for 10 min at ambient temperature. The mixture was cooled to 0 °C and *N*-methylmorpholine (9.3 ml, 84 mmol) was added dropwise to the solution. The reaction mixture was warmed to room temperature and stirred for 24 h. After quenching with 1M HCl (100 ml) the resulting mixture was extracted with DCM and water and washed with brine. The organic layer was dried over $MgSO_4$ and vacuum filtered. The solvent was removed *in vacuo* and the desired product was isolated using flash chromatography (hexane – ethyl acetate 50:50 v/v increasing to 40:60 v/v) giving the desired colourless oil product (82%, 5.084 g).

1H NMR ($CDCl_3$, 500 MHz): δ 7.13 (4H, s, ArH), 3.66 (3H, s, OCH_3), 3.21 (3H, s, NCH_3), 2.68 (2H, t, $J = 7.5$ Hz, $PhCH_2CH_2$), 2.48 (2H, t, $J = 7$ Hz, $COCH_2$), 2.35 (3H, s, $PhCH_3$), 2.00 (2H, quin, $J = 7.5$ Hz, $CH_2CH_2CH_2$). ^{13}C NMR ($CDCl_3$, 125 MHz): δ 175.80 ($C=O$), 138.70 ($C-Ar$), 135.31 ($C-Ar$), 129.22 ($CH-Ar$), 129.05 ($CH-Ar$), 128.72 ($CH-Ar$), 129.61 ($CH-Ar$), 61.16 (CH_3ON), 34.90 ($PhCH_2$), 32.19 (CH_3N), 31.21 ($CH_2CH_2CH_2$), 27.20 ($COCH_2$), 21.33 ($PhCH_3$).

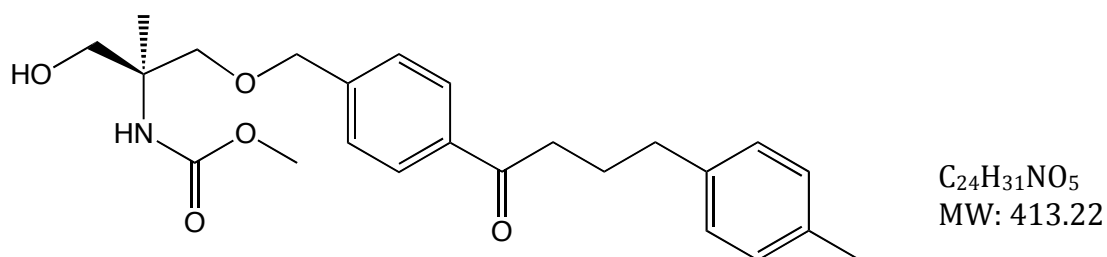
Synthesis of (4R)-methyl 2-(tert-butyl)-4-methyl-4-(((4-(4-(p-tolyl)butanoyl) benzyl) oxy) methyl) oxazolidine-3-carboxylate



To a solution of (4R)-methyl 4-(((4-bromobenzyl)oxy)methyl)-2-(tert-butyl)-4-methyloxazolidine-3-carboxylate (7.618 g, 19.09 mmol) in THF (60 ml) was slowly added *n*-BuLi (1.6 M *n*-hexane solution, 18.01 ml, 28.64 mmol) at -78 °C under argon. The mixture was stirred for 30 min at the same temperature. A solution of *N*-methoxy-*N*-methyl-4-(p-tolyl)butanamide (8.443 g, 38.18 mmol) in THF (10 ml) was added to the solution and the reaction mixture was gradually warmed to ambient temperature and then stirred for 2 h. After quenching with saturated ammonium chloride solution the resulting mixture was poured into water and extracted with AcOEt. The combined organic layer was washed with water and brine, dried over MgSO₄ and vacuum filtered. The solvent was removed *in vacuo* and the desired product was isolated using flash chromatography (hexane – ethyl acetate 100:0 v/v increasing to 50:50 v/v) giving the desired brown oil product (38%, 3.518 g).

¹H NMR (CDCl₃, 500 MHz): δ 7.78 (2H, d, *J* = 8.5 Hz, *ArH*), 7.25 (2H, d, *J* = 8.5 Hz, *ArH*), 6.97 (4H, s, *ArH*), 5.02 (1H, s, OCH), 4.45 (2H, m, PhCH₂O), 4.07 (1H, d, *J* = 9 Hz, CCH₂O), 3.76 (1H, d, *J* = 8 Hz, CCH₂O), 3.64 (1H, d, *J* = 8.5 Hz, CCH₂O), 3.57 (1H, d, *J* = 8.5 Hz, CCH₂O), 3.54 (3H, s, OCH₃), 2.83 (2H, t, *J* = 7 Hz, COCH₂), 2.56 (2H, t, *J* = 7.5 Hz, PhCH₂CH₂), 2.19 (3H, s, PhCH₃), 1.93 (2H, quin, *J* = 7.5 Hz, CH₂CH₂CH₂), 1.31 (3H, s, CCH₃), 0.80 (9H, s, CCH₃). ¹³C NMR (CDCl₃, 125 MHz): δ 199.81 (C=O), 143.51 (C=O, ester), 138.57 (C-Ar), 136.35 (C-Ar), 135.40 (C-Ar), 129.09 (CH-Ar), 128.72 (CH-Ar), 128.40 (CH-Ar), 128.35 (CH-Ar), 128.29 (CH-Ar), 128.29 (CH-Ar), 128.19 (CH-Ar), 127.54 (CH-Ar), 127.23 (CH-Ar), 97.27 (OCHC(CH₃)₃), 75.34 (OCH₂C), 73.17 (OCH₂C), 63.35 (PhCH₂O), 52.04 (OCH₃, ester), 48.59 (COCH₂), 37.75 (C(CH₃)₃), 34.76 (PhCH₂), 29.37 (C(CH₃)₃), 26.37 (CH₂CH₂CH₂), 21.01 (PhCH₃), 14.13 (NCCH₃). MS (ES⁺) *m/z* 482.3 (MH⁺) and 520.3 (MNa⁺).

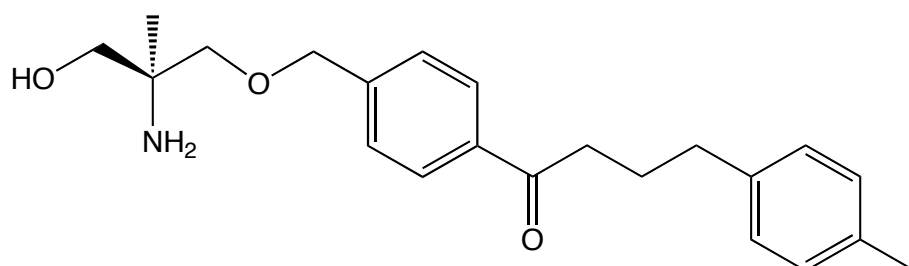
Synthesis of (S)-methyl (1-hydroxy-2-methyl-3-((4-(4-(p-tolyl) butanoyl) benzyl) oxy) propan-2-yl) carbamate



To a solution of (4R)-methyl 2-(tert-butyl)-4-methyl-4-(((4-(4-(p-tolyl) butanoyl) benzyl) oxy) methyl) oxazolidine-3-carboxylate (3.518 g, 7.31 mmol) in MeOH (35 ml) was added p-toluenesulfonic acid monohydrate (2.343 g, 12.32 mmol). The mixture was stirred for 3 h at 50 °C. The solvent was removed *in vacuo* and the desired product was isolated using flash chromatography (hexane – ethyl acetate 60:40 v/v increasing to 20:80 v/v) giving the desired yellow/brown oil product (89%, 2.691 g).

¹H NMR (CDCl₃, 500 MHz): δ 7.92 (2H, d, *J* = 8 Hz, *ArH*), 7.40 (2H, d, *J* = 8.5 Hz, *ArH*), 7.11 (4H, s, *ArH*), 5.42 (1H, b, *NH*), 4.51 (2H, s, PhCH₂O), 3.76 (1H, d, *J* = 11.5 Hz, CCH₂OH), 3.66 (1H, s, CCH₂O), 3.64 (3H, s, OCH₃), 3.62 (1H, s, CCH₂O), 3.59 (1H, d, *J* = 9 Hz, CCH₂OH), 2.97 (2H, t, *J* = 7 Hz, COCH₂), 2.69 (2H, t, *J* = 7 Hz, PhCH₂CH₂), 2.33 (3H, s, PhCH₃), 2.07 (2H, quin, *J* = 7.5 Hz, CH₂CH₂CH₂), 1.30 (3H, s, CCH₃).

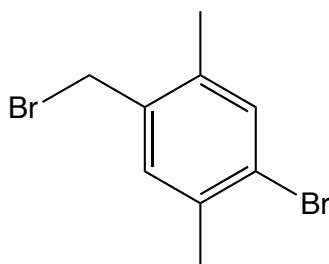
Synthesis of (S)-1-(4-((2-amino-3-hydroxy-2-methylpropoxy) methyl) phenyl)-4-(p-tolyl) butan-1-one



C₂₂H₂₉NO₃
MW: 355.21

To a solution of (S)-methyl (1-hydroxy-2-methyl-3-((4-(4-(p-tolyl)butanoyl)benzyl)oxy)propan-2-yl)carbamate (2.691 g, 6.51 mmol) in EtOH (150 ml) was added KOH solution (8 M, 70 ml, 10 mmol). Mixture heated under reflux at 90 °C for 24 h. The solvent was removed *in vacuo* and the resulting mixture was extracted with brine and DCM, dried over MgSO₄ and vacuum filtered. The solvent was removed *in vacuo* yielding the final yellow solid product (73%, 1.69 g).

¹H NMR (CDCl₃, 500 MHz): δ 7.83 (2H, d, *J* = 8 Hz, ArH), 7.31 (2H, d, *J* = 8.5 Hz, ArH), 7.02 (4H, s, ArH), 4.50 (2H, s, PhCH₂O), 3.47 (1H, d, *J* = 10.5 Hz, CCH₂OH), 3.66 (1H, d, *J* = 8.5 Hz, CCH₂O), 3.31 (1H, d, *J* = 10.5 Hz, CCH₂O), 3.27 (1H, d, *J* = 9 Hz, CCH₂OH), 2.88 (2H, t, *J* = 7 Hz, COCH₂), 2.60 (2H, t, *J* = 7 Hz, PhCH₂CH₂), 2.56 (2H, b, NH₂), 2.24 (3H, s, PhCH₃), 1.98 (2H, quin, *J* = 7 Hz, CH₂CH₂CH₂), 1.02 (3H, s, CCH₃).
¹³C NMR (CDCl₃, 125 MHz): δ 199.86 (C=O), 143.58 (C-Ar), 138.56 (C-Ar), 136.34 (C-Ar), 135.36 (C-Ar), 129.11 (CH-Ar), 128.58 (CH-Ar), 128.45 (CH-Ar), 128.42 (CH-Ar), 128.26 (CH-Ar), 127.71 (CH-Ar), 127.57 (CH-Ar), 127.26 (CH-Ar), 73.48 (OCH₂C), 72.80 (PhCH₂O), 68.23 (HOCH₂C), 53.47 (NH₂C), 37.74 (COCH₂), 34.75 (PhCH₂), 25.84 (CH₂CH₂CH₂), 22.71 (NH₂CCH₃), 21.03 (PhCH₃). MS (ES⁺) *m/z* 356.2 (MH⁺). [α]_D²⁴ = 0.5 (c = 0.21, CHCl₃).

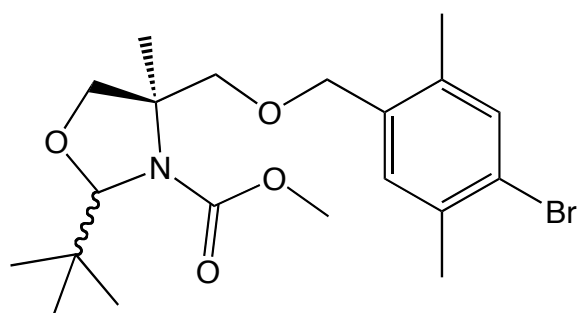
Synthesis of 1-bromo-4-(bromomethyl)-2,5-dimethylbenzene

C₉H₁₀Br₂
MW: 275.91

A mixture of paraformaldehyde (5.5 g, 183.16 mmol), 2-bromo-1,4-dimethylbenzene (25 g, 18.66 ml, 135.1 mmol), glacial acetic acid (32.5 ml), phosphoric acid (85%, 10 ml, 146.14 mmol) and hydrobromic acid (48%, 32.5 ml, 287.28 mmol) was heated under reflux at 130 °C for 24 h. To the mixture was added deionised water and extracted with diethyl ether. The organic layer was washed with saturated NaHCO₃ solution and then washed with distilled water. The organic layer was dried over MgSO₄ and vacuum filtered. The desired product was isolated using flash chromatography (hexane – ethyl acetate 100:0 v/v increasing to 70:30 v/v) giving the desired dark oil product (42%, 15.749 g).

¹H NMR (CDCl₃, 500 MHz): δ 7.40 (1H, s, ArH), 7.19 (1H, s, ArH), 4.46 (2H, s, PhCH₂Br), 2.38 (6H, s, PhCH₃).

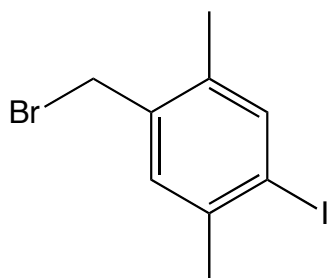
Synthesis of (4*R*)-methyl 4-(((4-bromobenzyl) oxy) methyl)-2-(*tert*-butyl)-4-methyloxazolidine-3-carboxylate



C₂₀H₃₀BrNO₄
MW: 427.14

Sodium hydride (60%, 1.171 g, 29.28 mmol) was added to a solution of (4*R*)-methyl 2-(*tert*-butyl)-4-(hydroxymethyl)-4-methyloxazolidine-3-carboxylate (4.513 g, 19.52 mmol) in DMF (52 ml) at 0 °C. The reaction mixture was stirred for 25 min, at which time 1-bromo-4-(bromomethyl)-2,5-dimethylbenzene (8.079 g, 29.28 mmol) in DMF (27 ml) was added. The resultant mixture was stirred at 0 °C for 20 min and then warmed to ambient temperature for 24 h. After 24 h the reaction mixture was quenched with saturated ammonium chloride solution and extracted with AcOEt and water and washed with brine. The organic layer was dried over MgSO₄ and vacuum filtered. The solvent was removed *in vacuo* and the desired product was isolated using flash chromatography (hexane – ethyl acetate 100:0 v/v increasing to 80:20 v/v) giving the desired dark oil product (53%, 4.402 g).

¹H NMR (CDCl₃, 500 MHz): δ 7.26 (1H, s, ArH), 7.05 (1H, s, ArH), 5.06 (1H, s, OCH), 4.36 (2H, m, PhCH₂O), 4.05 (1H, m, CCH₂O), 3.79 (1H, m, CCH₂O), 3.65 (1H, d, *J* = 8.5 Hz, CCH₂O), 3.60 (3H, s, OCH₃), 3.59 (1H, d, *J* = 9 Hz, CCH₂O), 2.28 (3H, s, PhCH₃), 2.17 (3H, s, PhCH₃), 1.33 (3H, s, CCH₃), 0.85 (9H, s, CCH₃).

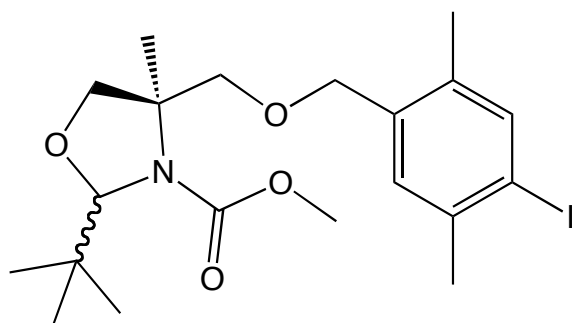
Synthesis of 1-(bromomethyl)-4-iodo-2,5-dimethylbenzene

C₉H₁₀BrI
MW: 323.90

A mixture of paraformaldehyde (3.559 g, 30.03 mmol), 1,4-dimethyl-2-iodobenzene (25 g, 107.73 mmol), glacial acetic acid (26 ml), phosphoric acid (85%, 8.11 ml, 118.5 mmol) and hydrobromic acid (48%, 26 ml, 226.23 mmol) was heated under reflux at 130 °C for 24 h. To the mixture was added deionised water and extracted with diethyl ether. The organic layer was washed with saturated NaHCO₃ solution and then washed with distilled water. The organic layer was dried over MgSO₄ and vacuum filtered. The desired product was isolated using flash chromatography (hexane – ethyl acetate 100:0 v/v increasing to 70:30 v/v) giving the desired red/brown product (42%, 14.522 g).

¹H NMR (CDCl₃, 500 MHz): δ 7.68 (1H, s, ArH), 7.19 (1H, s, ArH), 4.45 (2H, s, PhCH₂Br), 2.41 (3H, s, PhCH₃), 2.36 (3H, s, PhCH₃).

Synthesis of (4*R*)-methyl 2-(*tert*-butyl)-4-(((4-iodo-2,5-dimethylbenzyl)oxy)methyl)-4-methyloxazolidine-3-carboxylate

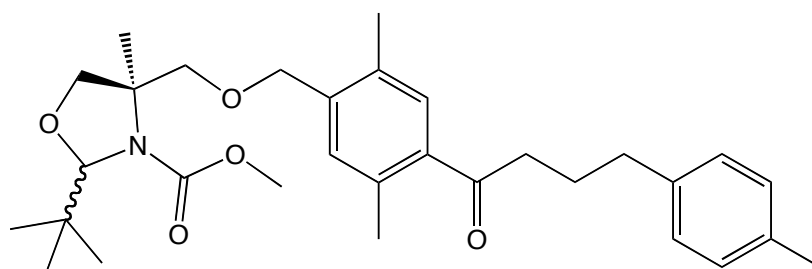


C₂₀H₃₀INO₄
MW: 475.12

Sodium hydride (60%, 1.793 g, 44.83 mmol) was added to a solution of (4*R*)-methyl 2-(*tert*-butyl)-4-(hydroxymethyl)-4-methyloxazolidine-3-carboxylate (8.298 g, 35.9 mmol) in DMF (50 ml) at 0 °C. The reaction mixture was stirred for 25 min, at which time 1-(bromomethyl)-4-iodo-2,5-dimethylbenzene (14.522 g, 44.83 mmol) in DMF (40 ml) was added. The resultant mixture was stirred at 0 °C for 20 min and then warmed to ambient temperature for 24 h. After 24 h the reaction mixture was quenched slowly with saturated ammonium chloride solution and extracted with AcOEt and water and washed with brine. The organic layer was dried over MgSO₄ and vacuum filtered. The solvent was removed *in vacuo* and the desired product was isolated using flash chromatography (hexane – ethyl acetate 100:0 v/v increasing to 70:30 v/v) giving the desired dark oil product (77%, 13.172 g).

¹H NMR (CDCl₃, 500 MHz): δ 7.51 (1H, s, ArH), 7.03 (1H, s, ArH), 5.04 (1H, s, OCH), 4.33 (2H, m, PhCH₂O), 4.03 (2H, m, CCH₂O), 3.77 (1H, m, CCH₂O), 3.63 (1H, m, CCH₂O), 3.58 (3H, s, OCH₃), 2.28 (3H, s, PhCH₃), 2.12 (3H, s, PhCH₃), 1.31 (3H, s, CCH₃), 0.84 (9H, s, CCH₃).

Synthesis of (4*R*)-methyl 2-(*tert*-butyl) -4-(((2,5-dimethyl-4-(4-(*p*-tolyl) butanoyl) benzyl) oxy) methyl)-4-methyloxazolidine-3-carboxylate



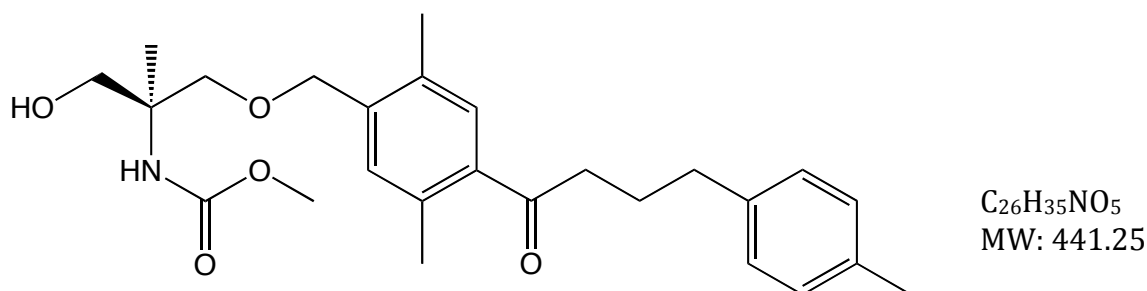
C₃₁H₄₃NO₅
MW: 509.31

To a solution of (4*R*)-methyl 2-(*tert*-butyl)-4-(((4-iodo-2,5-dimethylbenzyl)oxy)methyl)-4-methyloxazolidine-3-carboxylate (13.172 g, 27.72 mmol) in THF (30 ml) was slowly added *i*PrMgCl (27.72 ml, 55.44 mmol) at -78 °C under argon. The mixture was stirred for 30 min at the same temperature. A solution of *N*-methoxy-*N*-methyl-4-(*p*-tolyl)butanamide (12.26 g, 55.44 mmol) in THF (30 ml) was added to the solution and the reaction mixture was stirred at -78 °C and then allowed to gradually warm to ambient temperature and then stirred for 2 h. After quenching with saturated ammonium chloride solution the resulting mixture was poured into water and extracted with AcOEt. The combined organic layer was washed with water and brine, dried over MgSO₄ and vacuum filtered. The solvent was removed *in vacuo* and the desired product was isolated using flash chromatography (hexane – ethyl acetate 100:0 v/v increasing to 70:30 v/v) giving the desired dark oil product (41.5%, 5.855 g).

¹H NMR (CDCl₃, 500 MHz): δ 7.26 (1H, s, ArH), 7.08 (1H, s, ArH), 7.02 (4H, s, ArH), 5.07 (1H, s, OCH), 4.42 (2H, m, PhCH₂O), 4.08 (1H, d, *J* = 9 Hz, CCH₂O), 3.81 (1H, d, *J* = 9 Hz, CCH₂O), 3.67 (1H, d, *J* = 9 Hz, CCH₂O), 3.62 (1H, d, *J* = 9 Hz, CCH₂O), 3.60 (3H, s, OCH₃), 2.80 (2H, t, *J* = 7 Hz, COCH₂), 2.59 (2H, t, *J* = 7.5 Hz, PhCH₂CH₂), 2.36 (3H, s, PhCH₃), 2.25 (3H, s, PhCH₃), 2.20 (3H, s, PhCH₃), 1.94 (2H, quin, *J* = 7.5 Hz, CH₂CH₂CH₂), 1.35 (3H, s, CCH₃), 0.85 (9H, s, CCH₃). ¹³C NMR (CDCl₃, 125 MHz): δ 204.23 (C=O), 139.15 (C=O, ester), 138.59 (C-Ar), 137.39 (C-Ar), 135.39 (C-Ar), 135.27 (C-Ar), 133.51 (C-Ar), 133.46 (C-Ar), 131.67 (CH-Ar), 130.25 (CH-Ar), 129.08 (CH-Ar), 128.40 (CH-Ar), 97.27 (OCHC(CH₃)₃), 75.04 (OCH₂C), 71.44 (OCH₂C), 63.35 (PhCH₂O), 52.03 (OCH₃, ester), 40.73 (COCH₂), 38.61 (C(CH₃)₃),

34.75 (PhCH₂), 26.53 (C(CH₃)₃), 25.99 (CH₂CH₂CH₂), 21.01 (PhCH₃), 20.82 (PhCH₃), 18.31 (NCCH₃).

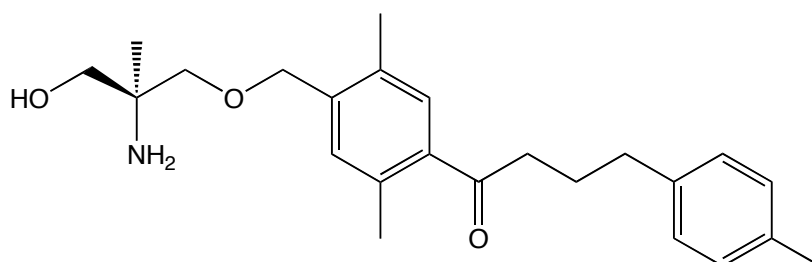
Synthesis of (*S*)-methyl (1-((2,5-dimethyl-4-(4-(*p*-tolyl) butanoyl) benzyl) oxy)-3-hydroxy-2-methylpropan-2-yl)carbamate



To a solution of (4*R*)-methyl 2-(*tert*-butyl) -4-(((2,5-dimethyl-4-(4-(*p*-tolyl) butanoyl) benzyl) oxy) methyl)-4-methyloxazolidine-3-carboxylate (5.855 g, 11.5 mmol) in MeOH (200 ml) was added *p*-toluenesulfonic acid monohydrate (4.375 g, 23 mmol). The mixture was stirred for 24 h at 50 °C. The solvent was removed *in vacuo* and the desired product was isolated using flash chromatography (hexane – ethyl acetate 50:50 v/v increasing to 40:60 v/v) giving the desired dark oil product (85%, 4.32 g).

¹H NMR (CDCl₃, 500 MHz): δ 7.36 (1H, s, ArH), 7.15 (1H, s, ArH), 7.12 (4H, s, ArH), 5.34 (1H, b, NH), 4.26 (2H, s, PhCH₂O), 3.76 (1H, d, *J* = 11 Hz, CCH₂OH), 3.69 (2H, m, CCH₂O), 3.67 (3H, s, OCH₃), 3.64 (1H, s, OH), 3.57 (1H, d, *J* = 9 Hz, CCH₂OH), 2.90 (2H, t, *J* = 7.5 Hz, COCH₂), 2.69 (2H, t, *J* = 7.5 Hz, PhCH₂CH₂), 2.47 (3H, s, PhCH₃), 2.35 (3H, s, PhCH₃), 2.32 (3H, s, PhCH₃), 2.05 (2H, quin, *J* = 7.5 Hz, CH₂CH₂CH₂), 1.30 (3H, s, CCH₃). ¹³C NMR (CDCl₃, 125 MHz): δ 204.25 (C=O), 156.71 (C=O), 138.57 (C-Ar), 138.47 (C-Ar), 137.77 (C-Ar), 135.40 (C-Ar), 135.32 (C-Ar), 133.76 (C-Ar), 132.01 (CH-Ar), 130.35 (CH-Ar), 129.08 (CH-Ar), 128.40 (CH-Ar), 74.65 (OCH₂C), 71.63 (PhCH₂O), 68.43 (HOCH₂C), 56.50 (NHC), 51.97 (OCH₃), 40.76 (COCH₂), 34.73 (PhCH₂), 25.95 (CH₂CH₂CH₂), 21.01 (PhCH₃), 20.76 (PhCH₃), 19.93 (PhCH₃), 18.31 (NHCCH₃).

Synthesis of (S)-1-(4-((2-amino-3-hydroxy-2-methylpropoxy) methyl) -2,5-dimethylphenyl)-4-(p-tolyl) butan-1-one



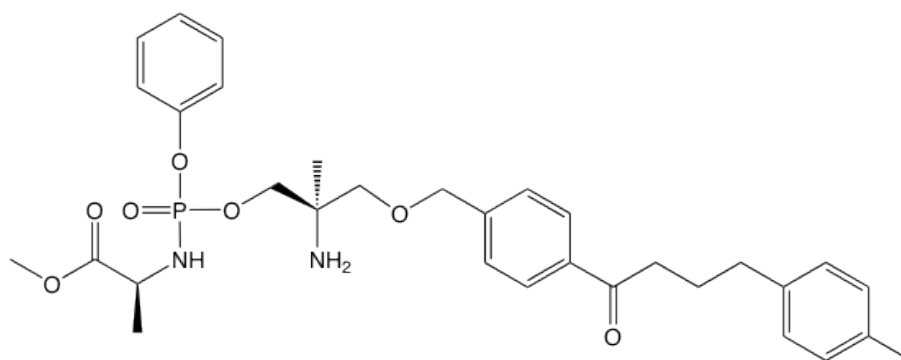
C₂₄H₃₃NO₃
MW: 383.25

To a solution of (S)-methyl (1-((2,5-dimethyl-4-(4-(p-tolyl)butanoyl)benzyl)oxy)-3-hydroxy-2-methylpropan-2-yl)carbamate (4.32 g, 9.79 mmol) in EtOH (200 ml) was added KOH solution (8 M, 61.19 ml, 489.5 mmol). Mixture heated under reflux at 90 °C for 24 h. The solvent was removed *in vacuo* and the resulting mixture was extracted with brine and DCM, dried over MgSO₄ and vacuum filtered. The solvent was removed *in vacuo* and the desired product was isolated using flash chromatography (methanol – dichloromethane 0:100 v/v increasing to 10:90 v/v) giving the desired brown oil product (56%, 2.09 g).

¹H NMR (CDCl₃, 500 MHz): δ 7.24 (H, s, ArH), 7.10 (H, s, ArH), 7.01 (4H, s, ArH), 4.43 (2H, s, PhCH₂O), 3.87 (2H, b, NH₂), 3.54 (1H, d, *J* = 11 Hz, CCH₂OH), 3.43 (1H, d, *J* = 9.5 Hz, CCH₂O), 3.41 (1H, s, OH), 3.40 (1H, d, *J* = 11.5 Hz, CCH₂OH), 3.34 (1H, d, *J* = 9.5 Hz, CCH₂O), 2.78 (2H, t, *J* = 7.5 Hz, COCH₂), 2.58 (2H, t, *J* = 7.5 Hz, PhCH₂CH₂), 2.36 (3H, s, PhCH₃), 2.24 (3H, s, PhCH₃), 2.20 (3H, s, PhCH₃), 1.93 (2H, quin, *J* = 7.5 Hz, CH₂CH₂CH₂), 1.11 (3H, s, CCH₃). ¹³C NMR (CDCl₃, 125 MHz): δ 204.28 (C=O), 138.65 (C-Ar), 138.58 (C-Ar), 137.68 (C-Ar), 135.41 (C-Ar), 135.29 (C-Ar), 133.61 (C-Ar), 131.87 (CH-Ar), 130.26 (CH-Ar), 129.09 (CH-Ar), 128.41 (CH-Ar), 75.48 (OCH₂C), 71.56 (PhCH₂O), 67.26 (HOCH₂C), 55.44 (NH₂C), 40.79 (COCH₂), 34.75 (PhCH₂), 25.97 (CH₂CH₂CH₂), 21.13 (NH₂CCH₃), 21.03 (PhCH₃), 20.78 (PhCH₃), 18.40 (PhCH₃). MS (ES⁺) *m/z* 384.17 (MH⁺) and 406.15 (MNa⁺).

9.8 Syntheses of BED Compound Derived Phosphoramidates

Synthesis of (2S)-methyl 2-((((R)-2-amino-2-methyl-3-((4-(4-(p-tolyl) butanoyl) benzyl) oxy) propoxy) (phenoxy) phosphoryl) amino) propanoate (12)



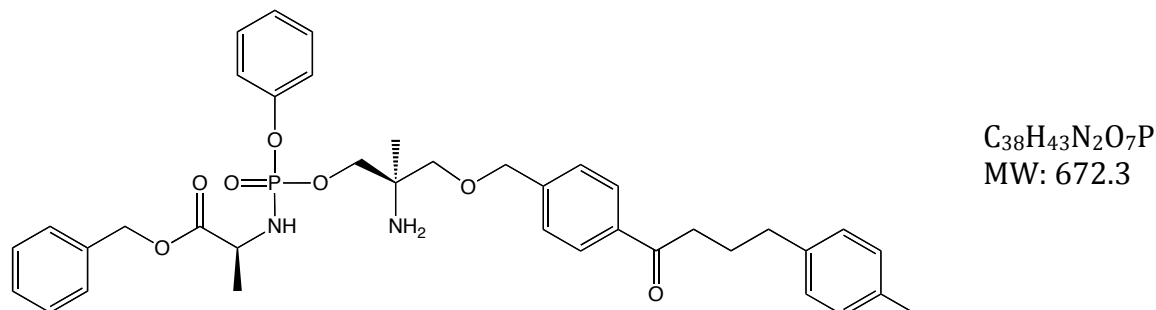
C₃₂H₄₁N₂O₇P
MW: 596.27

tBuMgCl (0.72 ml, 0.72 mmol) was added dropwise to a solution of (S)-1-(4-((2-amino-3-hydroxy-2-methylpropoxy)methyl)phenyl)-4-(p-tolyl)butan-1-one (254 mg, 0.72 mmol) in anhydrous THF (20 ml) under anhydrous conditions. The mixture was stirred at room temperature for one hour. After one hour the phosphorochloridate (199 mg, 0.72 mmol) in anhydrous THF (3 ml) was added dropwise to the stirring reaction mixture. The reaction was left to stir for 24 hours. After 24 hours the solvent was removed *in vacuo* and the desired product was isolated using flash chromatography (methanol – ethyl acetate 0:100 v/v increasing to 10:90 v/v) giving the desired oil product as a mixture of 2 diastereoisomers (44%, 0.188 g). The resulting oil was further purified using preparative reverse-phase HPLC (0.1% TFA in H₂O – ACN 20:80 v/v increasing to 100:0 v/v in 35 min) giving the desired product (6%, 0.026 g).

³¹P NMR (MeOD, 202 MHz): δ 3.74, 3.37, 3.30. ¹H NMR (MeOD, 500 MHz): δ 7.84 (2H, m, ArH), 7.41 (2H, m, ArH), 7.27 (2H, t, *J* = 8.5 Hz, ArH), 7.12 (3H, m, ArH), 6.97 (4H, s, ArH), 4.57 (2H, m, PhCH₂O), 4.09 (2H, m, CH₂OP), 3.88 (1H, m, CH₃CH), 3.56 (3H, m, OCH₃), 3.46 (2H, m, CCH₂O), 2.90 (2H, m, COCH₂), 2.55 (2H, t, *J* = 7.5 Hz, PhCH₂), 2.19 (3H, s, PhCH₃), 1.88 (2H, quin, *J* = 7 Hz, CH₂CH₂CH₂), 1.24 (3H, m, CHCH₃), 1.21 (3H, m, CCH₃). ¹³C NMR (MeOD, 125 MHz): δ 200.62 (C=O), 175.04 (C=O), 142.74 (2d, ²*J*_{C-P} = 3.3 Hz, POC-Ar), 138.57 (C-Ar), 136.51 (C-Ar), 136.0 (C-Ar), 129.52 (CH-Ar), 128.64 (CH-Ar), 128.02 (CH-Ar), 127.59 (CH-Ar), 127.57 (CH-

Ar), 125.08 (CH-Ar), 120.03 (2d, $^3J_{C-P} = 4.9$ Hz, CH-Ar), 72.55 (OCH₂C), 70.81 (d, $^2J_{C-P} = 3.6$ Hz, CH₂OP), 70.66 (PhCH₂O), 51.50 (OCH₃), 50.11 (CHCH₃), 41.71 (NH₂C), 37.31 (COCH₂), 34.30 (PhCH₂), 25.94 (CH₂CH₂CH₂), 19.69 (PhCH₃), 19.04 (m, CH₃C), 17.14 (CHCH₃). MS (ES+) m/z 597.3 (MH⁺). Reverse-phase analytical HPLC (0.1% TFA in H₂O – ACN 20:80 v/v increasing to 0:100 v/v in 35 min), 1 ml/min, $\lambda = 263$ nm showed a peak with a $t_R = 14.84$ min (99.1%).

Synthesis of (2*S*)-benzyl 2-((((*R*)-2-amino-2-methyl-3-((4-(4-(*p*-tolyl) butanoyl) benzyl) oxy) propoxy) (phenoxy) phosphoryl) amino) propanoate (13)

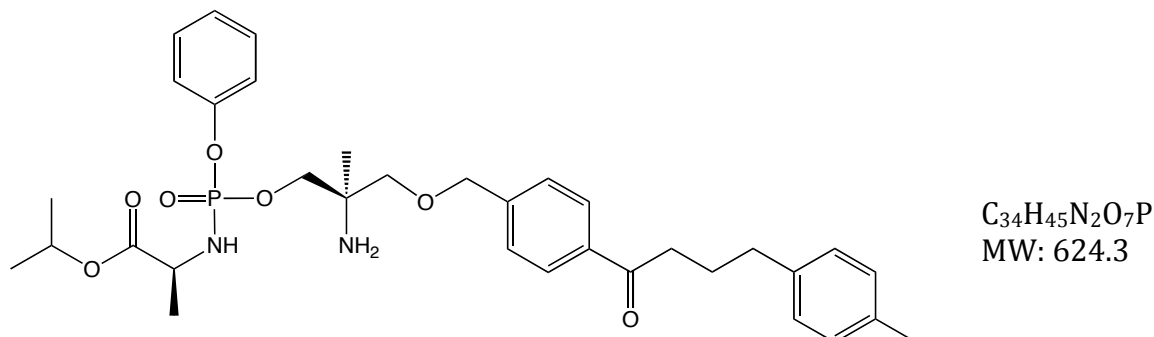


tBuMgCl (0.84 ml, 0.84 mmol) was added dropwise to a solution of (S)-1-(4-((2-amino-3-hydroxy-2-methylpropoxy)methyl)phenyl)-4-(*p*-tolyl)butan-1-one (300 mg, 0.84 mmol) in anhydrous THF (20 ml) under anhydrous conditions. The mixture was stirred at room temperature for one hour. After one hour the phosphorochloridate (297 mg, 0.84 mmol) in anhydrous THF (3 ml) was added dropwise to the stirring reaction mixture. The reaction was left to stir for 24 hours. After 24 hours the solvent was removed *in vacuo* and the desired product was isolated using flash chromatography (methanol – ethyl acetate 0:100 v/v increasing to 10:90 v/v) giving the desired oil product as a mixture of 2 diastereoisomers (65%, 0.365 g). The resulting oil was further purified using preparative reverse-phase HPLC (0.1% TFA in H₂O – ACN 20:80 v/v increasing to 100:0 v/v in 35 min) twice giving the desired product (3%, 0.015 g).

³¹P NMR (MeOD, 202 MHz): δ 3.71, 3.31, 3.32. ¹H NMR (CDCl₃, 500 MHz): δ 7.78 (2H, m, ArH), 7.30-6.94 (17H, m, ArH), 5.02 (2H, m, PhCH₂O), 4.39 (2H, m, PhCH₂O), 3.94 (2H, m, CH₂OP), 3.89 (1H, m, CHCH₃), 3.26 (1H, m, NH), 3.19 (2H, s, CCH₂O), 2.83 (2H, t, *J* = 7 Hz, COCH₂), 2.58 (2H, t, *J* = 7.5 Hz, PhCH₂), 2.22 (3H, s, PhCH₃), 1.95 (2H, quin, *J* = 7 Hz, CH₂CH₂CH₂), 1.21 (3H, m, CHCH₃), 1.02 (3H, m, CCH₃). ¹³C NMR (CDCl₃, 125 MHz): δ 199.80 (C=O), 173.42 (C=O), 150.85 (d, ²*J*_{C-P} = 6.75 Hz, POC-Ar), 143.42 (C-Ar), 138.61 (C-Ar), 136.34 (C-Ar), 135.81 (C-Ar), 135.39 (C-Ar), 129.69 (CH-Ar), 129.65 (CH-Ar), 129.12 (CH-Ar), 128.68 (CH-Ar), 128.65 (CH-Ar), 128.52 (CH-Ar), 128.43 (CH-Ar), 128.27 (CH-Ar), 128.24 (CH-Ar), 128.21 (CH-Ar), 128.05 (CH-Ar), 127.98 (CH-Ar), 127.29 (CH-Ar), 126.02 (CH-Ar), 124.93 (CH-Ar), 122.93 (CH-Ar), 120.81 (CH-Ar), 120.33 (CH-Ar), 74.77 (OCH₂C), 72.73 (d, ²*J*_{C-P} = 6.88 Hz,

CH₂OP), 71.40 (PhCH₂O), 67.18 (PhCH₂O), 60.43 (NH₂C), 50.33 (CHCH₃), 37.76 (COCH₂), 34.79 (PhCH₂), 25.85 (CH₂CH₂CH₂), 21.05 (PhCH₃), 20.85 (CH₃C), 14.26 (CHCH₃). MS (ES+) m/z 673.3 (MH⁺) and 695.3 (MNa⁺). Reverse-phase analytical HPLC (0.1% TFA in H₂O – ACN 20:80 v/v increasing to 0:100 v/v in 35 min), 1 ml/min, λ = 263 nm showed a peak with a t_R = 17.67 min (99.2%).

Synthesis of (2*S*)-isopropyl 2-((((*R*)-2-amino-2-methyl-3-((4-(4-(*p*-tolyl) butanoyl) benzyl) oxy) propoxy)(phenoxy) phosphoryl) amino) propanoate (14)

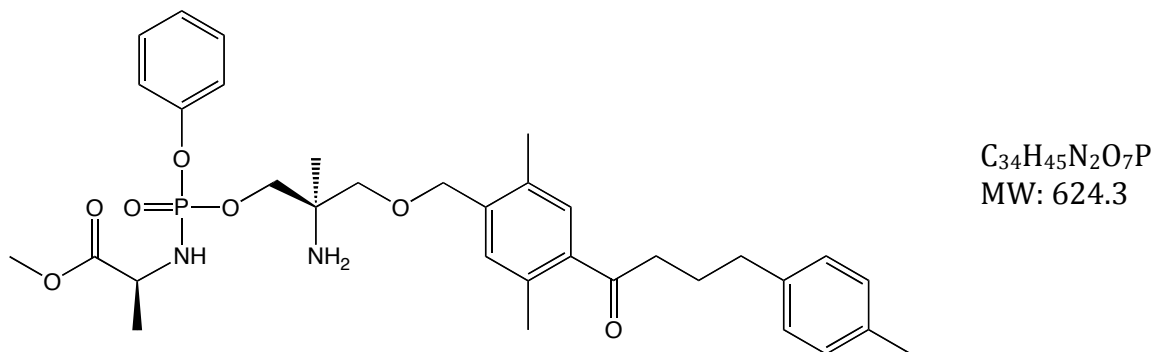


tBuMgCl (0.75 ml, 0.75 mmol) was added dropwise to a solution of (S)-1-(4-((2-amino-3-hydroxy-2-methylpropoxy)methyl)phenyl)-4-(*p*-tolyl)butan-1-one (265 mg, 0.75 mmol) in anhydrous THF (22 ml) under anhydrous conditions. The mixture was stirred at room temperature for one hour. After one hour the phosphorochloridate (229 mg, 0.75 mmol) in anhydrous THF (5 ml) was added dropwise to the stirring reaction mixture. The reaction was left to stir for 24 hours. After 24 hours the solvent was removed *in vacuo* and the desired product was isolated using flash chromatography (methanol – ethyl acetate 0:100 v/v increasing to 10:90 v/v) giving the desired oil product as a mixture of 2 diastereoisomers (50%, 0.234 g). The resulting oil was further purified using preparative reverse-phase HPLC (0.1% TFA in H₂O – ACN 20:80 v/v increasing to 100:0 v/v in 35 min) giving the desired product (14%, 0.065 g).

³¹P NMR (MeOD, 202 MHz): δ 3.79, 3.49, 3.41. ¹H NMR (MeOD, 500 MHz): δ 7.83 (2H, m, ArH), 7.39 (2H, m, ArH), 7.26 (2H, m, ArH), 7.12 (3H, m, ArH), 6.97 (4H, s, ArH), 4.91 (1H, m, CH(CH₃)₂), 4.56 (2H, m, PhCH₂O), 4.11 (2H, m, CH₂OP), 3.81 (1H, m, CHCH₃), 3.50 (2H, m, CCH₂O), 2.89 (2H, m, COCH₂), 2.54 (2H, t, *J* = 7.5 Hz, PhCH₂), 2.18 (3H, s, PhCH₃), 2.05 (1H, s, NH), 1.88 (2H, quin, *J* = 7.5 Hz, CH₂CH₂CH₂), 1.25 (3H, m, CHCH₃), 1.19 (3H, m, CCH₃), 1.11 (3H, m, CHCH₃), 1.10 (3H, m, CHCH₃). ¹³C NMR (MeOD, 125 MHz): δ 200.62 (C=O), 172.99 (C=O), 142.73 (2d, ²*J*_{C-P} = 2 Hz, POC-Ar), 138.56 (C-Ar), 136.47 (C-Ar), 135.06 (C-Ar), 129.52 (CH-Ar), 128.65 (CH-Ar), 128.03 (CH-Ar), 127.58 (CH-Ar), 127.55 (CH-Ar), 125.08 (CH-Ar), 125.04 (CH-Ar), 120.04 (2d, ³*J*_{C-P} = 4.75 Hz, CH-Ar), 72.54 (OCH₂C), 70.77

(PhCH₂O), 70.61 (d, $^2J_{C-P}$ = 1.63 Hz, CH₂OP), 68.98 (OCH(CH₃)₂), 56.21 (NH₂C), 50.54 (CHCH₃), 37.31 (COCH₂), 34.30 (PhCH₂), 25.94 (CH₂CH₂CH₂), 20.60 (OCHCH₃), 20.52 (OCHCH₃), 19.72 (PhCH₃), 19.14 (m, CH₃C), 17.11 (CHCH₃). MS (ES+) m/z 625.3 (MH⁺) and 647.3 (MNa⁺). Reverse-phase analytical HPLC (0.1% TFA in H₂O – ACN 20:80 v/v increasing to 0:100 v/v in 35 min), 1 ml/min, λ = 263 nm showed a peak with a t_R = 17.30 min (95.5%).

Synthesis of (2*S*)-methyl 2-((((*R*)-2-amino-3-((2,5-dimethyl-4-(4-(*p*-tolyl) butanoyl) benzyl) oxy)-2-methylpropoxy) (phenoxy) phosphoryl) amino) propanoate (15)

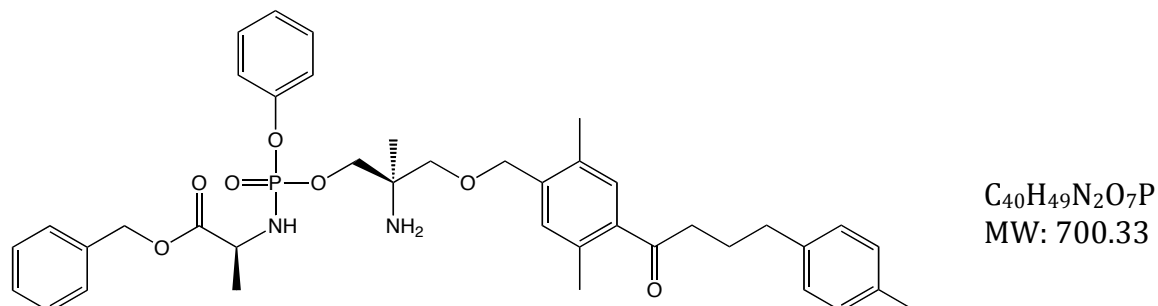


tBuMgCl (1.3 ml, 1.3 mmol) was added dropwise to a solution of (*S*)-1-(4-((2-amino-3-hydroxy-2-methylpropoxy) methyl) -2,5-dimethylphenyl)-4-(*p*-tolyl) butan-1-one (500 mg, 1.3 mmol) in anhydrous THF (23 ml) under anhydrous conditions. The mixture was stirred at room temperature for one hour. After one hour the phosphorochloridate (360 mg, 1.3 mmol) in anhydrous THF (2 ml) was added dropwise to the stirring reaction mixture. The reaction was left to stir for 24 hours. After 24 hours the solvent was removed *in vacuo* and the desired product was isolated using flash chromatography (methanol – ethyl acetate 0:100 v/v increasing to 10:90 v/v) giving the desired oil product as a mixture of 2 diastereoisomers (99%, 0.803 g). The resulting oil was further purified using preparative reverse-phase HPLC (0.1% TFA in H₂O – ACN 20:80 v/v increasing to 100:0 v/v in 35 min) twice giving the desired product (11%, 0.087 g).

³¹P NMR (MeOD, 202 MHz): δ 3.73, 3.43, 3.31. ¹H NMR (MeOD, 500 MHz): δ 7.44 (1H, m, ArH), 7.38 (2H, t, *J* = 8 Hz, ArH), 7.27 (4H, m, ArH), 7.07 (4H, m, ArH), 4.63 (2H, m, PhCH₂O), 4.25 (2H, m, CH₂OP), 3.99 (1H, m, CH₃CH), 3.68 (3H, m, OCH₃), 3.60 (2H, m, CCH₂O), 3.33 (1H, m, NH), 2.90 (2H, m, COCH₂), 2.63 (2H, t, *J* = 7.5 Hz, PhCH₂), 2.40 (3H, m, PhCH₃), 2.35 (3H, m, PhCH₃), 2.30 (3H, s, PhCH₃), 1.96 (2H, quin, *J* = 7 Hz, CH₂CH₂CH₂), 1.40 (3H, m, CHCH₃), 1.35 (3H, m, CCH₃). ¹³C NMR (MeOD, 125 MHz): δ 205.25 (C=O), 173.89 (C=O), 150.50 (2d, ²*J*_{C-P} = 4.88 Hz, POC-Ar), 138.51 (C-Ar), 138.31 (C-Ar), 137.71 (C-Ar), 135.08 (C-Ar), 134.81 (C-Ar), 134.19 (C-Ar), 131.92 (CH-Ar), 130.07 (CH-Ar), 129.52 (CH-Ar), 128.66 (CH-Ar), 128.05 (CH-Ar), 125.08 (CH-Ar), 120.07 (2d, ³*J*_{C-P} = 4.75 Hz, CH-Ar), 71.17 (OCH₂C),

70.72 (d, $^2J_{C-P} = 2.6$ Hz, CH_2OP), 70.57 ($PhCH_2O$), 56.18 (NH_2C), 51.50 (OCH_3), 50.34 ($CHCH_3$), 40.31 ($COCH_2$), 34.25 ($PhCH_2$), 26.00 ($CH_2CH_2CH_2$), 19.73 ($PhCH_3$), 19.44 ($PhCH_3$), 19.06 ($PhCH_3$), 18.87 (CH_3C), 17.12 ($CHCH_3$). MS (ES+) m/z 625.3 (MH^+) and 647.3 (MNa^+). Reverse-phase analytical HPLC (0.1% TFA in H_2O – ACN 20:80 v/v increasing to 0:100 v/v in 35 min), 1 ml/min, $\lambda = 245$ nm showed a peak with a $t_R = 17.03$ min (94.6%).

Synthesis of (2*S*)-benzyl 2-((((*R*)-2-amino-3-((2,5-dimethyl-4-(4-(*p*-tolyl) butanoyl) benzyl) oxy)-2-methylpropoxy) (phenoxy) phosphoryl) amino) propanoate (16)

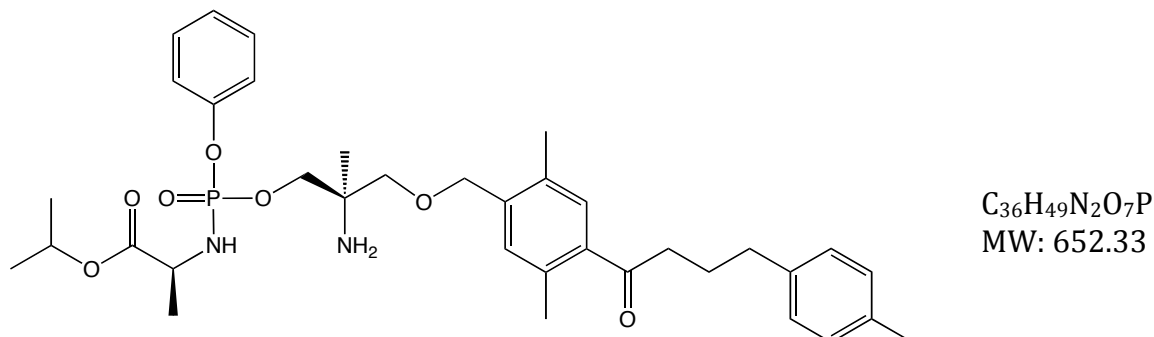


tBuMgCl (1.3 ml, 1.3 mmol) was added dropwise to a solution of (*S*)-1-(4-((2-amino-3-hydroxy-2-methylpropoxy) methyl) -2,5-dimethylphenyl)-4-(*p*-tolyl) butan-1-one (500 mg, 1.3 mmol) in anhydrous THF (20 ml) under anhydrous conditions. The mixture was stirred at room temperature for one hour. After one hour the phosphorochloridate (459 mg, 1.3 mmol) in anhydrous THF (5 ml) was added dropwise to the stirring reaction mixture. The reaction was left to stir for 24 hours. After 24 hours the solvent was removed *in vacuo* and the desired product was isolated using flash chromatography (methanol – ethyl acetate 0:100 v/v increasing to 10:90 v/v) giving the desired oil product as a mixture of 2 diastereoisomers (87%, 0.791 g). The resulting oil was further purified using preparative reverse-phase HPLC (0.1% TFA in H₂O – ACN 20:80 v/v increasing to 100:0 v/v in 35 min) giving the desired product (8%, 0.07 g).

³¹P NMR (MeOD, 202 MHz): δ 3.73, 3.37, 3.29. ¹H NMR (MeOD, 500 MHz): δ 7.42 (1H, m, ArH), 7.33 (7H, m, ArH), 7.23 (4H, m, ArH), 7.07 (1H, m, ArH), 5.11 (2H, m, PhCH₂O), 4.61 (2H, m, PhCH₂O), 4.22 (2H, m, CH₂OP), 4.04 (1H, m, CHCH₃), 3.60 (2H, m, CCH₂O), 3.37 (1H, m, NH), 2.88 (2H, t, *J* = 7 Hz, COCH₂), 2.63 (2H, t, *J* = 7.5 Hz, PhCH₂), 2.40 (3H, s, PhCH₃), 2.34 (3H, s, PhCH₃), 2.30 (3H, s, PhCH₃), 2.04 (2H, s, NH₂), 1.95 (2H, quin, *J* = 7.5 Hz, CH₂CH₂CH₂), 1.34 (3H, m, CHCH₃), 1.33 (3H, m, CCH₃). ¹³C NMR (MeOD, 125 MHz): δ 207.18 (C=O), 175.67 (C=O), 152.48 (d, ²*J*_{C-P} = 6.5 Hz, POC-Ar), 140.50 (C-Ar), 140.28 (C-Ar), 139.69 (C-Ar), 137.76 (C-Ar), 137.07 (C-Ar), 137.81 (C-Ar), 136.16 (C-Ar), 133.89 (CH-Ar), 133.84 (CH-Ar), 132.07 (CH-Ar), 131.50 (CH-Ar), 130.66 (CH-Ar), 130.25 (CH-Ar), 130.04 (CH-Ar), 130.03 (CH-

Ar), 129.94 (CH-Ar), 129.86 (CH-Ar), 129.84 (CH-Ar), 127.08 (CH-Ar), 127.03 (CH-Ar), 122.11 (2d, $^3J_{C-P} = 4.63$ Hz, CH-Ar), 73.17 (OCH₂C), 72.70 (PhCH₂O), 69.50 (d, $^2J_{C-P} = 5.38$ Hz, CH₂OP), 68.68 (PhCH₂O), 58.23 (NH₂C), 50.50 (CHCH₃), 42.29 (COCH₂), 36.24 (PhCH₂), 27.98 (CH₂CH₂CH₂), 21.73 (PhCH₃), 21.45 (PhCH₃), 21.05 (PhCH₃), 20.85 (CH₃C), 19.13 (CHCH₃). MS (ES+) m/z 701.5 (MH⁺) and 723.4 (MNa⁺). Reverse-phase analytical HPLC (0.1% TFA in H₂O – ACN 20:80 v/v increasing to 0:100 v/v in 35 min), 1 ml/min, $\lambda = 245$ nm showed a peak with a $t_R = 19.88$ min (97.3%).

Synthesis of (2S)-isopropyl 2-((((R)-2-amino-3-((2,5-dimethyl-4-(4-(p-tolyl) butanoyl) benzyl) oxy)-2-methylpropoxy) (phenoxy) phosphoryl) amino) propanoate (17)



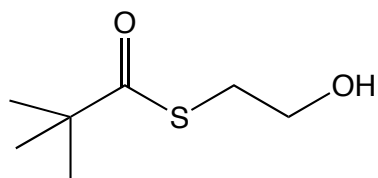
tBuMgCl (1.3 ml, 1.3 mmol) was added dropwise to a solution of (S)-1-(4-((2-amino-3-hydroxy-2-methylpropoxy) methyl) -2,5-dimethylphenyl)-4-(p-tolyl) butan-1-one (499 mg, 1.3 mmol) in anhydrous THF (25 ml) under anhydrous conditions. The mixture was stirred at room temperature for one hour. After one hour the phosphorochloridate (397 mg, 1.3 mmol) in anhydrous THF (6 ml) was added dropwise to the stirring reaction mixture. The reaction was left to stir for 24 hours. After 24 hours the solvent was removed *in vacuo* and the desired product was isolated using flash chromatography (methanol – dichloromethane 0:100 v/v increasing to 10:90 v/v) giving the desired oil product as a mixture of 2 diastereoisomers (15%, 0.129 g). The resulting oil was further purified using preparative reverse-phase HPLC (0.1% TFA in H₂O – ACN 20:80 v/v increasing to 100:0 v/v in 35 min) giving the desired product (8%, 0.065 g).

³¹P NMR (MeOD, 202 MHz): δ 3.78, 3.51, 3.43. ¹H NMR (MeOD, 500 MHz): δ 7.31 (1H, d, *J* = 3.5 Hz, Ar*H*), 7.26 (2H, m, Ar*H*), 7.15 (1H, m, Ar*H*), 7.12 (3H, m, Ar*H*), 6.96 (4H, s, Ar*H*), 4.85 (1H, m, CH(CH₃)₂), 4.51 (2H, m, PhCH₂O), 4.13 (2H, m, CH₂OP), 3.80 (1H, m, CHCH₃), 3.51 (1H, m, CCH₂O), 3.47 (1H, m, CCH₂O), 2.78 (2H, t, *J* = 7.5 Hz, COCH₂), 2.51 (2H, t, *J* = 7.5 Hz, PhCH₂), 2.28 (3H, s, PhCH₃), 2.23 (3H, s, PhCH₃), 2.18 (3H, s, PhCH₃), 1.84 (2H, quin, *J* = 7.5 Hz, CH₂CH₂CH₂), 1.18 (6H, m, CHCH₃), 1.12 (3H, m, CCH₃), 1.11 (3H, m, CHCH₃). ¹³C NMR (MeOD, 125 MHz): δ 205.24 (C=O), 173.54 (C=O), 150.53 (2d, ²*J*_{C-P} = 2 Hz, POC-Ar), 138.51 (C-Ar), 138.32 (C-Ar), 137.70 (C-Ar), 135.08 (C-Ar), 138.56 (C-Ar), 134.80 (C-Ar), 134.17 (C-Ar), 131.88 (CH-Ar), 130.07 (CH-Ar), 129.52 (CH-Ar), 128.66 (CH-Ar), 128.05

(CH-Ar), 125.09 (CH-Ar), 120.14 (2d, $^3J_{C-P} = 4.75$ Hz, CH-Ar), 71.18 (OCH₂C), 70.74 (PhCH₂O), 68.98 (OCH(CH₃)₂), 67.59 (2d, $^2J_{C-P} = 5.13$ Hz, CH₂OP), 56.22 (NH₂C), 50.52 (CHCH₃), 40.31 (COCH₂), 34.25 (PhCH₂), 26.00 (CH₂CH₂CH₂), 20.58 (OCHCH₃), 20.53 (OCHCH₃), 19.73 (PhCH₃), 19.44 (PhCH₃), 18.92 (PhCH₃), 18.84 (CH₃C), 17.13 (CHCH₃). MS (ES+) m/z 653.3 (MH⁺) and 675.3 (MNa⁺). Reverse-phase analytical HPLC (0.1% TFA in H₂O – ACN 20:80 v/v increasing to 0:100 v/v in 35 min), 1 ml/min, $\lambda = 245$ nm showed a peak with a $t_R = 18.64$ min (98.2%).

9.9 SATE Phosphorus Prodrugs

Synthesis of 2,2-Dimethyl-thiopropionic acid S-(2-hydroxy-ethyl) ester

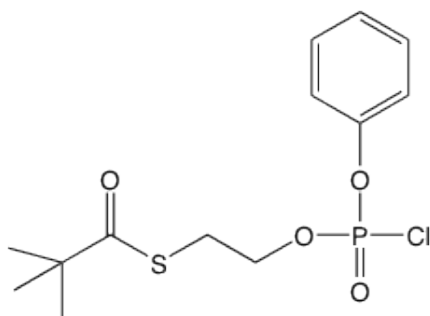


C₇H₁₄O₂S
MW: 162.07

Pivaloyl chloride (2.5 ml, 20.3 mmol) was added to a stirred solution of 2-mercaptoethanol (1.42 ml, 20.3 mmol) and triethylamine (2.83 ml, 20.3 mmol) in DCM, cooled at -78 °C. The mixture was stirred at -78 °C for 1 h. After 1 h the mixture was extracted with water and DCM (3 x 20 ml). The combined organic extracts were dried over MgSO₄ and concentrated in vacuo. The oily residue was purified by flash column chromatography (eluting with hexane - ethyl acetate 80:20 v/v increasing to 70:30 v/v) giving the desired compound (75%, 2.481 g).

¹H NMR (CDCl₃, 500 MHz): δ 3.98 (2H, m, HOCH₂), 3.03 (2H, m, SCH₂), 2.85 (1H, b, OH), 1.23 (9H, s, CCH₃).

Synthesis of 2,2-Dimethyl-thiopropionic acid S-(chloro-phenoxy-phosphoryloxy)-ethyl ester

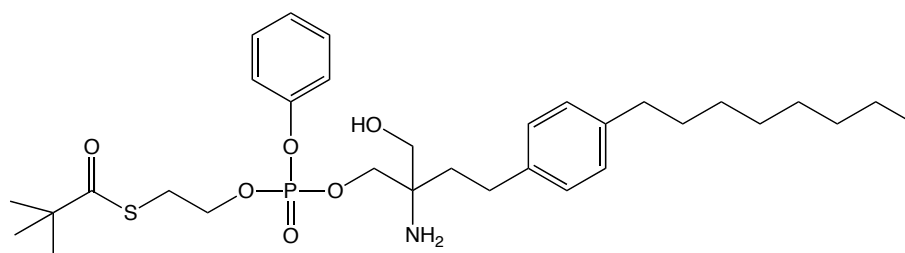


C₁₃H₁₈ClO₄PS
MW: 336.04

Phenyl dichlorophosphate (2.29ml, 15.31 mmol) was added dropwise into a cooled solution at -78 °C of 2,2-Dimethyl-thiopropionic acid S-(2-hydroxy-ethyl) ester (2.481 g, 15.31 mmol) and triethylamine (2.13 ml, 15.31 mmol) in THF (20 ml). The reaction was left to warm to room temperature and stirred overnight. The white precipitate was filtered off and the solution was concentrated in vacuo. The crude oil was used for the next step without further purification.

³¹P NMR (CDCl₃, 202 MHz): δ -0.69. ¹H NMR (CDCl₃, 500 MHz): δ 7.31 (2H, m, ArH), 7.18 (3H, m, ArH), 4.28 (2H, m, OCH₂), 3.15 (2H, t, *J* = 6.5 Hz, SCH₂), 1.17 (9H, s, CCH₃).

Synthesis of S-(2-(((2-amino-2-(hydroxymethyl)-4-(4-octylphenyl) butoxy) (phenoxy) phosphoryl)oxy) ethyl) 2,2-dimethylpropanethioate

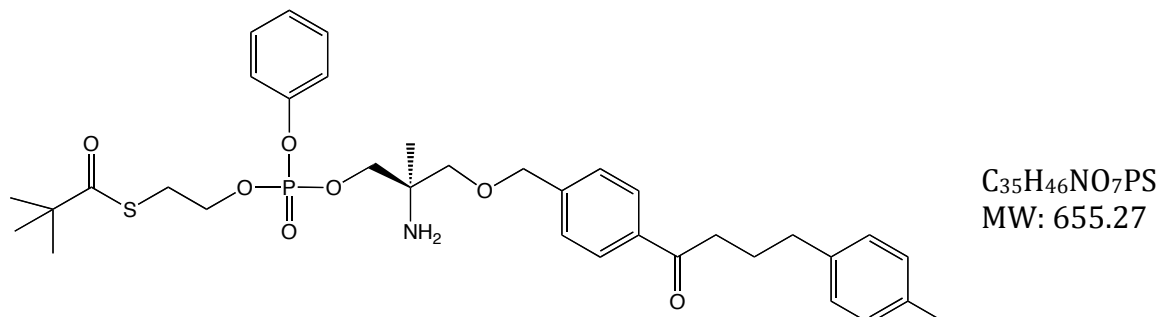


C₃₂H₅₀NO₆PS
MW: 607.31

tBuMgCl (1.45 ml, 1.454 mmol) was added dropwise to a solution of fingolimod HCl (500 mg, 1.454 mmol) in anhydrous THF (20 ml) under anhydrous conditions. The mixture was stirred at room temperature for one hour. After one hour 2,2-Dimethyl-thiopropionic acid S-(chloro-phenoxy-phosphoryloxy)-ethyl ester (489 mg, 1.454 mmol) in anhydrous THF (5 ml) was added dropwise to the stirring reaction mixture. The reaction was left to stir for 24 hours. After 24 hours the solvent was removed *in vacuo* and the desired product was isolated using flash chromatography (methanol – dichloromethane 0:100 v/v increasing to 10:90 v/v) and (methanol - dichloromethane 2:98 v/v) giving the desired compound as a mixture of four different diastereoisomers (7%, 0.076 g).

³¹P NMR (CDCl₃, 202 MHz): δ -5.88. ¹H NMR (CDCl₃, 500 MHz): δ 7.17 (4H, m, ArH), 7.03 (4H, s, ArH), 6.98 (1H, m, ArH), 6.38 (2H, b, NH₂), 3.96 (1H, t, *J* = 7 Hz, SCH₂CH₂), 3.94 (1H, t, *J* = 7 Hz, SCH₂CH₂), 3.74 (2H, m, CH₂OP), 3.1 2H, m, CH₂OP), 3.42 (1H, s, OH), 2.95 (2H, t, *J* = 7 Hz, OCH₂CH₂), 2.55 (4H, t, *J* = 7.5 Hz, PhCH₂), 1.89 (2H, m, CCH₂CH₂), 1.59 (2H, quin, *J* = 7.5 Hz, CH₂CH₂CH₂), 1.38-1.27 (10H, m, CH₂CH₂CH₂), 1.16 (9H, s, CCH₃), 0.91 (3H, m, CH₂CH₃). ¹³C NMR (CDCl₃, 125 MHz): δ 206.41 (C=O), 152.33 (d, ²*J*_{C-P} = 6.88 Hz, POC-Ar), 140.62 (C-Ar), 137.90 (C-Ar), 129.41 (CH-Ar), 128.45 (CH-Ar), 128.22 (CH-Ar), 123.53 (CH-Ar), 120.09 (CH-Ar), 120.05 (CH-Ar), 65.00 (d, ²*J*_{C-P} = 5.5 Hz, CCH₂OP), 62.80 (CCH₂OH), 60.86 (d, ²*J*_{C-P} = 3.88, CH₂CH₂OP), 46.39 (C(CH₃)₃), 35.63 (NH₂C), 33.83 (SCH₂), 31.96 (CCH₂), 31.65 (PhCH₂), 28.76 (PhCH₂), 28.69 (CH₂CH₂CH₂), 28.63 (CH₂CH₂CH₂), 27.33 (C(CH₃)₃), 22.72 (CH₂CH₃), 14.15 (CH₂CH₃). MS (ES+) *m/z* 648.3 (M+H₂+K⁺).

Synthesis of S-(2-((((R)-2-amino-2-methyl-3-((4-(4-(p-tolyl) butanoyl) benzyl) oxy) propoxy) (phenoxy)phosphoryl) oxy) ethyl) 2,2-dimethylpropanethioate

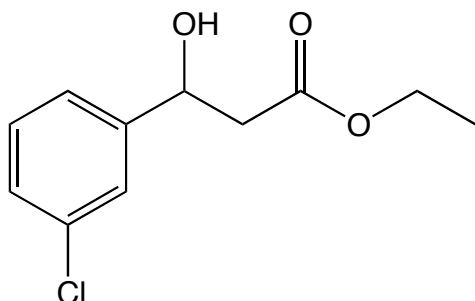


tBuMgCl (0.84 ml, 0.84 mmol) was added dropwise to a solution of (S)-1-(4-((2-amino-3-hydroxy-2-methylpropoxy) methyl) phenyl)-4-(p-tolyl) butan-1-one (300 mg, 0.84 mmol) in anhydrous THF (20 ml) under anhydrous conditions. The mixture was stirred at room temperature for one hour. After one hour 2,2-Dimethyl-thiopropionic acid S-(chloro-phenoxy-phosphoryloxy)-ethyl ester (282 mg, 0.84 mmol) in anhydrous THF (5 ml) was added dropwise to the stirring reaction mixture. The reaction was left to stir for 24 hours. After 24 hours the solvent was removed *in vacuo* and the desired product was isolated using flash chromatography (methanol – ethyl acetate 0:100 v/v increasing to 10:90 v/v) and (methanol - chloroform 0:100 v/v increasing to 10:90 v/v) giving the desired oil product as a mixture of 2 diastereoisomers (3%, 0.014g).

³¹P NMR (CDCl₃, 202 MHz): δ -7.54. ¹H NMR (CDCl₃, 500 MHz): δ 7.80 (2H, d, *J* = 8 Hz, ArH), 7.27 (2H, d, *J* = 8 Hz, ArH), 7.19 (2H, d, *J* = 9 Hz, ArH), 7.11 (2H, t, *J* = 7 Hz, ArH), 7.02 (4H, s, ArH), 6.90 (1H, t, *J* = 7.5 Hz, ArH), 4.44 (2H, s, CH₂Ph), 3.91 (2H, m, SCH₂CH₂), 3.51 (1H, m, CCH₂OP), 3.39 (2H, m, CCH₂O), 3.27 (1H, m, CCH₂OP), 2.92 (2H, m, OCH₂CH₂), 2.87 (2H, t, *J* = 7.5 Hz, COCH₂), 2.60 (2H, t, *J* = 7.5 Hz, PhCH₂CH₂), 2.25 (3H, s, PhCH₃), 1.98 (2H, quin, *J* = 7.5 Hz, CH₂CH₂CH₂), 1.19 (3H, s, CCH₃), 1.06 (9H, s, CCH₃). MS (ES+) *m/z* 674.29 (M+H₂O+H⁺).

9.10 HepDirect Phosphorus Prodrugs

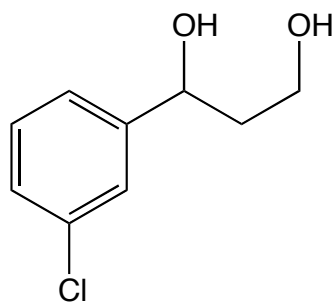
Synthesis of ethyl 3-(3-chlorophenyl)-3-hydroxypropanoate



C₁₁H₁₃ClO₃
MW: 228.06

N-butyllithium (14.25 ml, 35.6 mmol) was added slowly to a -78 °C solution of diisopropylamine (4.98 ml, 35.6 mmol) in anhydrous THF (35 ml) under anhydrous conditions. The mixture was stirred for 15 min and then a solution of AcOEt (3.5 ml, 35.6 mmol) in THF (5 ml) was added slowly and left to stir for 30 min. After 30 min a solution of 3-chlorobenzaldehyde (2.02 ml, 17.8 mmol) in THF (5 ml) was added slowly. The mixture was left to stir at -78 °C for 30 min and then removed from the dry ice bath and allowed to warm to ambient temperature over 2 h. 0.5 M HCl solution (200 ml) was then poured into the reaction mixture and then the mixture was extracted with AcOEt. The combined organic layers were dried over MgSO₄, vacuum filtered and the solvent was removed *in vacuo* giving the final crude product as an oil.

¹H NMR (CDCl₃, 500 MHz): δ 7.42 (1H, s, ArH), 7.29 (3H, m, ArH), 5.13 (1H, m, CHOH), 4.22 (2H, q, *J* = 7 Hz, OCH₂CH₃), 3.51 (1H, s, OH), 2.72 (2H, m CH₂CO), 1.29 (3H, t, *J* = 7 Hz, CH₂CH₃).

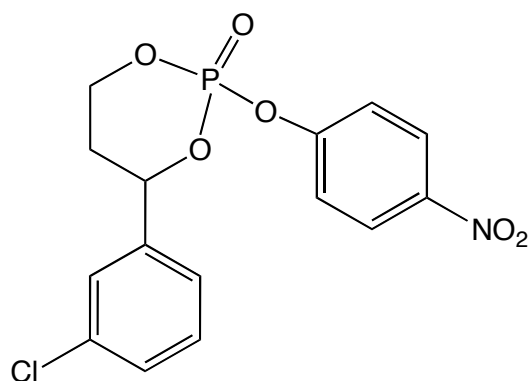
Synthesis of 1-(3-chlorophenyl) propane-1,3-diol

$C_9H_{11}ClO_2$
MW: 186.04

Crude ethyl 3-(3-chlorophenyl)-3-hydroxypropanoate (< 17.8 mmol) was dissolved in diethyl ether (40 ml) and cooled to 0 °C. A solution of $LiAlH_4$ (1M in THF, 52.5 ml, 52.5 mmol) was added slowly and the mixture was left to slowly warm to ambient temperature overnight. The mixture was cooled in an ice bath and the reaction was quenched slowly with AcOEt and treated with 0.5 M HCl. The mixture was stirred vigorously and then extracted with AcOEt. The combined organic extracts were dried over $MgSO_4$ and concentrated *in vacuo*. The crude product was purified by flash column chromatography (eluting with hexane - ethyl acetate 75:25 v/v increasing to 50:50 v/v) giving the desired compound (15%, 0.503 g).

1H NMR ($CDCl_3$, 500 MHz): δ 7.39 (1H, s, ArH), 7.27 (3H, m, ArH), 4.95 (1H, m, CHOH), 3.87 (2H, m, CH_2OH), 3.44 (1H, b, CHOH), 2.63 (1H, b, CH_2OH), 1.95 (2H, m, $CHCH_2CH_2$).

Synthesis of 4-(3-chlorophenyl)-2-(4-nitrophenoxy)-1,3,2-dioxaphosphinane 2-oxide



C₁₅H₁₃ClNO₆P
MW: 369.02

To a solution of 4-nitrophenyl phosphorodichloridate (760 mg, 2.97 mmol), triethylamine (1.5 ml, 10.8 mmol) in THF (12 ml) was added 1-(3-chlorophenyl) propane-1,3-diol (503 mg, 2.7 mmol) at 0 °C. After 1 h 4-nitrophenol (1.5 g, 10.8 mmol) in THF (6 ml) was added followed by triethylamine (1.5 ml, 10.8 mmol). The mixture was then allowed to warm to ambient temperature overnight. The solvent was then removed *in vacuo* and the crude product was extracted with AcOEt and water. The organic phase was then washed with 0.4 M NaOH solution, brine, water and then dried over MgSO₄. The crude product was then concentrated *in vacuo* and purified by flash column chromatography (eluting with hexane - ethyl acetate 50:50 v/v increasing to 25:75 v/v) giving the desired compound (69%, 0.685 g).

³¹P NMR (CDCl₃, 202 MHz): δ -14.51, -14.71. ¹H NMR (CDCl₃, 500 MHz): δ 8.19 (2H, d, *J* = 9 Hz, ArH), 7.39 (2H, m, ArH), 7.34 (1H, m, ArH), 7.29 (2H, m, ArH), 7.21 (1H, m, ArH), 5.52 (1H, m, PhCHO), 4.56 (2H, m, POCH₂), 2.33 (1H, m, CHCH₂CH₂), 2.06 (1H, m, CHCH₂CH₂).